Cork Open Research Archive
Cartlann Taighde Oscailte Chorcaí

| | |
|---|---|
| **Title** | Feasibility of combined wind-wave energy platforms |
| **Author(s)** | O'Sullivan, Keith Patrick |
| **Publication date** | 2014 |
| **Original citation** | O'Sullivan, K. 2014. Feasibility of combined wind-wave energy platforms. PhD Thesis, University College Cork. |
| **Type of publication** | Doctoral thesis |
| **Rights** | © 2014, Keith O' Sullivan. http://creativecommons.org/licenses/by-nc-nd/3.0/  |
| **Embargo information** | No embargo required |
| **Item downloaded from** | http://hdl.handle.net/10468/1897 |

University College Cork, Ireland
Coláiste na hOllscoile Corcaigh

**National University of Ireland – Cork (NUIC)**

**Department of Civil and Environmental Engineering**
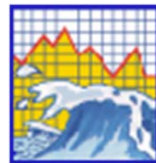




## "Feasibility of Combined Wind-Wave Energy Platforms"

Keith O'Sullivan BE(Hons) MEngSc

Supervisors: Dr. Jimmy Murphy, Prof. Tony Lewis
Head of Department: Prof. Gerald Kiely

Submitted in fulfilment of the requirements for the degree of

Doctor of Philosophy (PhD)

**September 2014**

*"Feasibility of Combined Wind-Wave Energy Platforms"*

# Contents

## Figures

## Tables

## Declaration

*"The work contained in this thesis has not been previously submitted to meet the requirements for an award at University College Cork (UCC) or any other higher education institution. To the best of my knowledge and belief, this thesis contains no material previously published or written by another person except where due reference is made."*

Signed:_____     Date:_____

        Keith O' Sullivan BE(Hons) MEngSc

## Acknowledgements

I would like to express my sincere gratitude to all those who aided me in the process of completing this work, including:

In particular Dr. Jimmy Murphy, my project supervisor, for affording me the opportunity to undertake this research work, for his valuable advice and encouragement throughout this study;

Prof. Tony Lewis for his support and guidance during the thesis preparation phase;

Prof. Alistair Borthwick and Prof. Gerald Kiely, for affording me the facilities of the Civil and Environmental Engineering Department, University College Cork to undertake this study;

The MARINA Platform team at Beaufort Research - Hydraulics and Maritime Research Centre (HMRC), Ms Katie Lynch, Dr. Fiona Devoy McAuliffe and Dr. Sara Armstrong for their assistance throughout the project;

The consortium members of the EU FP7 MARINA Platform project for their invaluable advice and guidance;

The staff of the Beaufort Research - HMRC, Mr. Tom Walsh, Mr. Niall O' Sullivan, Mr. Brian Holmes and Mr. Florent Thiebaut for their technical expertise and assistance throughout the various tank testing campaigns, and Mrs. Cora Edwards, Mrs. Mary Ryan, Ms. Mary Coleman and Ms. Emma Knowles for their administrative support;

My fellow students, Michael O' Shea, Richard O' Shea, Aaron Barker and Andrew Clarke for their assistance throughout the years in data analysis and tank testing;

Mr. Andy Baldock, Director Sustainable Energy Solutions, for his patience, understanding and flexibility during the final stages of the preparation of this thesis while working for Black & Veatch Ltd., and also Mr. Andy Jones, Chief Maritime Engineer, for his guidance on all things marine energy related;

And finally, the most important of all, my family, Parents and sisters, for their unwavering support and encouragement when needed most, particularly following my move to London in January 2014.

## Abstract

The European Union has set out an ambitious 20% target for renewable energy use by 2020. It is expected that this will be met mainly by wind energy. Looking towards 2050, reductions in greenhouse gas emissions of 80-95% are to be sought. Given the issues securing this target in the transport and agriculture sectors, it may only be possible to achieve this target if the power sector is carbon neutral well in advance of 2050. This has permitted the vast expansion of offshore renewables, wind, wave and tidal energy.

Offshore wind has undergone rapid development in recent years however faces significant challenges up to 2020 to ensure commercial viability without the need for government subsidies. Wave energy is still in the very early stages of development so as yet there has been no commercial roll out.

As both of these technologies are to face similar challenges in ensuring they are a viable alternative power generation method to fossil fuels, capitalising on the synergies is potentially a significant cost saving initiative. The advent of hybrid solutions in a variety of configurations is the subject of this thesis. A singular wind-wave energy platform embodies all the attributes of a hybrid system, including sharing space, transmission infrastructure, O&M activities and a platform/foundation. This configuration is the subject of this thesis, and it is found that an OWC Array platform with multi-MegaWatt wind turbines is a technically feasible, and potentially an economically feasible solution in the long term. Methods of design and analysis adopted in this thesis include numerical and physical modelling of power performance, structural analysis, fabrication cost modelling, simplified project economic modelling and time domain reliability modelling of a 210MW hybrid farm. The application of these design and analysis methods has resulted in a hybrid solution capable of producing energy at a cost between €0.22/kWh and €0.31/kWh depending on the source of funding for the project. Further optimisation through detailed design is expected to lower this further.

This thesis develops new and existing methods of design and analysis of wind and wave energy devices. This streamlines the process of early stage development, while adhering to the widely adopted Concept Development Protocol, to develop a technically and economically feasible, combined wind-wave energy hybrid solution.

## Acronyms

| | |
|---|---|
| ABS | American Bureau of Shipping |
| AC | Alternating current |
| AEO | Annual energy output |
| AHT | Anchor handling tug |
| AMETS | Atlantic Marine Energy Test Site |
| ATN | Attenuators |
| AWECS | Amplified Wave Energy Conversion System |
| B2D2 | Backward bent duct device |
| BBDB | Backward bent duct buoy |
| BIEM | Boundary integral element method |
| BM | Bending moment |
| BV | Bureau Veritas |
| BW | Bulge Wave Devices |
| CALM | Catenary anchor leg mooring |
| CAPEX | Capital expenditure |
| CCOB | Cantabria Coastal and Ocean Basin |
| CFD | Computational fluid dynamics |
| CM | Corrective Maintenance |
| COE | Cost of energy |
| COG | Centre of gravity |
| CORES | Components for Offshore Renewable Energy |
| CWR | Capture width ratio |
| DANWEC | Danish Wave Energy Centre |
| DCF | Discounted cash flow |
| DDF | Deep Draught Floating |
| DF | Device factor |
| DNV | Det Norsk Veritas |
| DONG | Danish Oil and Natural Gas Energy A/S |
| EC | Embedded controller |

| | |
|---|---|
| ECN | Ecole Centrale de Nantes |
| EHS | Extra high strength steels |
| EIA | Environmental impact assessment |
| EMEC | European Marine Energy Centre |
| Equimar | Equitable Testing and Evaluation of Marine Energy Extraction Devices in terms of Performance, Cost and Environmental Impact |
| ETA | Event Tree Analysis |
| ETS | Emissions Trading System |
| EU | European Union |
| EU FP7 | European Union Seventh Framework Programme |
| EWEA | European Wind Energy Association |
| F2T | Frequency to time domain |
| FAST | Fatigue, Aerodynamics, Structures and Turbulence |
| FEM | Finite element method |
| FHR | Flanders Hydraulics Research |
| FLS | Fatigue limit state |
| FMEA | Failure modes and effects analysis |
| FMEA | Failure Modes and Effects Analysis |
| FOS | Factor of Safety |
| FPP | Floating Power Plant |
| FPSO | Floating, production, storage offshore |
| FTA | Fault Tree Analysis |
| GBS | Gravity based structure |
| GH | Garrad Hassan |
| GL | Germanischer Lloyd |
| GYD | Gyroscopic Devices |
| HAWT | Horizontal axis wind turbine |
| HAZOP | Hazard and operability study |
| HMRC | Hydraulics and Maritime Research Centre |
| HRA | Human Reliability Analysis Techniques |

| | |
|---|---|
| HS | High strength steels |
| HSE | Health, safety and environment |
| HV | High voltage |
| IEA-OES | International Energy Agency – Ocean Energy System |
| IEC | International Electrotechnical Commission |
| IEEE | Institute of Electrical and Electronic Engineers |
| IRF | Impulse response function |
| IRR | Internal Rate of Return |
| ISO | International Organisation for Standardisation |
| IST | Instituto Superior Technico |
| IWS | Internal water surface |
| JONSWAP | Joint North Sea Wave Project |
| LCCA | Life cycle cost analysis |
| LCOE | Levelised cost of energy |
| LRFD | Load and Resistance Factor Design |
| MARINA | MArine Renewable INtegrated Application |
| MATLAB | Matrix Laboratory |
| MC | Monte Carlo |
| MI&T | Marine Innovation and Technology |
| MII | Motion induced interruption |
| MPA | Multiple Point Absorber |
| MRE | Marine renewable energy |
| MSP | Marine spatial planning |
| MTTF | Mean time to failure |
| MTTR | Mean time to repair |
| MWP | McCabe Wave Pump |
| NaREC | National Renewable Energy Centre |
| NASA | National Aeronautics and Space Administration |
| NATO | North Atlantic Treaty Organisation |
| NPV | Net Present Value |

| | |
|---|---|
| NREL | National Renewable Energy Laboratory |
| NS | Normal Strength Steel |
| O&M | Operations and maintenance |
| OES | Ocean Energy Systems |
| OPEX | Operational expenditure |
| OPT | Ocean Power Technologies |
| Orecca | Offshore Renewable Energy Conversion platforms Co-ordinated Action |
| OS | Offshore Standards |
| OSS | Offshore Service Standards |
| OTD | Overtopping devices |
| OTEC | Ocean thermal energy conversion |
| OWC | Oscillating water columns |
| OWEL | Offshore Wave Energy Limited |
| OWSC | Oscillating wave surge converters |
| OWWE | Ocean Wave and Wind Energy |
| PA | Point absorbers |
| PDF | Probability density function |
| PM | Preventative Maintenance |
| PRA | Probabilistic risk assessment |
| PTO | power take-off |
| R&D | Research and development |
| RANS | Reynolds-Averaged Navier-Stokes |
| RAO | Response amplitude operators |
| RBI | Risk Based Inspection |
| RC | Reinforced concrete |
| RCM | Reliability Centred Maintenance |
| REFIT | Renewable Energy Feed-In-Tariffs |
| RMS | Root mean square |
| RNA | Rotor-Nacelle Assembly |
| RP | Recommended Practices |

| | |
|---|---|
| SEAI | Sustainable Energy Authority of Ireland |
| SPD | Submerged Pressure Differential |
| SPH | Smooth Particle Hydrodynamics |
| SSG | Seawave Slot-Cone Generator |
| STANAG | Standardisation agreement |
| Standpoint | Standardisation of Point absorbers wave energy converters by demonstration |
| SURGE | Simple underwater renewable generation of electricity |
| TC | Technical Committee |
| Tc | Tipping coefficient |
| TLP | Tension leg platforms |
| TP | Transition piece |
| TRL | Technology Readiness Level |
| UCC | University College Cork |
| UDL | Uniformly distributed load |
| UK | United Kingdom |
| ULS | Ultimate limit state |
| UoE | University of Edinburgh |
| VAWT | Vertical axis wind turbine |
| VOF | Volume Of Fluid |
| WEC | Wave energy converter |
| WRASPA | Wave-driven, Resonant, Arcuate action, Surging Point Absorber |
| WSD | Working Stress Design |
| WTG | Wind turbine generators |

# 1   Introduction

This chapter outlines the current status of European renewable energy policy and associated targets, the commercial offshore wind market share, the current status of wave energy technology development and the challenges facing the offshore wind and wave energy industries. Furthermore, the potential solutions to these challenges are postulated and the contribution of this thesis is outlined.

## 1.1   European Renewable Energy Policy to 2050

In 2009, the European Union (EU), through its Renewable Energy Directive, has set out an ambitious 20% renewable energy target by 2020. This target has resulted in differentiated legally binding national renewable energy targets for each Member State. Encouragingly, the vast majority of the Member States have recognised the importance of this Directive, with 25 of 27 States planning to either exceed or meet their renewable energy targets. Assuming these commitments are met, the EU will exceed its target of 20% by 0.7 percentage points. These will most likely, in the main, be met by wind power as indicated by the European Wind Energy Association (EWEA). Looking beyond 2020, to 2050, the EU Heads of States have agreed on reductions of 80-95% in greenhouse gas emissions, while the directive on EU Emissions Trading System (ETS) will continue to reduce the cap on ETS sectors by 1.74% each year [1]. Given the issues with reducing emissions in areas such as transport and agriculture, achieving the Heads of State agreement is only possible if the power sector is carbon neutral well before 2050. This has permitted the vast expansion of renewable energy generation offshore, namely through wind, wave and tidal energy.

## 1.2   Offshore Wind Development

In recent years, significant funding has been put into developing the offshore wind energy industry in order for it to become a source of commercially exploitable renewable energy. The current status of European offshore wind power is at ~4GW of capacity [2], located mainly close to shore in depths of approximately 30m. Figure 1-1illustrates the recently developed 630MW London Array offshore wind farm located in the mouth of the Thames Estuary.



**Figure 1-1: London Array monopile offshore wind farm in the Thames Estuary [3]**

The wind turbine generators (WTG) themselves are very similar to their onshore counterparts using gearbox drivetrains and rotor diameters ranging from 60-120m with capacities of 2-5MW as illustrated in Figure 1-2.
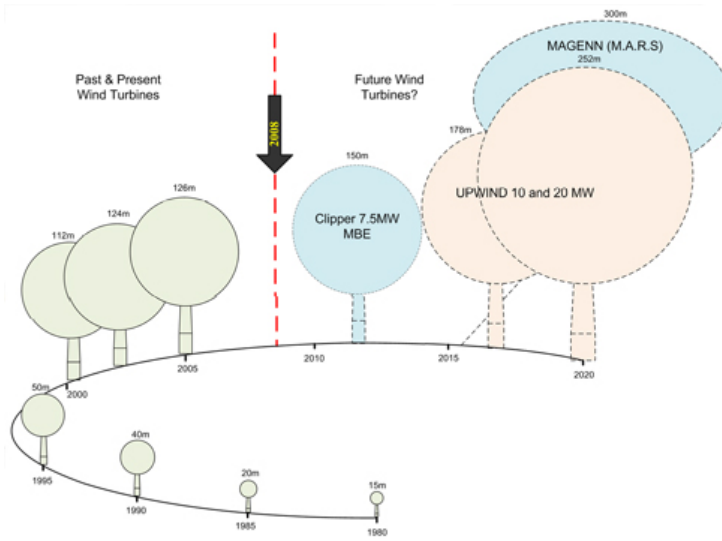


**Figure 1-2: Wind turbine sizes development with year [4]**

The drivetrain systems currently include gearbox systems while some have direct drive systems. Current developments seem to be that larger turbines, >5MW, will be direct drive system wind turbines which is a significant shift in standards up to 2012. Siemens have the majority of the offshore market up to now as indicated in Figure 1-3, with Vestas the next largest manufacturer.
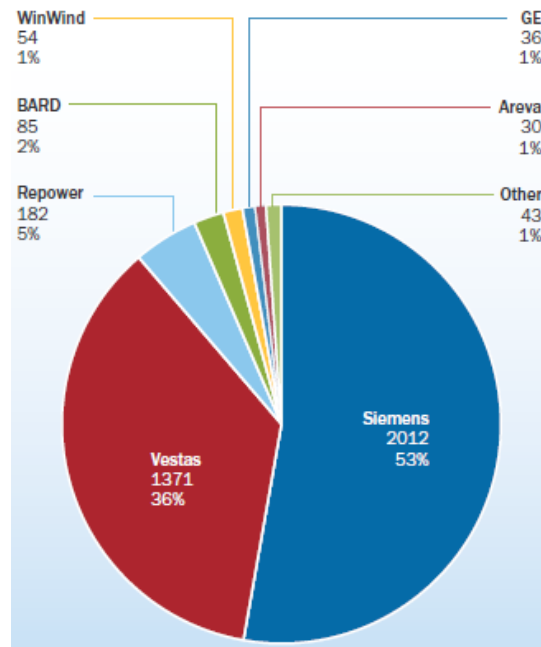


**Figure 1-3: Market share of wind turbine manufacturers [2]**

2

The foundations typically deployed offshore are illustrated in Figure 1-4 and Figure 1-5, whilst Figure 1-6 indicates the percentage market share of these foundations up to 2012.
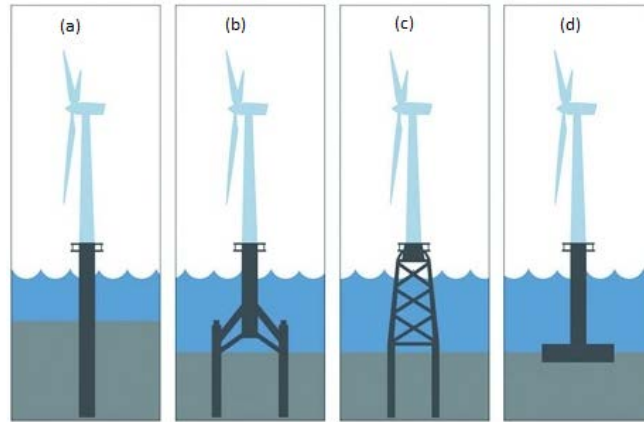


**Figure 1-4: Wind turbine foundations currently in use by industry, (a) monopile, (b) tripod, (c) jacket, (d) gravity based system [5]**



**Figure 1-5: Ormonde, Beatrice and Nysted Wind Farm foundations**
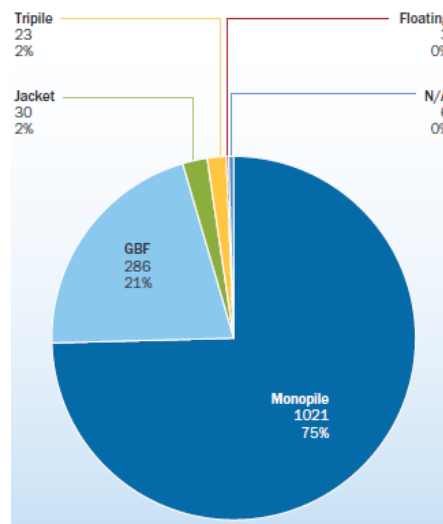


**Figure 1-6: Market share of offshore wind turbine foundations [2]**

The installation of these foundations have thus far utilised large heavy lift vessels for the installation of the foundations and wind turbines, like that in Figure 1-7, while a fleet of smaller service vessels tend to grouting and electrical rigging works.

**Figure 1-7: Wind turbine installation vessel at the Sheringham Shoal wind farm [6]**

Within the offshore wind development market, there are a significant number of developers/owners. However, the market share is far from even, with three developers owning over 50% and six developers owning 74% as illustrated in Figure 1-8. DONG Energy was the main developer in 2012, with significant plans for increasing their installed capacity up to 2020.
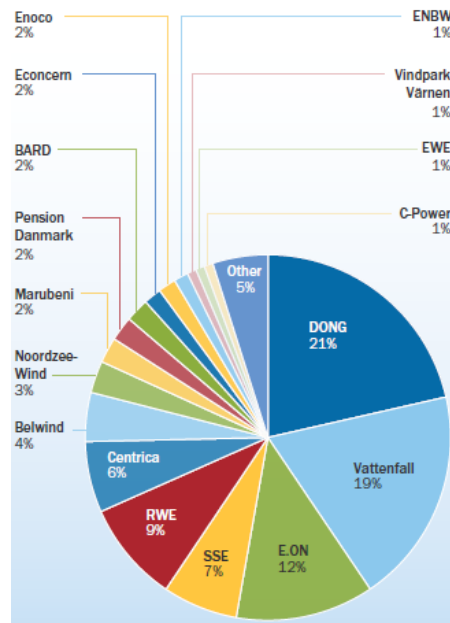


**Figure 1-8: Developers/Owners market share of offshore wind [2]**

The most active geographical market is the UK with 87% of new capacity in 2011. The recent Round 3 leases have set significant technical challenges for the industry with water depths of up to 70m and distances from shore up to 100km. Existing technology for offshore wind may be used for the sites nominated in Round 3 however, these farms will be under pressure to be financially viable due to the increase in costs of foundations and transmission systems with increasing water depth and distance offshore. The installed capacity due under this leasing round, 32GW, will help achieve the UK's 2020 targets. Looking beyond Round 3, it is expected that the next sites will exceed the economic feasibility of existing foundation technology. From Figure 1-6, it is noted that floating foundations are

included and these are the foundation types that are likely to feature in offshore wind farms beyond 2020. The design of these foundations have closely followed the experience of oil and gas exploration and extraction platforms, with semi-submersible, spar and tension leg platforms (TLP). Figure 1-9 illustrates the basic floating foundation concepts used for floating wind turbines.
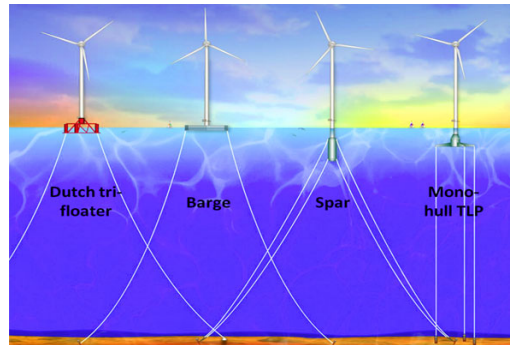


**Figure 1-9: Floating foundations used for wind turbines [7]**

This technology is at demonstration stage with both scaled and full-scale prototypes being deployed offshore. The best known of these include Statoil Hydro's Hywind spar concept, Blue H Group's TLP concept and Principle Power's WindFloat semi-submersible concept. Figure 1-10 illustrates these demonstration scale prototypes.
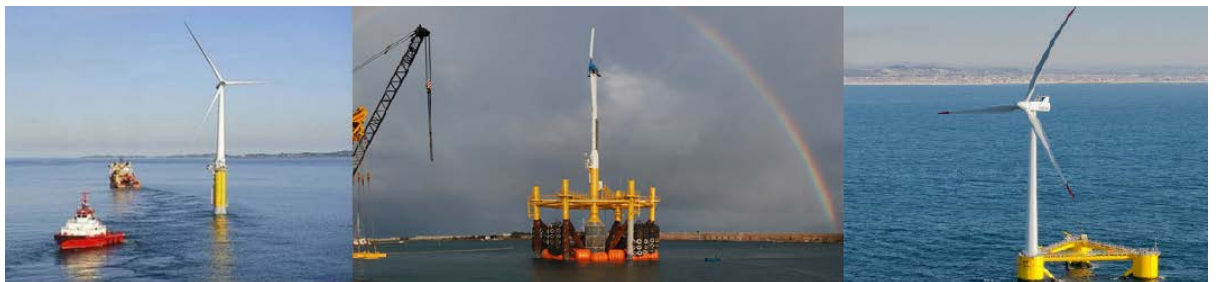


**Figure 1-10: Demonstration prototypes, Hywind, Blue H TLP, WindFloat**

These technologies will undoubtedly feature prominently in the development of offshore wind installations in the future. It is expected though, just as fixed offshore wind was more expensive than onshore wind [8], that floating offshore wind will be even more expensive and technological advances and cost saving efforts will be required in order to make these foundations commercially viable [9].

## 1.3 Wave Energy Development

The development of wave energy technology has not seen the same level of attention amongst commercial developers as wind energy. Since the early 1990's, following a series of unsuccessful deployments of wave energy platform concepts, a renewed interest in the development of wave energy devices has emerged. Unlike wind turbine technology, wave energy converter (WEC) technologies have not converged to one solution. A variety of primary absorption methods exist including oscillating water columns (OWC), wave activated bodies which include point absorbers (PA), attenuators (ATN) and oscillating wave surge converters (OWSC), and overtopping

devices (OTD). Figure 1-11 illustrates the primary methods of wave energy absorption [10].
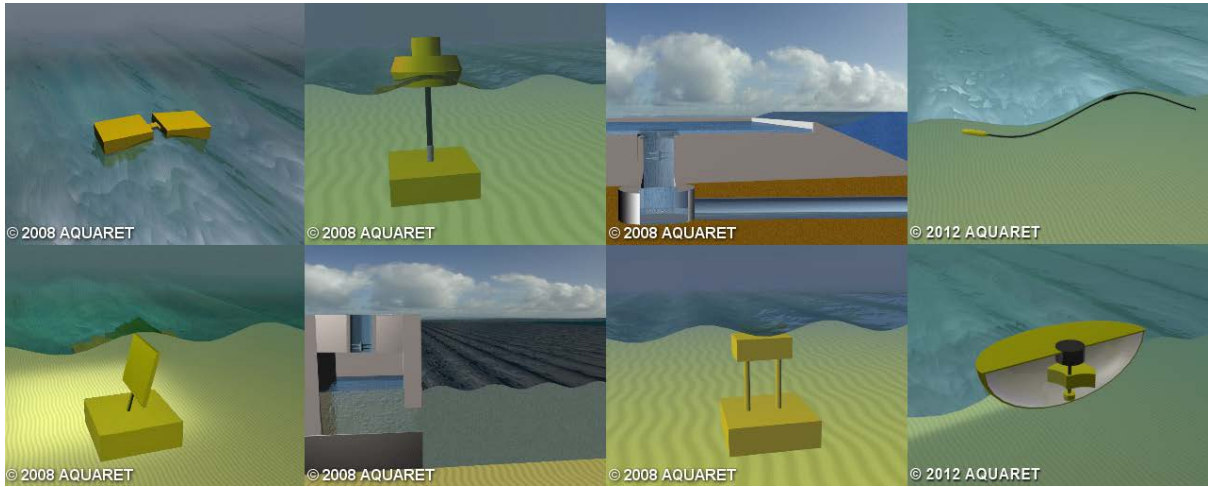


**Figure 1-11: Basic principles of wave energy conversion, clockwise from top left, ATN, PA, OTD, Bulge Wave, Gyroscopic, Submerged Pressure Differential, OWC, OWSC**

Each of these concepts, each in a number of different forms, has been demonstrated at either scale or full-scale at sea. Figure 1-12 illustrates WEC's that have been deployed at sea for trials. The OE Buoy floating OWC by Ocean Energy Ltd. at Galway Bay Ireland, WaveBob floating PA by WaveBob Ltd. at Galway Bay Ireland, Oyster OWSC by Aquamarine Ltd. at the European Marine Energy Centre (EMEC) Orkney, Wave Dragon floating OTD at Nissum Bredning in Denmark, Pelamis ATN at EMEC and Archimedes Wave Swing submerged PA in Portugal.
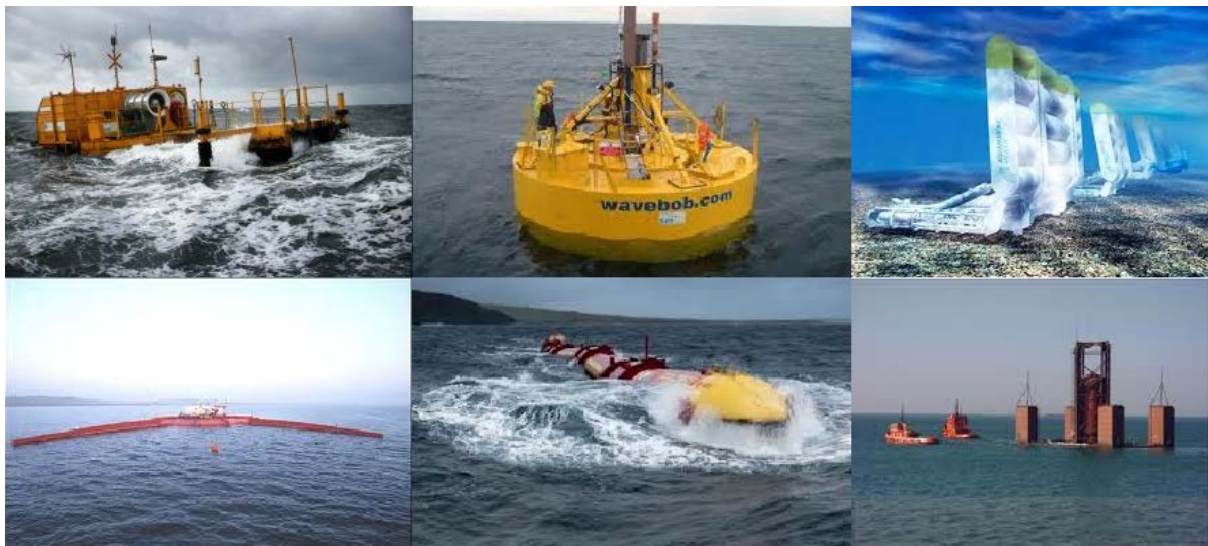


**Figure 1-12: Wave energy converters during sea trials, clockwise from top left, OE Buoy, WaveBob, Oyster, Archimedes Wave Swing, Pelamis and Wave Dragon**

These deployments have increased confidence in the industry and have encouraged investment in the sector from national governments, the EU and industrial companies, but have also highlighted that there remain a lot of technical issues to be resolved. These developments in the past decade have not resulted in significant

interest being displayed by large scale offshore developers. WEC development companies are typically small-medium sized enterprises with limited access to financing, and will struggle to bring wave energy to a commercial stage. In 2011, there was a significant development between DONG Energy A/S and Wave Star A/S in Denmark, who have entered into a research and development collaborative agreement investigating the possibility of combining wind and wave energy [11]. The wave energy sector will rely heavily on the offshore wind sector, both from an operations and maintenance (O&M) experience perspective but also from a financing perspective.

## 1.4  Issues Facing Wind and Wave Energy Industry

A EWEA report in 2009 quotes 150GW of installed wind capacity by 2030 as an achievable scenario for European waters [12] and it is well documented that the EU stresses that wind power can and must make a significant contribution to meeting the EU's energy policy objectives. The issue is that suitable sites will become scarce following the planned build out to 2020 and the technology will be forced into deeper waters farther from shore. This will challenge the current status of "fixed" foundation technology. The installation of these fixed foundation technologies requires significant mobilisation of large vessels and man-power and as such bears a significant cost. Economic feasibility of offshore wind currently relies on subsidies and investing in larger foundations with the same energy yield will then make it a loss making investment. The commercial exploitation potential for wind farms in deeper water is immense and existing plans for the next generation of wind farms suggest that the typical capacity will be of the order of 1000MW per farm, tens of kilometres from shore. With this in mind, the floating foundations, like those in Figure 1-9, will become prominent beyond 2020. Yet these will be far more capital intense than current foundations, and as such will require larger turbines to be installed. Even then, given the quantity of material required for floating foundations, energy yield from larger turbines may not be sufficient in order to make the venture worthwhile.

Wave energy has had a number of setbacks in the past, with developers eager to deploy prototypes at sea, without due consideration of the significant risks associated with such activities. As a consequence wave energy technology developers struggle to secure funding for the continued development of their technology. One criticism that must be said about developers at present, is that the experiences of the past do not seem to be taken into account with concepts with high levels of innovative mechanisms being deployed. This, in the view of investors, translates directly to increased risk. The Equitable Testing and Evaluation of Marine Energy Extraction Devices in terms of Performance, Cost and Environmental Impact (Equimar) Concept Development Protocol [13] has set out guidelines for the development of WEC concepts through tank testing and sea trials. For successful sea trials, risk reduction must be prioritised. This is achievable through, firstly, using proven technology for the platform on which the WEC is based. The survivability of this

platform is critical to the success of the technology. Secondary to this, is efficiency of the WEC in generating power. The development of WEC technology is quite diverse, ranging from small to very large devices. It remains to be seen which is the better approach, however it seems that the assessment methodologies have not progressed sufficiently to enable a definitive conclusion to be made, nor, have the prototype deployments significantly contributed to this argument.

## 1.5 Potential Solutions to the Offshore Wind and Wave Industry Challenges

There are a number of strategies which would result in cost and risk reduction for both the offshore wind and wave energy industries in the short term. However, due to the distinct possibility that wave energy may not feature substantially before 2030, this thesis considers a long term solution to significantly reducing cost and risks for both wind and wave energy industries. This is the design of hybrid wind-wave energy conversion concepts. Hybrid solutions can be realised in a number of different arrangements including,

- Sharing space
- Sharing power transmission infrastructure
- Sharing O&M strategies
- Sharing a foundation/platform

The concepts considered in this thesis involve a structural platform, either seabed mounted or floating, with a wind turbine and one or more of the wave energy absorption concepts mounted on the platform. This type of hybrid satisfies all the arrangements noted above and satisfies two of the main barriers to development of both technologies. Firstly, with the integration of wave energy converters to a platform it would require additional strength and reliability, such that it would provide a safe and potentially over-designed platform for the wind turbine. Secondly, by constructing a suitable platform with WEC's integrated on it, the addition of a wind turbine ensures a revenue stream from a more developed technology. These are the primary attractions to the development of hybrids in the short term, but these platforms have longer term benefits assuming they are deployed in commercial scale. These benefits include increased capacity per installation, a reduction in the per MW capital expenditure (CAPEX), and potentially smoother power output from the platform considering the wind resource leads the wave resource by a number of hours. EU projects focussing on multi-purpose offshore platforms are currently underway, one in particular investigating renewable energy, is the MARINA Platform project.

## 1.6 EU FP7 MARINA Platform Project

The MArine Renewable INtegrated Application (MARINA) Platform project is a European Union funded project under the seventh framework programme (EU FP7) and is dedicated to bringing offshore renewable energy applications closer to the market by creating new infrastructures for both offshore wind and ocean energy

converters. One of the primary objectives of MARINA is to produce a cost-effective technology development basis from which the future marine renewable energy industry in Europe may grow. Crucial to the success of MARINA is the inclusion of deep-water engineering experience from consortium members from the oil and gas industry. It is recognised that for ocean energy technology to become sufficiently reliable, both in terms of energy production and survivability, early stage concepts must be based on the vast body of marine technical knowledge gained through experience in one of the most hostile environments in the world, the Northern European seas. The primary objectives of MARINA may be summarised in an extract from Annex 1 – "Description of Work" for the project:

*Research in the MARINA Platform project will establish a set of equitable and transparent criteria for the evaluation of multi-purpose platforms for marine renewable energy (MRE). Using these criteria, the project will produce a novel, whole-system set of design and optimisation tools addressing, inter alia, new platform design, component engineering, risk assessment, spatial planning, platform-related grid connection concepts, all focussed on system integration and reducing costs. These tools will be used, incorporating into the evaluation all, presently known proposed designs including (but not limited to) concepts originated by the project partners, to produce two or three realisations of multi-purpose renewable energy platforms. These will be brought to the level of preliminary engineering designs with estimates for energy output, material sizes and weights, platform dimensions, component specifications and other relevant factors. This will allow the resultant new multi-purpose MRE platform designs, validated by advanced modelling and tank-testing at reduced scale, to be taken to the next stage of development, which is the construction of pilot scale platforms for testing at sea.*

## 1.7 The Contribution this Thesis will make to the Solutions of the Challenges Facing the Offshore Wind and Wave Energy Industries

This thesis has closely followed the work plan of the MARINA Platform project, and has developed a number of innovative methodologies of assessment of hybrid offshore renewable energy platforms, both within and outside the scope of the MARINA project. Innovative items of particular interest include;

- Simplified numerical and structural analysis of preliminary outline designs of floating WECs and WTGs for determination of economic feasibility,
- Innovative use of outputs from current state of the art numerical frequency domain modelling tools to determine on-site maintainability of floating WECs and WTGs,
- Development of a dedicated suite of economic modelling tools for hybrid wind-wave energy devices ranging from preliminary deterministic levelised cost of energy (LCOE) models, to probabilistic LCOE models to time domain probabilistic reliability models for accurate life cycle cost analysis (LCCA) modelling.

While each of these methods of assessment have been designed and developed for hybrid solutions, it is important to note that they are equally applicable to individual WEC and WTG concepts. In fact, application to one or the other is easier than the hybrid application and therefore it is hoped that these innovative methods of assessment will be adopted by developers in the earlier stages of development to optimise their respective solutions prior to progression to sea trials. Furthermore, while these items are well beyond the current state of the art in terms of analysis techniques, this thesis proves that they can be developed and applied relatively quickly to preliminary designs. For this reason, adoption into mainstream analysis protocols is anticipated in the near future.

## 1.8    Outline of Thesis

Chapter 1 has outlined the status of offshore wind and wave energy industries and acknowledges the technical and financial challenges facing these industries. A potential solution, through the design of hybrid devices, has been postulated.

Chapter 2 reviews the literature and studies relevant to the development of this thesis. This includes a description of the International Energy Agency – Ocean Energy System (IEA-OES) Concept Development Protocol, the available guidelines and standards for design of wave and wind energy devices, an overview of the device categories, their attributes and advantages and disadvantages and developers who have come through this development process. The sources of information and methods of assessment of innovative offshore renewable energy devices through tank testing, numerical modelling and economic modelling are also included for each device category. The currently available power take-off systems for WECs are described and conversion efficiencies for each presented for use in power performance predictions. Simplified methods of structural analysis are described and methods of determining concept related risk outlined. Finally the potential indicators of concept feasibility are discussed from the information determined from the methods of assessment.

Chapter 3 takes the current state of the art from Chapter 2 and applies this to wind and wave energy concepts to determine a baseline in terms of structural design, power performance from numerical modelling and tank testing etc. Furthermore, innovative methods of assessment for determining unit costs of fabrication of structures and potential for on-site maintenance of floating structures have also been developed and applied to wind and wave energy devices.

Chapter 4 then takes all available information from previous chapters to inform the outline design of a number of hybrid wave-wind energy hybrid devices. Each are illustrated and described and estimates of structural mass and power performance are suggested based on simplified methods. An innovative economic model, specifically designed for hybrid wind-wave energy concepts, is described and applied to each concept to deterministically estimate the LCOE. During the development of the hybrid concepts, a number of additional issues arose in terms of estimates of power

output or structural mass of some concepts. Therefore tank testing experiments were carried out to address these concerns and are described in this chapter. Other criteria, as well as LCOE, were also included in the ranking process, which are described. Finally, the result is presented and the chosen hybrid device for further analysis, the OWC Array, is discussed.

Chapter 5 describes the evolution of the OWC Array concept and the reasoning behind the design changes. The design process prioritised simplicity, robustness, reliability, constructability, deployability and maintainability. Simplified numerical analysis was carried out to predict power performance, motion characteristics and maintainability of the platform. The maintainability criteria resulted in a reconfiguration of the WTGs onboard the OWC Array platform to ensure on-site maintenance could be reasonably carried out. Tank testing of the OWC Array platform was carried out and is described in detail. This data was used as validation of the power and motion characteristics predictions. The final design configuration of the platform is then summarised.

Chapter 6 describes the LCCA carried out on the OWC Array platform. A probabilistic time domain reliability model was developed for the OWC Array platform in an array layout. Each module within the model is described and the links between each outlined. The O&M activities have been modelled accurately through crew and vessel tracking modules based on corrective maintenance requirements, which are based on applied failure rates for subsystems within the platform. Hindcast data of wind and wave conditions have been used to drive the model.

Chapter 7 concludes the thesis and summarises the work carried out. This chapter also suggests areas for further research and development in the future.

## 2 Literature Review

As with every product destined for commercialisation, with a remit for revenue generation for the developer, the ultimate assessment criteria is the lifetime cost of the product. Furthermore, knowledge of whether the revenue generated from the product is sufficient to add value to the company and provide a sufficient level of return on the investment is required. In order to determine these factors for renewable energy devices, a number of sub-assessments are undertaken. These sub-assessments relate to specific aspects of the design of the WTG or WEC. This chapter will describe the various assessments typically carried out in the design of offshore renewable energy devices as well as how these assessments fit into current European and American Marine Renewable Energy Concept Development Protocols. This chapter lists and describes the relevant standards and codes available for the design of offshore renewable energy platforms. Furthermore, a comprehensive review of the available and recent literature on studies using the various methods of assessment is provided.

### 2.1 Concept Development Protocol

The scope of this thesis is to address methodologies of assessment of combined floating wave and wind energy platforms in conjunction with the development of a specific platform which adheres to the specific criteria necessary for the development of a successful hybrid wave-wind device for deployment in high energy sites. This section outlines the development protocol of the IEA-OES, to which both European and American developers are urged to adhere during the process of development of marine energy technologies. Since the device development process extends from applying fundamental laws of physics at the proof of concept stage to implementing heavy offshore engineering design and fabrication at the prototype sea trial stage, it lends itself to following a structured, phased programme similar to the National Aeronautics and Space Administration's (NASA) Technology Readiness Level (TRL) approach [14]. The principle idea of such a development schedule is to sequence the design development through various levels so the required knowledge is obtained at different stages. In the case of ocean energy devices the stages can conveniently be linked to different device scales by following Froude Similitude Laws and geometric similarity. This scaling law however does not account for all physical phenomena correctly at each scale, hence the various stages of development. The Structured Development Plan proposed is modified slightly from the NASA TRL approach in that some of the TRL levels are grouped into "Stages", based on the application of Froude scaling to the WEC model, whereby five Stages now form the Structured Development Plan incorporating the nine TRL levels as illustrated in Figure 2-1.
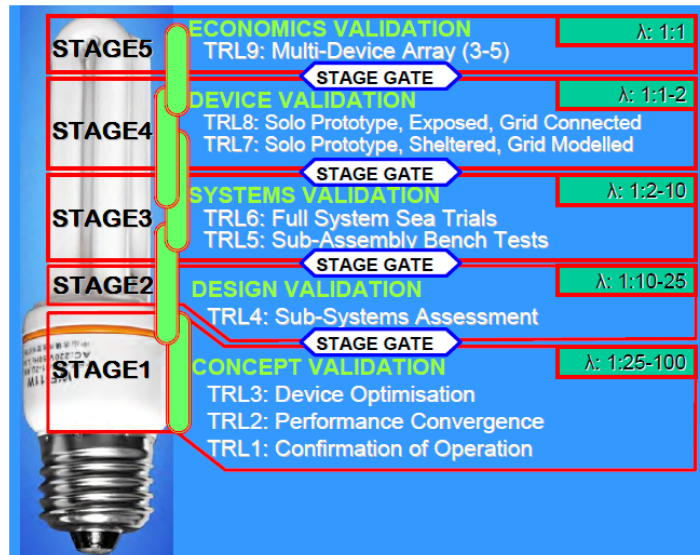
**Figure 2-1: IEA-OES 5 Stage Structured Development Plan [14]**

A comprehensive description of each Stage is given in an IEA-OES Annex II report [14]. For clarity and for structure of this chapter, a description of each of the five Stages is included below from the aforementioned report. Reference [15] also outlined the development of wave energy devices in Denmark. The approach is similar to the concept development protocol as outlined.

### 2.1.1 Stage 1 (TRL 1-3) – Concept Validation

This development stage consists of testing the idea as an idealised small scale (~ 1:50) model in a set of monochromatic, regular waves followed by panchromatic, irregular sea states. The former tests are to identify and describe the physical processes in relation to the design variables such that the device geometry can be optimised. The latter are to estimate the performance potential in realistic seaways. Hull seaworthiness and mooring suitability can also be established.

### 2.1.2 Stage 2 (TRL 4) Design Validation

This development stage uses a more sophisticated model (~1:10) and tests cover a more extensive range of sea states, including realistic survival conditions. During this phase engineering is introduced in the form of a preliminary design and an elementary costing of the system components is established. Based on the measured power absorption in a range of sea states the annual energy production is calculated using a set of generic wave conditions.

### 2.1.3 Stage 3 (TRL 5-6) Systems Validation

This development stage includes the testing of all sub-systems incorporating a fully operational power take-off (PTO) that enables demonstration of the energy conversion process from wave to wire. If the projected cost of energy production is acceptable, Stage 3 is entered in more detail with the aim to test the complete wave energy converter at a selected sub-prototype size (~ 1:4) that can safely be deployed

at sea and produce power. The device is still small enough to facilitate easier handling and operation but large enough to experience deployment, recovery and maintenance techniques at sea. The first involvement with licenses, permissions, certification and environmental requirements will be encountered. Also, design teams will experience manufacturing and production and supply chain issues, though the device may not be grid connected. Productivity remains a key stage gate requirement in these tests.

### 2.1.4   Stage 4 (TRL 7-8) Device Validation

This development stage is a critical part of the process and covers a solo machine pilot plant validation at sea in a scale approaching the final full scale (~ 1:1). This stage is a proving programme of designs already established rather than actually experimenting with new options. Tests can be initially conducted at a moderate sea state site prior to extending to proving at an exposed ocean location. This is a very exacting requirement however, since it involves all components from each sub-systems conversion process. The device as a whole must be proven fit for purpose before this stage is concluded and must also be grid connected before the end of the proving trials. Heavy engineering operations at sea are involved so health and safety requirements become important, as do O&M of the plant under realistic conditions. Since only a simple unit is involved, environmental impact will be minimal but monitoring of the machine's presence in a given location must be undertaken.

### 2.1.5   Stage 5 (TRL 9) Economics Validation

This final development stage involves multiple device testing, initially in small arrays (~3-5 machines) which can be expanded as appropriate. By the conclusion of the previous sea trials, the technology and engineering of a device should be well established and proven. The technical risk of Stage 5 should, therefore, be minimised. However, the consequence of failure would be significant and the financial risks are less certain since it is the economic potential of the devices deployed as a generating wave park that are under investigation. Initially the hydrodynamic interactions of the devices will be investigated, together with the combined electricity supply stability possible via the power electronics. Availability and service scenarios will be important issues as more machines are deployed as will onshore and offshore O&M requirements. Environmental aspects, both physical and biological, can now be studied in detail as well as the socio-economic effect the wave park will have on the local areas. Early stakeholder involvement is recommended.

It should be noted here that while the above development processes may only refer directly to WECs, they are also the recommended development protocol for floating offshore wind energy converters.

Each of the stages of development described briefly above, incorporate a number of tank testing procedures, mathematical/numerical modelling for power absorption and

structural analysis as well as economic modelling as detailed in Figure 2-2. The following section of this chapter is dedicated to establishing the state of the art in each of these topics relating specifically to Stage 1 and 2.

This thesis is focussed on the provision of methods of assessment of early stage offshore wind, wave and combined energy devices through LCCA modelling. In the early stages of development of concepts, the information required for LCCA modelling may not be available. This thesis is dedicated to determining the information required and how this information is attained while satisfying the development protocol.

| DEVELOPMENT PROTOCOL | STAGE 1 — CONCEPT VALIDATION | | | STAGE 2 — DESIGN VALIDATION | STAGE 3 — SYSTEMS VALIDATION | | STAGE 4 — DEVICE VALIDATION | | STAGE 5 — ECONOMICS VALIDATION |
|---|---|---|---|---|---|---|---|---|---|
| | TRL 1: Confirmation of Operation | TRL 2: Performance Convergence | TRL 3: Device Optimisation | TRL 4: Sub-Systems Assessment | TRL 5: Sub-Assembly Bench Tests | TRL 6: Full System Sea Trials | TRL 7: Solo, Sheltered, Grid Emulator | TRL 8: Solo, Exposed, Grid Connected | TRL 9: Multi-device Array (3-5) |
| Objectives/ Investigations | Op. Verification Design Variables Physical Process Validate/Calibrate Maths Model Damping Effect Signal Phase | Real Generic Seas Design variables Damping PTO Natural Periods Power Absorption Wave to Devise Response Phase | Hull Geometry Components Configurations Power Take-Off Characteristics Design Eng. (Naval Architects) | Final Design Accurate PTO [Active Control] Mooring system Survival Options Power Production Added mass | PTO Method Options & Control Inst. Power Absorption Electricity Production & Quality | Scale effects of Overall Performance Characteristics Mooring & Anchorage Security Environmental Influences & Factors | Oper & Mains Procedures Electrical Output Quality Grid Supply, Stability & Security PTO Performance at all phases Control Strategy Seaworthiness, Survival & Lifecycle Analysis Device Array Interaction (Stages 1 & 2) | | Grid Connection Array Interaction Maintenance Service Schedules Component Life Economics |
| Output/ Measurement | Vessel Motion Response Amplitude Operators & Stability Pressure / Force, Velocity RAOs with Phase Diagrams Power Conversion Characteristic Time Histories Hull Seaworthiness; Excessive Rotations or Submergence Water Surface Elevation Abeam of Devices | | | Motion RAOs Phase Diagrams Power v Time Wave Climates @ *head, beam, follow* | PTO Forces & Power Conversion Control Strategies | Incident Wave Field 6 D of F Body Motion & Phase Seaworthiness of Hull & Mooring [Survival Strategies] | Full On-Board Monitoring Kit for Extended Physical Parameters Power Matrix Supply forecasting | Array Interaction Annual Power Prod. Elec. Power Perfrm. Failure Rates Grid EIA reviews | Service, Maintenance & Production Monitor, Telemetry for Periodic checks & Evaluation |
| Primary Scale ($\lambda$) | $\lambda = 1 : 25 - 100$ ($\therefore \lambda_4 = 1 : 5 - 10$) | | | $\lambda = 1 : 10 - 25$ | $\lambda = 1 : 2 - 10$ | | $\lambda = 1 : 1 - 2$ | | $\lambda = 1:1$, Full size |
| Facility | 2D Flume or 3D Basin | | | 3D Basin | Power Electronics Lab | Benign Site | Sheltered Full Scale Site | Exposed Full Scale Site | Open Location |
| Duration –*inc* Analysis | 1-3months | 1-3months | 1 3 months | 6 – 12 months | 6 – 18 months | | 12 – 36 months | | 1 – 5 years |
| Typical No. Tests | 250 - 750 | 250 - 500 | 100 - 250 | 100 - 250 | 50 - 250 | | Continuous | | Statistical Sample |
| Budget (€,000) | 1 – 5 | 25-75 | 25-50 | 50 - 250 | 1,000 – 2,500 | | 10,000 – 20,000 | | 2,500 – 7,500 |
| Device | Idealised with Quick Change Options Simulated PTO (0-∞ Damping Range) Std Mooring & Mass Distribution | | Distributed Mass Minimal Drag Design Dynamics | Final design (internal view) Mooring Layout | Advanced PTO Simulation Special Materials | Full Fabrication True PTO & Elec Generator | Grid Control Electronics or Emulator Emergency Response Strategies Pre-Production         Pre-Commercial | | Operational Multi-Device |
| Excitation / Waves | Monochromatic Linear (10-25Δf) (25-100 waves) | Panchromatic Waves (20min scale) +ve 15 Classical Seaways Spectra Long crested Head Seas | | Deployment -Pilot Site Sea Spectra Long, Short Crested Classical Seas Select Mean wave Approach Angle | | Extended Test Period to Ensure all Seaways inc. | Full Scatter Diagram for initial Evaluation Continuous Thereafter Time & Frequency Domain Analysis | | |
| Specials | DofF (heave only) 2-Dimentional Solo & Multi Hull | Short Crest Seas Angled Waves As Required | Storm Seas (3hr) Finite Regular As required | Power Take-Off Bench Test PTO & Generator | Device Output Repeatability Survival Forces | Salt Corrosion Marine Growth Permissions | Grid Emulator Quick Release Cable Service Ops | Stakeholder Consult. Health & Safety Issues | Small Array (Up-grade to Generating Station)? |
| Maths Methods (Computer) | Hydrodynamic, Numerical Frequency Domain to Solve the Model Undamped Linear Equations of Motion | | Finite Waves Applied Damping Multi Freq Inputs | Time Domain Response Model & Control Strategy Naval Architects Design Codes for Hull, Mooring & Anchorage System.  Economic & Business Plan | | | Economic Model Electrical Stab. Array Interaction | Grid Simulation Wave forecasting | Array Interaction Market Projection for Devise Sales |

**EVALUATION [Stage Gates]**

| | | | | | | | | | |
|---|---|---|---|---|---|---|---|---|---|
| Absorbed Power Converted [kW] | | | | | | | | | |
| Weight, [tonnes] | | | | | | | | | |
| Manufacturing Cost [€] | | | | | | | | | |
| Capture [kW/tonne] or [kW/m^3] | [200-50 m^3] | | | | | | | | |
| Production [c/kW] | < 25 €c / kW | | | ≤ 15 €c / kW | | | ≤ 10 €c / kW | | ≤ 5 €c / kW |

**Figure 2-2: Concept Development Protocol**

16

## 2.2 Available Design Guidelines and Standards

The following section gives an overview of the status of standards and guidelines developed by various classification and certification societies and organisations which are applicable in the design of wave and wind energy foundations and drivetrain systems. The development of adequate standards and guidelines for offshore renewable energy structures is critical to the development of cost effective structures which will secure inward investment in the technology and ultimately result in deployment at sea. Initial versions of certain standards are claimed to be overly conservative in terms of the safety standards expected to be adhered to in the design phase of the technology. This results in structural designs which are unfeasible when matched with the energy yield of the technology. They are however, state of the art or best practice at the current time. It is only through further open sea deployments and full scale measurements that these standards and codes can be refined and improved. A number of internationally recognised classification and certification organisations which have published standards in the field of offshore renewable energy include:

1. International Electrotechnical Commission (IEC)
2. Germanischer Lloyd (GL)
3. Det Norsk Veritas (DNV)
4. American Bureau of Shipping (ABS)
5. Bureau Veritas (BV)
6. International Organisation for Standardisation (ISO)

Other organisations or collaborative projects have published a number of guidelines relevant to the development of marine energy. These include:

1. EMEC
2. EquiMar

The following sections will itemise the relevant standards and guidelines for design and evaluation of offshore renewable energy installations, particularly wind and wave energy installations, from each of the classifications organisations, similar to [16] with the addition of recently published documents.

### 2.2.1 Offshore Wind Turbines

#### 2.2.1.1 International Electrotechnical Commission (IEC) standards on offshore wind energy

The IEC publishes several standards for certification and evaluation of onshore and offshore WTG's. These standards are prepared by the IEC Technical Committee (TC) 88: Wind Turbines (IEC TC88). The following outlines the standards with relevance to offshore wind.

2.2.1.1.1  IEC-61400-1: Wind Turbines – Part 1: Design Requirements

This standard document specifies essential design requirements to ensure the engineering integrity of wind turbines such that it provides an appropriate level of protection against damage from all hazards during the planned lifetime. The standard is concerned with all subsystems of wind turbines such as control and protection mechanisms, internal electrical systems, mechanical systems and support structures and applies to wind turbines of all sizes

2.2.1.1.2  IEC-61400-3: Wind Turbines – Part 3: Design Requirements for Offshore Wind Turbines

This standard specifies additional requirements for assessment of the external conditions at an offshore wind turbine site and specifies essential design requirements to ensure the engineering integrity of offshore wind turbines. Its purpose is to provide an appropriate level of protection against damage from all hazards during the planned lifetime. The standard focuses on the engineering integrity of the structural components of an offshore wind turbine but is also concerned with subsystems such as control and protection mechanisms, internal electrical systems and mechanical systems. It should be used together with the appropriate IEC and ISO standards, in particular with IEC 61400-1.

2.2.1.1.3  IEC/TC 61400-13: Wind Turbine Generator Systems – Part 13: Measurement of Mechanical Loads

This standard acts as a guide for carrying out measurements used for verification of codes and for direct determination of the structural loading. It focuses mainly on large electricity generating horizontal axis wind turbines.

2.2.1.1.4  IEC 61400-21: Wind Turbines – Part 21: Measurement and Assessment of Power Quality Characteristics of Grid Connected Wind Turbines

This standard covers the definition and specification of the quantities to be determined for characterising the power quality of a grid connected wind turbine; measurement procedures for quantifying the characteristics; and procedures for assessing compliance with power quality requirements, including estimation of the power quality expected from the wind turbine type.

2.2.1.1.5  IEC 61400-22: Wind Turbines – Part 22: Conformity Testing and Certification

This standard defines rules and procedures for a certification system for WTG's that comprises both type certification and certification of wind turbine projects installed on land or off-shore. This system specifies rules for procedures and management for carrying out conformity evaluation of WTG's and wind farms, with respect to specific standards and other technical requirements, relating to safety, reliability, performance, testing and interaction with electrical power networks

2.2.1.1.6  IEC/TC 61400-23: Wind Turbines – Part 23: Full Scale Structural Testing
       of Rotor Blades

This standard is a technical specification providing guidelines for the full-scale structural testing of wind turbine blades and for the interpretation or evaluation of results, as a possible part of a design verification of the integrity of the blade. It includes static strength tests, fatigue tests, and other tests determining blade properties.

**2.2.1.2  Germanischer Lloyd (GL) guidelines for offshore wind energy**

GL has published a document, "Guidelines for the Certification of Offshore Wind Turbines" addressing both type and project certification. The type certification confirms that the WTG complies with the given WTG class, fulfils the design assumptions and confirms that the manufacturing process, the component specifications, the inspection, the test procedures and the documentation are in agreement with the design documentation. There are four levels of assessment which are called C- and D-Design Assessment for prototypes and A- and B-Design Assessment for the final machine. Project certification confirms that the type-certified WTG's meet the site-specific requirements relating to site design conditions, foundation, surveillance during transport and erection, commissioning and operation (production).

**2.2.1.3  Det Norsk Veritas (DNV) guidelines on offshore wind energy**

DNV have a unique methodology for the arrangement of the development of technical standards. The guidelines are organised hierarchically as follows:

1. Offshore Service Standards (OSS) cover basic principles and procedures of the certification processed
2. Offshore Standards (OS) describe the common technical regulations and criteria for approval as a basis for the technical certification. Together with other DNV guidelines and international codes and standards, they form the basis for ,
3. Recommended Practices (RP) which contain detailed information in line with actual practice. They accompany the DNV guidelines and other international recommended practices.

The following is a list of relevant DNV guidelines for offshore wind applications.

2.2.1.3.1  DNV-OSS-901: Project Certification of Offshore Wind Farms

This document has a dual function in that it provides a common communication platform for describing the scope and extent of activities performed for project certification of wind farms and also forms a reference document for defining the scope of work in accordance with requirements by the applicable certification system. The project certification concept for offshore wind farms constitutes a robust means to provide, through independent verification, evidence to stakeholders that a

set of requirements laid down in standards are met during design and construction, and maintained during operation, of an offshore wind farm.

### 2.2.1.3.2 DNV-OS-J101: Design of Offshore Wind Turbine Structures

This offshore standard provides principles, technical requirements and guidance for design, construction and in-service inspection of offshore wind turbine structures. The standard is to be used for the design of support structures and foundations for offshore WTG's as well as other support structures such as meteorological masts.

### 2.2.1.3.3 DNV-DS-J102: Design and Manufacture of Wind Turbine Blades, Offshore and Onshore Wind Turbines

This standard provides principles, technical requirements and guidance for the design and manufacture of wind turbine blades.

### 2.2.1.4 ABS Guidelines for building and classification of offshore wind turbine installations

The ABS has recently published two guideline documents relating to the building and classification of both bottom-fixed and floating wind turbines.

### 2.2.1.4.1 Guide for Building and Classing Bottom-Founded Offshore Wind Turbine Installations

This ABS guide provides criteria for the design, construction, installation and survey of bottom-founded offshore wind turbine installations which comprise permanently sited support structures and foundations of offshore wind turbines attached on and supported by the sea floor. The design criteria specified in this guide are intended for the bottom-founded offshore wind turbine installation to achieve the normal safety class as defined in IEC 61400-3 (2009).

### 2.2.1.4.2 Guide for Building and Classing Floating Offshore Wind Turbine Installations

This ABS guide provides criteria for the design, construction, installation and survey of permanently sited floating offshore wind turbine installations. It addresses three principle area: the floating support structure, the station-keeping system, and onboard machinery, equipment and systems that are not part of the Rotor-Nacelle Assembly (RNA).

### 2.2.1.5 BV Guidance note for classification and certification of floating offshore wind turbines

BV offer services in the type and project certification based on the IEC standards, in particular IEC 61400-22.

## 2.2.2 Wave Energy Converters

### 2.2.2.1 IEC Standard development on wave energy

The IEC have taken a pro-active approach to establishing standards and guidelines for marine energy through the establishment of the IEC TC114: Marine Energy –

Wave, Tidal and other Water Current Converters (TC114). The following outlines the standards, both published and under development, with relevance to wave energy technologies.

2.2.2.1.1 IEC/TS 62600-1: Marine Energy – Wave, Tidal and other Water Current Converters – Part 1: Terminology

This standard defines the terms relevant to ocean and marine renewable energy. For the purposes of this Technical Specification, sources of ocean and marine renewable energy are taken to include wave, tidal current, and other water current energy converters. This Technical Specification is intended to provide uniform terminology to facilitate communication between organisations and individuals in the marine renewable energy industry and those who interact with them.

2.2.2.1.2 IEC/TS 62600-100: Marine Energy – Wave, Tidal and other Water Current Converters – Part 100: Electricity Producing Wave Energy Converters – Power Performance Assessment

This standard provides a method for assessing the electrical power production performance of a WEC, based on the performance at a testing site. It provides a systematic method which includes: measurement of WEC power output in a range of sea states; WEC power matrix development; an agreed framework for reporting the results of power and wave measurements.

2.2.2.1.3 Standards due to be published in 2013/14
- IEC/TS 62600-2: Marine Energy – Wave, Tidal and other Water Current Converters – Part 2: Design Requirements for Marine Energy Systems
- IEC/TS 62600-101: Marine Energy – Wave, Tidal and other Water Current Converters – Part 101: Wave Energy Resource Assessment and Characterisation
- IEC/TS 62600-10: Marine Energy – Wave, Tidal and other Water Current Converters – Part 10: The Assessment of Mooring Systems for Marine Energy Converters
- IEC/TS 62600-103: Marine Energy – Wave, Tidal and other Water Current Converters – Part 103: Guidelines for the Early Stage Development of Wave Energy Converters: Best Practices and Recommended Procedures for Testing of Pre-Prototype Scale Devices

**2.2.2.2 Det Norsk Veritas Guidelines on Wave Energy Development**
The DNV have recently published an OSS document on the certification of wave and tidal energy converters.

2.2.2.2.1 DNV-OSS-312: Certification of Tidal and Wave Energy Converters
This OSS presents the principles and procedures for DNV services with respect to Certification of tidal and wave energy converters. Due to the specific needs and characteristics of this industry, the certification concept is extended such that it can be defined as a robust process to provide, through independent verification, evidence

to stakeholders that the marine energy converter will perform adequately within acceptable levels of safety, availability, reliability, asset integrity and environmental impact, within limits specified in the certification basis and complying, where applicable, to relevant standards.

**2.2.2.3    European Marine Energy Centre (EMEC) documents on wave energy devices**
EMEC have co-ordinated the development of a suite of guidelines on behalf of the marine renewable energy industry. Each document has been written by an acknowledged expert and progressed by a working group with individuals representing technology developers, regulators, academia, utilities and project developers. Some of the guidelines published have been submitted as suggested work programmes for the IEC TC 114. A list of guidelines and a short abstract are included below.

2.2.2.3.1   Assessment of Performance of Wave Energy Conversion Systems
This guideline outlines a methodology for assessing the performance of WEC's at open sea test sites. The purposes of the performance assessment are to provide a methodology for the measurement of the power output of the WECs in a range of sea states, to provide a framework for the reporting of the results of these measurements and to enable the estimation of the energy production of a WEC at a prospective site where wave power resource information of sufficient detail and quality exists.

2.2.2.3.2   Assessment of Wave Energy Resource
This guideline document specifies techniques which can be used to determine how much wave energy is available at a particular location in a particular region. The guidance given includes the derivation of wave energy resource information from both wave model results and from wave measurements. In the case of wave measurements the treatment includes descriptions of a number of measuring systems as well as the principles of quality control and spectral analysis.

2.2.2.3.3   Guidelines for Marine Energy Certification Schemes
This guideline document establishes a certification scheme for marine energy converter units or a farm consisting of several energy converter units. It gives guidelines for procedures and management to carry out conformity evaluation of such devices, in compliance with standards and other technical requirements agreed between the applicant and the certification body, relating to safety, reliability, performance, testing and interaction with electrical power networks.

2.2.2.3.4   Guidelines for Design Basis of Marine Energy Conversion Schemes
This guideline establishes general principles for producing a design basis document for a device. The aim of the document is to provide simple step by step guidance that can be followed by a device designer, in order to understand the factors that influence the design of a device, and design procedures that can be followed. By following the guidance in this document, it is hoped not only will the designer have a conforming design but will also be in a position to comply with the Certification

Scheme. It is applicable to all stages from prototype design stage (after the initial concept has been proven to work) up to final design.

### 2.2.2.3.5 Guidelines for Reliability, Maintainability and Survivability of Marine Energy Conversion Systems

This guideline document is intended to give guidance that can be used to improve and/or demonstrate the reliability, maintainability and survivability of marine energy converters that extract energy from waves and from tides and tidal streams.

### 2.2.2.3.6 Tank Testing of Wave Energy Conversion Systems

This guidance document specifies a structured development programme and specific test procedures for the early stages of a wave energy converter development. The format is based on traditional engineering methods similar to the TRL introduced by NASA.

### 2.2.2.3.7 Guidelines for Project Development in the Marine Energy Industry

This guideline establishes guidelines for the development of a marine power project. The document outlines the recommended processes and procedures to be followed in completing a marine power project from its conception through to decommissioning. It makes recommendations on the technical, environmental, Health and Safety and commercial issues that need to be considered through the phases of feasibility, conceptual and detailed design, manufacture, installation, operation, maintenance and decommissioning. It highlights regulations that are applicable to each stage of the process.

### 2.2.2.3.8 Guidelines for Manufacturing, Assembly and Testing of Marine Energy Conversion Systems

This guidance document specifies techniques for planning and building quality into the manufacturing processes and so provides an initial framework for providing consistency within the industry. It covers the manufacture of tidal stream generators, wave energy converters, offshore wind energy converters and devices generating power from a renewable source in the marine environment. This document may also be used for assessing manufacturer's capability for producing equipment for the demanding renewable energy market and providing a basis for acceptance by interested parties.

### 2.2.2.4 EU FP7 EquiMar Protocols

The EquiMar project has delivered a suite of protocols for the equitable evaluation of marine energy converters. These protocols harmonise testing and evaluation procedures across the wide variety of devices presently available with the aim of accelerating adoption through technology matching and improved understanding of environmental and economic impacts associated with the deployment of arrays of devices. A list of the protocols and a brief abstract is included below. The EquiMar project has produced a significant number of project deliverables, each contributing

to the development of the protocols. These deliverables are not described in this section, but will be referenced throughout this thesis.

### 2.2.2.4.1  Resource Assessment Protocol

This protocol provides methodologies for providing an estimate of the available energy resource as well as an assessment of the operating and survival characteristics of a specific site.

### 2.2.2.4.2  Environmental Assessment Protocol

This protocol addresses a number of topics including environmental assessment approaches, adaptive management, site selection, environmental impact assessment (EIA) guidelines, potential impacts and mitigation options, impact analysis tools and environmental key issues. This protocol is a key document in the planning and design phase of a project.

### 2.2.2.4.3  Tank Testing Protocol

This protocol document includes a number of issues critical to the design of a successful tank testing campaign for a marine renewable energy device. The document addresses specifications such as appropriate scales and associated effects, measurements, analysis and presentation of results, power performance ad model verification. This protocol will feature significantly in this thesis.

### 2.2.2.4.4  Sea Trials Protocol

This document is similar in structure to the tank testing protocol with the addition of specific topics including system integrity and functionality, temporal and spatial test site considerations and monitoring of system integrity and survivability.

### 2.2.2.4.5  Deployment and Performance Assessment of Multi-MegaWatt Device Array Protocol

This protocol document addresses array level considerations such as pre-deployment issues such as classification of devices, supply chain assessment, export and inter-array electrical connection design and spatial layout of the array. The protocol also consider the assessment of the performance of the array by providing methods for systematic quantification of the performance and approaches to recording and reporting of the temporal information including device performance, service and inspection logs and reliability data.

### 2.2.2.4.6  Project Assessment Protocol

This protocol provides a methodology for assessing the economic viability of a marine energy conversion project. The objective is to define a procedure that can be followed by a technology developer to obtain an economic assessment that is directly comparable to that produced by any other developer. It addresses CAPEX and operational expenditure (OPEX), revenue (methodology), risk assessment and performance and revenue.

2.2.2.4.7 Market Assessment Protocol

This protocol provides guidelines for estimating technology specific limitations to possible cost reduction mechanisms including CAPEX, OPEX and performance and revenue.

## 2.2.3 Structural Design Standards

The following is a non-exhaustive list and description of structural design standards from the DNV certification body which are available online. As this thesis is not solely focussed on structural design, it will only consider standards from the DNV where possible as no comparison between codes will be carried out.

2.2.3.1.1 DNV-OS-C101: Design of Steel Structures

This standard provides principles, technical requirements and guidance for the structural design of offshore structures. DNV-OS-C101 is the general part of the DNV offshore standards for structures. The design principles and overall requirements are defined in this standard. The standard is primarily intended to be used in design of a structure where a supporting object standard exists, but may also be used as a stand-alone document for objects where no object standard exists.

2.2.3.1.2 DNV-OS-C102: Structural Design of Offshore Ships

This standard comprises sections with provisions applicable to all types of offshore floating ship shaped units, and sections with provisions for specific types of units such as well intervention/drilling units and floating, production, storage offshore (FPSO) facilities. This standard is based on the Working Stress Design (WSD) method. In WSD the target component level stress is achieved by keeping the calculated stress for different load combinations equal to or lower than the maximum stress. The maximum permissible stress is defined by the multiplication of the capacity of the structural member with permissible usage factors.

2.2.3.1.3 DNV-OS-C103: Structural Design of Column Stabilised Units (LRFD Method)

This standard provides requirements and guidance for the structural design of column-stabilised units constructed in steel using the Load and Resistance Factor Design (LRFD) method. The requirements and guidelines in this document are generally applicable to all configurations of column-stabilised units including those with ring pontoons and twin pontoons.

2.2.3.1.4 DNV-OS-C104: Structural Design of Self-Elevating Units (LRFD Method)

This standard provides principles, technical requirements and guidance for the design and construction of self-elevating units. The design is based on the LRFD method. Self-elevating units may also be designed to the WSD method defined in DNV-OS-C201.

2.2.3.1.5  DNV-OS-C105: Structural Design of TLPs (LRFD Method)

This standard provides requirements and guidance to the structural design of TLPs. The requirements and guidance documented in this standard are generally applicable to all configurations of TLPs. This standard is based on the LRFD method. A TLP may be designed to the WSD method in accordance with DNV-OS-C201.

2.2.3.1.6  DNV-OS-C106: Structural Design of Deep Draught Floating Units (LRFD Method)

This standard provides requirements for the design of Deep Draught Floating (DDF) units, fabricated in steel, in accordance with the provisions of DNV-OS-C101 utilising the LRFD method. This standard is written for general worldwide application.

2.2.3.1.7  DNV-OS-C201: Structural Design of Offshore Units (WSD Method)

This standard provides principles, technical requirements and guidance for the structural design of offshore structures, based on the WSD method. The standard is written for worldwide general application and is applicable to structures such as column-stabilised units, self-elevating units, tension leg platforms and deep draught floaters.

2.2.3.1.8  DNV-OS-C502: Offshore Concrete Structures

This offshore standard provides principles, technical requirements and guidelines for the design, construction and in-service inspection of Offshore Concrete Structures. The Concrete Structures may be floating or ground supported structures. This standard shall be used with the general offshore design standards for steel structures, DNV-OS-C101, DNV-OS-C102, DNV-OS-C103, DNV-OS-C105 and DNV-OS-C106. The standard covers design, fabrication/construction, installation and inspection of Offshore Concrete Structures.

2.2.3.1.9  DNV-RP-C205: Environmental Conditions and Environmental Loads

This recommended practice document provides guidance for modelling, analysis and prediction of environmental conditions as well as guidance for calculating environmental loads acting on structures. The loads are limited to wind, wave and current. The guidance is based on state of the art within modelling and analysis of environmental conditions and loads and technical developments in recent R&D projects, as well as design experience from recent and ongoing projects.

2.2.3.1.10 DNV-RP-H103: Modelling and Analysis of Marine Operations

This recommended practice document provides guidance for modelling and analysis of marine operations, in particular for lifting operations including lifting through the wave zone and lowering of objects in deep water to landing on the seabed.

### 2.2.4  Qualification of New Technology

In the case of, primarily, wave energy devices, the PTO systems are regarded as new technologies and as such no standards exist on which to base the design process. In

that case, specific standards exist which aim to outline the process by which new technology may become certified. The following is a list of standards which do this.

#### 2.2.4.1 DNV-RP-A203: Qualification of New Technology

The objective of this procedure is to provide a systematic approach to the qualification of new technology, ensuring that the technology functions reliably within specified limits. The procedure is applicable for components, equipment and assemblies, which can be defined as new technology, in hydrocarbon exploration and exploitation, offshore.

#### 2.2.4.2 Bureau Veritas BV-NI525: Risk Based Qualification of New Technology

The qualification process is intended to prove with an acceptable level of confidence and in a cost-effective manner, that a technology is fit for purpose, that it complies with the specifications that the designer has developed and that it is sufficiently reliable and safe for people and the environment.

## 2.3 Concept Development Methodology

This section presents an overview of the wave and wind energy technologies under development presently. Current state of the art methods of assessment and development are discussed for each category of wave energy device and examples of commercial companies developing concepts within each category are described and briefly analysed.

### 2.3.1 Wave Energy Technology Overview

The wave energy industry has typically found it more difficult to progress through the Development Protocol than other technologies. This is symptomatic it seems of an industry which is still very much in the embryonic stage of development. This can be seen simply from the diverse range of technology types or categories under development as illustrated in Chapter 1 and furthermore in the range of configurations of devices in each category. The number of concepts therefore is large with funding not available to significantly progress any one of the categories. The underlying structures in use for wave energy generation are common in general, i.e. barges, semi-submersibles etc., however, they have specific appendages or connections which are not typical of existing offshore structures in other industries. This therefore equates to uncertainty in design, and to achieve certification for deployment requires overly conservative structural designs which lead to unfavourable economic potential projections for full scale deployments. The solution for this of course is further testing in offshore conditions to remedy the conservative design process.

This chapter is dedicated to the review and brief analysis of the various wave energy conversion concepts which are currently under development by technology development companies. The review consists of examples of all categories of devices and any available information specific to these. The review is not intended to be exhaustive, but sufficiently detailed to provide a thorough understanding and

appreciation of the performance of each category and device. Insofar as is possible, the devices investigated within each category are at prototype or reduced scale deployments at sea (which is a "loose" indicator of concept success) while ensuring a sufficient mix of concept variations within a category. The primary categories of wave energy devices, as listed by Aqua-RET [10], include:

- Attenuators (ATN)
- Point Absorbers (PA)
- Oscillating Wave Surge Converters (OWSC)
- Oscillating Water Columns (OWC)
- Wave Overtopping Devices (OTD)
- Submerged Pressure Differential (SPD)
- Bulge Wave Devices (BW)
- Gyroscopic Devices (GYD)

In terms of power performance of each of these categories, reference [17] presents the range and mean capture width ratio (CWR) for each. It is acknowledged that the CWR used in the preliminary assessment of the devices mentioned in this section may not necessarily accurately represent the concept specific CWR which may be achieved. The purpose of this section is to present typical examples of the various embodiments of devices and present an averaged representation of the device power performance using the mean CWR presented in [17]. This section outlines the development methodologies used by developers in the process of progressing through the Development Protocol.

### 2.3.1.1 Experimental Modelling

To date, the progress of all WECs and floating WTGs through the Development Protocol has relied heavily on the performance of the system during tank testing campaigns at various scales. As noted in the Development Protocol, the testing of WECs may be carried out in a number of different scales depending on the stage of development. This section reviews some of the available literature on the methods of physical testing of each category of WECs.

A detailed account of laboratory equipment and methods of experimental modelling of WECs may be found in [18]. The following are a range of discrete studies on the basic types of WECs and WTGs and how the testing and measurement setup was arranged.

### 2.3.1.2 Numerical Simulation

While experimental tests provide reliable results with regard to power absorption, floating body motions, mooring loads etc., a complementary and parallel process of developing a numerical model of the marine energy converter concept is required. This section outlines the various theories applied to floating bodies for assessment of the frequency and time domain responses, power absorption and mooring loads. Also listed are the numerical codes which are either commercially available or under development by academic institutes. This section is similar to the overview of

numerical methods given in the EU FP7 Offshore Renewable Energy Conversion platforms Co-ordinated Action (Orecca) Project [16].

2.3.1.2.1   Potential Theory Approaches

The design and optimisation of WECs and floating structures commonly uses the potential theory approach for the description of the wave-structure interaction. The linear potential theory corresponds to a linear regime of incident forces and resulting body forces and is only valid if the following assumptions are satisfied: incompressible and inviscid fluid, irrotational flow, small amplitude waves and small amplitude motions of the floating system. The potential solution of the fluid-structure interaction problem usually consists of a set of frequency dependent hydrodynamic coefficients which can be described with simplicity as:

- The excitation force caused by the incident wave on the body
- The added mass related with the water accelerated with the body during its oscillations
- The radiation damping, related to the waves that the body radiates through its oscillations

As many WECs and floating structures are complex hull shapes, numerical codes, such as those listed below, are required to solve the potential flow problem. In the event that a hull may be a very simple shape, the solution to the potential flow problem may be obtained analytically.

- ANSYS AQWA
- AQUAPLUS/AQUADYN/ACHIL3D
- DIODORE
- MOSES
- OrcaFlex
- SACS
- WAMIT
- Wadam

A comprehensive description of each of these software tools may be found at the website links above or alternatively a brief description is included in [16].

2.3.1.2.2   Advanced Numerical Approaches

For more detailed representation of WECs and floating bodies, computational fluid dynamics (CFD) may be used to solve the Reynolds-Averaged Navier-Stokes equation. Conveniently, unlike the potential theory methods, viscous forces are taken into account through the relative motion of the floating body and incident wave field. However, this method of numerical modelling is expensive in terms of computational effort. A number of both open source and commercially available CFD methods exist and are listed below. It should be noted that such methods would only be incorporated into the development process beyond Stage 1.

- ANSYS CFD/Fluent
- OpenFoam
- ICARE
- FLOW-3D
- Star-CCM+

Further to the advanced numerical methods mentioned above, a meshless particle based method is now attracting attention for use in modelling of WECs. Smooth Particle Hydrodynamics (SPH) is a mesh free method capable of modelling physical phenomena such as breaking waves, sloshing, splashing and slamming. This capability will allow accurate modelling of survivability conditions of WECs and floating WTGs. A list of the available SPH codes is included below. These methods again are computationally expensive.

- SPHysics
- Dual SPHysics

The following section outlines the various studies that have been undertaken in the analysis of both WECs and floating wind turbine structures. The studies are briefly described and include details of the numerical tools used, the structure being modelled and the results from the analysis.

### 2.3.1.3 Oscillating Water Columns (OWC)

This section outlines the OWC operating principle and the methods of analysis applied to the development of the OWC concept for power production. Furthermore an example of an OWC device currently under development is included and described in detail.

#### 2.3.1.3.1 Operating Principle

As shown in the figure below, the OWC type device is a structure which is open to the ocean and thus wave action which drives the water column in a primarily heave motion periodically compressing and expanding a pocket of air in and out through an orifice holding an air turbine.
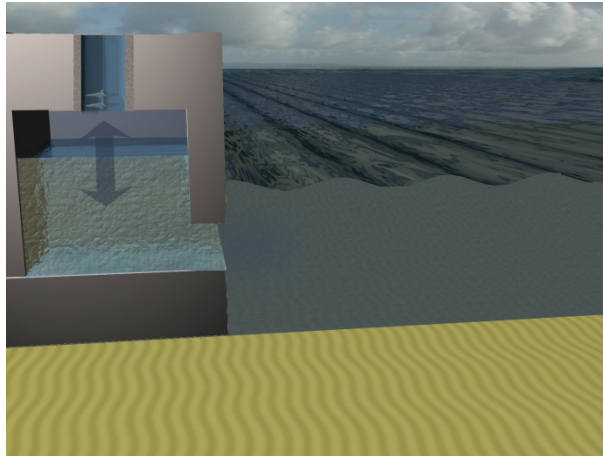
**Figure 2-3: Principle of Operation of an OWC Device [10]**

The OWC type concept is by far one of the best known and researched concepts for wave energy conversion. The OWC concept has found itself incorporated into many different variations of structural configuration, ranging from shoreline fixed reinforced concrete (RC) devices, floating ship hulls, small barges and large multi-OWC array platforms. This concept is clearly an exceptionally versatile concept and due to its PTO type, the air turbine, with very simple and effective components, has found favour amongst developers particularly in Ireland and Australia. The following is an outline of studies carried out on various configurations of OWC devices both numerically and physically to determine the performance of each.

2.3.1.3.2  Experimental Modelling of OWC Devices

Reference [19] investigated the performance of a cylindrical floating OWC model in the ocean wave basin at the Hydraulics and Maritime Research Centre (HMRC), University College Cork (UCC). The buoy motions were monitored by a Qualysis OQUS camera system operating at a sampling rate of 32Hz. Four markers mounted on a light frame connected to the buoy were used to monitor the rigid body motions of the buoy, while a fifth marker, connected to a float inside the OWC chamber on the free surface monitored the motion of the internal water surface (IWS) relative to the buoy motion. A Honeywell pressure transducer with a range of $\pm356$mm $H_2O$ was mounted onto the sealed lid of the buoy and measured the instantaneous chamber air pressure at a sampling rate of 32Hz. The motion of the IWS was damped using orifice plates of varying diameter connected to the main sealed lid of the buoy. The study calculates the absorbed power from the OWC by different methods based on the measurements made and concludes they are all acceptably close to one another. The study also reveals the nonlinear behaviour of the IWS and buoy heave and pitch motions around the resonant frequencies. It is found that the area ratio of chamber to orifice of 1.7% and 2.28% produce the best power absorption. No validation of the flow coefficients for each orifice used for the power calculations is reported.

Reference [20] carried out small scale tank testing of a spar-type OWC device at a scale of 1:120 in the wave flume at the Laboratory of Hydraulics and Environment of

Instituto Superior Technico (IST). The motions of the buoy were monitored by a motion tracking system with infrared cameras developed by Qualysis operating at a sampling frequency of 50Hz. A high-accuracy low-pressure sensor monitored the chamber air pressure at a sampling frequency of 100Hz. Standard resistive wave gauges were used to monitor the water elevation at different positions in the tank, as well as one positioned inside the buoy to monitor the relative motion between the buoy and IWS. These wave probes also operated at a frequency of 100Hz. The IWS motion was damped by an orifice with a porous filter material between the air chamber and the atmosphere. This membrane ensures a laminar flow of air through the orifice and thus a linear relationship between the pressure difference and air flow rate. Again no validation of the orifice and porous material flow coefficients were presented.

Reference [21] carried out a substantial tank testing campaign on the Offshore Wave Energy Limited (OWEL) device at the ocean wave basin at the HMRC, UCC at a scale of 1:100. The operation of the OWEL device is fairly similar to the operation of a typical OWC. The testing campaign consisted of firstly assessing the performance of the WEC in a fixed condition, or idealised conditions. Secondly the device was assessed in the more realistic floating condition in regular and irregular waves. The air flow from the compression chambers were damped by the use of orifice plates in the exhaust pipes located approximately ten times the diameter from the compression chamber. Differential pressure sensors were located in the exhaust pipes to calculate the pneumatic power. Strain gauges were used to measure the deflection of components of the model and calculate structural loads. Load cells were located in line with the mooring lines to monitor the loads. The motions of the platform were monitored by a Qualysis motion capture system operating at 32Hz.

### 2.3.1.3.3   Numerical Modelling of OWC Devices

Reference [22] carried out an investigation into the interaction between waves and three different OWC structures. The study utilised the commercially available boundary integral element method (BIEM) code WAMIT. The additional difficulty with OWC structures is the presence of an interior domain within the chamber. This study applied two different approaches to the representation of the behaviour of the IWS. The direct approach consists of adapting the dynamic boundary conditions on the free surface of the aperture. The second approach is based on the application of generalised modes, which are extra modes of motions that are introduced to describe the motion of a virtual, weightless and deformable piston, representing the free surface of the OWC chamber.

Reference [23] presented an adaptation of the BEM code AQUADYN to study OWCs. The direct approach has been implemented in the code to account for the oscillatory pressure within the chamber of the OWC. A comparison between the outputs from the new formulation in AQUADYN and the outputs from WAMIT are compared and it is noted that a satisfactory comparison is achieved.

Reference [24] carried out an investigation into the 3D hydrodynamic modelling and optimisation of a bottom-fixed OWC chamber using the BIEM code WAMIT. The results of the numerical simulations were compared with physical model tests and found to be satisfactory.

Reference [25] carried out a frequency domain numerical investigation into the performance and motion characteristics of a moored floating backward bent duct buoy (BBDB) WEC using WAMIT. In this analysis, a simplification of the mooring line stiffness has been proposed such that the equivalent mooring spring stiffness coefficients may be directly input into WAMIT to represent the limitations in surge, pitch and heave motions due to the mooring system. Physical model tests were carried out to validate the numerical model results.

Reference [26] again carried out a numerical investigation in the frequency domain, using WAMIT, to determine the performance and motion characteristics of a floating cylindrical OWC. The study analysed methods for the tuning of damping coefficients for heave, pitch and IWS response amplitude operators (RAO). The investigation attempted to overcome the nonlinearities by assuming that they are induced purely by non-linear damping. Therefore additional damping is added to the frequency domain equation to reproduce the motion responses and IWS motion. The numerical model tests were compared to physical model tests as detailed in the previous section and found to be accurate following the correct tuning of the damping coefficients.

Reference [27] investigated the potential for use of the commercially available Fluent CFD code to simulate the performance of an OWC. The model was a two-phase model i.e. includes both the air and water phases as well as the interface, through the Volume Of Fluid (VOF) method to track the free surface. The flow is assumed to be viscous, unsteady and incompressible. The IWS motions were found to be in good agreement with a mathematical model of the OWC system, while the air velocity through the nozzle was incompatible. For this reason, a separate 3D model of the OWC was created using the time dependent motion of the IWS from the original simulation as input and adopting a piston-like motion within the OWC chamber. The air flow through the nozzle was then much closer to that calculated from the mathematical model.

### 2.3.1.3.4 Example OWC Device - OE Buoy

Ocean Energy Ltd. is an Irish technology developer, currently developing a floating OWC type device of the BBDB type. This is essentially a barge structure with a hollow tube or duct wrapped around the buoyancy module in an "L" shape. The duct then is open to the sea at the stern of the buoy and terminates at the bow above sea level, therefore enclosing an air pocket between the duct roof and sea level. As the buoy is excited by the incident wave field, the water within the duct oscillates and compresses and expands the air volume in the duct. A turbine is connected to the air pocket through the duct walls and allows the compressed air to flow out through the turbine and air in during the expansion of the air pocket. Typically a bi-directional

turbine is used such as a Well's turbine or an impulse turbine with either fixed or moveable guide vanes.



**Figure 2-4: OE Buoy 1:15 Model at ECN**



**Figure 2-5: OE Buoy 1:4 Device at Galway Bay in '08-09, Ireland**

The OE Buoy has been developed over 10 years. The company has remained small, employing essentially only its board of directors. The company has relied on self funding as well as support from Irish governmental and European funding. The original BBDB concept was pioneered by Yoshio Masuda, a former Japanese naval commander who used the OWC concept for design of navigation buoys. The device development has strictly adhered to the IEA-OES concept development protocol having being tested in UCC at a scale of 1:50 (2002-2003) and in Ecole Centrale de Nantes (ECN) at a scale of 1:15 (2004) as illustrated in Figure 2-4. The first Stage 3 deployment occurred between 2006-2008 at the Sustainable Energy Authority of Ireland (SEAI) Galway Bay test site when the 1:4 scale steel hull was tested using only an orifice plate to simulate PTO damping. A Well's Turbine was fitted to the hull and the unit redeployed between 2008-2009 as illustrated in Figure 2-5. The device was the subject of the EU FP7 Components for Offshore Renewable Energy (CORES) project and the hull was deployed for 3 months in Galway Bay in 2012 with an Impulse Air Turbine with moveable guide vanes as illustrated in Figure 2-6.

**Figure 2-6: Webcam pictures of the OE Buoy during deployment for CORES in Galway Bay**

A number of studies have been carried out on the BBDB (or backward bent duct device – B2D2) previously. Reference [28] compared the performance of the B2D2 device numerically and physically and determined a method of applying additional damping in the frequency domain to correct the RAOs of the device at resonance. Reference [29] investigated the effects on performance when testing at different scales and the OE Buoy was a specific case study. More recently, [30] numerically analysed the BBDB device for energy production in the frequency domain. The BBDB device was also one of the devices analysed in the study carried out by [31] and the absorbed power matrix illustrated in Figure 2-7was produced for a 24m wide buoy.
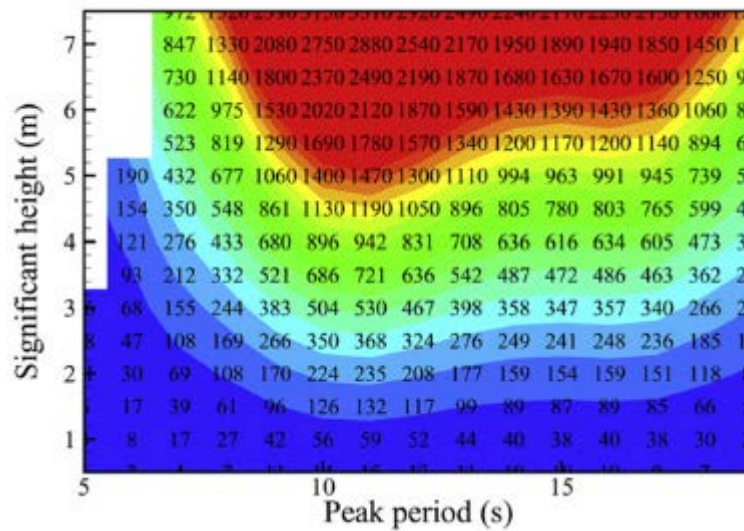


**Figure 2-7: Absorbed Power Matrix for BBDB type device**

The device is estimated to produce ~320kW of average power in a 65kW/m site assuming a PTO efficiency of 54% which translates to a capture width ratio (CWR) of ~38%. This is very close to the average figure quoted for OWC type devices in [17].

Like most other devices, very little information is available on the structural design of the BBDB device. Given the typical dimensions of the buoy used by OE and in [31] a steel plate and stiffener style construction is required. Assuming an equivalent steel plate thickness of 35mm, the buoy would weigh approximately 1500t of steel. The device makes use of three standard catenary mooring lines, with steel chain to a surface buoy and synthetic rope to the hull fairleads.

**2.3.1.4  Wave Activated Bodies**

This section outlines the principle of operation of wave activated bodies. This category includes a number of sub-categories including attenuators, point absorbers, oscillating wave surge converters and submerged pressure differential devices. Numerical and physical modelling of these device types is included as well as a selection of existing devices currently under development.

2.3.1.4.1  Operating Principle

The operating principle of wave activated bodies is essentially the movement of the device relative to another object such as the seabed or alternatively another floating object. This principle has been realised in a number of different configurations as illustrated below. The floating attenuator illustrated Figure 2-8 operates on the basis of one floating buoy moving relative to a downstream buoy in a number of degrees of freedom. This is an example of an attenuator, a long slender device of greater than two bodies orientated perpendicular to the incident waves.
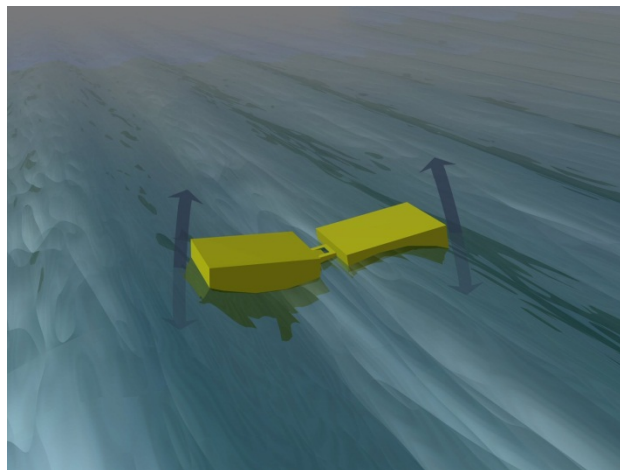


**Figure 2-8: Operating Principle of a 2-body Attenuator [10]**

The point absorber is another configuration of wave activated body device. This essentially consists of a surface floating buoy moved by the incident waves relative to either the seabed as illustrated below or alternatively relative to another floating buoy with substantially different motion characteristics to ensure relative movement

between the buoys. These primarily operate in a single degree of freedom such as heave as illustrated in Figure 2-9.
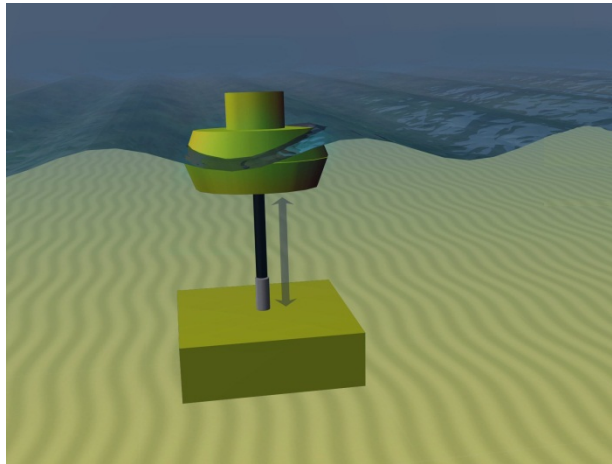


**Figure 2-9: Operating Principle of a Heaving Point Absorber [10]**

Another form of wave activated body device is the oscillating wave surge converter, or oscillating flap as illustrated Figure 2-10. This device type may be fixed to the seabed or floating. Essentially waves move the flap relative to another reference object in a pitch motion.
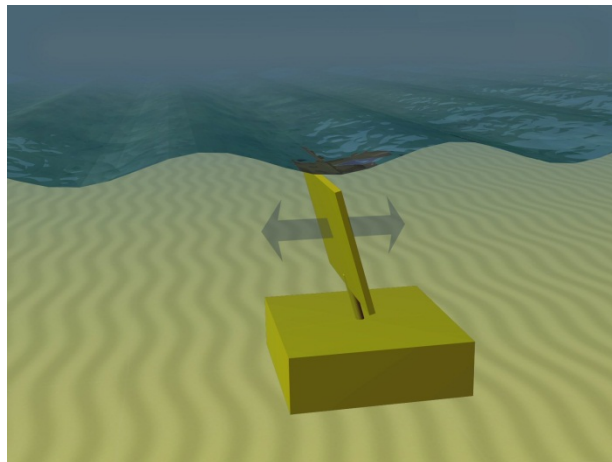


**Figure 2-10: Operating Principle of an Oscillating Wave Surge Converter (OWSC) [10]**

Finally in the wave activated body category is the submerged pressure differential device as illustrated in Figure 2-11. This is again a buoy, submerged below the water surface, embodying a fluid under pressure between the buoy and another reference object. As waves pass the buoy it increases and decreases the pressure in the fluid in a heave motion which generates pressurised motion and therefore power. These devices are less well developed in comparison to the other wave activated body types.
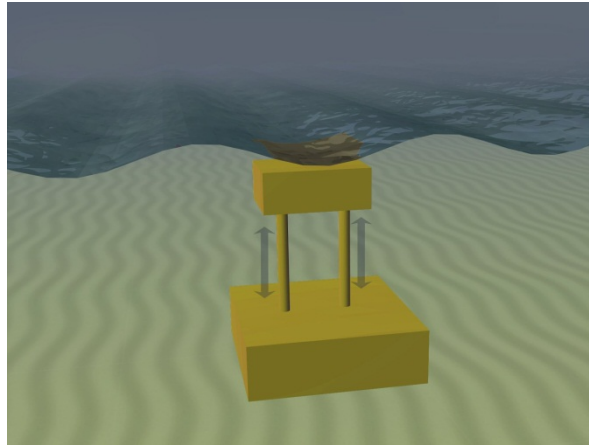
**Figure 2-11: Operating Principle of a Submerged Pressure Differential Device [10]**

2.3.1.4.2  Physical Modelling of Wave Activated Bodies

Reference [32] carried out physical model tests on a single point absorber buoy to provide validation material for the numerical model. The model tests were carried out in the wave flume at the Flanders Hydraulics Research (FHR) in Antwerp, Belgium at a scale of 1:15.9. The floating buoy is restricted to a single degree of freedom heave motion. This is achieved by connecting the buoy to a connecting rod (con-rod) which in turn is connected to a rotating belt, which is connected to a rotating shaft. The measurement equipment is mounted on this shaft. The con-rod is a rectangular cross-section to ensure bending does not occur under wave loading and thus reduces the load on the bearings on the rig. The motion of the buoy is monitored by an optical encoder mounted on a horizontal rotating shaft connected to the pulley. The damping force is applied by a mechanical brake consisting of a circular element covered by a felt that is pressed on a wheel that is mounted on the rotating shaft. The damping force is monitored by a force transducer and torque sensor. A tuning force proportional to the acceleration of the buoy was applied by adding a supplementary mass on the other side of the belt. All motions and forces required for the assessment of the performance of the system have been accounted for in this setup. This is a much more complex system than that of the OWC.

Reference [33] carried out physical model test on a three-body point absorber WEC, CPT Manta WEC, at the Hinsdale Wave Research Laboratory at Oregon State University, USA at a scale of 1:33. The tests were carried out in conjunction with the development of a numerical model as detailed in the next section. The model was constructed in three parts, the two surface floats and the central spar buoy. The surface floats are connected to the spar via a rotating shaft. Each float has a separate damping mechanism in the form of rotary DC motor-generator dampers. A custom designed embedded controller (EC) was located in the nacelle of the WEC. A six-degrees-of-freedom inertial sensor was used to monitor the linear acceleration and angular velocity of the central spar in three-axes. The EC was also connected to two high-resolution encoders attached to each of the DC motor-generator dampers to monitor the angular position and velocities of the generator shaft relative to the central spar. In addition, the EC monitors the torque at each generator shaft via two

torque transducers integrated into the WEC. The data was recorded every 2ms by the EC. The motions of the buoys were also monitored by a PhaseSpace optical motion tracking system and provided additional redundancy in the data collection.

Reference [34] reported on a physical testing campaign carried out on the Wavebob point absorber WEC at the MARIN tank facilities in the Netherlands. The novel aspect of this testing campaign was the assessment of a pitch controlling mechanism for the stability of the Wavebob device. The Mathieu analysis has shown that periodic multipliers that have significant components at twice the resonant pitch frequency of the pitch dynamics are of most concern. The Wavebob device suffers from this parametric resonance phenomenon. In order to test the pitch stability controller, a linear actuator was employed as the PTO mechanism. The linear motor satisfied the main velocity, force and stroke PTO requirements. In this study, a Copley Controls linear motor system consisting of a housing with windings, and a moving rod with magnets was used. The force between the bodies was measured with a six-degree-of-freedom force frame. The position was measured using an accurate position transducer and an acceleration sensor mounted on the lower body. The linear motor was controlled in current mode by a servo amplifier. The force is proportional to the applied electric current and is generated in the motor but was not equal to the force between the bodies due to losses in the bearings and Eddy currents. A feedback loop system of the measured force was used to control the linear motor to compensate for these losses. The force between the bodies was obtained using the six-component frame with a correction taking the acceleration of the frame mass into account.

2.3.1.4.3  Numerical Modelling of Wave Activated Bodies

The development of numerical models for the analysis of wave activated bodies such as point absorbers is well documented in literature. A substantial study by [32] investigated the performance of a single point absorber buoy using the BIEM code WAMIT in the frequency domain. The linear frequency to time domain (F2T) utility in WAMIT was used to determine the impulse response function (IRF). The F2T output was compared with output from ACHIL3D [35] and a satisfactory comparison was achieved. Further to this, a time domain model was developed in Matrix Laboratory (MATLAB). The equation of motion of the point absorber is described by the Cummins' integro-differential equations and converted into a set of ordinary differential equations using the Prony method to approximate the impulse response function (IRF) by a sum of exponential functions. Satisfactory agreement was achieved between the results from the time domain solver and the frequency domain results from WAMIT. WAMIT was again used to investigate the interactions of an array of closely spaced point absorbers and the superposition principle applied to determine the time-averaged power absorption in irregular waves. This study assessed the performance of the FO$^3$ device by Fred Olsen Ltd. Physical model tests were carried out as detailed in the previous section as validation material.

Reference [36] carried out a study of the point absorber type Aquabuoy WEC using WAMIT and a time domain solver developed in MATLAB. The aim of this study was to maximise the power output of the WEC as it is intended to be a commercial scale device. The outputs from WAMIT in the frequency domain are again input into the time domain solver in MATLAB whereby the time varying parameters are investigated and the non-linear damping and spring stiffness coefficients are optimised to produce the maximum power.

Reference [37] outlines the development of the SEAREV device through the development of an optimisation algorithm. For each geometry considered in the optimisation process, the frequency domain code AQUAPLUS [38] was used to determine the hydrodynamic coefficients. The calculation of the IRF was performed by the dedicated code ACHIL3D, however a second time domain solver was developed incorporating the method of Prony to avoid the use of the convolution integral in the numerical integration. Following the optimisation procedures, the power matrix for the SEAREV device was produced with and without latching control.

Reference [39] investigated the time domain modelling of single and two-body point absorber WECs. The frequency domain solver ANSYS AQWA was used to determine the hydrodynamic coefficients while a time domain solver was implemented in MATLAB/SIMULINK by calculating the IRF by trapezoidal integration to incorporate the effects of PTO forces and moorings for the OPT L10 WEC.

Reference [33] carried out a novel numerical investigation into the operation and performance of a 3-body floating point absorber, the Columbia Power Technologies (CPT) Manta WEC. The numerical framework included the coupling of WAMIT with Garrad Hassan (GH) WaveFarmer for assessment of performance in terms of power absorption, while the coupling of WAMIT with OrcaFlex analysed the mooring loads. The hydrodynamic coefficients were calculated by WAMIT for each geometrical representation of the device and passed to both GH WaveFarmer and OrcaFlex. GH WaveFarmer computes the equation of motion for each specific module, both frequency and time domain. The time domain solver allows non-linear external forces to be modelled and accurate representation of the absorbed power of the device.

Reference [40] evaluated the performance of a single degree of freedom surging point absorber using the commercial code Flow-3D. The WRASPA (Wave-driven, Resonant, Arcuate action, Surging Point Absorber) device is a pitching surge WEC developed at Lancaster University. The Flow-3D solver is based on the Reynolds-Averaged Navier-Stokes (RANS) equations. The solver makes use of a technique TruVOF to represent the free surface and does not require additional mesh cells at the free surface unlike general RANS solvers. The mesh is also fixed and thus reduces the time for computations. The pitching motion of the device was monitored

and the torque induced on the rotational joint calculated. The general moving object capability was used to optimise the shape of the primary absorber.

### 2.3.1.4.4 Example Attenuators

ATN devices are typically long slender devices floating on the sea surface. The primary dimension for energy absorption is not the width but the length of the device as the device width is generally much smaller than the length. The common mooring system used is the slack moored configuration. The power take-off (PTO) systems vary between pumped hydro and oil hydraulics. This section provides a more detailed description of a selection of ATN devices currently under development.

#### *2.3.1.4.4.1 Pelamis*

The Pelamis wave energy converter is quite possibly the best known device under development worldwide. This is due to the fact that it has been at the forefront of every progression the wave energy industry has made. The device is, like the OE Buoy, a barge type device, except with a number of barges connected together with a 2-degree of freedom connection, like a universal joint. The power take-off system is a hydraulic system extracting energy from the relative motion of the barges in pitch and yaw. The company originally began as Ocean Power Delivery Ltd in 1998 but became Pelamis Wave Power in 2007. The company has carried the attenuator concept through all stages of the Development Protocol. Pelamis pioneered the use of mathematical modelling for hydrodynamic and structural analysis and optimisation throughout the development process. The tank testing campaign began at 1:80 scale in University of Edinburgh (UoE) at Stage 1, 1:35 scale in UoE at Stage 2, 1:7 in both ECN (Figure 2-12) and Frith of Forth, Scotland in Stage 3, 1:1 at EMEC, Scotland in Stage 4, and 3 1:1 devices in Agucadoura in Portugal in Stage 5. Pelamis has also sold 2 devices to utility companies, namely E-ON and Iberdrola's Scottish Power Renewables. Like most companies, continuation of funding has been a struggle for Pelamis, with a significant and diverse list of shareholders already and talks of a stock market flotation in 2012 seemed unusual given the lag in progression the company has experienced since 2009.
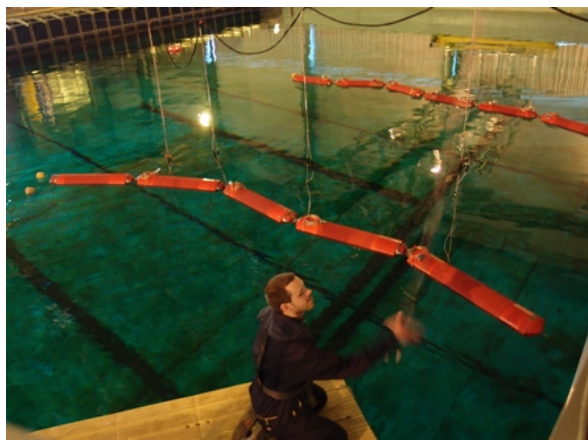


**Figure 2-12: Tank testing of a scale model Pelamis**

**Figure 2-13: Full scale Pelamis machine at EMEC**

The Pelamis is one of the frontrunners in the development of wave energy technology. This section intends to describe this device in more technical detail. Figure 2-13 illustrates the Pelamis P2 machine deployed in EMEC. The figure illustrates the machine is built from 5 cylindrical oblong sections of diameter 4m and length 35m. Each section is connected to the next by a 2-degree-of-freedom PTO mechanism operating in pitch and yaw modes. This joint is akin to a universal joint typically used in machinery and vehicle drive shafts. The figure also illustrates how this joint allows the machine to move with the wave field as both in plan and side elevation in this case, the machine has a curved profile.

The development of the Pelamis machine concept is outlined in [41] and states that the P2 machine weighs approximately 1300t. If it is assumed that 50% of the mass is sand ballast and 50% steel, the plate thickness is approximately 38mm, rounded to 40mm. Reference [42] investigated the potential for a project using the Pelamis P1 device in San Francisco which has a wave climate of ~20kW/m. The cost of that hull for the P1 4 section device was ~€600,000 for ~350t steel hull. Using the cost model developed and an equivalent steel plate thickness of ~25mm, which seems reasonable for that wave climate, results in a total steel mass of ~334t and unit a cost of ~€1800/t.

In the early development and marketing of the Pelamis P1 device, a power matrix was published on the company website and has been reproduced in many publications since. Fig. 4-2 is taken from the original Pelamis P1 brochure. Based on this power matrix, the P1 device could deliver ~188kW of power on average at 100% availability annually in a 65kW/m resource site. This equates to a maximum average annual capacity factor of 25%. The efficiency of the oil hydraulics PTO system is taken as 65% as indicated in Section 2.6.5. The absorbed power is then ~289kW on average. The CWR may then be assumed to be ~2.9%.

| $H_s$ (m) | $T_e$ (s) 5.0 | 5.5 | 6.0 | 6.5 | 7.0 | 7.5 | 8.0 | 8.5 | 9.0 | 9.5 | 10.0 | 10.5 | 11.0 | 11.5 | 12.0 | 12.5 | 13.0 |
|---|---|---|---|---|---|---|---|---|---|---|---|---|---|---|---|---|---|
| 0.5 | idle | idle | idle | idle | idle | idle | idle | idle | idle | idle | idle | idle | idle | idle | idle | idle | idle |
| 1.0 | idle | 22 | 29 | 34 | 37 | 38 | 38 | 37 | 35 | 32 | 29 | 26 | 23 | 21 | idle | idle | idle |
| 1.5 | 32 | 50 | 65 | 76 | 83 | 86 | 86 | 83 | 78 | 72 | 65 | 59 | 53 | 47 | 42 | 37 | 33 |
| 2.0 | 57 | 88 | 115 | 136 | 148 | 153 | 152 | 147 | 138 | 127 | 116 | 104 | 93 | 83 | 74 | 66 | 59 |
| 2.5 | 89 | 138 | 180 | 212 | 231 | 238 | 238 | 230 | 216 | 199 | 181 | 163 | 146 | 130 | 116 | 103 | 92 |
| 3.0 | 129 | 198 | 260 | 305 | 332 | 340 | 332 | 315 | 292 | 266 | 240 | 219 | 210 | 188 | 167 | 149 | 132 |
| 3.5 | - | 270 | 354 | 415 | 438 | 440 | 424 | 404 | 377 | 362 | 326 | 292 | 260 | 230 | 215 | 202 | 180 |
| 4.0 | - | - | 462 | 502 | 540 | 546 | 530 | 499 | 475 | 429 | 384 | 366 | 339 | 301 | 267 | 237 | 213 |
| 4.5 | - | - | 544 | 635 | 642 | 648 | 628 | 590 | 562 | 528 | 473 | 432 | 382 | 356 | 338 | 300 | 266 |
| 5.0 | - | - | - | 739 | 726 | 731 | 707 | 687 | 670 | 607 | 557 | 521 | 472 | 417 | 369 | 348 | 328 |
| 5.5 | - | - | - | 750 | 750 | 750 | 750 | 750 | 737 | 667 | 658 | 586 | 530 | 496 | 446 | 395 | 355 |
| 6.0 | - | - | - | - | 750 | 750 | 750 | 750 | 750 | 750 | 711 | 633 | 619 | 558 | 512 | 470 | 415 |
| 6.5 | - | - | - | - | 750 | 750 | 750 | 750 | 750 | 750 | 750 | 743 | 658 | 621 | 579 | 512 | 481 |
| 7.0 | - | - | - | - | - | 750 | 750 | 750 | 750 | 750 | 750 | 750 | 750 | 676 | 613 | 584 | 525 |
| 7.5 | - | - | - | - | - | - | 750 | 750 | 750 | 750 | 750 | 750 | 750 | 750 | 686 | 622 | 593 |
| 8.0 | - | - | - | - | - | - | - | 750 | 750 | 750 | 750 | 750 | 750 | 750 | 750 | 690 | 625 |

**Figure 2-14: Pelamis P1 Power Matrix**

The additional hazard with the use of hydraulic PTO systems is the reliability of the components. Availability is a direct function of accessibility and reliability and the performance of the components in a hydraulic system is critical to the feasibility of the device. Pelamis state that any maintenance necessary for the device would be carried out portside. This then requires the towing of the device from its installation site to port. The mooring attachment is then another critical component, which for the Pelamis is a subsea component as illustrated in Figure 2-15. No issues have been reported with this system, which is central to the success of the O&M philosophy for the Pelamis machine. No limits in terms of $H_s$ have been reported for (de)attachment of the device from the mooring, though it should be reasonable to assume 2m $H_s$ on the basis of O&M carried out on marine weather buoys.
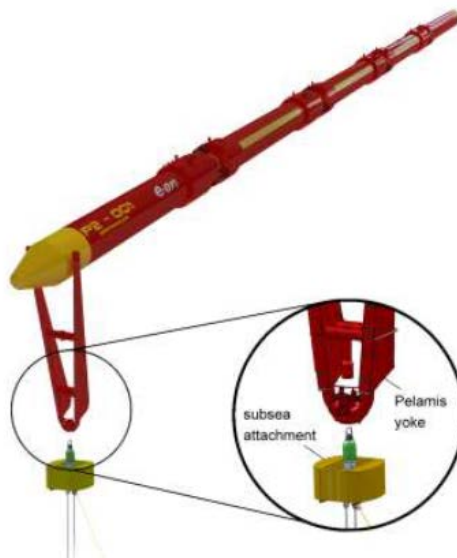
**Figure 2-15: Pelamis Mooring System**

### 2.3.1.4.4.2  McCabe Wave Pump

The McCabe Wave Pump (MWP) was originally patented under Hydam Technology in the US in 1992 under patent number US5132550 [43]. The system is composed of three articulated barges, a fore and aft barge and a central barge from which the fore and aft barge move in relation to primarily in pitch motion. The system is now under development by Ocean Energy Systems (OES) Inc. based in the US and is being marketed as a method of production of desalinated water under the name Amplified Wave Energy Conversion System (AWECS). The design was originally conceived in 1980 by Dr. Peter McCabe, and co-developed by Dr. Michael McCormick. The outline design is illustrated in Figure 2-16 and the Shannon Estuary prototype dimensions in Figure 2-17. [44] suggests that the performance of the MWP could reach an average of 150% CWR, which seems excessively high. [45] suggests that the MWP type unit would have a rating of 250-500kW. Assuming the 40m prototype unit was rated at 250kW and a capacity factor of 25% similar to the Pelamis machine previously, the CWR for the unit in 65kW/m resource is 3.7% using a PTO efficiency of 65%. This is a more reasonable estimate. The average output of the prototype in 65kW/m is approximately 60kW. The Shannon Estuary prototype is illustrated portside in Figure 2-18. The mooring system for the MWP is a typical catenary mooring layout with 4 lines. It has also been noted that the fore barge produces the majority of the power.
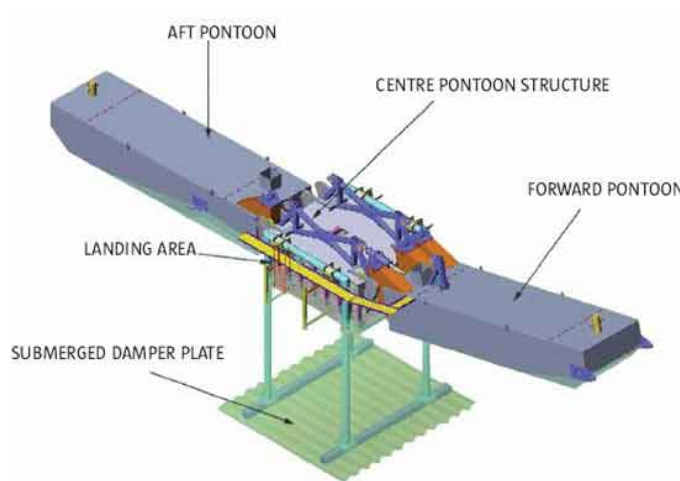


**Figure 2-16: MWP Concept**
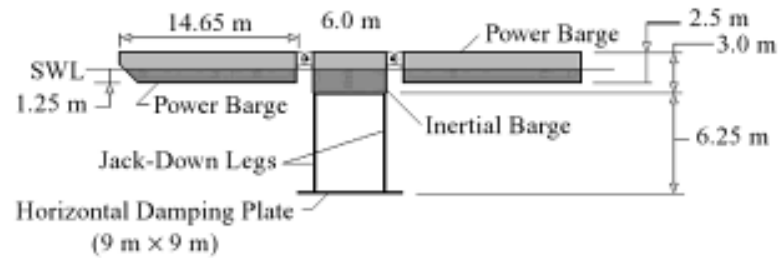
**Figure 2-17: MWP Dimensions for Shannon Estuary, Ireland [46]**



**Figure 2-18: MWP Prototype at the Shannon Estuary, Ireland**

The obvious advantages of the MWP type system is the simplicity of construction of the barge units. These are simple rectangular units and may be fabricated from steel plate and stiffeners or RC. As the device relies on relative motion between units the impact of using RC for fabrication on the power performance of the unit would need to be determined before a well informed choice may be made. Each barge for the prototype weighed approximately 60t, and therefore used 25-30mm steel plates.

### 2.3.1.4.4.3 *DexaWave*

The DexaWave wave energy device was under development by DexaWave ApS in Denmark established in 2008 but is reported to no longer be in business. The system is similar to that of the MWP with only a single power producing barge operating in relative pitch and therefore only one set of hydraulic PTOs. Currently, a 1:5 scale model is deployed at the Danish Wave Energy Centre (DANWEC) test site at Hanstholm, Denmark as illustrated in Figure 2-19. The device is ~8.9m long and ~3.25m wide weighing ~5t. The length to width ratio is considerably less for the DexWave device than for either the Pelamis or MWP. The power producing dimension would therefore need to consider both length and width through Pythagora's theorem. This results in an active dimension of ~9.4m. Reference [47] reported that the resource at the 17m deep berth at Hanstholm has an average annual resource of 7kW/m. The incident power is then ~66kW. The scale model is rated at 5kW, so a capacity factor of 25% results in an average power of 1.25kW. The CWR is then estimated to be 2.9% assuming a PTO efficiency of 65%.

**Figure 2-19: DexaWave 1:5 Device at Hanstholm, Denmark**

The mooring system for the DexaWave is anticipated to be a typical catenary system. The unit costs of the DexaWave are more difficult to assess than either the Pelamis or MWP hulls due to the shape of the sections and space frame nature of the structure, which is approximately 124t, as illustrated in Figure 2-20. The developers also suggest that this may be constructed from plastic or concrete materials. While plastic material is plausible for a space frame structure, the suggestion of concrete or RC for this configuration of device is questionable.
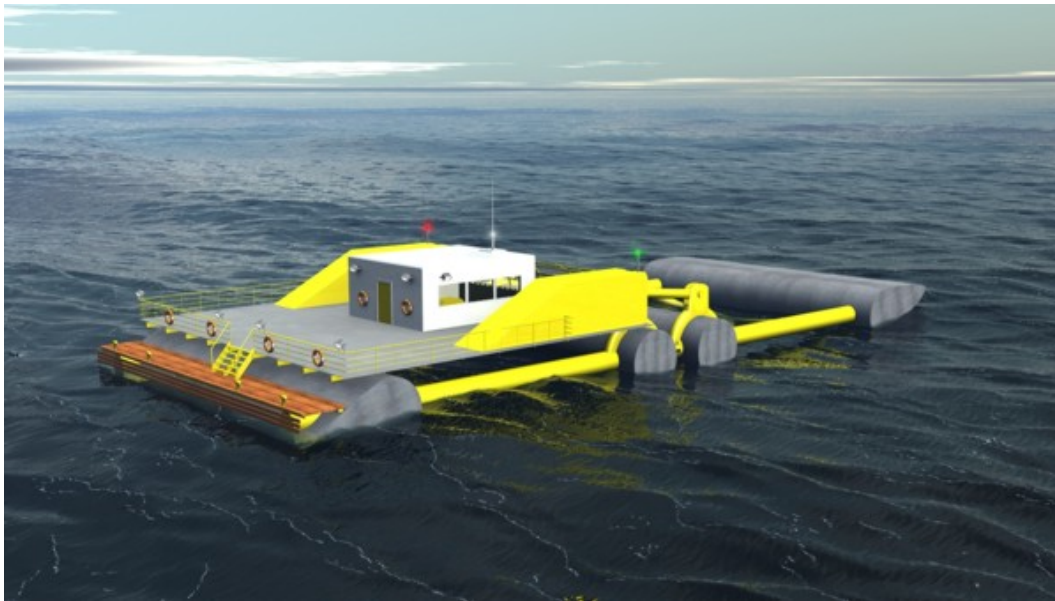


**Figure 2-20: DexaWave Prototype Illustration**

### 2.3.1.4.5 Example Point Absorbers

The PA wave energy device category is possibly the most populated in terms of concept number and variation as well as being the most researched category throughout wave energy development. Configurations vary from simple bottom referenced devices like the Seabased PA in Sweden, or a 2-body floating PA like the Wavebob in Ireland or an array type configuration like the Pontoon Power Converter

in Norway. This section aims to provide more detail on a selection of PA concepts and provides a reasonable cross-section of the category of devices which may be suitable for use in a hybrid scenario.

### 2.3.1.4.5.1 Wavebob

The Wavebob PA device is one of the best known examples of a 2-body floating PA for use in deep water. The device has been under development since 1999. A rigorous strategy for the development of the technology ensued and included numerical modelling and many tank testing campaigns across Europe. The device was also used as the test subject in the EU FP7 Standpoint project which aimed to accelerate the standardisation of wave energy harvesting through the use of the axisymmetric PA concept. This project also designed a hydraulic PTO system for the Wavebob for an Atlantic wave climate [48]. The device however, is known to suffer from parametric resonance in pitch thus significantly affecting the power performance of the device [34]. Efforts to control this have been carried out through novel control mechanisms and algorithms within the PTO system. Another issue of concern is the difficulties the concept experiences in keeping upright during steep wave conditions to ensure purely relative heave motion between body 1 and body 2 as illustrated in Figure 2-21. Considerable efforts have been carried out in the design of a mooring system which can rectify this issue as illustrated in Figure 2-22.
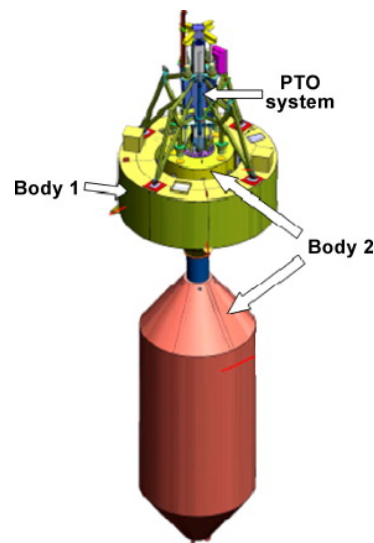


**Figure 2-21: Wavebob Concept Configuration**

**Figure 2-22: Wavebob Conceptual Mooring System**
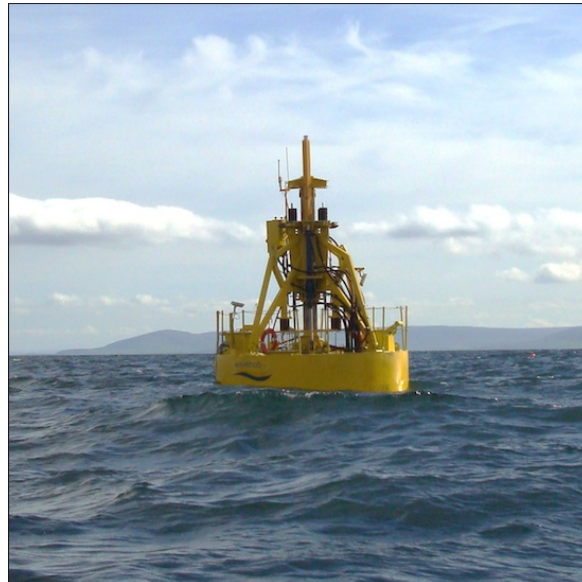


**Figure 2-23: Wavebob ¼ Scale Device in Galway Bay, Ireland**

Nonetheless, the Wavebob concept has progressed through the development protocol by securing funding from government and private sources. The company deployed a ¼ scale device at the Galway Bay test site, Ireland in 2006 as illustrated in Figure 2-23. The original device experienced mechanical failures [49] which were rectified and the machine was re-deployed in 2007 with a new mooring system.
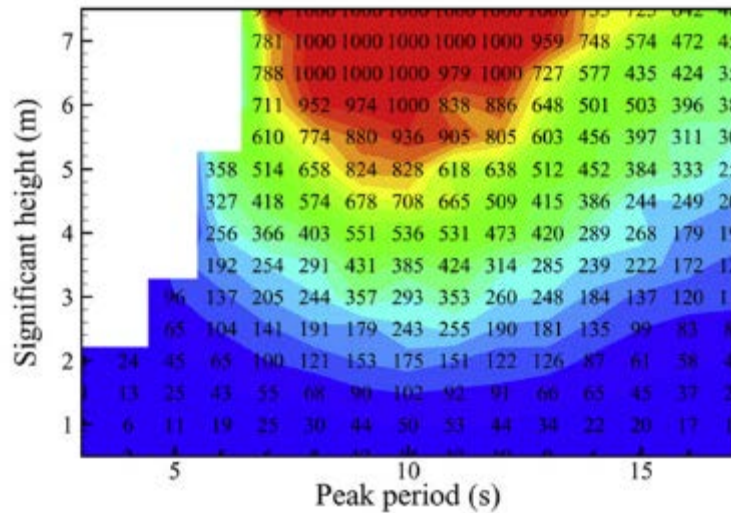


**Figure 2-24: 2-Body Point Absorber Power Matrix**

Very little information has been made public regarding the performance of the Wavebob system with the exception of some claims by the developer themselves. Reference [17] suggested a CWR range of 19-42%. Reference [31] carried out an assessment of a 2-body floating PA similar to the Wavebob system and produced the absorbed power matrix illustrated in Figure 2-24. In a 65kW/m wave climate, a 20m buoy would produce ~167kW. This corresponds to a CWR of 20% assuming a hydraulic PTO of 65%. This figure is at the lower end of the scale suggested.

The construction of the Wavebob device, despite its tubular nature, would require a steel plate and stiffener design given the dimensions of the parts. The surface torus buoy (body 1) is 20m in diameter with a central void for attachment of the PTO frame to the submerged inertial buoy (body 2).

### 2.3.1.4.5.2  OPT

Ocean Power Technologies (OPT) Inc. in the US has been in operation since 1994. This company is developing a system, similar to the Wavebob system, but smaller in size. The company has an impressive track record in terms of technology development and securing of funds for continuation of their development strategy for the PowerBuoy concept. The company was listed on the NASDAQ as OPTT in 1997. The Mark 3 PowerBuoy has a diameter of 11m and a generator of peak rating 866kW. The company claim capacity factors of 30-45%. In a news release regarding the performance of the PB150 device in the North Sea in Scotland, it is noted that the device produced highs of 400kW and an average of 45kW. The device was nominally rated at 150kW. This would suggest a capacity factor of 30% in line with

that claimed by the company. The PTO system is a direct drive system and it is assumed that an efficiency of 85% is achievable. Therefore the CWR of the PB150in Scotland assuming a 30-40kW/m resource is 16- 12% respectively. These values are between the ranges suggested by [17] for large and small PAs, which is appropriate as the buoy dimension is between the typical dimensions suggested.



**Figure 2-25: OPT PB150 Device docked in Scotland Awaiting Deployment**

As the PB150 is smaller than the Wavebob device, the options for construction are wider and make it difficult to assess costs for the hull, particularly the lower heave plate and truss structure as illustrated on the PB150 to be deployed in Scotland in Figure 2-25. The total mass of the structure is quoted to be 180t.

### 2.3.1.4.5.3 Wavestar

The concept of the Wavestar wave energy device originated in 2000 and the rights to the IP were bought out in 2003. The device marked a shift in the conception of wave energy devices at the time, from individual small devices to an array of devices hosted on a singular platform. Testing of the concept began at Aalborg University in Denmark in 2004-2005 at a scale of 1:40 with float diameters of 250mm as illustrated Figure 2-26. Following the performance of the device in these tank tests, the results were deemed acceptable to proceed to the next stage of development. This entailed design and deployment of a 1:10 model at the Nissum Bredning small scale test site in Denmark. The device is illustrated in Figure 2-27 following installation in 2005-2006. The concept has now moved to a 1:2 scale part deployment at the Hanstholm test site in Denmark. The machine installed has 2 floats on the jack-up platform as illustrated in Figure 2-28 and is grid connected.

**Figure 2-26: Wavestar 1:40 Model at Aalborg University**

The resource at Hanstholm in the location that Wavestar is installed is 3kW/m as reported in [47]. Wavestar publishes a monthly report on the performance of the machine since installation in 2009. An assessment of these figures provides some interesting performance indicators. The device has an average availability of ~75%. The individual buoy performance is ~28% CWR which is well above the range suggested for a 5m buoy in [17]. The average electrical energy supplied to the grid is ~1.9kW per buoy, thus a total efficiency of 12% and an average PTO efficiency of 45%. This is well below the 65% assumption made previously. However, the maximum PTO efficiency recorded is 62% which is close to the assumption made and indicates that this can be achieved. Further developments should bring the average higher.



**Figure 2-27: Wavestar 1:10 Model at Nissum Bredning**

51

**Figure 2-28: Wavestar 1:2 Part Deployment at Hanstholm**

In [31] a study was carried out on a Wavestar like device. The absorbed power matrix illustrated in Figure 2-29 was produced. The annual average power produced by this device in a 65kW/m resource is 343kW assuming a PTO efficiency of 65%. However, a 65kW/m resource is unlikely in shallow water of ~20m. As indicated in [50] for the Atlantic Marine Energy Test Site (AMETS), the wave resource in water depths of >45m is ~65kW/m while the resource at 20m is ~30kW/m. Applying the ratio of incident resource in deeper water to shallow waters, the Wavestar device is anticipated to produce ~158kW. This corresponds to a CWR of ~8% which is more in line with that indicated by [17]. The difference in the performances reported for the full scale device needs to be investigated. There are two main reasons why this discrepancy may exist. Firstly the numerical modelling of this system may be inaccurate. Secondly, the CWR of this type of device is not constant with resource as is suggested by [17]. In the same paper, the performance of an ideal PA is presented. Figure 2-30 presents some of this data and approximates the CWR of the ideal PA using a dimension of 20m guided by the suggestions in the paper.
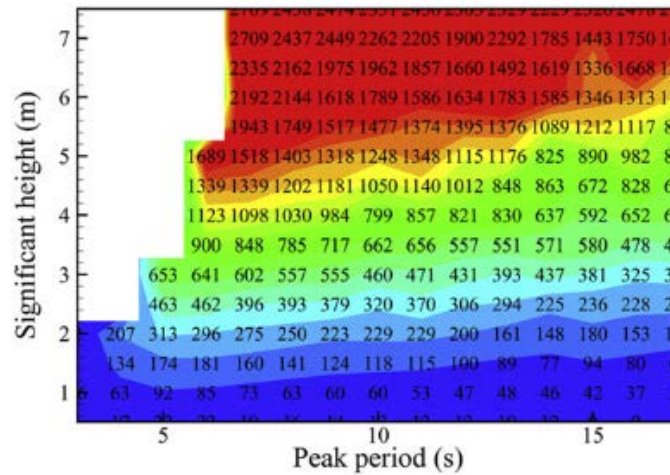
**Figure 2-29: Absorbed Power Matrix for a Wavestar Type Device**
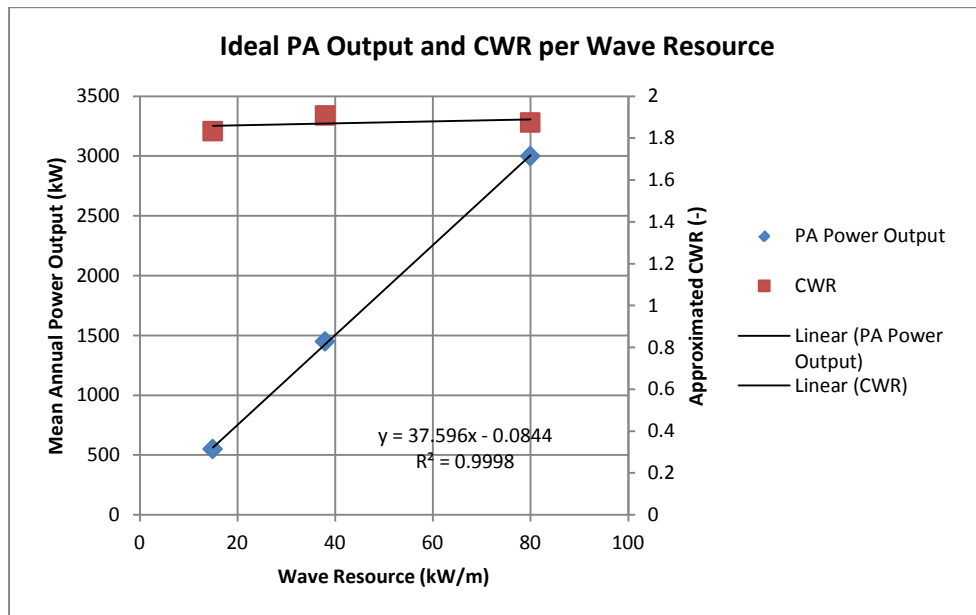


**Figure 2-30: Ideal PA Performance**

The mean output of the PA in Figure 2-30 has taken account of the practical performance of a PA by considering the output to be 30% of the ideal for all resource levels. This naturally translates to a constant CWR. If however, the percentage reduction in power from the idealised case is bounded by the motion constraints of the PA, which is certain to occur, the CWR could not remain constant with increasing resource levels. Increasing resource level implies larger wave heights. The motion excursions of a PA are fixed for a specific device configuration. If this device is placed in many different resource levels, the PA can only produce power within the excursion limits. Therefore in higher waves, the PA performance relative to the incident resource will be less with all other considerations equal, e.g. PTO damping. This could cause the different performance figures quoted previously. In contrast, [31] report that the Wavestar type device has a CWR of 12-17% for resource levels of between 15-80kW/m.

**Figure 2-31: Wavestar in storm protection mode at Hanstholm**

The Wavestar device has a unique survivability mode as illustrated in Figure 2-31. Each buoy is retracted from the water by the hydraulic system in storm conditions. Thus only the foundation pile structure is exposed to extreme conditions assuming the hydraulic system does not fail. The structural design of this device is difficult due to this fact. A number of considerations need to be taken account of in the event of buoy and jack-up hydraulics systems failure. These include, designing the total structure, piles, body, buoys and buoy connections for extreme loads un-retracted from the water. Or alternatively, install back-up hydraulics systems. A full probabilistic economic assessment would be required to determine the cheapest and most effective method. [31] suggest the characteristic mass of the Wavestar type device is 1600t. As it is a fixed structure, it may be assumed to be all structural steel.

2.3.1.4.6  Example Oscillating Wave Surge Converters

The OWSC device type is again another category which has seen a lot of interest and research in the last two decades. The concept has been incorporated into a number of very different device configurations each with its pros and cons. The hydrodynamic performance of the fixed version is exceptional as will be discussed, while the operational concept of the OWSC is not very well suited to floating systems. The following is a description of a selection of OWSC type devices.

*2.3.1.4.6.1 Oyster*

In 2001, the research team at Queens University Belfast began researching the possibility of using flap-type devices for wave energy production. The founder of Wavegen, the UK's first wave energy company, Allan Thompson, co-funded further research and development (R&D) into the technology. In 2005, Thompson established Aquamarine Power to bring the Oyster technology to the commercial market. In 2007, funding from SSE and venture capitalist firm Sigma Capital Group provided the company with the resources required to continue developing the Oyster from scale model tank tests to full scale prototypes, illustrated in Figure 2-32, at sea.

**Figure 2-32: The Oyster 800 device**

The Oyster wave energy converter is now under development at Aquamarine Power Ltd. The device is bottom-fixed, i.e. the device is connected to the seafloor through steel/concrete piles. The "flap" is hinged at the foundation and the passing waves cause the flap to rotate backwards, a motion which is resisted by the attachment of open-loop seawater hydraulic systems. This is essentially a hydroelectric power system. The flap rises back to the surface in the trough of the wave due to the buoyancy modules built into the flap itself. The other primary difference between this concept and floating systems is that the initial stage of power take-off, i.e. the hydraulic actuators, resisting the flap motion are completely submerged. The device is intended for nearshore sites, which would typically have breaking waves more frequently than offshore sites which may make O&M activities very difficult indeed. The concept originated at Queen's University in Belfast when Stage 1 testing began at a scale of 1:40 illustrated in Figure 2-33. Aquamarine Power Ltd. was founded in 2005 shortly afterwards and continued development of the concept through Stage 2 testing at Queen's University at a scale of 1:20, Stage 3 testing was carried out on the PTO system only at National Renewable Energy Centre (NaREC) in the UK. The Oyster 1 system was deployed in EMEC in 2009 at a scale of 1:1 during Stage 4 testing as illustrated in Figure 2-34. ABB became an investor which allowed a further redesigned device, the Oyster 800, was deployed at EMEC in 2012 for further Stage 4 testing. It is reported that issues with the subsea components are delaying progress. However, Aquamarine Power secured full consent to develop a 40MW farm in the north west of Lewis in Scotland in 2013, making it the largest fully permitted site in the world.
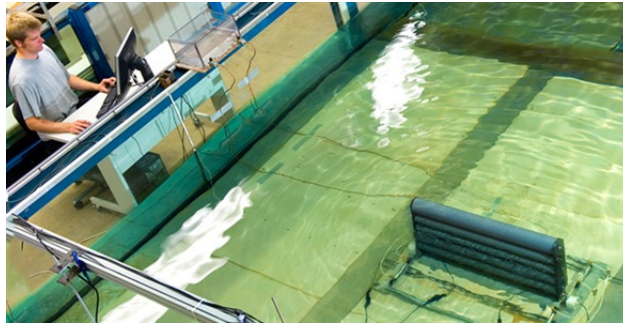
**Figure 2-33: Oyster device under test at Queen's University during Stage 2**



**Figure 2-34: Oyster 1 full scale device deployed in EMEC in 2009**

The CWR for this device is very large as indicated by [17] at ~41%. The ability of the device to absorb this amount of power naturally leads to significant loading on the structure and foundation piles. This type of device was included in the study by [31] and the absorbed power matrix for the device is illustrated in Figure 2-35. In a 65kW/m site, the device would produce ~333kW assuming a PTO efficiency of 65%. Like the analysis for the Wavestar, the Oyster would be situated in water depths of 10-15m. From [50] the resource at AMETS in 15m is ~20kW/m. It is anticipated that the Oyster would produce ~102kW in that location.
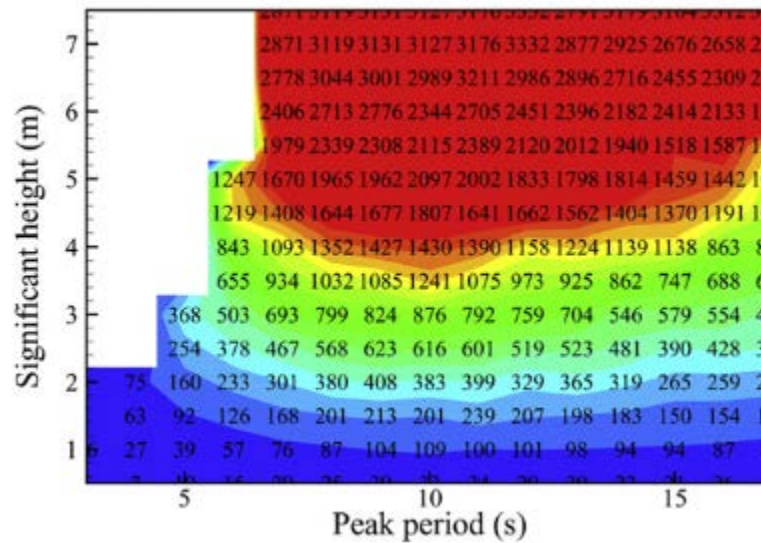
**Figure 2-35: Absorbed Power Matrix for a Bottom Mounted Pitching Flap Device**

In extreme conditions the Oyster has the capability of being rotated onto its foundation on the seabed well below any breaking waves, therefore the flap itself need only be designed for operational loads. However similar to the design issues mentioned for the Wavestar, a number of design issues should be considered. In the event of hydraulics system failure, the flap is exposed to extreme waves and large breakers and must be structurally designed to cope with the extreme loads. Alternatively a back-up hydraulic system may be considered. The design of the current Oyster 800 is such that no simplified methodology can be used to approximate the steel design. Reference [31] suggested that the characteristic mass of the device is 150t which may be assumed to represent all structural steel as it is a fixed device.

### 2.3.1.4.6.2  WaveRoller

AW-Energy Ltd. is the developer of the WaveRoller wave energy device, founded in Finland in 2002. The original concept development was initiated in 1999 by the inventor Rauno Koivusaari. The concept underwent continual development stages and the company received investment from a number of sources, which now include Aura Capital, Fortum, John Nurminen Oy and Sitra. The first prototype was installed in EMEC in 2005 and following encouraging performance, the next stage of prototype development in Portugal was initiated. In 2007, a WaveRoller unit with a hydraulic PTO was installed. The hydraulic rams were replaced with larger rams and redeployed again in 2007. A second WaveRoller unit was deployed in 2008 with more powerful rams and provided data for the development of the 300kW WaveRoller unit. The device became the subject of the EU FP7 SURGE project in 2009 which aimed to deploy the WaveRoller 300kW device in Portugal. The 3 flap unit was deployed in 2012 in Peniche, Portugal. An illustration of a WaveRoller farm is shown in Figure 2-36while the deployment of the 300kW unit in Portugal is illustrated in Figure 2-37.
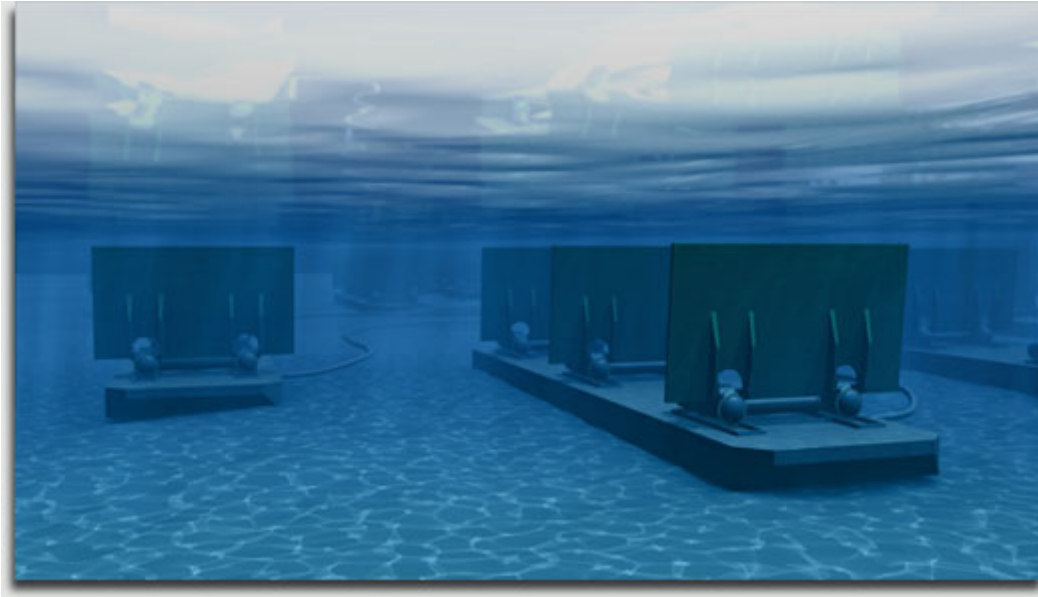
**Figure 2-36: WaveRoller Farm**



**Figure 2-37: Deployment of the 300kW WaveRoller Unit**

The WaveRoller deployed in 2008 in Portugal weighed 20t including the concrete base. This can be estimated to be ~1.5t of steel for the flap and ~18t of concrete ballast. The dimensions of the flap are estimated to be 3.5x4m and it is suggested to produce ~13kW of nominal power. In a good wave site, like AMETS in 10m water depth, this would translate to a CWR of ~57% which is again in the range suggested by [17] for flap devices but is well above the average. The deployment in 2012 was of a 300kW device which would produce ~100kW assuming similar conversion performance.

### *2.3.1.4.6.3  Langlee*

The Langlee wave energy device is a departure from the previous two OWSC type devices, though this was not always the case. Langlee Wave Power AS in Norway began investigating the fixed "water wing" concept in 2006 but concluded that this option was too expensive due to foundations etc. In co-operation with the Norwegian offshore industry, a floating concept using two flaps was developed. The initial floating concept is illustrated in Figure 2-38and suggests a semi-submersible platform. This configuration was tested at Aalborg University at a scale of 1:20 and characterised the performance of the device [51].
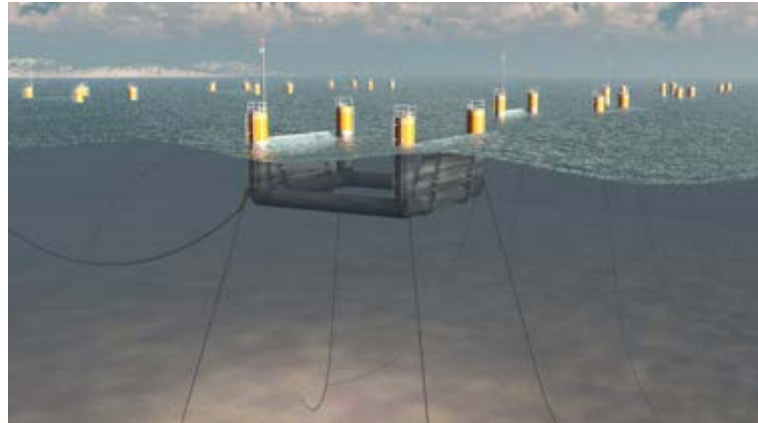


**Figure 2-38: Initial Langlee Device**
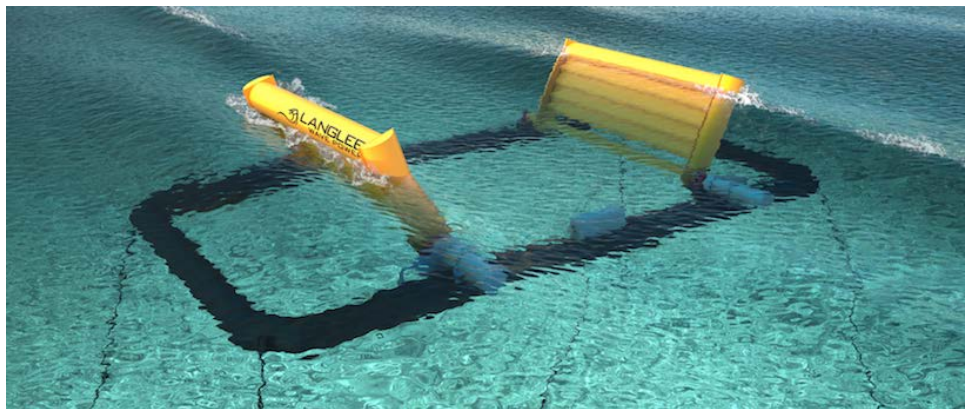


**Figure 2-39: New "streamlined" Langlee device**

The company has established a subsidiary in the Canary Islands and is planning a deployment of the newly developed Langlee device at the PLOCAN facility. The new device, illustrated in Figure 2-39, has the appearance of a TLP platform. This would provide more resistance against the loading applied to the flaps and direct this energy through the PTO rather than causing the platform to move excessively. The disadvantage of this is that the moorings will inevitably be more expensive. The original Langlee semi-sub device was included in the study carried out by [31] and the resulting power matrix for that device is illustrated in Figure 2-40.
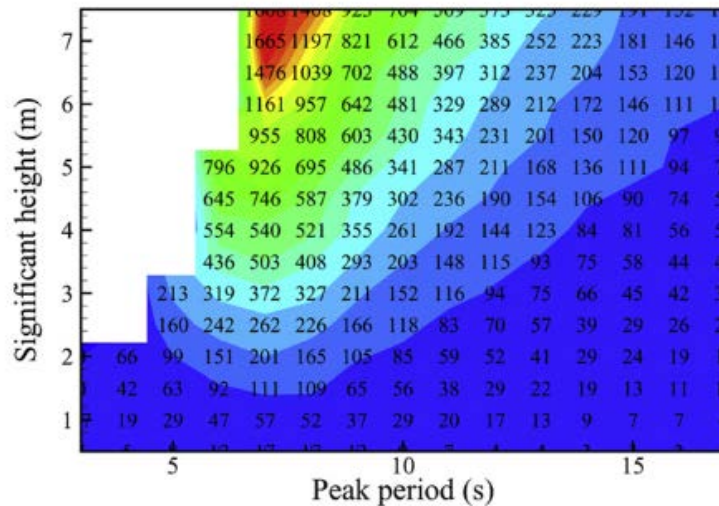
**Figure 2-40: Original Langlee Absorbed Power Matrix**

Using this power matrix and the efficiency of a direct drive PTO of 85%, which is mentioned on the company website, the performance of the device in a 65kW/m site is ~214kW. This equates to a CWR of 20% taking into consideration that the device has two flaps, which is equal to the average CWR suggested for floating pitching devices in [17]. The semi-sub platform is suggested to be 1600t characteristic mass. The breakdown of steel and ballast is unclear. If it is assumed that the equivalent steel plate thickness is similar to previous devices at 35mm, the semi-sub version would weigh ~770t of steel including bulkheads. The platform dimensions in this case are most likely in the range for use of ring stiffened steel tubes for the hull. This may result in lower steel masses. The new configuration would have considerably less structural steel, however the costs of the mooring system for this platform would have a significant impact on the CAPEX costs. A full LCCA analysis of such a system would be required to assess the benefits.

### 2.3.1.5 Overtopping Devices

This section outlines the operating principle of overtopping devices and the methods of analysis applied to the overtopping concept for power production. Furthermore an example of an overtopping device currently under development is included and described in detail.

#### 2.3.1.5.1 Operating Principle

These devices behave essentially like a shoreline beach allowing waves to break on the front ramp and flow into a reservoir situated a predetermined height above sea level. The water then flows back into the sea through the low head hydro turbines at the base of the reservoir. Figure 2-41 below illustrates the principle. These devices may be shoreline fixed or floating offshore devices.
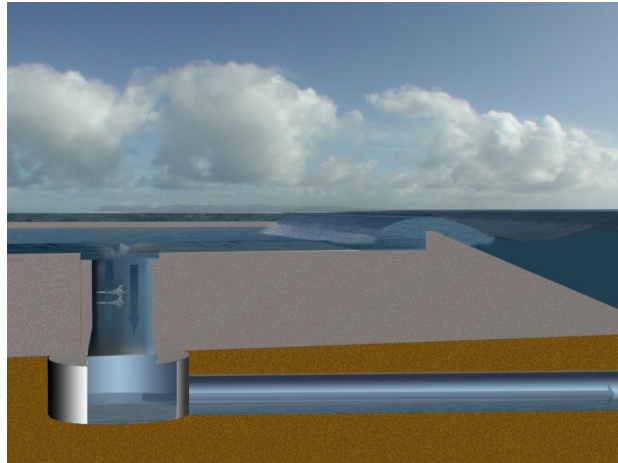
**Figure 2-41: Operating Principle of an Overtopping Device**

2.3.1.5.2   Physical Modelling of Overtopping Devices

Reference [52] conducted physical scaled model tests on the Wave Dragon WEC to examine the effects of the reflecting arms and their attachments to the main body of the device. The tests were carried out at the wave tank facilities in Aalborg University, Denmark at a scale of 1:51.8. The tests were carried out in response to a finding during sea trials of the 1:4 scale Wave Dragon that the method of attaching the reflecting arms had an influence on the overtopping flows into the main reservoir. During the tests, various methods of connecting the arms were investigated, either no arms, rigid arms and moveable arms. The forces in the connections for the arms were not measured in this study but are reported in [53]. The measurements setup during the tests included the measurement of the overtopping volume, the force at the main mooring point, the heave, pitch and surge motion of the device and the surface elevation in several points of the wave basin. The overtopping flow was expelled from the main reservoir through three main exhaust pipes which directed the flow into a storage tank. The water level in the tank was measured by a surface elevation gauge. The tank contained a pump controlled by the data acquisition system. When the water level reached a certain level, the pump automatically ran for three seconds and reduces the water level in the tank. The volume taken by the pump back to the basin was calibrated for that operating time. The total overtopping volume is then calculated by the number of cycles the pump operates times the calibrated volume plus the water volume in the tank at the end of the test. Two force transducers were used to monitor the mooring line forces at the connection points. The motions of the device were measured by three ultra-sound displacement sensors. Two aluminium plates were added to the device in order to show vertical and horizontal movements by measuring the distance from the plates. Two sensors recorded the vertical movements of the front and rear of the device, subsequently pitch and heave around the centre of gravity was deduced. The waves were measured with a linear set of wave gauges. All signals were set at a recording rate of 10Hz.

Reference [54] carried out physical scale model tests on the WaveCat WEC at the tank facilities at the Faculty of Engineering at the University of Porto, Spain at a scale of 1:30. The tests covered a comprehensive investigation into the behaviour of the WaveCat device through monochromatic and panchromatic waves. A number of variations in the device configuration were tested. The measurement setup included a water level control system in each of the reservoirs in the model hulls. The control system consisted of a bilge pump mechanism operating at a constant flow rate and a control system to determine the time and duration of the operation of the pump. The water levels in the reservoirs were measured by resistant wave gauges. The surface elevation was measured by six additional wave gauges aligned along the central axis of the wave tank. A motion capture system was employed to monitor the main motions of the device. The system was composed of three infra-red cameras monitoring the position of five reflective markers placed on the model.

2.3.1.5.3   Numerical Modelling of Overtopping Devices
The analysis of overtopping type WECs is a significant departure from the state of the art in the analysis of the other WEC types through BIEM codes primarily. The ability to accurately predict the nature of wave run-up and overtopping is a significant challenge and requires the use of the more advanced numerical techniques that are slowly appearing in the analysis of the other WEC types such as RANS based CFD solvers.

Reference [55] employed the use of Flow-3D software to analyse the overtopping volumes from individual waves over a structure with a specific crest height. This is the primary operating principle of the Seawave Slot-Cone Generator (SSG) and the Wave Dragon WEC. The VOF method is used to track the free surface. The study concludes that the method is applicable and that comparable results are achieved for the average individual overtopping volumes.

Reference [56] reported the development of both 2D and 3D numerical models are under development for the WaveCat WEC using the parallel RANS based Star-CCM+ code again using the VOF method. No further information has been found.

2.3.1.5.4   Example Overtopping Devices
The Wave Dragon is the best known example of an overtopping device. This particular configuration is a large floating barge with a doubly curved ramp and two reflecting arms directing the incident waves onto the ramp. The concept was in invented by Erik Friis-Madsen and was patented in 1999 [57] [58]. The concept underwent significant tank testing both in Aalborg University in 1998-1999 and University College Cork 1999-2000 both at 1:50 scale. The early stage development of the Wave Dragon is detailed in [59]. Following these, a 1:3.5 scale low head Kaplan turbine was testing in Munich. The device then progressed to a 1:4.5 scale demonstrator in Nissum Bredning in Denmark from 2003-2011 when it was decommissioned despite being designed for a 3 year life time.

**Figure 2-42: 1:4.5 Scale Model of Wave Dragon at Nissum Bredning**

Wave Dragon is currently in the process of securing funding to construct a full scale demonstrator. In c.2006 significant work went into planning the development of a 4MW demonstrator to be installed the Pembrokeshire coast in Wales. This however has not materialised.

From [17], the average CWR of overtopping devices is 13%. Based on a device width of 300m, an incident wave resource of 65kW/m and a conversion efficiency of 65%, the Wave Dragon would be expected to produce 1647kW. The platform in this environment may be ~60,000t, most likely constructed from RC.

### 2.3.2 Offshore Wind Energy Technology Overview

As discussed in Chapter 1, the fixed offshore wind industry is now well established reaching installed capacity of the order of gigawatts across Europe. While this industry is not the subject of this thesis, important design processes and cost estimations are to be taken from experience in this industry and will be dealt with in this Chapter. Floating wind concept development is however addressed in this Chapter owing to its similar status to wave energy concept development.

This Chapter is dedicated to the review and brief analysis of existing offshore wind systems, both fixed and floating. The methods employed for the design and assessment are both existing and innovative procedures. The analysis is focussed on connecting the deployment site extreme conditions to the foundation design and then to the costs of the foundation fabrication. This is a common assessment carried out at the detailed design stage whereby quotes from fabricators trained in the specific fabrication area can provide such information. This kind of information however, is almost impossible to attain by the public nor is it easy to apply such quotes to different structures should they be attained. In general, in the early stages of development of a concept, the structural mass, depending on the primary structural material, is estimated as a percentage of displaced mass. This method does not directly connect the deployment site extreme conditions to the structural mass and the certainty around this figure is low. Furthermore, the breakdown of the structural mass is not evident from such a crude estimate. For a detailed and accurate

fabrication cost to be attributed to the structure, a detailed account of the structural material breakdown is required. This chapter aims to show that this can be done for offshore wind structures and uses any available public or confidential information to validate the process so far as reasonably practicable. Firstly, an introduction to the offshore wind turbine types available on the market currently is provided.

### 2.3.2.1 Experimental Modelling

The experimental modelling of floating wind concepts is broadly similar to that of wave energy devices. However, the difference is the application of wind loads and a number of methods are available for this and are described below.

Reference [60] reported on the physical model testing of the WindFloat WTG at the tank testing facility at UC Berkeley at a scale of 1:105. The challenge with the testing of floating WTGs is the scaling of the wind forces. In this case, a disc fabricated from foam material with an area of one third of the total area occupied by the equivalent scaled rotor area is mounted on top of the tower. Turbulent wind is produced by a wind fan located upstream of the model. The wind hits the disc and creates a thrust force on the floater. This thrust force is measured by a load cell mounted between the disc and tower. The drag coefficient for the disc is assumed to be 1.2, and may have been measured prior to mounting on the floater. To create the gyroscopic loads which may be a limiting criteria on the design of the tower, a DC motor was mounted on the tower top. The motor was connected to an aluminium rod with two weights connected to the ends. The motor was set to rotate at the Froude scaled rotational frequency of 2Hz, approximately 12 rpm in prototype scale. The floater was connected to four soft springs which were connected to four mooring lines. This equivalent mooring system gave a resonant period of approximately 65 seconds in surge. The mooring loads were not monitored. The platform motion was measured using a digital video camera tracking the motion of light emitting diodes placed on the model. The system provides three-degrees-of-freedom measurements of the motion in the plane of the camera.

Reference [61] described the development of a scaled model version of the National Renewable Energy Laboratory (NREL) 5MW Reference Turbine for use in validation testing for simulation tools at a scale of 1:50. The thesis outlines the rationale behind maintaining Froude Similitude throughout the scaling of the turbine components and the effects this had on the Reynolds number of the equivalent prototype WTG. Methods of adjusting the various parameters of the turbine and incident wind field are addressed which modify the lift and drag forces on the turbine blades and result in the correct thrust and torque produced by the turbine while maintaining the relevant Froude scaled parameters for platform global dynamics. The nacelle is equipped with a substantial number of sensors and controllers allowing thrust load and torque measurement, blade pitch control for adjustment of lift and drag forces, a motor and a gearbox. The turbine unit was mounted on a tension leg, spar and semi-submersible platform for assessment of the system. This method of representation of the WTG is rather complex and would typically be used

following a comprehensive study of the floater it is to be mounted on has already taken place. This is in order to clearly identify the effects of the systems incorporated in a real WTG such as blade pitch, tip-speed ratio, and yawing mechanisms. For the purposes of the investigations in this thesis, this method is deemed unfeasible.

A third option for the simulation of the thrust load from the WTG on the floating platform is through the use of a ducted fan mechanism which has been used in tank testing in the EOLIA project co-ordinated by Acciona Energia, Spain. Information regarding such a system has not been found and therefore a study is being carried out in parallel to this thesis to investigate the feasibility of such a system. Essentially the system would be comprised of a ducted axial fan capable of producing thrust equivalent to the scaled thrust curve of the NREL Reference Turbine, connected to a load cell to monitor the instantaneous value of the thrust delivered. This unit would then be mounted on an appropriately scaled tower. The fan would be connected to a micro-controller such that a time series of voltage/current may be directed into the fan through a power supply to deliver time varying thrust based on the velocity at the hub. The system would be calibrated in the fully fixed conditions to determine the relationship between voltage/current input, rotational speed of the fan and the thrust delivered to the load cell. This option will apply the required thrust to the platform without the need for wind generation and also provide sufficient control to deliver a time varying thrust signal for simulation of wind spectra.

### 2.3.2.2 Numerical Simulation

The concept of a hybrid wave-wind energy concept in this thesis involves the design of a suitable floating platform for the WTG while integrating a WEC technology to that platform. The design and operation of the WTG itself is not considered in this work. For this reason, the review of the numerical tools focusses on the tools for the simulation of the floater but also includes reference to the simulation tools for the WTG.

Reference [62] described the development of a time domain numerical model for the analysis of floating WTGs, Fatigue, Aerodynamics, Structures and Turbulence (FAST). The code incorporates an aerodynamics subroutine package, AeroDyn, and a hydrodynamics subroutine package, HydroDyn. HydroDyn is used to calculate the hydrodynamic forces in FAST using linear wave theory. The hydrodynamic loading includes contributions from linear hydrostatic restoring, nonlinear viscous drag from Morison's equation, added mass and damping contributions from linear wave radiation and incident wave excitation from linear wave diffraction [63]. HydroDyn requires hydrodynamic coefficients from WAMIT as inputs. The mooring line loads are calculated using a quasi-static system which accounts for the apparent weight of the line, the elastic stretching and friction at the sea bed.

Reference [64] coupled FAST and AeroDyn with Charm3D hydrodynamic code. The first and second-order hydrodynamic coefficients are calculated in the frequency

domain by an external solver, WAMIT in this case. In the time domain, similar loading and nonlinearities are included as in [62].

Reference [65] again coupled FAST and AeroDyn with TimeFloat (time domain code for analysis for the WindFloat platform) for the analysis of the WindFloat floating WTG. The hydrodynamic coefficients are calculated in the frequency domain by WAMIT and passed to TimeFloat for use in the time domain solver where aerodynamic, hydrodynamic and mooring system forces on the system are calculated simultaneously.

Reference [66] extended the SIMO code developed by MARINTEK for the simulation of floating wind turbines through the addition of an external module for calculation of the rotor aerodynamic forces. Reference [67] also coupled SIMO with RIFLEX, a nonlinear FEM code for the analysis of slender marine bodies such as risers and mooring lines. [68] and [69] coupled SIMO/RIFLEX with HAWC2 developed by Risoe National Laboratory.

More detail regarding the coupling of various numerical solvers for the simulation of floating WTGs may be found in the review by [70] and [71].

### 2.3.2.3 Offshore Wind Turbines

The wind industry in the early 1990's quickly converged on a single configuration of wind turbine in the horizontal axis wind turbine (HAWT) design. This type was installed in large number onshore in Sweden, Germany and Denmark. Since then, the HAWT configuration has enjoyed majority market share over its counterpart, the vertical axis wind turbine (VAWT). The VAWT design is again becoming of interest to offshore technology developers as the mass distribution is more favourable for floating foundations. This is however, still an emerging technology and to provide some level of certainty to a hybrid wind-wave device, the HAWT system has been chosen for use in this thesis. This section provides a brief introduction to the three main turbines currently available on the commercial market for use in offshore conditions.

#### 2.3.2.3.1 Vestas V90 3.0MW

The Vestas V90 3.0MW offshore turbine, illustrated in Figure 2-43, has over 1300 units installed since launch as illustrated in Figure 1-3. The turbine proved popular in the early Round 1 UK wind farms being installed in five of the nine farms [72]. The turbine however did not keep up with the competing Siemens SWT-3.6-120 turbine due largely to its smaller capacity and market share is now standing at 36%. The turbine specifications are tabulated in Table 2-1.

**Table 2-1: Vestas V90 3.0MW Turbine Specifications**

| Turbine Characteristic | Value |
|---|---|
| Power Regulation | Pitch Regulated w/ Variable Speed |
| Rated Power | 3000 kW |
| Rotor Diameter | 90 m |
| Cut-In, Rated and Cut-Out Wind Speeds | 3.5, 15, 25 m/s |
| Nominal and Operating Range Revs. | 16.1, 8.6-18.4 rpm |
| Airbrake | Full blade feathering w/ 3 pitch cylinders |
| Electrical Frequency and Generator Type | 50/60 Hz 4 pole asynchronous w/ variable speed |
| Gearbox Type | 3 Stage Planetary and 1 Stage Helical |
| Blade Length and Mass | 44m, 6.7 t |
| Nacelle Mass | 22 t |
| Tower Specifications | Site Specific Design |



**Figure 2-43: The Vestas V90 3.0MW Turbine**

### 2.3.2.3.2 Siemens SWT-3.6-120 3.6MW

The Siemens SWT-3.6-120 3.6MW, illustrated in Figure 2-44, turbine is currently the most successful turbine in the offshore sector as illustrated in Figure 1-3. The turbine boasts over 2000 installations up to 2012 with an impressive 53% of the market. The turbine class faces challenges for its continued success as larger turbines are finding favour amongst developers for deeper water sites. The turbine specifications are tabulated in Table 2-2.

**Table 2-2: Siemens SWT-3.6-120 3.6MW Turbine Specifications**

| Turbine Characteristic | Value |
|---|---|
| Power Regulation | Pitch Regulated w/ Variable Speed |
| Rated Power | 3600 kW |
| Rotor Diameter | 120 m |
| Cut-In, Rated and Cut-Out Wind Speeds | 3, 12.5, 25 m/s |
| Operating Range Revs. | 5-13 rpm |
| Airbrake | Full span pitching |
| Generator Type | Asynchronous |
| Gearbox Type | 3 Stage Planetary/Helical |
| Blade Length | 58.5 m |
| Nacelle Mass | 125 t |
| Tower Specifications | Site Specific Design |

2.3.2.3.3   NREL 5MW Reference Turbine

NREL 5MW reference turbine is based largely on the RE Power 5M machine illustrated in Figure 2-45. The 5M is the more successful of the larger machines on the market with 5% market share and 182 installations up to 2012. The current trend is towards 5-7/8MW turbines and the continued success of the model is largely dependent on the market take up of the Siemens 6MW offshore turbine. The specifications of the NREL reference 5MW turbine are tabulated in Table 2-3.



**Figure 2-44: The Siemens SWT-3.6-120 3.6MW Turbine**

68

**Table 2-3: NREL 5.0MW Reference Turbine Specification**

| Turbine Characteristic | Value |
|---|---|
| Power Regulation | Pitch Regulated w/ Variable Speed |
| Rated Power | 5000 kW |
| Rotor Diameter | 126 m |
| Cut-In, Rated and Cut-Out Wind Speeds | 3, 11.4, 25 m/s |
| Operating Range Revs. | 6.9-12.1 rpm |
| Airbrake | Collective Pitch |
| Generator Type | Asynchronous |
| Gearbox Type | Multiple-Stage |
| Blade Length | 61.5 m |
| Nacelle Mass | 240 t |
| Tower Height and Specifications | 87.6 m, 347 t |



**Figure 2-45: The RE Power 5M 5.0MW Turbine**

### 2.3.2.4 Monopile Fixed Foundation

As illustrated in Figure 1-6, the monopile foundation has the greatest market share in terms of installed offshore wind turbine foundations at 75%. The foundation comprises two individual parts, namely the monopile itself and the transition piece (TP) illustrated in Figure 2-46. The monopile is installed initially by a large installation vessel using a hammer. This operation typically takes between 4-8 hours depending on the subsea soil conditions. Following this, the TP is installed by the same vessel or by a slightly smaller vessel as the mass of the TP is generally considerably less than the monopile. The TP acts as the connection between the monopile and the wind turbine tower and thus allows any eccentricities or angular

deviations in the monopile foundation orientation following installation to be corrected before attachment of the wind turbine tower. This is achieved by using wedges between the outer pile surface and inner TP surface and filling the void with grout. This foundation has all the typical characteristics required for use in a commercial industry including,

- Simplicity
- Robustness
- Mass production ability
- Low cost
- Relatively simple and quick installation
- Multiple choices for transport to installation site etc.



**Figure 2-46: A typical monopile foundation**

The foundation does however embody some disadvantages in its design. Most notably the attachment of the TP does not provide a lot of resistance to yaw movement induced by the yaw mechanism in the wind turbine nacelle. The grouted connection can fail and can inflict significant financial losses in the process of correcting the failure. In recent times, the use of shear keys has been promoted with the continued use of grout as well as tapering the top and bottom of the monopile and TP respectively. Both these modifications provide a fail-safe in the event of grout bond failure. If this happens, the shear keys are activated to resist movements in the TP and the conical sections allow recompression of the grouted connection under the self weight of the TP and wind turbine against the monopile. DNV has initiated a joint industry project looking into design practices for grouted connections with shear keys.

**2.3.2.5    Gravity Based Fixed Foundation**

From Figure 1-6, the foundation with the second largest market share following the monopile is the gravity based structure (GBS). The GBS found favour amongst developers in the early stages of development of offshore wind, being used in farms such as Middelgrunden in Denmark and Nysted in Denmark. These farms are very close to shore in depths of <10m and therefore have relatively small and light foundations. The GBS is typically manufactured from RC in a conical shape. The overall dimensions of the foundation are determined from global structural analysis ensuring resistance to soil bearing failure, sliding and overturning. The foundation, as the name suggests, relies on its self-weight to resist hydrodynamic and aerodynamic loading from waves and wind acting on the foundation and turbine respectively. The installation process for this foundation type is an area undergoing significant research currently with the desire that the reliance on large heavy lift vessels may be diminished through the design of a self-installing system. This would require the foundation to be watertight during tow-out as well as hydrostatically stable either with or without the turbine installed. The seabed does require preparation for this foundation as settlement of the foundation may cause failure and result in it being deemed unsafe. Therefore in the case of sand and clay seabed, dredging must take place to remove some of this material to be replaced with rock. Seabed surveys must then take place to ensure that a sufficiently level platform has been made to sit the foundation. Figure 2-48 below illustrates the final seabed configuration of a foundation location at the Thornton Bank offshore wind farm, which utilised a conical GBS system illustrated in Figure 2-47.



**Figure 2-47: Typical GBS Foundation**
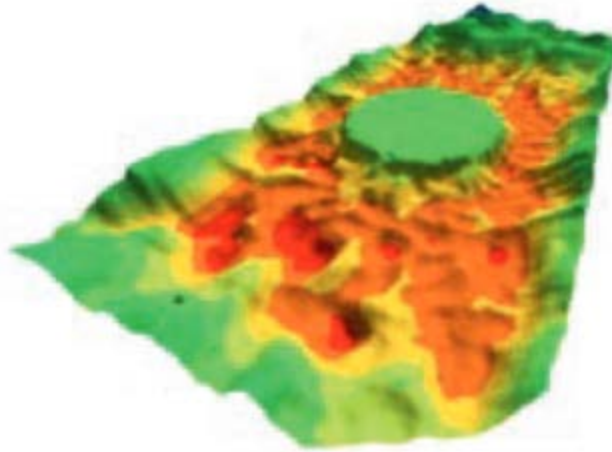
**Figure 2-48: Seabed Configuration for GBS Installation**

The design of the GBS is different from the monopile as not only does the process require a global analysis approach, but also a localised design based on hydrodynamic and hydrostatic pressures on the foundation during service and installation if it is the "float-out and sink" type installation. This is the type of foundation which will be investigated here. A number of companies are actively marketing their solution similar to this for water depths between 35-60m, including Arup in conjunction with Costain and Hochteif and BAM in conjunction with Van Oord. These systems are similar and employ the "float-out and sink" methodology.

### 2.3.2.6 Floating Wind Concepts

The development of floating offshore wind systems has experienced substantial, rigorous development over the last 5-10 years. This is most certainly due to the vast expansion of the fixed offshore wind industry throughout Europe. The turbines systems themselves have been progressed quickly from onshore small systems to much larger marinised offshore turbine systems. These have up to now been mounted on fixed foundations as illustrated in Chapter 1. Following the success of the industry, further developments in the manufacture of larger turbines and sites farther offshore in deeper waters, initiated the race for development of floating systems. Large utility companies entered the market such as Statoil Hydro in Norway. The floating wind industry has enjoyed significant development as a result, however, it is perhaps going in the same direction as the wave energy industry now. Almost on a continuous basis, new concepts are developed which are based on the typical oil and gas floating system foundations like spars, semi-submersibles and tension leg platforms. As a result, funding again becomes an issue for small technology development companies and it is only large companies such as Statoil that can maintain the required investment for continued development. The following is an overview of some concepts that have progressed through the Development Protocol, which is to an extent relaxed for floating wind systems as typical oil and gas standards can apply as the foundations are simply smaller rigs and storage facilities.

### 2.3.2.7 Example Floating Wind Turbine Foundations

2.3.2.7.1 Semi-submersible Floating Foundation

The semi-submersible floating foundation concept is primarily being driven by Principle Power Inc. in the USA. The concept under development is the Windfloat concept, a three column semi-submersible platform with large heave or water entrapment plates attached to the columns underwater. The concept was originally created and designed for marginal oil and gas fields by Marine Innovation and Technology (MI&T) in 2003 following proof of concept tank testing. The development of the Minifloat platform is outlined in [73]. Two patents for the "Minifloat" concept were lodged by MI&T in 2003 and 2007 until Principle Power Inc. exclusively licensed the "Windfloat" technology from MI&T in 2008. In 2009, Principle Power bought outright the intellectual property (IP) for the Windfloat concept from MI&T. Development of the concept has continued through dedicated tank testing at UC Berkeley in 2009 and numerical hydrodynamic and structural analysis as detailed in [65] and [60]. An illustration of both the Minifloat and Windfloat concepts is shown in Figure 2-49 and Figure 2-50.
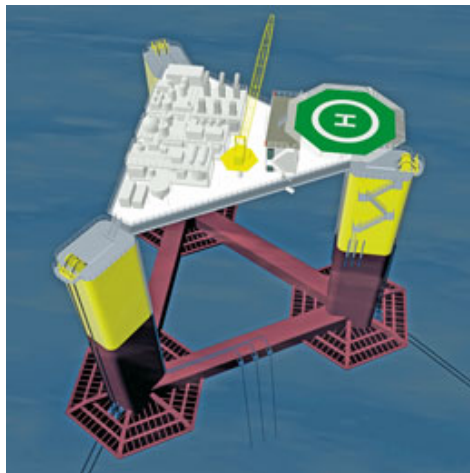


**Figure 2-49: MI&T Minifloat Concept**

**Figure 2-50: MI&T Original Windfloat Concept**

This concept has undergone significant analysis and design throughout the concept development protocol and has now reached TRL 5-6, scaled deployment at sea. In early 2011, construction of the floating foundation began in the Lisnave facility near Setubal in Portugal as illustrated in Figure 2-51. The illustration shows the two bow columns with the turbine installed on the stern column. The water entrapment or heave plates are clearly visible on the bottoms of the two bow columns. The structure is a space frame type structure with the main columns connected by a tubular truss configuration.



**Figure 2-51: Windfloat prototype under construction in 2011 in Setubal, Portugal**

Following completion of the foundation, the 2.0MW Vestas V80 HAWT turbine was installed portside and commissioned. The dry dock was filled and the hydrostatic certification of the platform was carried out prior to tow-out to the deployment site. The deployment site at Aguçadoura is 400km away from Setubal. A single anchor handling tug (AHT), which was used for the mooring system installation, was used

to tow the structure (Figure 2-52) to the site and connect to the pre-installed moorings.



**Figure 2-52: Towing of the Windfloat from Setubal by the AHT**

The installation was completed in November 2011 ahead of schedule and the machine has been operating since. This project confirmed that the installation of floating foundations could be significantly simpler than conventional fixed foundation concepts.

2.3.2.7.2  Spar Floating Foundation

The first spar floating foundation used for deployment of offshore wind was developed by Statoil Hydro in Norway. The concept underwent the necessary stages of development prior to the design and deployment of a multi-MegaWatt prototype off the coast of Karmoy in Norway. The selection of the spar foundation by Statoil was primarily driven by the experience gained with these structures in the offshore oil and gas activities of the company. The deep draft structure suits the topography of the Norwegian coastline as it may be constructed and "upended" close to shore in a fjord. The deep draft will not suit many coastlines unless further solutions to the deployment of the foundation are designed. However, due to its deep draft, the foundation exhibits favourable motion characteristics in heave and pitch modes as illustrated in [74] and [75]. The typical wave period at heave and pitch resonance is far beyond the typical wave energy range. Similar to the monopile foundation in a way, the foundation suffers from very little yaw inertia to resist the yaw motion of the nacelle of the turbine when wind-vaning. The mooring system has been designed using a "Delta Line" configuration to provide the floater with resistance to yaw motion. Figure 2-53 illustrates the concept of the spar floater and the delta mooring lines.
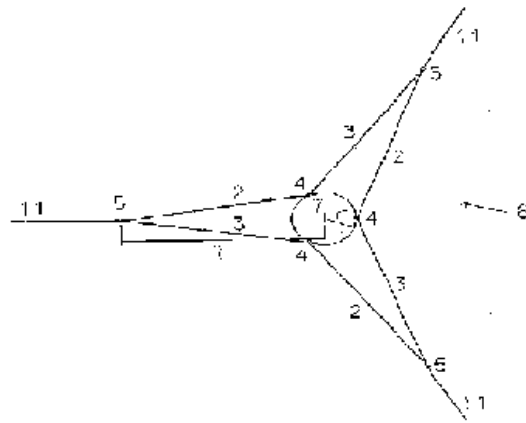
**Figure 2-53: The Spar Floating Wind Turbine and Delta Mooring Line Concept ( [76], [77])**

The foundation, due to its deep draft, will experience significant hydrostatic pressures and this may indeed be the design pressure for sizing steel plates and stiffeners. As well as this the foundation will undergo a number of operations and lifts during construction, transportation and deployment. Any one of these load cases may be the governing design case and all need to be considered in a detailed design situation. Figure 2-54 shows the foundation in preparation for tow-out to the upending site. Figure 2-55 shows the foundation nearing the end of the upending procedure. Figure 2-56 shows the installation of the wind turbine on the floater while Figure 2-57shows the completed floating wind turbine concept following final tow-out to the deployment site and connection to the mooring lines.



**Figure 2-54: Hywind foundation during tow-out**

**Figure 2-55: Hywind foundation during "upending" procedure**



**Figure 2-56: Hywind foundation during wind turbine installation**

**Figure 2-57: Hywind foundation following final installation at Karmoy**

The figures illustrate the number of complex steps associated with the installation of the spar floating wind turbine concept. This then makes for a risky and expensive process. Consider the scenario whereby the deployment site is off the west coast of Ireland. The point at which the upending process may take place is actually at the installation site in deep water. This may in fact be a prohibitive technical concern given the nature of the resource in that location. For widespread deployment of the spar concept, an alternative means of installation is critical to its success.

### 2.3.3 Hybrid Wave and Wind Energy Technology Overview

The following section is a brief review of the existing combined wind and wave energy hybrid devices currently under development by technology developers worldwide. This forms the basis for proposing new configurations of hybrids for consideration in this thesis.

### 2.3.3.1 Wave Dragon and Wind Turbines
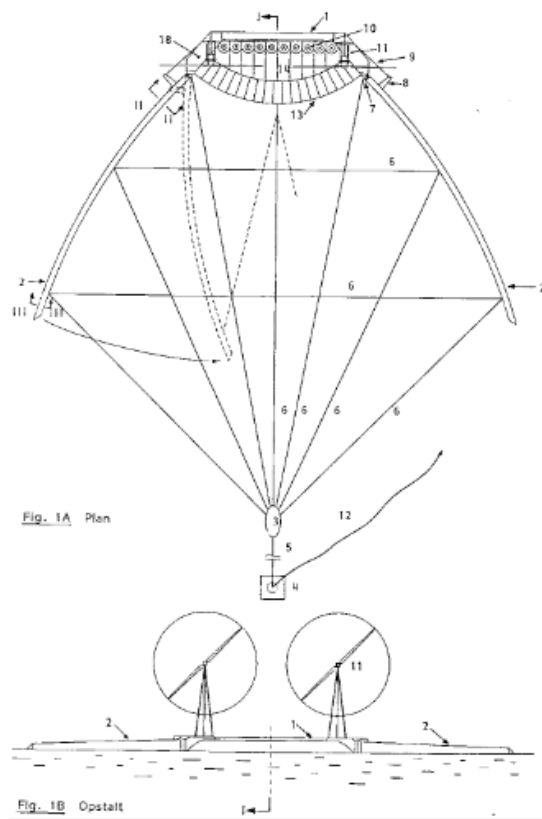


Figure 2-58: Wave Dragon and Wind Turbines Illustration [58]

In its original 1996 patent application, Wave Dragon included the sketch illustrated in Figure 2-58 showing the inclusion of two wind turbines on the Wave Dragon hull. The continued development of the hull did not include any further analysis of the attachment of WT's.

### 2.3.3.2 Floating Power Plant (FPP) – Poseidon

FPP was formed in 2004 and secured all IP rights for the platform concept and design from inventor Hans Marius Pederson in 2007. The concept has been developed through various tank testing campaigns at varying scales from 1998-2002. In 2007, the 37m 1:6 scale hull was constructed and deployed at DONG Energy's offshore turbine park in Onsevig, Denmark in 2008. This was the Phase 1 stage of sea trials for the Poseidon 37 device which focussed on the characterisation of the WEC system. In 2009, Risø-DTU confirmed the stability of the platform for the attachment of wind turbines. Phase 2 of the sea trials was carried out in 2009/2010 with the installation of the platform with three 2-bladed down-wind turbines rated at 11kW each as illustrated in Figure 2-59. The test phase was focussed on further confirming the hydrodynamic efficiency and PTO performance of the WECs while now also considering the influence of the turbines on exported power. [78] reported that the turbines acted to stabilise the platform in larger wave conditions in pitch motion, while in smaller wave conditions they acted to increase motion in both pitch and roll. The loads on the WT tower increase with increasing platform motion as

anticipated but the blade loads were largely unaffected. Phase 3 testing began in September 2012 and was deployed to analyse the performance again of combined wind and wave energy production, but now the WECs has a newly designed PTO system. The PTO was redesigned to allow each WEC buoy to generate power independently through a closed hydraulic circuit. This system was designed in cooperation with Siemens and others. Phase 4 testing began in September 2013 and was deployed to monitor the performance of a new condition monitoring system and further validate reliable power production from wind and waves.

The hydrodynamic performance of the Poseidon WEC system is reported in [79] where it states that the system achieves ~27% hydrodynamic efficiency. Assuming an incident resource of ~2.5kW/m and a PTO efficiency of 65%, the WEC would produce on average 16kW of wave power. The wind turbines may produce ~4kW of power assuming a load factor of ~35%. The total output on average is then 20kW for a 280t structure.



**Figure 2-59: FPP Poseidon 37 1:6 scale device at sea**

### 2.3.3.3 Ocean Wave and Wind Energy (OWWE)
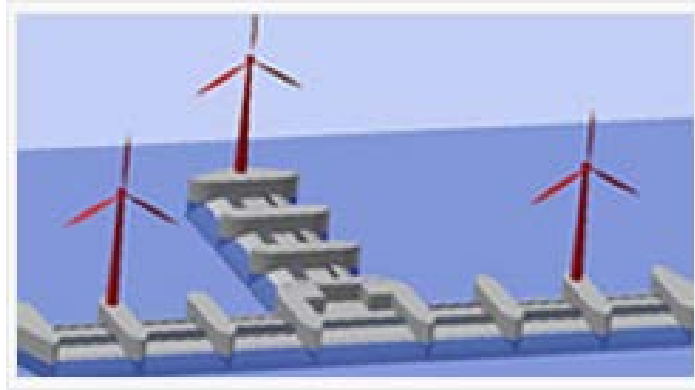


**Figure 2-60: OWWE 2Wave1Wind Concept**
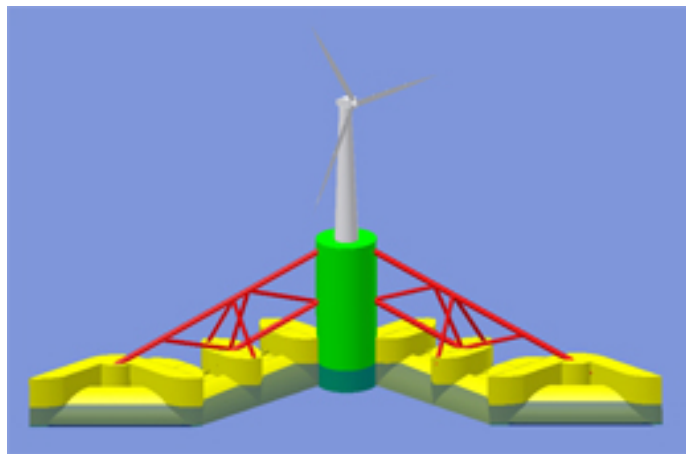


**Figure 2-61: OWWE Combined Overtopping and WT Concept**
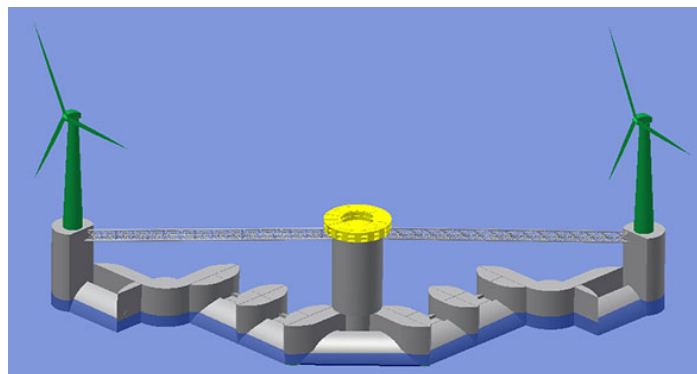


**Figure 2-62: OWWE 2Wave1Wind Concept Redesign**

The Norwegian company, Ocean Wave and Wind Energy (OWWE Ltd.), is currently developing a concept similar in style to the Wave Dragon overtopping WEC. The OWWE 2Wave1Wind concept is illustrated in Figure 2-60 and shows the large multiple overtopping sections joined together in a "T" formation with three WTs. The overtopping concept is slightly different from the Wave Dragon type. While the Wave Dragon uses compressed air in air pockets under the hull to raise and lower the freeboard of the device, the OWWE concept uses a variable freeboard ramp which is documented in a patent from 2005. The ramp level is controlled by the overtopping

rate and reservoir size. This allows the system to be a self-regulating system, however sealing of the moveable ramp sides is a concern. The second WEC incorporated into the structure is a form of PA which pumps water. The original concept was to be 600m in width, one of the largest known devices for wave energy. The company website states that one 600m unit can produce 1TWh of energy per annum in a 40kW/m resource. Assuming the WTs are 3.6MW turbines at a load factor of 35%, the overtopping WEC, assuming an active absorbing dimension of 1800m, would have a CWR of ~20% assuming a PTO efficiency of 52%. This is on the higher end of the scale proposed by [17], but the new freeboard design for overtopping regulation is expected to perform better than the Wave Dragon system. A newer concept illustration was shown on [80] as illustrated in Figure 2-61. The unit shown is 300m in width as is claimed to be capable of withstanding severe storm conditions. A further reconfiguration of the 2Wave1Wind concept was published in [80] as illustrated in Figure 2-62.

### 2.3.3.4    Green Ocean Energy - Wave Treader
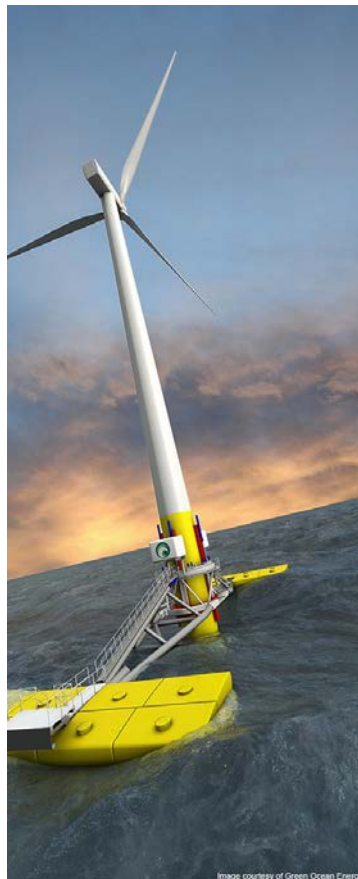


**Figure 2-63: Green Ocean Energy Wave Treader on a WT Illustration**

The Scottish company Green Ocean Energy founded in 2005 and based in Aberdeen, is currently developing a WEC device which can be mounted onto existing offshore wind platforms as illustrated in Figure 2-63. The device is based on the ATN class with a fore and aft float each driving a hydraulic PTO. Little is known in terms of the specifications of the device. Assuming that the floats are approximately 20m in

width, and that the CWR is 17% [17] for pitching wave activated bodies, in a 20kW/m site the Wave Treader might produce ~88kW assuming a PTO efficiency of 65%. And assuming a load factor of 30%, the machine would be rated at ~300kW. The concept is very much at the lower end of the scale of a hybrid that might be considered "worthwhile".

### 2.3.3.5    Pelagic Power – W2Power



**Figure 2-64: Pelagic Power W2Power Concept**

Pelagic Power is a Norwegian based company developing a combined wind and wave energy platform for deep water. Unlike any other platform, two "counter rotating" WTs are mounted on a light semi-submersible platform as illustrated in Figure 2-64. The company claims the counter rotating nature of the turbine reduces the wake interference from the WTs. Furthermore the WTGs do not have an active yaw control mechanism. The semi-sub has a turret mooring system in the bow column allowing full rotation about that point. The ability of the wind loads to shift the platform into the wind against the waves is questionable. The WTGs used are two 3.6MW WTGs which would provide a maximum of ~1.2MN thrust on the hubs at rated power. Using Morison's Equation for estimation of hydrodynamic loads on the hull, even a $H_s$ of 0.5m and $T_p$ of 2.5s provides a 3.6MN load on the hull which will try to streamline itself based on wave loading. The WECs are an array of 18 small diameter buoys, which have a CWR of ~9% [17]. The PTO is linked to all buoys which drive a closed loop sea water hydraulic pump system through a Pelton Wheel turbine. In a 30kW/m site, the WECs would produce approximately 158kW assuming a PTO efficiency of 65%, and be rated at ~500kW.

### 2.3.3.6 Wavestar - WindWaveStar
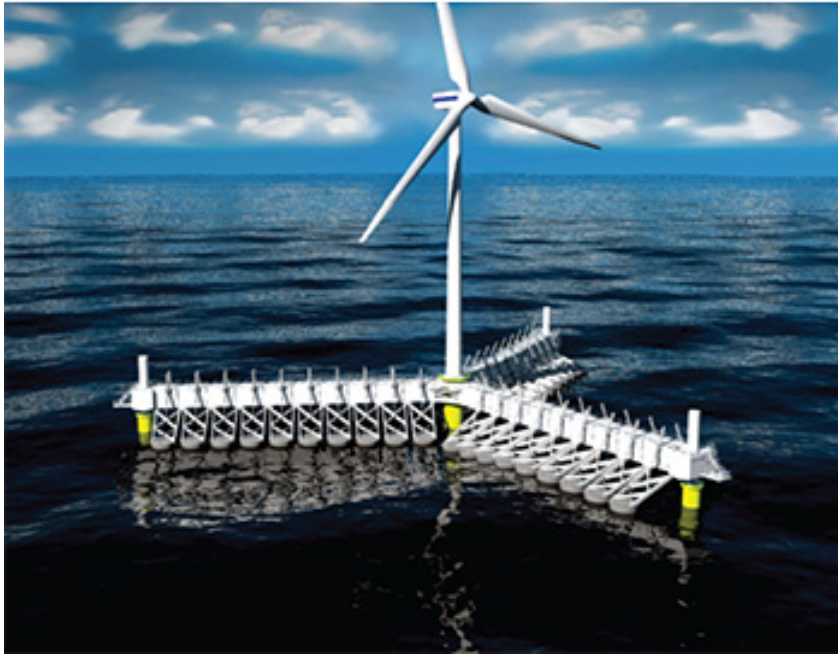


**Figure 2-65: Wavestar Combined Concept**

The Wavestar WEC has been discussed in detail in Chapter 2 and is shown in Figure 2-65 surrounding a fixed WTG. DONG Energy and Wavestar have entered into an agreement to install a Wavestar machine at the Horns Rev 1 wind farm in Denmark, signalling the first co-operation between wind and wave energy developer. Initially the Wavestar will share space with the wind farm, but could potentially develop to the concept illustrated above.

### 2.3.4 Power Take-Off (PTO) System Design and Modelling

This section describes the various PTO systems proposed for use in WECs and studies which have investigated each system. Typically the effects of PTOs are accounted for in hydrodynamic models or physical models by a mathematical representation of the damping mechanism or an equivalent physical system which is most applicable to the ultimate PTO system to be used. The outputs from the hydrodynamic and physical models, such as stroke and pressure or velocity and pressure, act as inputs to the detailed PTO system model. This section outlines the various PTO systems and cites studies which have investigated in detail the characteristics of those systems. For the purposes of this thesis, a preliminary failure modes and effects analysis (FMEA) is carried out for each system on a high level as this will be a significant contributing element to the LCCA model.

### 2.3.4.1 Hydraulic PTO

A conventional hydraulic system consists of hydraulic cylinders, control manifolds, motors, pipelines and accumulators. The operation of a generic hydraulic PTO requires the prime mover (e.g. buoy etc.) to drive the hydraulic cylinders which pump the hydraulic fluid, via the control manifold, into high-pressure accumulators

for short term energy storage. Hydraulic motors use the smooth supply of high-pressure fluid from the accumulators to drive grid-connected electric generators. Many WECs have incorporated this PTO system which in general, delivers a high efficiency transmission of mechanical power to electrical power. The hydraulic system suits the nature of wave power in that waves impose large forces at low speeds, and hydraulic systems with pressures of 350-500 bar, are suitable to absorb energy under this regime. In comparison to other types of PTO mechanisms, hydraulic machinery can supply much larger net forces to the prime mover, which makes its size and weight much smaller and lighter. The use of hydraulic systems in WECs was proposed quite early [81], but significant research into the system was not carried out until the advent of the Pelamis device in the 1990's [82]. Further work investigated the use of hydraulic systems for point absorber devices [83], [84], [85], [86]. The disadvantage of the hydraulic system is the number of components required in the transmission of mechanical power to the hydraulic fluid and to the hydraulic motors. This system is prone to leaks, corrosion of cylinders and rotational/translational connections/bearings and failure of pipelines under the extreme pressures experienced by the system in higher wave conditions. More recent studies have investigated the effects of the various components on the transmission of power through the system [87], [88].

### 2.3.4.2 Air Turbine PTO

The air turbine is probably the simplest PTO system amongst the options for WECs, with the exception that it is required to operate in reciprocating or bi-directional flows. The system is composed of a rotor with characteristics matched to the nature of the air flow in the OWC chamber, a main shaft linking the rotor to an optional flywheel for short-term inertial energy storage to an electric generator. The shaft is supported by axial and thrust bearings depending on the orientation and connection of the turbine casing to the OWC chamber. There are two main categories, the Wells turbine [89] and the self-rectifying impulse turbine [90].

The development of the Wells turbine initially included investigations into the geometric variables, blade profile and number of rotor planes [91] and also the use of guide vanes [92]. Wells turbines with standard NACA blade profiles have been used in the 75kW Islay plant [93], [94]. The Wells turbine system is simple and robust and consists of one moving part, the rotor. However, a disadvantage of the Wells turbine is the short range of flow rates within which the rotor can provide high efficiencies as well as the fact that the turbine is not self-starting and requires input power to initiate rotation. In flow rates below the optimum range the rotor experiences negative torque, while above the optimum flow rate range the rotor experiences aerodynamic stall. While stall is regarded a disadvantage in operational conditions, in survival conditions this can be seen as an advantage as the turbine does not reach a run-away speed and therefore require a mechanical brake.

The development of the impulse turbine has focussed on the development of the guide vane systems and whether these should be fixed, pitching or even self-pitching

[95]. The impulse turbine is slightly more complex than the Wells turbine but does deliver a wider band of operational flow rates at higher efficiencies. The impulse turbine is also self-starting, therefore does not require input power to initiate rotation. The impulse turbine however, does not experience stall. This is certainly an advantage in operational conditions, but is a significant disadvantage in survival conditions as a mechanical brake is required to control the rotational speed of the turbine. Should the mechanical brake fail, the rotor can reach run-away speed and cause damage to the whole PTO system.

In both instances, for each turbine, a further safety mechanism can be incorporated into the OWC chamber – a pressure relief valve (PRV). These can be fast or slow acting valves and essentially release air from the chamber when plenum pressure is greater than the safe threshold.

### 2.3.4.3   Hydro Turbine PTO

Hydro-turbines have been used in many applications worldwide for hydro-electric power plants of varying head ranges. The turbine types used have included Pelton, Francis and Kaplan turbine rotors. Unlike the air turbine, the hydro-turbine is required to operate only in uni-directional flows. The primary challenge with the use of hydro-turbines in WECs is that they are required to operate in low head ranges. The hydro-turbines have been used in conjunction with overtopping type WECs such as the Wave Dragon. The turbine head in this WEC is between 1.0 and 4.0m, and moreover, there is a significant variation in overtopping rates in random seas [96]. In the high head range, speed control of the hydro turbine is vital in achieving high turbine efficiencies. With such constraints on the operation of the WEC, the Kaplan turbine has been deemed the only suitable choice of rotor. In order to adapt to the varying operating conditions mentioned, the double regulated Kaplan turbine might be considered, where both guide vanes and runner blades are adjustable. The efficiency of such a system ranges between 0.6 and 0.9 for the aforementioned head range [97]. The issue with such a system is the maintenance effort required due to the large number of submerged moving parts. For this reason, options such as the Kaplan turbines with fixed guide vanes, fixed runner blades and unregulated systems are considered. A full LCCA analysis would be required to determine the most feasible option. As well as the specifications of the individual turbines, another consideration is the number of turbines to use within the reservoir. In the Wave Dragon WEC, it is proposed to use 16-24 small turbines resulting in several advantages such as redundancy in the design, as well as CAPEX and control considerations. Flow rates may be optimised by shutting turbines down and maintain a high overall efficiency. Smaller turbines also have higher speeds allowing off-the-shelf generators to be used.

### 2.3.4.4   Direct Drive – Linear Generator PTO

Direct drive PTO systems in wave energy conversion are similar in principle to that currently in use in the wind energy industry. The prime mover is linked directly to the generator whereby the prime mover may have magnets connected to the shaft

and oscillates through the generator coils under the influence of the incident waves. With the continued progression of permanent magnet materials and power electronics, direct drive generators have appeared to become one of the most popular PTO systems for point absorber WECs such as the OPT as described in Chapter 2 [98], [99], [100]. There exists three main classes of linear machines investigated for wave energy conversion, the longitudinal flux permanent magnet machine (LFPM), traverse flux permanent magnet machine (TFPM) and the tubular air cored permanent magnet machine (TAPM) [101]. The generator is considered as a damper, and as such the energy absorbed depends on the generator. Various approaches may be used to increase the absorption by the WEC and these may vary from active control or tuning of the resonance frequency to optimise energy absorption or a passive system acting far from resonance. Parameters of particular importance for design of direct drive PTOs are the peak-to-average power output ratio and the achievable load factor.

### 2.3.4.5   Typical PTO Efficiencies

Reference [79] carried out an investigation into the WEC types under development by Danish developers. The study assessed the main PTO types mentioned above and attributed an efficiency to the main constituent components of the PTOs. Table 2-4 outlines the results of the study.

**Table 2-4: Typical PTO Efficiencies**

| PTO | Direct | Air | Water | Hydraulics | Wave Dragon |
|---|---|---|---|---|---|
| Reservoir | | | | | 0.64 |
| Pumps | | | | 0.9 | |
| Turbine | | 0.6 | 0.9 | 0.85 | 0.9 |
| Gears | 0.95 | | | | |
| Generator | 0.9 | 0.9 | 0.9 | 0.85 | 0.9 |
| Total | **0.85** | **0.54** | **0.81** | **0.65** | **0.52** |

The average PTO efficiencies quoted above will be used in the preliminary assessments of various WEC concepts as well as the development of electrical power matrices of new concepts created in Chapter 4.

### 2.3.5   Structural Analysis and Design

The structural modelling of WECs is a rather complicated process through which few devices have undergone in a detailed manner. There are a number of reasons for this, primarily the fact that numerical modelling of survival conditions is beyond the state of the art in numerical modelling methods used in the estimation of power absorption. BIEM codes rely on the assumption of linear wave theory, i.e. small amplitude waves relative to the wavelength. Survival conditions typically involve highly nonlinear wave forms and the reaction of the device following slamming and

splashing events. Emerging numerical techniques including CFD and meshless methods may provide the answer to this. In the past and for the near future, the analysis of device responses and loads in survival conditions have been carried out in physical model tests at a scale typically larger than that used in functionality tests. This process is time consuming and quite expensive due to the requirement for large basins to accommodate large models etc. This section will investigate the possible simplified methods of assessment of the structural loads in WECs from a number of perspectives and determine the most appropriate governing loads to use in the estimation of structural materials for its construction.

### 2.3.5.1 Breaking Wave Loads Estimations and Local Strength Design

One of the primary concerns for many WEC structures is the hydrodynamic pressures imposed on the structure during breaking wave events. While the occurrence of these events is typically seldom, the structure nonetheless must be designed to resist the large impact loads. One of the primary challenges faced by designers of conceptual structures, is the estimation of structural materials required for survivability of offshore structures. In many cases, this estimate is guided by experience of similar structures etc., however in the case of innovative MRE platforms, simplified estimates of the hydrodynamic pressures imposed on the structure are required, typically referred to as "basic scantlings". Reference [102] suggests a formula for the estimation of breaking wave loads on vertical piles in Equation 2-1,

$$F_{br} = \frac{1}{2} C_{db} \rho g D H_b^2 \qquad \text{Equation 2-1}$$

where $F_{br}$ is the breaking wave force acting at the stillwater line (N), $C_{db}$ is the drag coefficient, $\rho$ is the density of seawater ($kg/m^3$), g is the acceleration due to gravity ($m/s^2$), D is the pile diameter (m) and $H_b$ is the breaking wave height (m). The force estimated by this formula is a concentrated force acting at the stillwater line. To estimate the thickness of steel plate required for a small WEC, this force would be distributed over an area of the WEC structure as shown in Equation 2-2.

$$p = \frac{F_{br}}{A} \qquad \text{Equation 2-2}$$

where p is the hydrodynamic pressure imposed on the WEC structure ($N/m^2$) and A is the area affected by the breaking wave ($m^2$). Furthermore, if numerical modelling, even in the frequency domain, is carried out, the linearised response amplitude operator (RAO) of hydrodynamic pressure on each panel of the discretised wetted hull is produced. This can also be used to produce a local design of the hull.

The hydrodynamic pressure estimated from these methods may be used as an input into Equation 2-3 from [103] Subsection 6,

$$t = \frac{15.8 \, s \, k_a \, k_r \, \sqrt{p}}{\sqrt{\sigma_p k_p}} + t_k \qquad\qquad \textbf{Equation 2-3}$$

where t is the estimated plate thickness (mm), s is the stiffner spacing (mm), p is the hydrodynamic pressure ($kN/m^2$), $k_a$ is an aspect ratio, $k_p$ represents the long side (stiffner) boundary condition, $k_r$ is a curvature factor, $\sigma_p$ is the nominal yield based allowable stress ($kN/m^2$) and $t_k$ is the added plate thickness to resist corrosion (mm). For a conservative estimate, $k_a$, $k_r$ and $k_p$ may be assumed to be one, while assuming a suitable corrosion prevention system is in place on the structure, $t_k$ may be assumed to be zero. This plate thickness design method assumes that, e.g. column diameters are greater than 12m. Smaller members would most likely be ring stiffened and the equation is inapplicable. To estimate the stiffner mass, reference [103] Subsection 6 uses Equation 2-4,

$$Z = \frac{1000 \, l^2 \, s \, p}{m \, \sigma_p \, k_s} + Z_k \qquad\qquad \textbf{Equation 2-4}$$

where Z is the section modulus ($cm^3$), l is the plate length (m), s is the stiffner spacing (mm), p is the hydrodynamic pressure ($kN/m^2$), m is the denominator of the beam equation, $\sigma_p$ is the nominal yield based allowable stress ($kN/m^2$), $k_s$ is a stiffner factor and $Z_k$ is the additional steel to account for corrosion. This equation is coupled with a minimum requirement for Z to be $15cm^3$.

These equations provide a preliminary estimate of the required structural material required for local strength checks. This methodology may be used for smaller WEC structures, while a more global strength approach is appropriate for larger WEC structures.

### 2.3.5.2   Global Strength Design of Large Structures

The global strength of a large structure depends on the structural configuration. It may be a long slender vertical beam, such as a spar foundation, or a horizontal beam, such as a barge or ship, or a space frame structure such as semi-submersibles and tension leg platforms. Each of these structure types would require specific consideration depending on the fabrication methods, installation methods etc., to determine what the global loads distribution would be throughout the lifecycle. These load cases are required to determine the governing load case and the design would be such to satisfy the worst case scenario. To address all possibilities of worst case loading for each structure would result in an exhaustive report, therefore as an example, consider the global loading of a ship in extreme wave conditions. The vessel may be supported only at the bow and stern by a large wave with a wavelength equal to the length of the ship. This scenario results in the majority of the hull being unsupported. The ship essentially would be pinned at either end, and a simple static structural analysis may be carried out to give a preliminary estimate of the basic scantlings of the hull. The problem may be simplified further by considering the maximum load of the vessel, i.e. including ballast for stability and

containers full, and transform this into an equivalent uniformly distributed load (UDL) by dividing by the length between the bow and stern. The maximum longitudinal bending moment may then be estimated from Equation 2-5.

$$BM_{max} = \frac{\omega l^2}{8}$$

**Equation 2-5**

where $BM_{max}$ is the maximum longitudinal bending moment (kNm), $\omega$ is the UDL (kN/m) and l is the ship length (m). This preliminary estimate of the bending moment may be used to estimate the steel plate thickness required for the hull to resist global loading.
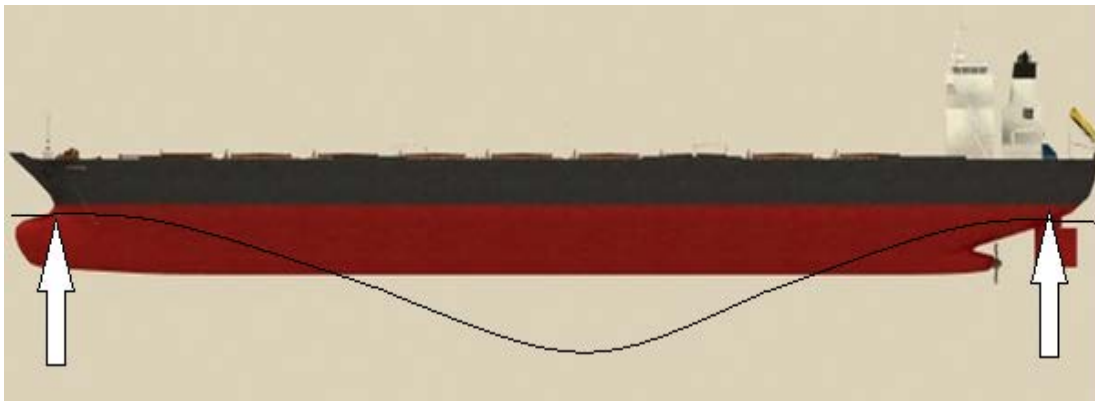


**Figure 2-66: Pinned oil tanker**

Reference [104] carried out physical model testing of the WEPTOS WEC at the Cantabria Coastal and Ocean Basin (CCOB) in Spain at a scale of 1:15. The WEPTOS is an innovative triangular shaped device with a number of "Salter Duck" type WECs mounted on each side of the "V" shape. The internal angle of the "V" can be changed dynamically through a sliding rail joined between the beams. The link between the two outer main beams is of a constant length and therefore as it slides towards the bow of the device it reduces the angle in the "V" shape. This is to reduce the loads on the mooring lines during survival sea states. The structural bending moments (BM) in the main beams have been monitored by strain gauges mounted on a measuring flange incorporated into the main beams. The BM was measured during both operational and survival sea states. It was found that the vertical BM in the main beams reduced to a value below the BM during operational conditions due to a reduction in the enclosed angle between the main beams from 90° in operational conditions to 30° in survival conditions. The longitudinal BM continued to increase significantly however due to the larger wave conditions. The largest recorded value of the longitudinal BM was 2151Nm. Reference [105] report that the 1:15 model weighed 1150kg with beam lengths of 7.4m, therefore each beam would have a uniform load of 762N/m. Treating the beam as simply supported at each end under its own self weight load, the maximum longitudinal BM would be 5216Nm. Therefore this 'simply supported' method of approximation provides an additional factor of safety of c. 2.5.

### 2.3.6 Mooring Loads

Many of the numerical methods mentioned in the previous section are capable of modelling sufficiently accurately the behaviour of moorings and the associated loads in nonlinear wave conditions.

For a preliminary design of the mooring lines and anchors, a simplified method of estimation of the mooring loads is required. The predominant method used in literature is the force estimated by Morison's Equation (Equation 2-6).

$$F_x(t) = \rho C_m V \dot{U} + \frac{1}{2} \rho C_d A U |U| \qquad \text{Equation 2-6}$$

where $F_x$ is the total horizontal force (N), $\rho$ is the fluid density (kg/m$^3$), $C_m$ is the inertia coefficient, V is the structure volume (m$^3$), and U is the fluid velocity (m/s), $C_d$ is the drag coefficient and A is the structure area perpendicular to the flow direction (m$^2$). As an example, consider the case of the Sevan FPSO facility. This structure has a diameter of 60m and a draft of 18m. Considering an inertial coefficient of 2, and a drag coefficient of 1.2, maximum wave height of 22m and period of 14s, the total load is approximately 628MN, as illustrated by Figure 2-67.
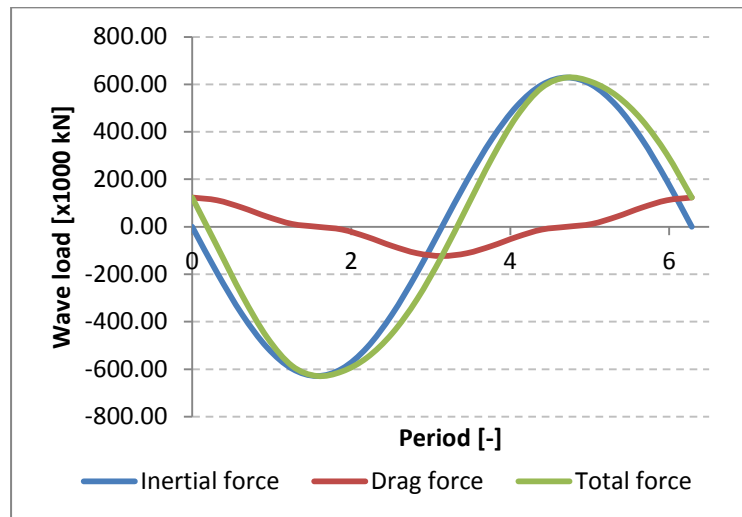


**Figure 2-67: Morison's Equation Example**

Based on the inputs noted above, the inertial forces clearly dominate. This would vary however depending on the structure type and design. The determination of the inertial and drag coefficients for new platform concepts will inevitably present a problem for designers at an early stage. Drag coefficients may be taken from [106].

### 2.3.7 Assessment of Concept Related Risk

The assessment of concept specific risk is not a typical undertaking in Stage 1 of the Concept Development Protocol, though this may need to be reviewed. There are many different methodologies of assessment of occurrence and severity of risks and hazardous events. Hazardous events typically mean threats to health, safety and environment (HSE). Common methodologies of risk identification include:

- Hazard and operability study (HAZOP)
- Failure Modes and Effects Analysis (FMEA)
- Fault Tree Analysis (FTA)
- Event Tree Analysis (ETA)
- Human Reliability Analysis Techniques (HRA)
- Markov Analysis
- Risk Based Inspection (RBI)
- Reliability Centred Maintenance (RCM)

A non-exhaustive description of each of these methods follows with references to documents which provide further detailed reading. Documents of particular interest include the deliverables from the 'Structural Design of Wave Energy Devices' (SDWED) project, namely [107] and [108], relating to WEC system reliability.

### 2.3.7.1 HAZOP

HAZOP is a structured and systematic technique for examining a defined system with the objective of:

1. Identifying potential hazards in the system. The hazards involved may include both those essentially relevant only to the immediate area of the system and those with a much wider sphere of influence, e.g. some environmental hazards.
2. Identifying potential operability problems with the system and in particular identifying causes of operational disturbances and production deviations likely to lead to non-conforming products.

An important benefit of HAZOP studies is that the resulting knowledge, obtained by identifying potential hazards and operability problems in a structured and systematic way, is of great assistance in determining appropriate remedial measures.

A more detailed account of HAZOP studies may be found in the British Standards BS IEC 61882:2001.

### 2.3.7.2 FMEA

FMEA is often the first step in a systems reliability study. It involves reviewing as many components, assemblies and subsystems as possible to identify possible failure modes and the causes and effects of such failures. The FMEA is mainly a qualitative analysis, which is usually carried out in the design stage of a system. The purpose is then to identify design areas where improvements are required to meet reliability requirements. There are two main methods of carrying out an FMEA analysis:

1. "Bottom-Up" Approach – this method involves beginning at the component level and expanding upwards towards system level.
2. "Top-Down" Approach – this method involves beginning at the system level and working downwards towards component level.

It is a difficult task to define the component level at which an FMEA analysis may be regarded as complete, as the workload can be extreme even for a system of moderate size. It is however, a general rule to expand the analysis to a level at which failure rate estimates are available or can be obtained.

A more detailed account of FMEA analyses may be found in the British Standards BS EN 60812:2006.

### 2.3.7.3 FTA

FTA is a "top-down" based, deductive reasoning failure analysis in which an undesired state of a system is analysed using Boolean logic to combine a series of lower-level events. This analysis method is mainly used in the field of safety engineering to determine the probability of a safety accident of a particular system level failure.

A more detailed account of FTA may be found in IEC 61025:2006.

### 2.3.7.4 ETA

ETA, in contrast to FTA, is an inductive reasoning failure analysis. An event is analysed using Boolean logic to examine the chronological series of subsequent events or consequences.

A more detailed account of ETA may be found in IEC 62502:2010.

### 2.3.7.5 HRA

HRA is related to the field of human factors engineering and ergonomics, and refers to the reliability of humans in fields such as manufacturing, transportation, military or medicine. Human reliability is very important due to the contributions of humans to the resilience of systems and to possible adverse consequences of human error or oversights. User-centres design and error-tolerant design are just two of many terms used to describe efforts to make technology better suited to operation by humans. A variety of methods exist for HRA. Two general classes of methods are those based on probabilistic risk assessment (PRA) and those based on cognitive theory of control.

A guide on methods of incorporating HRA for Nuclear Power Generation Stations may be found in the IEEE Standard 1082:1997.

### 2.3.7.6 Markov Analysis

Markov analysis is used to model systems which have many different states. These states range from fully functional to a total faults state. The migration between the different states may often be described by a so-called Markov-model. The possible transitions between the states may further be described by a Markov-diagram, or a state diagram. This methodology is very detailed in its analysis, and would require isolating a specific system for use of Markov analysis.

### 2.3.7.7 RBI

RBI is usually and typically applied to floating production FPSO units. These installations are permanently moored systems which very rarely travel to dry-dock for maintenance activities. This challenge results in the need for specific Inspection, Maintenance and Repair (IMR) procedures. The process includes identification of the most critical components in the overall system, undertaking of RBI analysis, summary and recording of RBI analysis results, establishment and implementation of IMR plans.

### 2.3.7.8 RCM

RCM has been developed to define risk indices of equipment failures and to prevent the occurrence of these failures by establishing and implementing an optimised preventative maintenance and inspection plan. The RCM approach typically requires the results of an FMEA analysis for the identification of critical components of the system. RCM aims to design an optimised maintenance strategy for each critical component/system within the overall system. This can only be completed following a full and detailed design of the system is completed.

### 2.3.7.9 Calculation of Average Failure Rates of Mechanical and Electrical Systems

On carrying out an FMEA analysis of a system, one now has a list of critical components for that system. It follows that in order to assess quantitatively the risk associated with that system, the failure rates, both critical and overall, for each component within the system should be identified. In the case of MRE platforms, this presents a particular challenge. Many of the components, particularly within the PTO system, are innovative and untested component designs. Therefore, a component similar in design and to an extent, function, is required to provide an indicative failure rate. Additional factors may then be applied based on the expected number of cycles of the component in relation to the baseline component. This would be required for each component in the system, which finally can be summed to provide an average failure rate for the system.

There are a number of sources of failure rate data;

1. OREDA Handbook
2. CONCAWE
3. EIREDA
4. ZEDB
5. T-BOOK
6. PDS

Each of these sources provides operational experience of thousands of mechanical and electrical system components in industries such as offshore oil and gas and nuclear power plants.

### 2.3.8  Life Cycle Cost Analysis

The penultimate criteria for the assessment of concept feasibility is the cost of energy (COE) produced, which is determined through LCCA modelling. The true feasibility of a concept is measured by a combination of technical and economic feasibility. This in turn requires a sufficiently well balanced match between device efficiency and life cycle cost. By focussing on one individual aspect of feasibility may result in a significantly unsatisfactory value of the other. Striving for maximum efficiency may not result in a cost effective device. Reference [107] and [108] pioneered methods of evaluating the COE through estimation of CAPEX and OPEX. This method in its most simple form would add the CAPEX to the OPEX estimate for each year of operation and divide by the total energy produced as in Equation 2-7.

$$COE = \frac{CAPEX + \sum_1^n OPEX}{\sum_1^n Annual\ Energy} \left(\frac{€}{kWh}\right)$$

<div align="right">**Equation 2-7**</div>

where n is the total project years. This method has been further refined by several researchers by applying discounting techniques to the future costs and energy production in order to obtain the LCOE. The annual discounted cash flow (DCF) may be given by Equation 2-8.

$$DCF(y) = \frac{FCF(y)}{\left(1 + \frac{R_d}{100}\right)^y}$$

<div align="right">**Equation 2-8**</div>

where y is the year, Rd is the discount rate and FCF is the future cash flow (€). This method has been employed by [44], [42], [109] and [110]. The Equimar protocol and Carbon Trust also recommend the use of DCF techniques for estimation of LCOE. An open-source CoE model is described in [113].

In the estimation of life cycle costs, there are two primary elements, the CAPEX and annual OPEX costs which need to be estimated. There are numerous methods of estimating these parameters, ranging from simplistic to complex methods. These are discussed in the following sections.

#### 2.3.8.1  CAPEX Estimations

The estimations of the expected CAPEX costs of a project is typically the more simple of the two elements of project costs, although in itself presents significant challenges. The methodology used to calculate a project CAPEX typically depends on the ultimate goal of the study, be it the assessment of a specific projects lifetime costs breakdown and ultimate energy generation costs, or the assessment of a projects cash flow and interaction with the energy market. Both of these studies would typically use very different methods of CAPEX estimation. The former would typically have a detailed account of the various components of all technical elements of the project including foundations, turbines, installation methods etc. This method requires a substantial bank of unit costs of the various elements in a project cost

estimation, guided by experience and costs provided by consulting engineers, fabrications companies and experts in the specific area under study. This method has been used in [111] for the comparison of various WEC concepts LCOE. The latter method employs a very much simplified estimate of a nominal cost per unit capacity installed, e.g. €/MW. This method is used in many DCF models for the assessment of the performance of offshore wind farms at various sites. Such CAPEX costs typically rely heavily on a bank of information from past projects to guide the estimate of installed cost per unit capacity. This information is readily available for the offshore wind industry at [112]. The applicability of this latter method is questionable for the wave energy industry as there is no official final installed cost for any projects. This thesis will therefore focus on the former method of CAPEX estimation through the preliminary design of the primary technical elements of a project and application of various unit costs to these designs to estimate the project CAPEX.

### 2.3.8.2 OPEX Estimations

The estimation of operations and maintenance (O&M) costs is a very different challenge. This time varying parameter depends on an extensive number of parameters and project specific strategies. Reference [72] outlined the O&M costs for a number of UK Round 1 offshore wind farms, expressed as a cost per unit energy produced. This, similar to the latter method of CAPEX estimation above, is a very simplistic view of OPEX costs.

In reality, O&M costs are determined by the machinery used, the vessels available, the wind and wave resource at the site, the method of transfer of personnel to the platforms and in particular the distance to shore. With this in mind, a constant O&M cost per unit energy produced is a significant simplification as none of these factors are constant between farms in different sites. The current state of the art is the creation of models capable of modelling wind farms throughout their operational lives. These models are driven by time series of wind and wave conditions at the particular site of the study. Maintenance strategies are modelled with time, depending on the requirements specified by the user for the machinery under study. This methodology has been used extensively recently in the assessment of offshore wind farms [113]. In that publication, a number of O&M modelling tools are listed, including:

- CONTOFAX by DTU
- O2M by Garrad Hassan
- BMT SLOOP by BMT
- ECN O&M Tool by ECN Netherlands

Each of these models has an emphasis on the assessment of the various maintenance strategies and their associated costs. The maintenance strategy hierarchy is illustrated in Figure 2-68.
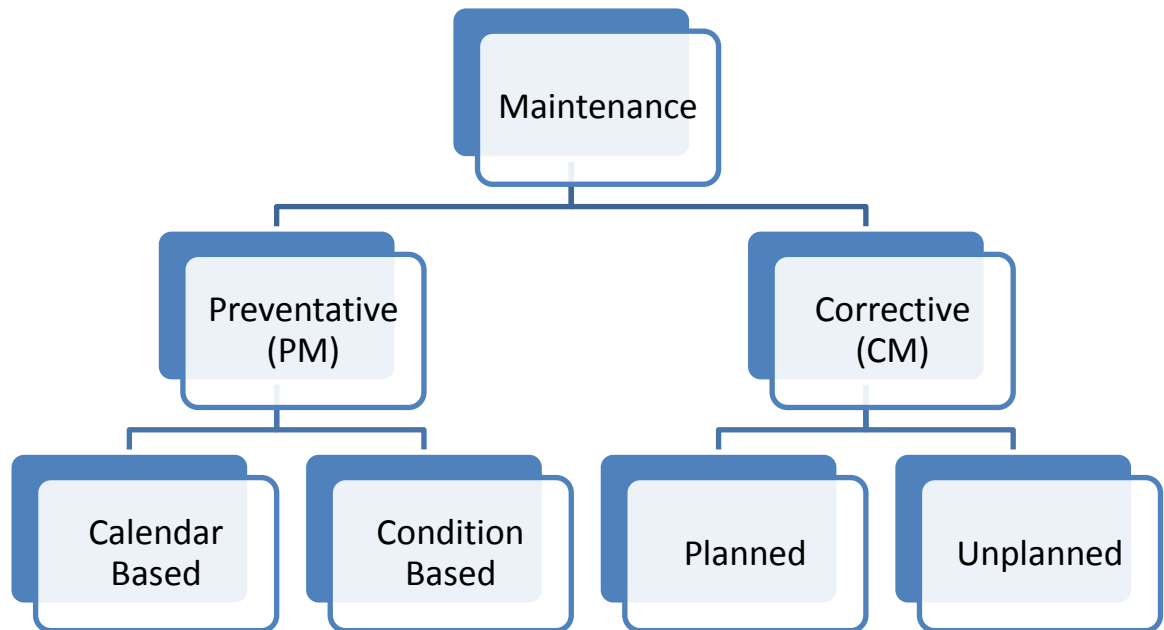
**Figure 2-68: Maintenance Categories and Sub-Categories**

### 2.3.8.3 Maintenance Classes

The primary sub-classes of a maintenance strategy include preventative and corrective. The secondary sub-classes of maintenance strategies include calendar and condition based maintenance for preventative and planned and unplanned for corrective maintenance. Each of these maintenance classes are described briefly below.

#### 2.3.8.3.1 Preventative

The preventative maintenance category essentially encapsulates all strategies which aim to prevent component failure within the energy generation device, including structure and drivetrain, i.e. any component which can stop the unit from generating power. This parent class includes two sub-classes of preventative maintenance strategy, i.e. Calendar Based and Condition Based.

#### 2.3.8.3.1.1 *Calendar Based*

Calendar based maintenance is the most common strategy employed today in the offshore wind industry for preventative maintenance. This method seeks to inspect, replace and "top-up" components as required before the component reaches its failure stage. The success of this method is tightly coupled to the operational experience of the wind farm operator, the O&M vessels at the operator's disposal and the annual weather conditions at the farm. Carrying out this type of maintenance is in general restricted to the summer months when wave and wind conditions are at a minimum and transfer of personnel can easily and quickly be carried out during daylight hours. Typically, three days of maintenance is required for each turbine between 2-4MW size. This approach has the disadvantage of no maintenance being carried out during the winter months when the machines are under most stress and

generating most of the annual distribution of power. Refinements to this method are ongoing through design of better vessels which can transfer personnel to the turbine in higher wave conditions thereby extending the season for maintenance.

### 2.3.8.3.1.2 *Condition Based*

Condition based maintenance is similar to calendar based maintenance, the difference being that maintenance of the turbine only occurs when components approach the end of their operational lifetime. This infers that monitoring equipment is necessary in the drivetrain on all components that can cause the turbine to shut down when they fail. This method requires significant investment in monitoring systems which in many cases cannot directly measure the degradation of the component, instead an indicator of possible component degradation. This presents a problem in that inspection is still required, thus posing the question whether this strategy should be considered at all. If inspection is still required despite monitoring equipment being installed, the more cost effective solution would then still be the calendar based strategy.

### 2.3.8.3.2 Corrective

The corrective maintenance strategy encapsulates all strategies which aim to bring a failed component back into service, and thus allow the turbine to resume production. Corrective maintenance strategies aim to reduce downtime as a result of failures, however, a cost benefit analysis should be carried out on whether a corrective maintenance strategy should be undertaken for large heavy components in a single turbine. This issue will be discussed in a later section.

### 2.3.8.3.2.1 *Planned*

Planned corrective maintenance is a strategy whereby a component or number of components, either in a single turbine or multiple turbines have failed, but is not detrimental to the survival of the turbine. This allows a time span to be attributed to the planning of the maintenance strategy to be undertaken in order to allow all components to be repaired or replaced to allow all associated turbines to resume production. These may be large or small components. In the situation where a large component such as generator requires replacement, a jack-up vessel is required which requires mobilisation time of the order of two weeks. In the event of this occurring, other tasks which may not be necessarily be required immediately can then be carried out when the large vessel is on site. This may be considered planned corrective maintenance. The generator is also used to draw power from the grid in extended periods of no wind to rotate the rotor to ensure even loading is placed on the main bearings of the main shaft. In the event of loss of a generator, a parallel planned maintenance strategy is put in place to bring a diesel generator to the turbine to rotate the rotor. During times of no access to the turbine in this case, further parts may need replacement.

*2.3.8.3.2.2 Unplanned*

Unplanned corrective maintenance is that which is completely unforeseen and is required to be carried out immediately as the survival of the machine or other equipment is at stake. This maintenance strategy is the most costly form of maintenance and takes place during the first available weather window.

### 2.3.8.4 Architecture of LCCA Models

The O&M costs for any offshore installation depends directly on the maintenance classes employed for that particular project. Many of the time based O&M models mentioned strive to incorporate each of these strategies in the operational simulations of the farms. This is a complex undertaking as it is believed that many decisions surrounding O&M activities, particularly in the corrective maintenance class, are made on an ad-hoc basis. Therefore it is difficult to pre-empt the decision making processes that determine the maintenance activities to be undertaken. Nonetheless, most models like the ECN O&M Tool and CONTOFAX are built as informative tools for comparing different maintenance strategies, thereby informing farm operators as to the most cost effective solution. These models are typically comprised of a number of sub-modules including, for e.g.,

- Environmental Module – Instantaneous environmental information as well as weather window information
- Preventative Maintenance Module – (PM) Strategy
- Corrective Maintenance Module – (CM) Strategy
- Resources Module – Availability of resources, vessels, crew, parts etc.

A brief description of each module and the definition of parameters and constraints held within them are outlined below.

2.3.8.4.1 Environmental Module

The environmental module of these O&M or operational simulation models can incorporate either manufactured time series of environmental conditions, such as hourly data of wind speeds, significant wave height and peak wave period. The most straightforward input is certainly measured data of the parameters required to drive the model, however, gaps in measured data can be difficult to replace on an hourly basis. Alternatively, monthly averaged data from a site may be used to generate a time series of the required data numerically. This method is used in some of the models mentioned. For the purposes of this thesis, numerical hindcast data generated from a regional scale hydrodynamic model will be used.

The major element within the environmental module is the specification of weather windows and what constitutes as a weather window. In the case of using hindcast data of, say, ten years, the average year from all ten would be used as the baseline. From this average time series, the monthly occurrences of weather windows may be determined. Typically, weather window "types" are specified by a significant wave height limit and time span length e.g. 1.5m Hs for min 4 hours. The specification of

the weather window types is dependent on the tasks to be carried out, the required machinery/vessels and the length of time for transit and repair of the fault. These are specified in the resources module.

### 2.3.8.4.2 PM Module

The PM module takes account of the PM strategy the user specifies for the farm under consideration. This is generally taken to be a specific number of trips with standard tasks carried out to each device in the farm annually. In some cases, the PM module can operate independently of the CM module assuming that in the event of CM maintenance being required, additional resources are hired in to carry out the required tasks. Alternatively, the PM strategy surrenders resources to the CM strategy, thus the need for both modules to be in contact at all times during the simulation. The module tracks all trips and man hours spent on each device and a report is generated at the end of each year stating how many resources were used for PM.

### 2.3.8.4.3 CM Module

The CM module operates on the basis of failures of components. Therefore, as an input, the list of components of the device are required and associated with each component, an average failure rate and standard deviation. Each simulation generates a random failure rate for each component and once the time step equals the failure rate of that component, it fails and the CM module is prompted. The CM module, in the event that resources are shared with the PM strategy, takes priority over PM. This is because generally in simplified models, components are either in a fully operational state or completely failed. There is no degraded performance state of a component. Therefore, if a component fails, the model tells the turbine to shut down. CM is required to bring the turbine back into production. During PM of a turbine, it is only shut down while personnel are on-board the turbine. The resources spent on CM and the turbines that require it are recorded and a report is generated at the end of each year.

### 2.3.8.4.4 Resources Module

The resources module keeps account of the deployment of all resources available to the operator of the farm at all timesteps. These include vessels, helicopters, spare parts, crew etc. In some cases, this acts as a central pool of resources when the PM and CM modules are in contact and share O&M resources. Otherwise, these resources are isolated to one or the other maintenance strategies, such as vessels to PM and spare parts to CM etc. When all resources are deployed in a timestep and maintenance is required on a turbine, the next time they become available they are deployed to that turbine. The resources module also keeps account of the hours kept by crews, and determines whether a crew has had sufficient time ashore before being redeployed to a maintenance activity.

As mentioned briefly in the Environmental Module description, the technical reasons for the weather window limits are held within the resources module. These are from

the technical specifications of the vessels or helicopters or equipment transfer constraints. Currently, only access systems to large floating oil and gas rigs and fixed offshore wind turbines have been investigated. Because these structures rely almost solely on the motion characteristics of the vessel for the transfer of personnel, their applicability to smaller floating structures is questionable. The benchmark will be the motions of the vessel on its own in typical transfer sea states for offshore wind turbines, which are currently limited to ~1.5m significant wave height. Actual relative motions between floating platforms and O&M vessels may lead to the redefining of the weather window constraints.

### 2.3.8.5   Probabilistic Economic Assessments with Monte Carlo Simulations

From the discussion before, the range of parameters which can affect the outcome of an O&M strategy is substantial. With this in mind, a deterministic simulation of the O&M strategy would be somewhat unrealistic bearing in mind the uncertainty associated with some of the values of these parameters, namely the component failure rates. For this reason, these models are made to be probabilistic in nature, i.e. they incorporate the uncertainty associated with each input parameter. The common method of Monte Carlo simulations is generally applied which essentially runs every possible combination of parameters within the ranges specified for each to determine the confidence interval for the output parameters. The number of simulations must also be investigated for each O&M strategy. This is to ensure that convergence is achieved in the output parameters of interest. One particular model in development currently is that described in [117] which is of the type described above.

### 2.3.9   Indicators of Project Feasibility

From the brief review of methods of assessment and development strategies undertaken by various technology developers for wave energy and floating wind energy devices, it is apparent that a significant number of criteria may be used to determine project feasibility. This section summarises the parameters determined from the methods of assessment described earlier, and presents a number of parameters which may be used as indicators of device or project feasibility. These parameters are based on both technical and economic performance, which are both critical indicators themselves.

### 2.3.9.1   Power Performance

Following the initial design of a wind or wave energy device geometry, the foremost parameter the developer aims to assess is the power performance and its dependence on specific geometry modifications. As discussed previously, and summarised below, this can be done in a number of ways. The ultimate aim of this assessment is to optimise the geometry with respect to power performance and seakeeping ability.

2.3.9.1.1  Methods of Estimation and Confidence

The main methods of assessment of power performance as discussed in Section 2.3.1.1, 2.3.1.2 and 2.3.4, are scaled model tank testing and/or numerical

simulations. It is generally recommended however, to carry out concept performance studies using both methods for cross comparison and validation. In terms of tank testing, the parameters to be measured are largely concept dependent. The main measurements to be taken include motion responses of the body in the case of floating systems and the main power absorbing degree of freedom(s) and damping applied to the system. Naturally, in numerical simulations all possible measurements of parameters are quite simple. Validation of the main parameters from tank testing is advised and therefore some degree of confidence can be taken from numerical simulation results. The type of numerical models used is also a primary consideration, particularly in the early stages of development. In Section 2.3.1.2 it was seen that the state of the art currently is the determination of the hydrodynamic coefficients from a frequency domain solver for input into a time domain solver developed for the specific characteristics of the concept under study. In many cases, the need for a time domain solver in Stage 1 of development is unnecessary as the information provided from the frequency domain solver, coupled with the use of empirical damping formulae to represent viscous damping, can provide a significant amount of information for optimisation studies. This can be used in conjunction with the 'principle of superposition' [114] to estimate a power matrix for a device and the initial structural design of the hull. This principle states that the response of a linear system from the sum of two stimuli is equal to the sum of the system responses from the individual stimuli. This allows a simple and fast analysis to be performed on real sea conditions if it assumed that a real sea state can be represented by the summation of an infinite number of sinusoidal waves each with a predetermined wave amplitude, frequency and phase shift. The uncertainties associated with the power output performance estimation in the early stage of development are significant. These uncertainties arise from a number of sources, including scale effects and measurement accuracy. These are very difficult parameters to estimate. The general solution is to express a confidence interval in the calculated LCOE which is discussed below.

### 2.3.9.1.2   Representing Power Output in Terms of Geometry

An indicator of the power performance of a device which has long been used is the CWR. This parameter is essentially a hydrodynamic efficiency as it relates the absorbed power of the device, the primary power absorbing dimension of the hull and the incident power per metre crest width as shown in Equation 2-9.

$$\eta = \frac{P_{abs}}{J \cdot w} \qquad \qquad \textbf{Equation 2-9}$$

where $\eta$ is the CWR, $P_{abs}$ is the absorbed power of the device (kW), J is the incident wave power (kW/m) and w is the primary power absorbing dimension of the device (m). A benchmarking study has been undertaken by [17] investigating the average CWR of each category of wave energy device. It is suggested that in the development of a new concept, the calculation of the CWR for the new concept should be broadly in line with the ranges suggested in that paper. If, for some reason

the calculated CWR is significantly different, independent verification should be sought.

### 2.3.9.2 Structural Requirements

A structural analysis is not commonly done in the early stages of concept development, due in part to the various modifications that are made to the hull shape to improve power performance. However, this particular assessment can be as significant as the power performance assessment. The structural mass is a significant indicator of the lifetime costs of a device and as such forms a major part of the concept feasibility both in terms of technical and economic feasibility. There are simplified rules of thumb available which estimate the structural mass in terms of displacement etc., but the applicability of these to wave energy devices has not been proven. During the assessment of a device hull for power performance numerically in the frequency domain, the hydrodynamic pressures are also calculated for each panel of the descretised wetted hull surface. These pressure RAOs may be used to more effect in carrying out a simplified linearised structural analysis again using the principle of superposition. This method will be demonstrated in following chapters.

#### 2.3.9.2.1 Structural Mass of Structure Relative to Geometry

Like that of the power performance criteria relative to the device geometry, the structural mass calculated from a simplified structural design must also be benchmarked relative to known ratios. These ratios are spread right across literature for oil and gas platforms as well as personal communications with developers. The design of structural steel is tightly coupled to the grade of steel that is used, i.e. the yield stress of steel. In [115], the various values of steel grade yield stress are outlined in Section 4.D Table D1. One should be cautious of the use of each of these as increasing the yield stress naturally reduces the ultimate tonnage of the hull but the unit cost is significantly different. A balance must be sought between the two parameters. A common indicator of the expected structural mass of a hull is a percentage range of the displaced mass. As an example, for a 3-column semi-submersible hull of displacement ~4000t with heave plates using steel grade NS (Normal Strength Steel), the structural mass should be ~2000t including heave plates. Such indicators can guide the preliminary design of a hull.

#### 2.3.9.2.2 Representing Power Output in Terms of Structural Mass

As the structural mass of a hull can be an indicator of the lifetime costs of the device, it is logical that the structural mass per unit power output would be an indicator of the LCOE. Reference [31] carried out the benchmarking of eight wave energy converters and suggested that the energy absorption per tonne is approximately 1 MWh/t for each device. It is unclear if a structural analysis was carried out on each device in the study, or whether this ratio refers only to the displaced mass of each device. Nonetheless, a similar indicator would provide guidance in early stage development.

2.3.9.2.3  Station-keeping Design and Estimated Loads

The station-keeping design of the wave energy devices or floating wind foundations currently under development is not that different from oil and gas platforms. Existing standards would in the main cover these designs. It is anticipated however, that in the design of much larger hulls, possibly manufactured from concrete, that the displaced mass and therefore loads experienced in extreme conditions will pose a significant challenge in the design of mooring systems. Maintaining position is one element of mooring design, i.e. ensuring lines do not break and anchors do not drag, but in the case of energy devices the maximum excursion is also a constraint due to the attachment of a flexible umbilical for power export. These limiting excursions can cause the lines to become taught and result in very high loads. While mooring systems can be designed to cater for any situation, the type of mooring lines used should so far as reasonable practicable be within the typical range used in the offshore sector currently. This is mainly for cost considerations but also for installation considerations. Should the required mooring design be outside current manufacturing and installation capabilities, it should be deemed technically unfeasible at that time.

**2.3.9.3  Concept Risk Assessment**

As it was discussed, risk assessments are not normally carried out in the early stages of development of a concept. However, in the case of ranking various concept types, naturally the one with least concept related risk would be a preferred option. This should in theory be reflected in the LCCA results of the various concepts but these models are limited in their abilities to cater for such detail. Therefore it may be necessary to carry out the risk assessment on a semi-quantitative or qualitative basis. The following sections outline both a qualitative and semi-quantitative analysis.

2.3.9.3.1  Application of Design Standards

In Section 2.2 the available guidelines and standards governing the design of offshore structures and wave and wind energy devices have been outlined. A rather simple risk assessment is whether or not any of these guidelines and standards apply to the concept or not. In the event that no standards exist in which to base a design process, standards designed to qualify new technology should be used. The number of items which these technology qualification standards need to be applied to in a concept may be an indicator of the level of risk associated with that particular concept.

2.3.9.3.2  Criticality of Components

The various methods of risk assessment of structures or components etc. are outlined in Section 2.3.7. These methods may be applied to any concept to determine the areas where risk of failure may occur. If however, in the early stages of development, the detailed configuration of a device is not defined or available, a semi-quantitative assessment may be undertaken. This would begin with an outline of the main components of the system, i.e. hull, PTOs, connections/joints etc., and determining which of these elements are the most critical to the continued survival of

the platform. Again, an indicator may be the number of components which are critical to the survival of the platform. Furthermore, from Section 2.3.9.3.1, how many of these components are then covered by design standards and guidelines would be a significant indicator of concept related risk.

### 2.3.9.4 Required Environmental Conditions

The feasibility of a concept is naturally tightly coupled to the resource level it is anticipated to be deployed in. In many cases, the LCOE of a concept is reported on the basis of deployment in a high energy site with very little regard for a technical assessment of O&M requirements and risk assessments of components etc. For this reason, it may be suitable to use the resource level as an indicator of risk, and therefore feasibility. Below are comments of how the resource level is related to the various elements that may affect overall platform/project feasibility.

#### 2.3.9.4.1 Average Wave and Wind Conditions for Power Performance

The average wind and/or wave conditions at a site are the typical resource information a developer investigates in the determination of the performance of a concept. While the average conditions indicate the power production possibilities for the device, or the revenue stream for the project, they too indicate the lifetime costs of a project.

#### 2.3.9.4.2 Extreme Conditions for Structural Design and Survivability

The extreme conditions for a site are the design criteria for structural integrity of the hull and mooring systems of a concept. These are the main cost drivers associated with the capital expenditure of a project. It thus would suggest that the lower the ratio between average and extreme wave heights at a site, the better the performance of a platform/project.

#### 2.3.9.4.3 Accessibility of Site Relative to Resource Level

At the current time, accessibility information for offshore energy devices is only available for fixed offshore wind turbine platforms. In the main, the access restrictions for transfer of personnel are related to the relative motion/accelerations between two bodies. As the offshore wind foundations are fixed, the motion and accelerations constraints are isolated to the motion and acceleration characteristics of the vessels used in certain sea states. For floating devices, the applicability of these sea state constraints are uncertain as a vessel and buoy may indeed have zero relative motion and accelerations in some sea states. As unlikely as this may seem, the process of redefining weather window limits must be entertained on the basis of two floating systems. The accessibility of a site will inevitably be a significant indicator of project feasibility due to the reliability issues surrounding PTO systems for both wave and floating wind energy devices.

#### 2.3.9.4.4 Anticipated Availability of Farm

A significant indicator of project feasibility for the wind industry has been the average availability of the devices for power generation. The availability of an

offshore installation can be assumed to be a function of reliability and accessibility. It may then be a case that the availability of the installation can be determined from the access limits imposed by the average site weather conditions and the concept related risk assessment. This provides the annual farm production and therefore revenue.

**2.3.9.5   Life Cycle Costs**

The anticipated cost of energy from the project is the most significant indicator of feasibility. This is considering the substantial increase in required effort to determine the real project feasibility indicators for a commercial entity, namely the Net Present Value (NPV) and Internal Rate of Return (IRR) (value of return on investment). The calculation of these parameters requires the specification of, in great detail, the revenue stream of the project. In many well developed industries, there are guidelines available for this. However, in terms of the renewable energy industry, there is more than one revenue stream and they are time dependent parameters in many countries, and furthermore in the case of Renewable Energy Feed-In-Tariffs (REFIT), their continued existence is not certain. The assessment of the revenue generation of a renewable installation requires up-to-date knowledge of short-term energy trading markets, rates and trends as well as REFIT rates and lifetime. This type of analysis is beyond the realm of an engineer's participation and therefore this thesis will focus only on the assessment of a projects life cycle costs and how this can be an indicator of project feasibility.

2.3.9.5.1  CAPEX per MWh Produced

The capital expenditure (CAPEX) for a platform/project concept is the relatively simplest of economic assessments. The approximation of a platform costs and the methods adopted to determine these is a function of the stage of development of a concept at the present time. In other words, in the early stages of concept development, very simplistic methods of determining CAPEX costs are used. As a concept progresses through the development stages, more detailed and accurate methods of determining CAPEX costs are employed. With the advent of a more holistic approach to concept development it may be possible to employ a more detailed method of determining CAPEX costs, particularly for the hull and mooring system designs. Following the determination of the CAPEX, relating this to the anticipated energy production would provide a good indication of the performance of the concept.

2.3.9.5.2  OPEX per MWh Produced

The operational expenditure (OPEX) for a platform/project concept is virtually unknown for emerging technologies such as wave energy. While the type of activities will essentially be similar to the existing offshore wind industry, the amount to be carried out may not. The determination of the OPEX costs over the lifetime of a project is by no means a trivial task and incorporates a significant number of variables ranging from labour costs, to spare parts supply to downtime costs etc. While models are emerging for the assessment of various O&M strategies

for various concepts, the computation time required to continually run these models for the thousands of simulations required to achieve convergence is still a barrier. So too are the limits associated with the saving of information. The use of these models in the earlier stages of development may be limited to the amount of uncertainty the model and hardware can cope with and therefore use in the initial stage of concept development may not be possible. Simplified methods of approximation of OPEX may be based on experience with other industries, or indeed from base case simulations of concepts using the time-based LCCA models. Relating this again to the energy production the concept is capable of in an average year would provide a good indication of the level of intensity of O&M operations per MWh produced and thus lifetime costs.

### 2.3.9.5.3  LCOE Produced

The combination of the CAPEX and OPEX costs can provide an annualised cashflow of the project costs and energy production. The use of a technology dependent discount rate, itself an indicator of risk, provides the levelised cost of energy (LCOE) the project/concept can deliver. The LCOE parameter is a link between all the technical indicators addressed previously. The power performance, structural design, concept related risk and the resource level and associated links between these are all considered in the determination of the LCOE. This will be the parameter this thesis will strive to produce for any concept developed, whether on a detailed or simplified basis.

### 2.3.9.6  **Ranking of All Indicators**

In many cases in early stage developments, the power performance, structural analysis, unit costs of the hull and LCOE are not linked in a seamless overall assessment but more on a stand-alone basis. For early stage development, the addition of full LCCA models may provide the link these analysis methods require. As an example, for the design of a device for operation in high energy sites, reliability, survivability and access will be significant contributors to the feasibility of the concept. The immediate ranking of the feasibility indicators is not obvious and may indeed be unique to every concept conceived. This thesis will investigate the sensitivity of these elements of feasibility to a number of concepts and try to determine if a constant trend emerges in terms of importance across various concepts.

# 3 Design and Analysis of Offshore Wind and Wave Energy Devices

This chapter applies the current state of the art in design methods to offshore wind turbine foundations and wave energy devices to assess their ability to potentially provide estimates to some of the feasibility indicators discussed in Chapter 2. It should be noted that the structural designs carried out in this chapter are only based on ultimate limit state (ULS) design. No fatigue limit state (FLS) design has been carried out as this is a time consuming process which requires specific knowledge of the installation location for determination of the number of stress/strain cycles the structure will undergo annually following a fatigue damage assessment from a rainflow analysis for all sea states. It may be considered sufficient to preliminarily size structures based on ULS design for this thesis.

## 3.1 Fixed Foundations Analysis

This section analyses the main offshore wind fixed foundation options, namely the monopile and the GBS. A stochastic parameterised hydrodynamic semi-empirical model based on Morison's Equation is used to determine the hydrodynamic loads. A simplified aerodynamic model based on stochastic wind velocity and turbine thrust curves is used to calculate the aerodynamic loads on the foundations. A simplified structural analysis and design has been carried out and unit costs calculated to determine the foundations costs for each and are compared.

### 3.1.1 Monopile Fixed Foundation

This section assesses the methodology of design of a monopile foundation and provides results from a parameterised model developed using Morison's Equation for hydrodynamic loads from spectral waves as well as turbulent wind loads at the hub for the three turbine types described above. The method of superposition, as first introduced in hydrodynamics by [114] is applied to both the wave spectra and wind spectra to provide a time series of representative loading on the structure. The variation of structural mass of the monopile foundation will be investigated for increasing water depth, turbine size and significant wave height and peak wave period. Only loading from spectral waves on the foundation and stochastic wind on the turbine rotor are considered for design of the monopile and TP using bending moment and shear checks in accordance with [116] as referred from [115]. A number of assumptions are made in the model and are outlined below.

- The thrust curve for the NREL 5MW reference turbine has been divided by the turbine rating to provide an approximation of thrust on the turbine hub depending on the rating of the turbine. This approximation may be updated with a correct thrust curve for the turbine under study.
- Only mean wind speeds of 12m/s are considered in the results below to allow for maximum thrust at the hub.

- The water depth determines the maximum significant wave height possible through

$$H_b = 0.42 d_b$$

where $H_b$ is the breaking wave height and $d_b$ is the breaker depth. The breaker depth is assumed to be the water depth under study. The maximum $H_s$ is limited to 15m.

- The design wave period is determined from the design wave height and is the minimum period allowed before breaking, thus giving the steepest wave possible to achieve maximum loading.

$$T_D = 11.1 \sqrt{\frac{H_b}{g}}$$

- The hub height of the turbine is assumed to be constant at 90m.
- The material factor for steel is constant at 1.15 as stated in [115].
- The yield strength of steel is 235MPa, representative of NS from [115].
- Monopile diameter is constant at 6m.
- The point of fixity of the monopile is assumed to be 5m below the seabed level.
- The drag and inertia coefficient for Morison's Equation are assumed to be 0.65 and 1.6 respectively as outlined in [117]
- No current profile is used in the calculation of hydrodynamic loads.

Therefore the study is primarily driven by the choice of,

1. Water depth,
2. Turbine rating,
3. Monopile steel plate thickness.

### 3.1.1.1 Results
This section presents the results of the study on the monopile foundation, beginning initially with a sample of the outputs from the parameterised model.

#### 3.1.1.1.1 Sample Output Plots from Model
In terms of the geometry of the monopile foundation, it was outlined that the diameter of the pile was kept constant. Two further parameters of the monopile geometry were required, the height above sea level and the depth of penetration below the seabed. These two parameters have been taken from a sample provided in [117]. The sample has been used to formulate the platform level and pile penetration depth as a function of water depth in which the foundation is installed. These are illustrated in Figure 3-1and Figure 3-2.
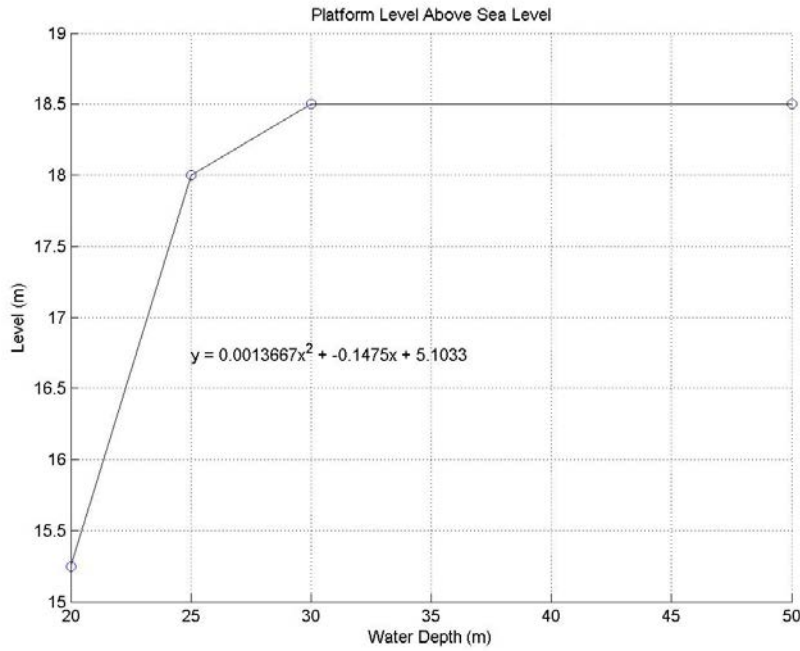
**Figure 3-1: Platform Level as a Function of Water Depth**
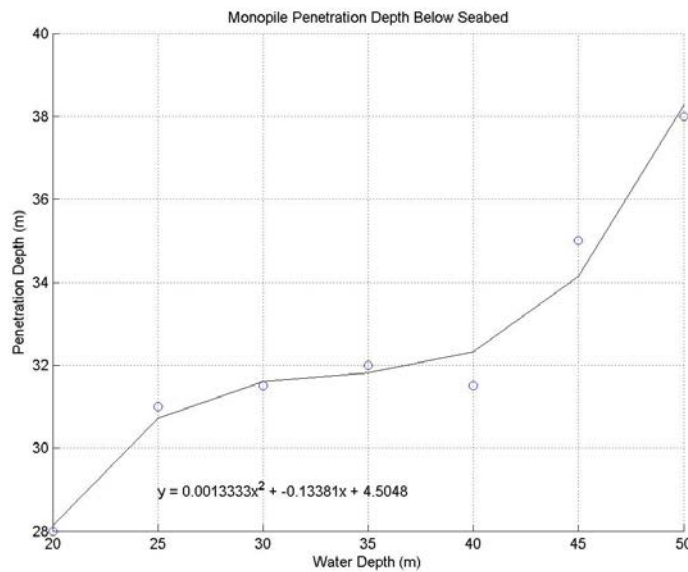


**Figure 3-2: Monopile Penetration Depth as a Function of Water Depth**

Following the determination of the pile geometry, the calculation of the loading was determined. As the model was required to analyse loading from spectral waves and stochastic wind, both a wave and wind spectrum was required as an input. The wave spectrum used was the Bretschneider Spectrum and the wind spectrum used was the Kaimal Spectrum as recommended by [118], while the Reference Turbulence Intensity Factor is given as a function of height above sea level by [119]. The "principle of superposition" has been applied to both spectra to create a representative time series of wave conditions based on linear wave theory and wind speeds. This principle involves determining the amplitude of the sinusoidal signal for

each frequency within the relevant spectrum and attributing a random phase shift to each sinusoid. The water level elevation, velocity and acceleration of a sample wave condition are illustrated in Figure 3-3. This process is carried out at depth increments of 1m so as a time series of velocity and acceleration can be determined at each depth. This allows the variation in loading with water depth to be applied to the foundation. The rationale behind the use of basic unmodified linear theory is to provide a simplified estimate of the order of magnitude of the loads which the structures are likely to experience. As the design progresses for any structure, more refined and detailed analysis techniques, theories and models should be used. The extreme wave conditions are potentially better represented using non-linear wave theories, but these require much more effort and time to implement. As a first approximation, linear theory is deemed reasonable to apply.

The instantaneous load on the foundation at each depth as determined from Morison's Equation is applied and the summation of these gives the lateral force applied to the foundation by the incoming waves. A sample output of the lateral force from wave loading applied at the point of fixity of the pile is illustrated in Figure 3-4. The associated bending moment at the point of fixity of the pile is then simply the force times the distance from the point of fixity. A sample output of the bending moment from wave loading is illustrated in Figure 3-5.
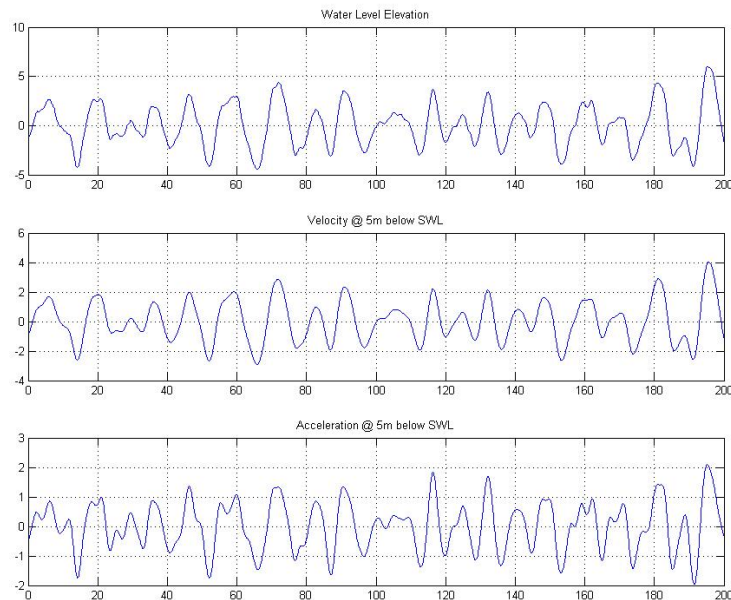


**Figure 3-3: Sample Time Series of Water Level Elevation, Velocity and Acceleration at 5m Below Surface**
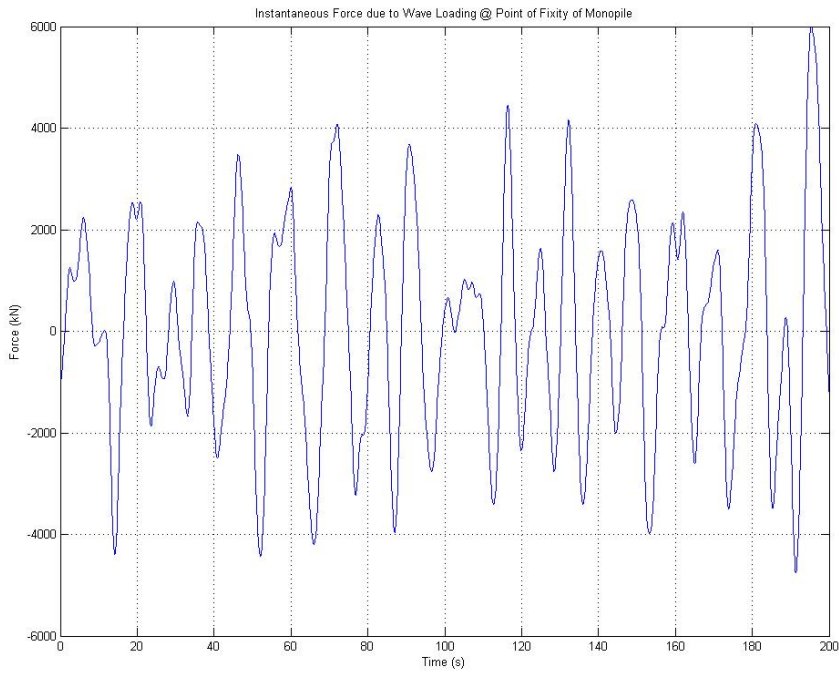
**Figure 3-4: Sample Instantaneous Lateral Force at the Point of Fixity of the Monopile from Wave Loading**
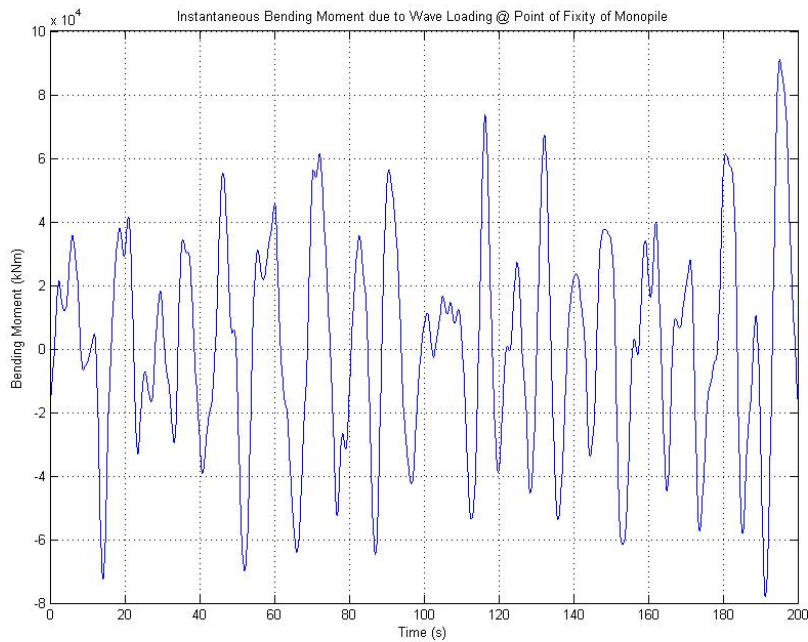


**Figure 3-5: Sample Instantaneous Bending Moment at the Point of Fixity of the Monopile from Wave Loading**

The other source of loading considered in this study is that of the thrust applied to the wind turbine at the hub. The hub height is constant at 90m above sea level while the thrust is determined from the wind speed, thrust per MW capacity curve and wind turbine rating. The instantaneous wind speed is determined from the Kaimal

Spectrum and superposition as discussed. Figure 3-6 illustrates a sample wind speed time series at hub height used in the model.



Instantaneous Wind Speed @ 90m Above Sea Level for Average Wind Speed of 12m/s
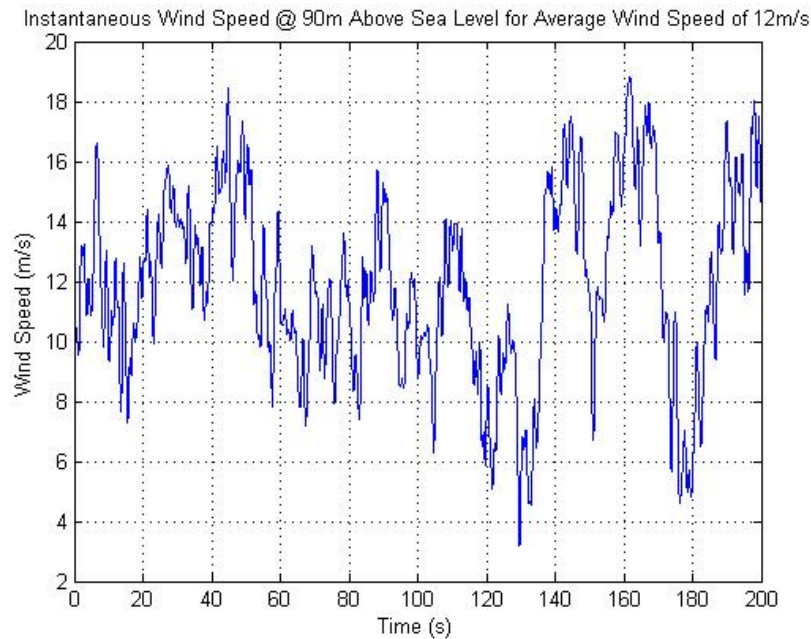
**Figure 3-6: Sample Instantaneous Wind Speed at Hub Height of the Turbine**

The wind speed time series is then used in conjunction with the thrust curve to determine the instantaneous lateral thrust load applied to the turbine at the hub height. A sample thrust time series is illustrated in Figure 3-7. It may be noticed that the thrust reaches a maximum value irrespective of the wind speed. This is due to the fact that the thrust curve is formed from an average thrust value for an averaged wind speed. In reality, the thrust at the rated wind speed may be higher depending on the speed at which the control mechanisms of blade pitch angle can react. For the purposes of this preliminary study, this method will suffice.
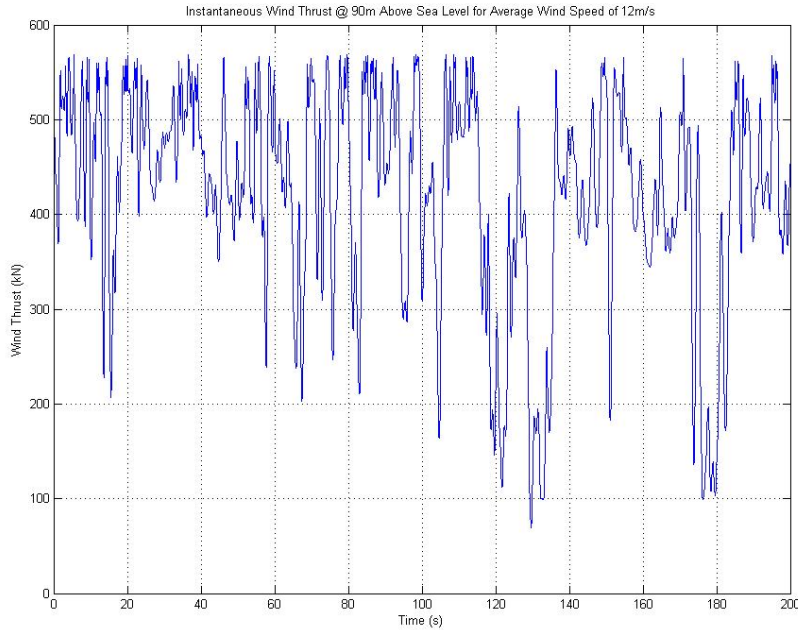
**Figure 3-7: Sample Instantaneous Wind Thrust at Hub Height of the Turbine**
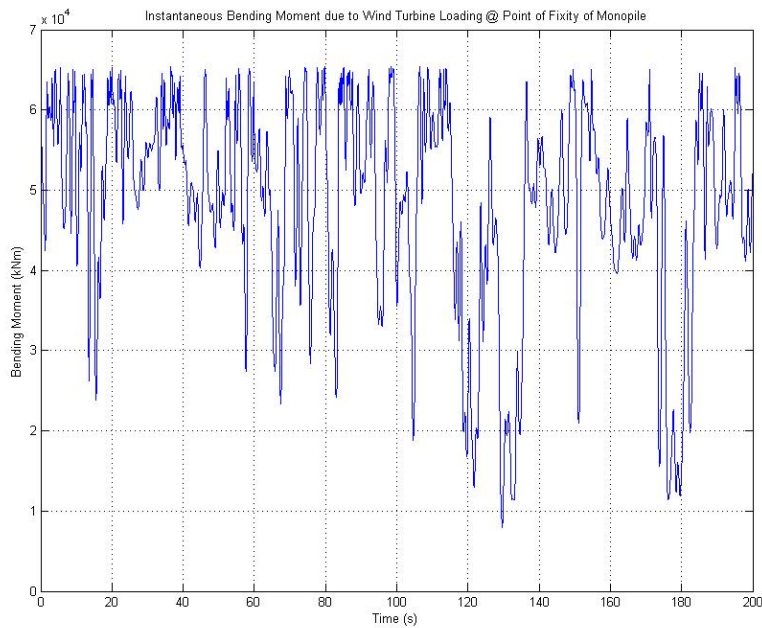


**Figure 3-8: Sample Instantaneous Bending Moment at the Point of Fixity of the Monopile due to Wind Loading**

The bending moment applied to the point of fixity of the pile may then be calculated by multiplying by the distance between the point of fixity of the pile and the hub height as illustrated in Figure 3-8. The contribution of both wind and wave loading on the pile are summed and the total shear force and bending moment applied to the pile at the point of fixity is determined. A sample plot of these is illustrated in Figure 3-9.
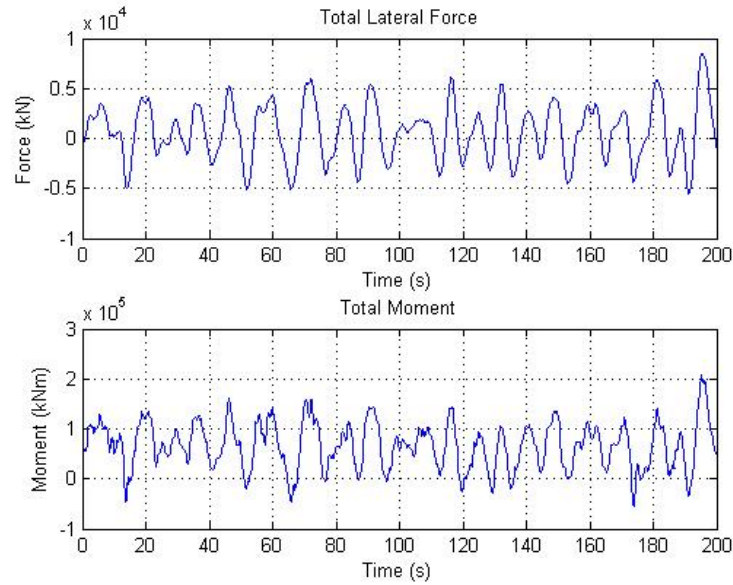
**Figure 3-9: Sample Total Lateral Force and Bending Moment on the Monopile**

The steel plate thickness from which the monopile must be fabricated to resist this loading is designed according to [116] following suitable load factors being applied to the design shear force and moment.

### 3.1.1.1.2 Model Validation

Simple tank testing has been carried out on a number of hybrid concepts to be discussed further in Chapter 4. One such model was a long slender pile with load cells incorporated into the pile to measure the hydrodynamic loading from incident waves described in APPENDIX C. The mathematical model described above has been used to estimate the loads likely to be experienced by the pile. The model configuration, in prototype scale, was a pile diameter of 3m in a water depth of 30m. The wave conditions were 3m $H_s$ and 10s $T_p$ Bretschneider Spectrum. The comparison between measured and modelled results is shown in Table 3-1.

**Table 3-1: Validation of Mathematical Model against Measured Data**

|  | Model (kN) | Measured (Scaled Up) (kN) | % Difference |
|---|---|---|---|
| Load @ -10m | 8.3 | 9.5 | -12.5 |
| Load @ -20m | 5.1 | 7.1 | -28 |

The results indicate that the mathematical model based on Morison's Equation underestimates the loads at both levels below water level. This may be due to several reasons including, incorrect drag and inertia coefficients used in the model, proportionately larger loads due to viscous effects at small scale tank testing which are then carried through in the scaled up figures. This is a common feature of tank testing in that such loads and damping are over-estimated relative to prototype due to scale effects of viscous forces and vortex shredding. As the figures are not an order

of magnitude larger than one another, this model may be deemed sufficient for preliminary design purposes.

### 3.1.1.1.3  Vestas V90 3MW Turbine Monopile Sizes

Figure 3-10 illustrates the dependency of monopile steel mass on water depth for the Vestas 3.0MW turbine. The results can be assumed to follow a linear trendline which is included in the plot as well as the equation for interpolation of further sizes depending on water depth.
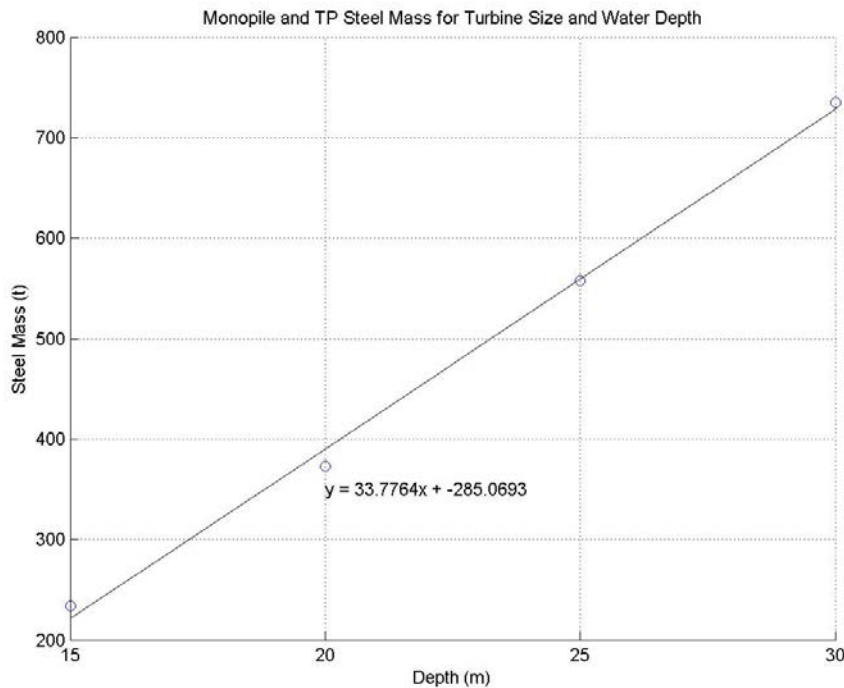


Figure 3-10: Dependency of Monopile Total Mass on Water Depth for 3.0MW Turbine

### 3.1.1.1.4  Siemens SWT 3.6-120 3.6MW Turbine Monopile Sizes

Figure 3-11 illustrates the dependency of monopile steel mass on water depth for the Siemens 3.6MW turbine. The results, similar to the 3.0MW turbine, may be assumed to follow a linear trendline which is plotted for illustrative purposes as well as the line equation for interpolation of other monopile sizes depending on the water depth of interest.
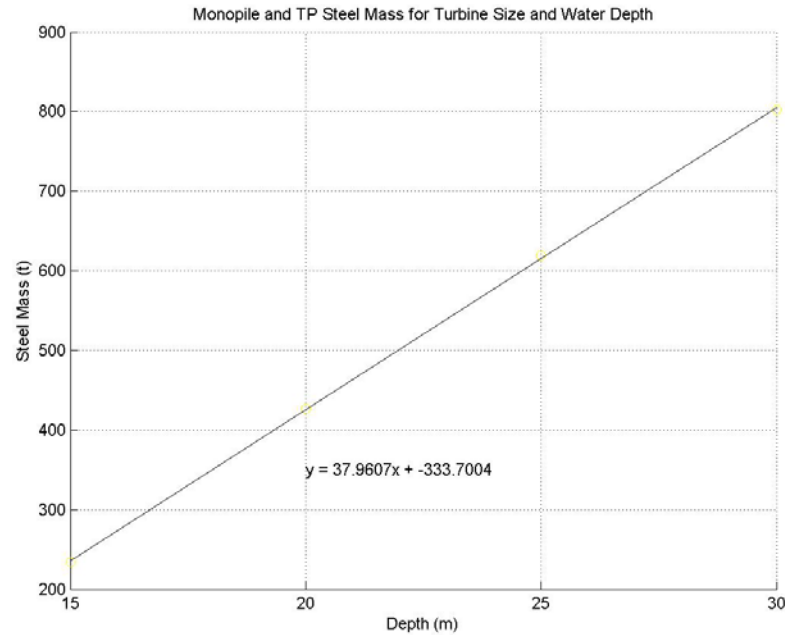
**Figure 3-11: Dependency of Monopile Total Mass on Water Depth for 3.6MW Turbine**

### 3.1.1.1.5  NREL 5MW Turbine Monopile Sizes

Figure 3-12 illustrates the dependency of monopile steel mass on water depth for the NREL 5.0MW turbine. The result is slightly different from the previous turbines as the lateral forces from the turbine are higher and contribute more to the steel requirements of the pile in lower water depths. As the water depth increases, the pile steel masses become similar to that required for the 3.6MW turbine in Figure 3-11 as wave loading again becomes the dominant force. The dependency of the pile mass for the 5.0MW turbine is a cubic function in this case and the equation is included in the plot for estimation of pile sizes in other water depths of interest.

### 3.1.1.2    Comments on Results

The results illustrate the trends to be expected in the design of monopile foundations for offshore wind farms, both existing and future farms. For the case of existing farms, take for example the results for the 3.6MW turbine in Figure 3-11. The foundation steel mass in shallow water of 15m is ~200t, while in 30m water depth this increases fourfold to ~800t while the depth has only doubled. The design appears to be weakly dependent on turbine size with the exception of designs in depths lower than 30m when the larger turbines provide significantly higher thrust loads and therefore bending moments at the foundation. It is anticipated that as the depth becomes higher that the foundation design will be dominated by wave loading and the turbine size will have a relatively weak effect. The results confirm the current train of thought surrounding monopile foundations by the industry. They simply cannot be feasible in deep water sites given the rate of increase of steel mass dependency on water depth. This is the reason for rigorous increase in efforts in design of alternatives including gravity based and steel jacket foundations.
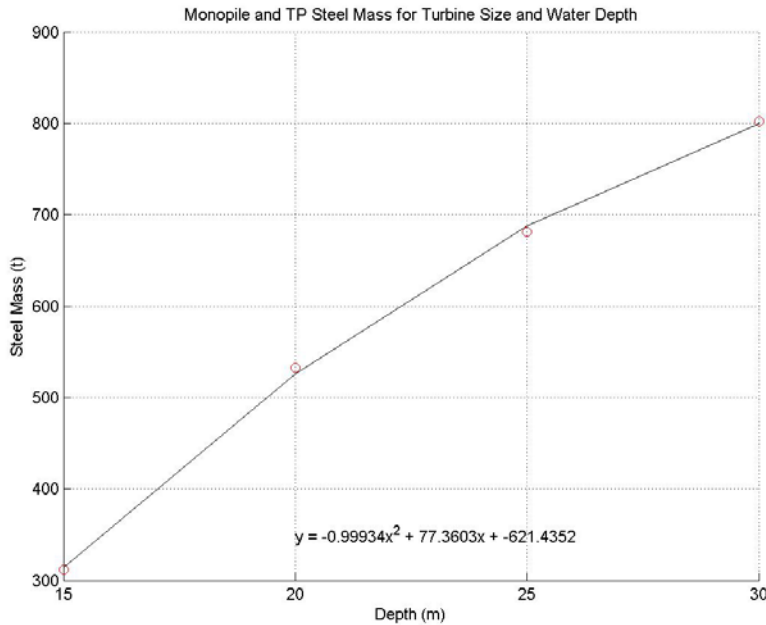
**Figure 3-12: Dependency of Monopile Mass on Water Depth for 5.0MW Turbine**

### 3.1.1.3    Unit Costs of Monopile Foundations

As the monopile foundation is the most widely used type, a generally accepted average unit cost per tonne production is approximately €2000/tonne steel mass. This is however a function of the steel plate sizes and the length of the monopile, as these imply the number of welds likely to be carried out during manufacturing which dictates the manufacturing costs. This section provides a means to estimate the variation in unit costs of monpiles using confidential information for a selected case, namely the 3.6MW turbine in 20m water depth. The case presumes the following details in Table 3-2.

**Table 3-2: Base Case Monopile Foundation Details**

| Item | Value |
|------|-------|
| **Monopile Mass** | 254.4 t |
| **TP Mass** | 118 t |
| **Pile Diameter** | 6 m |
| **Steel Plate Thickness** | 35 mm |
| **Monopile Length** | 49 m |
| **TP Length** | 22.9 m |

From a confidential percentage breakdown of the cost of manufacturing a monopile foundation, it is found that the approximate split of unit costs of a monopile and TP is 91% and 117% of the average respectively based on the Belwind Offshore Wind Farm average monopile and TP mass ratio of 30%. The market price of steel plate

and hot rolled sections is approximately €600/t currently [120]. Thus the fabrication cost of a monopile is ~€1230/t. Back calculating using these figures for the case study of the 3.6MW turbine in 20m water depth, it is found that the labour and overhead cost per hour is ~€31.20/hr based on the breakdown of fabrication costs from the [121], outlined in Table 3-3.

**Table 3-3: Steel Fabrication Costs Breakdown**

| Welding Costs Breakdown | % |
|---|---|
| **Labour and Overheads** | 85 |
| **Materials** | 9 |
| **Equipment Investment** | 4 |
| **Power and/or Gas** | 1 |

This cost of labour is determined from the time taken to weld all "cans" of a monopile together using standard steel plate sizes. The welding rates and operation times are taken from [122]. The preparation of a steel "can" for a monopile is illustrated in Figure 3-13 while a finished pile is illustrated in Figure 3-14. The rate breakdowns are used in the estimation of the unit costs of the other monopile sizes as calculated from the previous study.



**Figure 3-13: Monopile "Can" Rolling**

**Figure 3-14: Completed Monopile**

Figure 3-15 illustrates the dependency of the fabrication cost of the monopile on water depth for a 3.0MW turbine. Similar to the dependency of steel mass on depth, the unit cost of production has a linear dependency on depth.



Monopile Unit Cost for 3.0MW Turbine and Water Depth

$y = 104.22x + -200.7$
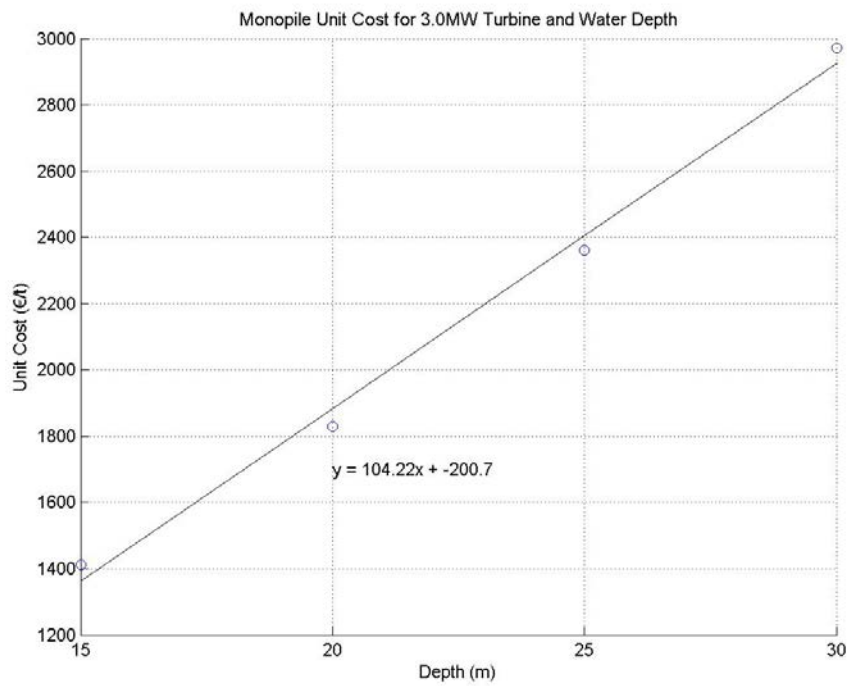
**Figure 3-15: Unit Costs of Monopile Only as a Function of Water Depth for 3.0MW Turbine**
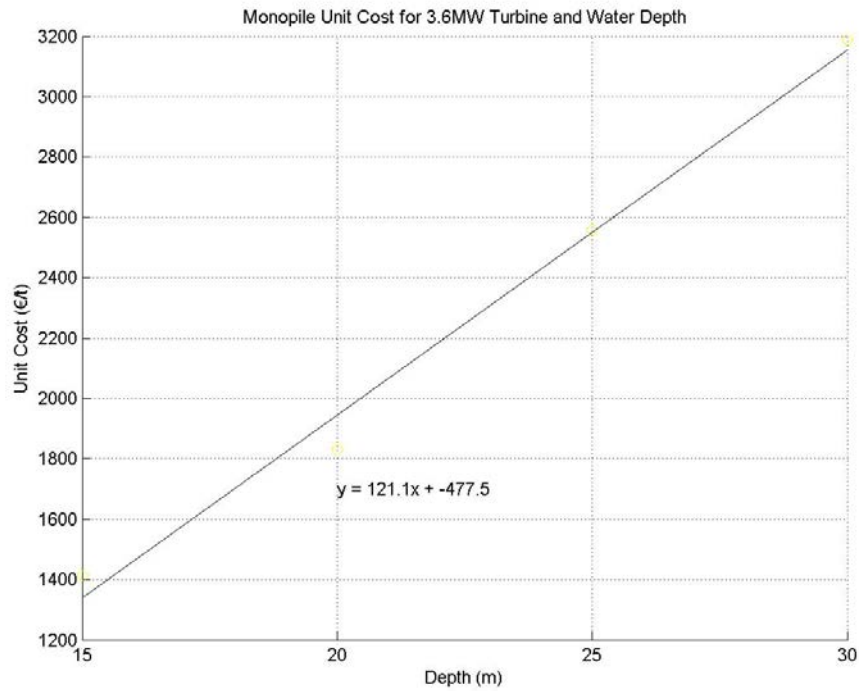
**Figure 3-16: Unit Costs of Monopile Only as a Function of Water Depth for 3.6MW Turbine**

Figure 3-16 illustrated the unit cost of production of a monopile dependency on water depth for a 3.6MW turbine. Again, a linear dependency is observed for the unit cost with water depth similar to the steel mass dependency.
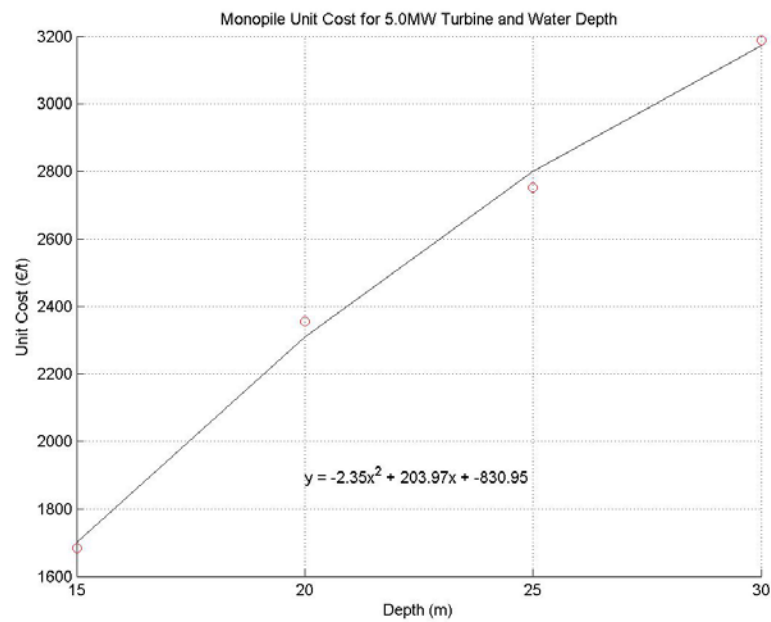


**Figure 3-17: Unit Costs of Monopile Only as a Function of Water Depth for 5.0MW Turbine**

It may be seen that the unit cost of the monopile is only weakly dependent on the turbine size, and mainly dictated by the water depth to be deployed in. The nature of the dependency of both monopile and TP mass and the unit costs of same can be seen to become more non-linear as the turbine size gets larger as illustrated in Figure 3-17 for the 5MW WT. This is similar to the mass dependency on depth and is likely to become linear again in deeper water depths as wave loading dominates. For the purposes of this thesis, these are the limits which will be investigated however, in the future as larger turbines come to market, the dependency of the mass and unit costs of the monopile foundation should be investigated and alternatives considered. One final observation, from both the structural mass dependency and unit cost of production dependency on depth is that as the depth gets larger, the piles become larger, heavier and progressively more expensive to produce.

### 3.1.2   Gravity Based Fixed Foundation

This section assesses the methodology of design of a GBS foundation and provides results from a parameterised model developed using Morison's Equation for hydrodynamic loads from spectral waves as well as turbulent wind loads at the hub for the three turbine types described above. The method of superposition is applied to both the wave spectra and wind spectra to provide a time series of representative loading on the structure. The variation of structural mass of the GBS foundation will be investigated for increasing water depth, turbine size and significant wave height and peak wave period.  The design of the GBS foundation is guided by [123] and [124]. A number of assumptions are made in the model are similar to those for the monopile with the exception of some specific assumptions relevant for the GBS foundation outlined below.

- The material factor for steel is constant at 1.15 as stated in [115] and the material factor for concrete is assumed to be 1.5 in accordance with [123].
- The yield strength of reinforcing steel is 460MPa.
- Upper cylindrical section of the GBS has a constant diameter of 6.5m.
- The base diameter of the GBS is related to the water depth by

$$\text{Base Diameter} = \frac{d}{1.5}$$

**Equation 3-3**

   where d is the water depth (m).
- The ultimate bearing capacity of the substrate is assumed to be 600kN/m$^2$.
- The Factor of Safety (FOS) against sliding, overturning and bearing capacity is > 1.5.

The outer shell of the GBS foundation is assumed to be constructed of one-way concrete slabs and beams. Therefore the study is primarily driven by the choice of,

1. Water depth,
2. Turbine rating,

3. Concrete wall thickness and,
4. Concrete beam width.

### 3.1.2.1  Results

This section presents the results of the simulations on the GBS foundation for each of the turbines considered. The values presented for the masses of the GBS are for structural masses only and do not include the ballast mass of sand which is pumped into the foundation following placement on the seabed.

#### 3.1.2.1.1  Vestas V90 3.0MW Turbine GBS Sizes

Figure 3-18 illustrates the GBS structural mass dependency on water depth for the 3.0MW turbine. Unlike the monopile, the dependency is not linear. A quadratic trendline is plotted as well as the equation for interpolation of GBS sizes for other water depths.



GBS Structural Mass for 3.0MW Turbine and Water Depth

$$y = 5.2196x^2 + -44.4143x + 125.4228$$
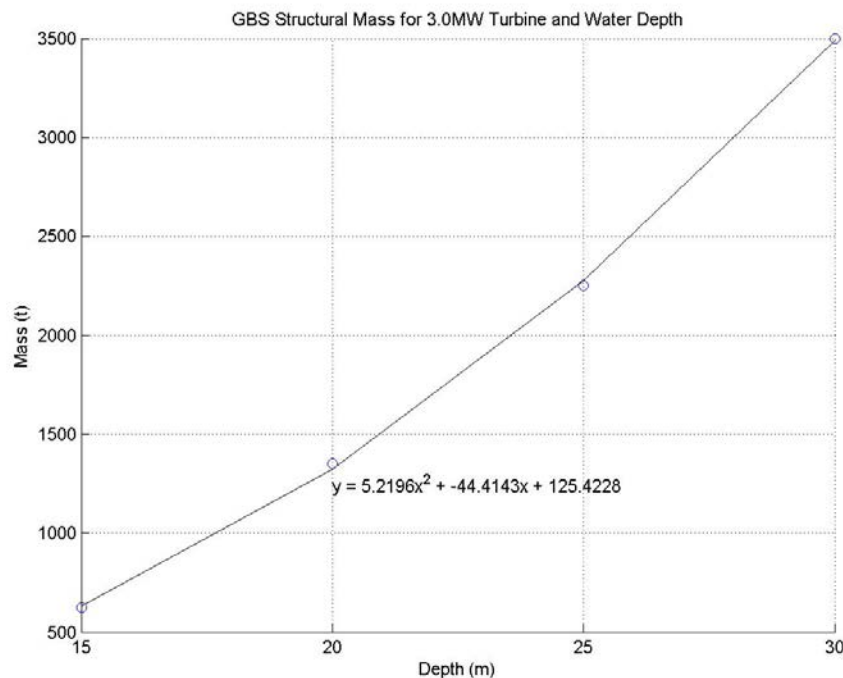
**Figure 3-18: GBS Structural Mass as a Function of Water Depth for 3.0MW Turbine**

#### 3.1.2.1.2  Siemens SWT3.6-120 3.6MW Turbine GBS Sizes

Figure 3-19 illustrates the dependency of GBS structural masses on water depth for the 3.6MW turbine. Similar to the 3.0MW turbine, a quadratic function is fitted to the values calculated and is plotted for interpolation of GBS sizes for other water depths.
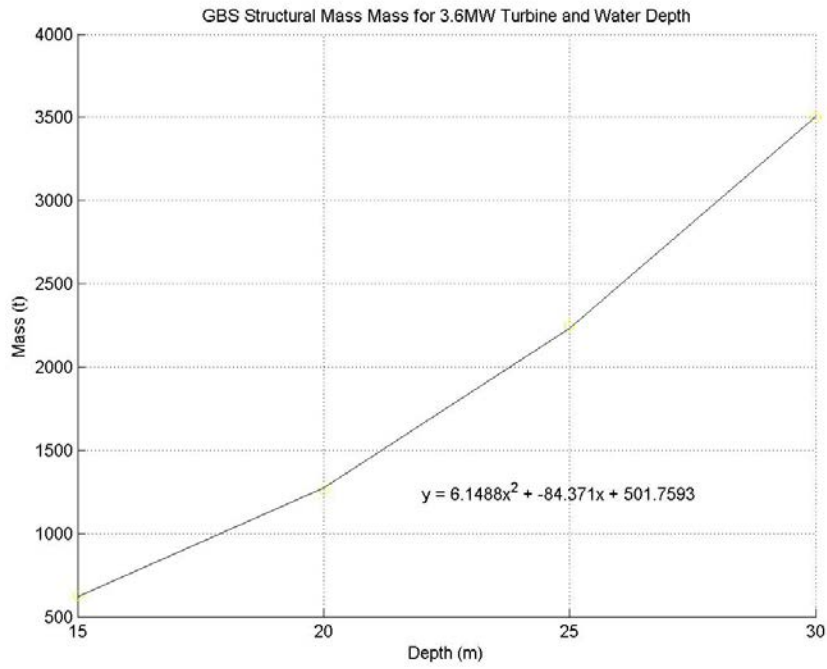
**Figure 3-19: GBS Structural Mass as a Function of Water Depth for 3.6MW Turbine**

### 3.1.2.1.3   NREL 5.0MW Turbine GBS Sizes

Figure 3-20 illustrates the dependency of GBS structural masses on water depths for the 5.0MW turbine. Again, a quadratic function is fitted to the dataset and is plotted for further interpolation of GBS sizes for other water depths.
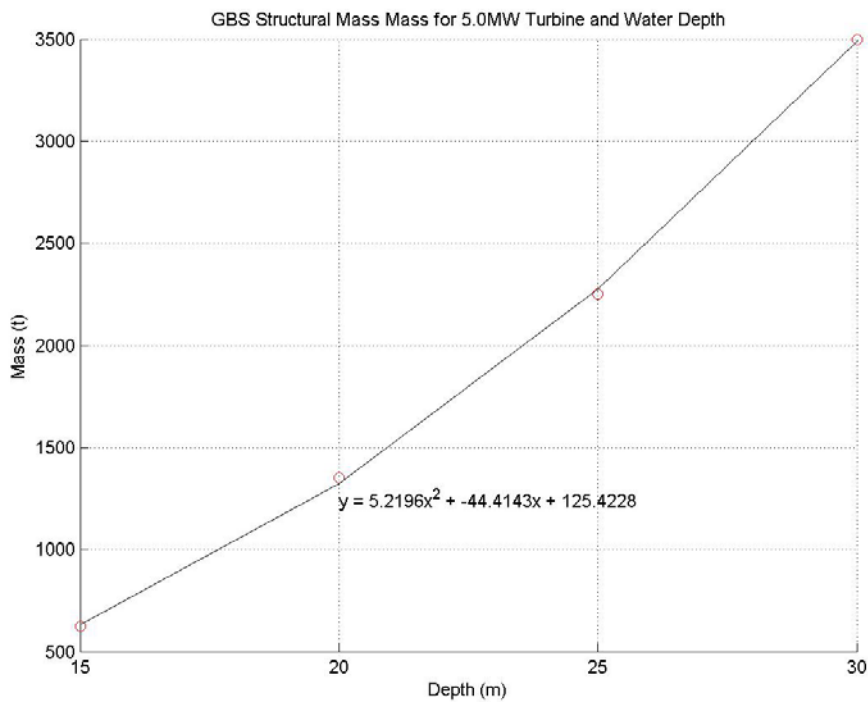


**Figure 3-20: GBS Structural Mass as a Function of Water Depth for 5.0MW Turbine**

### 3.1.2.2 Comments on Results

The GBS foundation structural mass is largely independent of wind turbine sizes used in this study. This may essentially be verified through the considerable difference in wave and wind loading experienced by the large volume submerged structure. No tank test validation data is available currently for the mathematical model, however a similar study carried out independently by a partner within the MARINA consortium has achieved similar results. The analysis has provided a basis for design of GBS foundations and/or other RC constructions through the global and local structural analysis carried out.

### 3.1.2.3 Unit Costs of GBS Foundations

The calculation of unit costs of RC construction is not a simple task given the range of options available for rebar preparation and installation, concreting etc. For the purposes of this study, the method of slip-form concreting has been chosen as it has been employed in conical RC structures previously, namely the Thornton Bank offshore wind farm illustrated in Figure 3-21 and the construction of the Troll and Heidrun oil platforms in Norway by Interform AS. This is a relatively expensive system compared to conventional formwork solutions, however saves considerably in time and labour costs, which are typical disadvantages of RC construction. The result can be an overall saving of 30-40% in comparison to conventional formwork construction methods for large and high structures [125]. Concreting rates of in excess of 100t/day and height increases of 2.5-3m/day are achievable using slip-form methods.

The time taken to construct one foundation for the Thornton Bank was 135 days on average, with ~2700t concrete and ~400t reinforcing steel. The steel content by volume is within the range of 4-6% which is the typical standard range for RC construction. Outside this range, i.e. >6%, the complexity increases considerably due to steel reinforcement spacing and the methods of approximating costs as carried out here may not be applicable. It is assumed that a team of four men can lay 1t of rebar in an eight hour day, at an unskilled labour cost of €10/hour. Thornton Bank, on average across the entire construction period, required 3t rebar to be laid per day, therefore the labour cost for steel was ~€1000/day. It is assumed that a two man team can lay 10t concrete per day, at a rate of €10/day. Thornton Bank required that 20t concrete per day be laid averaged across the entire construction period. Therefore, four men in an eight hour day will cost €320/day. The material cost of concrete is assumed to be €62.50/t while reinforcement steel is ~€600/t, therefore costing €1250/day and €1800/day respectively. On a per foundation basis, the port area costs are assumed to be ~€40,000 per foundation, therefore ~€300/day. It is assumed a tower crane and 300t crawler crane can service two foundations at a time. Based on standard day rates, these will cost in total €750/day. The formwork and associated works to be carried out in moving and preparing them and labour is assumed to be between 50-60% of the sum of these costs. Therefore, the total approximated cost per day for Thornton Bank per foundation was ~€9287/day including contingencies

of 10%. The total foundation cost was ~€1.25m and ~€400/t RC. Any further requirement of this figure will assume that if the steel volume content can be kept within the 4-6% range that this unit cost, or close to it, is applicable.

This simplified assessment of costs of RC construction suggests a percentage breakdown as tabulated in Table 3-4.

Table 3-4: Approximated Unit Cost Breakdown for RC Construction with 4-6% Steel Volume

| Costs Breakdown | % |
|---|---|
| Materials – Concrete | 13.5 |
| Materials – Steel | 19 |
| Materials Labour | 14.5 |
| Formwork and Labour | 32 |
| Equipment | 8 |
| Port Facilities | 3 |
| Contingencies | 10 |



Figure 3-21: Thornton Bank GBS Foundation Port-side construction site

### 3.1.3 Comparison of the Monopile and GBS Foundation in Deep Water

In the race to provide the next foundation capable of being deployed in deep water relatively cheaply, there have been many proposed solutions. These include the monopile and GBS foundations with some modifications to their respective designs. Using the simple models developed, a brief assessment of the potential for these

foundations in water depths of 40m with large turbines of 5MW capacity is investigated. The unit costs for these foundations are also determined using the respective methods proposed and a total production cost for each is determined and shown in Table 3-5.

**Table 3-5: GBS and Monopile Foundation Details for 5.0MW Turbine in 40m Water Depth**

| GBS | Value | Monopile | Value |
|---|---|---|---|
| **Concrete Mass** | 5266t | **Total Monopile Length** | 73.3m |
| **Concrete Thickness** | 700mm | **Steel Plate Thickness** | 80mm |
| **Steel Mass** | 961t | **Total Mass** | 1167t |
| **Total Cost** | €2.5m | **Total Cost** | €5.8m |

This simple assessment has illustrated that even in relatively shallow water depths of 40m, the monopile quickly becomes an unfavourable solution compared to other alternatives. This analysis has only considered two main options, the monopile and GBS foundations. There are of course additional alternatives such as the suction bucket foundation and the jacket foundation. The former requires detailed information on the substrate at the installation site and its successful design relies on complex calculations of soil-structure interactions. The latter also requires a detailed design process due to the 3D nature of the structure and number of members in the structure. The feasibility of the jacket is governed by number of members and the welding effort required. It must be noted however, that the installation process required for these large foundations should also be considered in the analysis of which foundation may be used.

## 3.2 Floating Foundations Analysis

This section analyses the main offshore wind floating foundation options, namely the semi-submersible and the spar floating foundations. Numerical frequency domain modelling has been used to assess the hydrodynamic motions and loads for each foundation. A simplified structural analysis and design has been carried out and hull costs calculated for each as a comparison.

### 3.2.1 Semi-submersible Floating Foundation

This section will analyse the Windfloat semi-submersible concept in terms of hydrodynamics and structural design to determine the hull construction costs of the platform using the methods discussed for the monopile and GBS systems.

#### 3.2.1.1 Hydrodynamics

The determination of the hydrodynamic loading on this occasion is carried out using the commercially available potential theory code WAMIT, which is considered the industry standard software for the frequency domain analysis of oil and gas floating and fixed platforms. The code is based on the hydrodynamic loading on the wetted

hull surface of the structure and allows the motion characteristics of the platform to be assessed assuming the geometry and mass matrix is input.

The wetted hull of the semi-sub was descretised into a number of rectangular panels, the size of which determines the accuracy of the results. The panel size reaches a limit after which, making the panel size any smaller, does not affect the results. The panel size and hull size directly affects the run-time of the simulations and so iterating to the optimum panel size is advised initially.

Following the specification of the geometrical properties of the structure, the frequency band of the assessment of the structure must be specified. For all concepts considered here, the frequency band considered is between 0.015rad/s to 3-4rad/s, i.e. ~150-200 points.

An additional input is required when the simulation results from the frequency domain analysis is to be used on their own, i.e. not as an input to a time-domain solver. This input is an external damping matrix itemising the damping to be applied to each mode. For head on seas for the semi-sub, motions in surge, heave and pitch are most important and therefore the damping to be applied at the resonant frequency may be calculated from [126]. Studies on a number of floating wind platforms by [74] and [75] have shown RAO and motion characteristics of a semi-sub platform based on the Windfloat design. The damping applied to the modes in this study has been guided by [126] but have been adjusted until similar results have been achieved as those in the [74] and [75].

The direct outputs of the frequency domain simulations include the motion RAOs of the platform, which for the semi-sub concept are illustrated in Figure 3-22. The translational (surge, sway and heave) and the rotational (roll, pitch and yaw) modes are shown for head on seas. Furthermore, the wetted hull panel pressure RAOs values at a wave period of ~8s are illustrated in Figure 3-23.
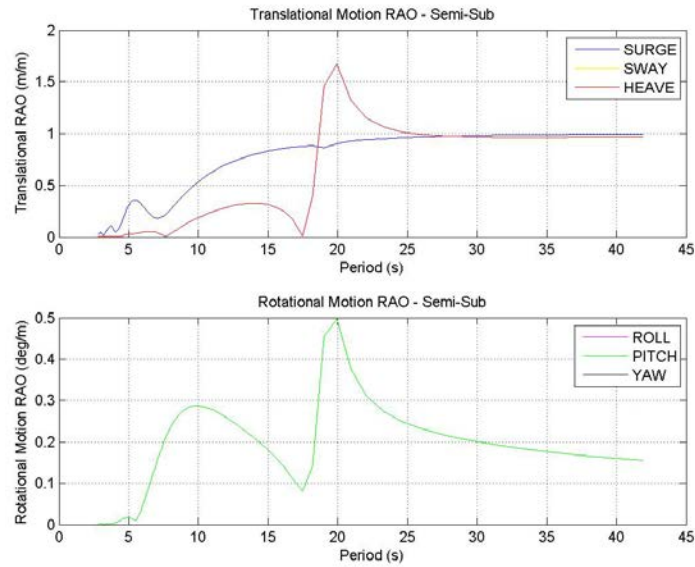
**Figure 3-22: Translational and Rotational Modes for the Semi-sub Platform**
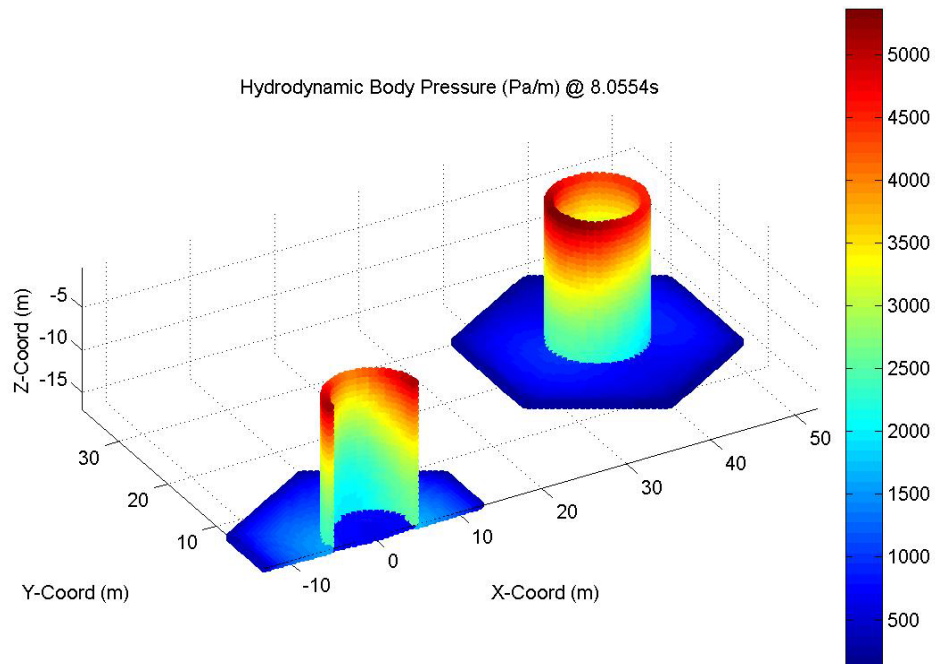


**Figure 3-23: Semi-Sub Wetted Hull Panel Pressures at 8s**

Following the calculation of the hydrodynamic motions and loads on the hull, an assessment of the structure may be carried out. Firstly, the motion characteristics of the semi-sub in terms of its response in the wave energy range of 5-15s wave periods. The heave response is at 20s which is significantly above the wave energy range. The pitch response is at 10s, but the magnitude is low. A true critique of the motion characteristics of the platform does require a full time domain solution to be carried out which is not within the scope of this chapter.

### 3.2.1.2 Structural Analysis

The panel pressures on the wetted hull can be used to perform, on a preliminary basis, a structural analysis of the hull. For this study, the method of superposition has been applied to the RAO of pressure at each panel for a design sea state of 15.0m $H_s$ and a $T_p$ value determined from guidance provided in [127]. The maximum pressure experienced on the hull on a specific panel is used as the design pressure. Reference [128] provides guidelines on the design of steel structures using steel plate and stiffeners. The method employed here varies the "T" beam stiffener spacing and calculates the steel plate thickness for each stiffener spacing to determine the optimum balance between the two in terms of minimum total structural mass of the hull for the given design pressure. The configuration of the structural members would resemble that in Figure 3-24.
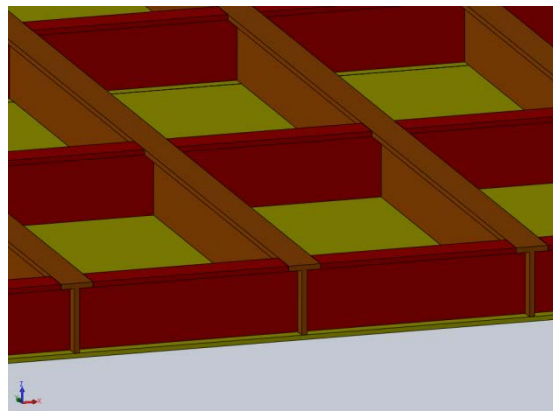


**Figure 3-24: Steel Plate and "T" Beam Stiffener Configuration**

The Monte Carlo (MC) simulation technique was used to assess a number of different realisations of short term sea state based on the random phase shift applied to each sinusoid to assess the impact on hull pressures and steel mass. The maximum mass calculated by this method is used as the final hull mass. The alternative to this method as described in [127] is to apply a 'multiplier' of between 1.1-1.3 to the response to account for the variations in short term sea state realisations. As it is unclear how an appropriate value for this parameter is determined, the MC simulation technique was used. Figure 3-25 illustrates the results of this analysis for the semi-submersible foundation considering NS of strength 235MPa as quoted by [128]. The optimum design was determined to have a stiffener spacing of 1.25m and an associated equivalent steel plate thickness of 23mm for the worst case of short term realisation of sea state for 20 MC simulations.
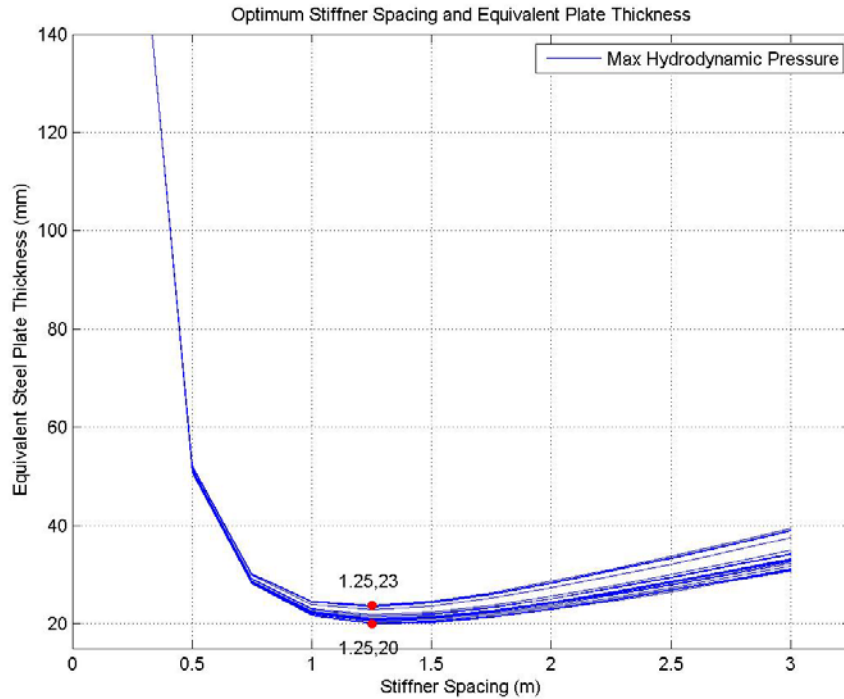
**Figure 3-25: Monte Carle simulation results of the equivalent steel plate thickness for optimum stiffener spacing**

As the simulations here have only considered a localised based design of the main columns of the semi-sub foundation, the steel mass of the foundation bracing structure is estimated to be 50% of the mass of the main columns and water entrapment plates. The actual design of the bracings requires a quasi-2D global design approach for which dedicated software and specialist analysis is required which is beyond the scope of this preliminary design exercise. For the purposes of preliminary design, a simple ratio can suffice. The total steel mass was determined to be ~1736t including a further 30% steel mass for internal bulkheads as illustrated in Figure 3-26.
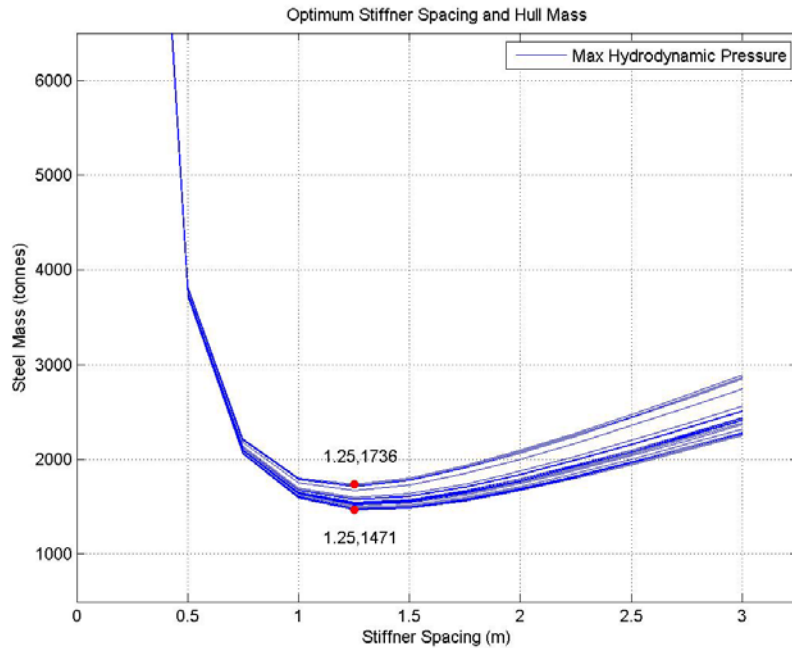
**Figure 3-26: Monte Carlo simulation results of the semi-sub hull total steel mass for optimum stiffener spacing**

The mooring loads on the structure have been assessed using the design wave conditions and the surge RAO of the platform through superposition. The catenary equations have been used as detailed in [129] to determine the mooring chain loads in order to size the chain. Approximations of the chain sizes and masses based on minimum breaking loads from [130] have been used. From the analysis, the mooring line total mass for a 4 line catenary system is ~80t in 100m water depth with a chain diameter of 45mm. The maximum mooring load was ~200t, and based on this information, using the [131], a Vryhof Stevin Mk3 or Mk5 anchor of mass 15t or 6t respectively would satisfy the design requirements assuming sea bed conditions of 'very soft clay'. These specifications are then used directly to determine the CAPEX cost of the hull and mooring system.

### 3.2.1.3    Unit Costs of the Semi Sub Foundation

The unit costs of the hull of the semi-sub foundation have been determined from the models developed previously for the monopile and GBS foundations. However, in the case of the steel plate and stiffener design method, a further uncertainty exists which is the radius of the fillet welds used to join the stiffener to the plate. This is a critical parameter as it directly affects the fabrication time and thus fabrication costs of the hull. This thesis has not considered localised fatigue design of the hulls which designs this parameter. For this reason, a simplification has been adopted. This is to consider both the maximum and minimum permissible weld sizes with respect to the stiffener and plate size being connected to determine the upper and lower bounds of the unit costs of fabrication. The upper and lower bound sizes of the weld are based on the root length and throat length of the weld. Based on the structural analysis carried out, the unit costs of fabrication for the semi-sub foundation are €1569-€5638/t. This gives a hull cost in the range of €2,723,784-€9,787,568.

### 3.2.2 Spar Floating Foundation

This section will analyse the spar type floating foundation in terms of hydrodynamics and structural design to determine the hull and mooring costs of the platform. Due to the considerations mentioned above regarding loads from both hydrodynamic and hydrostatic loads due to floater draft, both maximum anticipated hull pressures will be considered for design. The design with maximum steel requirements will be considered the governing design. The damping values were again guided by [126] and the studies carried out by [74] and [75].

#### 3.2.2.1 Hydrodynamics

The outputs of the WAMIT simulations are illustrated in Figure 3-27 and Figure 3-28. As mentioned, a thorough assessment of the motions of the platform would require a full time-domain simulation. As an indicator however, it would seem that the motions of the spar platform would be sufficiently outside the wave energy range as the heave period is in excess of 30s and the pitch period over 20s. The extreme responses would need to be considered in a full assessment.
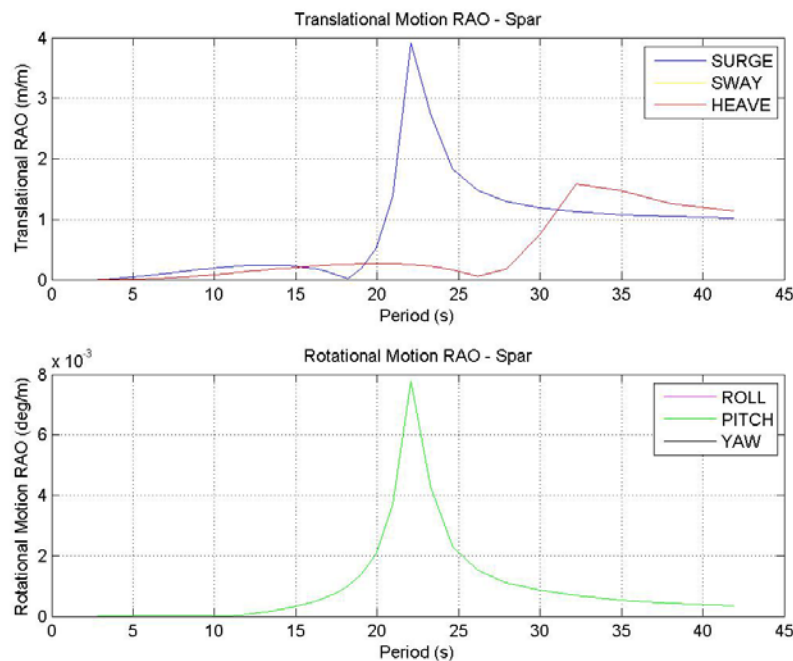


**Figure 3-27: Translational and Rotational Modes for the Spar Platform**

#### 3.2.2.2 Structural Analysis

The hydrodynamic pressures per metre wave height are illustrated in Figure 3-28 at a wave period of ~8s. It shows that the higher pressures on the hull are at the end of the spar close to the water level. In contrast the maximum hydrostatic pressure would be at the other end, at maximum draft. The structural design considering the hydrodynamic pressures are illustrated in Figure 3-29 and Figure 3-30 for a design $H_s$ of 15.0m and $T_p$ in the range specified by [127] for NS steel strength.
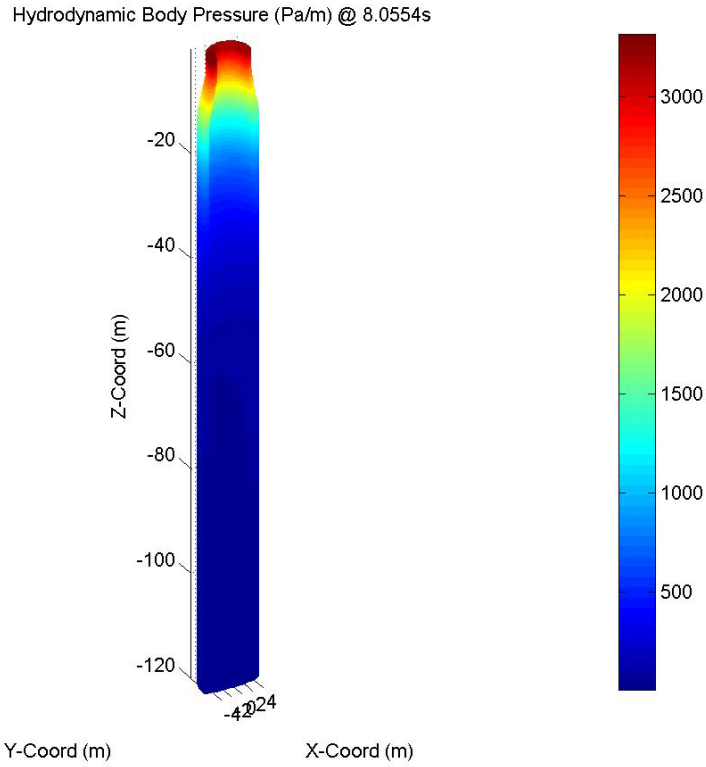
**Figure 3-28: Hydrodynamic Pressures per Metre Wave Height on the Spar Hull at ~8s**
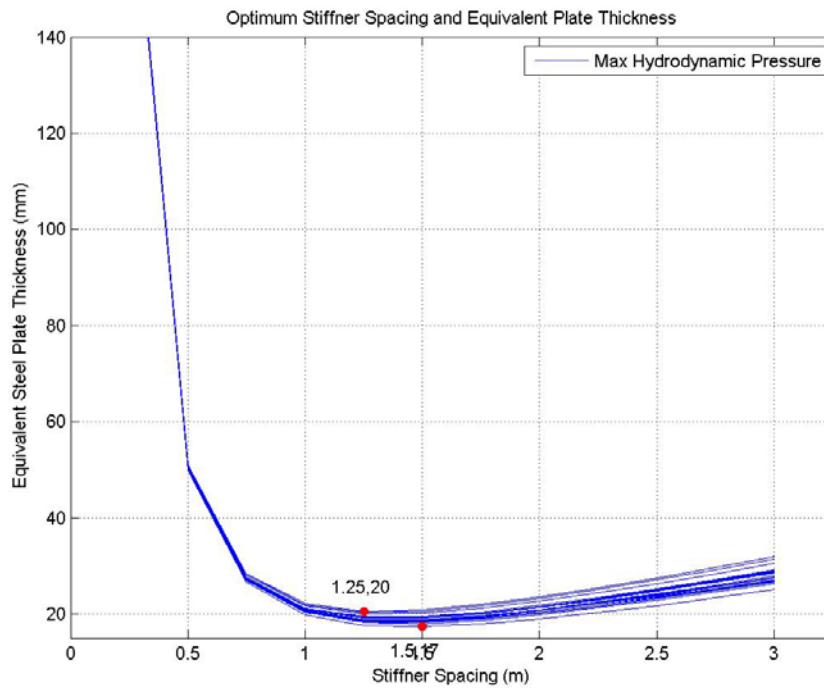


**Figure 3-29: Spar equivalent steel plate thickness for optimum stiffener spacing for hydrodynamic design pressure**
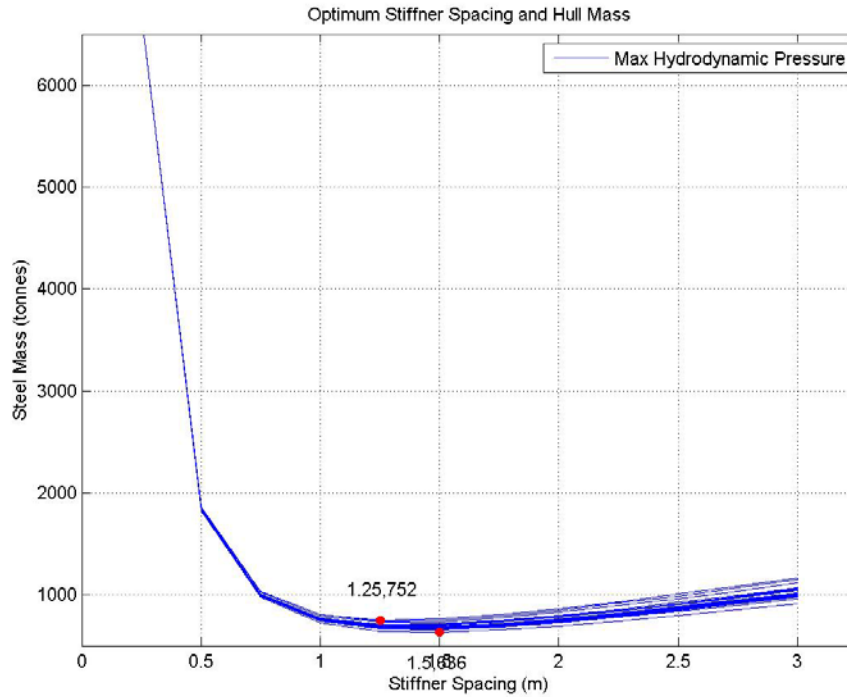
**Figure 3-30: Spar steel mass for optimum stiffener spacing for hydrodynamic design pressure**

The hydrodynamic design pressure results in an equivalent steel plate thickness of 20mm for a "T" beam stiffener spacing of 1.25m. Therefore a hull steel mass of 752t for the worst case scenario of 20 MC simulations considering different short term realisations of sea state is determined.

When the design pressure is taken to be the weighted hydrostatic pressure from 0-120m water depth, the required equivalent steel plate thickness is 57mm at a stiffener spacing of 0.75m as shown in Figure 3-31. The hull steel mass is then determined to be 2093t as shown in Figure 3-32.
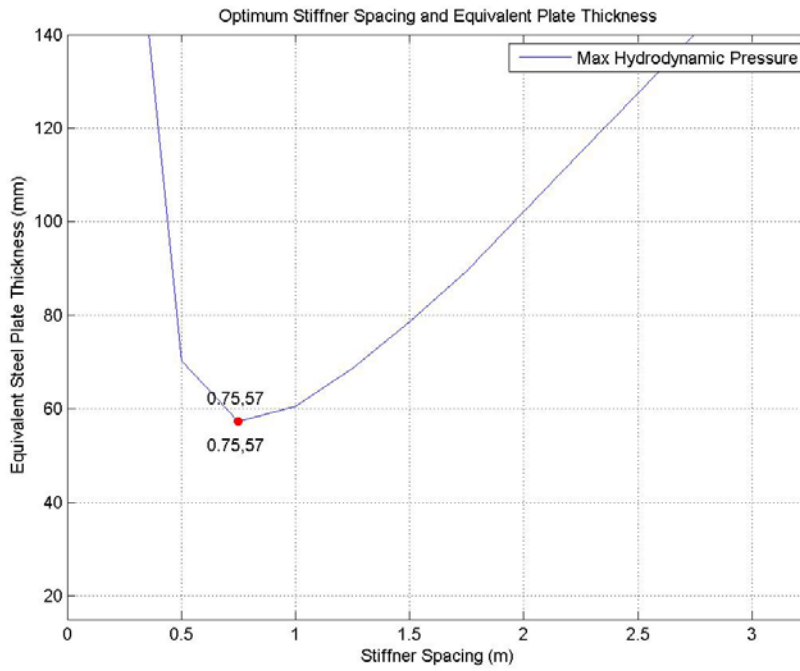
**Figure 3-31: Spar equivalent steel plate thickness and optimum stiffener spacing for weighted hydrostatic pressure**
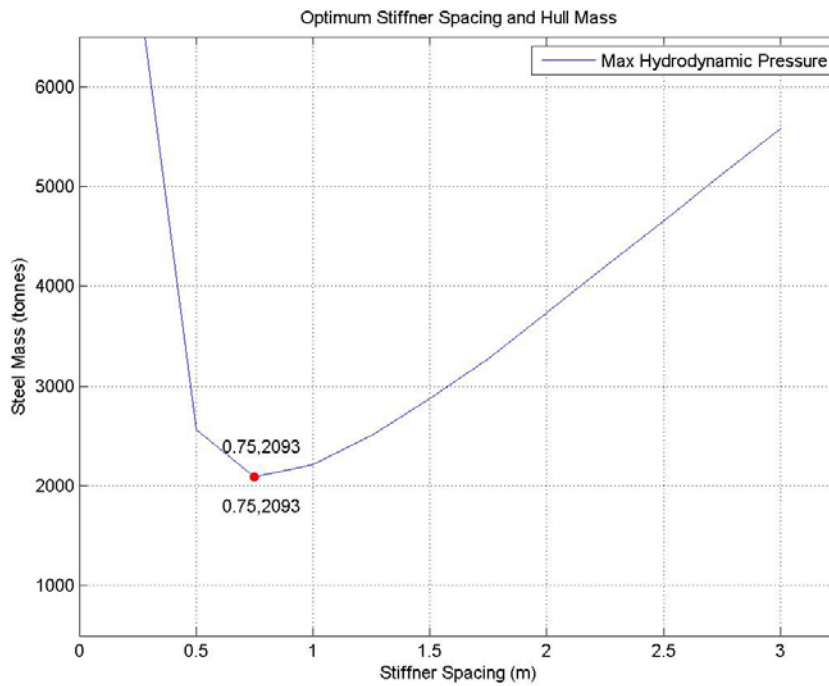


**Figure 3-32: Spar steel mass for optimum stiffener spacing for weighted hydrostatic pressure**

This design has incorporated the multiplier for variations in short term realisations of sea state as indicated by [127], and an additional 30% steel mass for internal bulkheads. A study carried out by [132] approximates that the OC3-Hywind spar platform has a steel mass of approximately 1900t. These two estimations are

acceptably close for the purposes of a validated preliminary design of the spar platform.

The design of the mooring lines has undergone the same process as that of the semi-submersible platform. The platform is assumed to be located in water depths of 200m for design $H_s$ of 15.0m. The catenary system consists of four mooring lines of chain diameter of 60mm, therefore a total mooring line mass of 287t. The maximum mooring load was ~390t, and based on this information, using [131], a Vryhof Stevin Mk3 or Mk5 anchor of mass 30t or 12t respectively would satisfy the design requirements assuming sea bed conditions of 'very soft clay'. These specifications are then used directly to determine the CAPEX cost of the hull and mooring system.

### 3.2.2.3 Unit Costs of the Spar Foundation

The unit costs have been determined in the same way as the semi-sub foundation, considering the upper and lower bound value based on the weld size limits. The unit costs have been determined to be between €1734-€3949/t. This results in a total hull cost in the range €3,629,262-€8,265,257.

## 3.3 Design Process for a Wave Energy Converter

As discussed early in this chapter, the design process for a wave energy converter is a rather complicated process. Currently, it seems that this process is confused and no clear strategy has emerged with the exception of the concept development protocol. This however relates to only one device configuration. The question is, how does one arrive at this device configuration, and is it a feasible option. The resource in Irish waters can vary from over 80kW/m in 150m water depth off the north-west coast to a mere 10kW/m in the Irish Sea. This makes for a perfect study as to what is the most feasible location for wave energy extraction, both in Ireland and worldwide, for a specific device. The device chosen for assessment in Ireland is the BBDB device, similar to the OE Buoy under development by Ocean Energy Ltd.

This section includes the selection of three sites around Ireland and the associated analysis for available power, weather windows and extreme conditions, the design of the BBDB type device for each site, and finally the performance of each device configuration at each site based on power production, structural masses and how the availability at each site may affect the ranking of these sites. The design process is illustrated in a flow diagram in APPENDIX A.

### 3.3.1 Irish Site Locations and Assessment

The three sites selected for analysis are located around Ireland as illustrated in Figure 3-33, each with significantly different wave climates.
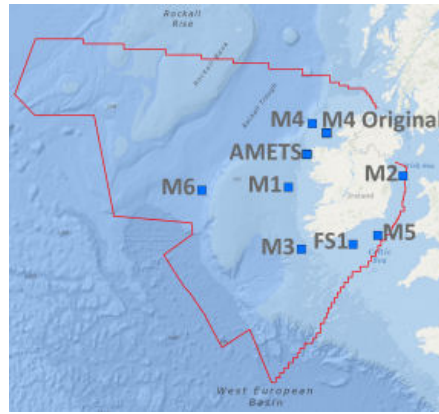
**Figure 3-33: Location of M buoys in Ireland [133]**

The location of the M1 data buoy is off the Galway coast in the west of Ireland (53°7.6'N 11°12'W) [134] in one of the world's most energetic seas, the North Atlantic. The annual average incident power is approximately 65kW/m. The annual average significant wave height ($H_s$) is approximately 3m while the $H_s$ with a 50 year return period ($H_{s,50}$) is approximately 15m. The M2 data buoy is located off the Dublin coast in the east of Ireland (53°28.8'N 5°25.5'W) [134] in the Irish Sea, in a rather benign wave climate relative to the M1 site. The annual average incident power is approximately 6.9kW/m. The annual average $H_s$ is approximately 1m while the $H_{s,50}$ is approximately 6m. The M5 data buoy is located off the Wexford coast in the south-east of Ireland (51°41.4'N 6°42.3'W) [134] where the North Atlantic meets the Irish Sea, in a medium level wave climate. The annual average incident power is approximately 18.7kW/m. The annual average $H_s$ is approximately 2m while the $H_{s,50}$ is approximately 11.5m. The averaged scatter diagrams of hourly occurrence of $H_s$ and upcrossing wave period ($T_z$) are illustrated in Figure 3-34, Figure 3-35and Figure 3-36. The typical annual average wave conditions and 50 year return wave conditions for each site are tabulated in Table 3-6. The water depth at each site has been assumed to be 100m for the design of mooring systems.

**Table 3-6: Site Characteristics Summary**

| Site | $H_s$ | $T_e$ | $H_{s,50}$ | Depth |
|------|-------|-------|------------|-------|
| M1 | 3 | 8 | 15 | 100 |
| M5 | 2 | 6 | 11.5 | 100 |
| M2 | 1 | 5 | 6 | 100 |
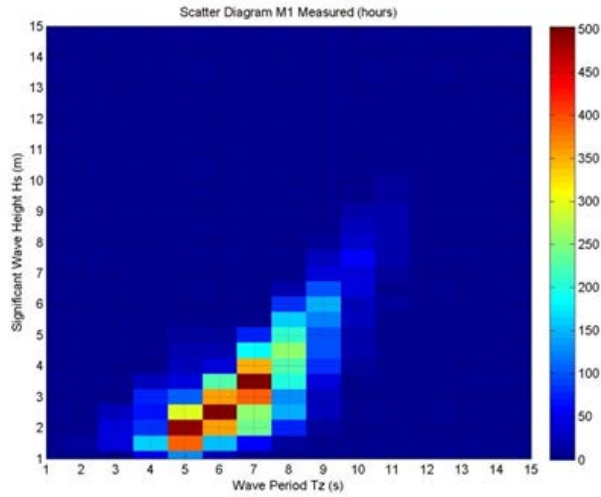
**Figure 3-34: Scatter Diagram for the M1 Location**
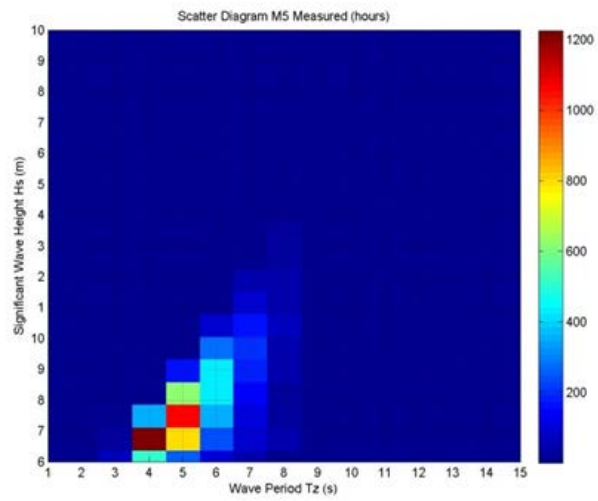


**Figure 3-35: Scatter Diagram for the M5 Location**
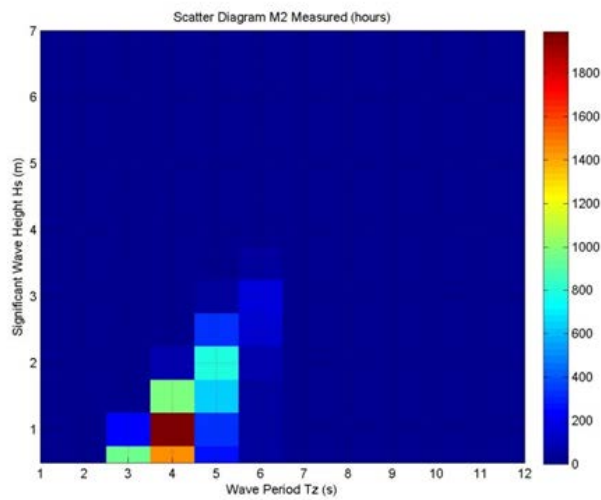


**Figure 3-36: Scatter Diagram for the M2 Location**

A weather window analysis has been carried out on the measured wave data from each of the M buoys specified. The constraints applied to the definition of a weather window are a $H_s$ limit of 1.5m for a time window of 12 hours. These constraints are typical of an offshore wind weather window definition, however their application to floating wave energy device access has not been verified. For simplicity, and for the purposes of demonstrating the methodology, the initial approximation of accessibility has considered these constraints sufficient and has applied them in the analysis. The M1 achieves accessibility of 11%, the M5 38% and the M2 58% based on these constraints annually. Ideally the maximum permissible WEC accelerations at the location of transfer for personnel and relative motion excursions between transfer vessel and WEC would be used. The relative acceleration and excursion constraints between vessel and WEC will result in redefining weather windows for floating wave energy devices and thus may significantly affect the current estimates of accessibility. It may be said that the issue of accessibility for WECs is extremely device dependent but generally speaking wave activated bodies without a floating reference structure will have extremely limited accessibility.

### 3.3.2 BBDB Device Design

The BBDB floating OWC device has been under development for more than 30 years. The primary benefit of the OWC device is the fact that only one moving part is required, i.e. the turbine rotor. Many configurations of the buoy have been proposed, both through tank testing campaigns [135] and numerical assessments [136] and [30] in order to optimise performance in terms of power absorption. Figure 3-37 defines the geometrical parameters of the BBDB.
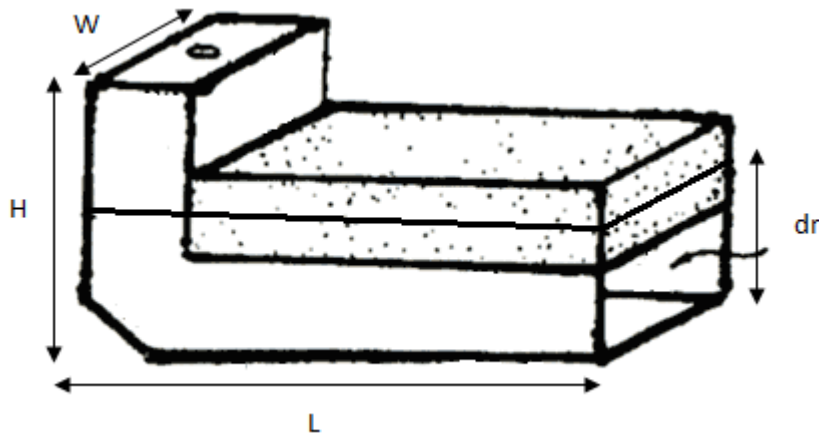


**Figure 3-37: Definition sketch of the BBDB geometrical parameters**

From the data provided by [135], three different configurations of BBDB were tested, each with a different duct length L. The device configuration with a near 1m duct length showed a resonance period of 1.1s. Assuming a scale of 1:50 for testing, it results in a full scale period of 8s, and a duct length of ~50m which is broadly in line with the required BBDB design for the North Atlantic Ocean wave regime. [31] carried out a study of the BBDB for Irish conditions and used a draft, dr, of ~13m for a ~50m duct. This is a L/dr ratio of ~3.9. Transferring back to 50th scale, the draft of

the models in [135] would have been approximately 240mm. Using this draft for the three configurations of duct length and relating the L/dr ratio to resonance period, the plot in Figure 3-38 is produced. A linear trendline is assumed for simplicity in the rage of 4-12s, the predominant design wave periods for most sites worldwide. This plot then allows the L/dr ratio to be determined for any site assuming the predominant wave period is known.



**L/dr Ratio Vs. IWS Resonant Period**

$y = 0.7019x - 1.3123$
$R^2 = 0.9789$
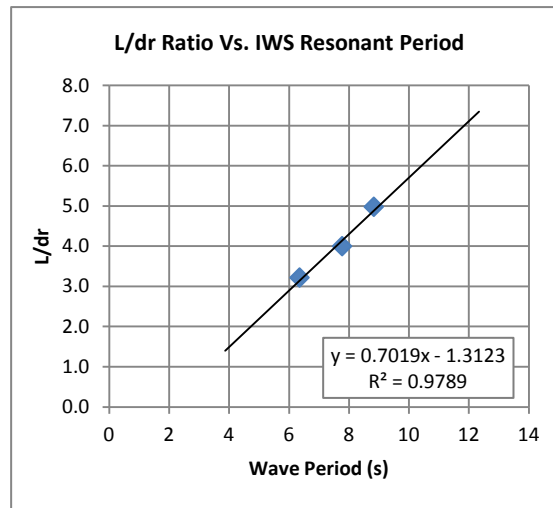
**Figure 3-38: L/dr Ratio for the BBDB**

The design process for the BBDB then requires a number of aspect ratios and dimensional ratios. The first is the shape of the bow plate. The aspect ratio of this plate for all designs is fixed at 1, i.e. the width W equals the height H of the bow plate. Secondly, the bow plate is submerged by 50%, i.e. dr = W/2 = H/2. Thirdly, the plenum width is set equal to W/3. The primary surface area of the buoy may be calculated from these dimensions, while an initial approximate primary mass can be determined by assigning an initial steel plate thickness. It was also determined that the additional steel for the two buoyancy tanks is approximately 10% of the primary surface area, this is then added to the primary steel mass and a further 15% mass added for additional equipment such as access platforms, turbine unit and associated electrical equipment. Using these basic guidelines, the designs for the BBDB's for each of the three sites are calculated and are tabulated in Table 3-7.

**Table 3-7: BBDB Designs for each Site**

| Site | Width | Draft | Plenum | Duct |
|------|-------|-------|--------|------|
| **M1** | 24 | 12 | 8 | 52 |
| **M5** | 18 | 9 | 6 | 26 |
| **M2** | 15 | 7.5 | 5 | 16 |

### 3.3.3 Hydrodynamic Numerical Modelling

This type of assessment would ideally be carried out in the early stages of technology development and as such would imply simplified methods of determining the main hydrodynamic responses and hull loads. For this reason, linearised frequency domain numerical modelling, using the industry standard

commercial code WAMIT, was carried out on each device configuration. The analysis was restricted to head seas as it is assumed that the BBDB mooring system will allow sufficient slack to weather vane into the incident waves during operational conditions. The surge, heave, pitch and IWS RAOs have been determined for each device configuration. The hydrodynamic pressure RAOs for each panel of the discretised hull have also been determined from WAMIT. As WAMIT is based on linear potential flow theory, it is unable to calculate viscous damping for the device. Therefore, empirical formulae for the estimation of the viscous damping in heave and pitch for the main hull structures have been estimated from [126]. The IWS also had to be rectified by the addition of empirical damping which was estimated from [106]. The linearised damping coefficient for moonpools is based on the water plane stiffness, added mass of the water plug and the damping ratio which depends on the geometry of the moonpool entrance. The following is the presentation of the results directly produced by WAMIT for this study.

### 3.3.3.1 Motion RAOs

The main hydrodynamic responses for the BBDB devices are illustrated in Figure 3-39, Figure 3-40 and Figure 3-41. It may be observed that in general, the response RAOs are reducing as the device becomes smaller which will have a significant impact on the power production and accessibility of the structures. The main observation however, is the resonance period of the IWS RAO plots. Overall, they are very much in line with the desired period for each intended site for each device configuration which builds confidence in the simplistic algorithm to estimate the buoy geometry based on predominant wave resource period.
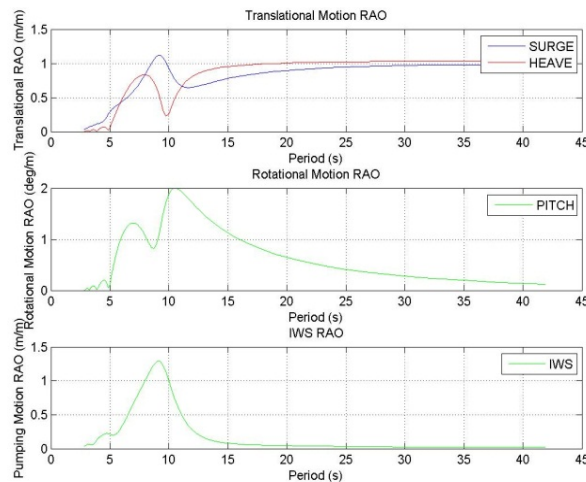


**Figure 3-39: BBDB RAOs for the M1 Location**
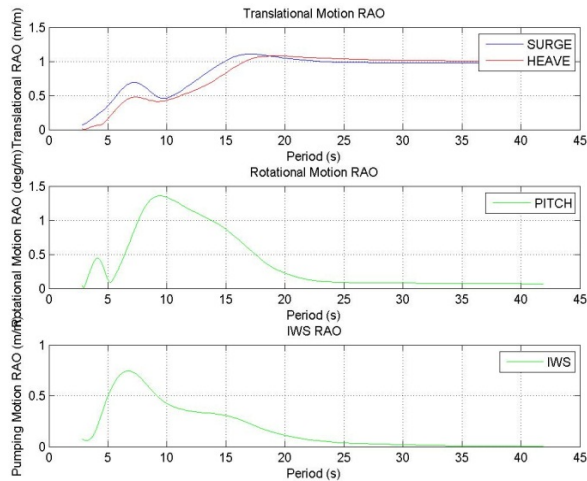
**Figure 3-40: BBDB RAOs for the M5 Location**
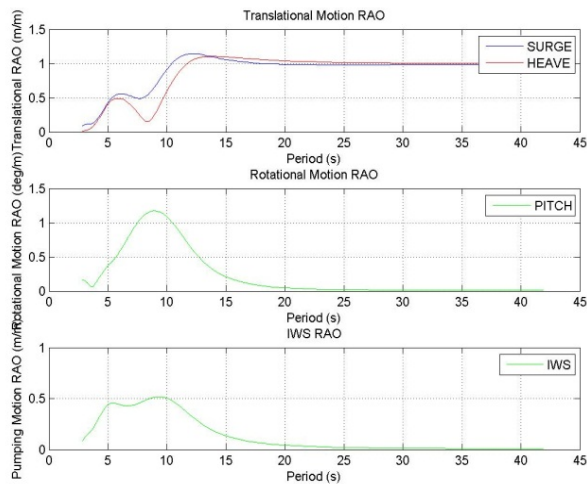


**Figure 3-41: BBDB RAOs for the M2 Location**

In order to validate these predictions made by WAMIT and the empirical damping applied from the various sources, a basic tank testing campaign was undertaken on one of the configurations of BBDB, namely the M1 device configuration. The model was fabricated from PVC sheeting and aluminium angle sections to provide stiffness to the hull. The model testing measured the motion responses of the buoy and IWS using a Qualysis Motion Capture system acquiring at 32 Hz, while the internal chamber air pressure was measured with a Honeywell pressure sensor with a range of ±175mm $H_2O$ again acquiring at 32 Hz. PTO damping was applied in the form of an orifice plate which was calibrated by a linear test rig to determine the discharge coefficient for a range of flows. The model is illustrated in Figure 3-42 in the wave flume at Beaufort Research - HMRC, University College Cork, Ireland.
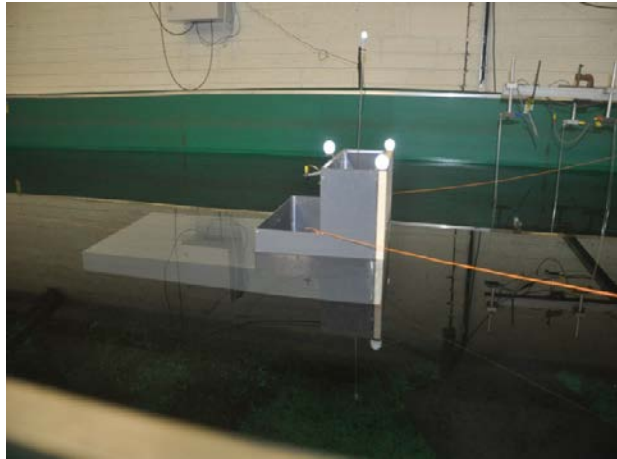
**Figure 3-42: BBDB Design for M1 Location at 1:50 Scale at UCC**

From initial results, it was found that the empirical damping calculated from [126] for heave, resulted in the device being over-damped. On removal of this heave damping and only applying damping in pitch, the results were better, though still over-damped in heave as illustrated in Figure 3-43.
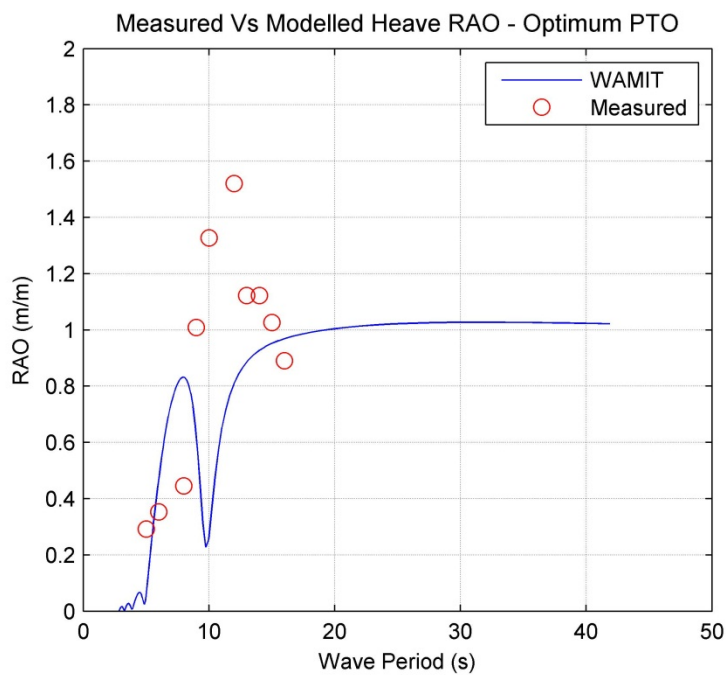


**Figure 3-43: Heave RAO for BBDB M1 Numerical and Physical Modelling Comparison**
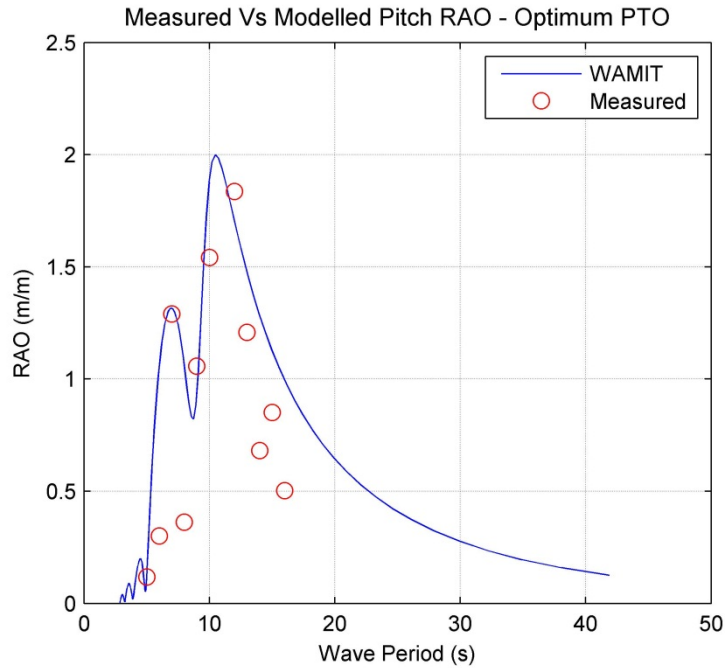
**Figure 3-44: Pitch RAO for BBDB M1 Numerical and Physical Modelling Comparison**
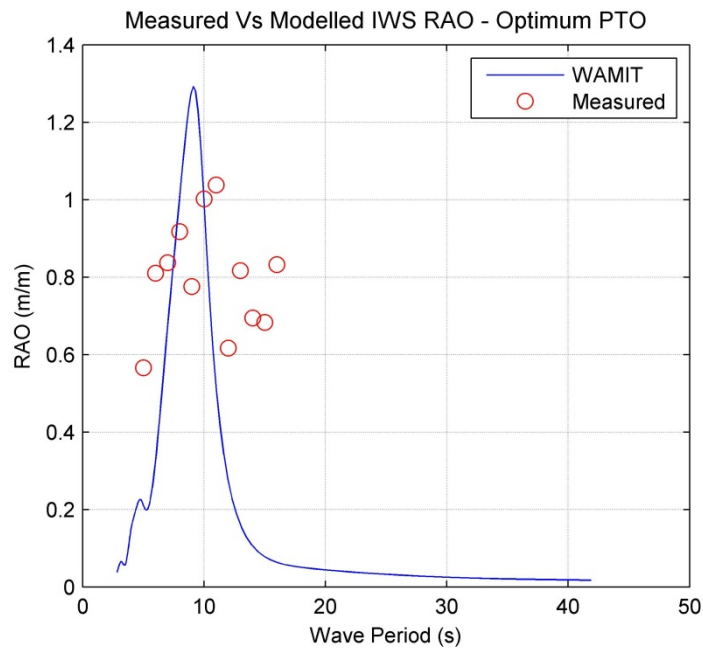


**Figure 3-45: IWS RAO for BBDB M1 Numerical and Physical Modelling Comparison**

The pitch RAO is acceptable with the exception of one outlier in the tank testing as illustrated in Figure 3-44. The IWS amplitude was also acceptable in relation to that measured as illustrated in Figure 3-45, however the scatter observed in the tank tests has been found to be more an issue with the method of measurement used rather than a true representation of the IWS motion. Nonetheless, the order of magnitude of both around the resonance period was encouraging.

The primary goal of the hydrodynamic simulation was the matching of the device designs determined from the experimental equation determined from Figure 3-38. Each device has been designed with the aim of ensuring optimum performance in each sea state considered. The following plots illustrate how this has been achieved. The aim has been to ensure the resonance period of the BBDB IWS coincides with the energy period of the sea state for which the device is intended. Figure 3-46, Figure 3-47and Figure 3-48 illustrate the performance of each device and confirms that the equation used to predict the geometry of the hull based on the target wave period is applicable and from these results, reliable. However, further simulations are required to confirm that different geometries can give the same resonance period at the target wave period.
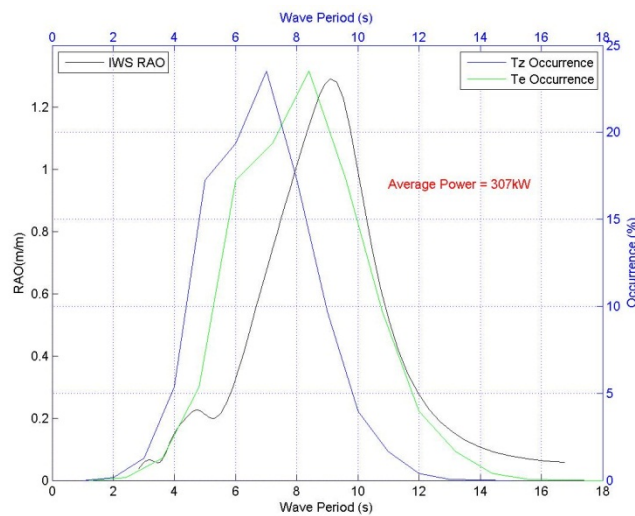


**Figure 3-46: Matching of BBDB M1 Device with M1 Sea State**
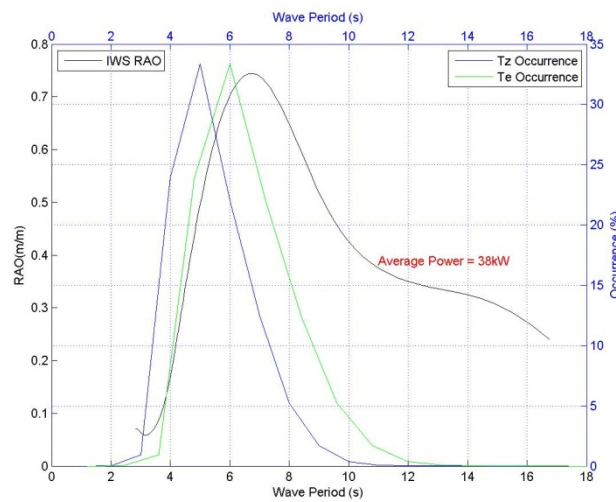


**Figure 3-47: Matching of BBDB M5 Device with M5 Sea State**
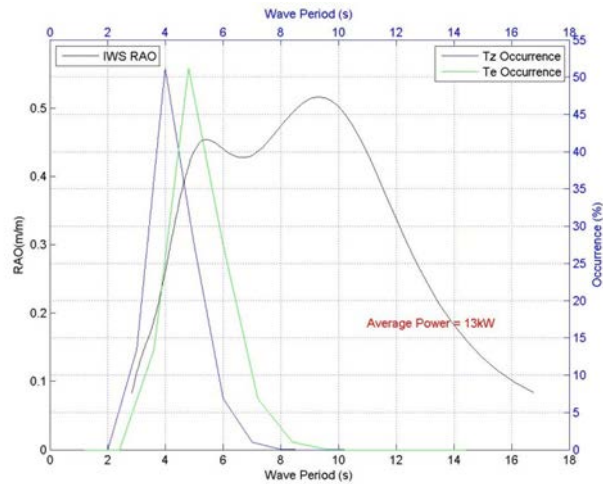
**Figure 3-48: Matching of the BBDB M2 Device with M2 Sea State**

### 3.3.3.2 Hydrodynamic Pressures

The excitation force on the hull shape in WAMIT is determined from the integration of the hydrodynamic pressures calculated at the centroid of each panel on the discretised wetted hull. The hydrodynamic pressure RAO for each panel is directly output and is used to determine the steel requirements of the hull in survival conditions. The information provided by the hydrodynamic pressures output is also critical for revealing the distribution of loads on the hull. Figure 3-49, Figure 3-50 and Figure 3-51 are an illustration of the hydrodynamic pressure distributions on each BBDB hull around the resonance wave period.
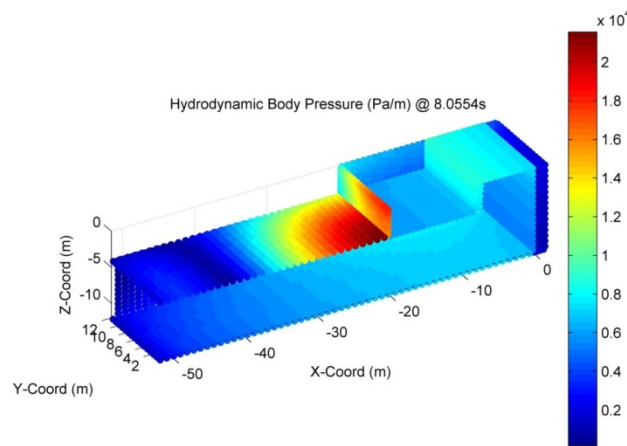


**Figure 3-49: BBDB for M1 Location Hydrodynamic Pressure RAO Values at ~8s**
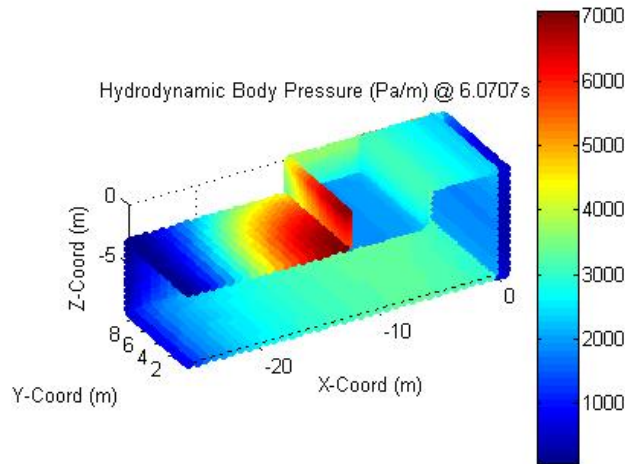
**Figure 3-50: BBDB for M5 Location Hydrodynamic Pressure RAO Values at ~6s**
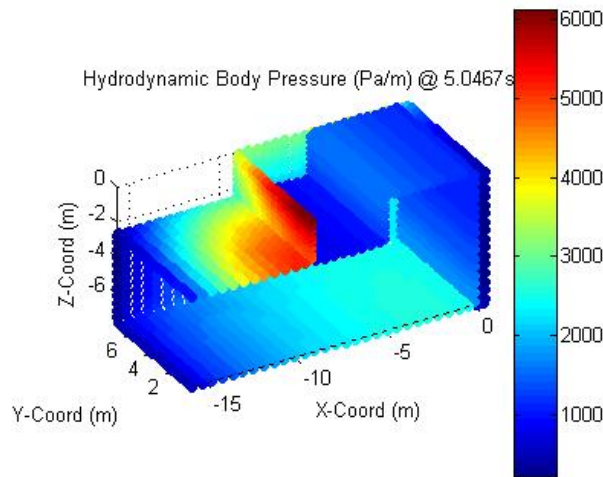


**Figure 3-51: BBDB for M2 Location Hydrodynamic Pressure RAO Values at ~5s**

### 3.3.4  Power Output Performance and Structural Design

For the assessment of the annual power output within defined operational limits and the determination of the indicative maximum structural loads on the hull for each device configuration, the 'principle of superposition', as first applied to hydrodynamics by [114], has been applied.

#### 3.3.4.1  Power Matrices

In the following analysis, this principle is applied in the determination of the power matrix of each device from the IWS response and the representation of each sea state within which the device may operate as a summation of sinusoidal waves. A random phase shift is applied to each sinusoidal wave, and as a result a Monte Carlo simulation technique is applied in the determination of the mean result for the power output at each sea state to account for the variation in each realisation of sea state through the effect of the attributed random phase shift between sinusoidal waves in

the principle of superposition. The number of simulations has been increased until convergence of the output is achieved. The resultant electrical power matrices are illustrated in Figure 3-52, Figure 3-53 and Figure 3-54 assuming a PTO efficiency of 54%. The annual power output of each device, at each site, is then determined by multiplying the power output in each cell of the power matrix by the hours of occurrence of that sea state determined from the scatter diagrams illustrated in Figure 3-34, Figure 3-35 and Figure 3-36. The results are tabulated in Table 3-8.
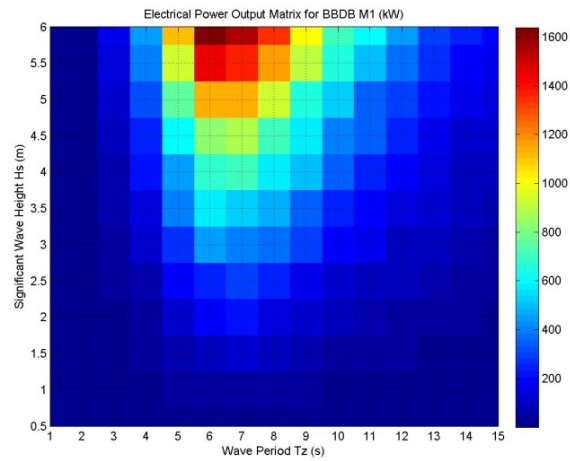


**Figure 3-52: Electrical Power Matrix for the BBDB M1 Location**
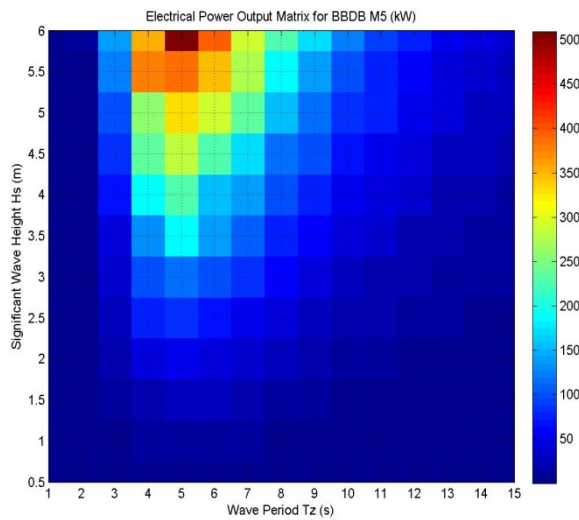


**Figure 3-53: Electrical Power Matrix for the BBDB M5 Location**
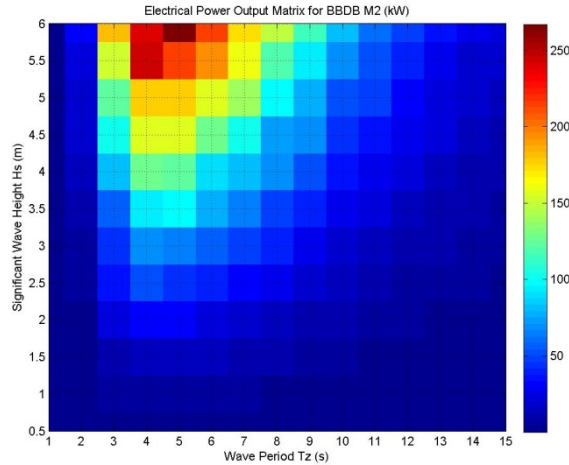
**Figure 3-54: Electrical Power Matrix for the BBDB M2 Location**

**Table 3-8: Power Output Performance of the BBDB's at each Site**

| Site | Power (kW) |
|------|-----------|
| M1 | 310 |
| M5 | 38 |
| M2 | 13 |

### 3.3.4.2 Hull Structural Analysis

The extreme $H_{s,50}$ conditions used for the structural design of the hull and mooring system are as tabulated in Table 3-6 for each site. These values were readily available from internal studies in the HMRC. However, design codes typically require return periods for individual environmental conditions of 100 years. In the case of the sites named in this study, similar studies have shown that the $H_{s,100}$ is c. 4% higher than $H_{s,50}$ [140], which it was thought was within the range of uncertainty in the analysis carried out on the raw data from the offshore M buoys. Thus $H_{s,50}$ was deemed sufficient to provide initial estimates of the hull structural mass. In [127], the range of wave periods to use with the extreme wave height is given in Section 3.7.4.2. The 'principle of superposition' was applied to the hydrodynamic pressure RAO of each panel of the discretised wetted hull of the structure to determine the hydrodynamic pressures during extreme conditions. The maximum panel pressure experienced by the hull during the extreme sea states was used as the design pressure. The LRFD design method was applied. A FOS of 2 was applied to the load, while a FOS of 0.95 was used on the yield strength of steel which was taken to be 235MPa for all designs as denoted for NS in [128]. A further FOS is applied to the load to account for extreme response variability from different short term sea state realisations as detailed by [127]. For this study, a multiplier of 1.3 could be considered to inflate the short term response. An alternative to the use of this multiplier is the use of the MC simulation technique to carry out many simulations to take account of the short terms variations in sea state realisations in the structural design. A simple comparison of these methods is included in the results. The configuration of the steel hulls were assumed to be constructed of standard steel plate sizes, with 'T' beam longitudinal and lateral stiffener beams welded to the plates as illustrated in Figure 3-24.

150

Based on the 'Plate and Stiffener' guidelines in [128], the minimum stiffener section modulus and stiffener spacing has been varied in order to achieve the optimum balance between steel plate thickness, stiffener size and spacing to achieve minimum steel mass for a specific simulation. The plots illustrating the variation in hull steel mass with stiffener spacing are shown in Figure 3-55, Figure 3-56 and Figure 3-57. The maximum optimum calculated structural mass for the hull is tabulated in Table 3-9 for both the MC Simulation technique using 20 simulations and the use of the DNV multiplier.
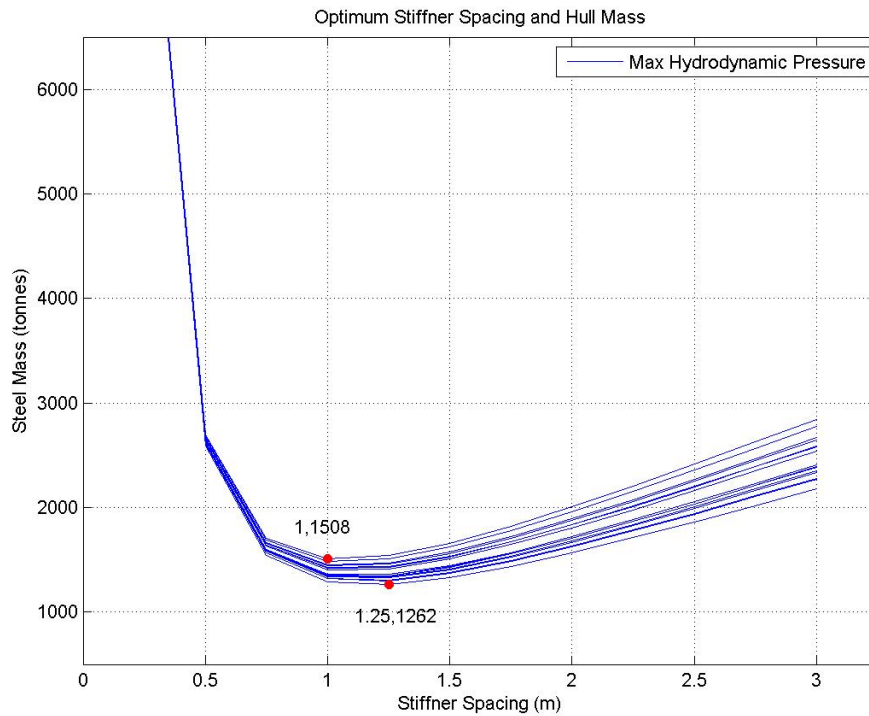


**Figure 3-55: M1 BBDB Hull Steel Mass for Optimum Stiffener Spacing**
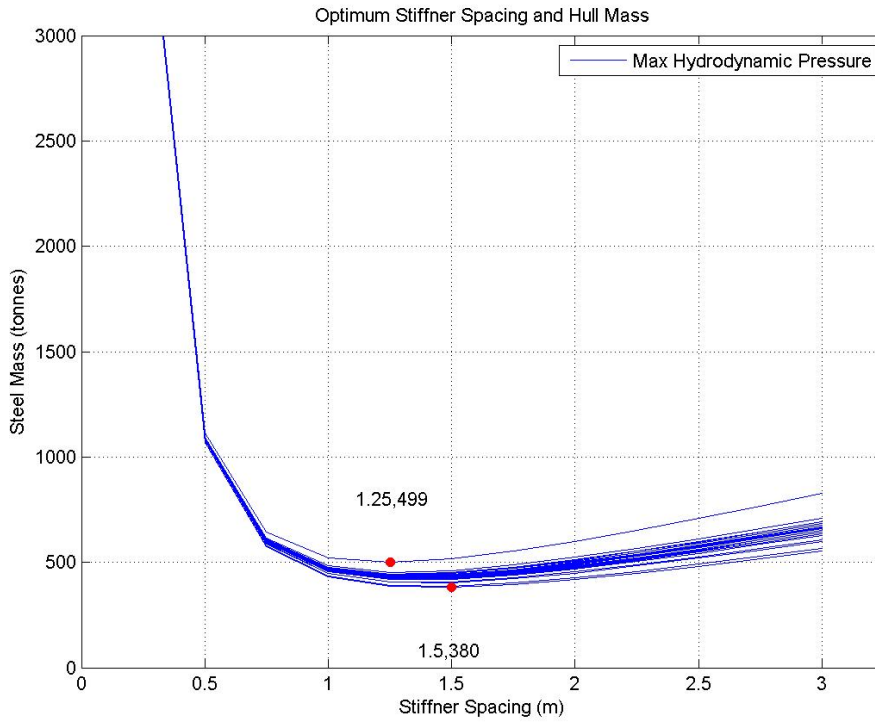
**Figure 3-56: M5 BBDB Hull Steel Mass for Optimum Stiffener Spacing**
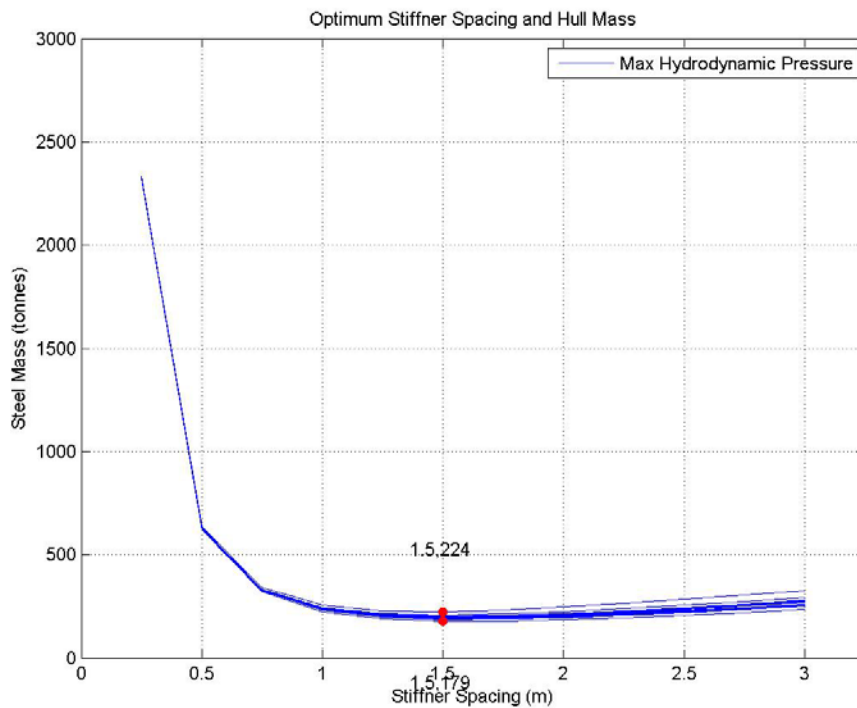


**Figure 3-57: M2 Hull Steel Mass for Optimum Stiffener Spacing**

### 3.3.4.3 Mooring System Design

The 'principle of superposition' was again applied to the surge motion RAO of the buoy to determine the mooring line loads during extreme conditions using the typical catenary line equations as listed in [129]. There was a FOS of 1.5 applied to the

mooring loads, as well as the aforementioned multiplier of 1.3 to account for extreme response variability due to different short term sea state realisations. The MC Simulation technique was also applied to the mooring system design to compare results. Guidelines provided by [130] for mooring chain design have been used to design the mooring chain size and mass required to resist extreme loading. The total mooring line masses as determined for each device at each site are tabulated in Table 3-9.

**Table 3-9: Structural Mass and Mooring Mass Summary**

| Site | Hull Mass (MC Sims) (t) | Hull Mass (DNV) (t) | Mooring Chain Mass (MC Sims) (t) | Mooring Chain Mass (DNV) (t) |
|------|------|------|------|------|
| **M1** | 1473 | 1434 | 120 | 143 |
| **M5** | 465 | 434 | 99.5 | 120 |
| **M2** | 215 | 223 | 80 | 99.5 |

### 3.3.5  Summary of Results

The results so far have presented the specifications of each device individually for each site. The following results combine them and relate the performance, both in terms of power output and structural design, to the incident resource the device is deployed in. The intention is to determine a parameter which may act as an indicator of site suitability using the available information at concept development stage. These results are specific to the geometry constraints applied to the BBDB hull designs considered in this study. Further simulations on the sensitivity of the power output to these geometry constraints will be considered. Firstly, the steel mass for each device is plotted against the incident wave resource in Figure 3-58. Although only three points exist on the plot, a linear dependence may be observed based on the constraints applied to the geometry. Furthermore, in Figure 3-59, the estimated annual energy production per tonne hull steel is presented. Although the power production per incident resource is non-linear in nature, the division by such a large number such as the total steel mass reduces this non-linearity such that an approximate linear relationship may be assumed. Between these two plots, an approximate steel hull mass and average annual power output may be estimated.
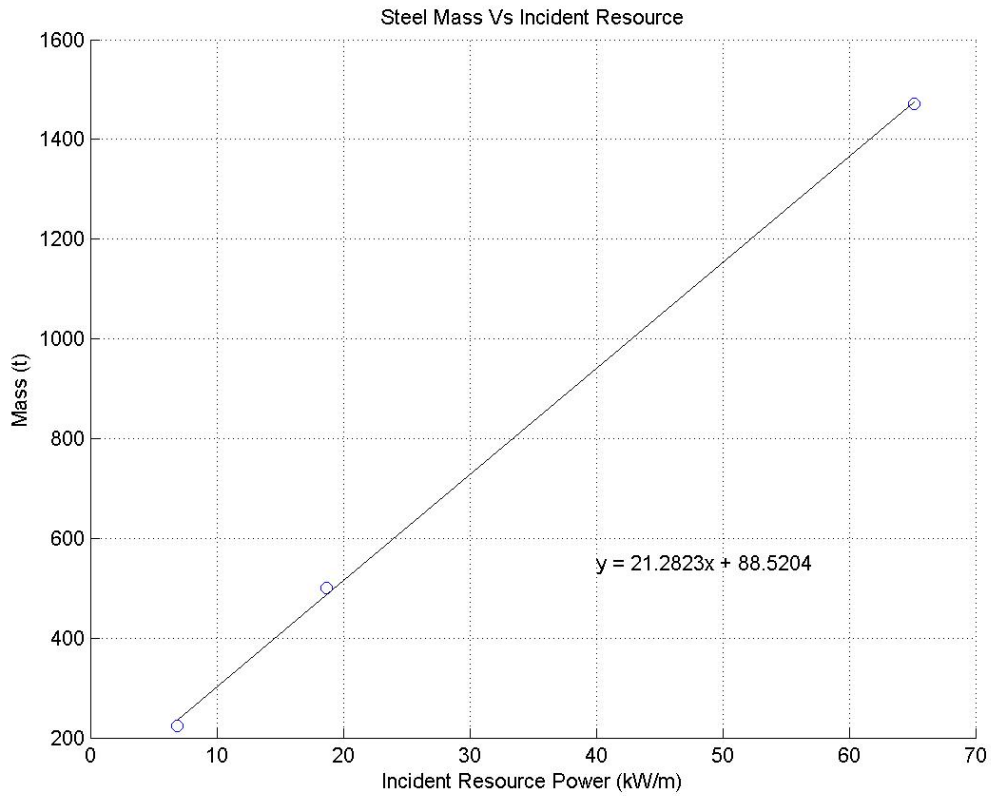
**Figure 3-58: Hull Steel Mass for each BBDB against Incident Resource**
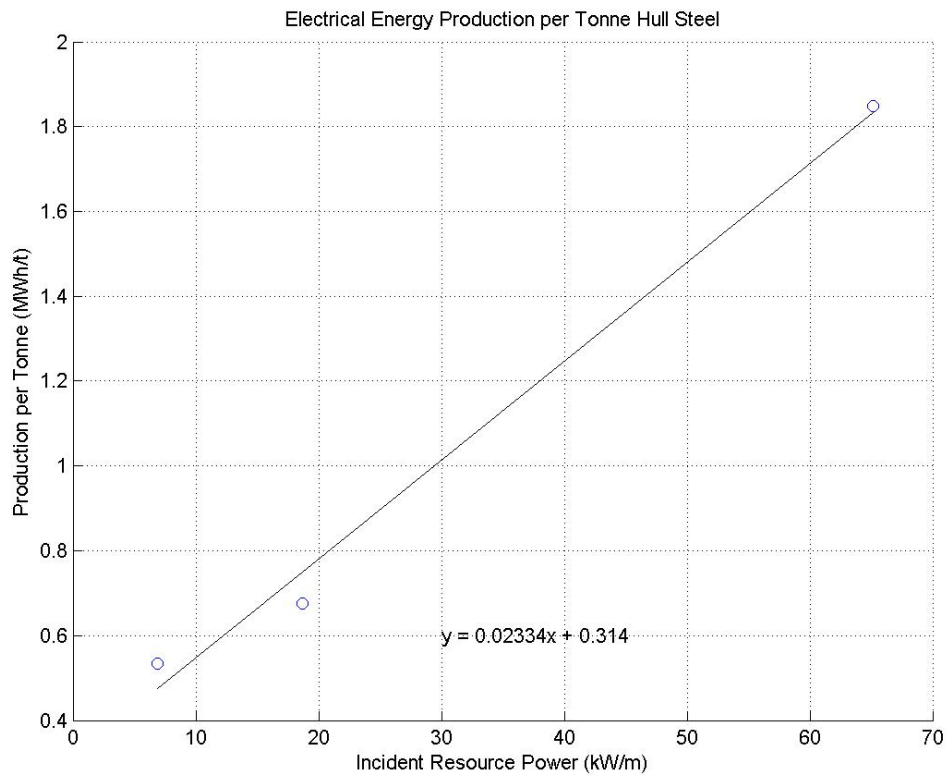


**Figure 3-59: Energy Production per Tonne of Steel for each BBDB against Incident Resource**

Figure 3-60 illustrates the approximate linear relationship between the steel mass and mooring mass ratio against incident resource. If a further parameter is added, the site accessibility, intended as an indicator of device availability, the anticipated energy production per tonne hull steel per site accessibility is given as in Figure 3-61. This is calculated by multiplying the annual energy output by the accessibility at that site. This rather surprising result reverses the expected annual energy production per tonne steel in Figure 3-59 in favour of the site with lowest resource. This result of course requires further validation from full site, device and O&M vessels assessments assuming PTO reliability is constant across all sites.
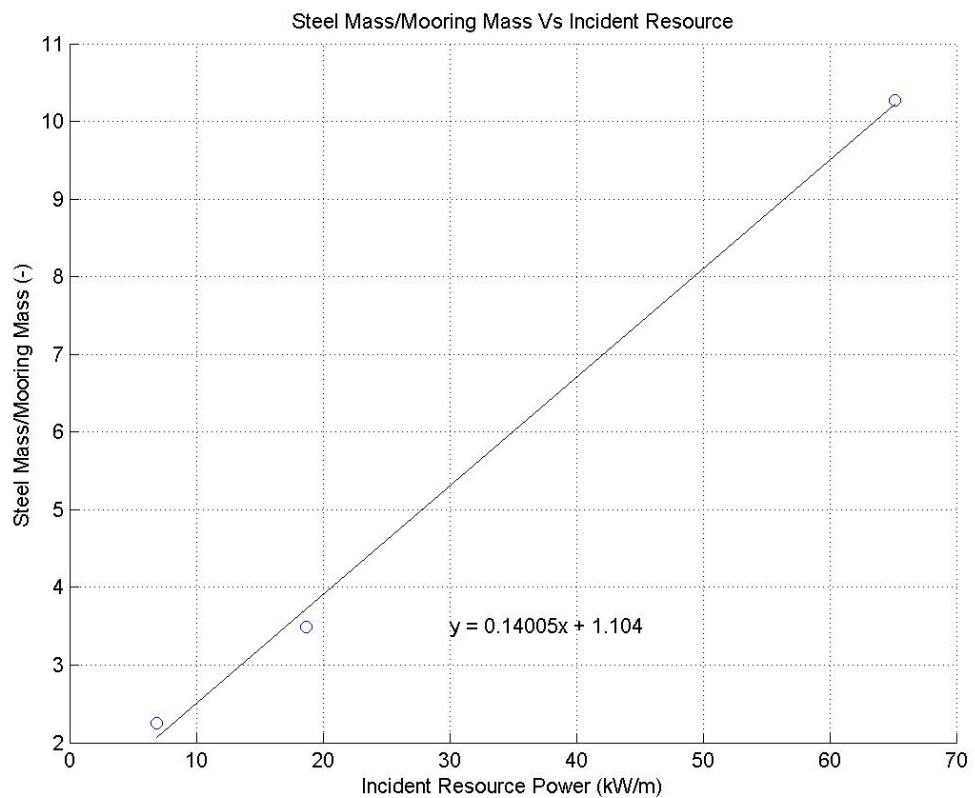


**Figure 3-60: Hull Steel Mass to Mooring Mass Ratio for each BBDB against Incident Resource**
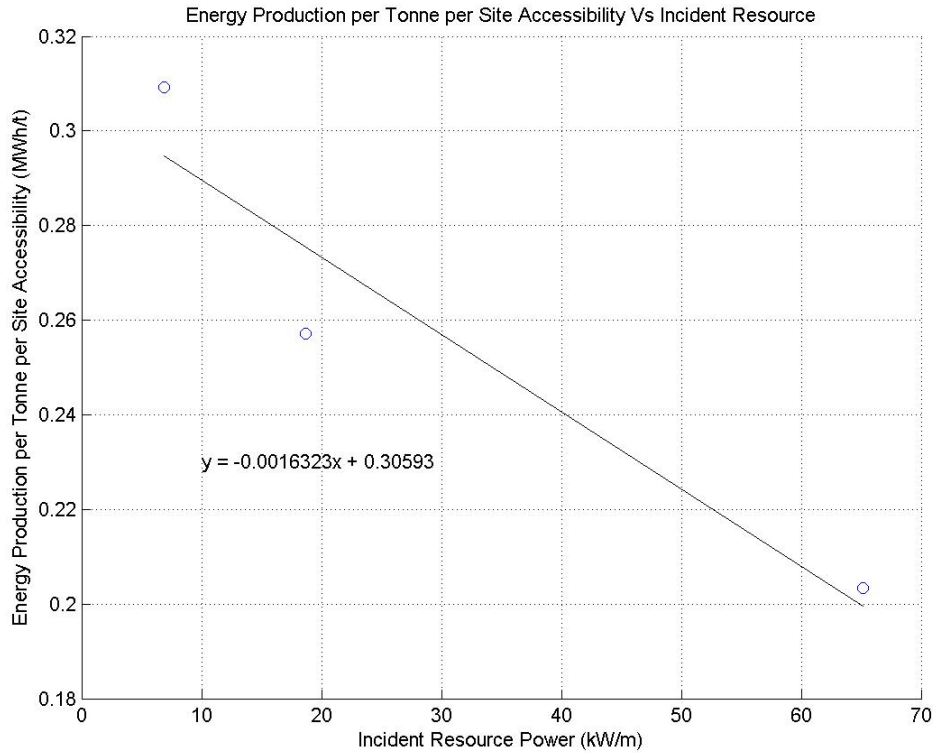
**Figure 3-61: Energy Production per Tonne Steel Mass per Site Accessibility for each BBDB against Incident Resource**

### 3.3.6 Unit Costs of the BBDB Hulls

The fabrication costs model developed in the previous chapter has been adopted to approximate the unit costs of steel fabrication of the hulls of the three BBDB designs considered in the previous sections. Central to the LCCA analysis for the BBDB design and selection of the most feasible option, is the correct assessment of costs of the devices. The model is based on the size of the steel members required and the associated welding activities that need to be carried out to fabricate the hull. Only the bow panel has been analysed, but due to the fact that the hull overall will be constructed from the same plates, stiffeners and spacings, this has been applied to the entire hull. A 10% contingency on the unit cost and hull mass has also been included for additional bracings etc. that may be required. The summary of the hull costs for each BBDB for each site is tabulated in Table 3-10 which are based on the maximum optimum total steel mass of the hull. It may be noticed that as the incident resource increases, the member sizes for each BBDB hull increase and as a result the unit costs of fabrication increase due to the complexity of the welding and amount of welding required for fabrication. Therefore, if data from the non-optimum steel plate and stiffener combination was used to minimise total cost, i.e. material and fabrication, rather than minimum overall mass, the hull costs could be reduced but potentially with an increase in total mass. The implications on power performance would need to be investigated as a result. If the costs of the hull are then related to the energy production for each site for 20 years, both considering 100% availability

and availability indicator, accessibility, the results are striking and are tabulated in Table 3-11.

**Table 3-10: Summary of the Costs of each BBDB for each Site**

| Site | Steel Hull Mass (t) | Steel Plate Thickness (mm) | Stiffener Thickness (mm) | Unit Cost of Fabrication Range (€/t) | Total Hull Cost Range (€) |
|------|------|------|------|------|------|
| **M1** | 1650 | 15 | 30 | 1403-6940 | 2.3m – 11.5m |
| **M5** | 550 | 13 | 25 | 1540-5916 | 0.85m – 3.25m |
| **M2** | 246 | 10 | 22 | 1618-5450 | 0.4m – 1.34m |

**Table 3-11: Summary of Cost of Energy Indicators Based on Site Characteristics and Hull Design**

| Site | Total Hull Cost (€) | 100% Availability Energy Production (MWh/yr) | Cost of Energy for 20 Years Based on Hull Cost (€/kWh) | Reduced Availability based on Accessibility Energy Production (MWh/yr) | Adjusted Cost of Energy for 20 Years Based on Hull Cost (€/kWh) |
|------|------|------|------|------|------|
| **M1** | 2.3m – 11.5m | 2715.6 | 0.04 – 0.21 | 298.7 | 0.39 – 1.93 |
| **M5** | 0.85m – 3.25m | 332.9 | 0.12 – 0.49 | 126.5 | 0.34 – 1.28 |
| **M2** | 0.4m – 1.34m | 113.9 | 0.18 – 0.59 | 66 | 0.3 – 1.0 |

The reason for using the site accessibility as an indicator of availability is that, this is the availability a developer could guarantee to an extent given that personnel can reach the device to ensure it works. This is also assuming that the reliability of the PTO is equal at all sites. This is also a cause for concern as it has been suggested in many case studies from the wind energy industry that failure rates increase, particularly of electrical systems, are correlated with higher average annual wind speed [137], [138], [139]. This may also occur for WEC PTO systems, i.e. higher incident resource may result in higher failure rates of the PTO components. This then presents a big problem as access is low in these locations. It is found from the analyses carried out above, that if the M1 site is to be the most economically feasible site, the availability needs to be four times the site accessibility, while the M5 site requires that the availability be twice the accessibility as illustrated in Figure 3-62. Reference [140] showed that for a site in the North Sea, availability can be expressed as a function of accessibility, and reaches values of up to twice the accessibility. Therefore, this would seem to suggest that the M2 site costs are too high and the M1 site cannot produce enough energy given the issues with accessibility. This then

leaves the M5 site which appears to have a reasonable balance between buoy structural design and costs and power production when considering potential availability at the site.
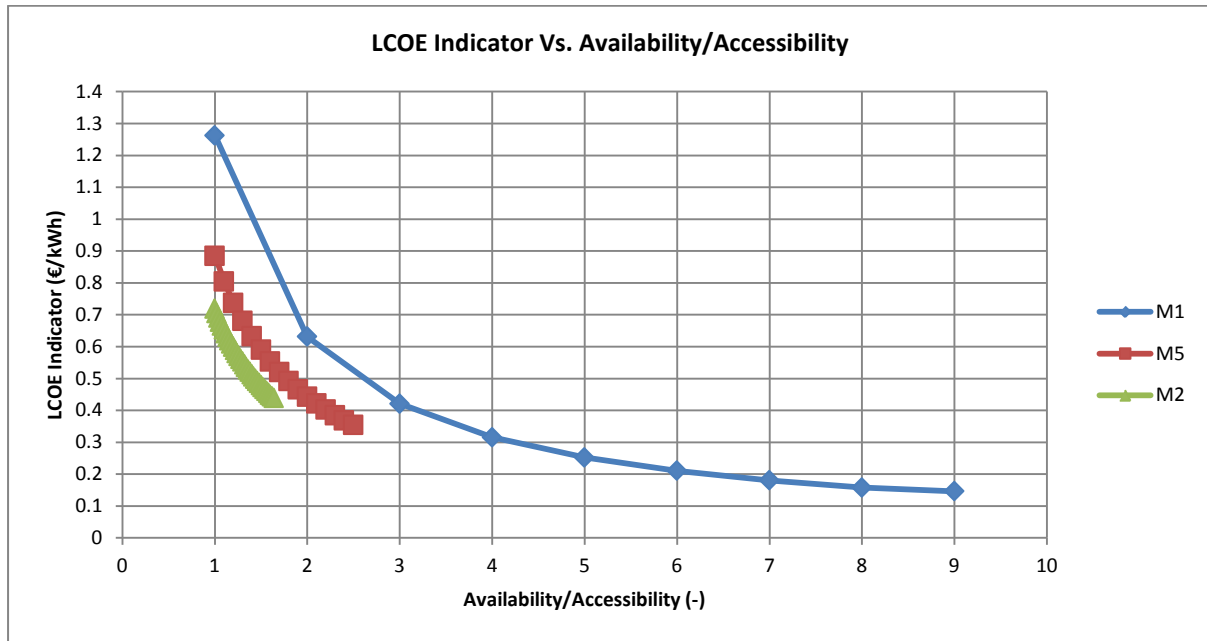


**Figure 3-62: LCOE Indicator as a function of Availability/Accessibility**

Central to this assumption, as was indicated previously is the definition of the access limits for the device under consideration. This will be addressed later in the thesis. For the moment, this result suggests that perhaps in the infancy of the wave energy industry that lower resource sites are better in terms of feasibility. Parameters that may improve the situation for higher energy sites are cheaper hull fabrication costs through either simple or radical reconfigurations of the hull, or more reliable machinery and better access systems subject to the issue regarding access limits already discussed.

### 3.3.7   Allowable Sea States for On-site Maintenance

In light of the significant impact the accessibility of devices can have on the selection of sites for deployment of WECs, a further study has been carried out on the potential for on-site maintenance on the BBDB device. The constraints for this study are different from those which are appropriate for the wind energy industry. This study has assumed that the transfer of personnel is achievable through various methods from a vessel to another floating platform. The primary constraint is the ability of technicians to perform maintenance tasks on-board a floating body. The main effects a technician will experience from working on a moving body are described in [141] and [142]. The parameter used in this study was the motion induced interruption (MII) index. This parameter includes three methods of occurrence,

1. Sliding
2. Stumbling or loss of balance

158

3. Individual becoming airborne due to large floating body accelerations

Sliding is usually easily catered for in ensuring sufficient friction provided between the technician's footwear and the deck finish. An individual becoming airborne is a very rare occurrence [143] and is unlikely to occur within the safe sea states identified for maintenance activities to be carried out. Therefore only the second effect has been considered, stumbling or loss of balance.

The stumbling criteria is governed by an individual's stance, i.e. location of centre of gravity (COG) relative to the distance between their feet. This ratio is referred to as the tipping coefficient (Tc) as described in [143]. The equation used for determining the value of the instantaneous Tc is given in [144] and is the ratio of horizontal acceleration to vertical acceleration. If this value exceeds the maximum permissible Tc, a MII occurs. The empirical value of the Tc is described in [145] and the average value determined as 0.222 has been adopted in this study. Reference [143] considered the 3s following an MII to constitute the MII event, however this study has considered that one MII can only occur for one half wave cycle. The MII limit imposed in this study was that defined by the US Coast Guard for the Cutter Certification plan at 2.1tips/minute [143]. The North Atlantic Treaty Organisation (NATO) standardisation agreement (STANAG) 4154 recommends a MII limit of 1tip/minute as it represents a reasonable level of risk for many shipboard tasks [146], while [147] recommend 3tips/min. The median value of 2.1tips/min has been chosen. The location on the BBDB at which the accelerations have been calculated are on the main deck adjacent to where the turbine housing would be. For a preliminary analysis, only heave and pitch modes have been considered. The heave and pitch frequency dependent RAO and phase functions have been used in conjunction with the superposition principle to estimate the accelerations at the turbine housing. A full time domain code would produce better estimations of the instantaneous accelerations, however this was not within the scope of this study. The occurrence of MII events per sea state are illustrated in Figure 3-63 for the BBDB at the M1 site, Figure 3-64 for the BBDB at the M5 site and Figure 3-65 for the BBDB at the M2 site.
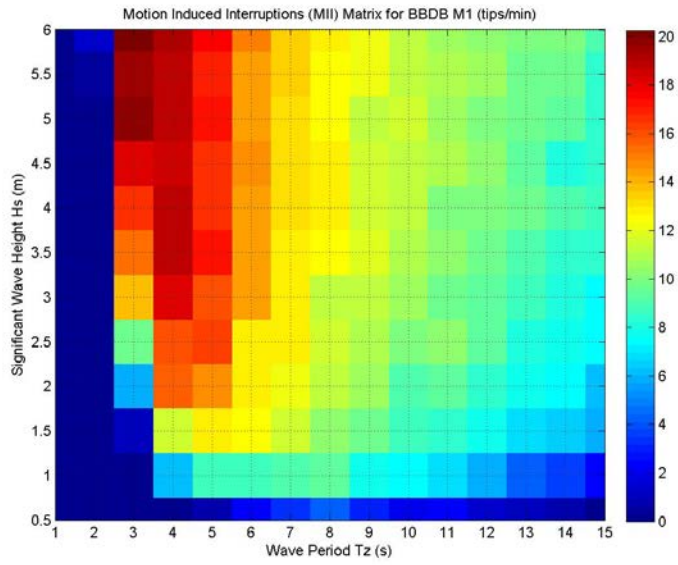
**Figure 3-63: MII Events for the BBDB M1 Device**
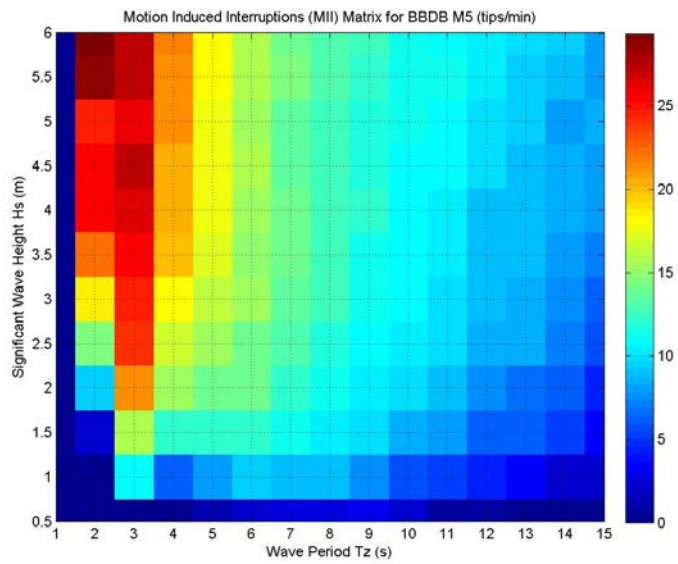


**Figure 3-64: MII Events for the BBDB M5 Device**
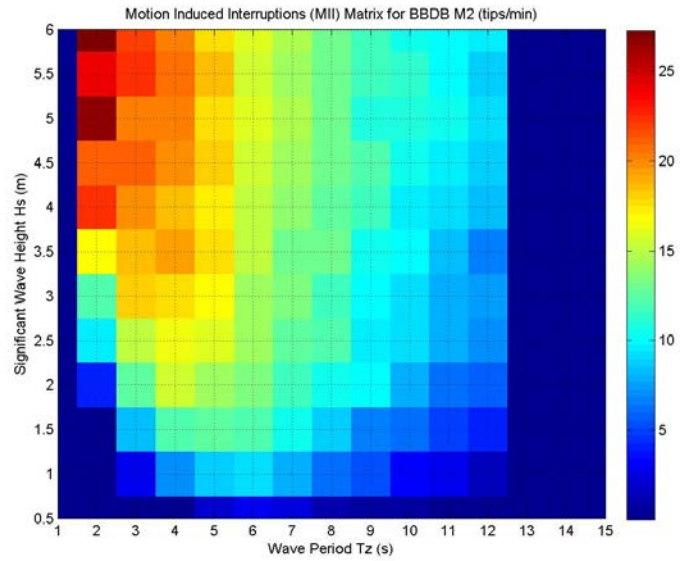
**Figure 3-65: MII Events for the BBDB M2 Device**

The number of hours at each site within which on-site maintenance is possible given the MII limits defined are illustrated in Figure 3-66 for the M1 site, Figure 3-67 for the M5 site and Figure 3-68 for the M2 site.
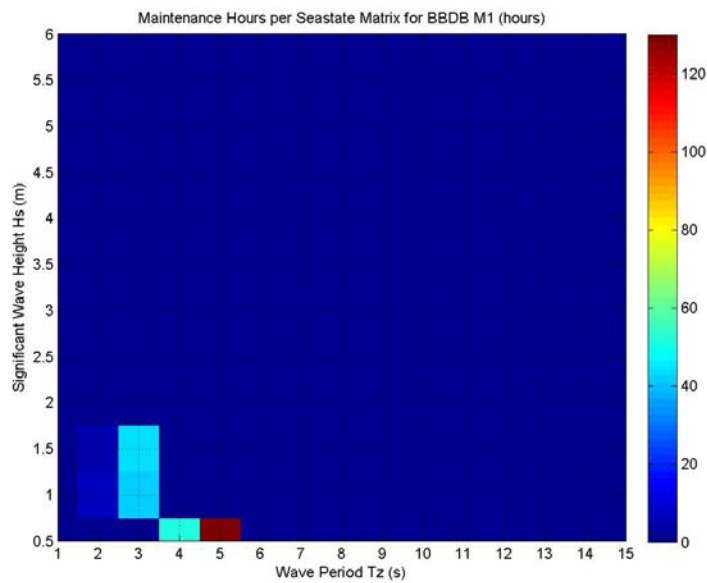


**Figure 3-66: Maintenance Hours Possible for the BBDB at the M1 Site**

161
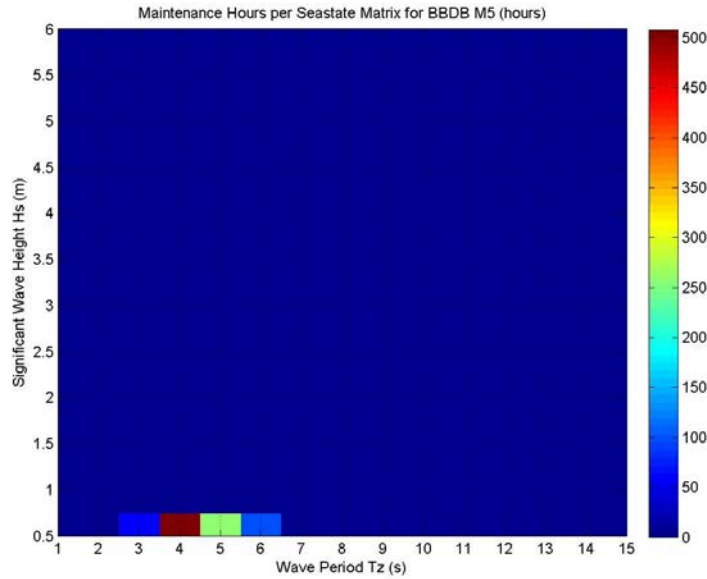
**Figure 3-67: Maintenance Hours Possible for the BBDB at the M5 Site**

One of the main observations from Figure 3-66, Figure 3-67 and Figure 3-68is that the conditions governing the maintenance activities aboard the buoy are both $H_s$ and $T_z$ dependent which has not been considered before. Reference [153] determined the weather windows at three sites based on a workboat $H_s$ and $T_p$ operating limits which were taken from [149]. The access limits for existing offshore wind are dependent only on the motions at the bow of the O&M vessel which are designed to minimise the motions. This is in stark contrast to the design philosophy for a WEC which relies on movement/relative movement for energy conversion.
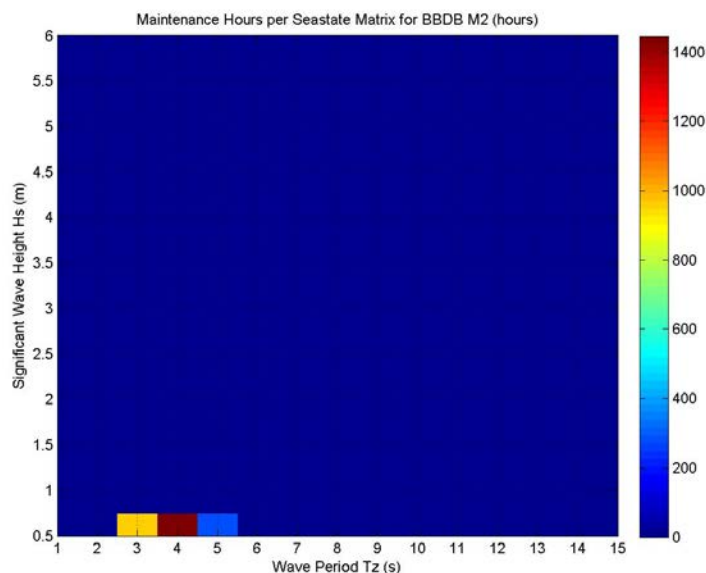


**Figure 3-68: Maintenance Hours Possible for the BBDB at the M2 Site**

This results in ~3%, or 280 hours, possibility of carrying out on-site maintenance on the BBDB at the M1 site due to the motions of the buoy assuming technicians can

board the buoy. At the M5 location, a total of ~10%, or 932 hours, of maintenance time is possible aboard the device. At the M2 location, a total of ~30%, or 2676 hours, of maintenance time is possible aboard the device.

It is potentially then prudent to consider concepts intended for high energy sites to be based on absorption methods which do not necessarily rely on maximising structure motions in order to achieve a suitable level of accessibility/maintainability. This may not be the only option to consider in striving to achieve overall concept feasibility in high energy sites but one which merits investigation.

### 3.3.8   Discussion

This section has presented the simplified early stage concept development methodology which is aimed at improving the economic feasibility of the basic concept. The methodology is intended to encapsulate all the available information at the early stage of concept development, including site resources and extreme conditions, preliminary hydrodynamic and structural modelling and preliminary tank tests for concept validation. The study has provided a substantial body of work which is then reduced into a select amount of summary parameters which it is hoped can act as indicators of concept feasibility in certain locations. These parameters, plotted against average annual incident resource level, have included:

1. Hull Steel Mass
2. Energy Production per Tonne of Hull Steel assuming 100% Availability
3. Hull Mass to Mooring Mass Ratio
4. Energy Production per Tonne of Hull Steel using Accessibility as an indicator of Availability

The result of the motions analysis with regard to possible on-site maintenance has significant implications for the selection of a device type for a specific site, and/or indeed the maintenance strategy adopted for that device at that site. Consider the BBDB design at the M1 site, the result of the motions analysis concludes that ~3% of time annually on-site maintenance can be carried out safely by technicians. The low percentage of time for on-site maintenance certainly does not discount the optimally designed BBDB from deployment at the M1 site, but does demand a further analysis of an alternative O&M strategy, namely off-site maintenance similar to that proposed by Pelamis. This strategy should not be regarded as a deterrent for deployment in high energy sites but requires a more detailed analysis in the LCCA models and also brings with it a number of technical issues. For the BBDB designed here, these would include,

- Tugboat bollard-pull capacity for efficient towing of the hull to and from the O&M location.
- Hull draft of 12m cannot be easily handled in ports, should a "nursery" site be used to carry out the O&M tasks? For example in the lee of the Aran Islands for the M1 location.

- Due to this O&M strategy, efficient towing will be critical. Should the hull be redesigned to accommodate this? For example streamlining of the hull to reduce drag while under tow.
- Perhaps even consider a large ship for lifting of the device out of the water for maintenance. Therefore lifting operations during high waves and lifting points need careful consideration.
- Mooring system design for (de)attachment to the surface buoys in high wave conditions.
- Flexible Riser connection design and location on the buoy for (de)attachment.

Each of these technical design conditions should be considered in the early stage of development to reduce the risk associated with operating a device in a high energy site. It follows that the economic feasibility of the device may change depending on the choices made in the early stage of development.

As the resource level reduces, the percentage time available to carry out maintenance on-site increases. At the M5 site, ~10% of the time this is possible. It is questionable whether this is a sufficient amount of time annually to carry out maintenance and it may be the case that the above considerations would also apply. In the case of the M2 location, the percentage time available to carry out on-site maintenance is ~30%. This is a more reasonable figure for adopting an on-site maintenance strategy, though the alternative of off-site maintenance should also be considered. Another alternative to the use of the BBDB and off-site maintenance option is the deployment of a device which has lower motion characteristics of the platform for on-site maintenance while maintaining sufficient relative movement with the incident wave field for power production.

These options will now be considered in selection of WECs depending on the site resource level which will be discussed in Chapter 4 for hybrid designs.

## 4    Hybrid Device Design and Assessment

The design and deployment of combined wave and wind energy devices, which aim to benefit economically from the obvious synergies between the two industries, is one initiative which is hoped can assist in the reduction in costs of energy from offshore renewable technologies. While many various combinations of ocean energy technologies are possible, amongst them wind, wave, ocean thermal energy conversion (OTEC), currents etc., this thesis will focus only on the combination of the major two, wind and wave energy. The design and assessment of combined wave and wind energy devices will embody the methods used for the design of both wave and wind energy devices individually. Firstly, this chapter will describe the basis for, and benefits of, hybrids and the likely technical and economic challenges they will face relative to the individual wind and wave technologies. The following section will then introduce a number of existing wind and wave hybrid devices under development by technology developers worldwide.

### 4.1    The Basis for Hybrid Wave and Wind Energy Devices

Ireland in 2009 was one of four countries in Europe to produce over 50% of its national electricity requirements from gas, while relying on 90% of this gas from imports [150]. A modest, and below EU average, 13% of electricity came from renewable sources. Before taxes, the Irish cost of electricity for households and industry in 2009 was the highest in Europe. After taxes, it remained one of the highest for households while becoming more on average for industry. Therefore there are two options for addressing this, reduce the reliance on gas imports through replacement of natural gas with biogas, or increase the renewable penetration. The ideal scenario is self-sufficiency on the basis of a renewable energy mix. But this is rather complicated on land, and therefore offshore becomes the necessary realm for mass renewable energy generation. The primary basis for the design and development of hybrid wind and wave energy systems in the offshore environment is the joint exploitation of both resources which may be more profitable compared to simply adding more of one or the other individual technologies. This essentially stems from the fact that the wind energy resource typically leads the wave resource by several hours [151]. This can be exploited in two ways, either spatially and/or temporally. In Chapter 1, the following list was given, describing the ways in which the concept of a hybrid may be realised.

- Sharing space
- Sharing power transmission infrastructure
- Sharing O&M strategies
- Sharing a foundation/platform

Reference [152] briefly outlined the benefits of these options. As is inferred by these various hybrid concepts, and combinations of them, the degree to which the wind and wave resource interacts through the hybrid varies substantially. The following is a brief description of each option and how it may be realised offshore.

### 4.1.1 Sharing Space

On its own, this would be the simplest realisation of a hybrid system. In most cases, installing a renewable energy farm offshore requires an annual payment to the state government for the amount of sea bed area used during the lifetime of the project. The effect these payments can have on the annual profits of the developer can be reduced by co-locating wind and wave energy devices within the same sea bed footprint, i.e. wave devices between the wind turbine foundations. Figure 4-1 illustrates the Wavestar device co-located in a wind farm [153].



**Figure 4-1: Co-located wind turbines and Wavestar WECs**

Reference [154] considered the benefits of variability reduction of renewable energy through energy mix diversification while considering a marine spatial planning (MSP) approach in the Danish North Sea which has significant benefits and constraints on offshore farm installation. Sharing space as a possible hybrid solution is unlikely in isolation as co-location would infer many more benefits than just reduction of sea bed rental costs per MWh produced. Nonetheless, even a simple solution like this can provide a positive synergy in terms of costs.

### 4.1.2 Sharing Power Transmission Infrastructure

Recently, many studies worldwide have investigated the potential for variability reduction of offshore renewable energy through combination of wave and wind energy resource utilisation [151], [155], [156], [157]. These studies essentially considered co-location of the extraction devices and the benefits in terms of power variability delivered to the grid. Reference [158] demonstrated that power transmission capacity could be reduced by up to 10% for a 1000MW offshore renewable energy farm comprised of any combination of wind and wave capacity

from 30-60km off the coast of California. The  showed that the combined farms delivered more power than a wave only farm and much less variable power than a wind only farm. The locations studies had correlation coefficients of 0.29-0.41 for wind and wave energy profiles.  Therefore the option of sharing power transmission networks is a significant positive synergy for offshore wind and wave farms. The use of DC cables for large farms far offshore has not been assessed in any great detail as of yet for the public domain.

### 4.1.3   Sharing Installation and O&M Strategies

On the outset, this option suggests a significant benefit. However, can it really deliver a substantial positive synergy for systems that do not share a foundation? The reason for this is that if the hybrid does not share a foundation, the farm is just comprised of more units. This requires more vessel travel time, more crew transfers etc. Ultimately with more machinery, more crews will be required for maintenance. And with more machinery, the possibility of CM increases which decreases the available crew to carry out PM. The increase in crew numbers may not however increase at the same rate as capacity increase. This can only be determined from a sophisticated LCCA model taking into consideration the CM and PM requirements of the farm. In a simple way, a positive synergy can be achieved by sharing the O&M port facilities. A similar argument is possible for installation activities and infrastructure. More units require more vessels for the same installation time. But in terms of the installation port, it may not be possible to share this facility due to the large space requirements of such infrastructure when in storage portside.

### 4.1.4   Sharing a Foundation/Platform

Sharing a platform or foundation embodies all the positive synergies outlined previously, from sharing space, transmission infrastructure and installation and O&M activities. For a floating solution mooring and anchor systems would also be shared. A number of these types of hybrid platforms are under development and will be discussed in another section. This type of solution for hybrids can also present negative synergies in terms of technical and economic performance. Each hybrid will be different depending on the combination of wind turbine, platform, WECs and mooring system. Therefore it is difficult to analyse from the outset which will provide all positive synergies.

### 4.2   Discussion of Hybrid Options

The possibilities of how hybrid wave and wind energy concepts can take shape are numerous. Many of these configurations do not require significant technical investigations to be carried out to prove their feasibility. For example, sharing space on its own is simple a modification in terms of cash flows in economic models for both farms. Sharing power transmission networks requires a technical investigation but does not require any modification of the individual technologies. An economic investigation should show a reduction in CAPEX for both transmission costs but also from sharing space. A detailed economic investigation of the installation and O&M

of a hybrid farm is the only way a definitive answer can be given in terms of worthwhile positive synergies being delivered from sharing installation and O&M infrastructures. The final form, a hybrid platform, embodies all possible positive synergies. As this form of hybrid has the potential for hosting all positive synergies, this thesis will consider this hybrid form. A number of configurations will be proposed and ranked in terms of known technical and economic performance of the relevant components of the hybrid concept. The foremost concept will then go through a more detailed investigation and conclusions drawn on the positive and if present, negative, synergies demonstrated.

## 4.3 Proposed Alternative Hybrid Wave and Wind Energy Devices

The following section introduces a selection of newly proposed hybrid wave and wind energy concepts. These concepts combine existing platforms, WECs and the turbines described in Chapter 2.

### 4.3.1 Single OWC Barge and WTG

The barge type floating wind turbine incorporating OWC chambers is illustrated in Figure 4-2. The barge is approximately 40m squared and 12m deep. The illustration includes focussing arms which may or may not be included. These have a secondary role in minimising pitch motion by applying a righting moment through additional mass upstream of the barge COG. The WTG used is the NREL 5MW WTG. Assuming the OWC is right across the full width of the barge, the WEC is anticipated to produce ~320kW of electrical power in a 45kW/m site. The WTG is anticipated to produce 1750kW in a high energy site. The barge is estimated to require ~2300t of steel for production.
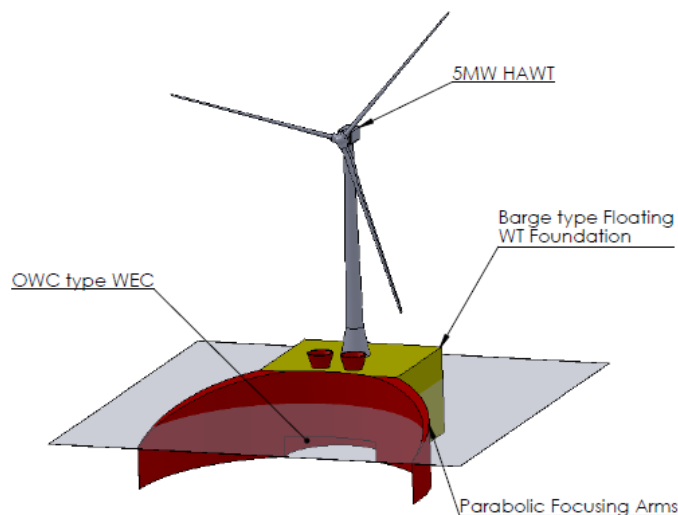


**Figure 4-2: Floating Barge Hybrid with OWC and 5MW WTG**

### 4.3.2 Large PA Spar and WTG
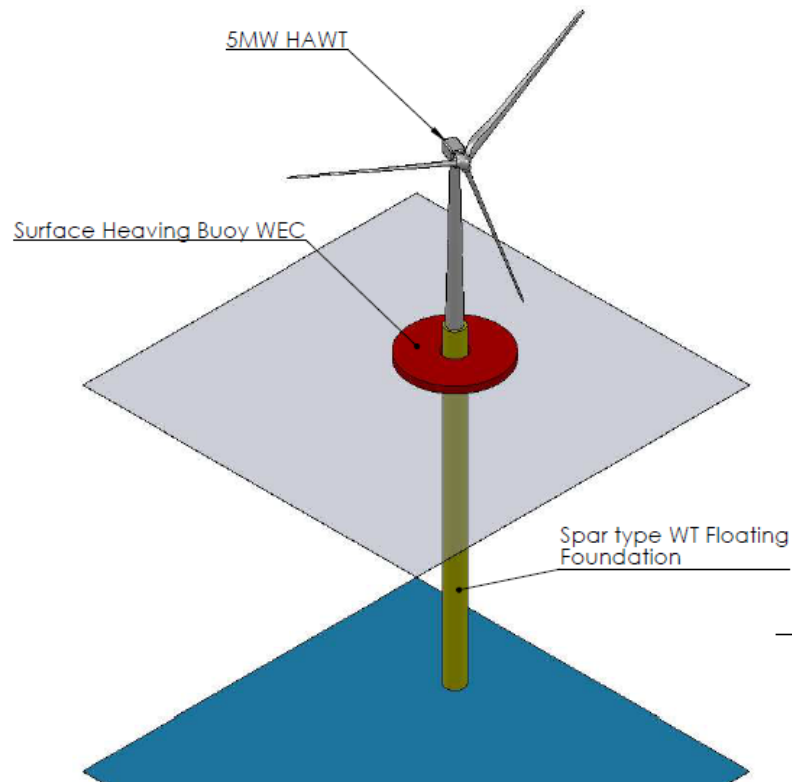


**Figure 4-3: Floating Spar Hybrid with Large PA and 5MW WTG**

A spar floating wind turbine foundation incorporating a large PA is illustrated in Figure 4-3. The spar has similar dimensions and mass characteristics as that of the Hywind platform discussed in Chapter 3. The WTG used is again the NREL 5MW machine. The PA has a diameter of 20m and in a 45kW/m site is anticipated to produce ~170kW. The PA is expected to have a structural steel mass of ~340t. Like the Wavebob concept, irregular motion characteristics may be a prohibitive reason for coupling the PA with the spar. Only detailed time domain modelling or tank testing can reveal this phenomenon. Furthermore, it is expected that accessibility of the WTG could be a significant issue unless the PA is locked in position for the duration of any necessary maintenance work. The practicalities of this are uncertain.

### 4.3.3   Twin OWC Spar and WTG
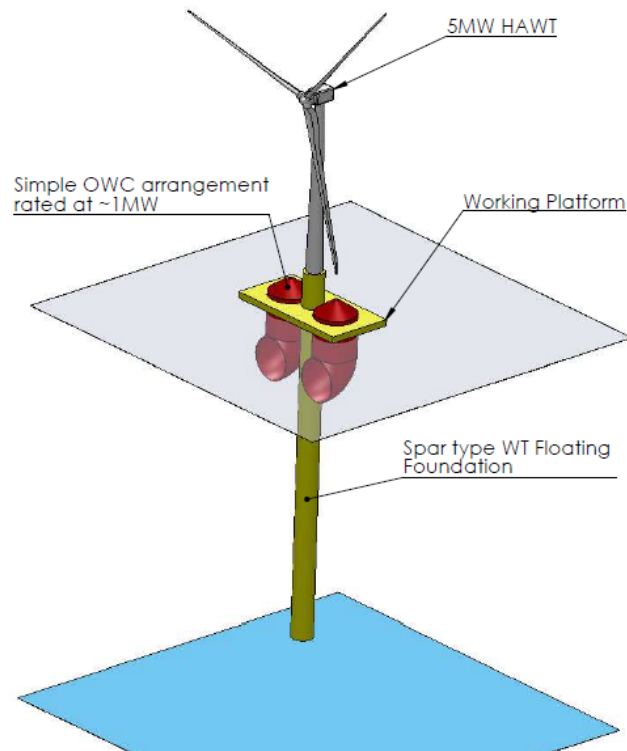


**Figure 4-4: Floating Spar Hybrid with 2 OWCs and 5MW WTG**

A spar floating wind turbine foundation incorporating two OWC chambers is illustrated in Figure 4-4. The WTG used is the NREL 5MW machine. The OWC chambers are ~20m in diameter and are expected to produce ~320kW in a 45kW/m site. Due to the large diameter of the tubes, a steel plate and stiffener design would be required. A structural steel mass of ~2200t would be necessary. Again, like the spar-PA coupling, the impact on motion characteristics of the spar would need to be thoroughly investigated.

### 4.3.4   Single OWC and Jacket WTG

Figure 4-5 illustrates the incorporation of a single OWC chamber into the void of a jacket foundation for a wind turbine. The cross-bracing members are not shown for clarity. The jacket would be similar to the design for the Ormonde Offshore Wind Farm in the UK which has used the RE Power 5M machine, on which the NREL machine is based. The turbine is expected to produce 1750kW while the OWC is expected to produce ~160kW in a 45kW/m site. The structural steel required would be ~1100t. It is expected that this concept would be prohibitively expensive due to the costs associated with the fabrication of a jacket foundation. Furthermore, as this thesis is intended to develop concepts geared towards deepwater deployment in high energy sites, fixed foundations are unlikely to feature.
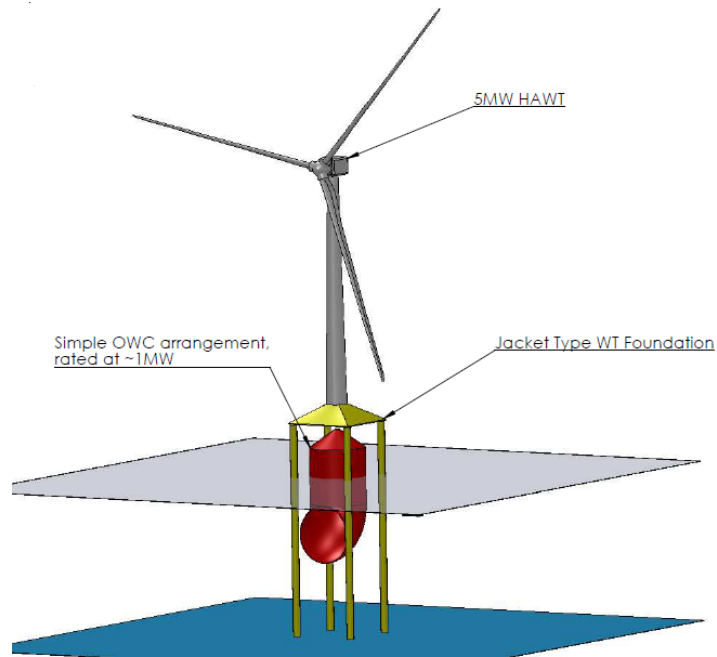
**Figure 4-5: Fixed Jacket Hybrid with OWC and 5MW WTG**

### 4.3.5 OWSC Array and WTG
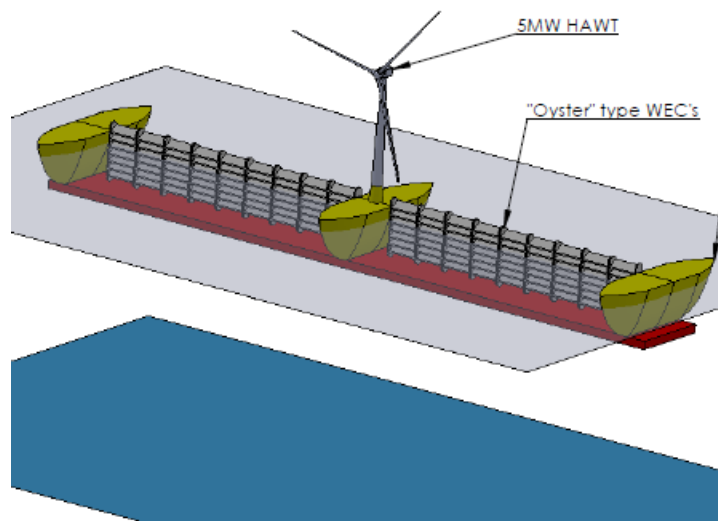


**Figure 4-6: Floating Semi-sub Hybrid with OWSC Array and 5MW WT**

Figure 4-6 illustrates the concept of a semi-sub platform incorporating an array of OWSC devices. The structure is 400m in width. The OWSC array is expected to produce ~2300kW of power. The WTG used is the NREL 5MW machine which is assumed to produce 1750kW. The structure is long and slender and the nature of loading applied to the OWSC devices may induce pitching motion to the overall platform depending on the level of damping applied through the PTO systems. The steel content is difficult to assess, but the flaps may weight ~2700t. The platform structure would require more modelling to accurately assess the steel mass.

### 4.3.6   OWC Modified Ship Hull and WTG
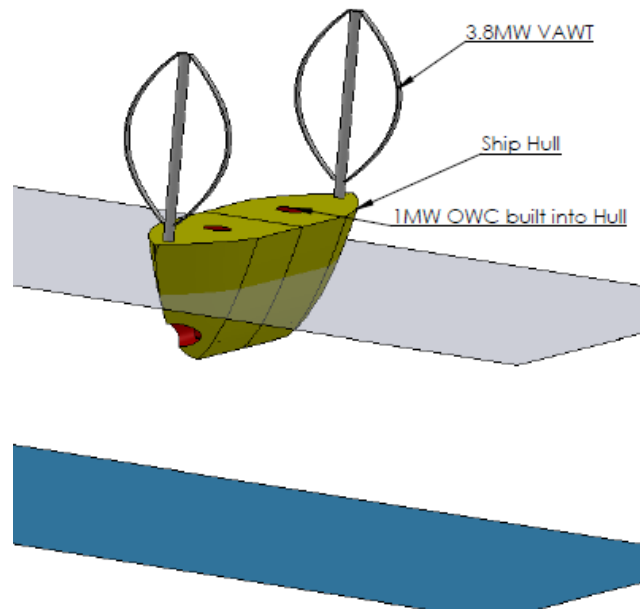


**Figure 4-7: Modified Ship Hull with 2 OWCs and 2 VAWTs**

Figure 4-7 illustrates one of the more unusual hybrid wind-wave energy concepts. The hull utilises a modified ship hull, with two OWC chambers built into it. This concept is similar to the Kaimei [159]. This device had rather disappointing results in terms of power absorption but it is possible that the OWC chamber were not correctly designed to account for the motions of the barge itself. This could be rectified with sufficient tank and numerical modelling. The OWCs are expected to be capable of producing 320kW in a 45kW/m resource. The WTGs shown are two VAWTs, but may be switched with a single 5WM HAWT as it is intended the ship hull should be moored head-on into the incident waves. The retrofit of the ship hull with OWCs and stripping of other unnecessary equipment is difficult to assess with any degree of certainty and is unlikely to be suitable for mass production.

### 4.3.7   Barge OWC Array and WTG
The barge OWC Array concept is a simple extension of the single OWC barge concept described in 4.3.1. Figure 4-8 illustrates an initial OWC Array barge and WT platform. The barge incorporates 9 OWC chambers of ~15m width. The OWCs are then expected to produce ~1000kW of power in a 45kW/m resource. Due to the large size of the platform it may be more economical to fabricate from RC rather than pure structural steel. The mass distribution of the platform and the ultimate mass will be critical in the design of the mooring system due to the size and dimensions of the platform. The large platform may be a suitable all-round solution due to stability, and RC construction capability. The power matching possible between WEC and NREL 5MW WTG is also an advantage for specific sites for power variability reduction.
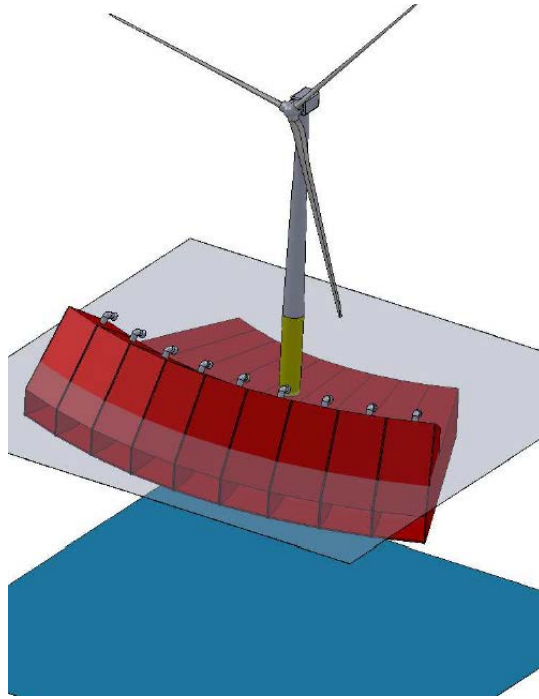
**Figure 4-8: Floating Barge Hybrid with OWC Array and 5MW WTG**

### 4.3.8   ATN Barge and WTG

The ATN and WTG concept is a modification of the Wave Treader and McCabe Wave Pump concepts and is illustrated in Figure 4-9. The ATN is much larger than the original concepts with a width of ~30m. Central to the success of this concept is ensuring the central barge is kept stationary. This has a twofold requirement for WEC power absorption to ensure maximum angular rotation of the fore and aft barges relative to the central barge, and, motion characteristics suitable for the attachment of a WTG. The WEC is expected to produce ~300kW in a 45kW/m site. The barge structure is approximately 2700t in structural steel mass not including the heave plate structure.
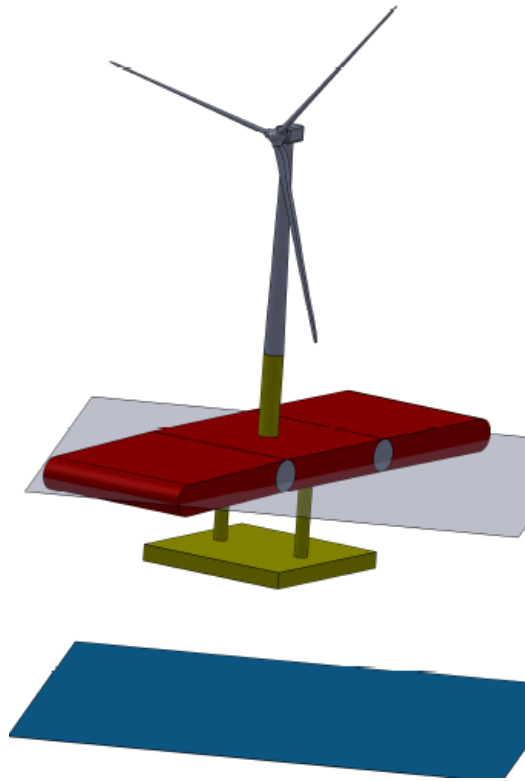
**Figure 4-9: Floating Barge Hybrid with ATN and 5MW WTG**

### 4.3.9 PA Array and Tripile WTG
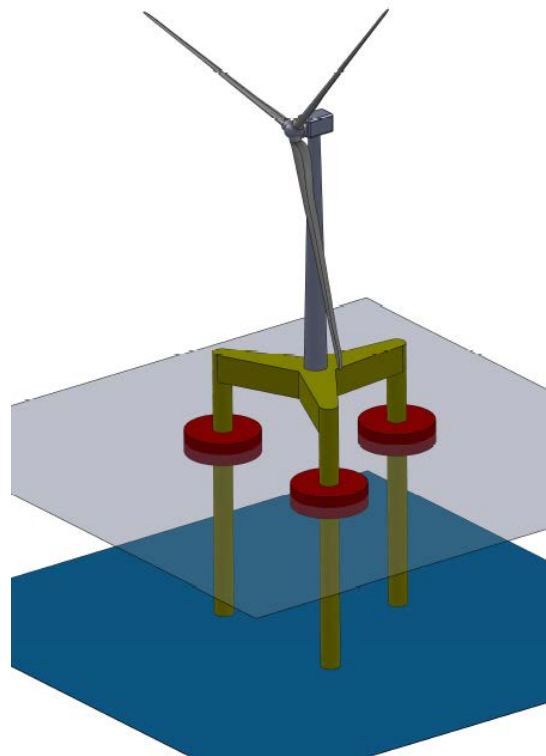


**Figure 4-10: Fixed Tripile Hybrid with 3 Medium PA and 5MW WTG**

The tripile solution for installation of large offshore wind turbines is a modification of the traditional monopile solution and is used in the BARD 1 offshore wind farm. Each pile is smaller than a typical monopile and each are connected by a transition piece which can weigh approximately 500t of welded steel. The piles are long and slender and act like a propped cantilever beam. The attachment of the medium sized PAs as illustrated in Figure 4-10 will induce a further load on the pile at sea level during operational and survivability conditions. The steel mass of the piles requires a structural design similar to that carried out for the monopile foundations in Chapter 3. This will be a function of water depth, soil conditions, PA size and resource. The PAs are expected to produce ~130kW in a 45kW/m site and weigh ~370t of structural steel. The solution is a rather neat and tidy solution compared to the attachment of a PA to a monopile as the structural configuration of the propped cantilever will reduce global bending moments at the point of fixity of the piles. Strict installation conditions apply to the tripile as the TP unit needs to fit into the three piles simultaneously and very little movement of the piles is possible following installation.

### 4.3.10 PA Array and Large Semi-sub WTG (1)
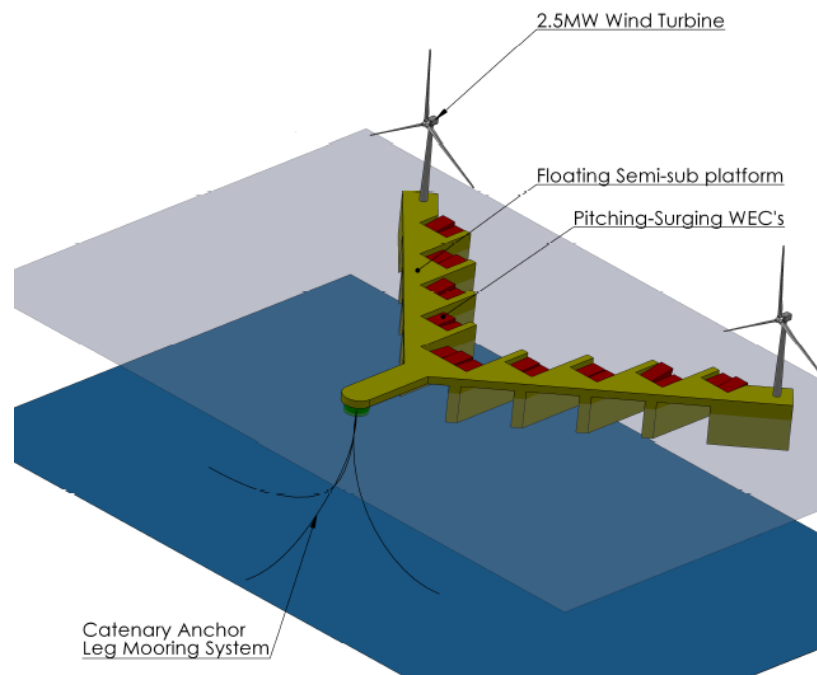


**Figure 4-11: Floating Semi-sub Hybrid with Surging/Pitching PA Array and 2 WTGs**

The floating semi-sub hybrid with downstream pitching PAs as illustrated in Figure 4-11 is a modification of the Poseidon concept with two WTGs. The "V" shape provides a downstream shift in location of rotation of the PTO systems for the buoys and as such acts to smooth the power output. The WTGs are located at either end of the structure so as to minimise the wake interference in angular differences in direction of wind and waves. The structure is moored with a catenary anchor leg

mooring (CALM) mooring system to allow weather-vaning of the platform from the influence of incident waves. The steel plate and stiffener design of this structure would be difficult given the long, narrow and numerous semi-sub components of the hull. The WECs are expected to produce ~1500kW of power in a 45kW/m resource, while the two WTs are expected to produce ~2100kW of power.

### 4.3.11 PA Array and Large Semi-sub WTG (2)
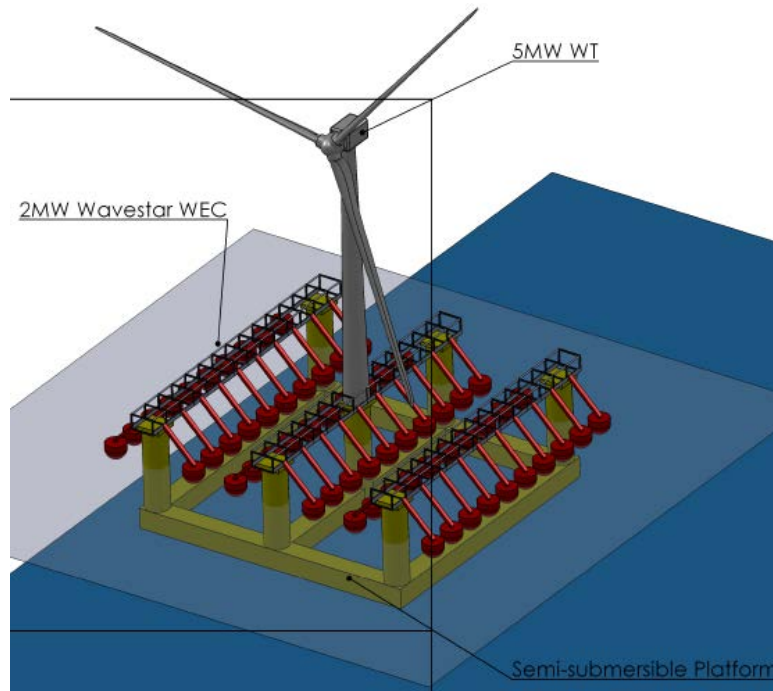


**Figure 4-12: Floating Semi-sub Hybrid with Small PA Array and 5MW WTG**

Figure 4-12 illustrates a hybrid device combining a large semi-sub platform, a 5MW WTG and a large array of small PA's. The buoys are approximately 5m in diameter and are configured in 6 rows of 10, 60 in total. The buoy configurations are based on the Wavestar WEC described in Chapter 3. A number of observations can be made from the figure, including that the platform has large dimensions and displaced mass and should provide a stable base for the WTG, secondly the number of buoys in close proximity to one another will prove very difficult to assess accurately the power output of the system due to the interactions amongst them. Neglecting this interaction, a preliminary estimate of the power output suggests the WECs will produce ~800kW in a 45kW/m site. In typical cases, the steel mass for small semi-sub platforms is 50% of the displaced mass for NS steel. Assuming similar estimates for this platform, the structural steel mass would be ~4400t. The WECs would be a similar design to the Wavestar design.

### 4.3.12 PA Array and TLP WTG
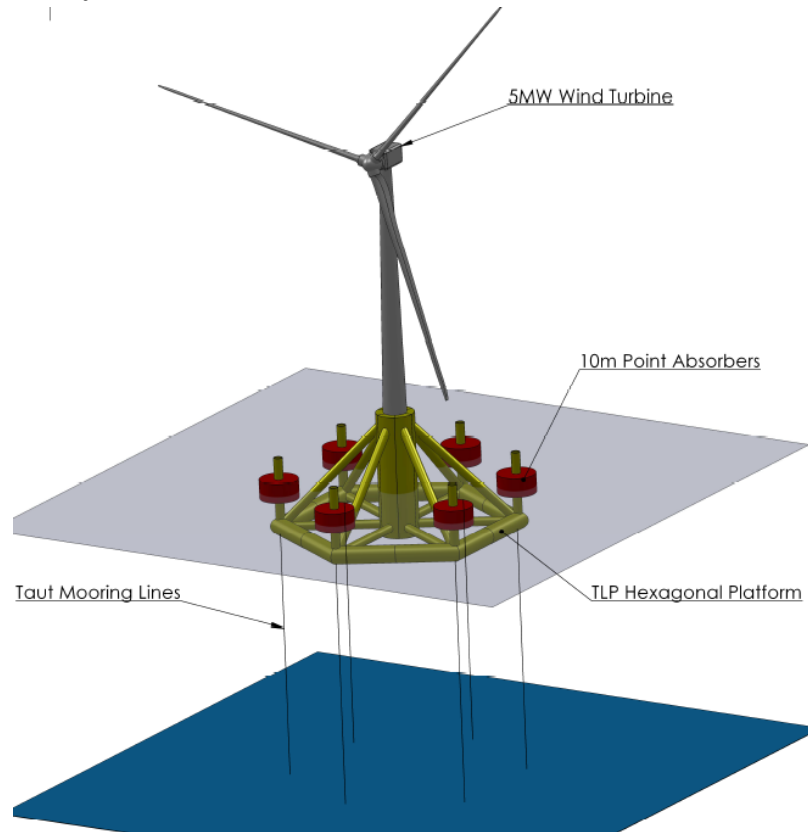


**Figure 4-13: Floating TLP Hybrid with Medium PA Array and 5MW WTG**

Figure 4-13 illustrates a space frame type TLP platform with a 5MW WTG and an array of medium sized PA's. The platform is hexagonal in shape allowing redundancy in the mooring system. The TLP will act primarily in surge motion at periods well above the wave energy regime, while well designed PA's will act only in heave along the guides attached to the platform within the wave energy regime. The TLP mooring system provides significant resistance to heave motion and provides a stable reference about which the PA can move to generate power. The PA's are expected to produce ~263kW in a 45kW/m resource. The method of estimating the TLP platform structural mass may be similar to the method used for the semi-sub if the TLP is designed to be self-installing. The benefit of such a system would need to be economically confirmed as the TLP mooring system is a much more expensive alternative to the catenary system for the semi-sub. The TLP would then have a similar cost foundation and more expensive mooring system than a semi-sub alternative.

## 4.4   Assessment of Hybrid Concepts with New and Existing Methods

This section assesses the hybrid concepts described and applies both existing and newly developed methods of assessment to rank the various designs in terms of the best indicator of feasibility, LCOE.

### 4.4.1 Power Output Estimation Methodology

The proposed power output estimation methodology is based on the concept of the CWR but extended to include the secondary dimension of the primary hydrodynamic plane of the device. The new measure is described below and an example calculation is provided.

#### 4.4.1.1 The Device Type Factor (DF)

An average power output matrix for a specific device is obtained and coupled with a scatter diagram of a specific site, to give an average power output for that device at that site. Typically, the scatter diagram will also be used to estimate the average annual power per metre at the site. Using these incident power and output power figures, as well as the device width, the total efficiency of the device may be estimated from Equation 4-1.

$$\eta\ (\%) = \frac{P_{out}}{J_{incident}.B}x100 \qquad \text{Equation 4-1}$$

Typically this type of calculation has been used to describe the ability of a device to convert energy, and not for sizing various devices as it accounts for only one dimension of the device. In the conversion of energy, a device occupies a certain area. This area is device specific, i.e. for an OWC it is the area occupied by the plenum chamber in the X-Y plane, for an overtopping device it is the area the ramp occupies in the X-Z plane. By altering the size and shape of this area, the power output of the device changes. Therefore, it is proposed to include the second dimension of the main power conversion plane in the above equation. This results in a dimensional factor as given in Equation 4-2.

$$DF = \frac{P_{out}}{J_{incident}.B.D} \qquad \text{Equation 4-2}$$

The variable D (m) now refers to the dimension of the device power conversion plane in the Y or Z direction, depending on the device type. The DF has dimensions of per metre ($m^{-1}$). From model tests, it has been found that this DF remains constant across both device size and incident resource. The simple physical model tests included the testing of three fixed OWC's in the wave flume and monitoring the instantaneous pressure in the plenum chamber. A picture of the three OWC's is shown in Figure 4-14.

**Figure 4-14: Different OWC's Sizes Tested**

The absorbed power may be estimated using a modified Bernoulli equation. Each OWC had the same area ratio of plenum area to orifice area, and the same device draft. The calculated device factor for each OWC diameter at full scale is plotted in Figure 4-15. It can be seen that this parameter remains quite constant between 7.5-10m and reduces thereafter at a constant rate. This can be explained due to the lower extraction per square metre of OWC area as the dimension in line with the wave direction increases. This may also offer a reason for the range of CWRs suggested by [17] for each WEC type.
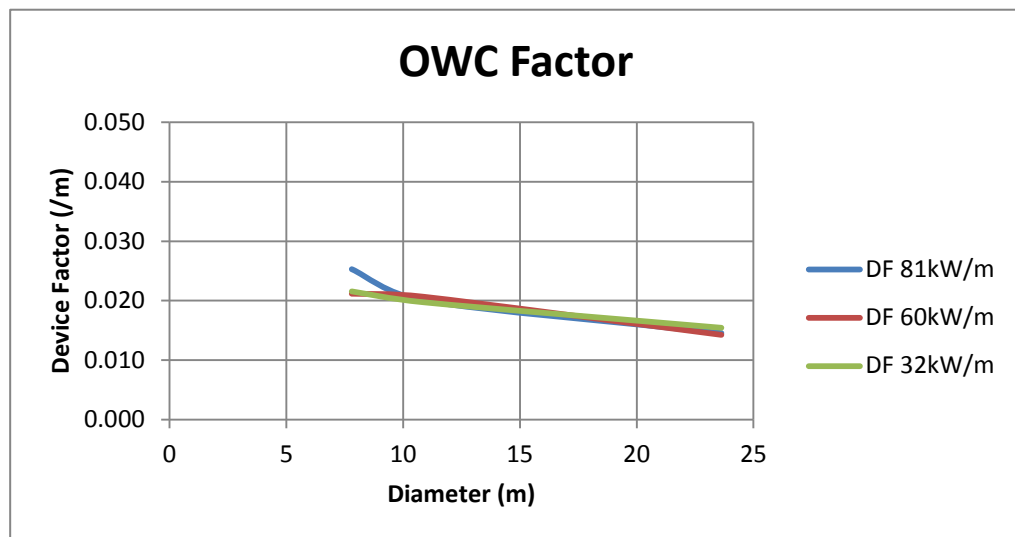


**Figure 4-15: Device Factor against OWC diameter in various incident wave resources**

Simple physical testing was also carried out on a number of OWSCs. These included three flap widths and two flap depths, each damped with two 16mm diameter pneumatic cylinders. The device factor was calculated for each flap depth and plotted against flap width full scale. The results for the 13.0m flap depth are illustrated in Figure 4-16. A similar trend as that observed for the OWC is noted as the depth of the flap increases.
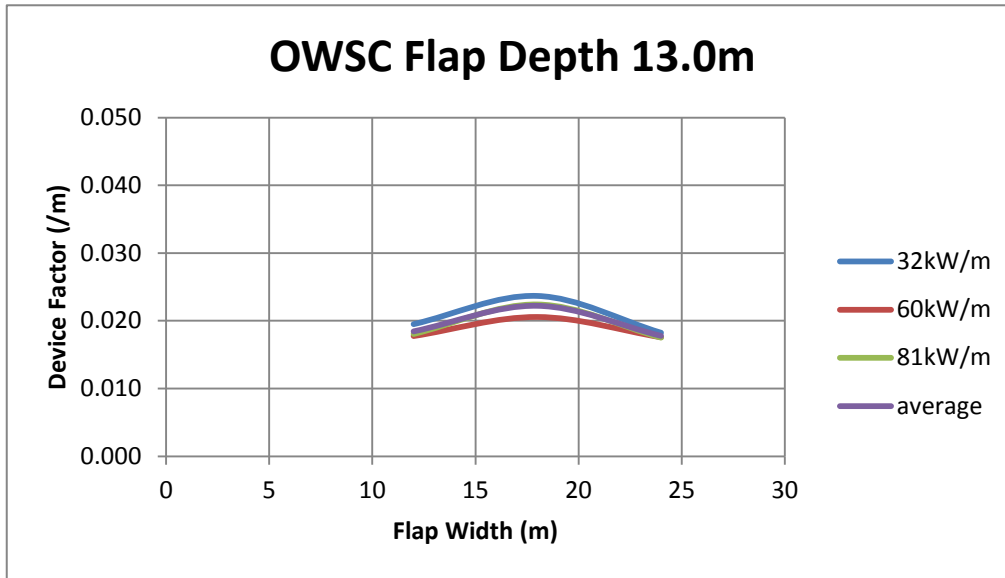
**Figure 4-16: Device Factor against OWSC flap width for 13.0m deep flap in various incident wave resources**

This device factor can be determined from a reference device power matrix. In the current method of power output estimation, it is proposed to use the power matrices of devices which are available. Therefore, the limits of the power matrix and the overall size proportions of the new device will remain the same as the reference device.



| | | | | | | | | | OE Buoy 2MW Average Power Matrix (kW) | | | | | | | | |
| --- | --- | --- | --- | --- | --- | --- | --- | --- | --- | --- | --- | --- | --- | --- | --- | --- | --- |
| | | | | | | | | | Average Period Tz (s) | | | | | | | | |
| | 1 | 2 | 3 | 4 | 5 | 6 | 7 | 8 | 9 | 10 | 11 | 12 | 13 | 14 | 15 | 16 | 17 |
| 1 | 0 | 0 | 0 | 0 | 7.4 | 15.9 | 27.5 | 42.3 | 57.1 | 64.1 | 61.0 | 52.8 | 46.5 | 43.9 | 43.5 | 42.5 | 36.2 |
| 1.5 | 0 | 0 | 0 | 0 | 15.5 | 33.5 | 57.9 | 89.0 | 120.3 | 135.2 | 128.4 | 111.5 | 98.4 | 92.9 | 92.4 | 89.9 | 76.6 |
| 2 | 0 | 0 | 0 | 0 | 26.8 | 58.5 | 100.6 | 153.9 | 208.9 | 235.1 | 223.1 | 193.6 | 171.0 | 161.4 | 160.7 | 155.8 | 133.0 |
| 2.5 | 0 | 0 | 0 | 0 | 41.6 | 90.4 | 155.5 | 237.7 | 323.1 | 363.7 | 344.8 | 299.2 | 264.4 | 249.8 | 248.6 | 240.9 | 205.9 |
| 3 | 0 | 0 | 0 | 0 | 59.5 | 129.1 | 222.7 | 340.7 | 462.6 | 520.7 | 493.3 | 428.8 | 378.5 | 357.3 | 355.9 | 345.0 | 295.1 |
| 3.5 | 0 | 0 | 0 | 0 | 80.5 | 174.7 | 301.9 | 461.9 | 627.2 | 706.0 | 669.2 | 581.8 | 513.4 | 484.3 | 482.7 | 468.1 | 400.2 |
| 4 | 0 | 0 | 0 | 0 | 104.8 | 227.6 | 393.1 | 601.5 | 817.0 | 919.3 | 871.9 | 757.8 | 668.9 | 630.8 | 629.0 | 610.2 | 521.2 |
| 4.5 | 0 | 0 | 0 | 0 | 132.6 | 287.9 | 496.9 | 759.7 | 1031.5 | 1160.9 | 1101.6 | 958.2 | 845.6 | 796.8 | 794.8 | 770.9 | 658.5 |
| 5 | 0 | 0 | 0 | 0 | 163.6 | 355.1 | 612.9 | 937.2 | 1272.4 | 1432.2 | 1359.2 | 1182.6 | 1043.3 | 983.3 | 980.7 | 950.2 | 811.6 |
| 5.5 | 0 | 0 | 0 | 0 | 197.3 | 429.5 | 741.2 | 1134.0 | 1539.4 | 1732.8 | 1643.6 | 1428.5 | 1260.4 | 1189.4 | 1186.6 | 1148.4 | 980.1 |
| 6 | 0 | 0 | 0 | 0 | 234.6 | 510.8 | 881.0 | 1348.9 | 1832.8 | 2000.0 | 1954.5 | 1697.4 | 1498.2 | 1414.3 | 1410.9 | 1366.3 | 1166.2 |
| 6.5 | 0 | 0 | 0 | 0 | 275.0 | 599.0 | 1033.3 | 1582.1 | 2000.0 | 2000.0 | 2000.0 | 1991.0 | 1758.4 | 1658.9 | 1653.2 | 1602.6 | 1369.7 |
| 7 | 0 | 0 | 0 | 0 | 318.6 | 694.5 | 1198.1 | 1833.5 | 2000.0 | 2000.0 | 2000.0 | 2000.0 | 2000.0 | 1923.6 | 1916.3 | 1857.8 | 1588.2 |

**Figure 4-17: Average Power Output Matrix for a BBDB type OWC device**

The average power matrix of a BBDB device is presented in Figure 4-17, based on [31] and calculated through numerical modelling. Figure 4-18 is a scatter diagram developed from site measurements on the west coast of Ireland. By coupling these two matrices, an average power output of the floating OWC may be estimated.

Ireland (West Coast) Scatter Diagram
Annual Hours of Occurrence (hours)

| Significant Wave Height (Hs) / Wave Period (Tz) | 1 | 2 | 3 | 4 | 5 | 6 | 7 | 8 | 9 | 10 | 11 | 12 | 13 | 14 | 15 |
|---|---|---|---|---|---|---|---|---|---|---|---|---|---|---|---|
| 0.5 | 0 | 0 | 0 | 52 | 130 | 25 | 0 | 0 | 0 | 0 | 0 | 0 | 0 | 0 | 0 |
| 1 | 0 | 8 | 41 | 164 | 387 | 151 | 59 | 11 | 0 | 0 | 0 | 0 | 0 | 0 | 0 |
| 1.5 | 0 | 5 | 44 | 82 | 488 | 360 | 236 | 75 | 12 | 0 | 0 | 0 | 0 | 0 | 0 |
| 2 | 0 | 0 | 26 | 65 | 293 | 503 | 258 | 142 | 31 | 4 | 0 | 0 | 0 | 0 | 0 |
| 2.5 | 0 | 0 | 0 | 76 | 107 | 354 | 386 | 129 | 26 | 5 | 3 | 1 | 0 | 0 | 0 |
| 3 | 0 | 0 | 0 | 30 | 45 | 226 | 496 | 201 | 41 | 1 | 2 | 0 | 0 | 0 | 0 |
| 3.5 | 0 | 0 | 0 | 1 | 26 | 44 | 352 | 227 | 82 | 9 | 0 | 0 | 0 | 0 | 0 |
| 4 | 0 | 0 | 0 | 0 | 23 | 19 | 181 | 252 | 99 | 19 | 3 | 1 | 0 | 0 | 0 |
| 4.5 | 0 | 0 | 0 | 0 | 9 | 9 | 71 | 210 | 99 | 19 | 4 | 0 | 0 | 0 | 0 |
| 5 | 0 | 0 | 0 | 0 | 2 | 6 | 6 | 158 | 123 | 30 | 3 | 1 | 0 | 0 | 0 |
| 5.5 | 0 | 0 | 0 | 0 | 0 | 0 | 3 | 81 | 144 | 29 | 10 | 3 | 0 | 1 | 0 |
| 6 | 0 | 0 | 0 | 0 | 0 | 0 | 4 | 21 | 100 | 44 | 7 | 4 | 0 | 1 | 0 |
| 6.5 | 0 | 0 | 0 | 0 | 0 | 0 | 4 | 6 | 47 | 42 | 11 | 4 | 0 | 0 | 0 |
| 7 | 0 | 0 | 0 | 0 | 0 | 0 | 4 | 0 | 27 | 57 | 16 | 3 | 0 | 0 | 0 |
| 7.5 | 0 | 0 | 0 | 0 | 0 | 0 | 0 | 3 | 14 | 33 | 19 | 0 | 0 | 0 | 0 |
| 8 | 0 | 0 | 0 | 0 | 0 | 0 | 0 | 0 | 3 | 29 | 21 | 5 | 0 | 0 | 0 |
| 8.5 | 0 | 0 | 0 | 0 | 0 | 0 | 0 | 0 | 1 | 21 | 17 | 2 | 0 | 0 | 0 |
| 9 | 0 | 0 | 0 | 0 | 0 | 0 | 0 | 0 | 0 | 4 | 15 | 2 | 2 | 0 | 0 |
| 9.5 | 0 | 0 | 0 | 0 | 0 | 0 | 0 | 0 | 0 | 1 | 9 | 1 | 0 | 0 | 0 |
| 10 | 0 | 0 | 0 | 0 | 0 | 0 | 0 | 0 | 0 | 0 | 2 | 3 | 1 | 0 | 0 |
| 10.5 | 0 | 0 | 0 | 0 | 0 | 0 | 0 | 0 | 0 | 0 | 2 | 1 | 0 | 0 | 0 |
| 11 | 0 | 0 | 0 | 0 | 0 | 0 | 0 | 0 | 0 | 0 | 0 | 2 | 0 | 0 | 0 |
| 11.5 | 0 | 0 | 0 | 0 | 0 | 0 | 0 | 0 | 0 | 0 | 0 | 0 | 1 | 0 | 0 |
| 12 | 0 | 0 | 0 | 0 | 0 | 0 | 0 | 0 | 0 | 0 | 0 | 0 | 0 | 0 | 0 |
| 12.5 | 0 | 0 | 0 | 0 | 0 | 0 | 0 | 0 | 0 | 0 | 0 | 1 | 0 | 0 | 0 |

**Figure 4-18: Measured Scatter Diagram for the West Coast of Ireland**

The average power output for this device has been calculated as 337kW on the west coast of Ireland. The total efficiency and device factor may be calculated taking the average resource to be 73kW/m, the width of the plenum chamber as 24.0m (X-direction) and the length to be 8.0m (Y-direction) as given in Equation 4-3 and Equation 4-4.

$$\eta = \frac{337}{73x24} x\ 100 = 19.3\%$$

<div align="right">**Equation 4-3**</div>

$$DF = \frac{337}{73x24x8} x100 = 0.024\ (m^{-1})$$

<div align="right">**Equation 4-4**</div>

As noted above, this device factor is independent of both device size and incident resource and may be used to size any floating OWC similar in operating principle to the BBDB.

### 4.4.1.2 Example Calculations

As an example, a floating OWC of the BBDB type of dimensions 35.0m wide (X-direction) and 10.0m length (Y-direction) in an incident resource of 60kW/m can be estimated to produce on average 504kW.

However, for a device that operates in the X-Z plane, an additional consideration must be taken into account. As the draft of a device increases, the incident power changes, but not at the same scale as the physical dimensions due to the exponential decay of wave power beneath the water surface assuming all waves are in deepwater. In order to account for this, a form of weighted area is utilised. The reference device is used to derive the device factor. By changing the dimension of the device in the Z-

181

direction, the new device and reference device will have a certain ratio of incident power and a ratio of Z-dimensions. Due to the exponential decay of wave power in the Z-direction, the ratios are unlikely to be the same. Therefore, it is the ratio of the incident power that is employed for power output estimations of the new device.

As an example, the 7MW Wave Dragon device has a width of 300.0m and a draft of 14.0m and is estimated to produce 1844kW on the west coast of Ireland. The device factor is calculated to be 0.006 m$^{-1}$. If a new device of dimensions 340.0m wide and a draft of 20.0m is deployed in a resource of 60kW/m, the power output may be estimated from Equation 4-5, Equation 4-6 and Equation 4-7.

$$X \ dimension \ ratio = \frac{340}{300} = 1.133$$

Equation 4-5

$$Y \ dimension \ ratio = 1$$

Equation 4-6

$$Z \ dimension \ ratio = 1.43$$

Equation 4-7

The power incident on the original device ramp may be calculated as 36.8kW/m, the power incident on the new device ramp may be calculated as 45kW/m giving a ratio of 1.22. Therefore the Z-dimension ratio is taken as 1.22 rather than 1.43 for power output estimation. The weighted draft is taken as 17.08m. The average power output may be estimated from Equation 4-8. The method of accounting for draft change is similar to that described in [53].

$$P_{avg} = 60x340x17.08x0.006$$
$$= 2090kW$$

Equation 4-8

The method suggested above for the estimation of power output of various devices is simple and effective, while indicating the varying potential of every device type and size in all resources. This will ensure that every device will inherit a ranking representative of the device design and deployment site. The power matrices of various devices are available from literature and from numerical modelling studies of devices. The device factor calculated above is directly derived from these, and can be used to reproduce another power matrix for a new device with a new hydrodynamic plane area.

There are alternatives to this method, including non-dimensionalising a reference power matrix using the $H_s$ and resonant $T_p$ for the reference machine. This method would also require using a new machine capture area etc. so in theory, both these methods should give similar results.

### 4.4.2 Development of a Simplified LCCA Model for Hybrids

The objective of the economics tool is to estimate the power output of a combined wind/wave energy platform, couple this with estimations of the cost of the system, including CAPEX and OPEX, to generate an indicative LCOE.

### 4.4.2.1 Platform Structure Inputs

All concepts generated have been designed on SolidWorks software which may be used to calculate the surface area of any shape and size of component. The surface area of the platform structure and wave energy converter structure may be input, assuming they are separate components and/or materials. A materials choice of Steel Plate, Mass Concrete, Reinforced Concrete with Epoxy Coated Reinforcing Bars and Reinforced Concrete with Stainless Steel Reinforcing Bars may be specified for each component. The density of steel is assumed to be approximately 7000kg/m$^3$. The density of concrete is assumed to be 2400kg/m$^3$. The ratio of steel volume to concrete volume is assumed to be 5%. The steel plate is assumed to be 25mm thick in all cases. The volume of ballast within a hull structure may also be specified and is assumed to be sand with a density of 1630kg/m$^3$. The costs of each of these materials per tonne, taken from [160], [161], [162], [163] as the default value, may be changed in the model if required. The maintenance of steel structures annually is assumed to be 4% of the structure cost and 0.4% for concrete structures for the first unit.

### 4.4.2.2 WEC Power Take Off Inputs

Following the specification of the structural components, the PTO for the WEC is specified. The choices here include Air Turbines, Hydraulics, Water Turbines and Direct Drive PTOs. The costs of these components are not known, and therefore an estimated cost of €800/kW capacity has been assumed for all PTO's. It is acknowledged that while this is a crude estimate of PTO costs given the variety of PTO configurations which exist for WECs, a first estimate is required for ranking of various concepts. Following further research and consultation with manufacturers a better estimate of costs may be entered for specific PTO configurations. It is assumed there is a factorial reduction in costs for the PTO's up to 50% for any PTO thereafter. The maintenance of mechanical systems is assumed to 4% of the initial cost of the first PTO unit.

### 4.4.2.3 Wind Turbine Inputs

The wind turbine structure is assumed to be one single unit, i.e. the blades, rotor, nacelle and tower all are one component. The costs structure for this component is assumed to be €2.2m/MW capacity for the first turbine and a factorial reduction in cost for any turbine thereafter. If a wind turbine is installed, structural upgrades will need to be made to the platform. These are assumed to be a percentage of the wind turbine cost. The maintenance of the wind turbine is assumed to be 4% of the initial cost of the first turbine.

### 4.4.2.4 Mooring and Anchor System Inputs

For floating systems the mooring line lengths are directly related to the water depth of deployment. If the system is buoyancy or ballast stabilised, it is assumed the platform uses slack-moored systems or catenary moorings. The mooring line length for each line is then four times the water depth. In the event that the platform is mooring line stabilised, each mooring line is assumed to be the same as the water

depth. The mooring line materials may be selected to be Steel Chain, Wire Rope or Synthetic Rope. Each material has a different cost per metre per tonne of breaking force [164]. The cost is based on the calculation of the breaking force in the mooring line, estimated from the mass of the structure and the acceleration from linear wave theory, and the length of the mooring lines. The maintenance of the mooring system is assumed to be 3% of the initial cost.

The mooring lines selected may be coupled with suitable anchors, catenary systems tend to utilise Drag Embedment Anchors and taut-leg mooring systems use Suction Pile Anchors. Each anchor has different requirements based on the mooring load that is expected to be experienced. Therefore a basic calculation of mooring loads is made based on the acceleration of the maximum wave height, taken as twice the significant wave height specified in the inputs, times the mass of the platform, times a factor of safety taken to be two. The appropriate anchor may be designed based on this loading, and the appropriate costs associated with them and the installation of the anchors. The installation of the anchors is assumed to include the mooring lines. The minimum costs for anchors and the increasing cost per kN force are taken from [163]. The installation of the anchor and mooring systems are also taken from [163] and assume three anchors and mooring lines per day.

### 4.4.2.5 Platform Installation Inputs

The installation of floating platforms is assumed to take place using simple tug boats and labour. The costs for these are taken from [163] and are on a per day basis. The time required for installation is directly related to the distance from shore. From [163], it is assumed that three days is required for 100km offshore installation. This ratio of days per km is utilised in the economics tool, and is multiplied by the tug and labour day-rates and the distance offshore of the installation.

### 4.4.2.6 Offshore and Onshore Cabling Inputs

A very important consideration in the concept development process is the distance of the particular platform from shore. This has implications for installation as discussed above and also in particular for offshore cabling considerations. All cables are assumed to be alternating current (AC) cable and are trenched when being installed. There are a number of assumptions associated with cabling in the model which may need to be modified in due course, primarily, the use of offshore substations and the associated high voltage (HV) -AC cable to shore. It is assumed that an offshore substation will be required if the MW rating of the farm exceeds 100MW. A 150kV cable connects the onshore substation to the offshore substation. 33kV cable is used to connect the devices. If a wind turbine is installed in the platform the spacing is assumed to be 1km, if the platform is a WEC only, a spacing of 0.25km is assumed. If no offshore substation is required, 30MW maximum will come ashore via 33kV cable. In essence, maximum 3 no. 33kV cables will come ashore until an offshore substation is required. All farms will have an onshore substation with a basic cost per MW capacity. The costs of cabling have been estimated from [165]. The cable installation is assumed to be a flat rate per km of cable irrespective of the voltage.

The maintenance of the transmission system is broken into a number of parts. The maintenance of the cables is assumed to be a percentage of the cable system CAPEX. The maintenance of the offshore substation is assumed to be related to the MW capacity and the installation to be similar to the platform installation.

### 4.4.2.7  Replacement and Salvage

In the model inputs are the lifetime of the device and the project lifetime. In the event that these are different, i.e. the project lifetime exceeds the device lifetime, a replacement device will be required. The cost of the replacement device is taken as 90% of the original CAPEX. When the project expires, the device may be salvaged for scrap age or re-use. The percentage of the device cost recouped depends on the remaining lifetime of the device following the expiration of the project. Table 4-1lists the various percentages of the device costs recouped after salvage.

Table 4-1: Salvage Value on the Market based on Life Left

| Salvage Market Value | |
| --- | --- |
| % Life Left | % Value on Market |
| 0 | 50 |
| 10 | 50 |
| 20 | 50 |
| 30 | 60 |
| 40 | 70 |
| 50 | 75 |
| 60 | 80 |
| 70 | 85 |
| 80 | 90 |
| 90 | 95 |

The figures assumed for salvage are for steel structures and are based on estimates obtained by HMRC staff members following consultation with relevant industry personnel. The salvage value at zero lifetime may be high, and the actual figure would naturally be device configuration specific. The welding of structural elements together makes salvage considerably more difficult. The detailed design stage could present opportunities to specifically address methods of increasing the salvage value of the structures.

### 4.4.2.8  Other Operational Cost Inputs

Other basic OPEX costs include insurance of the platform taken to be 3% of the CAPEX, the rent of the seabed location is taken to be 2.5% of CAPEX and the utilities cost taken to be €3,500 per MW capacity per year.

### 4.4.2.9  Economics Tool Outputs

All these components are linked together through the economics tool depending on the specifications of the platform under study. A breakdown of the CAPEX and OPEX components is included in the model output for the comparison of various component costs between platform concepts.

To calculate the COE, the OPEX costs are discounted based on the MW capacity installed in the farm. Discount rates are derived from [166].

The Total Lifetime Cost (TLC) is the calculated by adding the CAPEX and the discounted lifetime OPEX. The COE is calculated by dividing the annualised costs by the annual energy output (AEO) of the platform.

### 4.4.2.10  Economics Tool Validation for WEC's

From [167], a number of CAPEX costs have been given for different WEC's. The economics tool has been used to approximate the costs for these WEC's to determine how accurate/close the figures are. Table 4-2 details the costs given in [167] and the results of the economics tool.

**Table 4-2: CAPEX Costs for various WEC's from developers and HMRC_UCC tool**

| | Device | | |
|---|---|---|---|
| | **Pelamis** | **WaveStar** | **Wave Dragon** |
| Developer – CAPEX | €12.6m | €24m | €32m |
| HMRC - CAPEX | €10.6 | €22.9m | €31.6m |

The comparisons of the costs produced for each device have relied on the adjustment of the prices of concrete and steel to include costs for fabrication. This has resulted in a reasonably good estimate of the CAPEX required for each WEC.

### 4.4.2.11  Economics Tool Example – Floating Platform

The platform described in 4.3.11 is illustrated in Figure 4-19 as an example for use in the economic model.



**Figure 4-19: Combined Floating Wind/Wave Energy Platform analysed**

NOTE: All required input cells are highlighted in yellow. All outputs are highlighted in green and blue.

4.4.2.11.1 Input 1: The Resource

| SPECIFY RESOURCE | | |
|---|---|---|
| | | |
| **Select Site or Specify Resource** | | **Specify Incident Resource** |
| | | |
| **Wave Spectral Type** | | **Bretschneider** |
| **Significant Wave Height** | m | 3.3 |
| **Average Wave Period** | s | 8 |

**Figure 4-20: Specify Incident Wave Resource Input Box**

Figure 4-20 illustrates the inputs for specifying the incident resource. In the first cell highlighted in yellow, there are three options, "Ireland", "Portugal" or "Specify Incident Resource". If either Ireland or Portugal is selected, the wave height and period are automatically input into the model. The three cells below do not change. If Specify Incident Resource is selected, a spectral type, either Bretschneider or Joint North Sea Wave Project (JONSWAP) is chosen, and a significant wave height and average wave period. The resource is then calculated based on these inputs as shown in Figure 4-21.

| AVERAGE RESOURCE | | |
|---|---|---|
| | | |
| **Incident Wave Resource** | kW/m | 50 |

**Figure 4-21: Calculated Average Incident Wave Resource Output Box**

4.4.2.11.2 Input 2: The Device Type and Size

The next set of inputs is critical for the calculation of the power output of the platform. Firstly, the type of WEC device is selected from a drop-down list. The list of WEC types is shown in Table 4-3.

**Table 4-3: WEC Type and Equivalent Devices**

| WEC Device Type | Device Based On |
|---|---|
| **Floating OWC** | OE Buoy |
| **Floating OWSC** | Langlee |
| **Fixed OWSC** | Oyster |
| **Multiple Point Absorber** | WaveStar |
| **Large Point Absorber** | WaveBob |
| **Floating/Fixed Overtopping** | Wave Dragon |
| **Attenuator** | Pelamis |

Each WEC device type is based on a power matrix available for a similar device outlined above. It is crucial that the dimensions entered represent the hydrodynamic

plane of the device, not the overall device dimensions. In Figure 4-22, the WEC type chosen is 'Multiple Point Absorber' (MPA), which is based on the WaveStar device.

| SPECIFY DEVICE TYPE & SIZE | | |
|---|---|---|
| Select WEC Device Type | | Multiple Point Absorber |
| WEC X Dimension | m | 5 |
| WEC Y Dimension | m | 300 |
| WEC Z Dimension | m | 2.5 |
| WEC Capacity/Load Factor | | 20% |
| Number of Wind Turbines per device | | 1 |
| Rating of Wind Turbines | kW | 5000 |
| WT Capacity/Load Factor | | 35% |
| Number of Units | | 10 |

**Figure 4-22: Specify Device Type and Size Input Box**

The WEC dimensions of the WaveStar are X-10m, Y-50m, Z-2.5m. In the platform above, there are three MPA devices, with the same dimensions as that of WaveStar. Therefore, only one dimension needs to change, either the X or Y dimension. In the example above, the X direction is changed to 300m to reflect the three rows of 10m, or the six rows of 5m buoys. The capacity factor expected from the device may also be input, here taken as 20%. The number of wind turbines to be installed in a single platform is input as one and the rating as 5000kW. The capacity factor of offshore wind turbines may also be input, here as 35%. The number of units to be analysed is also a required input, here taken to be ten.

| PLATFORM POWER OUTPUT | | |
|---|---|---|
| Average Power Output of WEC's (HMRC) | kW | 1044 |
| | GWh | 9.1 |
| Average Power Output of WEC's (CWF) | kW | 1044 |
| | GWh | 9.1 |
| Average Power Output of Wind Turbine | kW | 1750 |
| | GWh | 15.3 |
| Total Platform Energy Production | GWh | 24.5 |
| Total Farm Power Rating | MW | 10.221 |
| Total Farm Energy Production (TEP) | GWh | 24.5 |
| Households Powered | | 2,448 |

**Figure 4-23: Platform Power Output Calculation Box**

Figure 4-23 illustrates the output from the power calculations. For comparison, the HMRC method of power calculation and the CWR method are presented, but only the result of the HMRC method is used for the COE calculation. The average power output of the WEC and wind turbine is calculated, as well as the annual energy production in GWh. The combined platform energy production and the platform power rating are included also. The farm energy production is calculated by

multiplying the platform production by the number of devices. The number of households powered is calculated by assuming a household uses 10MWh of electricity per annum.

4.4.2.11.3 Input 3: The Platform Specifications

Following the calculation of the power output, the cost of the construction, deployment and maintenance of the system must be calculated. In this input field, the platform characteristics are input. Floating and fixed platforms are analysed on two separate tabs in the worksheet. The inputs for the example above are input on the 'Floating Platform' tab. These include, stabilisation method, water depth, structural materials, surface areas, PTO's, Anchors and mooring lines, distance offshore and project life span. For the platform above, it is a floating semi-submersible with buoyancy as its stabilisation method and deployed in a water depth of 50m. The floating platform structure is to be constructed of reinforced concrete with epoxy coated rebars, while the WEC is to be constructed of steel plate. The surface areas of both components are input also. The WEC uses a hydraulic PTO system. The mooring line material is to be of steel chain and the anchors are drag embedment anchors. Each corner of the platform will have a mooring line and anchor, i.e. four of each in total. The platform is to be deployed 10km offshore and the project lifespan is chosen to be 15 years. An approximate mass of 1000tonnes is allowed for the wind turbine. Figure 4-24 illustrates how these specifications are input.

| DEVICE SPECIFICATIONS | | |
|---|---|---|
| Floating or Fixed Platform | | Floating Platform |
| Platform Stabilisation Method | | Buoyancy Stabilised |
| Water Depth | m | 50 |
| Platform Structural Material | | Reinforced Concrete - Epoxy Coated Rebar |
| Surface Area of Platform | m² | 9,000.00 |
| Additional WEC Components Material | | Steel Plate |
| Additional WEC Components Area | m² | 8,950.00 |
| Ballast Required (Sand/Concrete) | m³ | - |
| WEC PTO Type | | Hydraulics |
| Mooring Line Material | | Chain |
| Anchor Type | | Drag Embedment Anchor |
| Number of Mooring Lines | | 4 |
| Number of Anchors | | 4 |
| Distance Offshore | km | 10 |
| Estimated Lifetime of Device (max 25 Years) | Years | 15 |

**Figure 4-24: Platform Specifications Input Box**

Following the specification of the platform components, the CAPEX and OPEX for the lifetime of one device in the farm is calculated and output. It is displayed in a cost breakdown table as shown in Figure 4-25. The costs subtotals are split into the cost of the device, the total CAPEX and the undiscounted OPEX.

| PLATFORM COSTS BREAKDOWN | | | | |
|---|---|---|---|---|
| **Platform Structural Costs Summary** | | | | |
| Platform Structural Costs (Number of Units) | USD $ | 13,838,175.00 | EURO I | 9,686,722.50 |
| Additional WEC Structure and Ancilliaries | USD $ | 2,632,500.00 | EURO I | 1,842,750.00 |
| WEC PTO Cost | USD $ | 5,967,603.00 | EURO I | 4,177,322.10 |
| Structure Upgrades | USD $ | 1,105,000.00 | EURO I | 773,500.00 |
| Wind Turbine Cost (Number of Units) | USD $ | 11,050,000.00 | EURO I | 7,735,000.00 |
| **DEVICE COST** | USD $ | 34,593,278.00 | EURO I | 24,215,294.60 |
| | | | | |
| Mooring/Anchor Cost including Installation | USD $ | 1,399,620.06 | EURO I | 979,734.04 |
| Device Installation Cost | USD $ | 14,528.00 | EURO I | 10,169.60 |
| Offshore Cabling Cost/Device | USD $ | 2,521,470.00 | EURO I | 1,765,029.00 |
| Offshore Cable Installation Cost/Device | USD $ | 5,054,285.71 | EURO I | 3,538,000.00 |
| Offshore Substation Cost/Device | USD $ | - | EURO I | - |
| Onshore Substation per Device | USD $ | 292,028.57 | EURO I | 204,420.00 |
| Onshore Cabling per Device | USD$ | 1,939,092.86 | EURO I | 1,357,365.00 |
| Project Management | USD $ | 4,358,318.18 | EURO I | 3,050,822.72 |
| **CAPEX** | USD $ | 50,172,621.38 | EURO I | 35,120,834.96 |
| | | | | |
| Structure Maintenance Costs | USD $ | 789,750.00 | EURO I | 552,825.00 |
| WEC PTO O&M Cost | USD $ | 3,580,561.80 | EURO I | 2,506,393.26 |
| Wind Turbine Maintenance | USD $ | 3,450,000.00 | EURO I | 2,415,000.00 |
| Transmission System O&M/Device | USD $ | 4,874,122.63 | EURO I | 3,411,885.84 |
| Insurance/Device | USD $ | 22,577,679.62 | EURO I | 15,804,375.73 |
| Rent/Device | USD $ | 1,254,315.53 | EURO I | 878,020.87 |
| Utilities/Device | USD $ | 536,602.50 | EURO I | 375,621.75 |
| | | | | |
| **Undiscounted OPEX** | USD $ | 37,063,032.08 | EURO I | 25,944,122.46 |
| | | | | |
| **Total Combined Platform Cost** | USD $ | 87,235,653.46 | EURO I | 61,064,957.42 |

**Figure 4-25: Platform Lifetime Costs Breakdown Output Box**

4.4.2.11.4 Main Output for Analysis - COE

Following the calculation of the various project components, the COE may be calculated. This incorporates the AEO of the platform and the total annualised costs. Figure 4-26 illustrates the output table.

| Cost of Electricity (COE) | | |
|---|---|---|
| Individual Device CAPEX | EURO ⎮ | 44,316,381.08 |
| Discounted Device Lifetime OPEX | EURO ⎮ | 19,779,886.31 |
| OPEX:CAPEX | | 45% |
| Total Individual Platform Lifetime Cost | EURO ⎮ | 64,096,267.39 |
| Total Individual Platform Lifetime Energy Production | GWh | 416.1 |
| COE | €/kWh | 0.18 |
| | | |
| Farm CAPEX | EURO ⎮ | 443,163,810.82 |
| Farm OPEX Discounted | EURO ⎮ | 197,798,863.07 |
| Farm Lifetime Cost (TLC) | EURO ⎮ | 640,962,673.89 |
| | | |
| Farm OPEX UnDiscounted | EURO ⎮ | 305,488,764.74 |

| Summary | | |
|---|---|---|
| CAPEX/GWh | €/GWh | 1,810,467.33 |
| OPEX/GWh | €/GWh | 80,807.23 |
| COE | €/kWh | 0.18 |
| Net Present Value (NPV) | € - | 457,791,320.13 |
| Internal Rate of Return (IRR) | | #DIV/0! |

**Figure 4-26: COE and Summary Output Box**

The summary table illustrates the predominant figures which are used to rank the various concepts, the CAPEX investment/GWh of energy produced, the discounted OPEX investment/GWh of energy produced and the COE. The NPV and IRR are not applicable here as no REFiT rates have been included in the calculation.

### 4.4.3 Further Evaluation of Aspects of Hybrid Platforms

During the evaluation of the hybrid concepts, a number of issues regarding power performance and structural loading arose with respect to a number of the specific concept configurations. This section addresses these issues, which are listed below.

1. Power performance and motion characteristics of the OWC Array Concept
2. Structural Load Implications of a PA on a Fixed Column Guide

The method applied to determining these issues was primarily tank testing due to a number of considerations outlined in each study.

#### 4.4.3.1 OWC Array Characterisation

As noted above, the characterisation of the OWC Array platform concept had significant uncertainties associated with the prediction of the performance in terms of power due to the unknown interactions between each OWC chamber on the one

platform. In early 2012, a developer with a similar device as that proposed carried out testing to characterise power performance at UCC. This developer had specific intellectual property (IP) incorporated into their device. For the testing carried out in this thesis, this IP was completely removed and the performance of an array of individual OWC chambers on a single structure was tested. This was with the permission of the developer and the overall system performance result was provided to the developer to act as a benchmark for their IP performance. The details of the testing are outlined below. The results of testing carried out specifically on the OWC Array platform basic concept provided the necessary information to predict the power performance of the OWC Array within typical tank testing confidence limits.

4.4.3.1.1 Model Description

The OWC array device considered here has the very same operating principle as the OE Buoy, but has a total of 32 OWC chambers, each connected together. The overall shape of the platform is a "V" shape in plan as illustrated in Figure 4-27, pointing directly into the waves similar to the 'Leancon' [168] wave energy device. The OWC array consists of 16 OWC chambers on each leg of the platform. The total width of the device is 6.9m with an angle of 90° between each leg and is designed to be at a scale of 1:50. Initially, the developer of this device, J.J. Campbell and Associates Ltd., used two plenum chambers on each leg of the platform to gather the positive pressure and negative pressure from each chamber into a single venturi flume. Both plenum chambers were connected to each other via the venturi flume. Therefore the air flow in the device was a closed system. The positive and negative pressures from the individual OWC chambers were allowed flow into the correct plenum chamber by using standard one directional air admittance valves. However, for the testing programme carried out to characterise the OWC interactions and performance of an OWC Array on a single platform, these plenum chambers were removed and each OWC chamber was treated individually. The individual chambers were damped using simple orifice plates of varying size. Furthermore, basic Froude scaled wind turbine towers were attached to the platform to assess the modifications to the motion characteristics. A more in depth description of the testing and analysis can be found in APPENDIX B, however the main outputs include the power matrix of the array and the fact that no measureable effect was seen on the motion characteristics from either configuration of wind turbine towers mounted on the platform with thrust loads applied.

**Figure 4-27: 32 Chamber OWC Array model**

### 4.4.3.1.2 Power Matrix

The testing programme produced a significant amount of data, not all of which has been utilised in this study. From this dataset, a power matrix has been determined for the OWC Array as illustrated in Figure 4-28. In this analysis, the average PTO and Electrical efficiencies have been taken to be 50% and an assumed load factor of 25%.

| OWC ARRAY - ELECTRICAL POWER OUTPUT MATRIX | | | | | | | | | | | | | | | | | |
|---|---|---|---|---|---|---|---|---|---|---|---|---|---|---|---|---|---|
| Peak Wave Period (T$_p$) (s) | | | | | | | | | | | | | | | | | |
| 1 | 2 | 3 | 4 | 5 | 6 | 7 | 8 | 9 | 10 | 11 | 12 | 13 | 14 | 15 | 16 | 17 | 18 |
| 6 | 14 | 23 | 35 | 47 | 61 | 75 | 91 | 97 | 101 | 104 | 104 | 101 | 97 | 91 | 79 | 66 | 54 |
| 24 | 55 | 93 | 138 | 190 | 243 | 302 | 366 | 388 | 405 | 417 | 414 | 404 | 386 | 362 | 317 | 264 | 217 |
| 54 | 124 | 210 | 311 | 427 | 547 | 679 | 823 | 873 | 912 | 939 | 932 | 908 | 869 | 815 | 714 | 594 | 489 |
| 97 | 221 | 373 | 552 | 759 | 973 | 1208 | 1463 | 1553 | 1622 | 1670 | 1656 | 1615 | 1546 | 1449 | 1270 | 1056 | 869 |
| 151 | 345 | 582 | 863 | 1186 | 1520 | 1887 | 2286 | 2426 | 2534 | 2609 | 2588 | 2523 | 2415 | 2264 | 1984 | 1650 | 1358 |
| 217 | 497 | 838 | 1242 | 1708 | 2189 | 2717 | 3291 | 3493 | 3648 | 3757 | 3726 | 3633 | 3478 | 3260 | 2857 | 2375 | 1956 |
| 296 | 676 | 1141 | 1691 | 2324 | 2980 | 3698 | 4480 | 4755 | 4966 | 5114 | 5072 | 4945 | 4733 | 4438 | 3888 | 3233 | 2663 |
| 386 | 883 | 1490 | 2208 | 3036 | 3892 | 4830 | 5851 | 6210 | 6486 | 6679 | 6624 | 6458 | 6182 | 5796 | 5078 | 4223 | 3478 |
| 489 | 1118 | 1886 | 2795 | 3842 | 4925 | 6113 | 7405 | 7860 | 8209 | 8453 | 8384 | 8174 | 7825 | 7336 | 6427 | 5344 | 4401 |
| 604 | 1380 | 2329 | 3450 | 4744 | 6081 | 7547 | 9143 | 9703 | 10134 | 10436 | 10350 | 10091 | 9660 | 9056 | 7935 | 6598 | 5434 |
| 731 | 1670 | 2818 | 4175 | 5740 | 7358 | 9132 | 11062 | 11741 | 12263 | 12628 | 12524 | 12210 | 11689 | 10958 | 9601 | 7984 | 6575 |
| 869 | 1987 | 3353 | 4968 | 6831 | 8756 | 10868 | 13165 | 13973 | 14594 | 15028 | 14904 | 14531 | 13910 | 13041 | 11426 | 9501 | 7825 |
| 1020 | 2332 | 3936 | 5831 | 8017 | 10276 | 12754 | 15451 | 16000 | 16000 | 16000 | 16000 | 16000 | 16000 | 15305 | 13410 | 11151 | 9183 |
| 1183 | 2705 | 4564 | 6762 | 9298 | 11918 | 14792 | 16000 | 16000 | 16000 | 16000 | 16000 | 16000 | 16000 | 16000 | 15553 | 12932 | 10650 |
| 1358 | 3105 | 5240 | 7763 | 10673 | 13681 | 16000 | 16000 | 16000 | 16000 | 16000 | 16000 | 16000 | 16000 | 16000 | 16000 | 14846 | 12226 |
| 1546 | 3533 | 5962 | 8832 | 12144 | 15566 | 16000 | 16000 | 16000 | 16000 | 16000 | 16000 | 16000 | 16000 | 16000 | 16000 | 16000 | 13910 |
| 1745 | 3988 | 6730 | 9971 | 13709 | 16000 | 16000 | 16000 | 16000 | 16000 | 16000 | 16000 | 16000 | 16000 | 16000 | 16000 | 16000 | 15704 |
| 1956 | 4471 | 7545 | 11178 | 15370 | 16000 | 16000 | 16000 | 16000 | 16000 | 16000 | 16000 | 16000 | 16000 | 16000 | 16000 | 16000 | 16000 |
| 2180 | 4982 | 8407 | 12455 | 16000 | 16000 | 16000 | 16000 | 16000 | 16000 | 16000 | 16000 | 16000 | 16000 | 16000 | 16000 | 16000 | 16000 |
| 2415 | 5520 | 9315 | 13800 | 16000 | 16000 | 16000 | 16000 | 16000 | 16000 | 16000 | 16000 | 16000 | 16000 | 16000 | 16000 | 16000 | 16000 |

*Significant Wave Height (H$_s$) (m): 0.5, 1, 1.5, 2, 2.5, 3, 3.5, 4, 4.5, 5, 5.5, 6, 6.5, 7, 7.5, 8, 8.5, 9, 9.5, 10*

**Figure 4-28: Electrical Power Output for OWC Array rated at 16MW**

### 4.4.3.2 PA and Monopile Foundation

This investigation was aimed at determining the effects of mounting a PA WEC on a monopile structure with regard to the change in structural loading on the monopile as well as the power absorbed by the point absorber. The testing was carried out on a 1:50 scale model in the HMRC, UCC.

### 4.4.3.2.1 Model Description

The PA model tested in this study consisted of a steel base with a vertical steel bar spine. The outer pile was constructed of 110mm diameter PVC tubing as illustrated in Figure 4-29. This outer tube was connected to the inner steel spine by four load cells. This allowed the horizontal load on the outer pile to be measured. A baseline set of tests were carried out with this configuration in both sinusoidal waves and uni-

directional 2-D wave spectra. The PA was a torus type buoy and was fabricated from two layers of 100mm insulation board, total depth 200mm. The outer diameter of the torus was 380mm and the internal diameter of the torus was 130mm. Lead weight was added to the lower section of the buoy to increase the draft. A number of configurations have been tested by adjusting the mass of the buoy. A more detailed account of the testing and analysis can be found in APPENDIX C.



**Figure 4-29: Point Absorber, Mono pile, Pistons, Gravity Base**

The motion of the buoy was restricted to heave only by using six guide rollers between the buoy and the main pile. The PTO was simulated by using two submerged pistons. These pistons damped the heave motion of the buoy by pumping water through an orifice. The diameter of this orifice was varied to calculate the optimum damping for power absorption. The pressure in the pistons was monitored by a pressure transducer tapping in an air pocket situated above the water surface. The power calculations have assumed the pressure in the air pocket was the same as that in the piston chamber.

The efficiency of the device was then calculated for each different wave period for the configuration which resulted in the maximum power absorbed. Figure 4-30 and Figure 4-31 display the power available to the PA, the power absorbed by the device and the efficiency of the device for the two differing configurations.

It is evident from Figure 4-30 and Figure 4-31 that the maximum efficiency of the PA device was 14.9% at a wave period of 8s with a PA Mass of 762.5t resulting in an absorbed power of 203.5 kW. The maximum absorbed power of 279 kW occured at a wave period of 11.0s with a PA mass of 762.5t and a device efficiency of 14.8%.
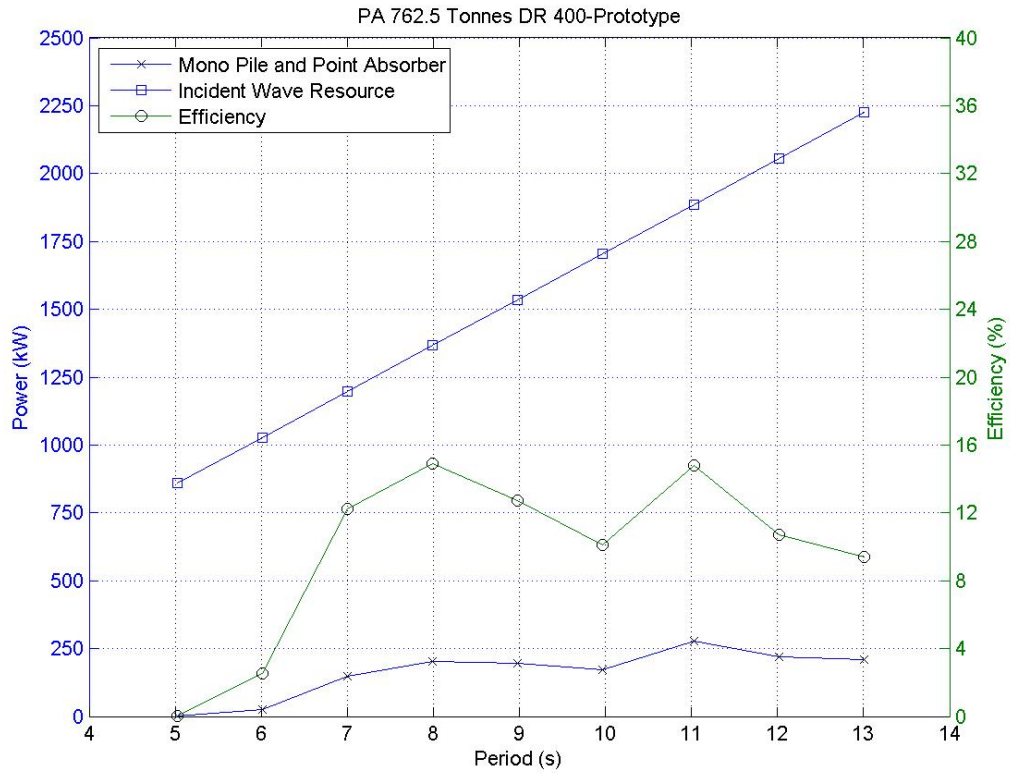
**Figure 4-30: Power Available, Power Absorbed and Efficiency of Device. PA Mass: 762.5t, Damping Ratio: 400**
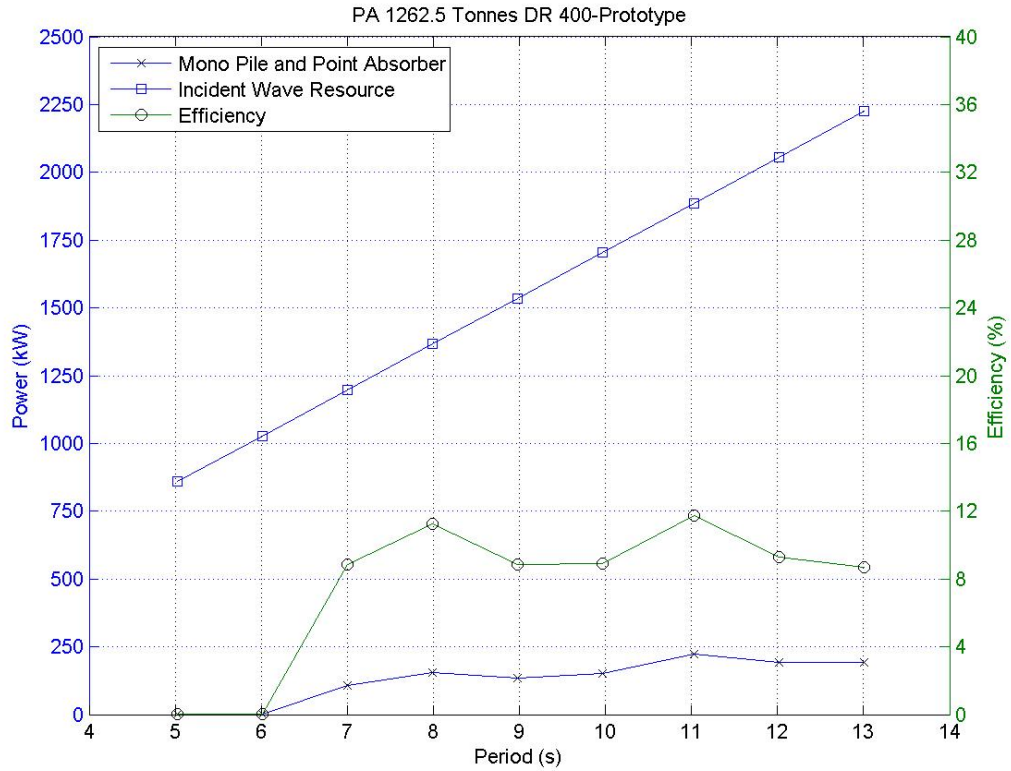


**Figure 4-31: Power Available, Power Absorbed and Efficiency of Device. PA Mass: 1262.5t, Damping Ratio: 400**

195

4.4.3.2.2   Increase in Load per kW of Absorbed Power

In order to determine if there exists any relationship between the absorbed power, the structural load on the monopile and the wave period, the increase in load from the base line case of the monopile alone was divided by the absorbed power at each period. The following tables display the increase in structural load per kW of power absorbed by the PA (kN/kW) for the two PA masses and wave periods. Figure 4-32 shows the variation of the increase in structural load per kW of absorbed power with wave period for a constant wave height of 3m.
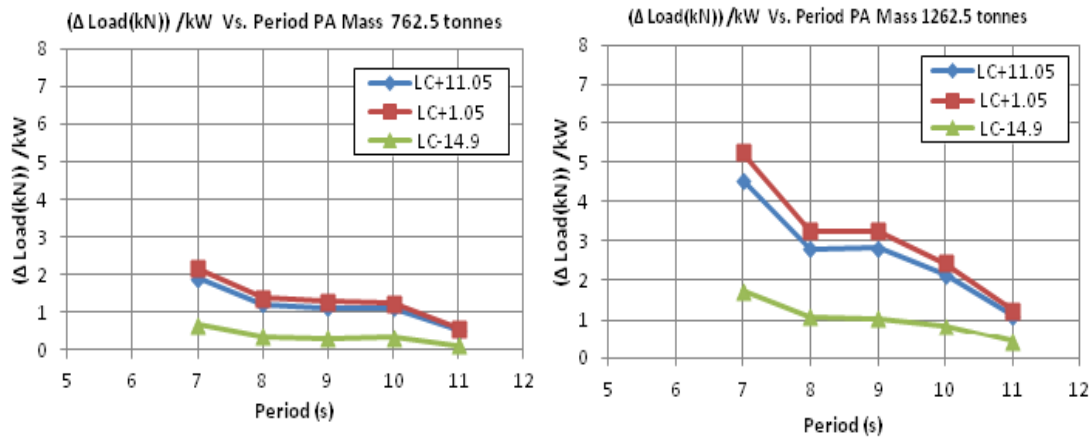


**Figure 4-32: kN/kW PA Mass: 762.5 tonnes and 1262.5 tonnes for Hₛ 3m**

It can be seen from Figure 4-32 that there was a gradual decrease in the ratio of structural load to absorbed power (kN/kW) as the wave period was incresased for both configurations of the PA. This reflected the decrease in structural load experienced by the load cells with an increase in wave period. In addition to this the kN/kW values for all load cells at all periods is lower for the configuration with a PA mass of 762.5t when compared to the configuration with a PA mass of 1262.5t. In fact,  not only was the structural load on the monopile lower for the 762.5t configuration but the power absorbed was greater also.

### 4.4.4   Ranking of Proposed Hybrid Concepts

The ranking process for the hybrid concepts involves taking into consideration all known information from the results of the assessment methods discussed while also taking into consideration a degree of engineering judgement with regard to the overall concept and its appropriateness for deployment in deepwater high energy sites. A number of quantitative and qualitative criteria have also been used to rank these concepts. The criteria include:

1.  Levelised Cost of Energy
2.  Constructability of Hull
3.  Operations and Maintenance
4.  Installability
5.  Survivability

In a detailed assessment level, only one of these criteria would be required, the LCOE. However, as this ranking of concepts is at the first stage of development the estimate of the LCOE cannot accurately represent that which will be delivered by the concept. With this in mind, the additional categories of assessment are added which specifically target areas which will ultimately affect the LCOE when the LCCA model can be correctly populated with information from a detailed assessment. Each category is introduced and briefly discussed below.

### 4.4.4.1 LCOE

The concept specific LCOE is generated from the simplified LCCA model discussed in 4.4.2. The inputs and outputs have been discussed at length.

### 4.4.4.2 Constructability of Hull

The constructability of the hull is a significant consideration for each concept depending on the installed capacity of the device and the ease of construction. In other words, for a platform with a low power capacity, mass production capability is critical to deploy a sufficient number of platforms to reach the farm capacity. For a platform with a high power capacity, this criteria can be relaxed to an extent. Furthermore, the type of construction will be of concern, i.e. a large platform with a steel plate and stiffener design will present a significant logistical challenge in delivering large stiffened plate to the main construction site for fabrication. Alternatively, an RC construction can be carried out in-situ similar to any large building. The decisions made in this section have cross-category effects with regard to mooring system design in survivability and O&M activities in operations and maintenance and should be carefully considered.

### 4.4.4.3 Operations and Maintenance

The O&M category is a significant contributor to the overall LCOE. In the first stage of development this is simplified to large extent due to lack of detailed information. Therefore, the concept related risk associated with the type of machinery to be used as the PTO, the access limits of the platform, and the resource in which it is intended to be deployed are all relevant considerations.

### 4.4.4.4 Installability

In specific cases, either a large or small platform can present installation challenges. For example, the installation process for the Hywind discussed in Chapter 2 was a significant challenge due to the number of processes and vessels required. For a large platform with a large displacement, the number of tugboats required for towing to sea is a significant consideration for risk reduction and timely installation depending on the distance offshore.

### 4.4.4.5 Survivability

The survivability of the platform in this case refers to the activities and machinery required to secure the platform, WECs and WTGs, during extreme wave conditions. For example, the process for securing the WECs on-board the Wavestar WEC

described in Chapter 2. The survival of the WECs relies on timely withdrawal from the sea by a hydraulics system. The failure of this hydraulics system would result in damage to the WECs. This category considers the ease by which the platform components can be secured against damage, but primarily the PTO. Structural survivability of the platform and moorings is assumed to be sufficiently covered by design standards if they apply to the concept.

Similar categories have also been used in the ranking of concepts in the MARINA project.

**4.4.4.6    Performance of Concepts**

The ranking criteria below include constructability, O&M, installability and survivability. O&M and survivability are considered the main criteria.

| | | | | | | |
|---|---|---|---|---|---|---|
| 1 | Wave Dragon and WTG | Large, heavy hull; May be difficult to assemble due to shape of central reservoir and draft of hull; Steel plate and stiffener or RC for reservoir; steel for arms | Large wake in leeside, boat docking should be easy even in high waves; Turbine PTO simple to maintain with the exception of rotor being 1-2m under water; biofouling in draft tube | Will require a number of tugboats for towing to installation site; will be very slow due to large displacement; installation time will be a significant concern | Loss of PTO not detrimental to hull survivability |  |
| 2 | FPP - Poseidon | WECs are block shaped, should be ok for mass production; Linear build possible, should be suitable for dry-docks; Deep-draft may be an issue in full scale; Steel plate and stiffener; | Large wake in leeside, boat docking should be easy even in high waves; moving WECs may be an issue for O&M | Will require a number of tugboats for towing to installation site; will be very slow due to large displacement; installation time will be a significant concern | Loss of PTO could be detrimental to hull integrity |  |
| 3 | OWWE | Large, heavy hull; May be difficult to assemble due to shape of central reservoir and draft of hull; Steel plate and stiffener or RC for reservoir; steel for arms | Large wake in leeside, boat docking should be easy even in high waves; Turbine PTO simple to maintain with the exception of rotor being 1-2m under water; biofouling in draft tube | Will require a number of tugboats for towing to installation site; will be very slow due to large displacement; installation time will be a significant concern | Loss of PTO not detrimental to hull survivability |  |
| 4 | Green Ocean Energy - Wave Treader | Simple; Mass production of main ATN possible; Connection to foundations may be specific; Steel plate and stiffener; | May limit access to WTG; Hydraulic PTO, complex and number of parts | Retro-fit? Requires a crane ship/jack-up | Loss of PTO could be detrimental to hull integrity |  |
| 5 | Pelagic Power - W2Power | Medium sized semi-sub, production in a dry-dock should be possible; bracing and heave plate are complicated structures; Steel plate and stiffener for columns and steel tubing for braces; | Space frame stucture, no shielding effect, boat motions critical; access to PAs difficult due to size; Helicopter access possible; | Installation should be straightforward with 2/3 tugboats | Loss of PTO could be detrimental to hull integrity |  |
| 6 | Wavestar - WindWaveStar | Mass production definitely required, difficult for hemisphere buoys?; | Depending on the location of buoys, access to turbine may be limited; all hydraulic equipment above water within hull | 4 piles to be installed, time consuming; lifting of WEC beams and turbine requires crane-ship or jack-up; | Loss of PTO could be detrimental to hull integrity |  |

| | | | | | | |
|---|---|---|---|---|---|---|
| 7 | Single OWC Barge and WTG | Without focussing arms, barge would be possible to build in a dry-dock; Simple shape for mass production; Steel plate and stiffener or RC | No moving parts under water; only access to hull is required | 2/3 tugboats would be sufficient depending on size of hull | Loss of PTO not detrimental to hull survivability |  |
| 8 | Large PA Spar and WTG | Diameter of spar requires a steel plate and stiffener construction; transportation etc difficult due to length of foundation | Access to the spar may be difficult if PA is operating; Depending on survival condition, PTO equipment may be over/under water | Installation of the spar is a complex and risky process, particularly in areas where nearshore deepwater is not available; | Loss of PTO could be detrimental to hull integrity; Instabilities like that experienced by the Wavebob may occur |  |
| 9 | Twin OWC Spar and WTG | Diameter of spar requires a steel plate and stiffener construction; transportation etc difficult due to length of foundation | All PTO above water; Access to rear of OWCs, wake may be provided for boat docking | Installation of the spar is a complex and risky process, particularly in areas where nearshore deepwater is not available; | Loss of PTO not detrimental to hull survivability; Loading on OWC chambers during extreme conditions may cause instabilities in spar motions |  |
| 10 | Single OWC and Jacket WTG | Jacket structure is already a complicated structure, addition of OWC chamber even moreso; Structural implications of additional load from OWC on jacket; | Wake may be provided by OWC for boat access; positioning of OWC turbine critical for ease of maintenance | The addition of the OWC into the jacket will make it heavier and more difficult to install; The limits of installtion of the jackets will be further reduced due to the additional loading from the OWC chamber; | Loss of PTO not detrimental to hull survivability; Loading on OWC chambers during extreme conditions may cause extreme loads on jacket piles and fracture of grout connection |  |
| 11 | OWSC Array and WTG | The construction of the flaps is complex like the Oyster; The semi-sub may be suitable for construction in 2 parts in a dry-dock; | Hydraulic hoses etc located underwater, difficult for O&M, need divers; Moving parts of hydraulic actuators underwater; PTO can be over water | Will require a number of tugboats for towing to installation site; will be very slow due to large displacement; installation time will be a significant concern | Loss of PTO could be detrimental to hull integrity |  |
| 12 | OWC Modified Ship Hull and WTG | Re-commissioning of a ship hull is unlikely to be a feasible option; retro-fit of OWC through the hull will be difficult; Mass production unlikely | No moving parts under water; only access to hull is required | 2/3 tugboats would be sufficient depending on size of hull | Loss of PTO not detrimental to hull survivability |  |

| 13 | Barge OWC Array and WTG | The barge structure can be fabricated from either RC or steel plate and stiffeners; each chamber can be made seperately and joined making the foundation modular in nature; This allows any number of OWCs to be attached to make a WEC of any capacity for variability reduction | No moving parts under water; only access to hull is required; Large wake in leeside, boat docking should be easy even in high waves; | Will require a number of tugboats for towing to installation site; will be very slow due to large displacement; installation time will be a significant concern | Loss of PTO not detrimental to hull survivability |  |
|----|----|----|----|----|----|----|
| 14 | ATN Barge and WTG | Straightforward construction of ATN, steel plate and stiffener; joints and higes this size may be problematic; more than likely FLS governed design | Access may be difficult due to fore and aft moving ATN; Higes semi-submerged | Assuming the heave plate can be retracted, the installation should be easy due to shallow draft of ATN; 2-3 tugboats would be sufficient | Loss of PTO could be detrimental to hull integrity |  |
| 15 | PA Array and Tripile WTG | The construction of the tripile is straightforward and has been demonstrated; Depending on size, the PAs may be more difficult; | Access would be difficult due to motion of PA; possibility of submerging PA? Time consuming; | The tripile requires 3 piles to be installed seperately and a TP installed; The tolerances are very small for the pile locations and can make this a risky operation as one pile may be lost if incorrectly installed; Requires a crane-ship or jack-up | Loss of PTO could be detrimental to hull integrity |  |
| 16 | PA Array and Large Semi-sub WTG | WECs are block shaped, should be ok for mass production; Linear build possible in 2 pieces, should be suitable for dry-docks; Deep-draft may be an issue in full scale; Steel plate and stiffener; | Large wake in leeside, boat docking should be easy even in high waves; Rotating shafts and hydraulic fluid transmission network above water | Will require a number of tugboats for towing to installation site; will be very slow due to large displacement; installation time will be a significant concern | Loss of PTO could be detrimental to hull integrity |  |
| 17 | PA Array and Large Semi-sub WTG | Mass production of buoys and connectors critical; may be difficult for hemisphere buoys; | Significant number of components in the hydraulic systems for O&M | Will require a number of tugboats for towing to installation site; will be very slow due to large displacement; installation time will be a significant concern | Loss of PTO could be detrimental to hull integrity |  |
| 18 | PA Array and TLP WTG | space-frame structure, difficult welding operations; fixed guides for PAs require significant strength even for operational conditions; FLS may be critical | Access to the buoys will be difficult unless individual gangways are provided to each buoy; | TLPs by nature are difficult to install due to tension in mooring lines; float-out using PAs as buoyancy at correct draft?; divers or ROV for "threading" of mooring line through fairlead? | Loss of PTO could be detrimental to hull integrity |  |

**Figure 4-33: Qualitative Ranking of Hybrid Concepts**

Due to the uncertainty associated with the approximations of the LCOE, it was decided that on the basis of two categories, O&M and Survivability, that a qualitative ranking of these would be the main method of reducing the number of concepts. From Figure 4-33 the overtopping and OWC concepts have received the better ranking from O&M and Survivability illustrated in colour. This is largely due to the PTO configuration of these concepts. The PTO for both overtopping and OWC concepts are turbine based and the turbine rotor and shaft is the only moving part along with the associated axial and thrust bearings. The survival of the PTO for these concepts is not required for the continued survival of the total hull. End-stops are not an issue for these systems either. Within the overtopping and OWC concepts, a distinguishing factor between them is that the overtopping turbine is submerged in 1-2m deep water in the reservoir making access more difficult and likely to suffer from biofouling of the rotor and draft tube. Furthermore, the power capture performance of the OWC is superior to that of the overtopping concepts as reported in [17] which should show directly in the LCOE estimations and has been confirmed with additional tank testing described in 4.4.3.1. Given the uncertainty surrounding the power performance of any particular concept in isolation based on average CWRs for that class of WEC, a brief account of the performance of both overtopping and OWCs can be undertaken. From [17], the maximum reported CWR for overtopping is c. 23% based on Wave Dragon and using the proposed 85% reservoir efficiency for a full scale Wave Dragon [53], and 90% for both the turbine and electrical efficiencies, the total efficiency of the overtopping system would be c. 15.8% maximum. Using the average efficiencies for an OWC, 33% CWR and 54% turbine and 90% electrical efficiency, the total average efficiency would be c. 16%. Even comparing maximum overtopping system efficiency with average OWC system efficiency in this instance, the OWC system presents a better opportunity to deliver high power performance. With these considerations in mind, the chosen concept is then the OWC concept with a WTG. The three concepts representing this category are the single OWC barge and WTG, the ship hull and WTG and the OWC barge array and WTG. The ship hull has been discarded also due to the issues surrounding retro-fits and sourcing of decommissioned hulls. The single OWC is a simplification of the OWC array concept, so therefore the chosen concept is the Barge OWC Array and WTG as described in 4.3.7.

# 5 Design and Assessment of an OWC Array Hybrid Platform

Following the initial conceptual design, ranking and selection of the OWC Array hybrid device in Chapter 4, this chapter focusses on the design and assessment methodologies for the OWC Array platform in the high energy west of Ireland conditions, or the M1 location as described in Chapter 3. This ranges from initial numerical modelling of hydrodynamics and structural analysis of reconfigured platform shapes and sizes of the OWC to a more detailed assessment of the final design. The chapter then addresses the design and fabrication of a 1:50 scaled model of the OWC Array platform for tank testing. The results and performance of the OWC Array is then discussed.

## 5.1 Reconfiguration of the Initial OWC Array Concept

During the ranking and preliminary analysis of the concepts in Chapter 4, the Wave Dragon concept with WTs stood out as one of the preferred options. This was mainly due to the fact that the company had already considered this in their original patent application, the motion characteristics of the large platform must be within an acceptable range to consider this and the O&M of the PTO is middle of the range between air turbines and fluid hydraulics. The issue with the concept is the power performance of the overtopping ramp which has a low CWR compared to OWCs. With this in mind, a new configuration of the OWC Array was envisaged which was derived from the Wave Dragon platform. It stands to reason that if the platform mass can be maintained, power performance improved and O&M simplified, the LCOE of the new concept would be lower. This is the intention for the concept illustrated in Figure 5-1.
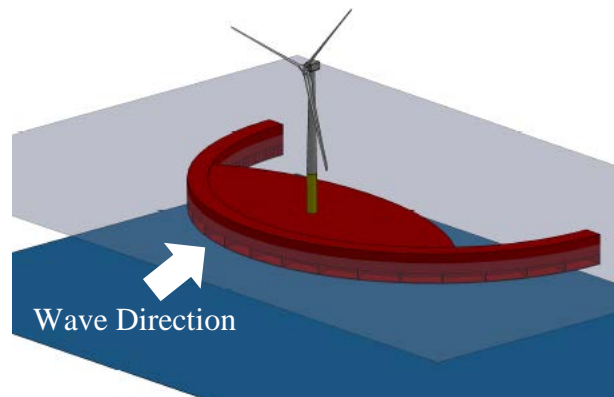


**Figure 5-1: Reconfiguration of the OWC Array based on the Wave Dragon Platform**

The platform in Figure 5-1 is referred to as the "Curved OWC Array". The platform incorporates 20 OWC chambers in the hull each measuring 24m long by 8m wide and the NREL 5MW reference turbine. The platform is 300m in width in total and is semi-circular in shape. The draft of the hull is approximately 12m. A preliminary analysis of the Curved OWC Array platform has been carried out numerically for assessment of hydrodynamics and structural design as well as the motion characteristics for the wind turbine and maintenance tasks. These assessments are

discussed in the following sections. The primary platform details are tabulated in Table 5-1.

**Table 5-1: Curved OWC Array Specifications**

| Curved OWC Array Parameter | Value |
|---|---|
| **Platform Width** | 300m |
| **Platform Length** | 150m |
| **Platform Depth** | 12m |
| **Platform Displacement** | 164,400t |
| **No OWC Chambers** | 20 |
| **Dimensions of OWC Chamber** | 24m x 8m |

### 5.1.1 Numerical Analysis of Power Performance

The analysis of power performance was similar to that carried out for the BBDB device in Chapter 3 using the commercially available linearised potential theory code WAMIT. In this instance however, the platform is composed of a single hull and 20 individual OWC chambers. Therefore, 20 'numerical lids' as detailed in [136] have been used to represent the IWS of the OWCs. Empirical damping was applied to the numerical lid from [106] to account for viscous damping and vortex shedding as well as PTO damping which was estimated from the tank testing carried out on an OWC Array device as discussed in Chapter 4. The chamber IWS motion has been restricted to one degree of freedom, i.e. vertical movement of the water column, no sloshing modes have been included. The chamber IWS RAOs that have been produced by the numerical analysis are illustrated in Figure 5-2.
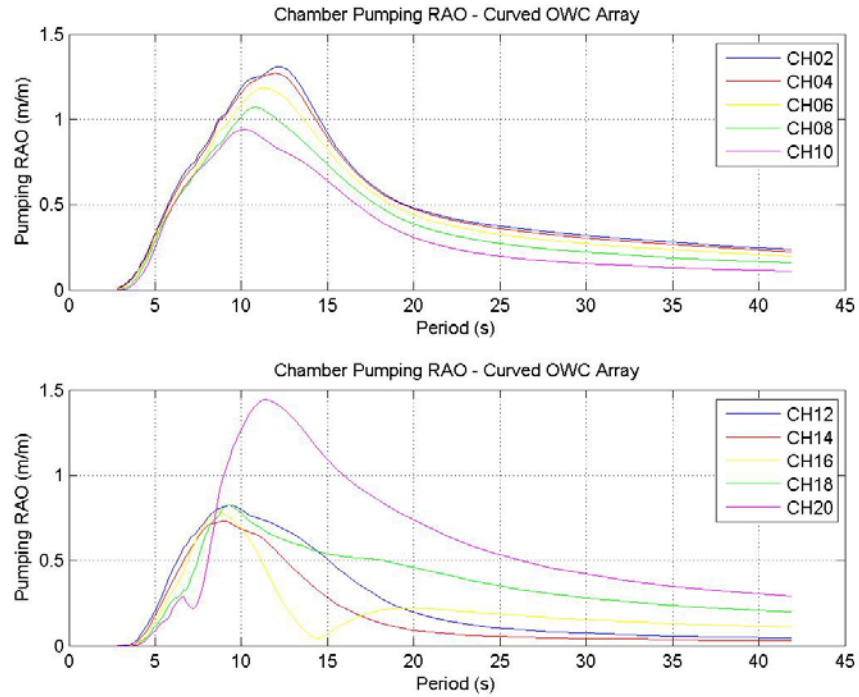
**Figure 5-2: Curved OWC Array Chamber IWS RAOs**

These RAOs have been used in conjunction with the principle of superposition to develop an average electrical power matrix for the Curved OWC Array platform. The resultant power matrix is illustrated in Figure 5-3 assuming an average PTO efficiency of 54%.
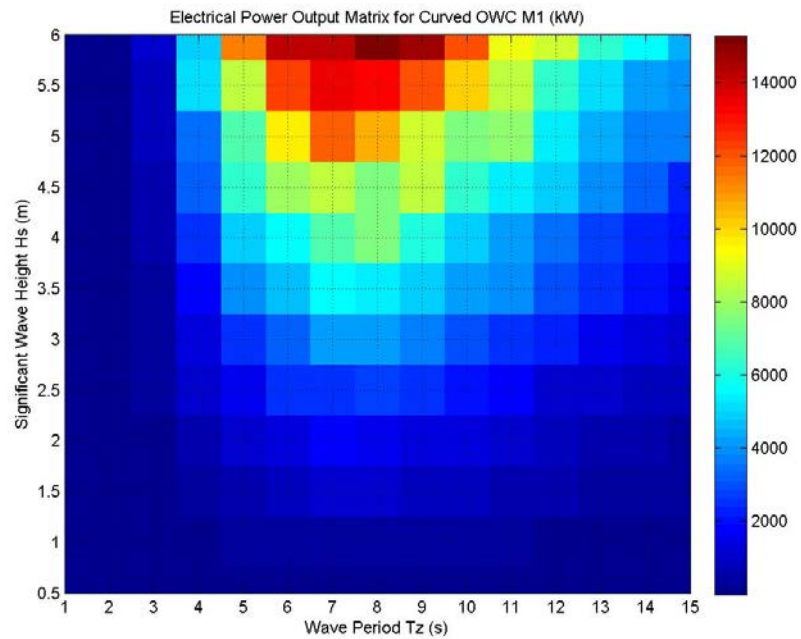


**Figure 5-3: Average Electrical Power Matrix for the Curved OWC Array**

From the IWS RAO plots in Figure 5-2 and the power matrix illustrated in Figure 5-3, the Curved OWC Array platform appears to be performing at the correct period range for the high energy site off the west coast of Ireland. Coupling this matrix with the scatter diagram for the M1 site, the annual average electrical power produced by the WEC is 3341kW.

## 5.1.2 Numerical Analysis of Structural Design Requirements

The frequency domain hydrodynamic analysis has also produced the hydrodynamic pressures on each panel of the wetted hull of the Curved OWC Array platform.
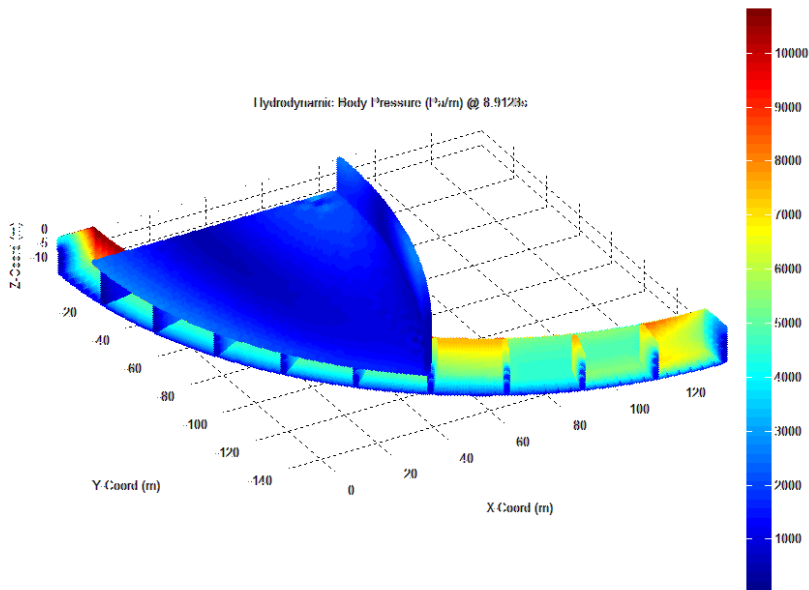


**Figure 5-4: Hydrodynamic Pressures on the Wetted Hull of the Curved OWC Array Platform at ~9s**

The panel pressure RAO distribution is illustrated in Figure 5-4 for a wave period of ~9s. The RAO for each panel has been used to design the structural material requirements in a simplified manner using the principle of superposition for the design wave conditions for the M1 site described in Chapter 4. The hull has been designed using structural steel initially to determine the platform mass and total cost.

### 5.1.2.1 Steel Construction

The first structural design configuration for the Curved OWC Array platform was the typical steel plate and stiffener fabrication method for estimation of structural steel mass. The method of design is similar to that outlined in Chapter 3. Figure 5-5 illustrates the results of the MC simulations for assessment of the effects of short term realisations of sea states on the structural mass of the platform for varying steel beam stiffener spacing based on [115]. The figures illustrated on the plot represent the best and worst case for the structural steel mass of the platform. Only the worst case scenario is considered in LCCA analysis, i.e. 13,672t. Figure 5-6 illustrates the equivalent steel plate thickness and stiffener spacing dependency for a number of

MC simulations. The worst case scenario suggests the equivalent plate thickness is 28mm. The details required for input into the steel fabrication costs model are listed in Table 5-2.
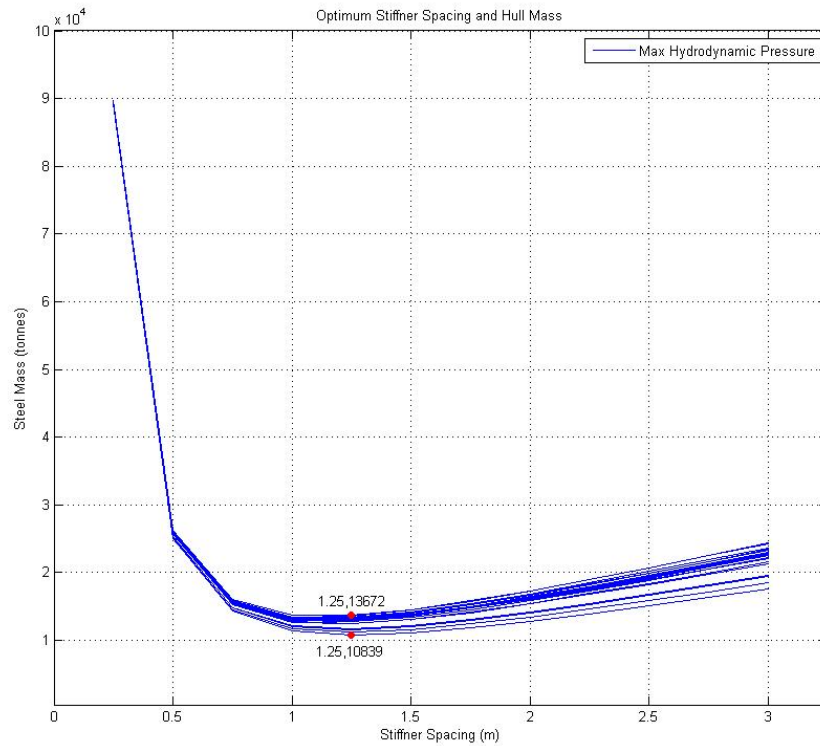


**Figure 5-5: Steel Mass and Stiffener Spacing for the Curved OWC Array Platform**
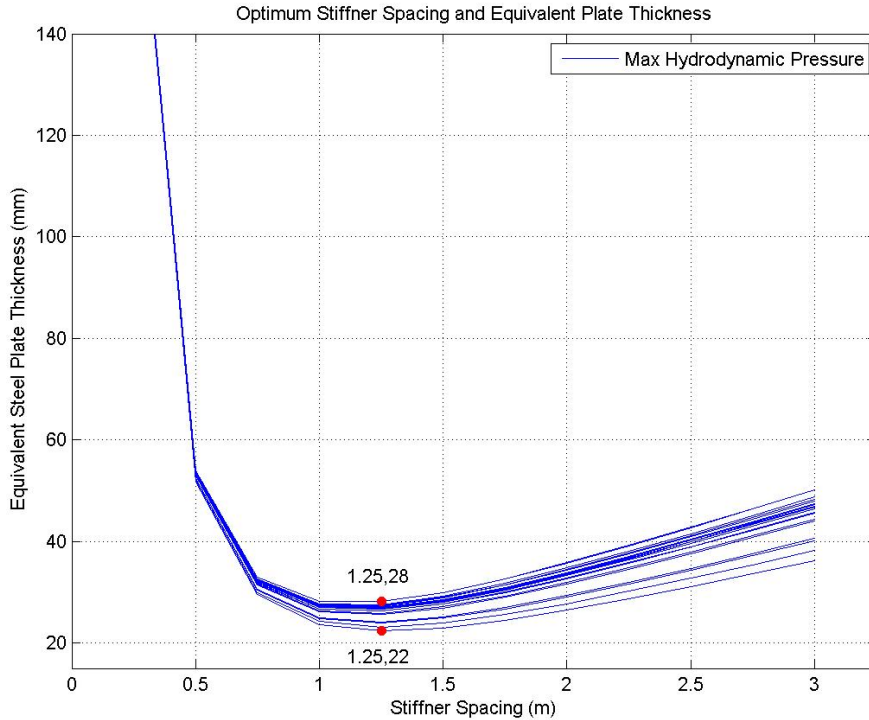
Figure 5-6: Equivalent Steel Plate Thickness and Stiffener Spacing for the Curved OWC Array Platform

Table 5-2: Steel Fabrication Model Specifications

| Item | Value |
|---|---|
| **Steel Plate Thickness (mm)** | 20 |
| **Steel T Beam Stiffener Thickness (mm)** | 23 |
| **Steel T Beam Stiffener Spacing (m)** | 1.25 |

The structural material specifications from Table 5-2 are input into the steel fabrication model described in Chapter 3. The unit cost range calculated for this steel hull is €1707 - €4747/t, resulting in a total hull steel CAPEX of range of €25.7m - €71.4m when additional steel for bulkheads and a 10% buffer on the steel unit cost is considered.

### 5.1.3   Numerical Analysis of Motion Characteristics and Maintainability

The frequency dependent motion RAOs calculated from WAMIT for the Curved OWC Array platform are illustrated in Figure 5-7 for surge, heave and pitch modes. On inspection, the platform appears to be over-damped in heave which affects the platform motions and the OWC IWS motions as they are tightly coupled. A further iteration would be required to accurately represent the platform heave RAO. For the purposes of this section, the RAOs illustrated have sufficed. This section presents the estimated MII matrix for the Curved OWC Array platform at the bow, or the farthest away turbine from the COG, which would represent the worst case scenario. This is then coupled with the scatter diagram for the M1 site off the Irish west coast to calculate the allowable maintenance hours for on-site maintenance. The motion

RAOs are also used to estimate the accelerations at the WTG hub to assess the acceptable operational range for the WTG as well as the access time for maintenance on the WTG.
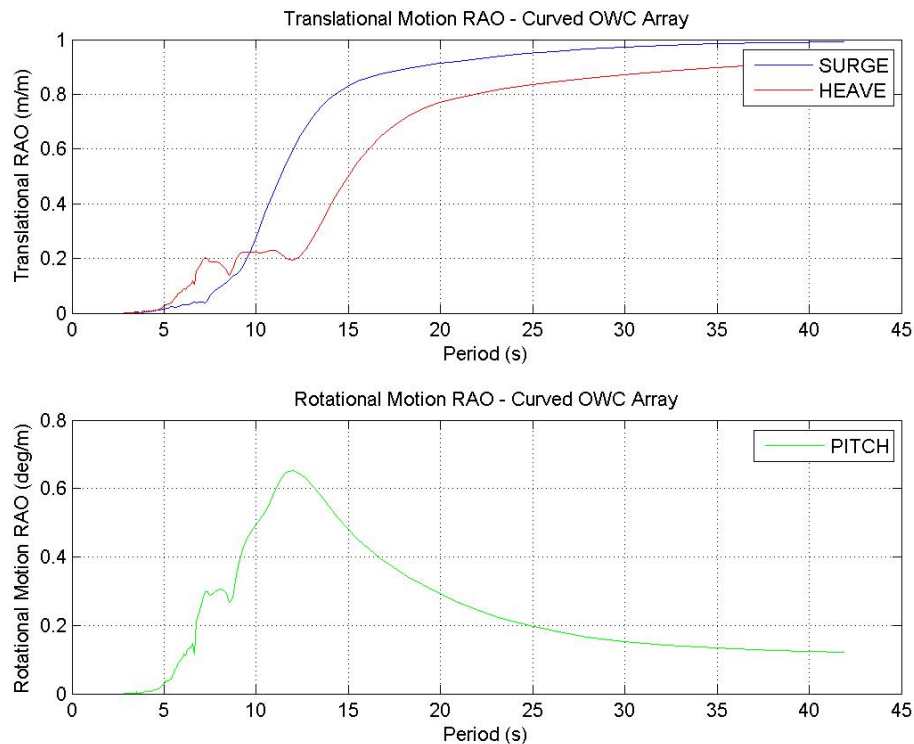


**Figure 5-7: Curved OWC Array Platform Motion RAOs**

### 5.1.3.1 WEC Maintainability

The maintainability criteria used in this section is the MII index as discussed in Chapter 3. The MII matrix for the Curved OWC Array platform bow turbines is illustrated in Figure 5-8. The Curved OWC Array platform would in fact have a number of these matrices, one for every turbine location as these locations will have different acceleration ranges due to varying distances from the COG. The bow turbines have been chosen here as they represent the worst case scenario for the Curved OWC Array platform in head-on wave conditions. The MII matrix looks considerably different from that calculated for the BBDB in Chapter 4 due to the vastly different motion characteristics of each platform. When coupling this matrix with the scatter diagram for the M1 site the allowable sea states and associated hours of occurrence for on-site maintenance are illustrated in Figure 5-9. The total allowable on-site maintenance time for the Curved OWC Array platform is ~6000 hours. This is significantly higher than that achievable for the BBDB at the M1 site and the 68% occurrence allows the use of an on-site maintenance strategy in the LCCA analysis for the platform.
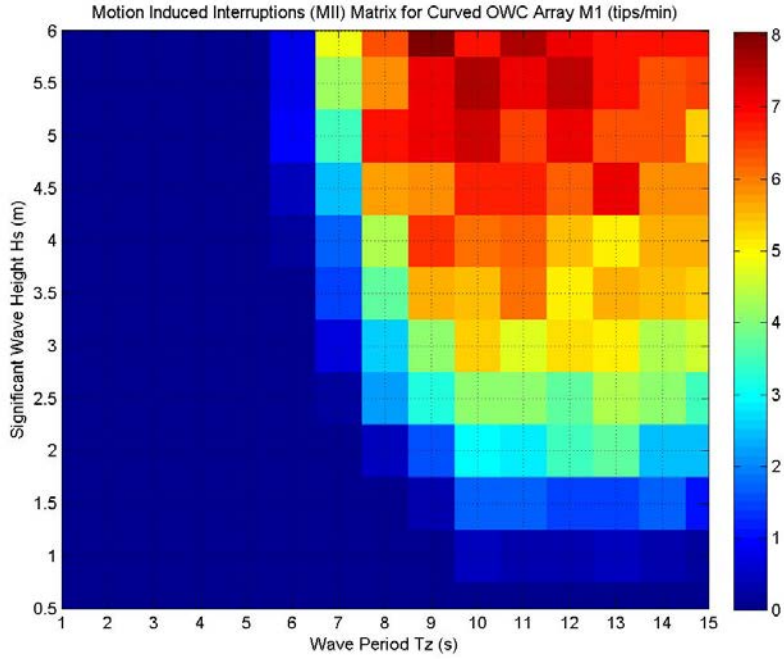
**Figure 5-8: MII Matrix for the Curved OWC Array Platform for the Bow Turbines**
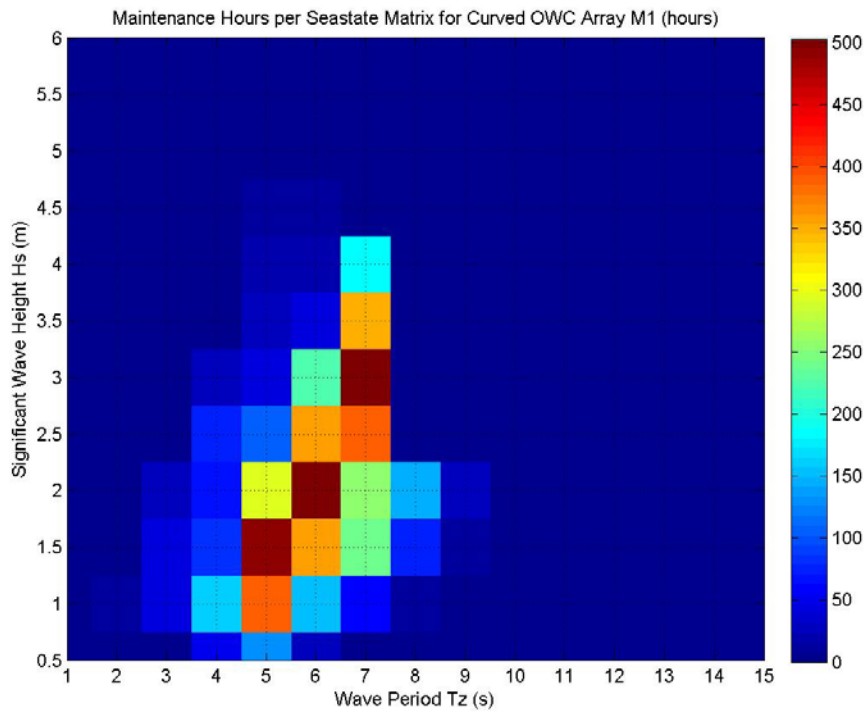


**Figure 5-9: Acceptable On-site Maintenance Sea States for the Curved OWC Array Platform Bow Turbines**

### 5.1.3.2 Accelerations at Hub Height

In the design standards for floating offshore wind turbine installations listed in Chapter 2, each consider the accelerations at the WTG hub to be a crucial consideration during the design process. However, no standard has placed a maximum limit on these accelerations. Reference [169] investigated a number of

configurations of TLP platform for offshore wind turbines. In that study, the root mean square (RMS) accelerations at the hub are presented as a percentage of gravitational acceleration. Most of the platforms have a low acceleration value however one specific shallow draft TLP has what is regarded by the author as a high acceleration value of 22.6% of gravity, or >2m/s$^2$. Having reviewed a number of other sources of information for such an operational limit, namely [175] and [176], no explicit statement is made on a hub acceleration limit. Reference [175] alludes to a limit based on the bending moment at the wind turbine tower base, which is not explicitly stated but is dependent on the accelerations at hub height. There are unsubstantiated reports that this 'limit' of 2m/s$^2$ is increasing but there is no guidance or reference for this. For the purposes of this section, 2m/s$^2$ is used as a maximum limit and also a mean limit for determining the operational wave conditions the WTG can operate when situated on the Curved OWC Array platform.



**Figure 5-10: Maximum Acceleration at Hub Matrix for the NREL 5MW WTG on the Curved OWC Array**
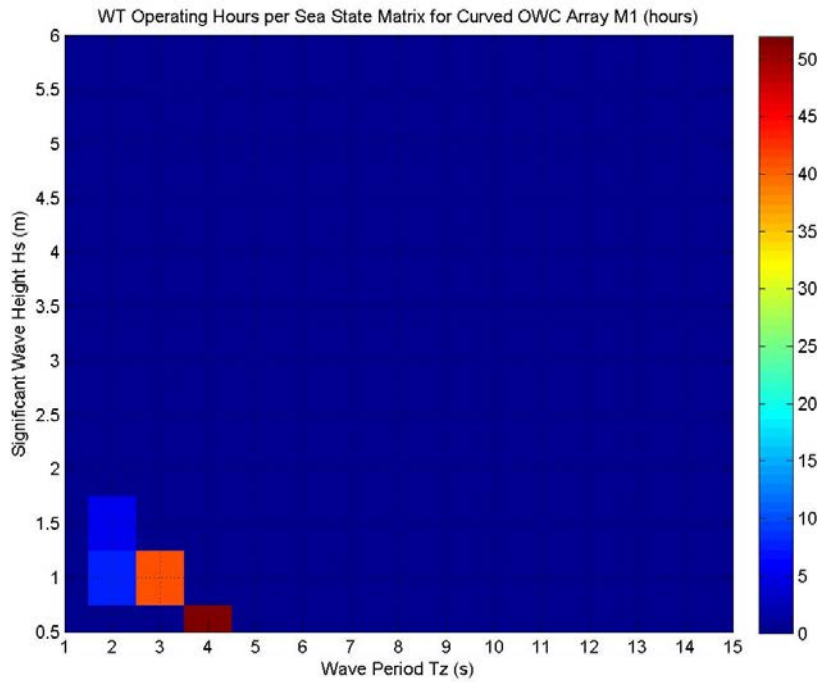
**Figure 5-11: Sea States and Total Hours of Operation for the NREL 5MW WTG on the Curved OWC Array (Max)**

The NREL 5MW WTG is assumed to be located directly above the COG of the platform with a hub height of 90m above water level. As the criteria is the maximum acceleration experienced at the hub during a sea state, the matrix illustrated in Figure 5-10 appears scattered and no obvious pattern is evident. Coupling this matrix with the scatter diagram for the M1 site, the sea states in which the turbine can operate under these constraints are calculated and illustrated in Figure 5-11. The total permissible operating time is ~106 hours. The maximum availability of the WTG under these constraints is ~1.21%.
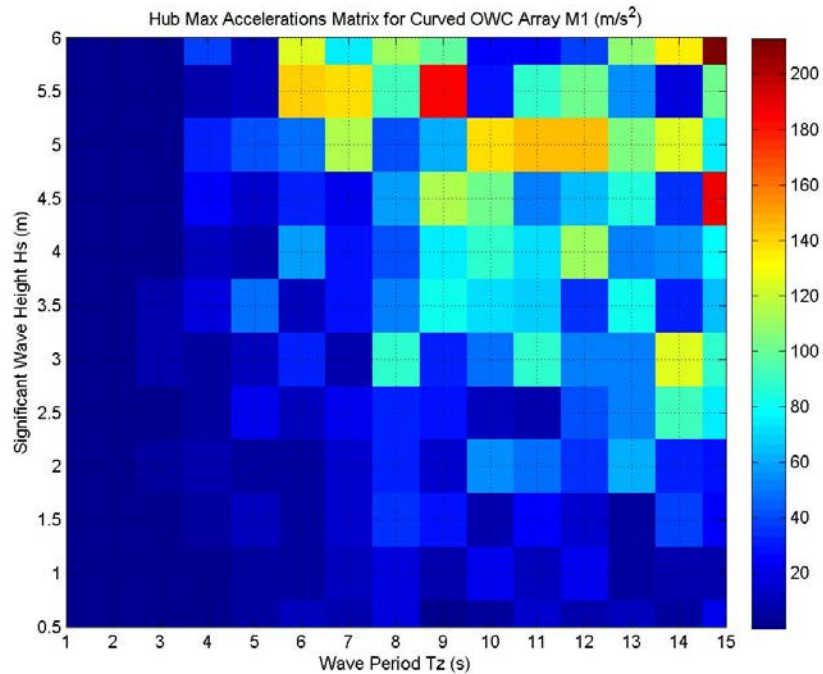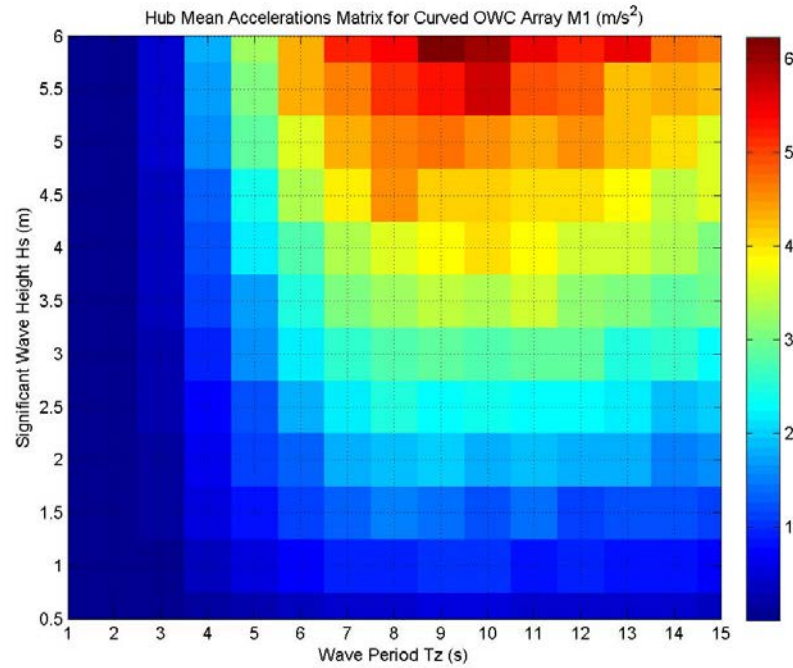
**Figure 5-12: Mean Acceleration at Hub Matrix for the NREL 5MW WTG on the Curved OWC Array**
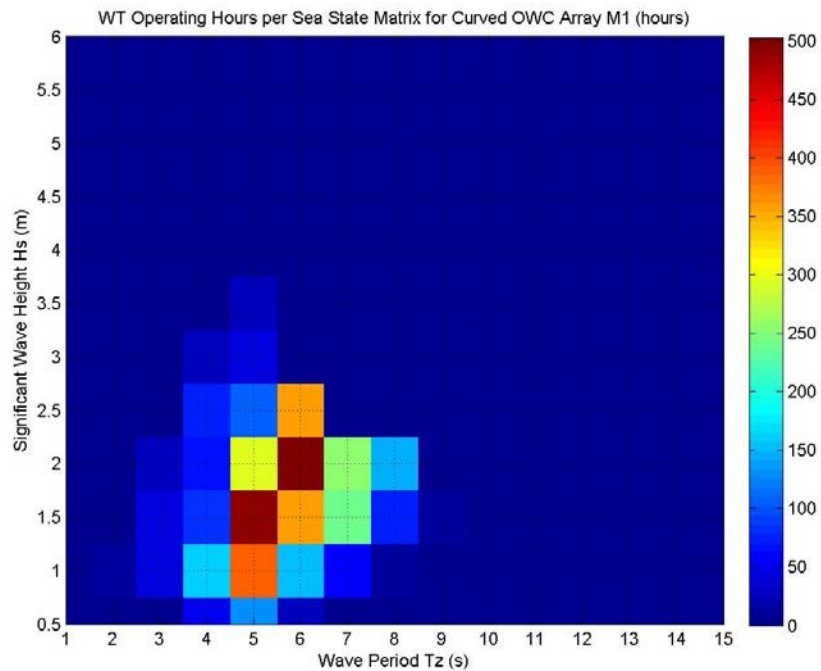


**Figure 5-13: Sea States and Total Hours of Operation for the NREL 5MW WTG on the Curved OWC Array (Mean)**

Figure 5-12 illustrates the mean acceleration at the hub matrix for the WTG on the Curved OWC Array platform. This matrix has a clear pattern with regard to dependency of hub accelerations with respect to sea state. Coupling this matrix with the scatter diagram for the M1 site, the sea states in which the WTG can operate under the mean acceleration limit is illustrated in Figure 5-13. The total operating

213

time for the WTG using the mean acceleration criteria is ~4260 hours. Thus the maximum availability for the WTG under these constraints is ~48.6%.

### 5.1.3.3  WT Maintainability

As well as the WEC and platform maintainability, the maintainability of the WTG must also be considered. In this case, the same limits imposed for the WEC maintainability apply to the WTG but now use the accelerations ratio at the rotor-nacelle assembly (RNA) location. The MII matrix for this location is illustrated in Figure 5-14. Coupling this with the scatter diagram for the M1 site, the sea states and number of hours in which on-site maintenance can take place is calculated and illustrated in Figure 5-15. The total on-site maintenance time for the 5MW WTG is ~54 hours which is far too low for consideration of this configuration for practical implementation. A reconfiguration was necessary based on this result.
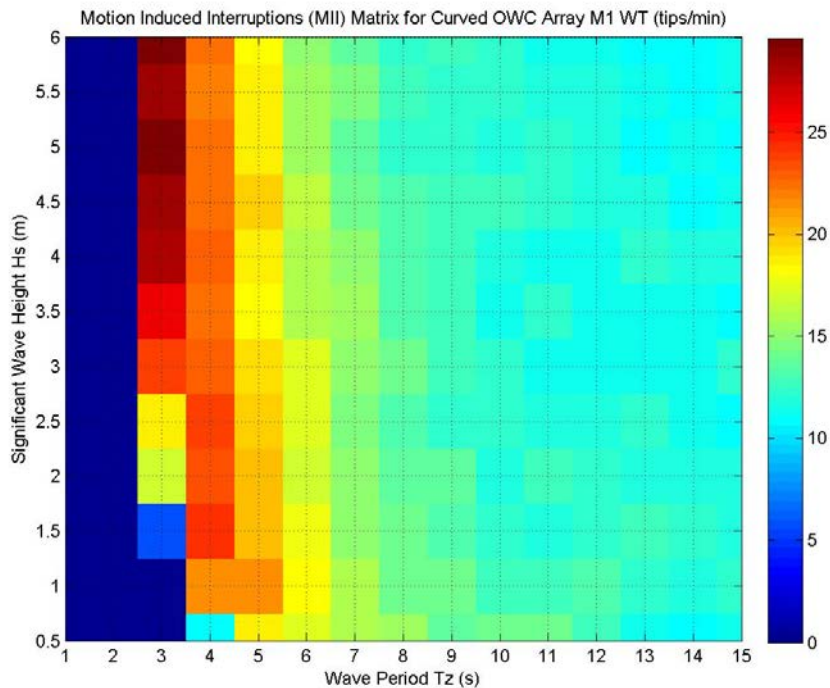


**Figure 5-14: MII Matrix for the WTG at the RNA Location on the Curved OWC Array**
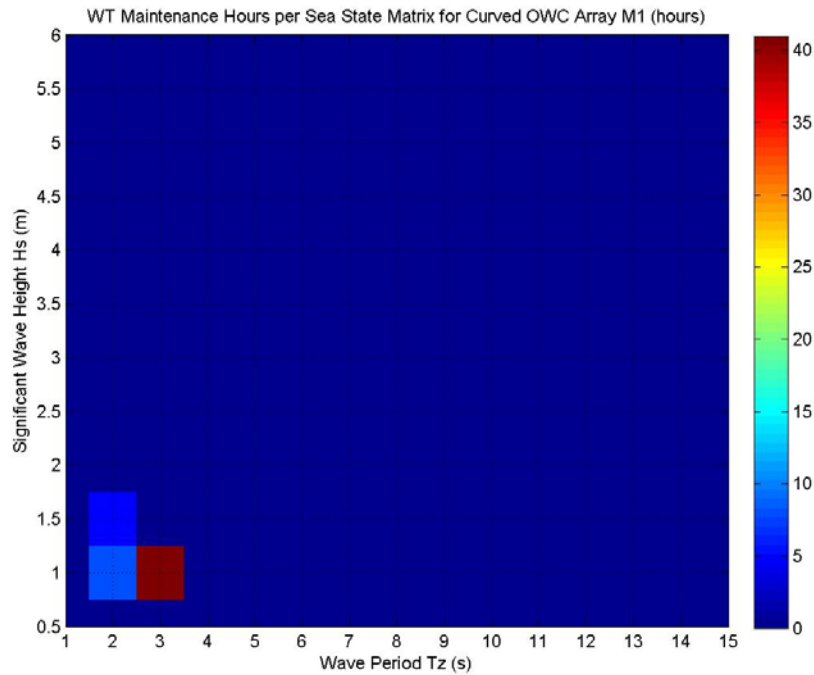
**Figure 5-15: Acceptable On-site Maintenance Sea States for the Curved OWC Array NREL 5MW WTG**

## 5.1.4 Assessment of the Curved OWC Array Platform

The assessment of the Curved OWC Array platform may be split into a number of individual performance metrics based on the assessments carried out previously. The following sections will consider these in isolation and then finally form an overall conclusion regarding the continuation of the Curved OWC Array platform.

### 5.1.4.1 Power Output Performance

The power output performance of the WEC and WTG will be considered separately in light of the additional constraints imposed on the WTG operability.

5.1.4.1.1 WEC

The WEC power matrix is well matched to the M1 site conditions and thus produces a significant amount of power, averaging at 3340kW. The availability of the platform is likely to be high, perhaps in line with current levels of availability for bottom fixed WTs due to the high level of maintainability hours. It should be reasonable to assume 90% availability on the basis of access and maintenance of 68%. The annual average power would then be ~3000kW.

5.1.4.1.2 WTG

Depending on the wind conditions at the site of deployment, the WTG will have a varying load factor. A quick estimate of the performance of the NREL 5MW WTG at the M1 site suggests that the WTG will have a load factor of ~40% and an average annual power output of ~2000kW. Applying the additional constraints from the hub accelerations, the annual average power is reduced to 972kW.

**5.1.4.2    Structural Design and Platform Costs**
The statistics of the structural steel construction of the Curved OWC Array platform and its constructability are addressed separately.

5.1.4.2.1   Structural Steel Construction
The preliminary structural steel design has calculated a steel plate and stiffener optimum design of 23mm stiffener beam thickness, 1.25m stiffener spacing and a steel plate thickness of 20mm. These member sizes are not very large and result in a unit production cost range of €1707 - €4747. The total steel mass is 13,672t. The addition of 30% additional steel mass for bulkheads and a 10% buffer on unit cost, the platform hull fabricated from steel will cost in the region of €33.3m - €92.8m. A global structural analysis would also be required to ensure sufficient structural strength during extreme conditions.

5.1.4.2.2   Constructability
Due to the large and bulky dimensions of the Curved OWC Array platform, the constructability of its current form is low. Very large dry dock facilities would be required to build the hull but are rare and very expensive. The potential for mass production is low, however as discussed previously, the need for this characteristic is lower as the platform power capacity increases.

**5.1.4.3    Motion Characteristics of the Platform for WEC Maintainability**
The motion characteristics for on-site maintenance of the WEC are sufficient to allow ~6000 hours of access and maintenance. This is sufficiently high to consider an on-site maintenance strategy for the platform.

**5.1.4.4    Accelerations at the RNA for WTG Operability**
Two criteria for determining the operational range of the WTG on the Curved OWC Array platform have been used. Firstly, using $2m/s^2$ as the maximum permissible acceleration at the hub and secondly, using $2m/s^2$ as the allowable mean acceleration at the hub for a 20 minute sea state. For the first criteria an operability of just ~1.2% is possible while for the second criteria an operability of ~48.6% is possible. As [169] only consider the RMS acceleration at the hub, the operability of the WTG using the mean acceleration has been used.

**5.1.4.5    Motion Characteristics at the RNA for WTG Maintainability**
The motion criteria used for the calculation of the allowable sea states in which on-site maintenance can be undertaken for the WTG reveals that only 54 hours annually this can be done. This essentially means that on-site maintenance for the WT on the Curved OWC Array platform at the M1 site is not possible. This is in contrast to that calculated for the WEC as the accelerations are amplified from the platform to the hub due to the large distance from the COG.

**5.1.4.6    Overall Conclusion on the Curved OWC Array Hybrid**
Based on the assessment criteria summarised, the immediate conclusions are,

- The hull requires a re-design to improve the constructability
- Based on the hull costs, RC material would be best suited to this large platform
- The motion characteristics of the platform need to be addressed in order to improve the maintainability of the 5MW WTG at the M1 site
- Alternatively, WTGs with a lower hub height should be considered to reduce the accelerations and improve operability and maintainability on-site

Each of these points is technically feasible to achieve and thus the OWC Array concept has undergone a further iteration to improve performance in each of these areas.

## 5.2 Structural Redesign of OWC Array for Constructability

Due to the bulky size of the Curved OWC Array platform i.e. plan dimensions of 300m x 150m, the constructability of the platform is questionable. The largest known dry docks include the H-Dock in Ulsan, South Korea by Hyundai at 490x115x13.5m shown in Figure 5-16 or the Harland and Wolff dry dock in Belfast, UK at 556x93x8m shown in Figure 5-17.



**Figure 5-16: H-Dock in South Korea**

**Figure 5-17: Harland and Wolff Dry Dock in Belfast Harbour**

Broadly speaking this would allow construction at each facility of just one platform at a time which is not ideal for deployment of tens of these devices to make a farm. Clearly then an alternative is required. The options are somewhat limited but include,

- Smaller devices,
- Modular construction and float out of sections of large devices

For the OWC Array concept, a smaller device implies more movement of the hull which is not acceptable for WTG operation or WEC and WTG maintenance operations. Therefore, only a single option exists for the OWC Array, modular construction of the platform.

The OWC Array concept is composed of a number of OWC chambers incorporated into a platform or hull which has buoyancy. The redesign of the concept envisaged splitting this buoyancy and attaching the relevant amount to each chamber for self-stabilisation in the free floating condition. Therefore the chamber cross-section had to be designed to be hydrostatically stable within a range of $\pm 25°$ roll angles as dictated by [170]. The initial cross-sectional design is illustrated in Figure 5-18. The chamber cross-section includes three buoyancy tanks which hold specific volumes of ballast to maintain static stability.
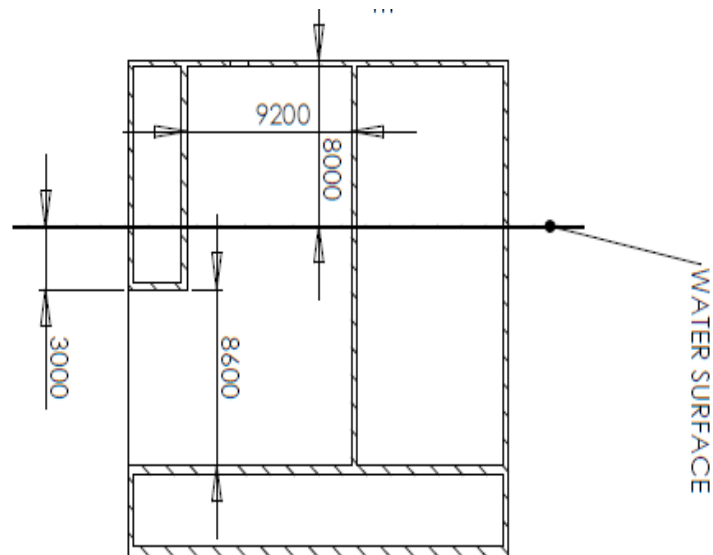
**Figure 5-18: Initial Redesigned OWC Chamber Cross-section**

It was envisaged then that each chamber, or a number of chambers, could be constructed together in a line simultaneously. This would result in a linear chamber beam. The OWC Array platform was then reconfigured to account for this linear construction method and the design illustrated in Figure 5-19 was defined.
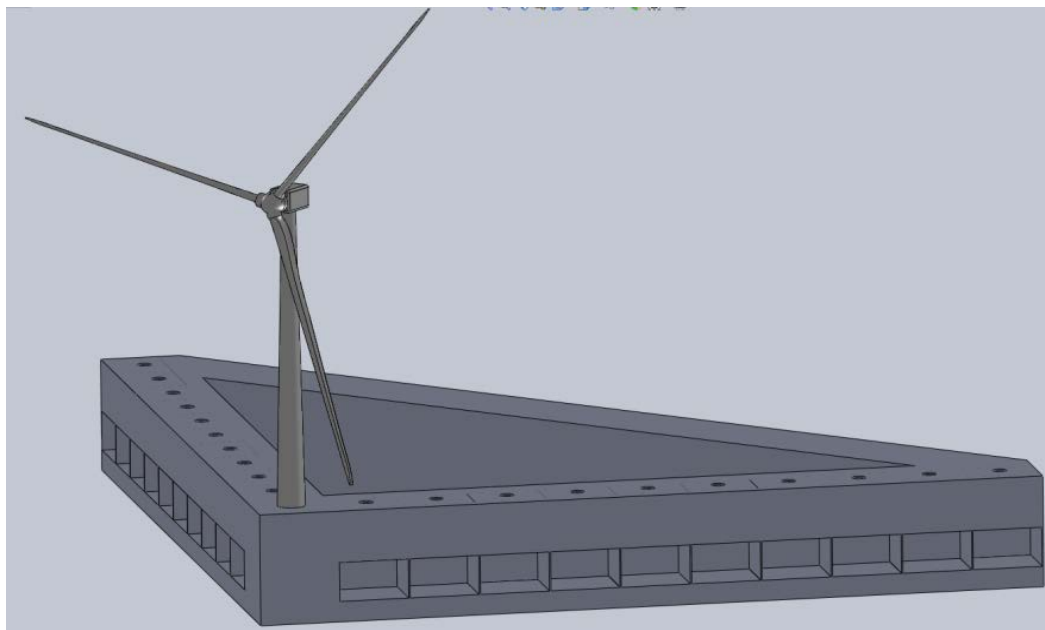


**Figure 5-19: Reconfigured OWC Array Platform for Constructability**

The configuration of the platform in this way allows for simpler construction processes to be used in a dry dock. By splitting the hull into three beams, the Harland and Wolff dry dock could construct two platforms simultaneously. The primary disadvantage of this method is that the final connection of the beams requires float out to a benign area where they are joined together in the delta shape illustrated in Figure 5-19. Furthermore, there remains an issue regarding the stable draft of the chamber beams which is 16.1m. This is deep in relation to the depth capacity of most harbours. One solution to this is to temporarily block the openings

to the chambers and float the beams to the connection site and then ballast them down to the correct draft using pumps.

**Table 5-3: Delta OWC Array Platform Dimensions**

| Delta OWC Array Parameter | Value |
|---|---|
| **Platform Width** | 245m |
| **Platform Length** | 135m |
| **Platform Depth** | 16.1m |
| **Platform Displacement** | 100,000t |
| **No OWC Chambers** | 20 |
| **Dimensions of OWC Chamber** | 15m x 9.2m |

## 5.3    Second Reconfiguration of the OWC Array

Following the reconfiguration of the OWC Array hull through constructability criteria and structural design, the new platform illustrated in Figure 5-19 and referred to as the Delta OWC Array has been subjected to the same analysis as the initial concept to determine the platform redesign effects on power absorption, motion characteristics etc.

### 5.3.1    Numerical Analysis of Power Performance

The power performance has been assessed in the same manner as the BBDB in Chapter 3 and the Curved OWC Array through linearised frequency domain modelling using WAMIT and the principle of superposition. The calculated IWS RAO for each chamber is illustrated in Figure 5-20.
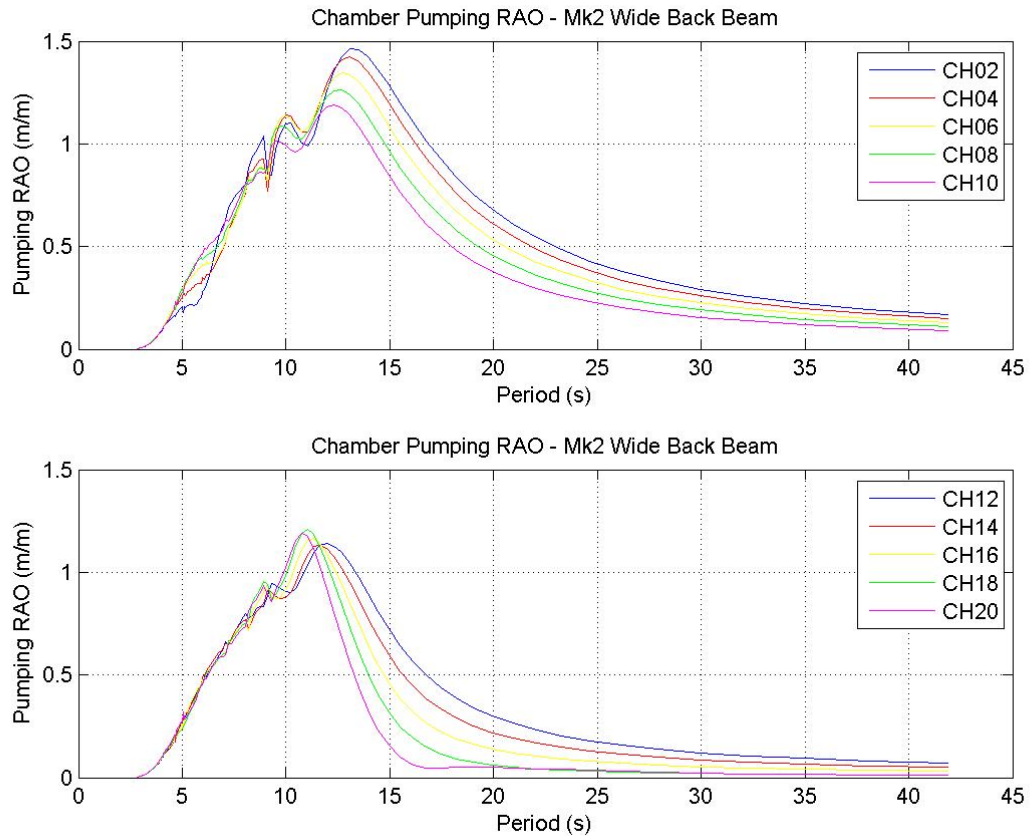
**Figure 5-20: Delta OWC Array Chamber IWS RAO's**

External damping was added to each IWS mode to restrain the responses around the resonant frequency as outlined in [106].

The principle of superposition has been applied to the IWS RAOs in Figure 5-20 for a range of sea states and the average power output calculated. The resultant average electrical power output matrix for the Delta OWC Array is illustrated in Figure 5-21. Coupling this with the averaged measured scatter diagram for the M1 site, the annual average power output is 2752kW. Broadly speaking, a ratio of 1:3 is indicative of the required capacity for a WEC, therefore an installed capacity of ~10MW is appropriate for this device.
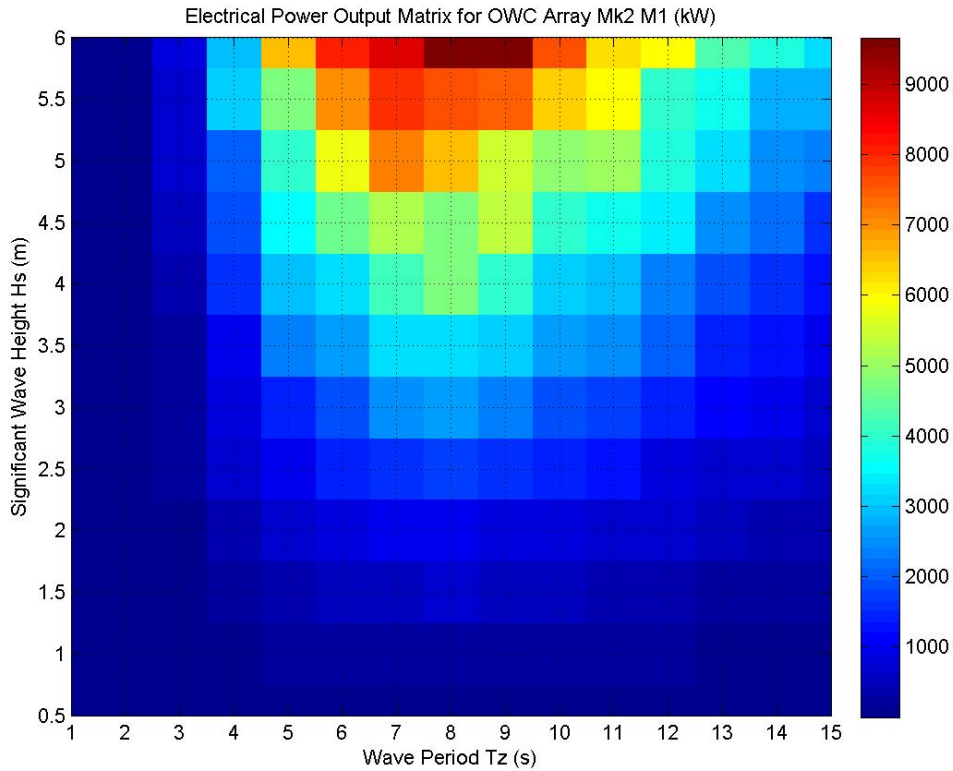
**Figure 5-21: Average Electrical Power Matrix for the Delta OWC Array**

### 5.3.2   Numerical Analysis of Structural Design Requirements

Though it has been decided on the basis of the hull costs of the Curved OWC Array that the primary structural material to be used is RC, both RC and structural steel have been considered here for the Delta OWC Array for completeness. It should be noted that the total displacement of the platform remains constant and the masses reported in this section relate only to structural masses. The same methodology has been applied using the hydrodynamic pressure RAOs for the wetted hull as shown in Figure 5-22 and superposition to approximate the loads during extreme conditions and using the [115] structural steel design standard and equivalent RC design standards, the steel and RC masses for the hull have been calculated using the MC simulation technique to account for short term variations in sea state realisations.
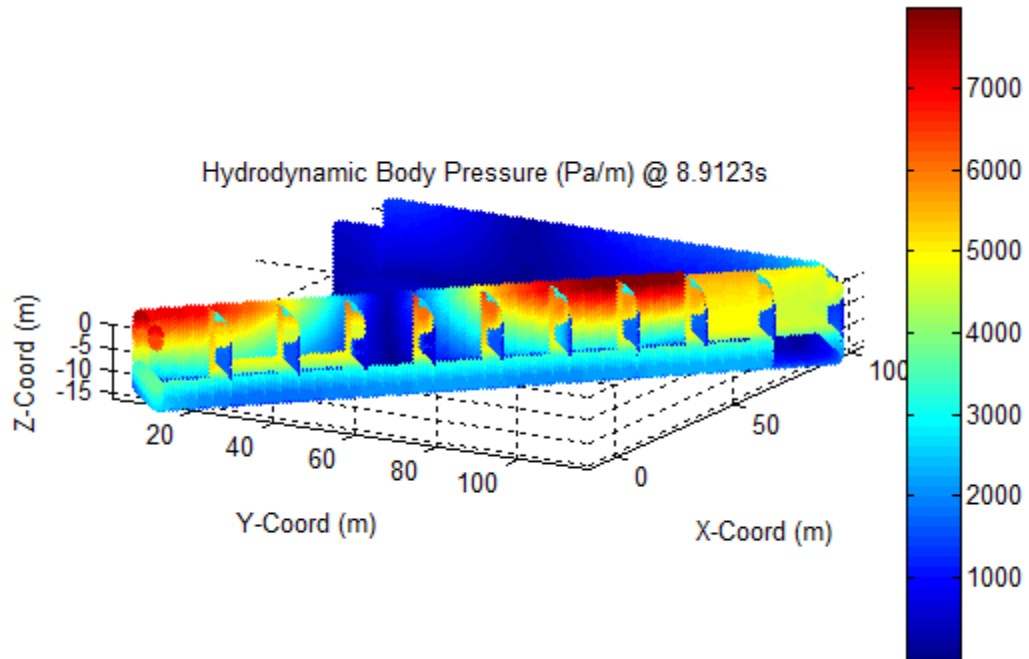
**Figure 5-22: Hydrodynamic Pressures on the Wetted Hull of the Delta OWC Array Platform at ~9s**

### 5.3.2.1 Steel Construction

The first structural design configuration for the Delta OWC Array platform was the typical steel plate and stiffener fabrication method for estimation of structural steel mass. Figure 5-23illustrates the results of the MC simulations for assessment of the effects of short term realisations of sea states on the structural mass of the platform for varying steel beam stiffener spacing based on [115]. The figures illustrated on the plot represent the best and worst case for the structural steel mass of the platform. Only the worst case scenario is considered in LCCA analysis, i.e. 14,392t. Figure 5-24 illustrates the equivalent steel plate thickness and stiffener spacing dependency for a number of MC simulations. The worst case scenario suggests the equivalent plate thickness is 29mm. The details required for input into the steel fabrication costs model are listed in Table 5-4.
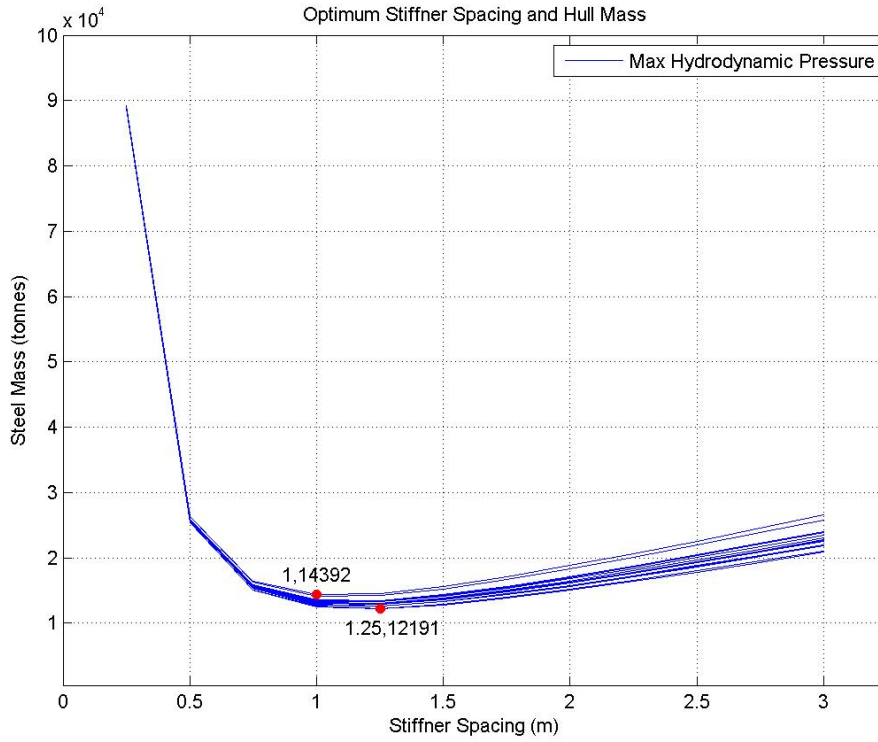
**Figure 5-23: Steel Mass and Stiffener Spacing for the Delta OWC Array Platform**
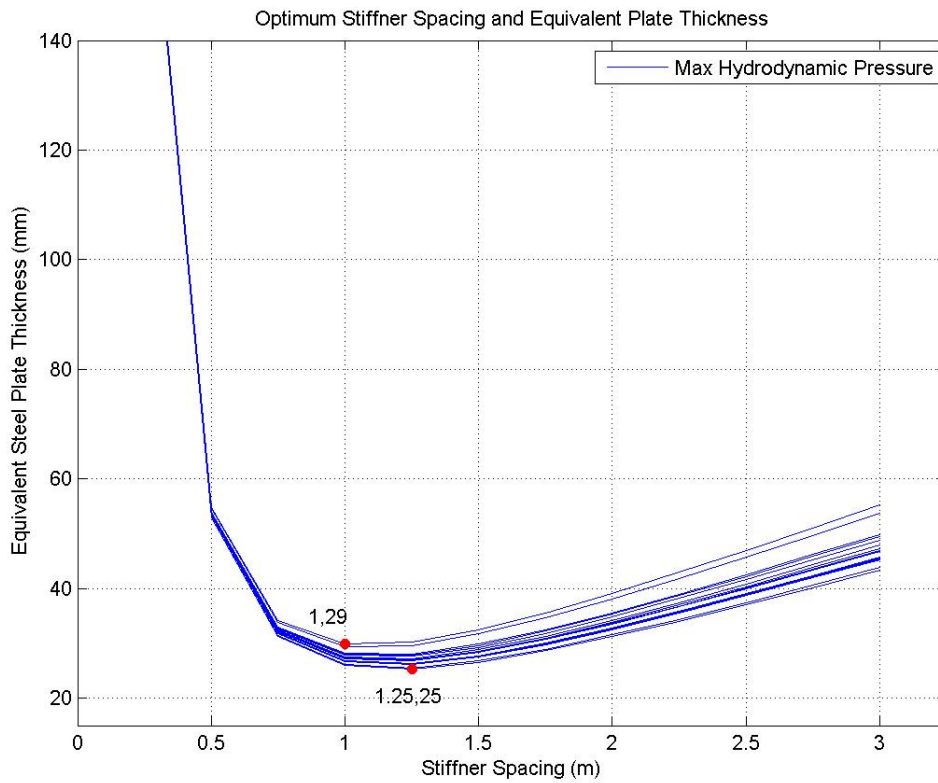


**Figure 5-24: Equivalent Steel Plate Thickness and Stiffener Spacing for the Delta OWC Array Platform**

**Table 5-4: Steel Fabrication Model Specifications for the Delta OWC Array Platform**

| Item | Value |
|---|---|
| **Steel Plate Thickness (mm)** | 16 |
| **Steel T Beam Stiffener Thickness (mm)** | 27 |
| **Steel T Beam Stiffener Spacing (m)** | 1.0 |

The structural material specifications from Table 5-4 are input into the steel fabrication model described in Chapter 3. The unit cost range calculated for this steel hull is €1516 - €6342/t, resulting in a total hull steel CAPEX of €31.2m - €130.5m when additional steel for bulkheads and a 10% buffer on the steel unit cost is considered.

### 5.3.2.2   Reinforced Concrete Construction

The total platform costs for the Delta OWC Array platform from structural steel are very high. An alternative construction of RC has been considered.

The methodology for the calculation of the global bending moments in the chamber beams was simplistic, assuming the chamber beams behave like a uniform section beam under a UDL equal to the structural mass and ballast mass per metre length of beam and simply supported at either end. This method would represent the platform behaviour in extreme conditions with the hull spanning between two wave crests. Due to the complex nature of the distribution of walls in the beam, further finite element method (FEM) analysis would need to be carried out to verify the design proposed by this methodology. The preliminary estimation of the tensile stress in the bottom wall of the chamber beam when simply supported on both ends is calculated using Equation 5-1.

$$BM = \frac{\omega L^2}{8}$$

**Equation 5-1**

BM is the longitudinal bending moment (Nm), L is the beam length (m) and $\omega$ is the uniformly distributed load (N/m).

The tensile stress is derived from the BM assuming the location of the neutral axis is known, i.e. the location of no stress, below which is tension and above is compression. Equation 5-2 is used.

$$\sigma_{max} = \frac{BM.z}{I}$$

**Equation 5-2**

$\sigma_{max}$ is the tensile stress (N/m$^2$), z is the distance of the neutral axis from the location of maximum stress (m) and I is the moment of inertia (m$^4$).

Using Equation 5-2, a cross-sectional area of steel for the bottom wall of the chamber beam may be calculated. The calculated parameters for the structural design of the OWC Array chamber and supporting beam are detailed in Table 5-5.

**Table 5-5: Results of the Calculation of Steel Reinforcement**

| Dimension | | Unit | Beams | Back-Piece |
|---|---|---|---|---|
| **Concrete Section in Wall** | $A_b$ | m$^2$ | 8.6 | 6.06 |
| **Max. Tension** | $\sigma_{max}$ | MPa | 17 | 6.8 |
| **Concrete Safety Factor** | $Y_b$ | | 1.5 | |
| **Tensile Strength of Steel** | $\sigma_e$ | MPa | 460 | 460 |
| **Steel Safety Factor** | $Y_s$ | | 1.15 | |
| **Reinforcing Steel Section** | $A_s$ $= \dfrac{Y_b \ x \ A_b \ x \ \sigma_{max}}{Y_s \ x \ \sigma_e}$ | m$^2$ | 0.41 | 0.12 |

Assuming a similar ratio of steel to concrete volume throughout the structure, the total mass breakdown of steel and concrete for the main chamber beams and supporting beam is tabulated in Table 5-6.

**Table 5-6: OWC Array Mk2 structural material breakdown (Bow ballast not included)**

| Material | Beams | Back-Beam | Total |
|---|---|---|---|
| | t | t | t |
| Concrete | 36230 | 9270 | 45500 |
| Longitudinal Steel | 4542 | 1100 | 5642 |
| Traversal Steel (est.) | 730 | 290 | 1020 |
| Total without Ballast | 41502 | 10660 | 52162 |
| | | | |
| Ballast | 2798 | 48161 | 50959 |
| Total Mass | 44300 | 58821 | 103121 |

By setting the wall thicknesses and number of chambers as constants and calculating the beam length which keeps the steel volume between 4-6%, the chamber dimensions have changed. The chambers are now 15m in length while calculation of the hydrostatic stability of the chamber cross-section allowed the chamber width to increase to 9.25m. This results in an area reduction of ~28% from the initial concept and power output is expected to reduce by a similar amount.

The localised hull loads from numerical modelling have been used in a similar manner as that in the steel design to determine the reinforcing steel and concrete mass required for the hull to resist extreme loads. Similar to the GBS design constraints in Chapter 3, the reinforcing steel volume has been restricted to 4-6% to maintain a reasonable level of simplicity/complexity in the construction of the hull. This allows the same unit cost to be applied to the design. This method has produced figures broadly in line with those calculated by using the global load approach and these have been adopted in the calculation of the cost of the RC hull. The approximate cost of the RC hull is ~€20m. It should be noted that the design proposed is from a simplified approach. An FLS analysis would need to be carried out and also the RC design would need to be checked to minimise the occurrence or susceptibility of the concrete to cracking.

### 5.3.3   Numerical Analysis of Motion Characteristics and Maintainability

The frequency dependent motion RAOs calculated from WAMIT for the Delta OWC Array platform are illustrated in Figure 5-25for surge, heave and pitch modes. This section presents the estimated MII matrix for the Delta OWC Array platform at the bow, or the farthest away turbine from the COG, which would represent the worst case scenario. This is then coupled with the scatter diagram for the M1 site off the Irish west coast to calculate the allowable maintenance hours for on-site maintenance. The motion RAOs are also used to estimate the accelerations at the WTG hub to assess the acceptable operational range for the WTG as well as the access time for maintenance on the WTG.
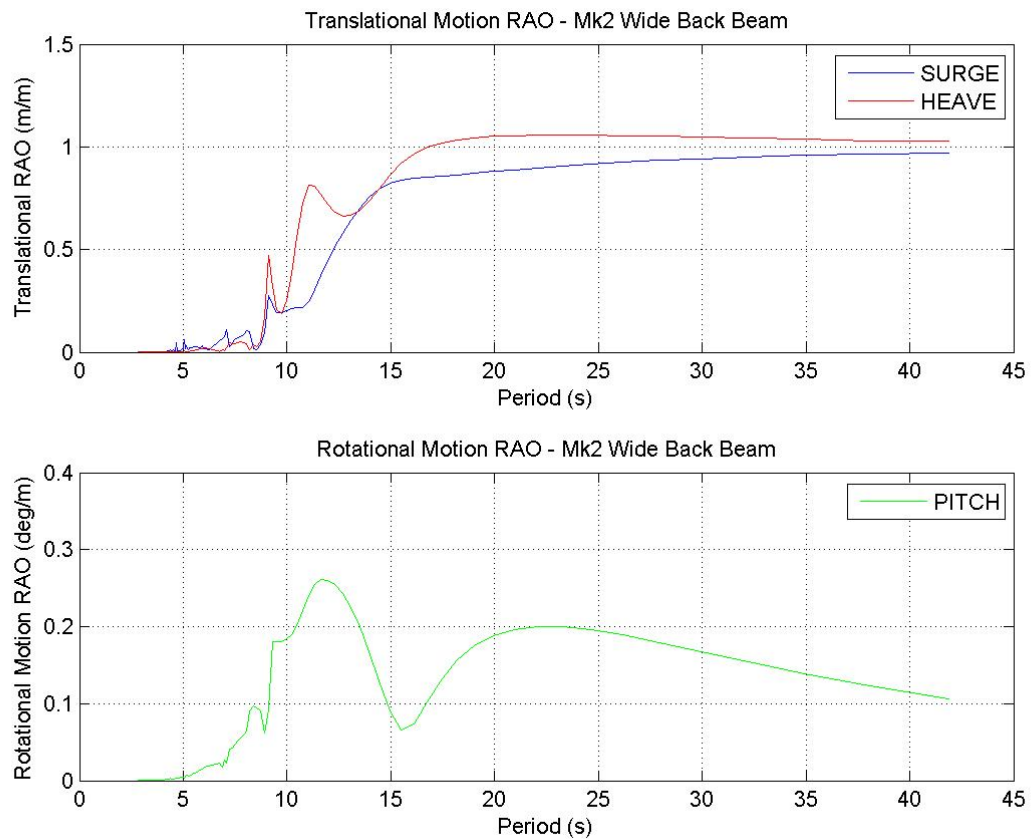


**Figure 5-25: Delta OWC Array Platform Motion RAO's**

### 5.3.3.1   WEC Maintainability

The maintainability criteria used in this section is the MII index as discussed in Chapter 3. The MII matrix for the Delta OWC Array platform bow turbines is illustrated in Figure 5-26. The Delta OWC Array platform, similar to the Curved OWC Array, would have a number of these matrices, one for every turbine location as these locations will have different acceleration ranges due to varying distances from the COG. The bow turbines have been chosen here as they represent the worst case scenario for the Delta OWC Array platform in head-on wave conditions. When coupling this matrix with the scatter diagram for the M1 site the allowable sea states and associated hours of occurrence for on-site maintenance are illustrated in Figure

5-27. The total allowable on-site maintenance time for the Delta OWC Array platform is ~7407 hours. This ~85% occurrence allows the use of an on-site maintenance strategy in the LCCA analysis for the platform.
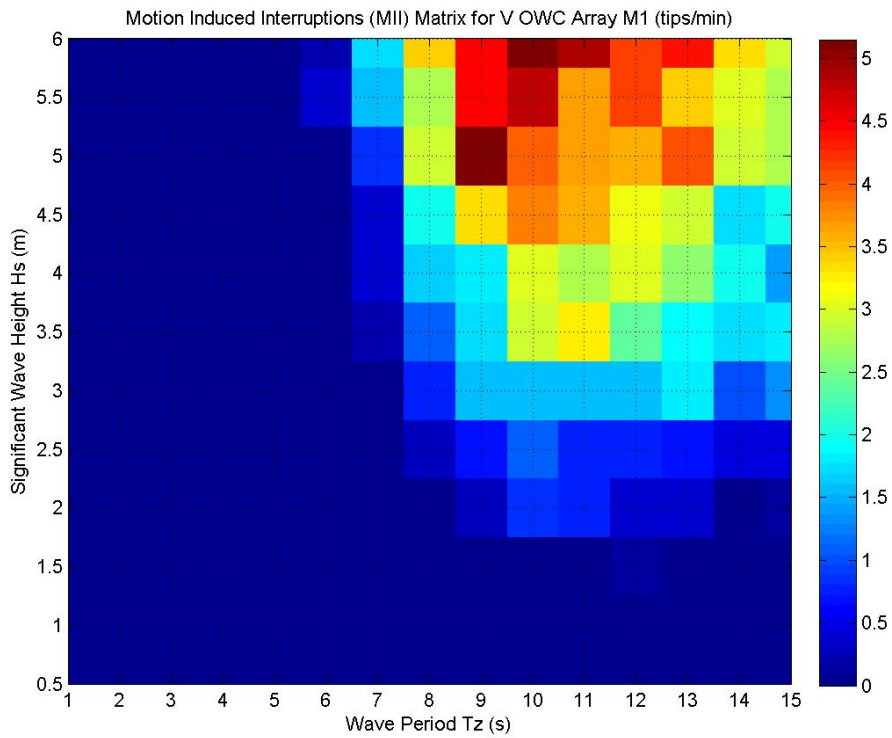


**Figure 5-26: MII Matrix for the Delta OWC Array Platform for the Bow Turbines**
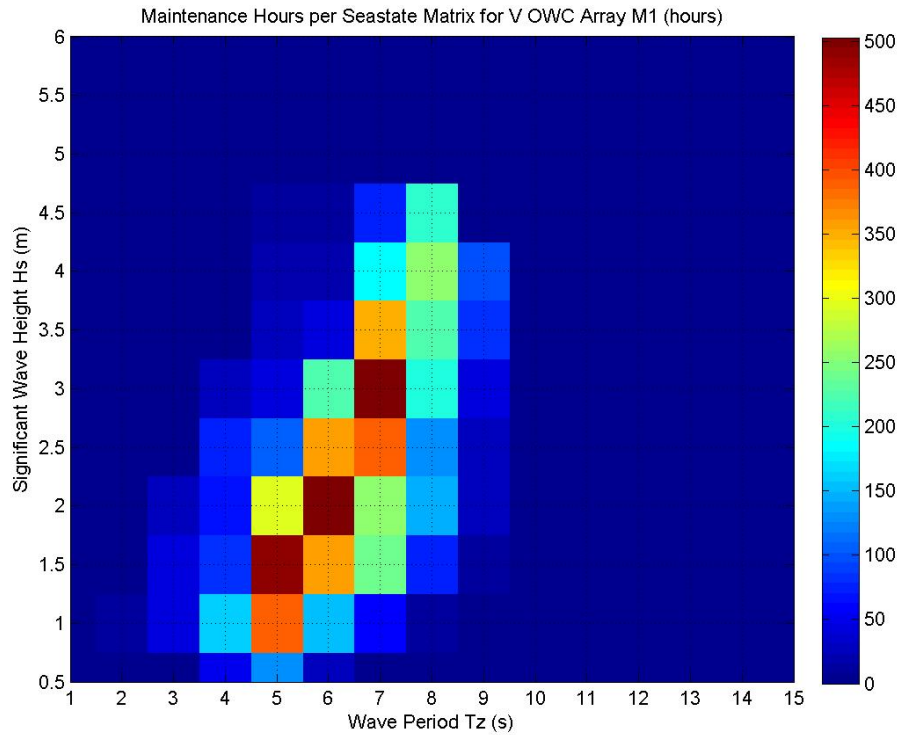
**Figure 5-27: Acceptable On-site Maintenance Sea States for the Delta OWC Array Platform Bow Turbines**

### 5.3.3.2 Accelerations at Hub Height

A similar analysis to that performed for the Curved OWC Array was carried out for the Delta OWC Array platform to assess the accelerations experienced at hub height of an NREL 5MW WTG situated on the bow. The maximum accelerations modelled for each sea state is illustrated in Figure 5-28. Following [169], using $2m/s^2$ as both a maximum limit and mean limit for hub accelerations, the allowable sea states for operation of the WTG using the $2m/s^2$ as a maximum limit is illustrated in Figure 5-29. The total allowable operating hours under these constraints for the WTG is ~671 hours. This represents a maximum ~8% availability of the WTG, which is too low to be feasible.
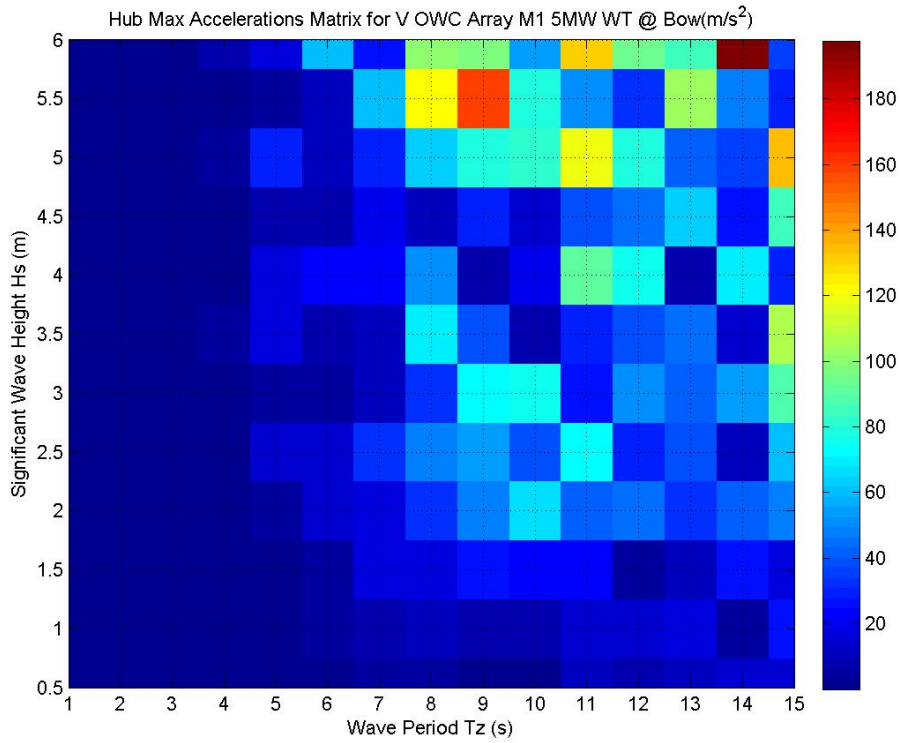
**Figure 5-28: Maximum Acceleration at Hub Matrix for the NREL 5MW WTG on the Delta OWC Array**
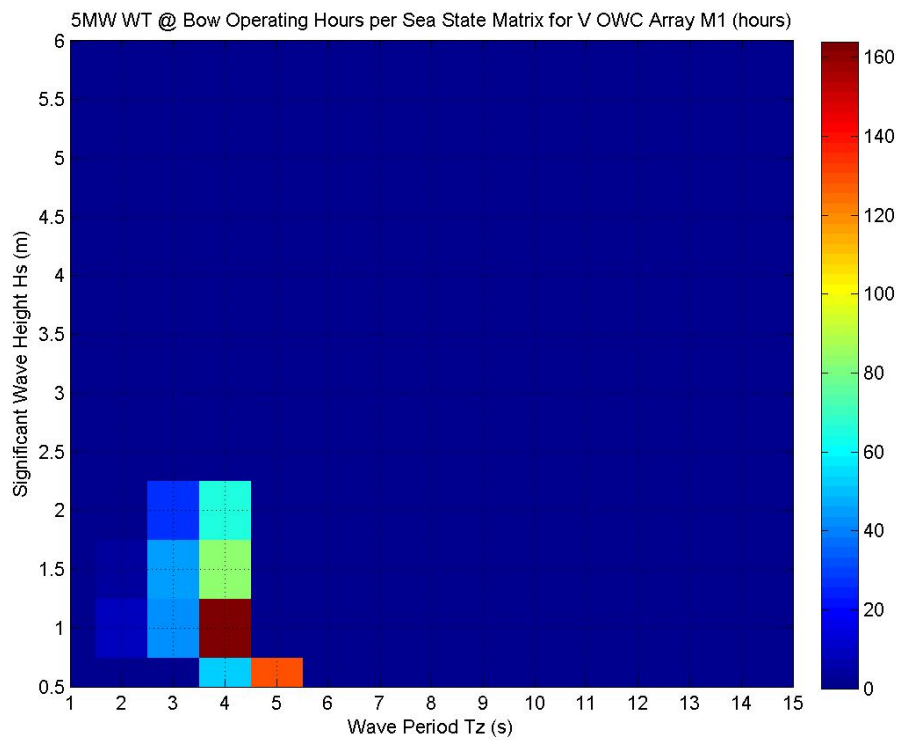


**Figure 5-29: Sea States and Total Hours of Operation for the NREL 5MW WTG on the Delta OWC Array (Max)**

230

Hub Mean Accelerations Matrix for V OWC Array M1 5MW WT @ Bow(m/s$^2$)
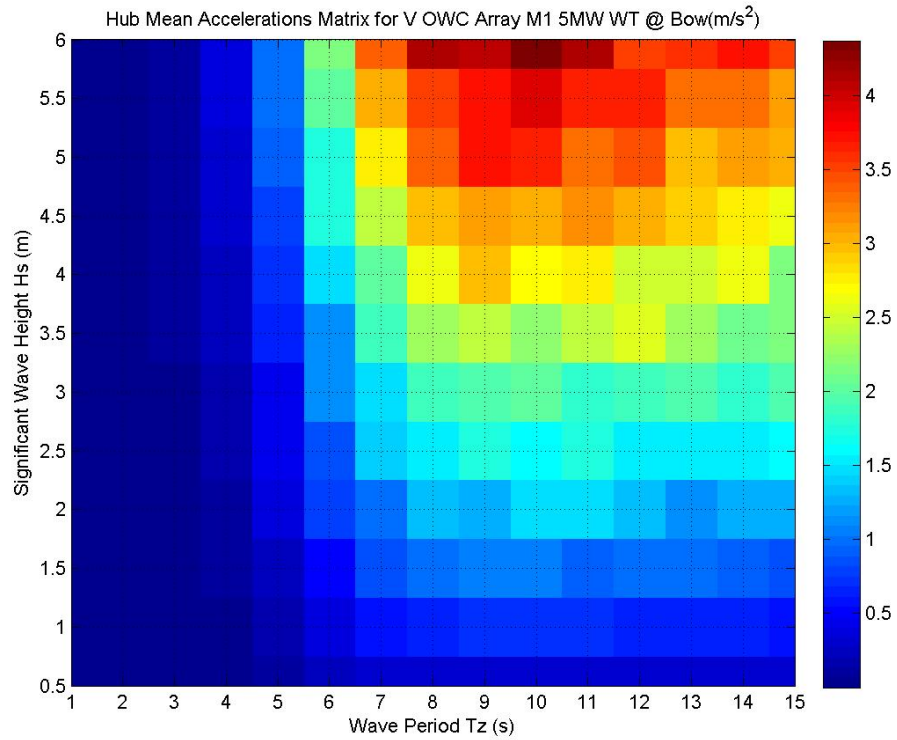
**Figure 5-30: Mean Acceleration at Hub Matrix for the NREL 5MW WTG on the Delta OWC Array**

5MW WT @ Bow Operating Hours per Sea State Matrix for V OWC Array M1 (hours)
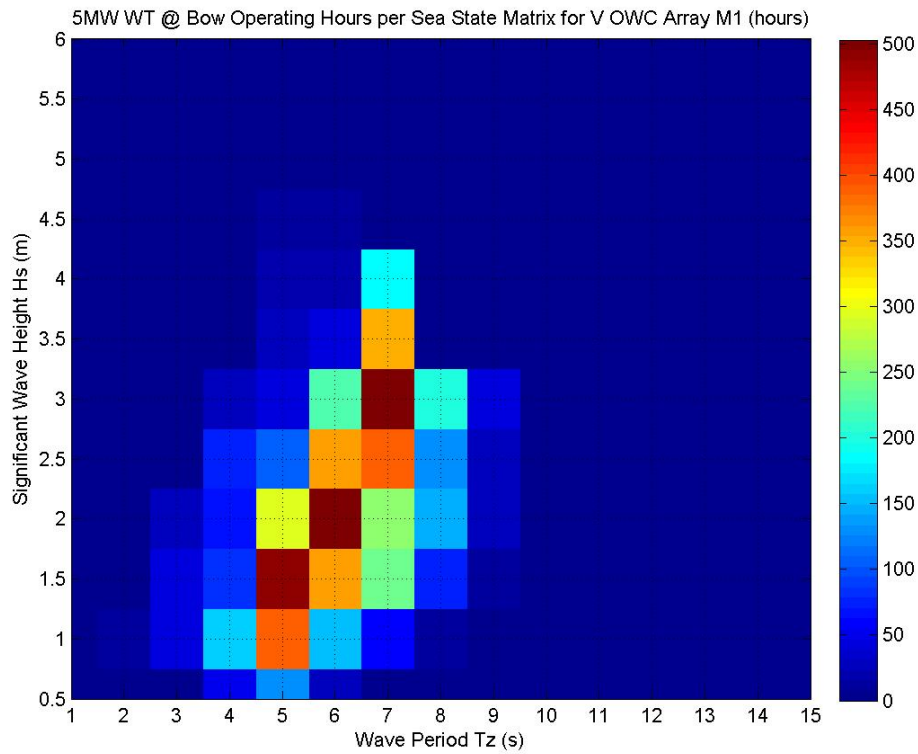
**Figure 5-31: Sea States and Total Hours of Operation for the NREL 5MW WTG on the Delta OWC Array (Mean)**

The mean accelerations experienced at the hub of the NREL WTG for a range of sea states is illustrated in Figure 5-30. Using the 2m/s$^2$ limit as a mean acceleration limit at the hub, the allowable sea states for WTG operability is illustrated in Figure 5-31. The total allowable operating hours under these constraints for the WTG is ~6453 hours. This represents a maximum ~74% availability of the WTG.

### 5.3.3.3 WTG Maintainability

As well as the WEC and platform maintainability, the maintainability of the WTG must also be considered. In this case, the same limits imposed for the WEC maintainability apply to the WTG but now use the accelerations ratio at the RNA location. The MII matrix for this location is illustrated in Figure 5-32. Coupling this with the scatter diagram for the M1 site, the sea states and number of hours in which on-site maintenance can take place is calculated and illustrated in Figure 5-33. The total on-site maintenance time for the 5MW WTG is ~1105 hours, representing a ~13% accessibility/maintainability.
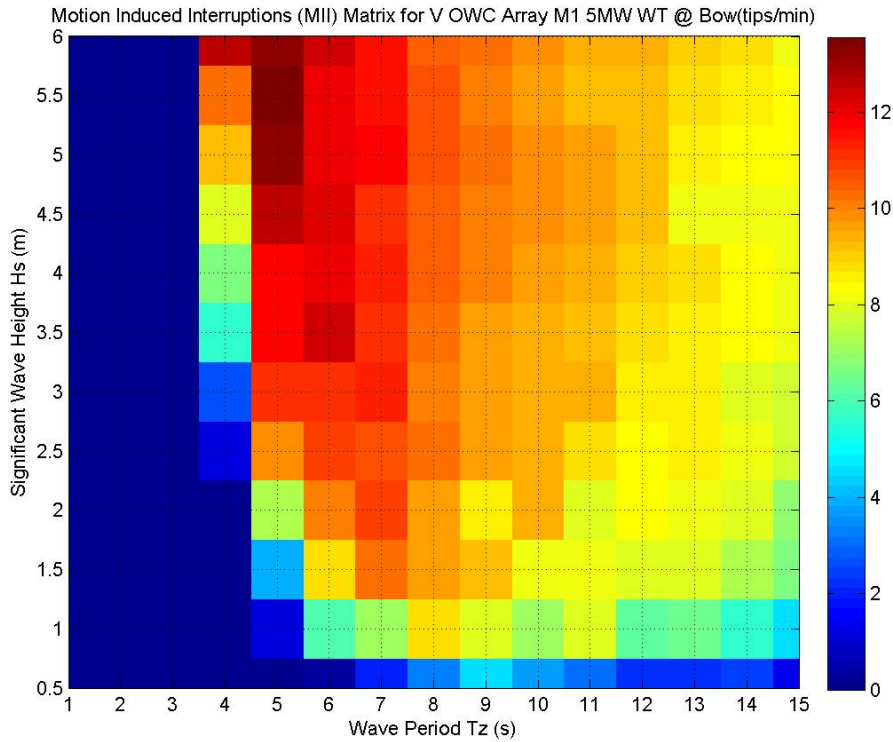


**Figure 5-32: MII Matrix for the WTG at the RNA Location on the Delta OWC Array**
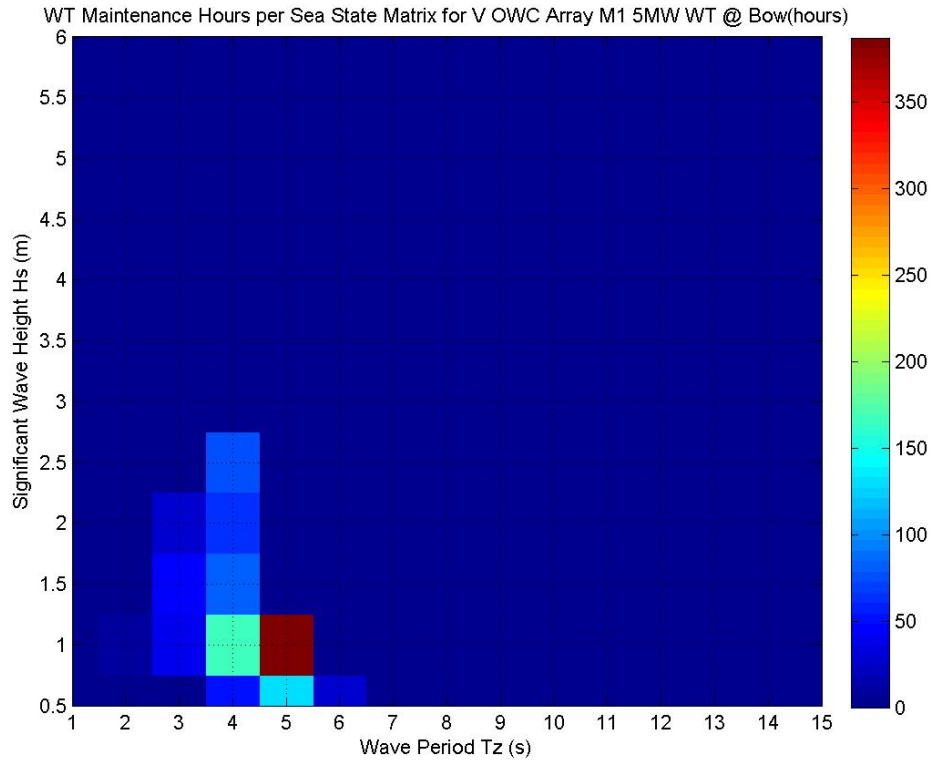
**Figure 5-33: Acceptable On-site Maintenance Sea States for the Delta OWC Array NREL 5MW WTG**

In respect of the low accessibility/maintainability of the NREL 5MW WTG situated on the bow of the Delta OWC Array platform, a further reconfiguration of the platform was envisaged to specifically target this short fall in the design. Due to the large width of the structure, two smaller turbines may be situated on the back beam as illustrated in Figure 5-34. These may range in size from 3MW to 5MW depending on the angular difference between incident waves and wind for the deployment site of interest. Keeping the WTG distance constant, the maximum angle between incident waves and wind without direct shadowing of the WTG in the lee is illustrated in Figure 5-35 based on turbine rotor diameter.
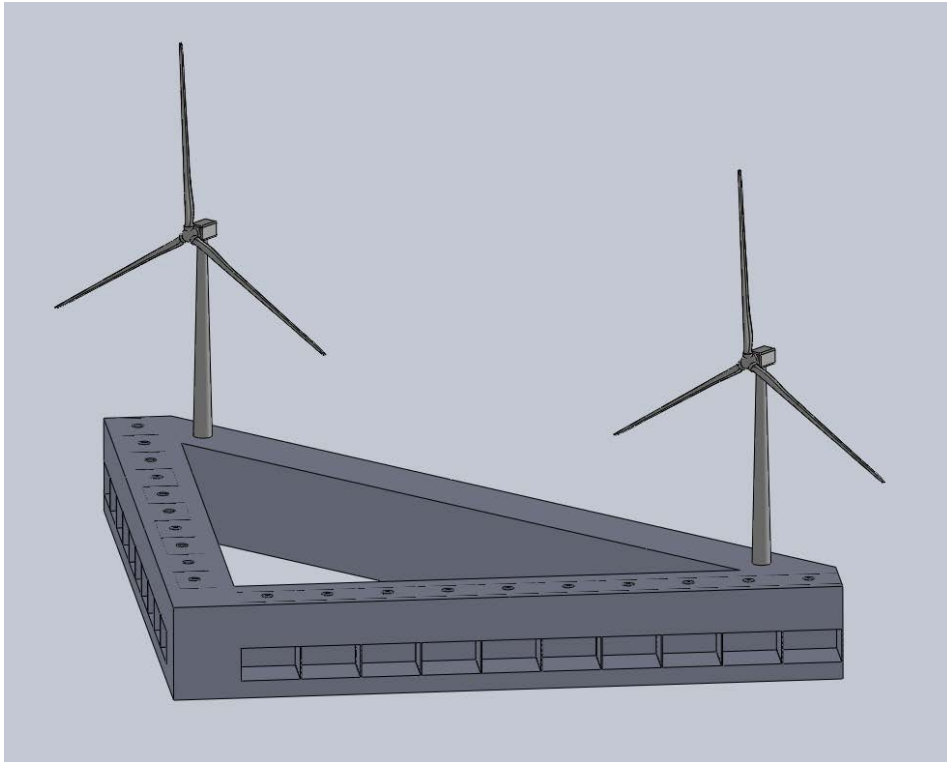
**Figure 5-34: Delta OWC Array Platform with Two WTG's on the Back Beam**
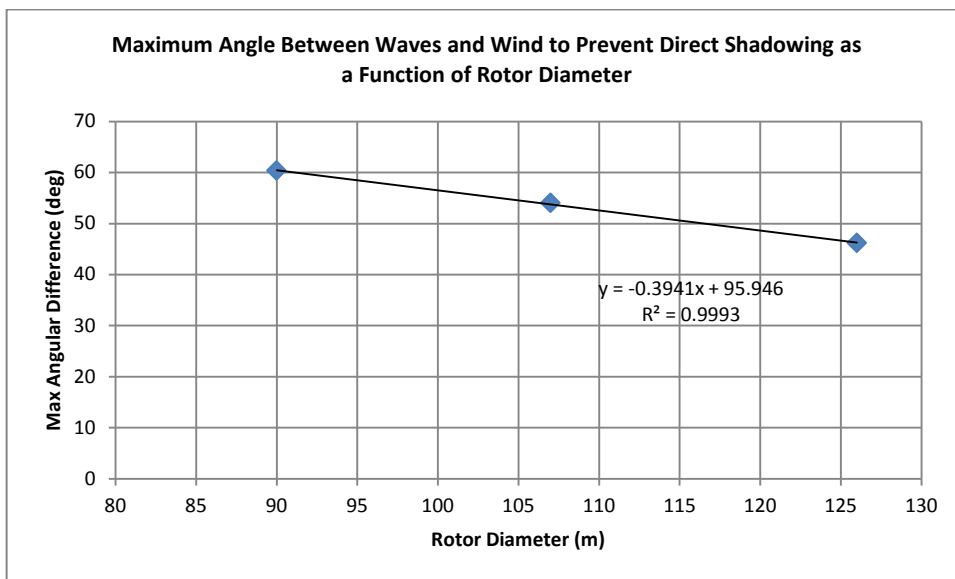


**Figure 5-35: Max Angular Difference Between Incident Waves and Wind to Prevent Direct Shadowing**

Due to time constraints the additional availability which may be possible due to the additional accessibility/maintainability of the WTGs when located at the stern of the platform has not been calculated. The code takes a significant amount of time to complete followed by post-processing. It is thought that due to the closer proximity of the WTGs to the platform COG, much lower accelerations will be experienced and thus higher accessibility/maintainability will be possible.

### 5.3.4 Extreme Response and Mooring System Design

The extreme response analysis was carried using Ansys AQWA software. The station-keeping system incorporates 20 mooring lines at a N-S-E-W configuration. Figure 5-36 illustrates the mooring system layout. Each mooring line is approximately 970.0m in length and assumed a typical size of steel spiral strand wire rope of 150mm diameter. The extreme response of the Delta OWC Array at the M1 site is outlined in Table 5-7.
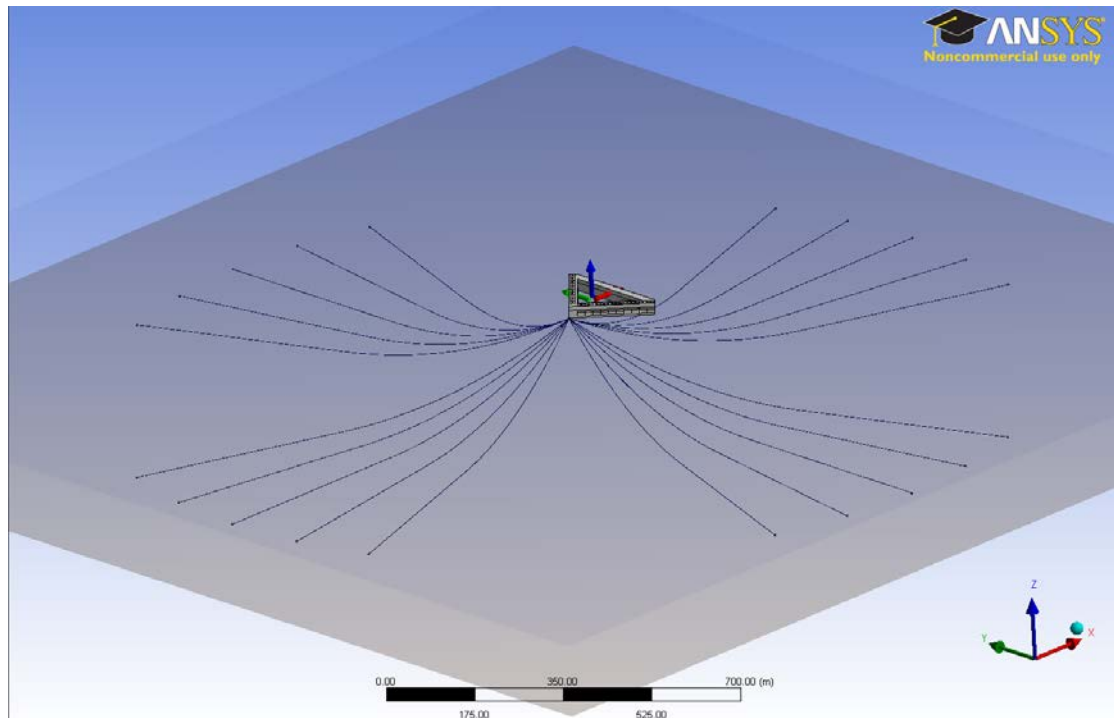


**Figure 5-36: OWC Array Mk2 Mooring System Layout**

**Table 5-7: Extreme Responses of OWC Array at the M1 Site**

|      | Z (m)  | RY (°) | X (m)  | Mooring Load (MN) | Acceleration (m/s$^2$) |
|------|--------|--------|--------|-------------------|------------------------|
| Max  | 4.15   | -0.09  | 121.46 | 29.8              | 5.76                   |
| Min  | -13.28 | -5.11  | 86.61  | -1.22             | 0                      |
| Mean | -4.82  | -2.53  | 102.47 | 2.7               | 0.58                   |

The response analysis results of the OWC Array in typical North Atlantic and Northern North Sea conditions are tabulated in Table 5-8. The wave conditions for this run were $H_s$ 3.5m and $T_p$ 10s.

**Table 5-8: Responses of OWC Array Mk2 in Operational Conditions**

|      | Z (m)  | RY (°) | X (m)  | Mooring Load (MN) | Acceleration (m/s$^2$) |
|------|--------|--------|--------|-------------------|------------------------|
| Max  | -4.06  | -1.85  | 102.01 | 2.3               | 1.04                   |
| Min  | -6.13  | -4.48  | 73.93  | 0.59              | 0                      |
| Mean | -4.80  | -2.56  | 90.52  | 1.07              | 0.023                  |

235

The extreme loads on the mooring system in extreme conditions have resulted in the requirement for a mooring system with substantial mass. The size of the mooring system is on the borderline of what is currently possible in the oil and gas industry. The mooring system specifications are summarised in Table 5-9.

**Table 5-9: Delta OWC Array Mooring Specifications**

| Item | Value |
|---|---|
| **Mooring Line Type** | Steel Spiral Strand Wire Rope |
| **Line Length** | 970m |
| **Rope Diameter** | 150mm |
| **No. of Lines** | 20 |
| **Anchor Type** | Vryhof Stevpris Mk5 or similar |
| **No. of Anchors** | 20 |
| **Anchor Mass** | ~100t |

The anchor mass has been very crudely estimated on the basis that the mooring line could go taut at some stage during the lifetime of the device in survivability conditions. This has resulted in extremely large anchors. This may result in a prohibitive mooring system cost. A dedicated mooring system design through thorough load case definitions in dynamic modelling software would provide a better estimate of what the mooring line and anchor loads would be. It is expected that this will be carried out through the MARINA Project.

### 5.3.5 Assessment of the Delta OWC Array

The assessment of the Curved OWC Array platform may be split into a number of individual performance metrics based on the assessments carried out previously. The following sections will consider these in isolation and then finally form an overall conclusion regarding the continuation of the Curved OWC Array platform.

#### 5.3.5.1 Power Output Performance

The power output performance of the WEC and WTG will be considered separately in light of the additional constraints imposed on the WTG operability.

5.3.5.1.1 WEC

The WEC power matrix is well matched to the M1 site conditions and thus produces a significant amount of power, averaging at 2752kW. The availability of the platform is likely to be high, perhaps in line with current levels of availability for bottom fixed WTs due to the high level of maintainability hours. It should be reasonable to assume 90% availability on the basis of access and maintenance of 85%. The annual average power would then be ~2476kW.

5.3.5.1.2 WTG

Depending on the wind conditions at the site of deployment, the WTG will have a varying load factor. A quick estimate of the performance of the NREL 5MW WTG

at the M1 site suggests that the WTG will have a load factor of ~40% and an average annual power output of ~2000kW. Applying the additional constraints from the hub accelerations, the annual average power is reduced to 1480kW.

**5.3.5.2    Structural Design and Platform Costs**
The statistics of the structural steel construction of the Curved OWC Array platform and its constructability are addressed separately.

5.3.5.2.1   Structural Steel Construction
The preliminary structural steel design has calculated a steel plate and stiffener optimum design of 27mm stiffener beam thickness, 1.0m stiffener spacing and a steel plate thickness of 16mm. These member sizes are not very large and result in a unit production cost range of €1516 - €6342/t. The total steel mass is 14,392t. The addition of 30% additional steel mass for bulkheads and a 10% buffer on unit cost, the platform hull fabricated from steel will cost in the region of €31.2m - €130.5m. A global structural analysis would also be required to ensure sufficient structural strength during extreme conditions.

5.3.5.2.2   Reinforced Concrete Construction
The preliminary structural RC design of the platform has calculated a structural mass of ~51,000t. The steel reinforcement is approximately 4% by volume which is at the range required for use of the €400/t unit cost. Therefore the hull cost from RC is estimated to be ~€20m.

5.3.5.2.3   Constructability
The constructability of the OWC Array has been improved through the redesign of the platform into the Delta configuration. The three sides can be constructed individually and floated to a benign location and connected. However, large dry dock facilities would be required to build the beams and are rare and very expensive. The potential for mass production is low, however as discussed previously, the need for this characteristic is lower as the platform power capacity increases.

**5.3.5.3    Motion Characteristics of the Platform for WEC Maintainability**
The motion characteristics for on-site maintenance of the WEC are sufficient to allow ~7407 hours of access and maintenance. This is sufficiently high to consider an on-site maintenance strategy for the platform.

**5.3.5.4    Accelerations at the RNA for WTG Operability**
Similar to the Curved OWC Array assessment, the limits of $2m/s^2$ as a maximum and mean limit for operability of the WTG have been considered. For the first criteria an operability of just ~8% is possible while for the second criteria an operability of ~74% is possible. The operability of the single 5MW WTG using the mean acceleration has been used.

Time constraints meant that the code for the determination of the accelerations at hub height for the two WTGs at the stern of the platform could not be calculated.

**5.3.5.5    Motion Characteristics at the RNA for WTG Maintainability**

The motion criteria used for the calculation of the allowable sea states in which on-site maintenance can be undertaken for the WTG reveals that only 1105 hours annually this can be done. This essentially means that on-site maintenance for the WTG on the Curved OWC Array platform at the M1 site is not possible. This is in contrast to that calculated for the WEC as the accelerations are amplified from the platform to the hub due to the large distance from the COG.

Time constraints meant that the code for the determination of the accelerations at hub height for the two WTGs at the stern of the platform, and thus RNA maintainability, could not be calculated.

**5.3.5.6    Overall Conclusion on the Delta OWC Array Hybrid**

Based on the assessment criteria summarised, the immediate conclusions are,

- The platform motions have been improved and allow 85% availability for maintenance
- The availability of the 5MW WTG has been improved significantly to 74%
- The maintainability of the RNA of the 5MW WTG on the bow is still low at 13%
- The availability of the two 3MW WTGs is likely to be higher but has not been calculated
- The maintainability of the RNA of the two 3MW WTGs is likely to be higher but has not been calculated
- The maximum directional difference between the incident wind and waves is 60° for two 3MW WTGs mounted on the stern of the platform
- The two WTG configuration has not been considered in any further sections of this thesis
- The RC hull cost is significantly lower than that for steel. Even for the optimistic steel case, RC is minimum ~50% less.

The platform design at this point has been deemed to be sufficiently analysed to warrant scale model testing. The next phase of development involved the design and construction of a suitably scaled platform for tank testing.

## 5.4    Scale Model Tank Testing of the Delta OWC Array

This section outlines the development of a Froude scaled model of the Delta OWC Array platform for tank testing at the Beaufort Research – HMRC, University College Cork Ocean Wave Basin in 2013. This section is divided into relevant sections describing the model design and construction, the testing carried out and main results and finally the comparison of the motion RAOs and power matrices from tank and numerical modelling.

### 5.4.1 Model Design and Construction

The model has been designed to ensure, so far as reasonably practicable, geometric similarity through Froude scaling has been conserved. Of course, like many model designs, compromise between accuracy and time and costs has been required. Furthermore, considerations such as handling and craning capability at the testing facility have had to be borne in mind during design as space is limited and the model is one of the largest, both in terms of geometrical size but also mass, tested at the facility. Therefore the model has had to be built in sections, similar to the design philosophy for the prototype, for craning into the tank and connected while floating. A 3D drawing of the model is illustrated in Figure 5-37.



**Figure 5-37: 3D Drawing of the Delta OWC Array Model**

The model has been designed to be 1:50 scale due to limitations in the tank size and wave making capabilities. The summary of the scaled geometrical quantities of the model are shown in Table 5-10.

**Table 5-10: Summary of Geometrical Quantities of the 1:50 Scale Model of the Delta OWC Array Platform**

| Platform Element | Dimension/Mass |
|---|---|
| **Total Width** | 4.9m |
| **Chamber Beam Length** | 3m |
| **Chamber Beam Width** | 352mm |
| **Back Beam Length** | 4m |
| **Back Beam Width** | 352mm |
| **Total Mass** | 815kg |
| **Chamber Beam Mass** | 186kg |
| **Back Beam Mass** | 413kg |

It may be seen from Table 5-10 that the dimensions and masses of the model sections are quite high. The model sections have been fabricated from polycarbonate material plates chemically bonded together with dichloromethane. Five chambers have been constructed together in one section as illustrated in Figure 5-38.



**Figure 5-38: 5 Chamber Polycarbonate Section**

The chamber cross section has been geometrically scaled from that illustrated in Figure 5-18. The ballast has been designed and placed within the ballast tanks to achieve the correct trim and draft. The chamber cross section dimensions and locations of the ballast are illustrated in Figure 5-39. The ballast blocks for each ballast chamber were specifically sized and cast from concrete. Lead was then used to fine tune the mass of each block. In total, there are 60 ballast/buoyancy tanks in the chamber beams. This is a significant number to ensure water tightness. In fact due to the accuracy of the laser cutting of the polycarbonate plates, the low viscosity adhesive was unable to fill any larger (~0.5-1mm) voids in the connections between adjacent plates. Therefore, it was decided to fill each tank with buoyant expandable foam to prevent leaks. Ballast mass was adjusted accordingly.
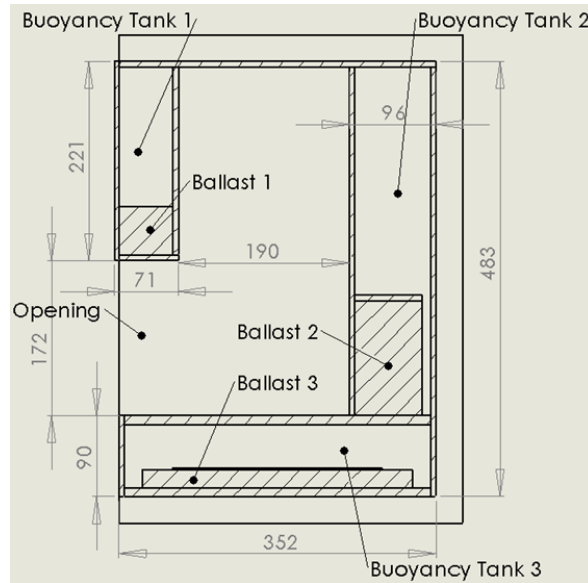
**Figure 5-39: Chamber Cross Section Dimensions and Ballast Locations**

The model has had further additional fixtures and fittings applied such as OWC chamber caps with a fitting to easily change the damping applied to the water column. A float and steel rod with a Qualysis marker has been fitted to ten chambers to monitor the chamber water level elevation. The steel rod has been guided by two guides above and below the orifice plate. Each chamber has been fitted with a pressure transducer to measure the air gauge pressure. Four further Qualysis markers have been installed at the bow to monitor the platform degrees of freedom. The final model installed in the tank and operating is illustrated in Figure 5-40.
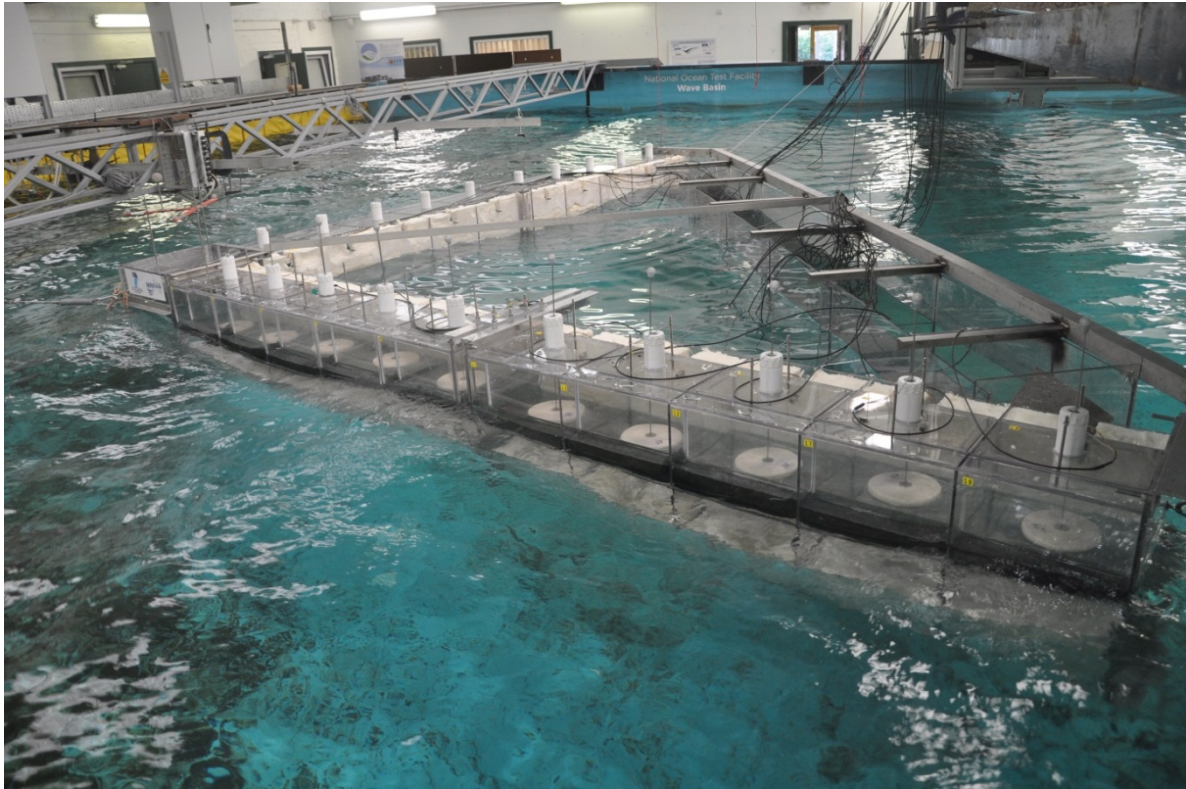
**Figure 5-40: Final Delta OWC Array Model Installed in the Tank and Operating**

In summary the measurements carried out on the model are;

- 4 No. Qualysis markers for platform motion
- 10 No. Qualysis markers for OWC water level elevation on one side of the model
- 20 No. pressure transducers in each chamber
- 3 No. wave probes to the fore of the model
- Strain gauge flange in the centre of the port side chamber beam to monitor global structural loads. The results of these measurements are not included in this thesis as the analysis is on-going due to the unexpected strongly non-linear behaviour of the flange.

The model was moored with three stainless steel mooring lines but as this test campaign was focussed on the performance of the platform in terms of power absorption, no load cells have been used to monitor mooring loads. A more detailed account of the model build and instrumentation is included in APPENDIX C.

### 5.4.2 Delta OWC Array Model Testing Campaign

The testing campaign for the Delta OWC Array platform has included all the typical first stage tests including;

- Monochromatic waves of varying height and period
- Panchromatic waves of varying $H_s$ and $T_p$
- Directional effects on chamber responses

- Effects of a scaled WT on the motion characteristics

Due to the size and mass of the platform, conducting decay tests was deemed unfeasible without the use of a gantry crane. These have not been carried out in this test series.

A more detailed account of the testing campaign is included in APPENDIX C.

### 5.4.3 Testing Results in Brief

The main objectives of the testing campaign were to measure the frequency dependent motion RAOs of the platform and the OWC chambers as well as calculate the power matrices of the platform for varying wave incident direction. This section presents in brief the RAO results for small amplitude waves. The data has been filtered with a Butterworth filter with an appropriate frequency band.

#### 5.4.3.1 Platform and Chamber Motion RAOs

The results presented here are for uni-directional waves with incident direction parallel to the symmetrical central axis of the platform. Figure 5-41, Figure 5-42 and Figure 5-43 illustrate the platform motion RAOs, chambers 01-09 water level elevation RAO and chamber 11-19 water level elevation RAOs respectively.
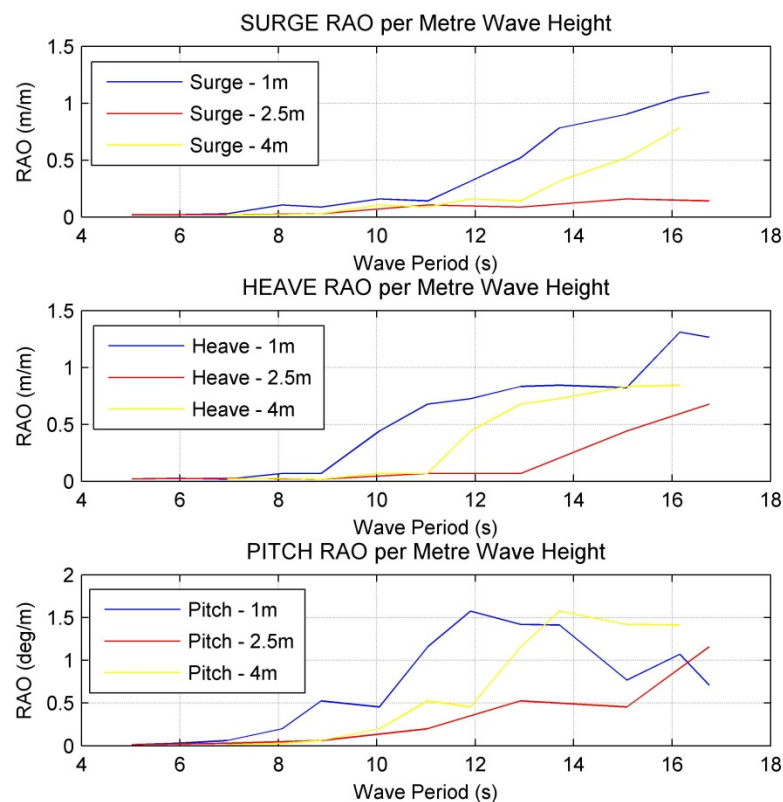


**Figure 5-41: Surge, Heave and Pitch Motion RAOs of the Delta OWC Array Platform for Varying Wave Heights**
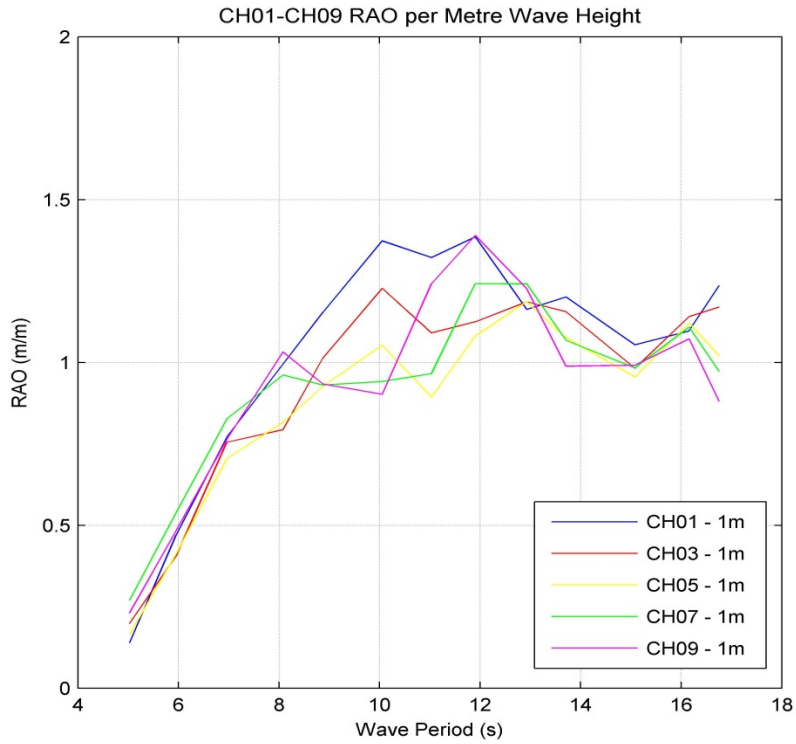
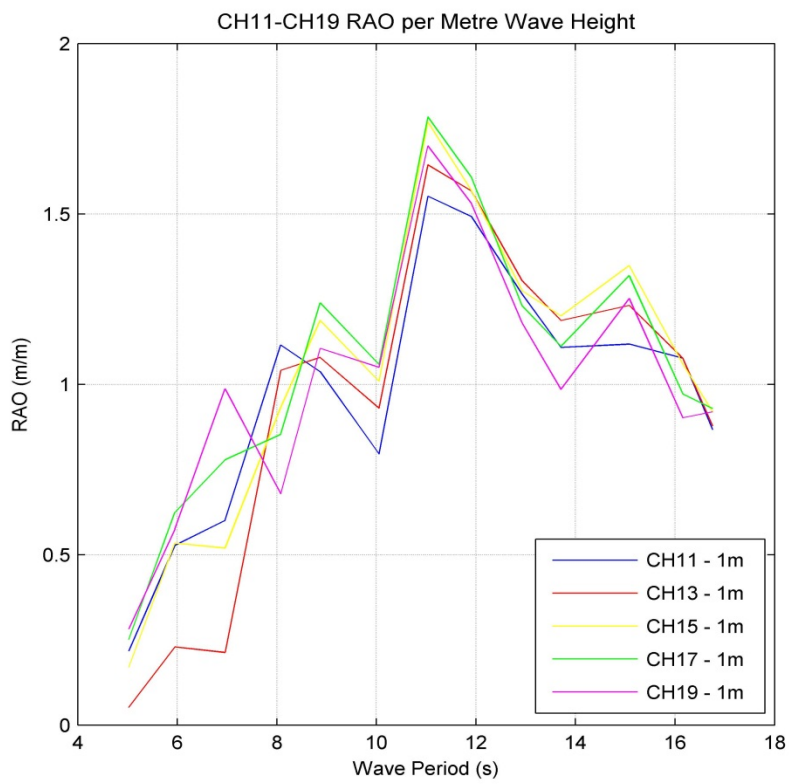**Figure 5-42: Delta OWC Array Chambers 01-09 RAO**



**Figure 5-43: Delta OWC Array Chambers 11-19 RAO**

### 5.4.3.2 Power Matrices for Varying Wave Direction

The results presented here are for uni-directional waves with incident directions of 0°, 22.5° and 45° to the symmetrical central axis of the platform.
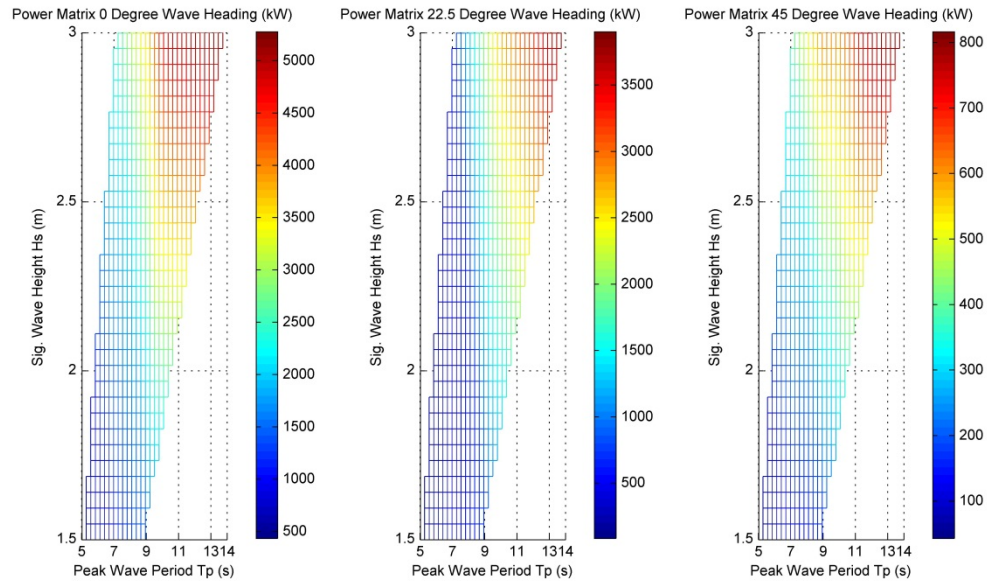


**Figure 5-44: Prototype Absorbed Power Matrices for the Delta OWC Array Platform for Varying Incident Wave Direction**

It may be seen from Figure 5-44 that the Delta OWC Array platform is capable of absorbing 5MW of power in 3m $H_s$ sea states. This may be adjusted according to the approximate PTO efficiency of 54% to give 2700kW which is broadly in line with that suggested by the numerical simulations. However, with increasing wave directional angle relative to the central axis of the platform, the absorbed power drops considerably to a mere 800kW in 3m $H_s$ sea states for a wave directional angle of 45°. This is a substantial drop and clearly indicates the directional dependence of the platform. This suggests that a weather vaning mooring system is preferred for this platform but a full cost-benefit analysis is required based on the mooring system design.

## 5.5 Comparison of Numerical and Scaled Tank Testing Results

This section compares the numerical and tank test results for the main parameters likely to affect platform feasibility, namely the motion characteristics and the power performance.

### 5.5.1 Platform and Chamber Motion Characteristics

Firstly, the platform motions are compared. The surge RAO comparison is illustrated in Figure 5-45. The correlation is acceptable overall with the exception of the modelled response at 15-17s which is estimated to be the resonance period of the platform. The model underestimates the response in this region. The heave RAO comparison is illustrated in Figure 5-46. The correlation is acceptable up to 10s whereby the measured and modelled responses deviate. The model again

underestimates the response between 12s and 15s. The more concerning however, is the pitch RAO illustrated in Figure 5-47 where the model clearly significantly underestimates the pitch response. Due to time constraints, the source of this error has not been identified but may well be to do with the definition of the mass matrix or the definition of the location of the COG with respect to the origin and co-ordinate systems of the geometrical model and hydrodynamic model. As the derivation of the maintainability of the WECs and WTG is based on the numerical pitch and heave response, the underestimated pitch response will have an influence on this parameter. Following identification of the source of the error, the maintainability analysis would have to be re-done. Figure 5-48, Figure 5-49, Figure 5-50 and Figure 5-51 illustrate the comparison between some of the Delta OWC chambers measured and modelled IWS response RAO. It may be noticed that a very good fit is achieved in the chambers close to the bow. In the chambers farther from the bow, the peak response is not as well predicted. This may be due to the under predicted pitching response.
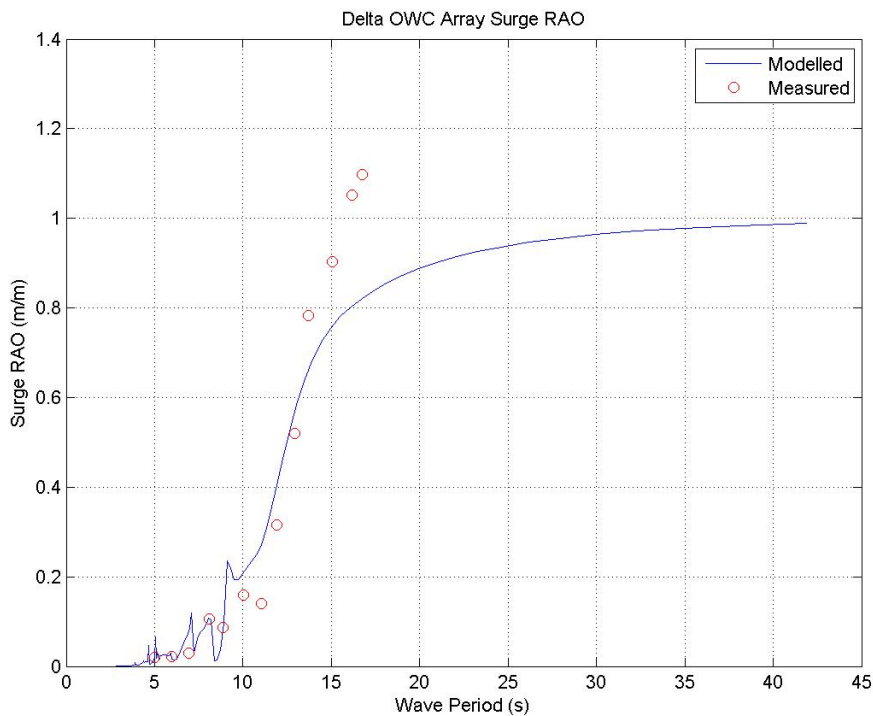


**Figure 5-45: Delta OWC Array Surge RAO Measured Vs Modelled**
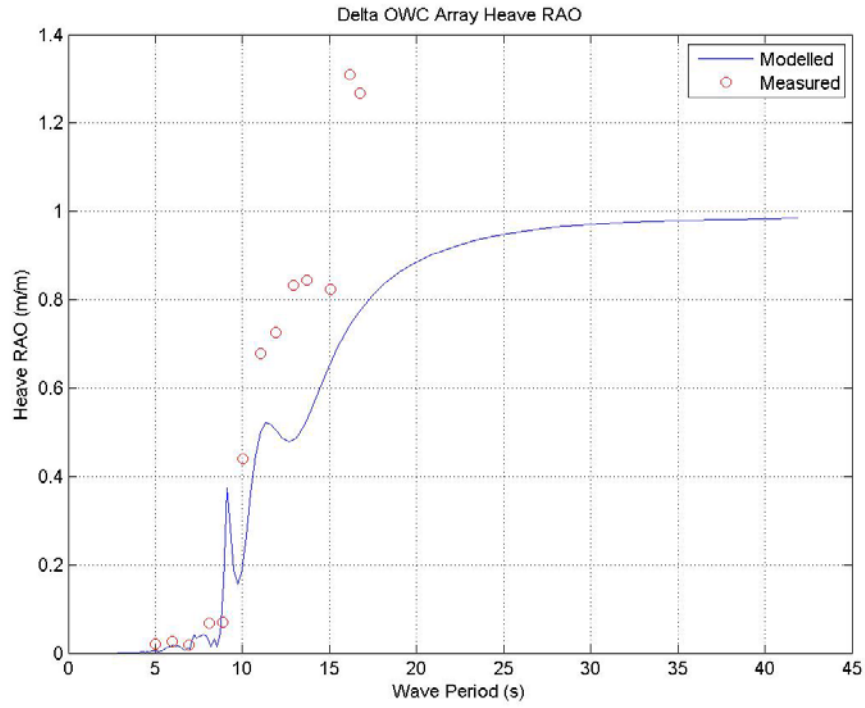
**Figure 5-46: Delta OWC Array Heave RAO Measured Vs Modelled**
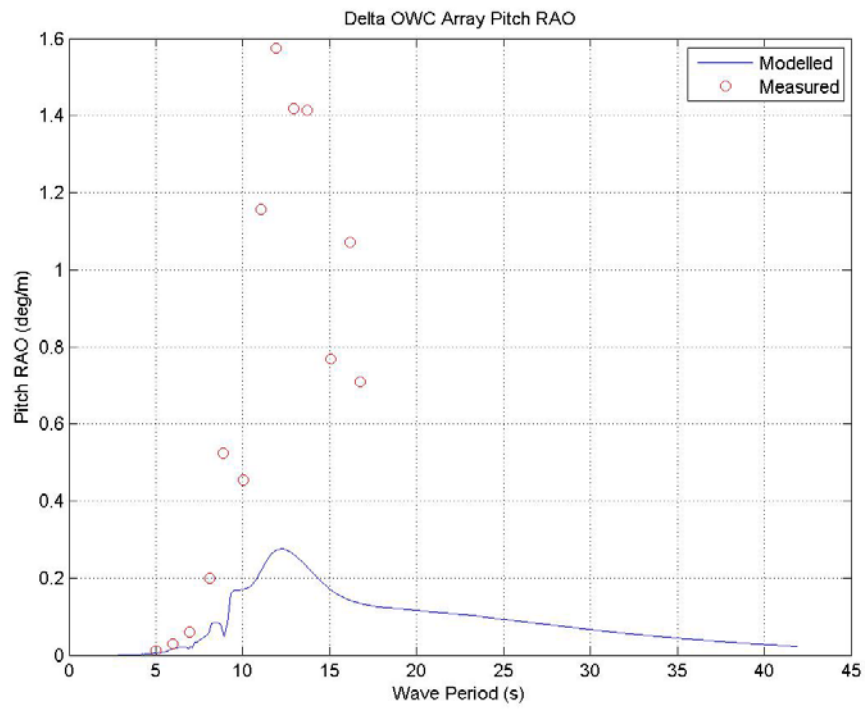


**Figure 5-47: Delta OWC Array Pitch RAO Measured Vs Modelled**

**Figure 5-48: Delta OWC Array Chamber 01 RAO Measured Vs Modelled**



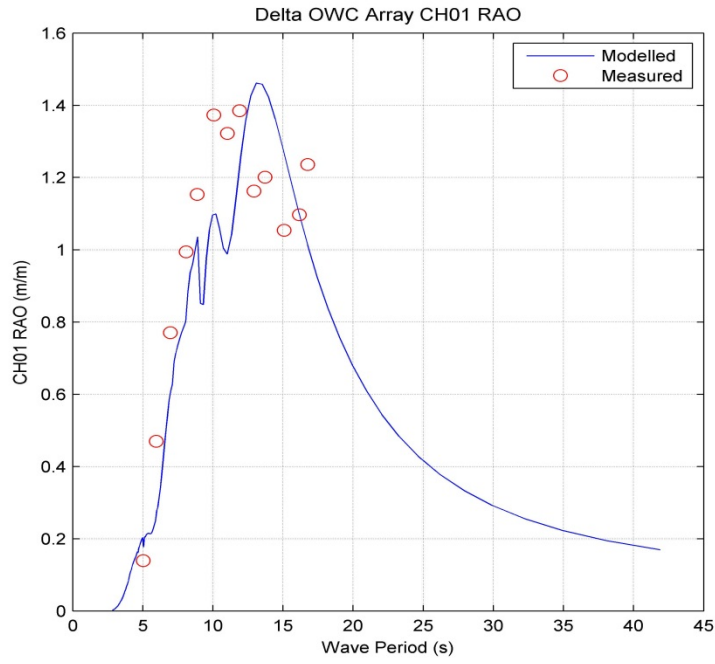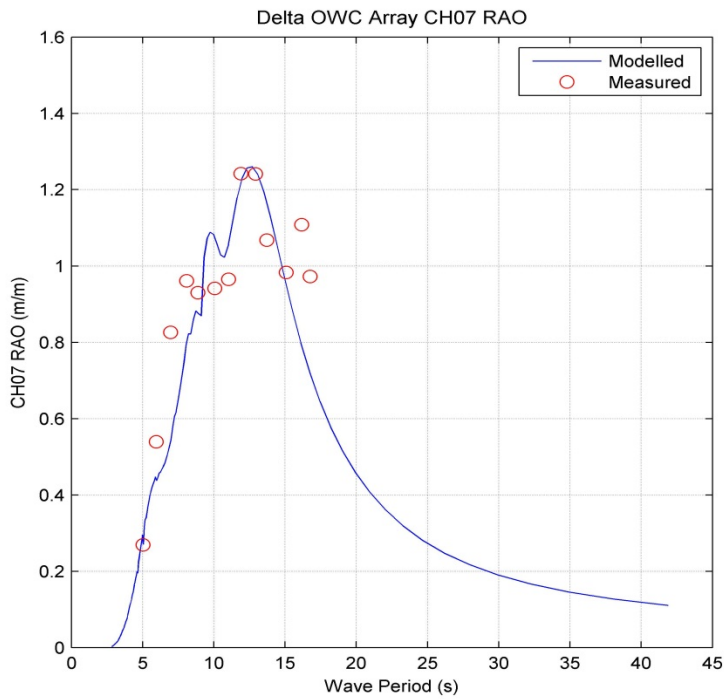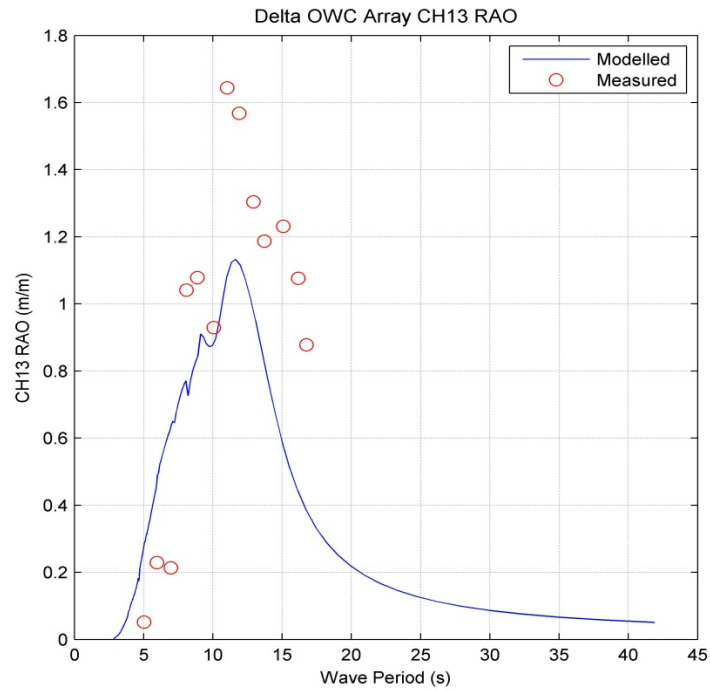**Figure 5-49: Delta OWC Array Chamber 07 RAO Measured Vs Modelled**

**Figure 5-50: Delta OWC Array Chamber 13 RAO Measured Vs Modelled**
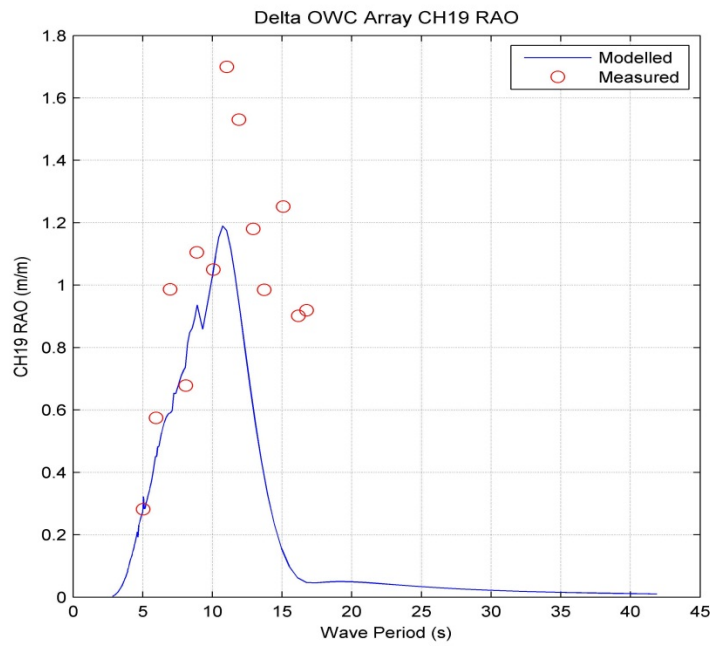


**Figure 5-51: Delta OWC Array Chamber 19 RAO Measured Vs Modelled**

### 5.5.2 Power Performance

The power performance comparison has been carried out in a rather simplistic manner by comparing regions of the numerically generated and measured power matrices with one another.

In the lower regions of the power matrix, i.e. low wave heights, the comparison is reasonable which is as expected as these wave conditions would be close to linear. However as the wave height increases and become progressively more non-linear the linearised approach naturally overestimates the power performance. There are five sea states which overlap and are itemised in Table 5-11below.

**Table 5-11: Comparison of Modelled and Measured Power Outputs**

| Sea State | | Modelled as a % of Measured |
|---|---|---|
| Hs (m) | **Tp (s)** | |
| **1.5** | 7 | 68 |
| **3** | 10 | 99 |
| **3** | 12 | 87 |
| **3** | 14 | 67 |
| **4.5** | 12 | 129 |

Further tests with the model are required to quantify the differences in each cell of the modelled power matrix.

## 5.6  Conclusions on the Delta OWC Array

This chapter has described the design and assessment methodology applied to the OWC Array platform with WTGs concept. This has resulted in two reconfigurations of the platform for power performance considerations initially and constructability reasons secondly. The design process has followed the process outlined in Chapter 3 for the design of a wave energy device but with modifications necessary for the consideration of the addition of WTGs. The following points conclude this chapter;

- The redesigned Delta OWC Array was an improvement on the Curved OWC Array platform in terms of constructability
- The Delta OWC Array platform was estimated to produce 2476kW based on a reasonably assumed 90% availability estimated based on accessibility/maintainability of 85% of the WEC platform
- The WTG output on the Delta OWC Array platform was estimated to produce 1480kW based on a calculated 74% availability based on a limit of 2m/s2 mean hub acceleration and a capacity factor of 40%
- The structural design of the Delta OWC Array platform in structural steel was estimated to be 14,672t with an additional 30% for bulkheads
- Based on the fabrication model the estimated platform cost was €131.2m - €130.5m
- The RC hull is ~51,000t in mass without ballast, and ~103,000t with sand ballast. The hull cost is therefore ~€20m
- The accessibility/maintainability of the Delta OWC Array platform was calculated to be 7407 hours while the WTG achieved 1105 hours

- Accessibility/maintainability of two 3MW WTGs on the platform stern is worth consideration but due to time constraints, it has not been possible to include this analysis in this thesis
- Extreme response analysis of the Delta OWC Array platform revealed large mooring loads
- The tank testing campaign revealed that the numerical model significantly underestimated the pitch response of the platform thus affecting the assumptions on accessibility/maintainability above
- The ability of the model to predict power performance is reasonable up to ~3m $H_s$, where after the estimates are above the measured power due to not accounting for non-linearity of power absorption
- Overall, the Delta OWC Array concept is a reasonably technically feasible concept to consider for further analysis

# 6   LCCA Analysis of the Delta OWC Array Concept

This chapter outlines the development of a time domain reliability model for the assessment of the performance of the OWC Array device in a project scenario. The simplified economic model described in Chapter 4 was unable to accurately model the annual OPEX costs, therefore the time domain model has been developed to model the costs of machinery failures, operations and maintenance throughout the project life span. This chapter describes the main attributes and functions of each module within the model and the importance of these modules in the determination of the LCOE of the OWC Array concept.

## 6.1   Model Description

The model is composed of three main components, namely the CAPEX and OPEX modeller and the discounted cash-flow modeller. Each of these, and their sub-modules, are described here.

### 6.1.1   CAPEX Modeller

The CAPEX modeller is similar to that described in Chapter 4 with a number of additions to account for uncertainty associated with the units costs employed in the CAPEX estimate. The CAPEX for the project as specified by the user are estimated from a large collection of unit costs collected from within the MARINA consortium and personal communications with various consulting engineering firms and advisors. The unit costs are coupled with a either a maximum and minimum unit cost or a standard deviation depending on the probability density function (PDF) used in conjunction with the mean unit cost to provide variability in the cost estimates. The PDF used for this study was the normal distribution, Figure 6-1, for all unit costs. This provides the year zero cash deficit for the project.
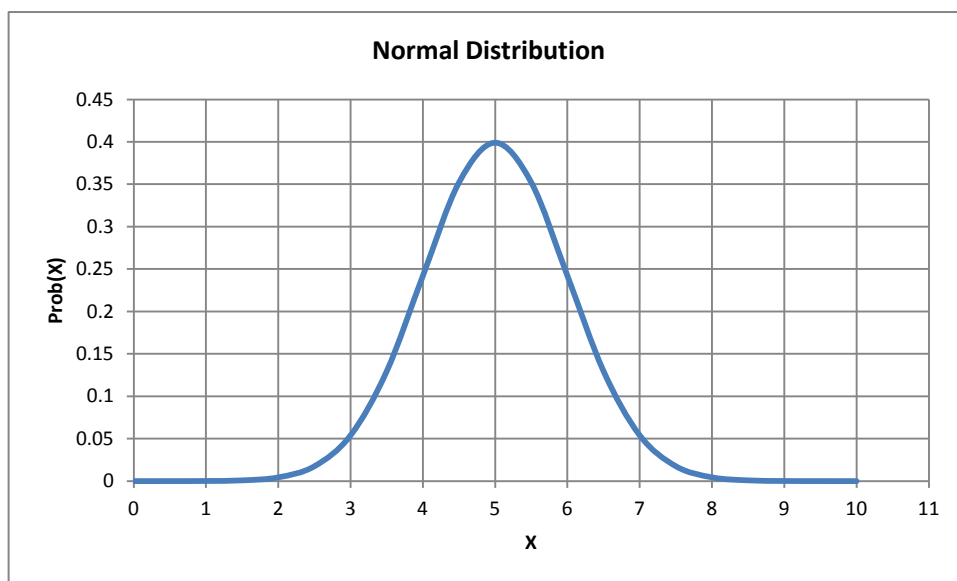


**Figure 6-1: Typical Normal Distribution used in the CAPEX Modeller**

### 6.1.2 OPEX Modeller

The OPEX modeller is the main addition to the economic modelling of the Delta OWC Array device in a project scenario. This model permits the departure from simplistic estimates of OPEX costs and more importantly, correctly reflects the time distribution of OPEX costs so as the weighted contribution to LCOE is calculated based on the discount rate applied. This section includes a description of each of the main elements of the OPEX model and how they are calculated.

#### 6.1.2.1 Environmental Inputs

The primary driver for the time domain OPEX modeller is the resource input. The input for the model is a 10-year hourly time series of wind and wave conditions at AMETS on the west coast of Ireland, which is doubled to create a 20-year time series. This hindcast data has been retrieved from the European region resource model developed within the MARINA project. The time series is for hourly statistics of sea state parameters including $H_s$ and $T_p$, while the wind speed is the hourly average wind speed at 100m above sea level. Each device is assumed to experience the same environmental conditions. This is naturally a simplification however this is not the primary focus of the model, as and when more refined datasets on the specific environmental conditions experienced by each device become available, these can easily be coded into the model. One of the main elements required from the environmental dataset is the calculation of the probability of weather windows of a specified time span throughout each month of the year. For this, an average of the ten years of data is used as the basis for calculation. From this average year, the occurrence of weather windows is determined and a probability of occurrence matrix is produced and acts as the basis for deciding when an offshore task may be carried out.

The environmental dataset is used to determine the hourly power performance of the Delta OWC Array device in a project. The power matrix and power curve for the WEC and WTG respectively are used in conjunction with the time series resource information and time keeping module records the annual energy production for the farm. The model does not account for spatial variation in resource as discussed above or electrical losses in the transmission system.

#### 6.1.2.2 Component Reliability Inputs

The operations module tracks the randomly generated failure times for each of the PTO sub-assemblies, both WEC and WTG, on each platform. These failures are generated from a normal distribution PDF based on the mean time to failure (MTTF) for each sub-assembly and a standard deviation. The LCCA model adopted a run-to-failure or unscheduled corrective maintenance (CM) strategy due to the significant lack of information regarding maintenance strategies for WEC PTO components etc. Furthermore, due to the fact that this process has been undertaken while the concept is within Stage 1 of the development protocol, the model adopted a simplified arrangement of the PTO systems for both the WEC turbines and WTG. These PTO systems are regarded as a single assembly which can encounter both a major or

minor failure. Each failure type (i.e. major or minor) has an associated MTTF and a standard deviation. The mean time to repair (MTTR) the fault is also specified with an associated standard deviation.

### 6.1.2.3    Accessibility and Maintainability Inputs

Currently, a single $H_s$ limit is defined by the user to specify when tasks may be carried out aboard the Delta OWC Array. The motion characteristics of the platform allow access by crews for maintenance in weather conditions up to $H_s$ 4.0m. This has a significant impact on the ability to maintain the devices and power output. Work is ongoing to build-in the capability of specifying an accessibility matrix as described in Chapter 3 for the BBDB device into this model for more accurate representation of accessibility limits.

### 6.1.2.4    Available Resources for O&M Activities

The resources required to correct the various faults encountered are deployed and monitored throughout each simulation. These include spare parts for major failures, available workboats and crew etc. Maintenance procedures are carried out based on the available weather windows. The weather window statistics are based on an average year as discussed previously. These statistics are used in the decision making processes in the operations module for each maintenance procedure, while incorporating an appropriate forecast time to inform the deployment time for maintenance teams. This forecast time is taken to be 12 hours while the required percentage probability of occurrence of the required weather window for deployment of the maintenance team is 15-20%.

### 6.1.3    Discounted Cash flow

The annual costs of maintenance and operations etc. are accounted for in an accounting module which tracks the annual spend on O&M. This vector is then imported into the discounted cash flow modeller as described in Chapter 4 in the simplified economic models. The annual cash flow and annual energy yield are discounted and finally divided to determine the LCOE. The discount rates used in these simulations is 15.5% in line with that suggested by [166] for commercially funded projects and 8% for government/publically funded proejcts.

## 6.2    Analysis of the Delta OWC Array Hybrid Device

The project scenario analysed consisted of a hybrid wind-wave farm with a nameplate capacity of 210MW. The centre of the farm was located 20km offshore while the devices were arranged on a grid with spacing of 1km$^2$, in two rows of six and seven devices staggered. The concept specifications utilised for informing the LCCA CAPEX model are outlined in Table 6-1. The WEC and WTG PTO assemblies have been assigned MTTF and MTTR values listed in Table 6-1. A mean MTTF and MTTR for the WTG have been assumed for major and minor failures [171]. The WEC MTTF and MTTR and estimated from these. For each Monte Carlo simulation, the MTTF and MTTR have been randomly generated from a normal

distribution with mean equal to the values quoted in Table 6-1and a standard deviation of 50% of the mean for the WECs and 10% of the mean for the WTGs. The larger deviation for the WEC is in response to the lack of guidance available for WEC PTO systems and general lack of operational experience with such systems.

**Table 6-1: Failure Rates of Sub-Assemblies for the Delta OWC Array Concept**

| FAILURE RATES FOR WEC AND WT DRIVETRAIN ASSEMBLIES | | |
|---|---|---|
| **Major** | **WEC** | **WT** |
| **MTTF (hours)** | 99,454 | 246,761 |
| **MTTR (hours)** | 24 | 157 |
| **Vessel** | Workboat | Floating Crane |
| | | |
| **Minor** | **WEC** | **WT** |
| **MTTF (hours)** | 50,057 | 93,991 |
| **MTTR (hours)** | 6 | 12 |
| **Vessel** | Workboat | Workboat |

A sensitivity analysis was carried out on the convergence of the results with increasing MC simulation numbers. A minimum simulation number was determined for the farm scenario. The primary outputs of interest from the LCCA model are the CAPEX breakdown for the device, the annual farm energy, the annual maintenance costs and the associated minimum and maximum values within each year. Figure 6-2 illustrates the CAPEX breakdown for the Delta OWC Array hybrid device. This plot clearly identifies the components within the device which contribute most to the total CAPEX.
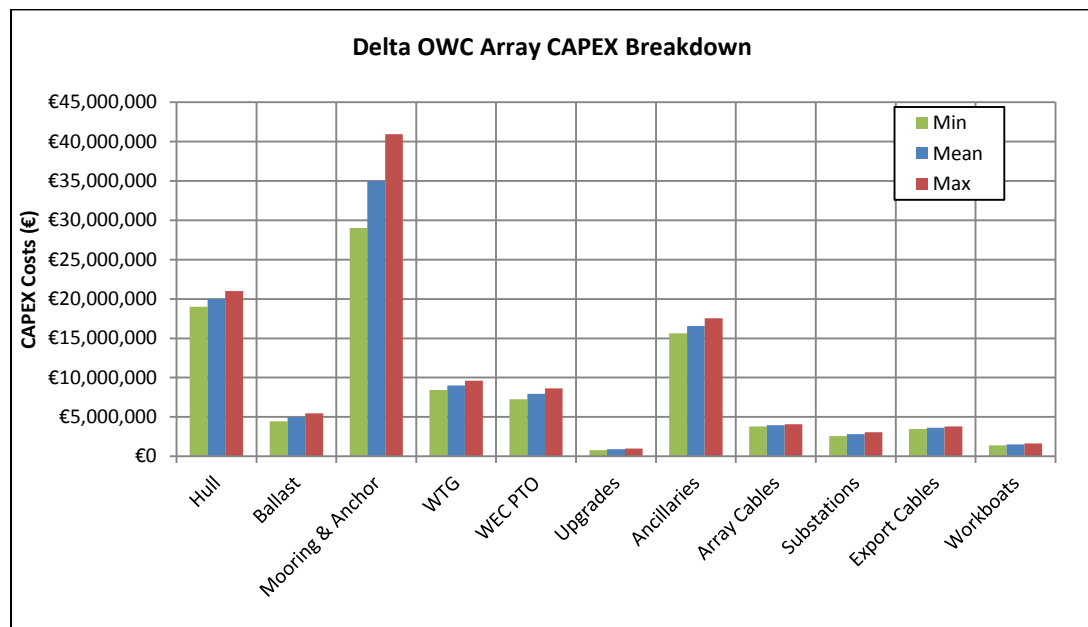


**Figure 6-2: Delta OWC Array CAPEX Breakdown**

In this case, the CALM mooring system is the most expensive component due to the requirement for each mooring line and anchor to be designed for the maximum load. Figure 6-3 illustrates the annual energy output from the farm of hybrid wind-wave

Delta OWC Array devices. The mean annual energy output is 597GWh or approximately 4.8MW of average power output per device. The variance in the annual power output is rather small, of the order of 1%. The reason for this is that no uncertainty has been incorporated into the power matrix or power curve for the WEC and WTG respectively nor the wave and wind resource. Following further analysis of the tank testing data and comparison with numerical assessments, the uncertainty in the power performance can be better quantified and incorporated into the model. Work is on-going in this respect.
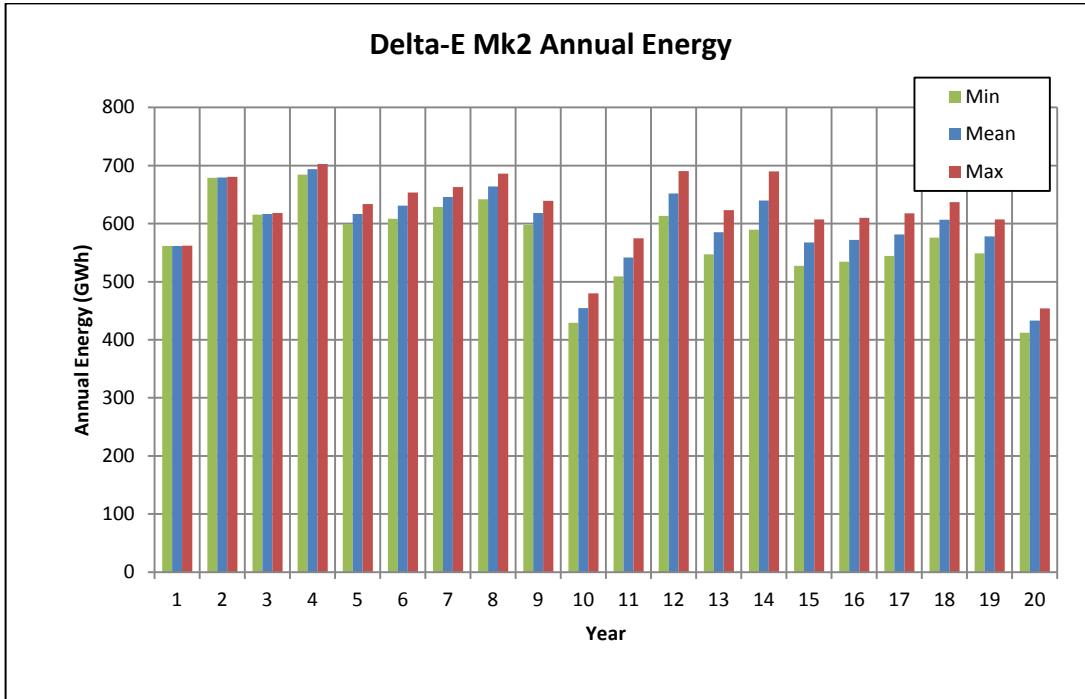


**Figure 6-3: Delta OWC Array Total Wind and Wave Energy Annual Output**
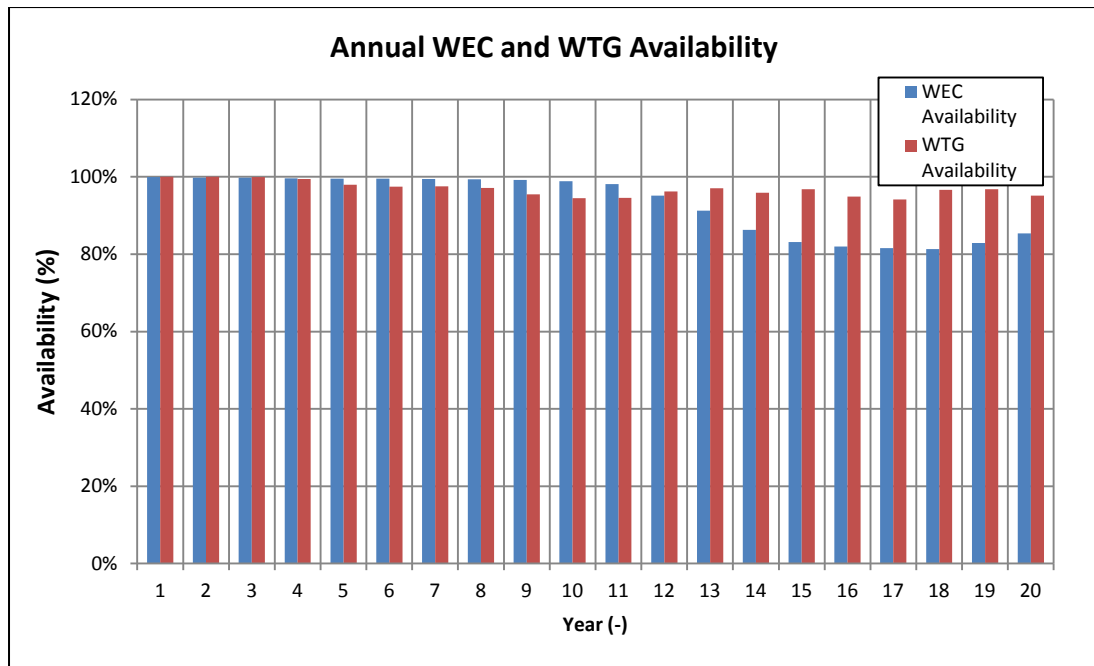
**Figure 6-4: Annual WEC and WTG Availability**

Based on the failure rates and the PDF function specified for the WEC and WTG sub-assemblies, the annual availability of the turbines has been calculated and is illustrated in Figure 6-4. It can be seen that due to the high access limits of 4m $H_s$, a high availability is achievable for both the WEC and WTG infrastructure.

Figure 6-5, Figure 6-6 and Figure 6-7 illustrate the annual variation and associated range of possible costs of crew, workboat and WEC spares costs for the farm. Figure 6-8 illustrates the annual CM costs for the Delta OWC Array 210MW farm. The plot indicates the true nature of the time dependent O&M costs annually. It may be seen that due to the large standard deviation applied to the MTTF of the WEC PTO systems, the O&M activities are highly variable throughout years 7-12 in particular. As more operational experience with WECs is gained, many failures may be planned for and shifted from a corrective to a preventative maintenance strategy and result in a more cost-effective maintenance programme for the farm. The wide variance in annual costs, in particular year 12, depicts a significant range of possible costs due to O&M activities, ranging from €450k to €1.4m. These values make it particularly difficult to design an effective preventative maintenance programme for WEC devices and assign the necessary resources to O&M.
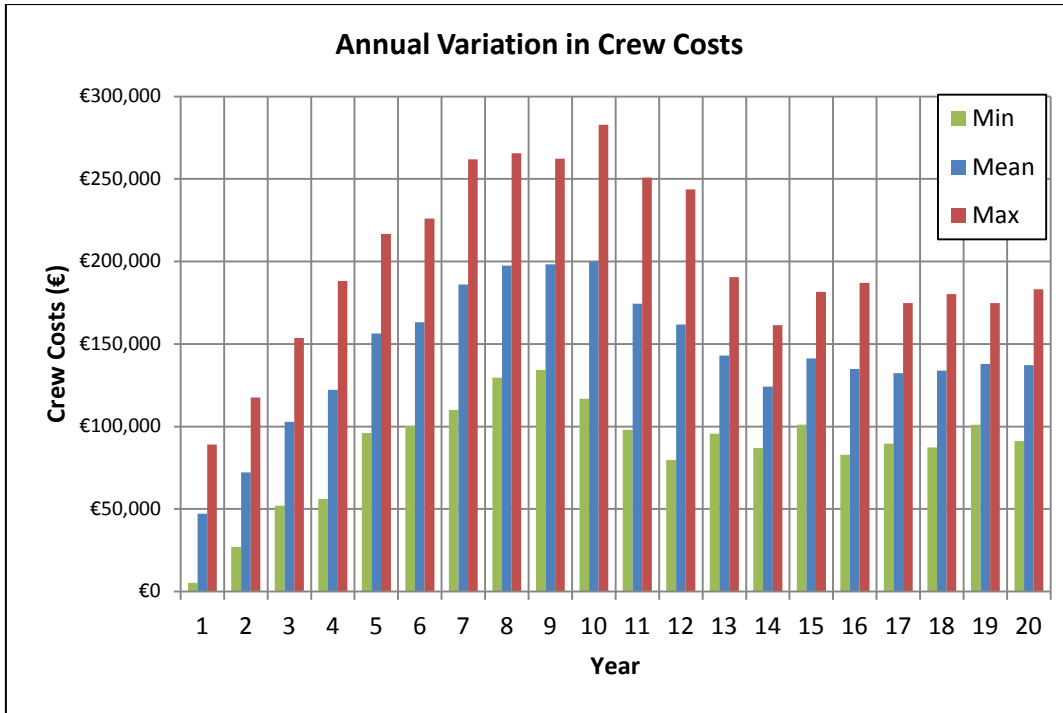
**Figure 6-5: Annual Variation and Associated Range in Crew Costs**
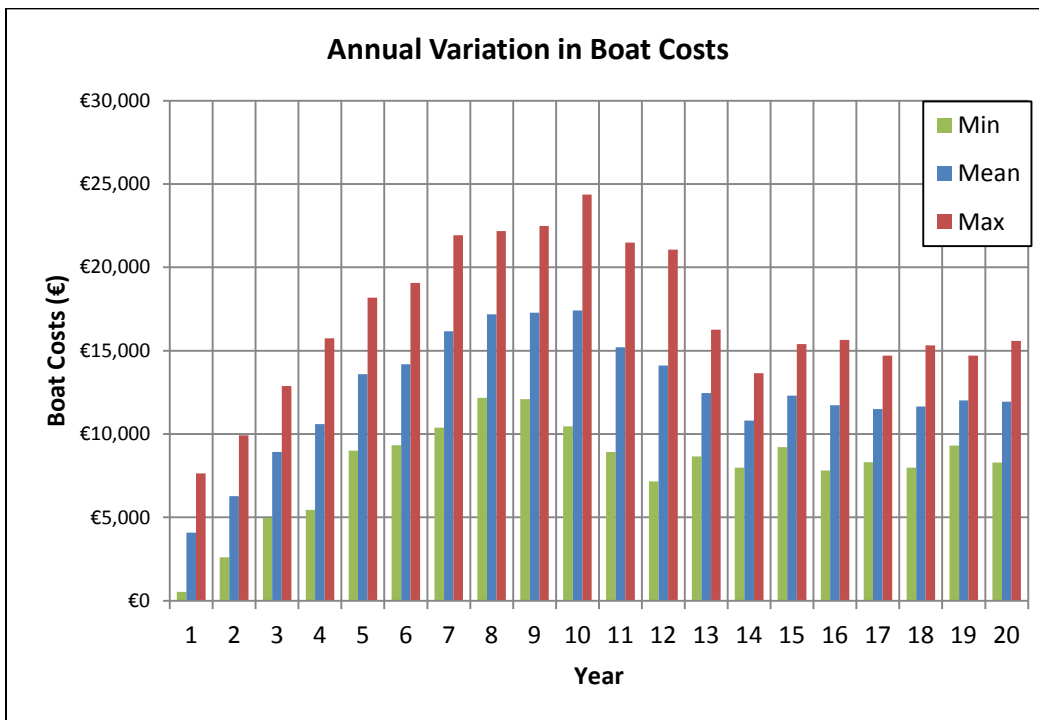


**Figure 6-6: Annual Variation and Associated Range in Boat Costs**
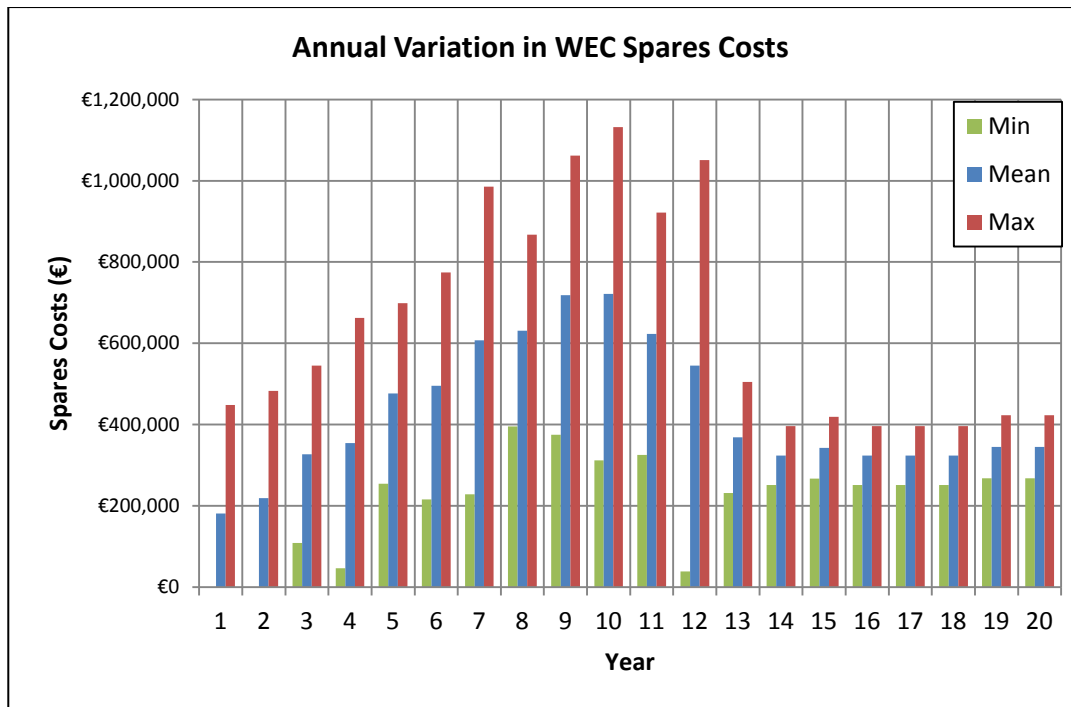
Figure 6-7: Annual Variation and Associated Range in WEC Spares Costs
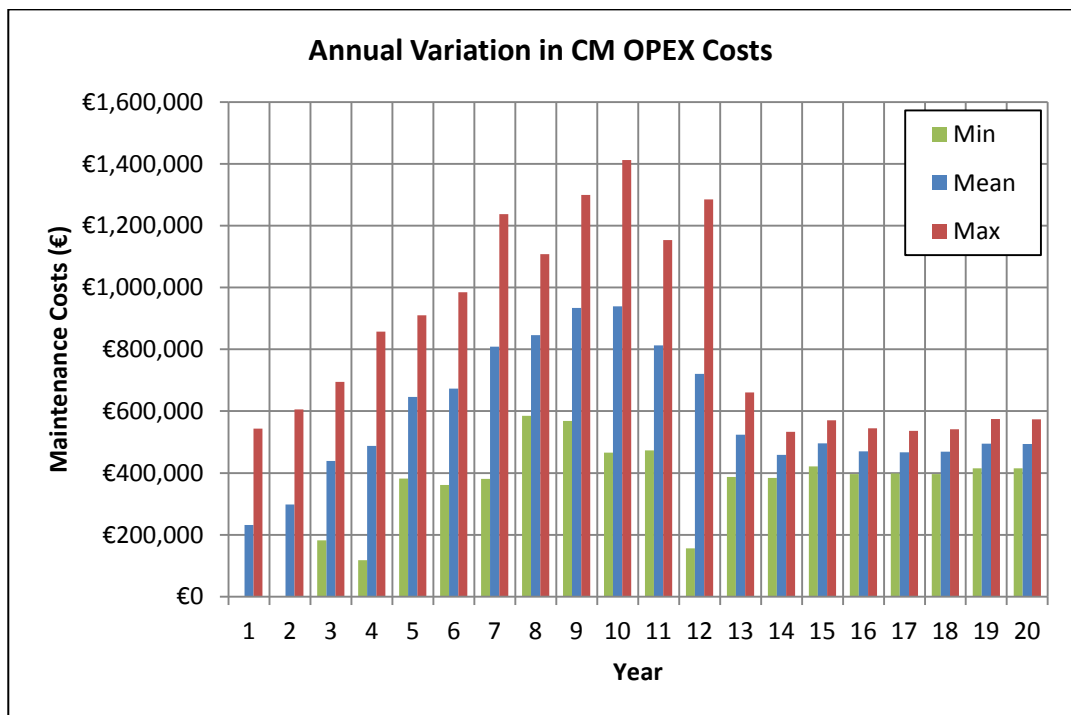


Figure 6-8: Annual Variation and Associated Range in CM OPEX Costs

## 6.3 Discussion and Conclusions

This chapter has briefly presented the development of a time domain economic model for the assessment of project OPEX costs by predicting the occurrence of machinery failures, accessibility of the platforms and availability of spare parts. The model components have been described in brief and include the CAPEX modeller, the OPEX modeller and the discounted cash flow modeller. The primary component

of the model developed is the OPEX modeller which is comprised of a number of sub-modules including;

- Environmental Inputs
- Component Reliability Inputs
- Accessibility and Maintainability Inputs
- Available Resources for O&M Activities

Each of these sub-modules and their associated inputs contribute significantly to the economic viability metrics. The model allows the necessary flexibility in optimising the O&M strategy of a project, however; for this study only a CM strategy has been adopted.

From the preliminary engineering design carried out on the Delta OWC Array platform in previous chapters, the CAPEX costs for the platform have been estimated. From the analysis carried out, it is clear that the governing design consideration for large platforms like the Delta OWC Array is the mooring or station-keeping system. Other CAPEX components for the platforms are much smaller than the CALM system. This is in contrast to the typical CAPEX breakdown expected for a ~ 1MW device where the platform would be ~ 40% and the mooring system ~ 10-20%.

In April 2014, as part of the MARINA Platform project, Technip reported on a dedicated analysis of two mooring systems for the Delta OWC Array platform. A weather-vaning turret mooring system and a fixed orientation spread mooring system. The conclusion of this study was surprising in that the turret system was more cost effect in CAPEX costs. Total CAPEX costs with up-to-date market prices were provided. The total system cost including anchors was ~€35m allowing some additional costs for the turret system on the bow of the platform but not including installation costs for the mooring lines and anchors. This has been used in the analysis of the LCOE of the platform. On comparison between the original design proposed in Chapter 5 and the redesigned system, it was indeed the anchor mass which was the cause of the majority of the overestimation of original mooring system costs. The new anchor size is ~20t Stevpris Mk6, 20% of the original estimate of 100t Stevpris Mk5. Though the Mk6 design achieves more Ultimate Holding Capacity (UHC) for less mass, the difference in cost is most certainly from overestimation of the anchor mass due to assuming the mooring lines would go taut and transfer all load to the anchor.

The OPEX model tracks the operating WEC and WTG turbines during each time step of the simulation which are based on the failure rates identified through the normal distribution inputs in the component reliability module. By tracking the operating turbines, an accurate representation of the instantaneous energy output of the farm is possible. Figure 6-3 illustrates the annual energy output of the farm and illustrates a ~ 20% drop in energy output around year 10 due to consecutive failures

of turbines at that time. A reduction in output is again seen in the latter years of the project as further turbines fail. In response to these failures, crews, workboats and spares resources are utilised in the process of bringing the turbines back into full operation again. The operations currently coded into this OPEX component of the economic model can be significantly improved and added to. Work is on-going on adding a PM module into the code which should better represent the current state of the art in the offshore wind energy industry in O&M strategies. This will naturally add to the projects costs as the failure rates used in the simulations for the WTG are based on datasets of WTG farms which have employed a PM and CM strategy.

The LCOE of the Delta OWC Array with the most recent designed weather-vaning mooring system was €0.31/kWh with a standard deviation of €0.02/kWh and €0.22/kWh with a standard deviation of €0.01/kWh for discount rates of 15.5% and 8% respectively after accounting for availability. The OPEX costs are ~10% of the COE which is low compared to wind which would be ~30% (the COE is undiscounted). The CAPEX/MW is ~€6.5m which is reasonable considering the large platform. In order to be competitive, the OPEX needs to be less than other industries with lower CAPEX/MW capacity statistics. The OPEX costs currently only account for a CM maintenance strategy. Following modification of the code to account for an additional PM strategy, the OPEX percentage will naturally increase further.

Aside from the lack of full and complete functionality in the model currently, it has demonstrated the ability to model time dependent energy production on the basis of operating machinery. Furthermore, the ability to model maintenance activities on the basis of these non-operating turbines and the accessibility limits imposed on the fulfilling of these activities has been demonstrated. In the case of wave energy devices and projects, the introduction of time based economic models is ahead of the state of the art. However, more advanced technology developers are known to be developing their own in-house versions of these tools to assist in providing more accurate availability figures for medium to long term economic projections for the machine and project roll-out the developer deems appropriate on the basis of investment potential and TRL level of the specific technology. It is the intention to continue developing this model to a point whereby early stage technology developers can avail of it despite not having specific information on PTO components or O&M strategies. This tool is envisaged to be a starting point to provide better estimates of availability and O&M costs for better medium to long term economic projections. It is hoped that this will contribute to improving the quality of technical information input into economic models and improve the transparency in developer economic viability projections for securing funding and investment.

# 7 Conclusions and Recommendations for Further Work

This chapter summarises the work of this thesis in the form of clear and concise conclusions and recommendations. The conclusions are presented firstly for each individual chapter and then for the thesis as a whole. For clarity the scope of each chapter is first stated and the conclusions are then listed. Recommendations for further work that will advance specific areas of the research undertaken in this thesis are also outlined.

## 7.1 Conclusions

Chapter 1 outlined the scope for this thesis and acknowledged the challenges facing the wind and wave energy industries and discussed how, through a hybrid solution, these challenges may be overcome. The contribution this thesis has made to the solution was outlined and their potential use in future design optimisation methodologies discussed.

Chapter 2 has provided a substantial bank of information to inform design decisions and methods for various wind, wave and hybrid wind-wave structure combinations. The acknowledgement of the state of the art in the following areas has underpinned the thesis and its work;

- Concept development protocol
- Available guidelines and standards
- Physical and numerical modelling techniques
- Fundamental wave energy conversion principles, their various embodiments by WEC developers and how they have been developed to sea trials (>TRL 5)
- Commercial wind turbines and associated fixed and floating foundation types and design methods
- WEC PTO types and conversion efficiencies
- Structural design techniques based on local and global loads
- Techniques for the assessment of concept related risk
- Life cycle cost analysis modelling and
- Indicators of project feasibility

Each of these items has provided input into the processes by which the hybrid device designed later in the thesis was initially conceptualised, assessed and ranked relative to the other hybrid concepts. It is postulated that a list such as this would form the basis of design for all offshore wind, wave and wind-wave hybrid concepts. It may be concluded from this chapter that a significant amount of information is available to guide preliminary designs of offshore renewable energy devices, yet specific guidelines and standards are still a necessity for the industry. The release of IEC standards currently under development for WECs and tidal energy converters are eagerly anticipated.

Chapter 3 has presented preliminary design methods for two fixed and two floating offshore wind turbine foundations and a wave energy device. The structural design for these structures has been based on ULS design only. No account of fatigue damage throughout the structure lifetime has been considered as it may be considered overly onerous at TRL2 stage of development. It is acknowledged that WEC structures are subjected to numerous load cycles throughout the lifetime of the installation and are likely to be fatigue governed in terms of structural material requirements. Further analysis on the structures in this thesis should consider some form of fatigue design as the concept progresses to TRL3. These may be simplified methods or more involved Rainflow Counting techniques coupled with Miner's Linear Damage Rule.

It may be concluded, from the design methods for the fixed wind turbine foundations presented, that;

- A preliminary structural design of a monopile and GBS fixed foundation, based on semi-empirical methods using Morison's equation and the principle of superposition, is feasible
- There is a relationship between water depth and structural mass for various turbine power capacities
- There is a relationship between water depth and steel production costs for various turbine power capacities on the basis of the preliminary structural designs of the foundations can be developed
- Based on a preliminary analysis in a relatively shallow water depth of 40m, the GBS foundation costs for a 5MW turbine can be less than 50% of a monopile foundation

It may be concluded, from the design methods for the floating wind turbine foundations presented, that;

- The frequency dependent response of the foundations can be used to determine the localised structural loads on the hull
- The steel plate and stiffeners in the hull construction can be preliminarily sized
- The mooring lines and anchors can be preliminarily sized
- The CAPEX costs of the hull based on the upper and lower bounds of the weld details based on the structural members may be preliminarily estimated

The design process of a wave energy converter in Chapter 3 has demonstrated an effective method of designing a WEC for various resource levels ranging from low to high. The design process has concluded that;

- Following identification of the parameters most appropriate for sizing the device, it may be designed to match the target wave energy resource

- The principle of superposition can be used to determine the linearised power matrix and structural design of the hull based on ULS
- Steel production costs for the hull, based on steel member sizes and upper and lower bound sizes of welds, can be estimated
- Frequency dependent motion characteristics can be used for a preliminary assessment of mooring loads and chain sizes
- Frequency dependent motion characteristics can be used for the assessment of the potential of on-site maintenance by technicians on-board the device

Chapter 4 has presented the basis for hybrid wind and wave energy hybrid devices and methods by which they may be realised including;

- Sharing space
- Sharing power transmission infrastructure
- Sharing installation and O&M strategies
- Sharing a foundation/platform

For the basis of this thesis, the latter form, sharing a foundation/platform was chosen as it embodies all other aspects of hybrids also. A selection of eleven potential hybrid devices for consideration for further work was presented. These devices varied substantially in combinations of WEC operating principles and host structures.

The assessment methods developed have been discussed and concluded that;

- The device type factor, which, based on preliminary tank testing of a variety of OWCs and surge flap WECs, can be used to design WECs of varying cross-sectional area, i.e. plan area of OWCs and PAs and surge flap frontal area and ramp frontal area of overtopping devices
- Simplified deterministic economic modelling can calculate the CAPEX, simplified OPEX and LCOE of various combinations of hybrid devices
- Simplified tank testing of specific aspects of a design of interest can assist in reducing uncertainty in power performance
- Ranking of concepts based on the following is possible qualitatively;
  - LCOE
  - Constructability of hull
  - Operations and maintenance
  - Installability
  - Survivability

The OWC Array was chosen through this process as a hybrid concept worth further design and analysis on the basis primarily of O&M and survivability performance.

Chapter 5 has carried out further design and analysis of the OWC Array concept. The analysis has concluded;

- The mean power performance of the WEC platform is ~3341kW at the M1
- The platform requires ~13,672t of structural steel
- On the basis of the structural members for the steel hull, the hull costs are estimated to be ~€33.3m-€92.8m
- The WEC accessibility/maintainability on the basis of allowable MII limits is estimated to be ~6000 hours, i.e. 68%
- The accelerations at the WTG RNA, using mean accelerations above $2m/s^2$ as a limit, result in a maximum availability of ~4206 hours, i.e. 48.6%
- The WTG accessibility/maintainability on the basis of allowable MII limits is estimated to be ~54 hours
- On the basis of the high accessibility/maintainability of the WEC, 90% availability is reasonable to assume and thus the mean power output of the WEC is ~3000kW
- Due to the maximum availability of the turbine, the maximum mean power output is expected to be ~972kW
- The low availability of the WTG and the large dimensions of the hull require a redesign of the hull to minimise the accelerations at the RNA for accessibility/maintainability of the WT and for constructability of the hull

The OWC Array platform was again redesigned focussing on constructability. The new configuration allows partial construction in a dry dock and connection of the main hull elements in a benign location. Further analysis of this reconfiguration has concluded;

- The mean power performance of the WEC platform is ~2752kW at the M1
- The platform is ~14,392of structural steel
- On the basis of the structural members for the steel hull, the hull costs are estimated to be ~€31.2m-€130.5m
- The WEC accessibility/maintainability on the basis of allowable MII limits is estimated to be ~7407 hours, i.e. 85%
- The accelerations at the WTG RNA, using mean accelerations above $2m/s^2$ as a limit, result in a maximum availability of ~6453 hours, i.e. 74%
- The WTG accessibility/maintainability on the basis of allowable MII limits is estimated to be ~1105 hours, i.e. 13%
- On the basis of the high accessibility/maintainability of the WEC, 90% availability is reasonable to assume and thus the mean power output of the WEC is ~2476kW
- Due to the maximum availability of the turbine, the maximum mean power output is expected to be ~1480kW
- The RC designed hull was estimated to be ~51,000t excluding ballast mass with a steel to concrete volume ratio of ~4%
- The RC hull is estimated to be ~€20m based on a unit cost of €400/t

- The mooring system designed initially for this platform was very heavy, i.e. 150mm diameter steel wire at 970m in length coupled with, it has transpired, significantly oversized anchors at 100t

The scale model testing of the OWC Array concluded that;

- The concept is a multi-MW output system in most wave conditions
- The concept is significantly affected by the incident wave direction if a fully fixed mooring system is adopted
- The numerical modelling of power performance is reasonably good even when using simplified linearised modelling
- Numerical prediction of pitch response is not sufficiently accurate

Chapter 6 has developed a time domain LCCA model to demonstrate the effectiveness of such models to assist in developing an O&M strategy for offshore renewable energy installations. It is concluded that the model has the ability to;

- Calculate the CAPEX breakdown for the concept
- Track the annual energy output of the farm based on the operating machinery at each timestep of the incident wave and wind resource
- Calculate the annual availability of the WEC and WTG machinery based on the machinery that has been operating and repaired
- Track the annual variation in crew costs, boat costs and, for this scenario, WEC spares costs
- Track the total annual variation in CM costs

The cost statistics of the OWC Array concept have been calculated to be;

- LCOE at a discount rate of 15.5% and 8% of €0.32/kWh and €0.22/kWh respectively
- The OPEX is approximately 10% of the COE which is low compared to typical rates for offshore wind however; these costs are only for a CM strategy
- The accessibility of the platform permits maintenance to be carried out almost continually year-round and thus ensures a high availability of machinery

In summary, from the work carried out in this thesis, it can be concluded that the design of hybrid wind-wave energy devices is a difficult task, most notably due to the motion constraints for the RNA. The design process for WECs as outlined in Chapter 3 is still in development and has not yet matured to a state where it may be considered a well defined process. This may indeed be due to the diverse cross-section of WECs in development and a single, well documented and sufficiently detailed process cannot be achieved unless convergence in WEC design occurs. With this in mind, the individual design methods developed in this thesis are of merit in

their own right and may be adapted to suit different design processes which may suit different devices. This in fact has been done in this thesis as the design process for the WEC in Chapter 3 has been adapted to form the development process for the OWC Array hybrid device but include a further assessment method for a design parameter of specific interest for the wind turbine, the accelerations at the RNA. This essentially reflects the current state of the art in device design as the methods employed vary substantially yet the high level themes of the methods applied are similar across all devices. This thesis has clarified the design process appropriate for Stage 1 (TRL 1-3) concept development for WECs, WTGs and wind-wave hybrid devices and, two devices, a floating BBDB WEC and the OWC Array wind-wave hybrid have been preliminarily designed. As a result, this thesis has made a substantial contribution to both streamlining early stage concept development processes and, through the OWC Array hybrid device, developed a technically feasible device for further consideration which can provide a cheaper alternative to fixed, nearshore offshore wind farms in the longer term.

## 7.2   Recommendations for Further Work

The recommendations for further work are listed below and are derived from the technical work carried out throughout this thesis.

- Chapter 3 outlined a design methodology for a particular WEC type. This methodology should be extended to other WEC types such that a common approach may be converged upon.
- The use of the suggested accessibility/maintainability parameter, the MII index, should be improved through time domain simulations of the instantaneous position of the machinery location relative to the device COG.
- The fabrication costs model should be coupled to the preliminary steel design code to determine the optimum hull mass and steel member type using the minimum hull costs as the reference rather than minimum total mass.
- NS steel was used for the design in this thesis. In design codes currently, there is very little benefit in using high strength steels (HS) or extra high strength steels (EHS) in fatigue limited designs such as WECs. The material properties of these steels need further analysis in fatigue performance. Use of HS or EHS steels may make lighter devices possible.
- A full LCCA model should be carried out on the BBDB devices designed for each Irish location and an optimum location determined.
- Furthermore, this device should be redesigned for the high energy location to include a semi-taut mooring system for mode suppression in pitch and heave and promote surge both for energy absorption and accessibility/maintainability reasons.
- Chapter 4 outlined a number of hybrid wind-wave concepts which could be further analysed using similar methods applied in this thesis to determine if they can also be competitive and/or suitable for specific resource types (low, medium or high).

- Chapter 5 applied the design methodology described in Chapter 3 to the OWC Array hybrid concept. Due to the significant number of degrees of freedom of the platform and WECs, time domain modelling has proved very difficult to implement. Further work is required in developing a time domain code for this concept, coupling both WECs and WTG(s).

- The use of RC in a dynamic marine environment in fatigue limited designs such as WECs requires substantial further analysis. The ability to dramatically reduce costs of a large platform has been demonstrated, yet its performance in these conditions is not well known.

- Mooring systems for very large floating structures need further work as the current design is just within the oil and gas industry limits of manufacture and installation due to the large loads in the lines. If WECs do continue to grow in size and mass, mooring systems will become a critical aspect of design.

- Motion characteristics of floating wind turbines require further work. While it seems that higher accelerations at the RNA are possible (reported to be ~3-4m/s$^2$), the ability to access/maintain the drivetrain by technicians in these conditions is not as straightforward as originally thought as illustrated by the MII index analysis

- The LCCA model as developed in Chapter 6 for the OWC Array farm has demonstrated its ability to be a very useful design tool for O&M strategies and identifying the required level of accessibility/maintainability/reliability at a specific site to achieve high availability of machinery. Further work is required in developing this code for more accurate representation of weather window statistics for a site, the incorporation of PM strategy code and better representation of costs incurred by O&M operations.

# 8 Bibliography

[1] EWEA, "EU Energy Policy to 2050 - Achieving 80-95% Emissions Reductions," European Wind Energy Association, 2011.

[2] EWEA, "The European Offshore Wind Industry - Key 2011 Trends and Statistics," European Wind Energy Association, 2012.

[3] M. Rowe, "Greener Ideal," 2012. [Online]. Available: http://www.greenerideal.com/alternative-energy/1029-worlds-largest-offshore-wind-farm-now-generating-power/. [Accessed 22 February 2014].

[4] "Wind Energy - The Facts," 2009. [Online]. Available: http://www.wind-energy-the-facts.org/en/part-i-technology/chapter-3-wind-turbine-technology/evolution-of-commercial-wind-turbine-technology/growth-of-wind-turbine-size.html. [Accessed 25 February 2014].

[5] A. Czyzewski, "The Engineer," 2012. [Online]. Available: http://www.theengineer.co.uk/in-depth/the-big-story/wind-energy-gets-serial/1012449.article. [Accessed 25 February 2014].

[6] "World Maritime News," 2011. [Online]. Available: http://worldmaritimenews.com/archives/41101. [Accessed 25 February 2014].

[7] D. Thorpe, "GT Global Trader," [Online]. Available: http://www.gtglobaltrader.com/news/britain-and-us-collaborate-floating-wind-turbines. [Accessed 25 February 2014].

[8] R. Green and N. Vasilakos, "The Economics of Offshore Wind," Birmingham, 2009.

[9] J. Slatte and M. Ebbesen, "The Crown Estate," 21 December 2012. [Online]. Available: http://www.thecrownestate.co.uk/media/428739/uk-floating-offshore-wind-power-report.pdf. [Accessed 28 February 2014].

[10] Aqua-RET, "Aqua-RET," 2013. [Online]. Available: http://www.aquaret.com. [Accessed 2013].

[11] DONG, "DONG Energy," 2014. [Online]. Available: http://www.dongenergy.com. [Accessed 21 February 2014].

[12] EWEA, "Oceans of Opportunity - Harnessing Europe's Largest Domestic Energy Resource," European Wind Energy Association, 2009.

[13]  Equimar, "Equimar," 2013. [Online]. Available: http://www.equimar.org/. [Accessed 2013].

[14]  B. Holmes and K. Nielsen, "Guidelines for the Development and Testing of Wave Energy Systems," OES-IA Annex II Task 2.1, 2010.

[15]  J. P. Kofoed, P. Frigaard and L. B. Hernandez, "Development of Wave Energy Devices - Past, Present and Future: The Danish Case," St. Johns, 2008.

[16]  L. Quesnel, J. Rabe, M. Brommundt and F. Vorpahl, "State of the art of design tools and standards for offshore renewable energy conversion systems," Report 3.4, EU FP7 Orecca Project, 2011.

[17]  A. Babarit and J. Hals, "On the maximum and actual capture width ratios of wave energy converters," Southampton, 2011.

[18]  M. F. Lopes, "Experimental Development of Wave Energy Converters," Universidade Technica De Lisboa Instituto Superior Technico, Lisbon, 2011.

[19]  W. Sheng and B. Flannery, "Experimental Investigation of a Cylindrical OWC, Part I: Floating OWC," Rio de Janeiro, 2012.

[20]  R. P. Gomes, J. C. Henrique, L. M. Gato and A. F. Falcao, "Testing of a small scale OWC model in a wave flume," Dublin, 2012.

[21]  M. Leybourne, W. Batten, A. S. Bahaj, N. Minns and J. O'Nians, "Experimental and Computational Modelling of the OWEL Wave Energy Converter," Dublin, 2012.

[22]  C. H. Lee, J. N. Newman and F. G. Nielsen, "Wave Interaction with an Oscillating Water Column," Los Angeles, 1996.

[23]  A. Brito-Melo and A. J. Sarmento, "Numerical modelling of OWC wave power plants of the oscillating water column type," in *Boundary Elements XXIV*, C. A. Brebbia, A. Tadeu and V. Popov, Eds., Southampton, WIT Press, 2002, pp. 25-34.

[24]  Y. Delaure and A. W. Lewis, "3D Hydrodynamic Modelling of Fixed Oscillating Water Column Wave Power Plant by a Boundary Element Method," *Ocean Engineering,* vol. 30, pp. 309-330, 2003.

[25]  W. Sheng, A. W. Lewis and R. Alcorn, "Numerical Investigation into the Hydrodynamics of Moored Floating Wave Energy Converters," Southampton, 2011.

[26] W. Sheng, A. Lewis and R. Alcorn, "Numerical Studies of a Floating Cylindrical OWC WEC," Rio de Janeiro, 2012.

[27] U. Senturk and A. Ozdamar, "Modelling the Interaction between Water Waves and the Oscillating Water Column Wave Energy Device," *Mathematical and Computational Applications,* vol. 16, no. 3, pp. 630-640, 2011.

[28] A. Lewis, T. Gilbaud and B. Holmes, "Modelling the backward bent duct device B2D2 - a comparison between physical and numerical models," Cork, 2003.

[29] J. M. Forestier, B. Holmes, S. Barret and A. Lewis, "Value and validation of small scale testing of floating wave energy converters," Porto, 2007.

[30] A. Kurniawan, J. Hals and T. Moan, "Modelling and Simulation of a Floating Oscillating Water Column," Rotterdam, 2011.

[31] A. Babarit, J. Hals, M. J. Muliawan, A. Kurniawan, T. Moan and J. Krokstad, "Numerical benchmarking studies of a selection of wave energy converters," *Renewable Energy,* vol. 41, pp. 44-63, 2012.

[32] G. de Backer, "Hydrodynamic Design Optimisation of Wave Energy Converters Consisting of Heaving Point Absorbers," Ghent University, Ghent, 2009.

[33] K. Rhinefrank, A. Schacher, J. Prudell, J. Cruz, N. Jorge, C. Stillinger, D. Naviaux, T. Brekken, A. von Jouanne, D. Newborn, S. Yim and D. Cox, "Numerical and Experimental Analysis of a Novel Wave Energy Converter," Shanghai, 2011.

[34] C. Villegas and H. van der Schaaf, "Implementation of a Pitch Stability Control for a Wave Energy Converter," EU FP7 Standpoint, 2012.

[35] A. H. Clément, "Using differential properties of the green function in seakeeping codes," *Proceedings of the 7th International Conference in Numerical Ship Hydrodynamics,* vol. 6, no. 5, pp. 1-15, 1999.

[36] A. Wacher and K. Nielsen, "Mathematical and Numerical Modelling of the AquaBuOY Wave Energy Converter," *Mathematics-In-Industry Case Studies,* vol. 2, pp. 16-33, 2010.

[37] A. Babarit, A. Clement, J. Reur and C. Tartivel, "SEAREV: A Fully Integrated Wave Energy Converter," Ecole Central de Nantes, Nantes, 2005.

[38] G. Delhommeau, P. Ferrant and M. Guilbaud, "Calculation and measurement

of forces on high speed vehicle in forced pitch and heave," *Applied Ocean Research,* vol. 14, no. 2, pp. 119-126, 1992.

[39]   K. Ruehl, "Time Domain Modelling of Heaving Point Absorber Wave Energy Converters, including Mooring and Power Take-Off," Oregon State University , Oregon, 2011.

[40]   M. Bhinder, C. G. Mingham, D. M. Causon, M. T. Rahmati, G. A. Aggidis and R. V. Chaplin, "Numerical and Experimental Modelling of a Surging Point Absorber Wave Energy Converter," Uppsala, 2009.

[41]   R. Yemm, D. Pizer, C. Retzler and R. Henderson, "Pelamis: experience from concept to connection," *Philosophical Transactions of the Royal Society A,* vol. 370, no. 1959, pp. 365-380, 2012.

[42]   M. Presivic, R. Bedard and G. Hagerman, "E2I EPRI Assessment - Offshore Wave Energy Conversion Devices," Electricity Innovation Institute, 2004.

[43]   R. P. McCabe, "Wave powered prime mover". United States of America Patent US5132550, 1992.

[44]   T. W. Thorpe, "A Brief Review of Wave Energy," UK Department of Trade and Industry ETSU-R120, Oxfordshire, 1999.

[45]   CRSES, "Centre for Renewable and Sustainable Energy Solutions," 5 October 2011. [Online]. Available: http://www.crses.sun.ac.za/files/technologies/ocean/WaveEnergyConvertors.pdf. [Accessed 28 February 2014].

[46]   M. McCormick, Ocean Engineering Mechanics with Applications, Cambridge University Press, 2009.

[47]   J. F. Chozas, M. Kramer, H. C. Sorensen and J. P. Kofoed, "Combined Production of a Full Scale Wave Energy Converter and a Full Scale Wind Turbine: a real case study," Dublin, 2012a.

[48]   K. Schlemmer, F. Fuchschumer, N. Bohmer, R. Costello and C. Villegas, "Design and Control of a Hydraulic Power Take Off for an Axi-symmetric Heaving Point Absorber," EU FP7 Standpoint, 2012.

[49]   F. Sharkey, "Engineers Ireland," 25 February 2012. [Online]. Available: https://www.engineersireland.ie/EngineersIreland/media/SiteMedia/groups/regions/midlands/Ocean-Energy-in-Ireland-Presentation-25-02-2013-Midland-Region-slides.pdf?ext=.pdf. [Accessed 26 February 2014].

[50] B. Cahill and A. Lewis, "Resource Variability and Extreme Wave Conditions at the Atlantic Marine Energy Test Site," Dublin, 2012.

[51] J. Lavelle and J. P. Kofoed, "Experimental Testing of the Langlee Wave Energy Converter," Southampton, 2011.

[52] B. Borgarino, J. P. Kofoed and J. Tedd, "Experimental Investigation for the Wave Dragon - effects of the reflectors and their attachements," Aalborg University, Aalborg, 2007.

[53] J. Tedd, "Testing, Analysis and Control of Wave Dragon, Wave Energy Converter," Aalborg University, Aalborg, 2007.

[54] H. Fernandez, G. Iglesias, R. Carballo, A. Castro, M. Sanchez and F. Taveiro-Pinto, "Optimisation of the WaveCat Wave Energy Converter," *Coastal Engineering,* 2012.

[55] L. Victor, P. Troch and J. P. Kofoed, "Prediction of individual wave overtopping volumes of a wave energy converter using experimental testing and first numerical model results," Uppsala, 2009.

[56] G. Iglesias, H. Fernandez, R. Corballo, A. Castro and F. Taveiro-Pinto, "The WaveCat - Development of a New Wave Energy Converter," Linkoping, 2011.

[57] E. Friis-Madsen, "Plant for extraction of wind/wave energy at open sea". Denmark Patent PR173018, 1999a.

[58] E. Friis-Madsen, "Offshore wind/wave energy converter". Europe Patent 95 923 202.6 2315, 1999b.

[59] J. P. Kofoed, P. Frigaard, H. C. Sorensen and E. Friis-Madsen, "Development of the wave energy converter - Wave Dragon," Seattle, 2000.

[60] D. Roddier, C. Cermelli, A. Aubault and A. Weinstein, "WindFloat: A floating foundation for offshore wind turbines," *Journal of Renewable and Sustainable Energy,* vol. 2, pp. 1-34, 2010.

[61] H. R. Martin, "Development of a Scale Model Wind Turbine for Testing of Offshore Floating Wind Turbines," University of Maine, Maine, 2011.

[62] J. M. Jonkman, "Dynamics Modeling and Loads Analysis of an Offshore Floating Wind Turbine," National Renewable Energy Laboratory (NREL), Colorado, 2007.

[63]     J. M. Jonkman, "Dynamics of Floating Offshore Wind Turbines - Model Development and Verification," *Wind Energy,* vol. 12, pp. 459-492, 2009.

[64]     S. Shim and M. H. Kim, "Rotor-Floater-Tether Coupled Dynamic Analysis of Offshore Floating Wind Turbines," Vancouver, 2008.

[65]     C. Cermelli, D. Roddier and A. Aubault, "WindFloat: A floating foundation for offshore wind turbines Part II: Hydrodynamic Analysis," Honolulu, 2009.

[66]     I. Fylling, K. Mo, K. Merz and N. Luxcey, "Floating wind turbine - response from a rigid body model," 2009.

[67]     F. G. Nielsen, T. D. Hansen and B. Skaare, "Integrated Dynamic Analysis of Floating Offshore Wind Turbines," Hamburg, 2006.

[68]     B. Skaare, T. D. Hansen, F. G. Nielsen, R. Yttervik, A. M. Hansen, K. Thomsen and T. J. Larsen, "Dynamics of Floating Wind Turbines Utilising Integrated Hydrodynamic and Aerodynamic Analysis," Milan, 2007.

[69]     T. J. Larsen and T. D. Hansen, "A method to avoid negative damped low frequent tower vibrations for a floating, pitch controlled wind turbine," 2007.

[70]     A. Cordle and J. M. Jonkman, "State of the Art in Floating Wind Turbine Design Tools," Maui, 2011.

[71]     C. M. Wang, T. Utsunomiya, S. C. Wee and Y. S. Choo, "Research on floating wind turbines: a literature survey," *The IES Journal Part A: Civil and Structural Engineering,* vol. 3, no. 4, pp. 267-277, 2010.

[72]     Y. Feng, P. J. Tavner and H. Long, "Early experiences with UK round 1 offshore wind farms," *Proceedings of the Institution of Civil Engineers,* vol. Energy 163, no. EN0, pp. 1-15, 2010.

[73]     C. Cermelli and D. Roddier, "Experimental and numerical investigations into the stabilising effects of a water entrapment plate on a deepwater minimal floating platform," Halkidi, 2005.

[74]     H. Bagbanci, "Dynamic Analysis of Offshore Floating Wind Turbines," Instituto Superior Technico, Lisbon, 2011.

[75]     ABS, "Floating Wind Turbines," American Bureau of Shipping, Houston, 2012.

[76]     C. Morris, "Experimentation," 2013. [Online]. Available: http://www.experimentation-online.co.uk/. [Accessed 13 August 2014].

[77] D. Sveen, "Anchoring arrangment for floating wind turbine installations". Europe Patent EP1881927 B1, 2013.

[78] B. S. Kallesoe, "Aero-Hydro-Elastic Simulation Platform for Wave Energy Systems and Floating Wind Turbines," Risoe DTU, Roskilde, 2011.

[79] N. I. Meyer, M. McDonald Arnskov, L. C. Vad Bennetzen, H. F. Burchart, J. Bunger, V. Jacobsen, P. Maegaard, S. Vindelov, K. Nielsen and J. N. Sorensen, "Blogekraftprogram: Afsluttende rapport fra Energistyrelsens Radgvinde Bolgekraftudvalg," Bolgekraftudvalgets Sekretariat, Ramboll, Virum, 2002.

[80] OWWE, "Offshore Wind and Wave Energy," 2014. [Online]. Available: http://www.owwe.net/?o=home. [Accessed 02 March 2014].

[81] S. Salter, "Wave power," *Nature,* vol. 249, pp. 720-724, 1974.

[82] R. Yemm, R. Henderson and C. Taylor, "The PWP Pelamis WEC: Current status and onward programme," Aalborg, Denmark, 2000.

[83] H. Eidsmoen, "On the theory and simulation of heaving-buoy wave-energy converters with control," PhD Thesis, NTH, Trondheim, Norway, 1995.

[84] T. Bjarte-Larsson and J. Falnes, "Laboratory experiment on heaving body with hydraulic power take-off and latching control," *Ocean Engineering,* vol. 33, pp. 847-877, 2006.

[85] A. F. d. O. Falcáo, "Modelling and control of oscillating-body wave energy converters with hydraulic power take-off and gas accumulator," *Ocean Engineering,* vol. 34, pp. 2021-2032, 2007.

[86] A. F. d. O. Falcáo, "Phase control through load control of oscillating-body wave energy converters with hydraulic PTO system," *Ocean Engineering,* vol. 35, pp. 358-366, 2008.

[87] L. Yang, J. Hals and T. Moan, "Analysis of dynamic effects relevent for the wear damage in hydraulic machines for wave energy conversion," *Ocean Engineering,* vol. 37, no. 13, pp. 1089-1012, 2010.

[88] L. Yang and T. Moan, "Dynamic analysis of wave energy converter by incorporating the effect of hydraulic transmission lines," *Ocean Enegineering,* vol. 38, no. 16, pp. 1849-1860, 2011.

[89] A. A. Wells, "Fluid driven rotary transducer". Britain Patent 1595700, 1976.

[90] T. W. Kim, K. Kaneko, T. Setoguchi and M. Inoue, "Aerodynamic performance of an impulse turbine with guide vanes for wave power generator," 1988.

[91] S. Raghunathan, "A methodology for Wells turbine design for wave energy conversion," *Journal of Power Energy IMechE,* no. 209, pp. 221-232, 1995.

[92] T. Setoguchi, M. Takao and K. Kaneko, "Hysteresis on Wells turbine characteristics in reciprocating flow," *International Journal of Rotating Machinery,* vol. 4, no. 1, pp. 17-24, 1998.

[93] T. J. Whittaker, W. C. Beattie, S. Raghunathan, A. Thompson, T. Stewart and R. Curran, "The Islay Wave Power Project: an engineering perspective," *Institute Civil Engineering - Water Maritime and Energy,* vol. 124, no. 3, pp. 189-201, 1997a.

[94] T. J. Whittaker, A. Thompson, R. Curran and T. Stewart, "Europoean Wave Energy Pilot Plant on Islay (UK)," European Commission, Directorate General VII, Science, Research and Development - Joint Research Centre, JOU-CT94-0267, 1997b.

[95] T. Setoguchi, S. Santhakumar, H. Maeda, M. Takao and K. Kaneko, "A review of impulse turbines for wave energy conversion," *Renewable Energy,* vol. 23, pp. 261-292, 2001.

[96] W. Knapp, "Water turbines for Overtopping Wave Energy Converters," CA-OE, Workshop on Component Technology and Power Take-Off, Uppsala, Sweden, 2005.

[97] W. Knapp, E. Holmén and R. Schilling, "Considerations for Water Turbines to be used in Wave Energy Converters," 2000.

[98] M. A. Mueller, "Electrical generators for direct drive wave energy converters," *IEE Proceedings Generation Transmission Distribution,* vol. 149, no. 4, pp. 446-456, 2002.

[99] M. Leijon, O. Danielsson, M. Eriksson, K. Thorburn, H. Bernhoff, J. Isberg, J. Sundberg, I. Ivanova, E. Sjostedt, O. Agren, K. E. Karlsson and A. Wolfbrandt, "An electrical approach to wave energy conversion," *Renewable Energy,* vol. 31, no. 9, pp. 1309-1319, 2006.

[100] M. G. Prado, F. Gardner, M. Damen and H. Polinder, "Modelling and test results of the archimedes wave swing," *Journal of Power Energy,* vol. 220, pp. 855-868, 2006.

[101] J. Cruz, Ocean wave energy, Berlin: Springer, 2008.

[102] W. Coulbourne, C. P. Jones, O. Kapur, V. Koumoudis, P. Line, D. K. Low, G. Overcash, S. Passman, A. Reeder, L. Seitz, T. Smith and S. Tezak, "Coastal Construction Manual: Principles and Practices of Planning, Siting, Designing, Constructing, and Maintaining Residential Buildings in Coastal Areas (Fourth Edition)," August 2011. [Online]. Available: http://lplonline.org/wp-content/uploads/2013/08/Coastal-Construction-Manual_vol-2_4th-Edition.pdf. [Accessed 02 March 2014].

[103] DNV, "Hull Structural Design: Ships with Length 100m and Above - Part 3 Chapter 1," Det Norsk Veritas (DNV), Oslo, 2003.

[104] A. Pecher, J. P. Kofoed and T. Larsen, "Design Specifications for the Hanstholm WEPTOS Wave Energy Converter," *Energies,* vol. 5, pp. 1001-1017, 2012a.

[105] A. Percher, J. P. Kofoed, T. Larsen and T. Marchalot, "Experimental Study of the WEPTOS Wave Energy Converter," Rio de Janeiro, 2012b.

[106] DNV, "DNV-RP-H103: Modelling and Analysis of Marine Operations," Det Norsk Veritas (DNV), Oslo, 2011a.

[107] B. Hamedni, C. Mathieu and C. Bittencourt Ferreira, "Generic WEC System Breakdown," SDWED, 2014.

[108] B. Hamedni and C. Bittencourt Ferreira, "Generic WEC Risk Ranking and Failure Mode Analysis," SDWED, 2014.

[109] T. Thorpe, "An Review of Wave Energy," UK Department of Trade and Industry ETSU Vol. 1 & 2, Oxfordshire, 1992.

[110] Atkins, "A parametric costing model for wave energy technology," UK Department of Trade and Industry ETSU-wv-1685, 1992.

[111] G. Dalton, R. Alcorn and T. Lewis, "Case study feasibility analysis of the Pelamis wave energy converter in Ireland, Portugal and North America," *Renewable Energy,* vol. 35, pp. 443-455, 2009.

[112] A. Raventos , A. Sarmento, F. Neumann and N. Matos, "Projected deployment and costs of wave energy in Europe," Bilbao, 2010.

[113] J. Fernandez-Chozas, J. P. Kofoed and N. E. Helstrup Jensen, "An Open-Access COE Calculation tool for Wave Energy Converters - the Danish approach," in *European Wave and Tidal Energy Conference (EWTEC),*

Aalborg, 2013.

[114] K. O' Sullivan and J. Murphy, "Deterministic Economic Model for Wind-Wave Hybrid Energy Conversion Systems," Dublin, 2012.

[115] 4COffshore, "4C Offshore," 2014. [Online]. Available: http://www.4coffshore.com. [Accessed 02 March 2014].

[116] L. W. Rademakers, H. Braam, T. S. Obdam, P. Frohbose and N. Kruse, "Tools for estimating operating and maintenance costs of offshore wind farms: state of the art," Brussels, 2008.

[117] B. Teillant, R. Costello, J. Weber and J. Ringwood, "Productivity and economic assessment of of wave energy projects through operational simulations," *Renewable Energy,* vol. 48, pp. 220-230, 2012.

[118] M. St. Denis and W. J. Pierson, "On the motion of ships in confused seas," *Transactions of the Society of Naval Arcitects and Marine Engineers (SNAME),* vol. 61, no. 1, pp. 1-53, 1953.

[119] DNV, " DNV-OS-C101: Design of Offshore Steel Structures," Det Norsk Veritas (DNV), Oslo, 2011b.

[120] NORSOK, "NORSOK-004: Design of steel structures," Standards Norway, Oslo, 2004.

[121] W. E. de Vries and V. D. Krolis, "Effects of Deep Water on Monopile Support Structures for Offshore Wind Turbines," Milan, 2007.

[122] IEC, "Wind Turbines - Part 1: Design Requirements," International Electrotechnical Commission (IEC), Geneva, 2005.

[123] NORSOK, "NORSOK 003: Actions and Actions Effects," Standards Norway, Oslo, 2007.

[124] WSI, "World Steel Index," 2013. [Online]. Available: http://www.worldsteelprices.com/. [Accessed 05 November 2013].

[125] AWS, "American Welding Society," 01 May 2002. [Online]. Available: http://www.aws.org/research/HIM.pdf. [Accessed 02 March 2014].

[126] K. Shreve and A. H. Basson, "Small Volume Fabrication Cost Estimation Models for Embodiment Design," *R&D Journal,* vol. 20, pp. 1-10, 2004.

[127] DNV, "DNV-OS-C502: Offshore Concrete Structures," Det Norsk Veritas

(DNV), Oslo, 2010a.

[128] DNV, "DNV-OS-J101: Design of Offshore Wind Turbines," Det Norsk Veritas (DNV), Oslo, 2011c.

[129] M. R. Sharifi, S. Baciu and T. Zayed, "Slip form porductivity analysis for concrete silos," Calgary, 2006.

[130] H. Cozijn, R. Uittenbogaard and E. ter Brake, "Heave, Roll and Pitch Damping of a Deepwater CALM Buoy with a Skirt," Seoul, 2005.

[131] DNV, "DNV-OS-C205: Environmental Conditions and Environmental Loads," Det Norsk Veritas (DNV), Oslo, 2010b.

[132] DNV, "DNV-OS-C201: Structural Design of Offshore Units (Working Stress Design)," Det Norsk Veritas (DNV), Oslo, 2011d.

[133] L. O. Garza-Rios, M. M. Bernitsas and K. Nishimoto, "Catenary Mooring Lines with Non-Linear Drag and Touchdown," University of Michigan, Michigan, 1997.

[134] Orcaflex, "Orcina," 2013. [Online]. Available: http://www.orcina.com/. [Accessed 03 March 2014].

[135] Vryhof, "Vryhof," November 2010. [Online]. Available: http://www.vryhof.com/. [Accessed 03 March 2014].

[136] T. A. Nygaard, A. Myhr and K. J. Maus, "A comparison of two conceptual designs for floating wind turbines," Stockholm, 2009.

[137] MI, "Marine Institute," 2012. [Online]. Available: http://data.marine.ie/. [Accessed 03 March 2014].

[138] MET, "Met Eireann," 2014. [Online]. Available: http://www.met.ie/. [Accessed 03 March 2014].

[139] Y. Masuda, T. Kuboki, A. Thakker, T. Lewis, X. Liang and P. Sun, "Prospect of Economical Wave Power Electric Generator by the Terminator Backward Bent Duct Buoy (BBDB)," Kitakyushu, 2002.

[140] W. Sheng, R. Alcorn and A. Lewis, "Numerical Studies on Hydrodynamics of a Floating Oscillating Water Column," Netherlands, 2011.

[141] PhysE Limited, "Wave mapping in UK waters," UK Health and Safety Executive, 2008.

[142] P. J. Tavner, C. Edwards, A. Brinkman and F. Spinato, "Influence of wind speed on wind turbine reliability," *Wind Engineering,* vol. 30, no. 1, 2006.

[143] P. J. Tavner, R. Gindele, S. Faulstich, B. Hahn, M. W. Whittle and D. M. Greenwood, "Study of Effects of Weather and Location on Wind Turbine Failure Rates," Brussels, 2010.

[144] S. Faulstich, P. Lyding and P. Tavner, "Influence of wind speed on wind turbine reliability," Brussels, 2011.

[145] G. J. van Bussel and W. A. Bierbooms, "The DOWEC offshore reference wind farm: analysis of transportation for operation and maintenance," *Wind Engineering,* vol. 27, no. 5, pp. 381-392, 2003.

[146] T. Dobie, "The Importance of the Human Element in Ship Design," University of New Orleans, New Orleans, 2000.

[147] J. Colwell, "Human factors in the naval environment: a review of motion sickness and biodynamic problems," Canada National Defence, 1989.

[148] S. C. Stevens and M. G. Parsons, "Effects of Motion at Sea on Crew Performance: A Survey," *Marine Technology,* vol. 39, no. 1, pp. 29-47, 2002.

[149] J. H. Pattinson and D. J. Sheridan, "Human performance factors and measures in hull form selection," Prague, 2004.

[150] P. Crossland and K. Rich, "Validating a model of the effects of ship motion on postural stability," UK Defense Evaluation and Research Agency, Gosport, 2000.

[151] NATO, "Common procedures for seakeeping in the ship design process - Chapter 7: seakeeping criteria for general application," NATO STANAG 4154, 1997.

[152] BV, "Rules for the classification of naval ships," Bureau Veritas (BV), Paris, 2011.

[153] M. O' Conner and G. Dalton, "Weather windows for operation and maintenance," *Renewable Energy,* vol. 52, no. 4, pp. 57-66, 2012.

[154] R. T. Walker, J. Johanning and R. Parkinson, "Weather windows for device deployment at UK sites: availability and cost implications," Southampton, 2011.

[155] EC, "European Commission," 01 June 2011. [Online]. Available: http://ec.europa.eu/energy/observatory/countries/doc/key_figures.pdf.

[Accessed 10 March 2014].

[156] L. Cradden, H. Mouslim, O. Duperray and D. Ingram, "Joint Exploitation of Wave and Offshore Wind Power," Southampton, 2011.

[157] C. P. Collazo, M. M. Jakobsen, H. Buckland and J. F. Chozas, "Synergies for a Wind-Wave Energy Concept," Vienna, 2013.

[158] L. Marquis, M. M. Kramer, J. Kringelum, J. F. Chozas and N. E. Helstrup, "Introduction of the Wavestar Wave Energy Converter at the Danish Offshore Wind Power Plant Horns Rev 2," Dublin, 2012.

[159] A. Azzellino, F. Ferrante, J. P. Kofoed, C. Lanfredi and D. Vicinanza, "Optimal Siting of Offshore Wind Power Combined with Wave Power Through a Marine Spatial Planning Approach," *International Journal of Marine Energy,* 2013.

[160] F. Fusco, G. Nolan and J. Ringwood, "Variability reduction through optimal combination of wind/wave resources - An Irish Case Study," *Energy,* vol. 35, pp. 314-325, 2010.

[161] J. F. Chozas, H. C. Sorensen and N. E. Helstrup Jensen, "Economic Benefit of Combining Wave and Wind Power Productions in Day Ahead Electricity Markets," Dublin, 2012b.

[162] E. Stoutenburg, N. Jenkins and M. Z. Jacobsen, "Power output variations of co-located offshore wind turbines and wave energy converters in California," *Renewable Energy,* no. 2781-2791, p. 35, 2010a.

[163] E. Stoutenburg and M. Z. Jacobsen, "Optimising Offshore Transmission Links for Marine Renewable Energy Farms," OCEANS 2010, 2010b.

[164] Y. Masuda, "Experimental full-scale results of wave power machine Kaimei in 1978," Gotenburg, 1979.

[165] E. Hoogendoorn, "Seasteading Engineering Report - Part 1: Assumptions and Methodology," Seasteading Institute, 2011.

[166] M. Yunovich, N. Thompson, T. Balvanyos and L. Lave, "Highway Bridges Appendix D".

[167] BSSA, "The Use of Stainless Steel Reinforcement in Bridges," British Stainless Steel Association, 2003.

[168] E. Wayman, P. Sclaounos, S. Butterfield, J. Jonkman and W. Musial,

"Coupled Dynamic Modelling of Floating Wind Turbines," Texas, 2006.

[169] R. Harris, L. Johanning and J. Wolfram, "Mooring Systems for Wave Energy Converters: A review of design issues and choices," International Conference on Marine Renewable Energy, Blyth, 2004.

[170] S. Lundberg, "Performance comparison of wind park configurations," Chalmers University of Technology, Sweden, 2003.

[171] Oxera, "Discount Rates for Low Carbon and Renewable Generation Technologies," Oxera Consulting for the Committee on Climate Change, London, 2011.

[172] G. Dalton and A. W. Lewis, "Performance and Economic Feasibility of 5 Wave Energy Devices off the West Coast of Ireland," Southampton, 2011.

[173] Leancon, "Leancon Wave Energy," 2014. [Online]. Available: http://www.leancon.com/. [Accessed 12 April 2014].

[174] P. Sclavounos, C. Tracy and S. Lee, "Floating Offshore Wind Turbines: Responses in a Seastate Pareto Optimal Designs and Economic Assessments," Massachusettes Institute of Technology (MIT), Massachusettes, 2007.

[175] B. J. Kallesoe, T. J. Larsen, U. S. Paulsen, A. Kohler, F. H. Dixen, C. B. Morch, J. Kringulum and H. F. Hansen, "Aero-hydro-elastic simulation platform for wave energy systems and floating wind turbines," Risoe DTU, 2011.

[176] Y. Zhao, J. Yang and Y. He, "Preliminary design of a multi-column TLP foundation for a 5MW offshore wind turbine," *Energies,* vol. 5, pp. 3874-3891, 2012.

[177] MCA, "MGN 427 (F): Stability Guidance for Fishing Vessels Under 15m Overall Length," [Online]. Available: Marine Guidance Note MGN 427 (F). . [Accessed 13 March 2014].

[178] S. Faulstich, B. Hahn and P. J. Tavner, "Wind turbine downtime and its importance for offshore deployment," *Wind Energy,* vol. 14, pp. 327-337, 2011.

[179] T. Moan, Z. Gao and M. Muliawan, "Modelling methodology for concept assessment," Report 4.1, EU FP7 MARINA Platform Project, 2013.

**APPENDIX A Design Process for a Wave Energy Converter Flow Diagram**
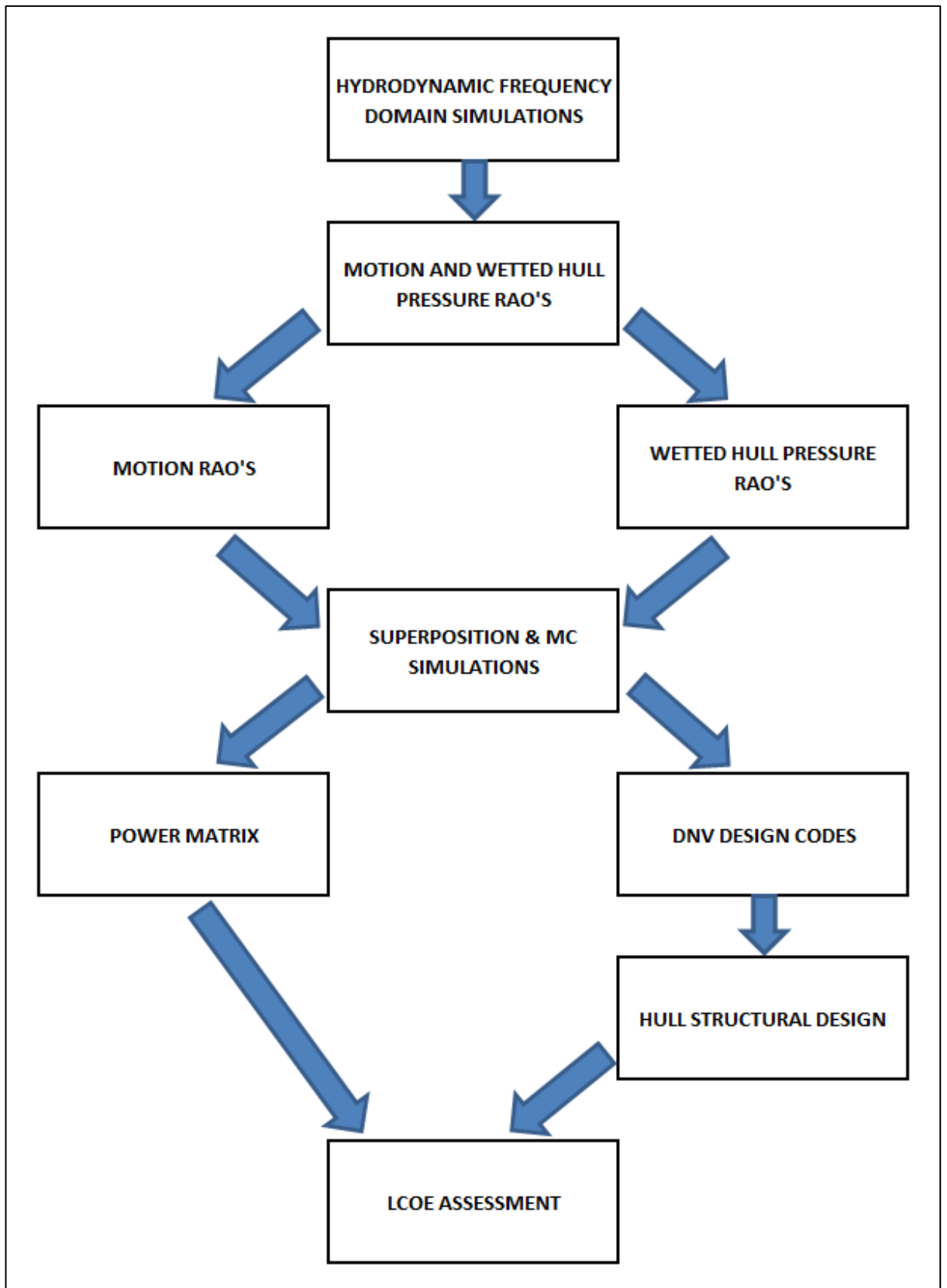
# APPENDIX B Tank Testing of the OWC Array

## B.1    Model Description

The OWC array device considered here has the very same operating principle as the OE Buoy, but has a total of 32 OWC chambers, each connected together. The overall shape of the platform is a "V" shape in plan as illustrated in Figure 4-27 and Figure B.1, pointing directly into the waves similar to the 'Leancon' [168] wave energy device. The OWC array consists of 16 OWC chambers on each leg of the platform. The total width of the device is 6.9m with an angle of 90° between each leg and is designed to be at a scale of 1:50. Initially, the developer of this device, J.J. Campbell and Associates Ltd., used two plenum chambers on each leg of the platform to gather the positive pressure and negative pressure from each chamber into a single venturi flume. Both plenum chambers were connected to each other via the venturi flume. Therefore the air flow in the device was a closed system. The positive and negative pressures from the individual OWC chambers were allowed flow into the correct plenum chamber by using standard one directional air admittance valves. However, for the testing programme carried out to characterise the OWC interactions and performance of an OWC Array on a single platform, these plenum chambers were removed and each OWC chamber was treated individually. The individual chambers were damped using simple orifice plates of varying size. Furthermore, basic Froude scaled wind turbine towers were attached to the platform to assess the modifications to the motion characteristics. The main outputs include the power matrix of the array and the fact that no measureable effect was seen on the motion characteristics from either configuration of wind turbine towers mounted on the platform as illustrated in Figure B.2 and Figure B.3.
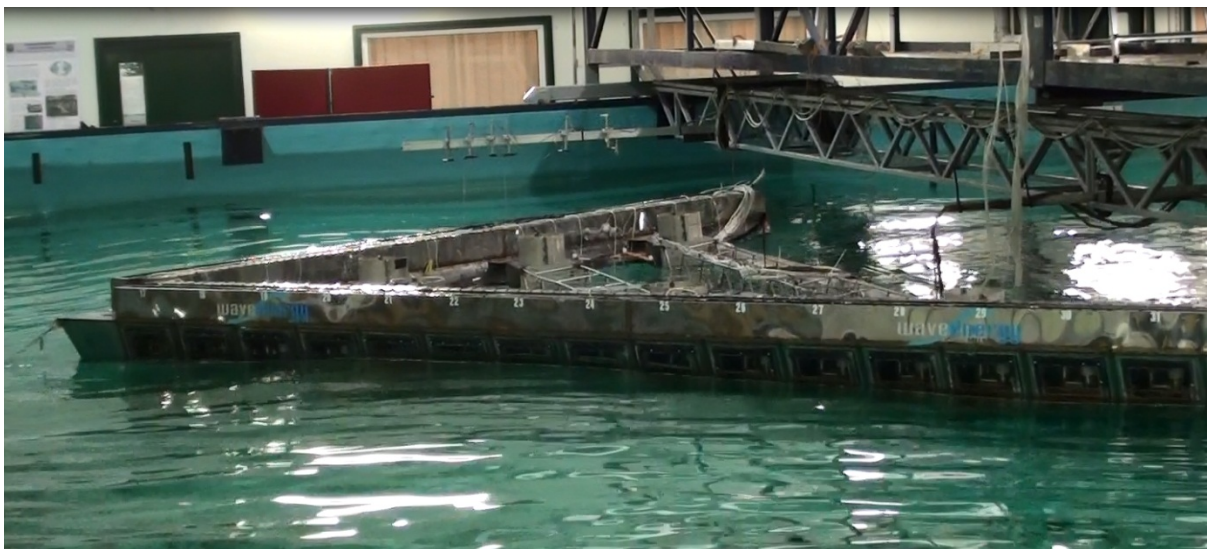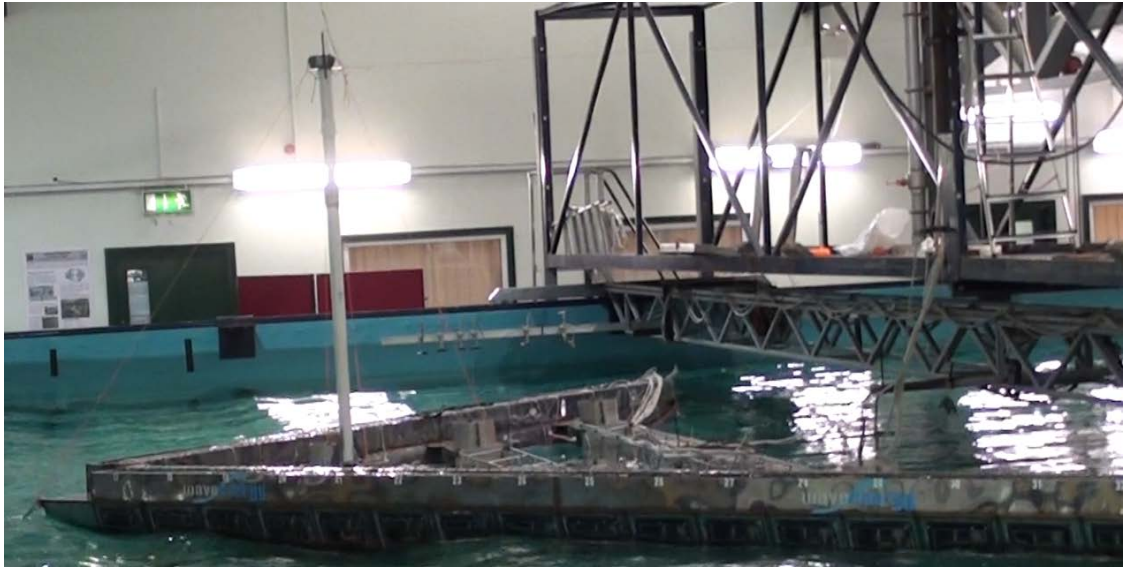


**Figure B.1: 'V' OWC Array Model**

**Figure B.2: 'V' OWC Array Model with WTG on Bow**



**Figure B.3: 'V' OWC Array Model with 2 N. WTG's on Stern**

## B.2    Testing Programme for OWC array

As this device will be a combined wind and wave energy platform, the motion characteristics of the platform are crucial for the effective operation of the wind turbine. For this reason, a number of platform arrangements were tested in the beginning to iterate to the platform arrangement with the best motion characteristics. These arrangements consisted of the redistribution of mass and buoyancy to alter the centre of gravity (COG) of the platform and the effective positions of the restoring buoyancy forces. These preliminary tests were carried out with a damping ratio of 1:59, i.e. the area of the orifice is 59 times smaller than the chamber water plane area. The various model arrangements were tested in uni-directional monochromatic waves of 60mm wave height and periods ranging from 0.71-2.26secs. Following the successful determination of the optimal platform arrangement, various levels of damping were applied to the OWC chambers, ranging from area ratio of 1:59 to

1:2714. The OWC array device was tested in uni-directional monochromatic and panchromatic wave fields for each damping ratio. The monochromatic waves included wave heights of 60, 90 and 120mm and wave periods ranging from 0.71-2.26secs. The panchromatic waves were generated from a Bretschneider wave spectrum, and were described by significant wave heights of 60 and 90mm and peak wave periods of 1.08, 1.52, 2.03, 2.5 and 2.72secs. Table outlines the various tests carried out on the WEC.

**Table B.1: Testing Programme Outline**

| Monochromatic Waves | |
|---|---|
| **Wave Heights (mm)** | 60, 90, 120 |
| **Wave Periods (s)** | 0.71, 0.85, 0.99, 1.13, 1.27, 1.41, 1.56, 1.70, 1.84, 1.98, 2.12, 2.26 |
| Panchromatic Waves | |
| **Significant Wave Heights (mm)** | 60, 90 |
| **Peak Wave Periods (s)** | 1.08, 1.52, 2.03, 2.50, 2.72 |
| **Spectral Shape** | Bretschneider |
| **Damping Ratios** | 59, 75, 109, 140, 265, 679, 2714 |

## B.3    Measuring and Sampling Equipment

Each of the 16 chambers on one leg of the device was fitted with a pressure transducer and wave probe. The pressure sensors were Honeywell S&C transducers, with a range of $\pm\sim$175mm, and measured the instantaneous air pressure inside the chamber with time. The wave probes were simple arrangements consisting of two lengths of conducting wire placed from the top of the chamber downwards below the water level in the chamber. These measured the instantaneous water level elevation in each of the 16 chambers.

## B.4    Physical Testing Results

### B.4.1    Orifice Calibration

In order to ensure accurate calculation of the absorbed power output from the OWC array device, each of the orifice plate arrangements were tested on the linear test rig at Beaufort Research - HMRC. This consists of a servo-motor driven arm connected to a piston, which is housed within a cylinder of diameter 300mm as shown in Figure B.4. The arm motion is controlled such that a known flow of air is driven through the orifice plate arrangement as shown in Figure B.5, connected to the top of the cylinder. The instantaneous pressure within the cylinder is monitored by a sensor as described. The time series of piston position and air pressure is output to a text file for analysis. The flow of air calculated from the piston position and the pressure time series using Bernoulli's equation are compared and the discharge coefficient is the non-dimensional coefficient applied to the flow rate as calculated from the pressure time series to match the flow rate calculated from the piston position. The results of

these tests are illustrated in Figure B.6. The 'DR' values refer to the damping ratio for the OWC array chambers and not the damping ratio for the linear test rig.
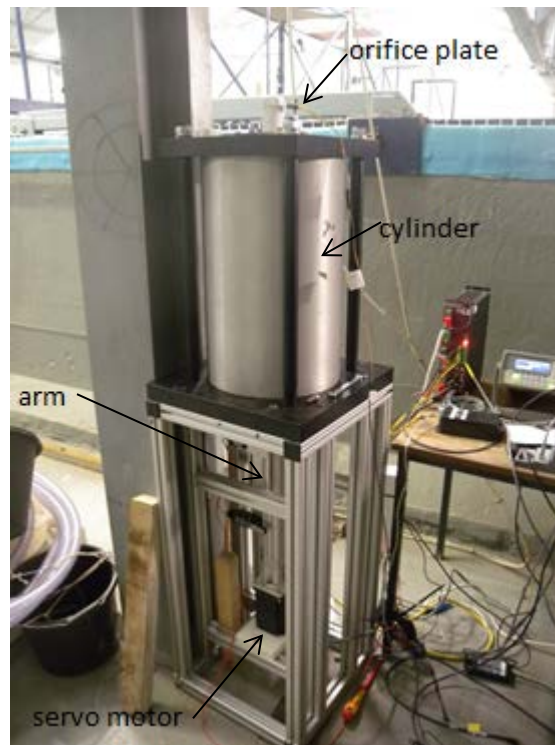


**Figure B.4: Linear Test Rig arrangement**



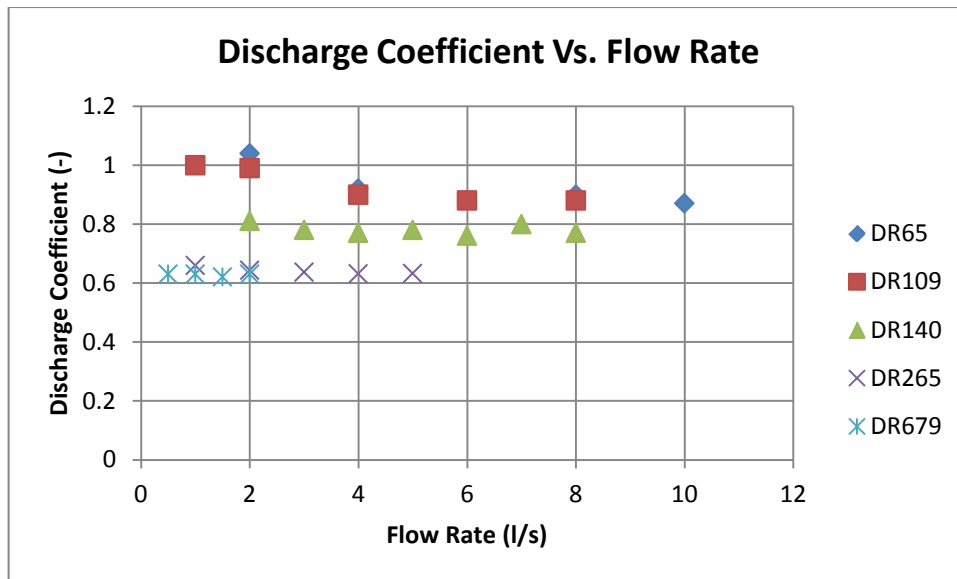**Figure B.5: Orifice Plate arrangement**

**Figure B.6: Discharge coefficient Vs. Air flow rate for each orifice plate**

Figure B.6 illustrates the relationship between discharge coefficient and air flow rate for each orifice plate arrangement. The graph shows a tendency for the discharge coefficient to reduce as the damping ratio increases and appears to reach a limit of 0.6.

**B.4.2   Motion Characteristics**

As outlined above a number of platform arrangements were tested originally, with the view to iterate to the platform arrangement with the most favourable motion characteristics for the addition of wind turbine structures. The results presented in this section are those measured for the best platform in monochromatic wave conditions.
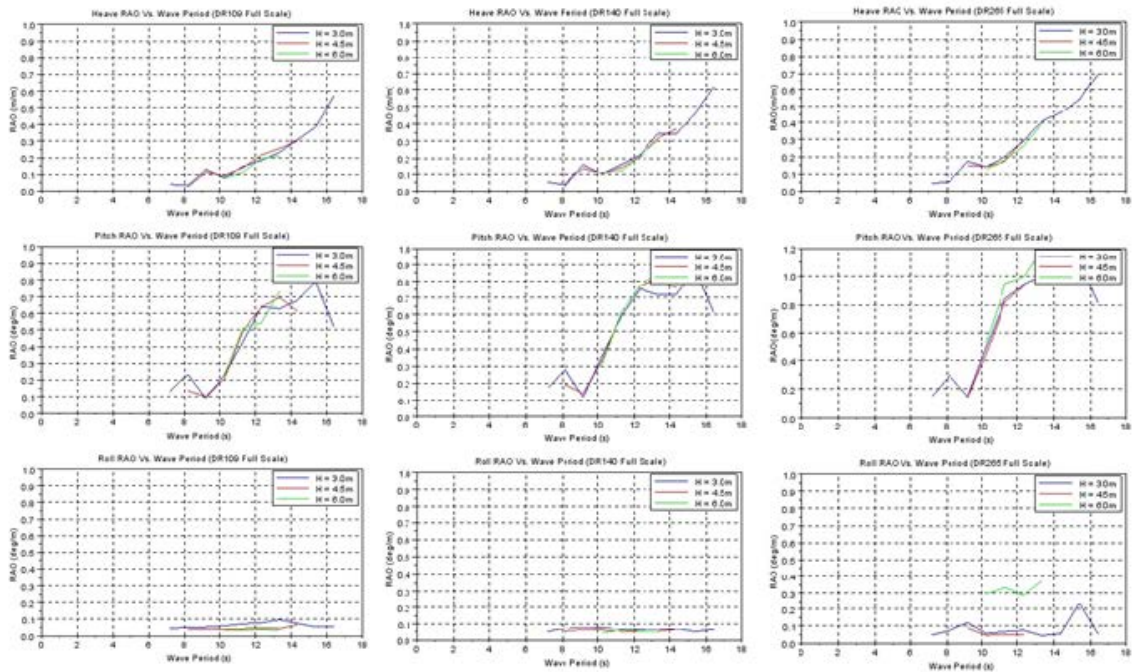
**Figure B.7: Primary motion characteristics, heave, pitch and roll, for the OWC array platform for DR109, DR140 and DR265**

The observation from Figure B.7, is that as the damping ratio increases, the motion RAOs increase for each wave period above 12s suggesting that the motions of the platform are tightly coupled to the damping applied to the platform.

After the main WEC testing was completed, a number of motion tests were carried out with Froude scaled wind turbine towers and nacelles attached to the main floating platform. These varied from a single Froude scaled 5MW turbine attached to the front of the device as illustrated in Figure B.2 and 2 No. Froude scaled 3MW turbines attached to the rear of the device at its extremities as illustrated in Figure B.3. No measureable difference in motion RAOs were obtained from either configuration on the platform.

### B.4.3   Power Output

The absorbed power from each chamber fitted with pressure sensors has been calculated using the following equations. The air velocity at the orifice is calculated from Equation B.1.

$$\frac{\rho v_1^2}{2} + p_1 = \frac{\rho v_2^2}{2} + p_2 \qquad \text{Equation B.1}$$

where $v_1$ is the velocity at the air water interface, $v_2$ is the velocity at the orifice, $P_1$ is the pressure within the chamber and $P_2$ is the pressure at the orifice. Assuming $v_1^2 \ll v_2^2$, and $P_2 = 0$, the velocity at the orifice may be simplified to Equation B.2.

$$v_2 = \sqrt{\frac{2p_1}{\rho}}$$

<div align="right">**Equation B.2**</div>

where ρ is the density of air, taken to be $1.285 \text{kg/m}^3$. The instantaneous absorbed power from each chamber may be calculated from Equation B.3.

$$P_i(t) = C_d . \sqrt{\frac{2}{\rho}} . p(t)^{\frac{3}{2}} . A_2$$

<div align="right">**Equation B.3**</div>

where $C_d$ is the relevant discharge coefficient for the orifice plate as determined from Figure B.6, $A_2$ is the orifice area and t is time. The total instantaneous absorbed power in Watts is calculated from Equation B.4.

$$P_{tot}(t) = 2 . \sum_{i=1}^{16} P_i(t)$$

<div align="right">**Equation B.4**</div>

### B.4.4 Summary Plots Monochromatic Waves

Each test run has been calculated individually and the RMS value of each total absorbed power output time series calculated. These have been plotted against each other for each wave height, period, and damping ratio for model and full scale, as well as the CWR.
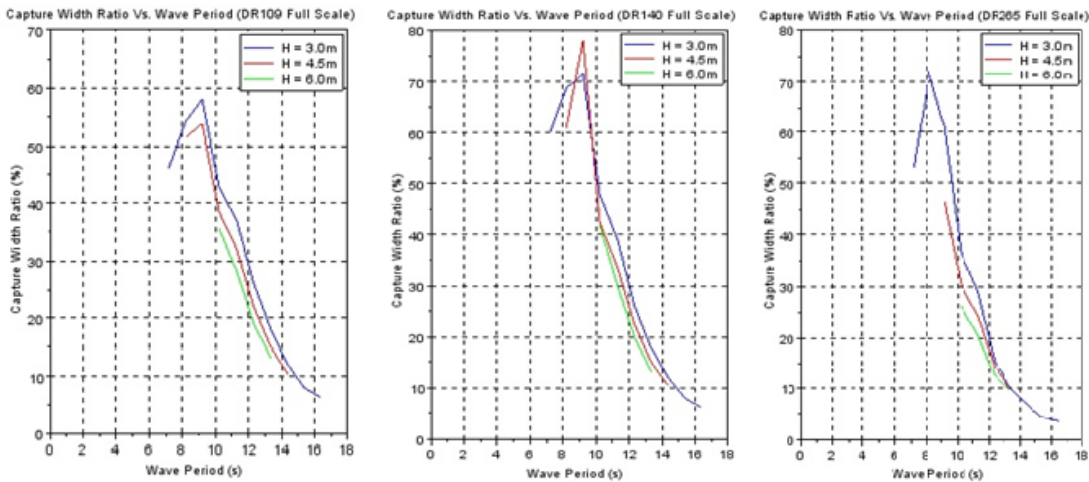


**Figure B.8: CWR Vs. Wave Period for each wave height and damping ratio DR109**

From Figure B.8, it suggests that the power absorption is a linear system, whereby there is very little, if any, dependency on wave amplitude. The damping ratio with the highest Capture Width Ratio (CWR) is DR140 with a CWR of between 70 and 80% at a wave period of 9secs.
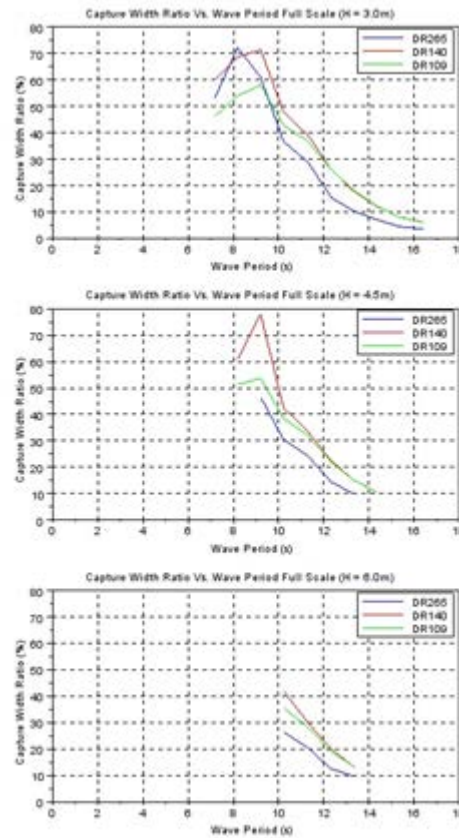
**Figure B.9: CWR Vs. Wave Period for each DR and Wave Height**

Figure B.9, at "H=60mm", shows that the CWR is very similar for both DR265 and DR140 due to the different $C_d$ values applied in the calculation of the absorbed power. For "H=4.5m" and "H=6.0m", the range of wave periods tested is reduced due to the reflections in the wave basin from the increasing wave steepness. This limits the analysis that may be performed around the resonance frequency as Figure B.9 shows.
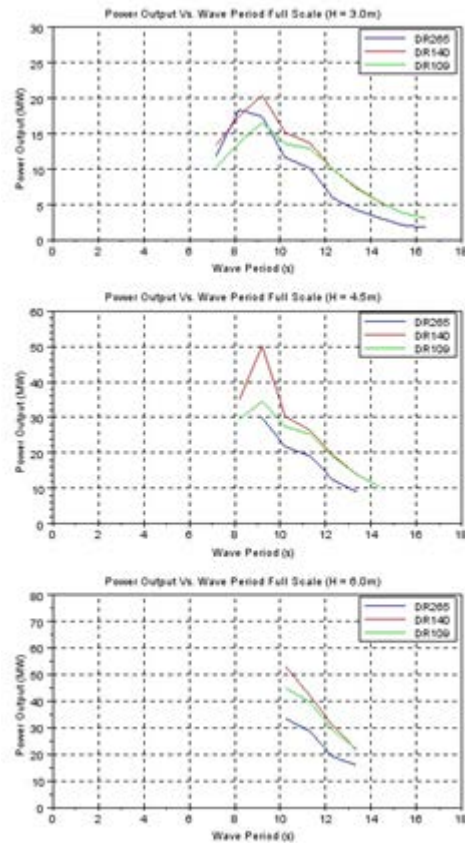
**Figure B.10: Absorbed Power Output Vs. Wave Period for each DR and Wave Height**

The absorbed power output for each DR is illustrated in Figure B.10. DR140 appears to have more absorbed power, approximately 20MW, than DR265 at approximately 18MW at "H=3.0m". This trend continues for "H=4.5m" and "H=6.0m".

**B.4.5   Summary Plots Panchromatic Waves**

The analysis for the panchromatic wave tests is the very same as for that performed in the monochromatic wave tests. The absorbed power and CWR is plotted for each significant wave height $H_s$, and peak wave period $T_p$, as well as for each DR.
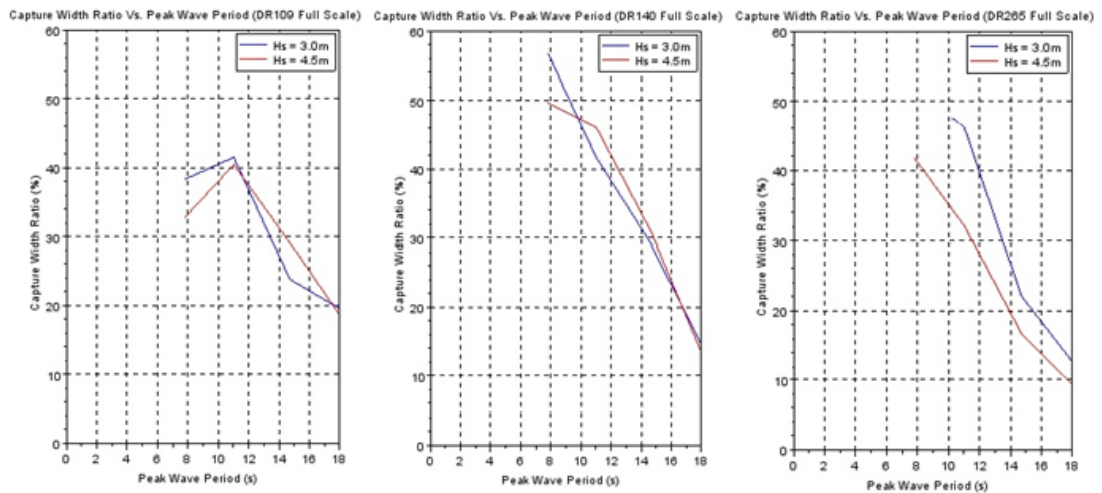
**Figure B.11: CWR Vs. Peak Wave Period for each significant wave height and DR109, DR140 and DR265**

From Figure B.11 and Figure B.12, DR140 performs the best in terms of CWR. In this scenario, the system is linear with little difference between the CWR values for each significant wave height within each peak wave period.
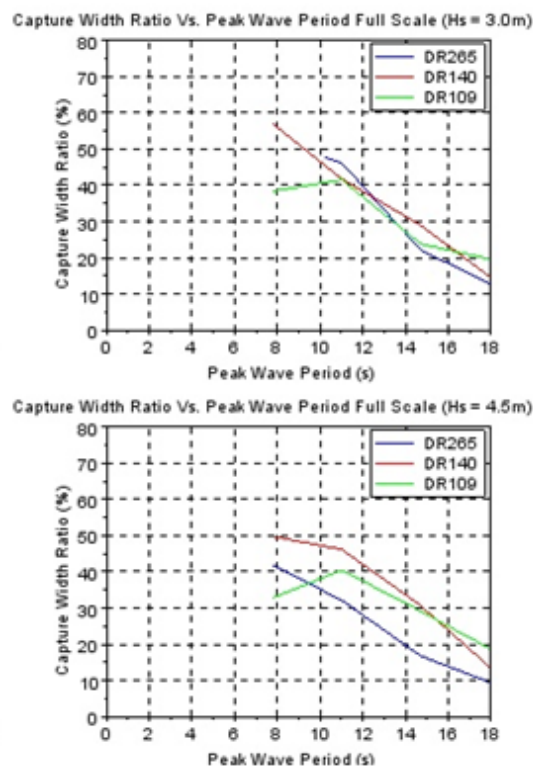


**Figure B.12: CWR Vs. Wave Period for each DR and significant wave height $H_s$**

## B.5    Summary

The tank testing of the OWC Array has shown that significant power output can be achieved from the large platform and that the motion characteristics may be suitable for attachment of commercial scale WTGs.

The power performance of the OWC Array is substantial and can be estimated to be ~3.6MW mean power output in a 50kW/m resource. The improvement of power quality exported from the platform is considerable in comparison to a single OWC chamber output. This topic is the subject of a paper associated with this thesis attached in APPENDIX E. For the purposes of the analysis of various hybrid concepts, the important output from this testing was the interpolated power matrix and the motion RAOs.

The potential for the addition of commercial scale WTGs on the platform is an attractive prospect in terms of power performance and also economic viability. The motion characteristics of the platform are critical in this respect as the accelerations induced at hub height need to limited so as to ensure the survivability of the WTG.

Further work is required on the structural loads imposed on such a large structure from extreme wave conditions to determine if the platform can be a feasible option in the future.

# APPENDIX C Tank Testing of a Point Absorber – Monopile
## C.1    Model Description

The point absorber (PA) model tested in this study consisted of a steel base with a vertical steel bar spine. The outer pile was constructed of 110mm diameter PVC tubing as illustrated in Figure C.1. This outer tube was connected to the inner steel spine by 4 load cells. This allowed the horizontal load on the outer pile to be measured. A baseline set of tests were carried out with this configuration in both sinusoidal waves and uni-directional 2-D wave spectra. The PA was a torus type buoy and was fabricated from two layers of 100mm insulation board, total depth 200mm. The outer diameter of the torus was 380mm and the internal diameter of the torus was 130mm. Lead weight was added to the lower section of the buoy to increase the draft. A number of configurations have been tested by adjusting the mass of the buoy.



**Figure C.1 : PA-Monopile Test Rig**

The PA model was tested under a number of wave conditions as detailed in Table C.1. The system response was monitored under sinusoidal wave conditions of constant wave amplitude and varying wave period, and various Bretschneider Wave Spectra. Due to time constraints, testing of the PAs under Bretschneider Wave Spectra could not be carried out.

**Table C.1: Table of Device Configuration and Test Conditions**

| Setup | H (m) | T (s) | T Increment(s) | Notes |
|---|---|---|---|---|
| **No Buoy** | 3 | 5-11 | 1 | - |
| | 4.5 | 6-11 | 1 | - |
| | 6 | 7-10 | 1 | - |
| | 3 | 7.6 | N/A | Bretschneider Spectrum |
| | 3 | 10.4 | N/A | Bretschneider Spectrum |
| | 3 | 14.4 | N/A | Bretschneider Spectrum |
| | 4.5 | 7.6 | N/A | Bretschneider Spectrum |
| | 4.5 | 10.4 | N/A | Bretschneider Spectrum |
| | 4.5 | 14.4 | N/A | Bretschneider Spectrum |
| **Buoy M=762.5t** | 3 | 5-11 | 1 | Pistons Not Attached |
| **Buoy M=762.5t** | 3 | 6-14 | 1 | Pistons Attached, No Orifice |
| **Buoy M=762.5t** | 3 | 5-13 | 1 | Orifice Diameter 0.05-0.1m |
| **Buoy M=1262.5t** | 3 | 5-13 | 1 | Orifice Diameter 0.05-0.1m |

## C.2    Measuring and Sampling Equipment

The measurements required for the effective analysis of the PA performance included the instantaneous motions of the PA torus buoy in heave, the loading on the outer pile, the incident wave field and the pressure in the piston chambers.

A single reflective marker was mounted on the point absorber, of which the instantaneous position was monitored by 4 Qualisys 3-Series Oqus Marker Tracking Cameras with a sampling frequency of 32Hz. Prior to testing each test setup, a still water measurement was recorded which allowed the deviation of the torus buoy positions and outer pile loads from the hydrostatic condition to be calculated for each hydrodynamic test.

The outer pile loads were measured with 4 No. Tedea-Huntleigh stainless steel single ended bending beam load cells with a maximum load of ~50N as illustrated in Figure C.2. The load cells were designated according to their position (in meters) relative to the water level and were located at varying heights along the monopile-steel frame interface. Table C.2 details the positions of the load cells.

**Table C.2: Position of Load Cells**

| Load Cell Name | Position Relative to Water Level (WL) |
|---|---|
| LC-30.85 | WL-30.85 |
| LC-14.95 | WL-14.95 |
| LC+1.05 | WL+1.05 |
| LC+11.05 | WL+11.05 |

**Figure C.2 : Tedea-Huntleigh Load Cell**

Each of the load cells was exposed to differing loads due to the variation in their positioning. An example of this is the constantly submerged state of LC-30.85 and the constantly above water state of LC+11.05. The incident wave field was measured by 2 wave probes, either side of the model. Figure C.3 is a dimensioned drawing that contains information regarding the configuration of the device and the location of the load cells relative to the base of the Ocean Wave Basin (Model Scale).
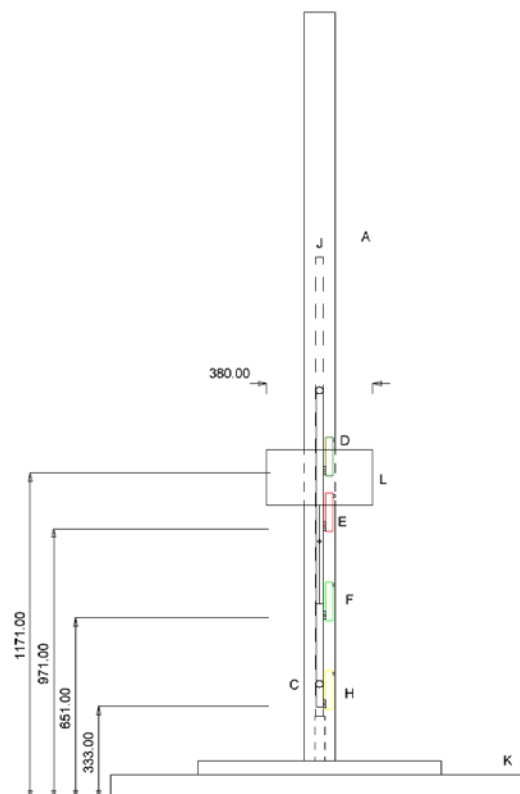


**Figure C.3 : A: Monopile, C: Drowned Orifice, D: LC+11.05, E: LC+1.05, F: LC-14.95, H: LC-30.85, J: Inner Steel Frame, K: Gravity Base, L: Point Absorber.**

### C.3    Physical Testing Results

#### C.3.1    RMS Load on Monopile (No PA Attached)

The first set of tests carried out involved exposing the monopile with no PA attached to regular waves. During testing the wave height was varied between 3m, 4.5m and 6m and the wave period was varied between 5-11s, 6-11s and 7-10s respectively.
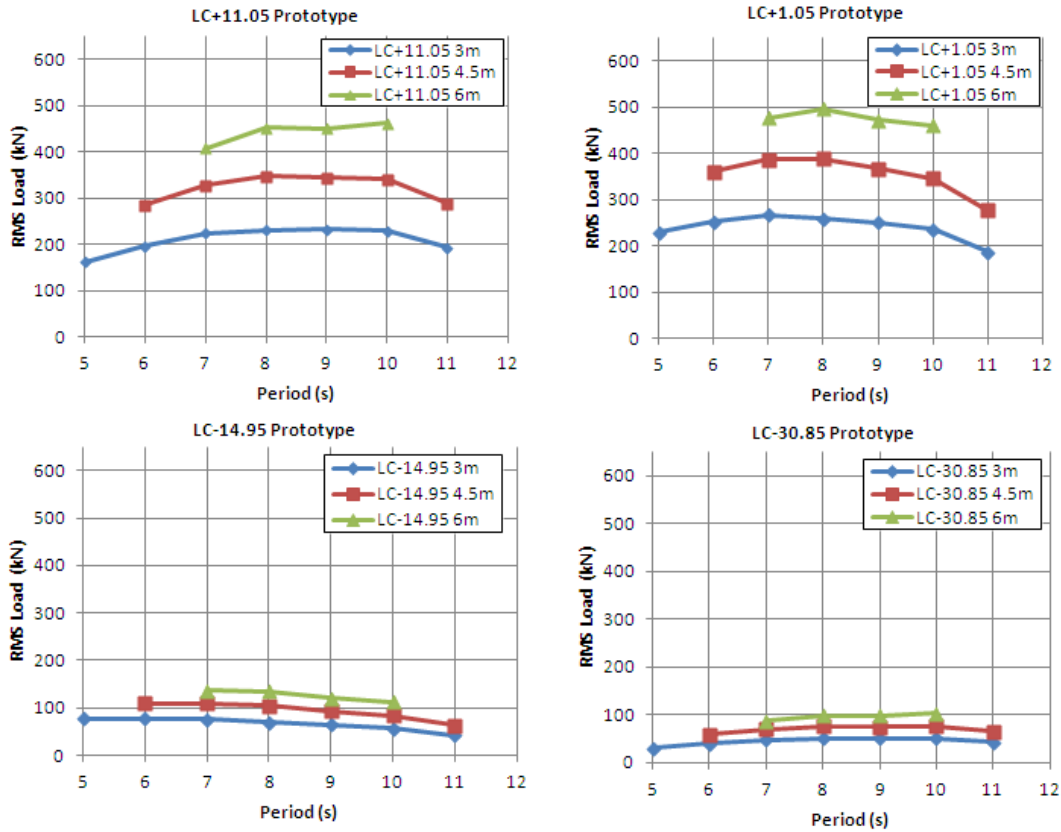


**Figure C.4 : Loadings on Monopile for varying wave heights**

Figure C.4 displays how the RMS load on all of the load cells increased across all wave periods with an increase in wave height. The maximum RMS load occurred at LC+1.05 followed by LC+11.05, LC-14.9 and LC-30.85 respectively.

In order to determine whether this increase can be modelled linearly or nonlinearly an RAO type analysis was carried out. This involved dividing the RMS load on each load cell at each period by the incident wave height; this produced a figure (with units of kN/m) which described the RMS load on each load cell per meter of wave height. In theory, if the RMS load scaled linearly then the RAO of each of the load cells, at each individual period, for the three differing wave heights in question, should be equal i.e. the kN/m of a load cell at a period should be the same irrespective of wave height. Figure C.5 shows the RAO for the four load cells.
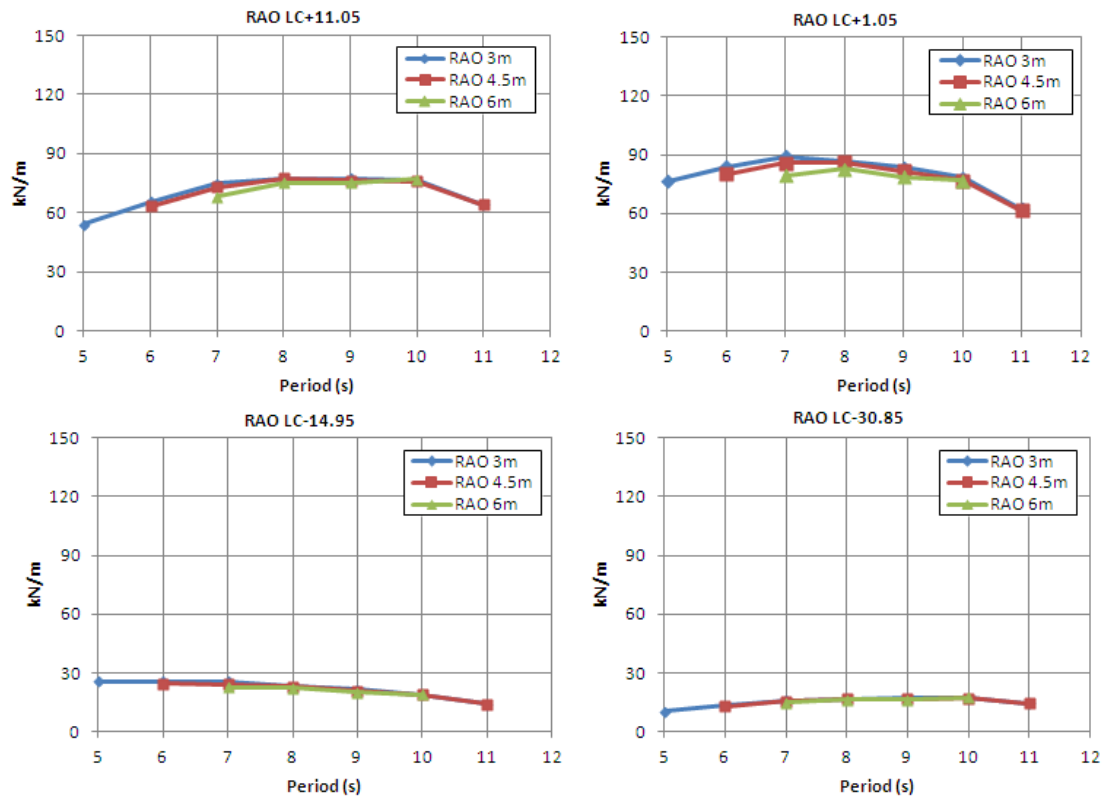
**Figure C.5: Loading RAO for Monopile only**

It can be seen from the above RAO plots that the RMS load on each load cell did indeed scale linearly as the RAO plots for the differing wave heights are very similar for each load cell in question. This linear nature allows the response load cells to be estimated for wave heights not used during the physical testing of the model by multiplying the RAO by the new wave height in question.

The second set of tests carried out on the monopile alone involved exposing the monopile to a number uni-directional 2D Bretschneider Wave Spectra. This set of tests was carried out in order to determine the RMS load on the monopile alone when exposed to irregular waves. The tests involved varying the significant wave height ($H_s$) and the peak wave period ($T_p$). The configuration of the device was not changed from the tests involving regular waves.

Figure C.6 shows the RMS load on each of the four load cells for the above wave conditions at prototype scale.
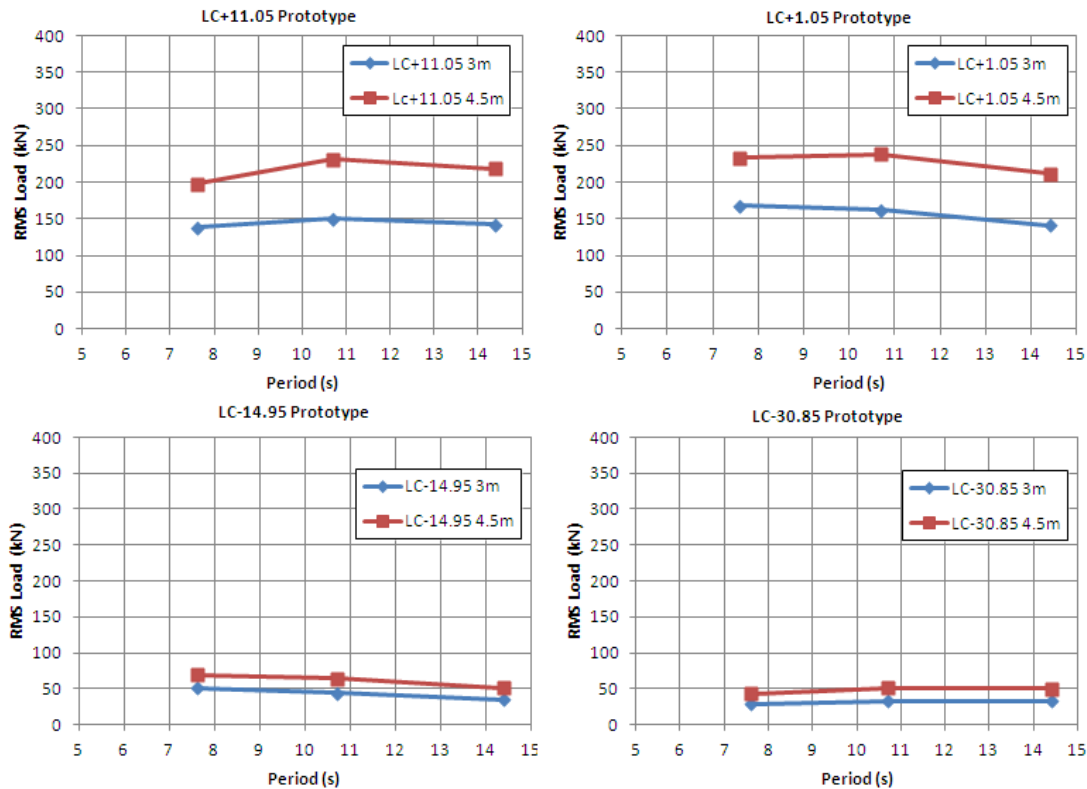
**Figure C.6 : Loadings on Monopile only for panchromatic waves**

From Figure C.6 it can be deduced that the RMS load on each of the load cells increased with an increase in Hs, this is in agreement with the variation in load with respect to wave height recorded for regular waves. In addition to this the maximum RMS load occurred at LC+1.05, followed by LC+11.05, LC-14.9 and LC-30.85 respectively. This is also in agreement with the variation in RMS load with respect to the load cell position seen in the regular wave tests.

### C.3.2 RMS Load on Monopile with PA Attached

As previously mentioned the configuration of the device was varied by adjusting the torus buoy mass and the damping ratio in order to maximise power absorption. The change in the RMS load on the outer pile versus the change in configuration and the absolute absorbed power was calculated.

Figure C.7 displays the variation in the RMS load on each of the four load cells for differing wave periods and for differing device configurations. The three configurations plotted are;

- The monopile alone,
- The monopile with the PA attached. This configuration consisted of a PA mass of 762.5t and a damping ratio (ratio of orifice area to piston block area) of 400 at prototype scale,

- The monopile with the PA attached. This configuration consisted of a PA mass of 1262.5t and a damping ratio (ratio of orifice area to piston block area) of 400 at prototype scale.
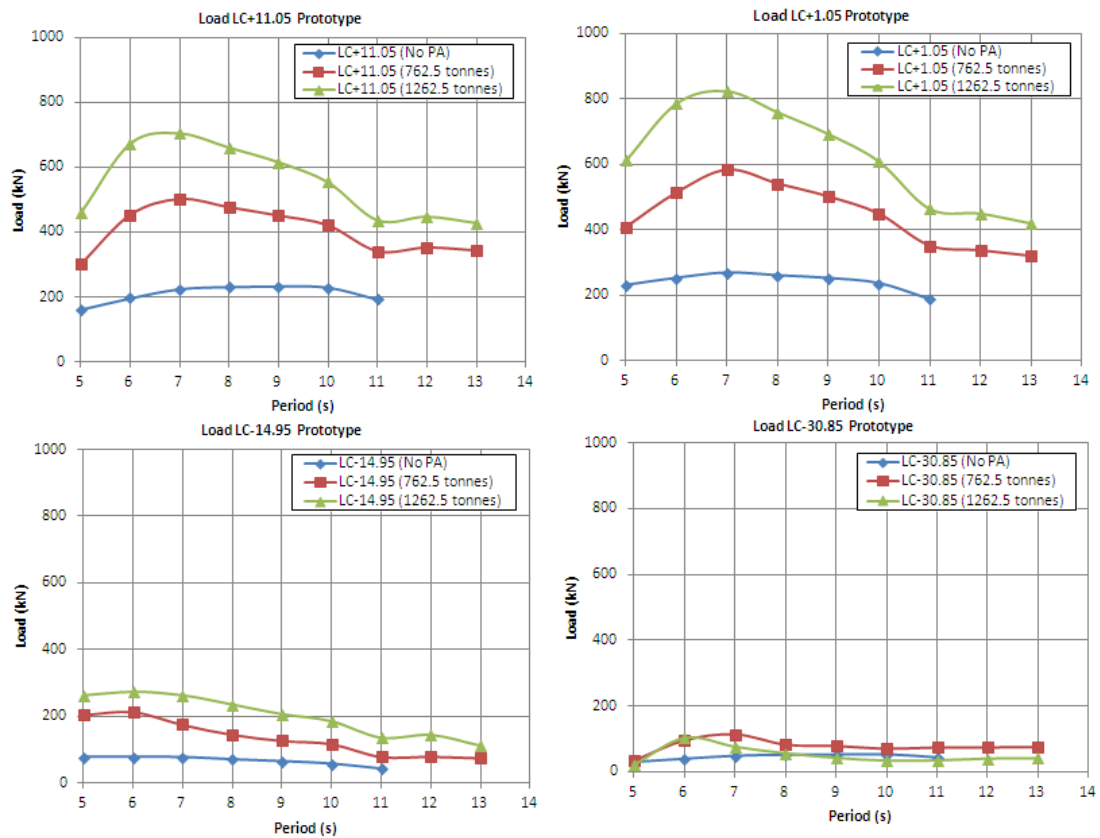


**Figure C.7 : Loading on Monopile only and with PA's**

It can be seen from Figure C.7 that the attachment of the point absorber to the monopile increased the structural load on the monopile. In addition to this it is evident that increasing the mass of the PA resulted in an increase in load on LC+11.05, LC+1.05 and LC-14.95. Figure C.8 illustrates the load RAOs for each of the load cells for the monopile baseline and both PA arrangements.
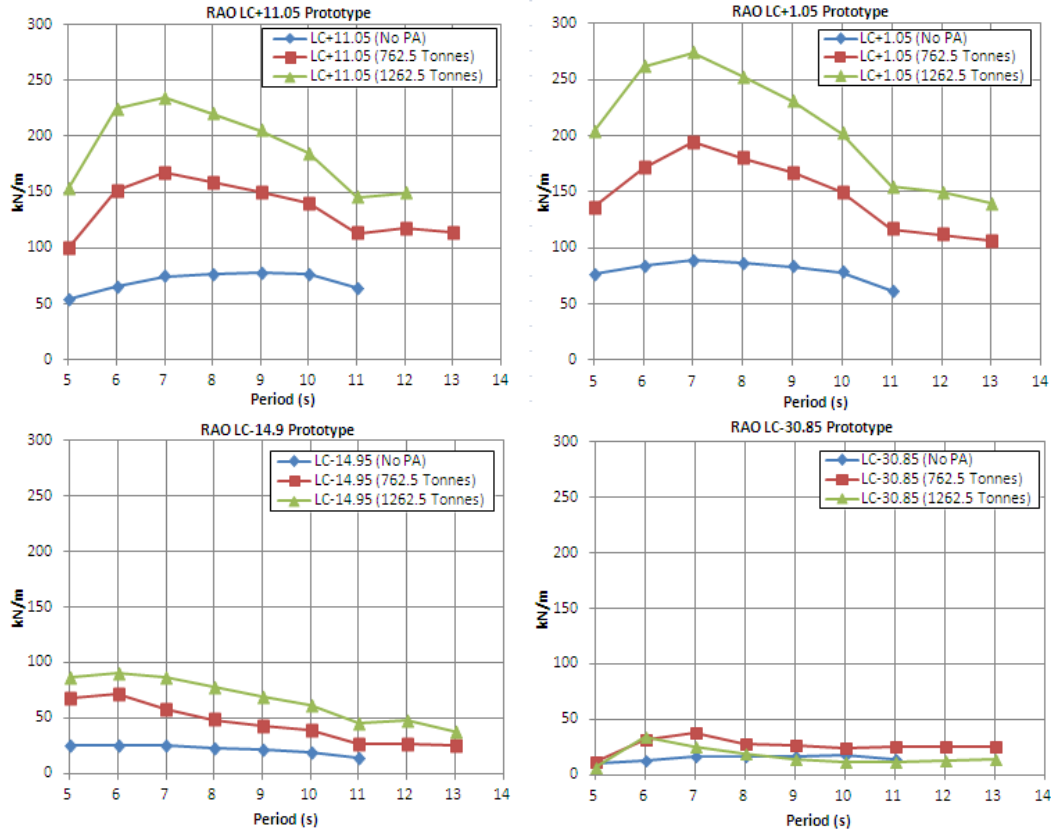
**Figure C.8 : Load RAO's for Monopile only and with PA's**

Figure C.9 displays the increase of load on each load cell with respect to wave period with a PA mass of 762.5t and 1262.5t.
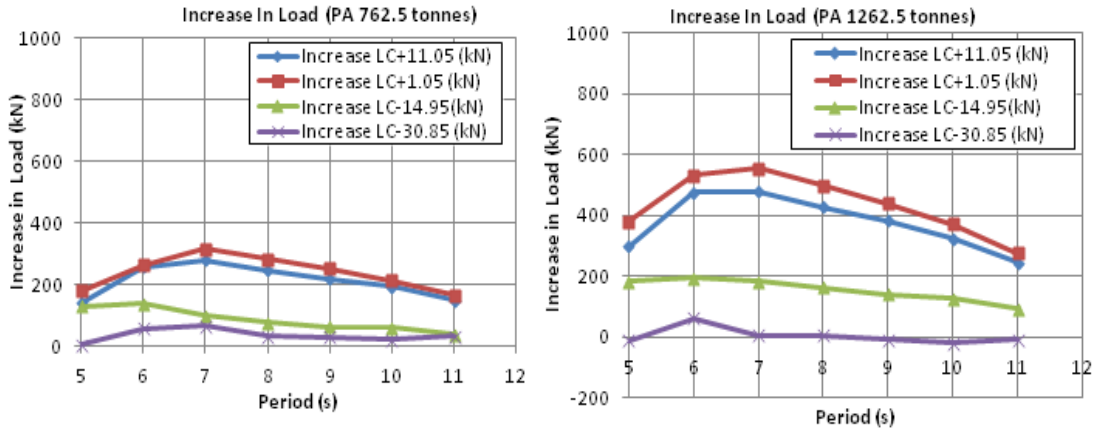


**Figure C.9: Increase in Load, PA mass 762.5 tonnes and 1262.5 tonnes**

Figure C.10 displays the percentage increase in load on each load cell with respect to wave period with a PA mass of 762.5t and 1262.5t. The percentage increase in load for LC-30.85 is not included in the graphs as a result of the initial load being less than 100 kN in magnitude. Any small increase or decrease in the magnitude of load on this load cell will result in a very large percentage increase or decrease in load on the load cell.
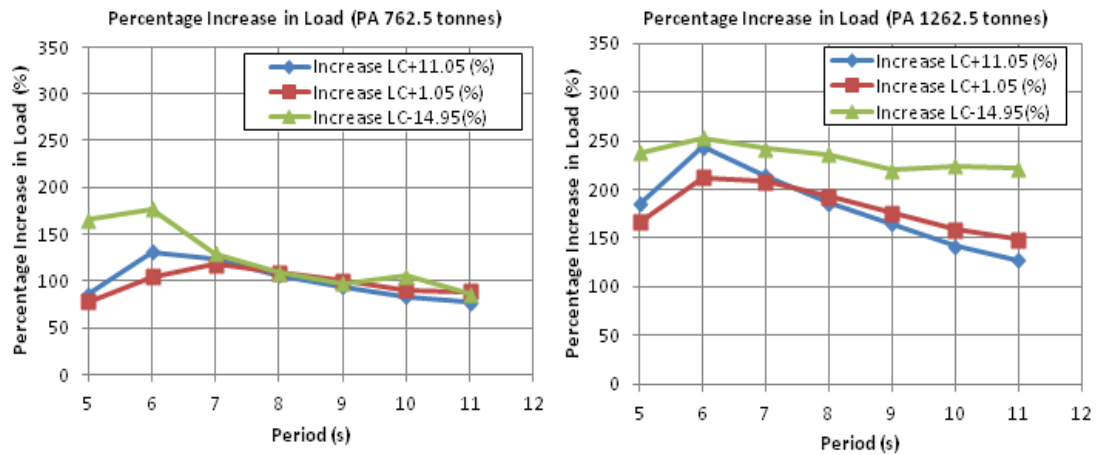
**Figure C.10 : Percentage Increase in Load, PA mass 762.5 tonnes**

## C.4    Summary

### C.4.1    RMS Load on Monopile (No PA Attached)

The RMS load on the load cells increases linearly with an increase in wave height for regular waves as can be seen from the RAO plots in Figure B.5. This allows for the RMS load on the monopile to be estimated for wave heights not used during the physical testing of the model by multiplying the RAO of each load cell at each wave period by the new wave height in question. In addition to this it is evident that the RMS load on each of the four load cells increased with an increase of Hs during the irregular wave tests. These tests provided a base line reading of RMS load on the monopile and allow the influence of the PA on the RMS load on the monopile to be quantified.

### C.4.2    RMS Load on Monopile with PA Attached.

Regarding the RMS load on the load cells it is clear that the attachment of the PA to the monopile resulted in a marked increase on the load on each load cell, this can be seen in Figure C.7. In addition to this, the increase in load varied with the position of the load cells as illustrated in Figure C.9. From Figure C.9, LC+1.05 experienced the largest overall increase in load across all periods for both of the configurations tested followed by LC+11.05 and LC-14.95. The load on LC-30.85 increased across all periods for the configuration with a PA mass of 762.5t but only increased for periods of 6s, 7s and 8s for the configuration with a PA mass of 1262.5t.

The large increase in load on LC+1.05 is to be expected as it is directly along the path of the PA when it is in motion. Regarding the percentage increase in load experienced by each load cell Figure C.10 shows that the largest percentage increase experienced for all of the load cells occurred at a wave period of 6.0s for both configurations of the PA. This is because at this wave period the PA was not moving significantly in heave as the wave period was not equal, or close to, the resonant frequency of the PA.

In relation to the variation of the PA mass and its influence on the structural load on the monopile it can be seen from Figure C.7 that an increased mass of the PA resulted in an increase in the structural load on the monopile.

# APPENDIX D Tank Testing of the Delta OWC Array

This APPENDIX outlines the development of a Froude scaled model of the Delta OWC Array platform for tank testing at the Beaufort Research – HMRC, University College Cork Ocean Wave Basin in 2013. This section is divided into relevant sections describing the model design and construction, the testing carried out and main results and finally the comparison of the motion RAOs and power matrices from tank and numerical modelling.

## D.1 Model Design and Construction

The model has been designed to ensure, so far as reasonably practicable, geometric similarity through Froude scaling has been conserved. Of course, like many model designs, compromise between accuracy and time and costs has been required. Furthermore, considerations such as handling and craning capability at the testing facility have had to be borne in mind during design as space is limited and the model is one of the largest, both in terms of geometrical size but also mass, tested at the facility. Therefore the model has had to be built in sections, similar to the design philosophy for the prototype, for craning into the tank and connected while floating. A 3D drawing of the model is illustrated in Figure 5-37.
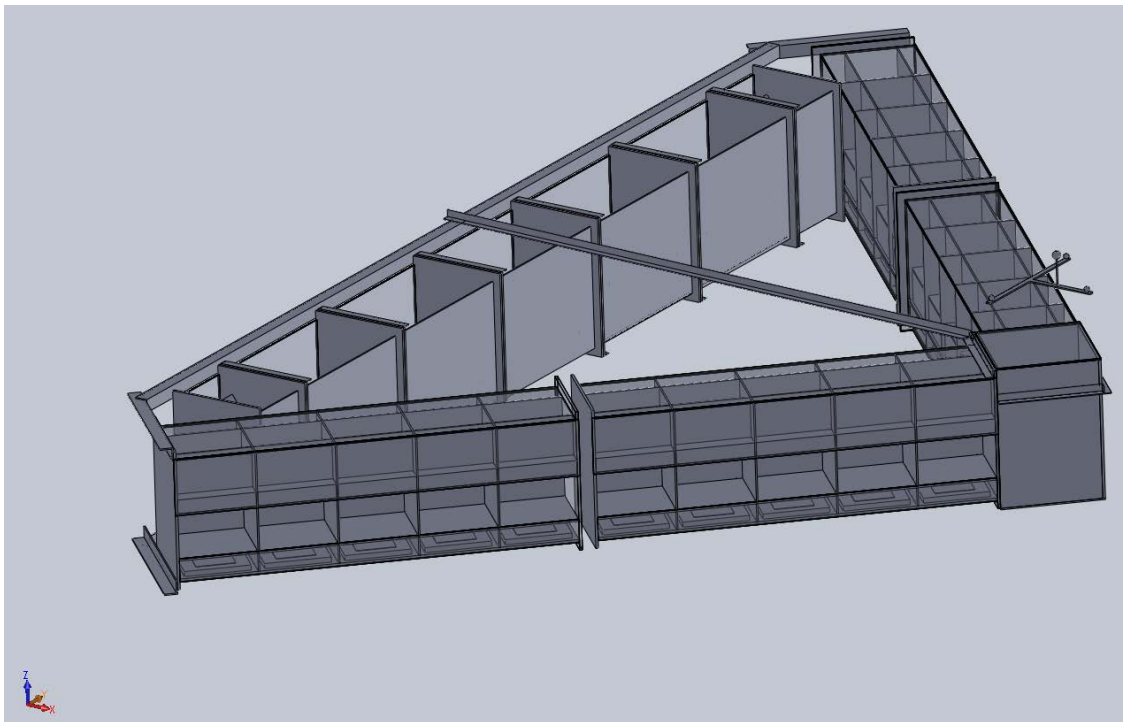


**Figure D.1: 3D Drawing of the Delta OWC Array Model**

The model has been designed to be 1:50 scale due to limitations in the tank size and wave making capabilities. The summary of the scaled geometrical quantities of the model are shown in Table 5-10.

**Table D.1: Summary of Geometrical Quantities of the 1:50 Scale Model of the Delta OWC Array Platform**

| Platform Element | Dimension/Mass |
|---|---|
| **Total Width** | 4.9m |
| **Chamber Beam Length** | 3m |
| **Chamber Beam Width** | 352mm |
| **Back Beam Length** | 4m |
| **Back Beam Width** | 352mm |
| **Total Mass** | 815kg |
| **Chamber Beam Mass** | 186kg |
| **Back Beam Mass** | 413kg |

It may be seen from Table 5-10 that the dimensions and masses of the model sections are quite high. The model sections have been fabricated from polycarbonate material plates chemically bonded together with dichloromethane. Five chambers have been constructed together in one section as illustrated in Figure 5-38.



**Figure D.2: 5 Chamber Polycarbonate Section**

The chamber cross section has been geometrically scaled from that illustrated in Figure 5-18. Specifically designed ballast blocks were cast from concrete as illustrated in Figure D.3 to allow accurate placing within the chamber cross-section. Lead was then used to fine tune the mass of each block. The ballast has been designed and placed within the ballast tanks to achieve the correct trim and draft. The chamber cross section dimensions and locations of the ballast are illustrated in Figure 5-39 and Figure D.4. In total, there are 60 ballast/buoyancy tanks in the chamber beams. This is a significant number to ensure water tightness. In fact due to the accuracy of the laser cutting of the polycarbonate plates, the low viscosity adhesive was unable to fill any larger (~0.5-1mm) voids in the connections between adjacent plates. Therefore, it was decided to fill each tank with buoyant expandable

foam to prevent leaks as shown in Figure D.5. Ballast mass was adjusted accordingly.
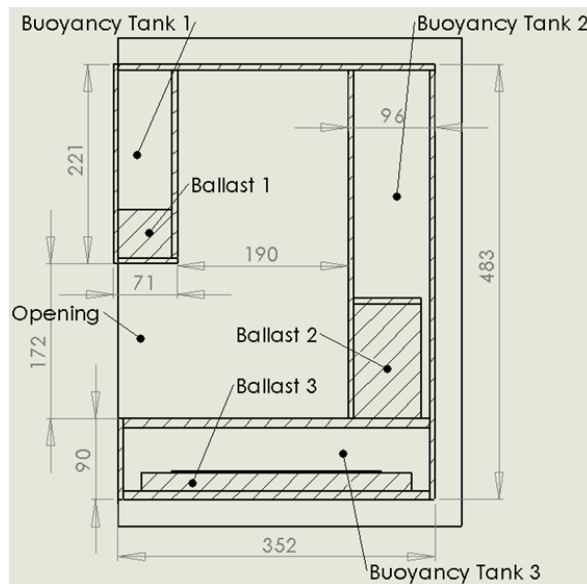


**Figure D.3: Casting of concrete ballast blocks**



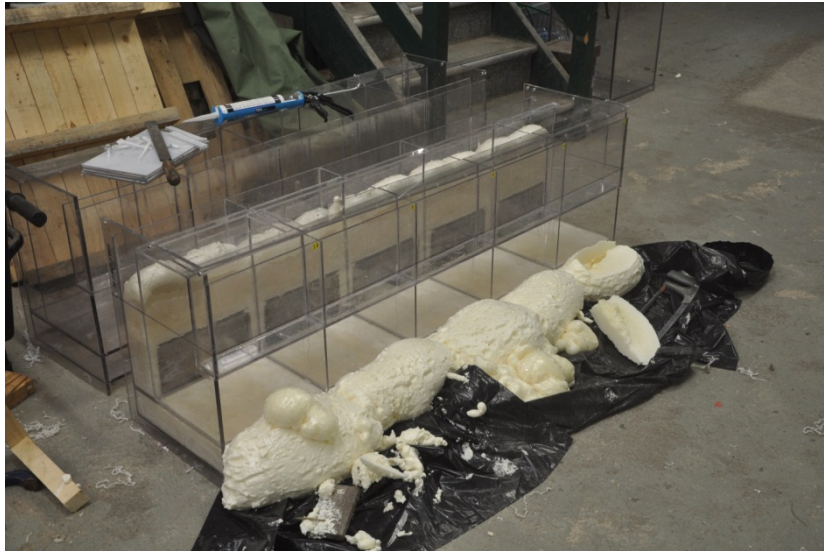**Figure D.4: Chamber Cross Section Dimensions and Ballast Locations**

**Figure D.5: Expandable foam and ballast blocks in the chamber ballast tanks**

The model has had further additional fixtures and fittings applied such as OWC chamber caps with a fitting to easily change the damping applied to the water column. This system was the same system as used in the original tank testing of an OWC Array discussed in APPENDIX A. The final model installed in the tank and operating is illustrated in Figure D.6.
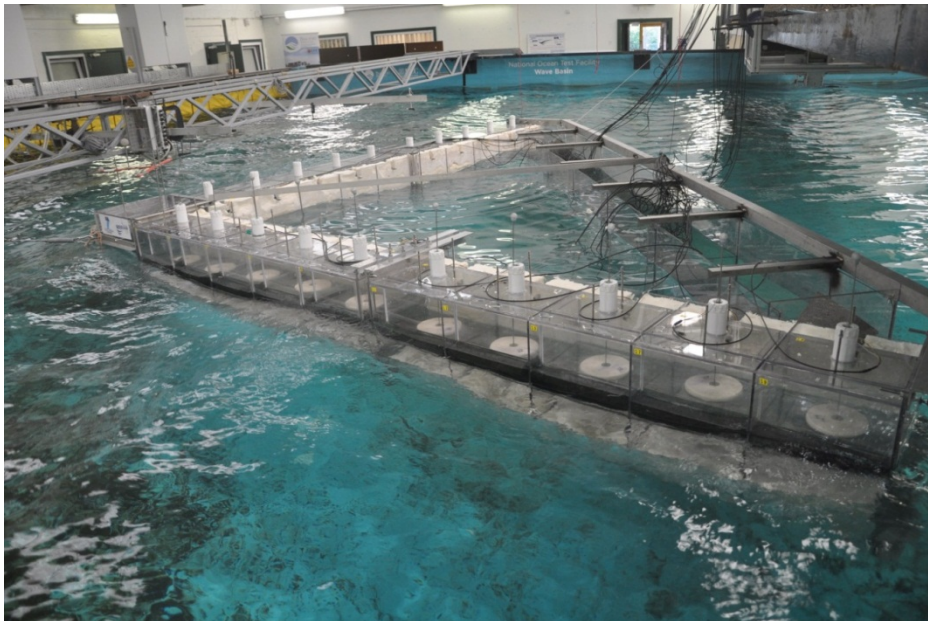


**Figure D.6: Final Delta OWC Array Model Installed in the Tank and Operating**

## D.2    Measurements and Instrumentation

A significant number of measurements have been taken from the tank testing campaign from the Delta OWC Array model. In summary the measurements carried out on the model were;

- 4 No. Qualysis markers for platform motion

- 10 No. Qualysis markers for OWC water level elevation on one side of the model
- 20 No. pressure transducers in each chamber
- 3 No. wave probes to the fore of the model
- Strain gauge flange in the centre of the port side chamber beam to monitor global structural loads. the results of these measurements are not included in this thesis as analysis is proving to be exceptionally difficult due to the non-linear behaviour of the flange.

The model was moored with three stainless steel mooring lines but as this test campaign was focussed on the performance of the platform in terms of power absorption, no load cells have been used to monitor mooring loads.

A more detailed discussion on each of the measurements taken is included below.

### D.2.1 Platform motion measurements

The 6 Degrees of Freedom (DOF) of the floating platform have been measured by a Qualisys OQUS motion capture camera system operating at a frequency of 32Hz. The rigid body marker template is illustrated in Fig. The BOW, TOP, PORT and STBD markers as shown in Fig., track the DOFs of the platform. The camera system is coded to track the 3D co-ordinates of each marker. The system may be set up to calculate the 6 DOFs directly by specifying 4 markers and the location of the COG of the model relative to one marker. However, in this instance, due to the fact that a further 10 markers were used for tracking the water level elevation within the chambers, only the 3D co-ordinates of the markers were exported from the system. The 6 DOFs of the platform are then calculated from the instantaneous position of 3 makers, namely, BOW, PORT and STBD. TOP acts as a "spare" marker in the event that the time signal from one of the other markers is of insufficient quality. The process of calculation of the 6DOFs is outline here using 3D vector mathematics.

### D.2.2 Internal Water Surface (IWS) elevation measurements

The internal water surface (IWS) elevation in the global co-ordinate reference frame has been measured using very light surface following floats attached to a stainless steel bar of pre-defined length with a Qualysis Motion Capture marker on top. The motion of the float is restricted to pumping motion perpendicular to the plenum roof. First order sloshing motion may not be accurately measured by the floats, however for the purposes of validation of numerical models, the pumping mode has been deemed sufficient as this is the only mode of motion attributed to the IWS in each chamber. The float and guide arrangement is illustrated in Figure D.7.

**Figure D.7: Float, guides and Qualysis maker arrangement in the chamber**

### D.2.3 Chamber pressure measurements

The pneumatic pressure fluctuation within each OWC chamber is measured with a Honeywell 0-7in differential pressure transducer illustrated in Figure D.8. The transducer is open to atmosphere on one end, thereby only measuring the increase or decrease in instantaneous pressure in the chamber relative to instantaneous atmospheric pressure. The sensors have been calibrated prior to testing for known pressures and scaling factors applied in the data acquisition system. Both chamber beams were instrumented with a transducer in each chamber.



**Figure D.8: Honeywell Differential Pressure Sensor**

### D.2.4 Global structural load measurements

Global structural loads have been measured with the use of a strain gauge flange as shown in Figure D.9 below. As the chamber beam was built in two sections, there was a requirement for a connection joint. It was decided that within this joint, a method of measuring the global bending moments was desirable. The flange was a

310

simple design, using aluminium angle connections between the main chamber beam sections and a polycarbonate plate joining the two angles. It was found post testing however, that this joint configuration exhibited substantial non-linear behaviour with respect to anticipated strain and measured strain. Due to this anomaly, a bench test was set-up to calibrate the flange through the range of strains it measured during testing and while the total chamber beam sections, joined by the flange, was simply supported at either end.
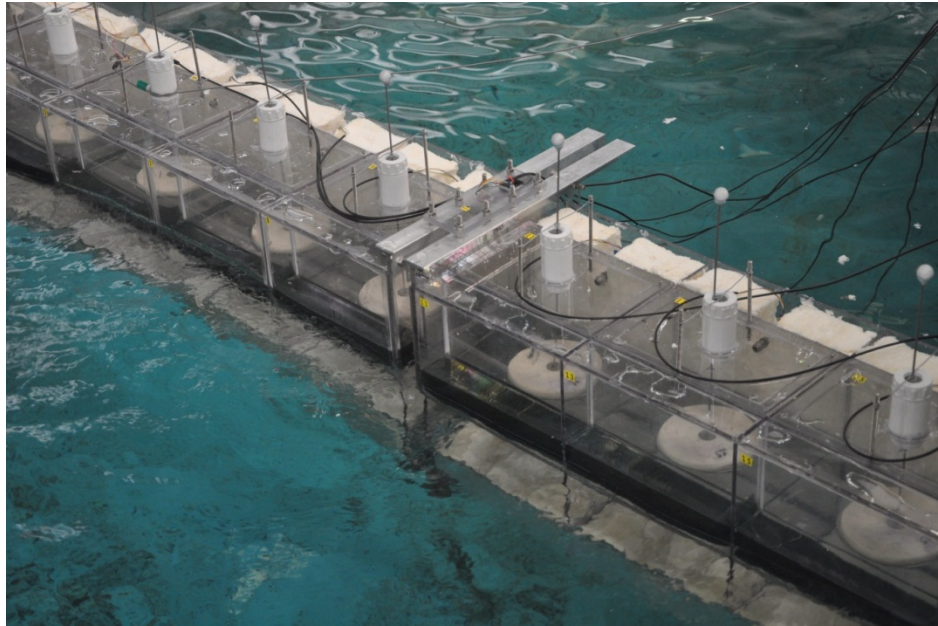


**Figure D.9: Strain gauge flange between the chamber beam sections**

Figure D.10 below illustrates the strain gauge flange undergoing a bench test. The flange is set up to act as a simple cantilever beam. The idealised beam equations are used to predict the strain ($\varepsilon$) imposed on the strain gauges based on the location of the load and the location of the gauges relative to the load and fixity point. A number of configurations of the flange were investigated to determine the linearity of the flange with respect to measured strain and calculated strain. These initial bench tests spanned a range of strain up to ~70$\mu\varepsilon$. The polycarbonate plate without aluminium angles supported as a simple cantilever acted as an ideal beam and the measured and calculated strain matched. When the aluminium angles were added, the flange exhibited non-linear behaviour.
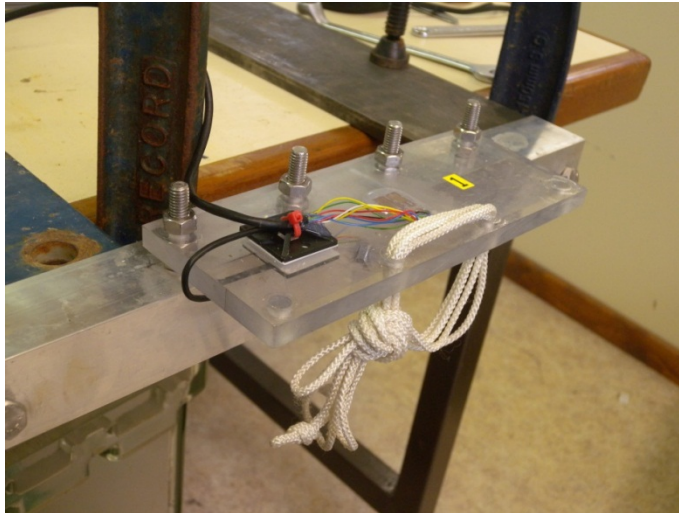
**Figure D.10: Strain gauge flange undergoing a bench test**

The loads applied resulted in rather low strains as compared to the condition when the entire chamber beam was simply supported as in Figure D.11. These strains reached values of ~2700με.



**Figure D.11: Full chamber beam in dry test simply supported**

Unfortunately, by the time of completing this thesis, the measurements of the global structural load have not been analysed in full. The behaviour of the flange has not been as expected and is complicated somewhat by the non-linear behaviour of the polycarbonate material and the full flange arrangement. Further work is on-going currently to resolve the issues with the measurements taken.

### D.2.5   Water Surface elevation measurements

The water surface elevation has been measured using standard conductivity based wave probes as shown in Figure D.12 below. Three in total were used to measure the surface elevation at the bow of the model. The waves were also measured without the model in the tank. The statistics from these surface elevation signals have been used to determine the Response Amplitude Operators (RAO) for each DOF.
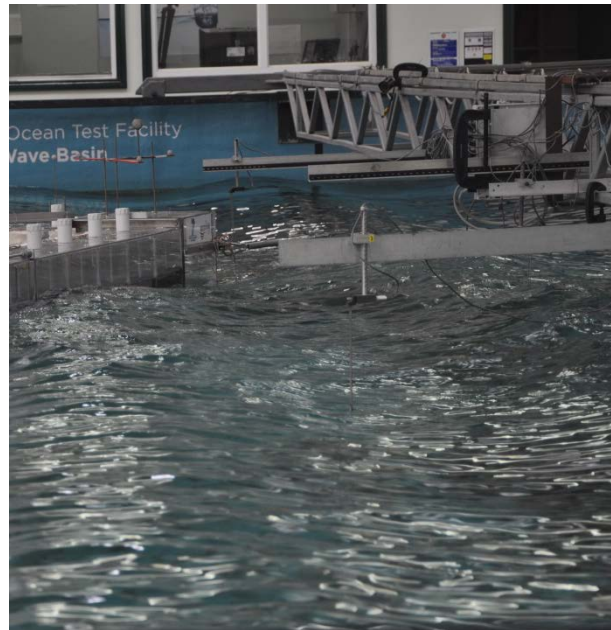
**Figure D.12: Wave probe arrangement used during testing**

### D.3    Delta OWC Array Model Testing Campaign

The testing campaign for the Delta OWC Array platform has included all the typical first stage tests including;

- Monochromatic waves of varying height and period
- Panchromatic waves of varying $H_s$ and $T_p$
- Directional effects on chamber responses
- Effects of a scaled WT on the motion characteristics

Due to the size and mass of the platform, conducting decay tests was deemed unfeasible without the use of a gantry crane. These have not been carried out in this test series.

**Set 1: Optimum Dampings, Determine Effect of Wave Directionality**

This test set is to determine the effects of wave directionality on power absorption.

| Wave Heights (mm) | No. Frequencies | Frequency Range |
|---|---|---|
| **20** | 14 | 1.41 - 0.4 |
| **50** | 7 | 1.41 – 0.4 |
| **80** | 10 | 1.00 – 0.44 |

| Damping Type | No. of Settings |
|---|---|
| **Non-Linear** | 1 |

| Directions |
|---|
| **0°** |
| **Heading** |
| **22.5°** |
| **45°** |
| **-22.5°** |
| **-45°** |

## Set 2: Optimum Dampings, Irregular Waves

This test set is designed to characterise the power absorption of the platform for wave conditions only.

| Significant Wave Heights (mm) | No. Frequencies | Peak Frequencies (Hz) |
|---|---|---|
| **30** | 3 | 1.41, 1.01, 0.79 |
| **60** | 5 | 1.01, 0.79, 0.71, 0.59, 0.51 |
| **90** | 5 | 1.01, 0.79, 0.71, 0.59, 0.51 |

| Damping Type | No. of Settings |
|---|---|
| **Non-Linear** | 1 |

| Directions |
|---|
| **0°** |
| **Heading** |
| **22.5°** |
| **45°** |
| **-22.5°** |
| **-45°** |

## Set 3: Optimum Dampings, Determine Effect of Wind Thrust and Wave Directionality

This test set is intended to determine the effects of wind thrust on the motions of the platform.

| Wave Heights (mm) | No. Frequencies | Frequency Range | Wind Speeds (m/s) |
|---|---|---|---|
| **20** | 14 | 1.41 - 0.4 | 0.97 |
| **50** | 7 | 1.41 – 0.4 | 1.23 |
| **80** | 10 | 1.00 – 0.44 | 1.5 |
| **110** | 8 | 0.78 – 0.44 | 1.67 |

| Damping Type | No. of Settings |
|---|---|
| **Non-Linear** | 1 |

| Directions |
|---|
| **0° Heading** |
| **22.5°** |
| **45°** |
| **-22.5°** |
| **-45°** |

## D.4    Results

The main objectives of the testing campaign were to measure the frequency dependent motion RAOs of the platform and the OWC chambers as well as calculate the power matrices of the platform for varying incident wave direction. This section presents in brief the RAO results for the platform and the chambers in three wave heights. The data has been filtered with a Butterworth filter with an appropriate frequency band. Firstly, hydrostatic stability tests on the chamber cross section design are outlined.

### D.4.1    Hydrostatic stability of Chamber Beam Section

The cross-section of the chamber beam has been designed to ensure that the beam is hydrostatically stable in the freely floating condition for constructability reasons discussed in Chapter 5. Through the MARINA Platform project, hydrostatic stability analysis was carried out by EOSEA SAS, a French engineering consultant, on the chamber cross section design using dedicated software. In order to confirm this, brief hydrostatic stability tests have been carried out in the 2D flume tank at the Beaufort Research Laboratory, University College Cork. Two conditions have been tested, roll forward and roll backwards. Roll forward refers to the tilt angle which tends to increasingly submerge the front buoyancy tank. Two 2kg masses were applied on the top of the beam over the COG. This initial position was recorded. The masses were then moved towards the front of the beam in steps of 20mm. This continued until the masses reached the edge of the beam. For roll backwards, it was slightly more difficult to get as many readings as the COG is much closer to the rear of the beam. One 6kg mass was applied directly over the COG and moved backwards two steps of 20mm. The resulting tilt angle was measured using two markers and the Qualysis OQUS motion capture camera system installed over the tank. The metacentric height is calculated from Equation D.1.

$$GM_z = \frac{w_j}{W}\frac{dx}{d\theta}$$

<div align="right">**Equation D.1**</div>

where dθ is the change in tilt angle and dx is the change in position of the jockey weight, $w_j$ is the mass of the jockey weight and W is the total mass of the chamber

beam section. The righting arm is the measure of the lateral distance between the COG and centre of buoyancy (COB) and is given by Equation D.2.

$$RA = GM_z . \sin \theta$$

where RA is the righting arm, $GM_z$ is the metacentric height and $\theta$ is the tilt angle. The righting arm is plotted against tilt angle in Figure D.13 below. The illustrations within the plot indicate the direction of tilt of the beam.
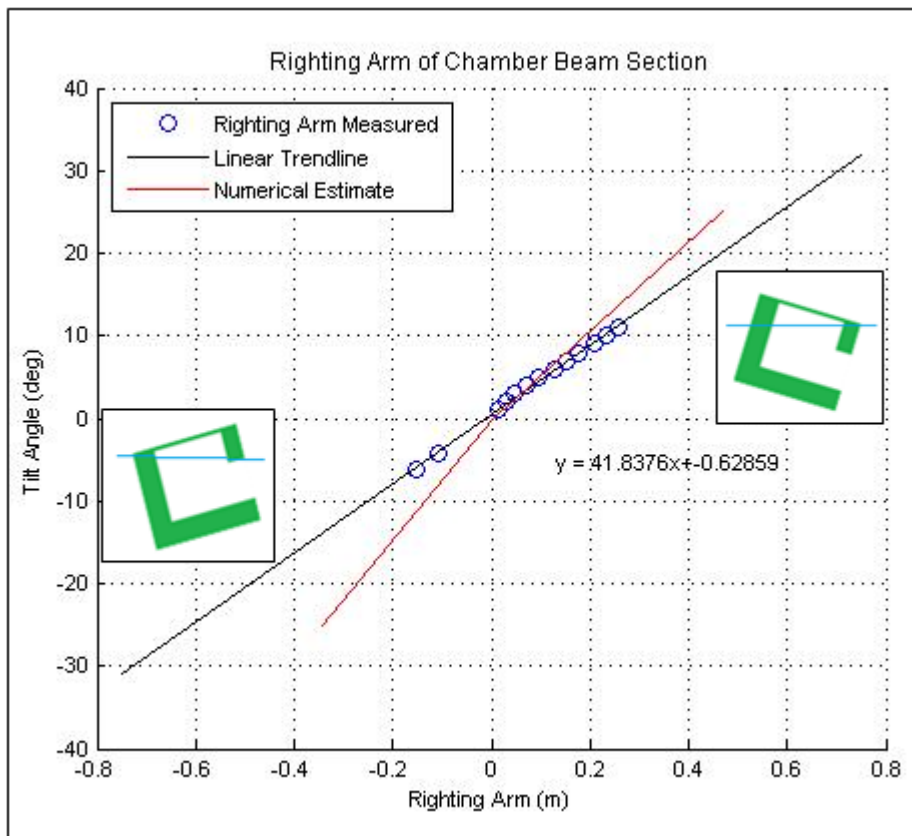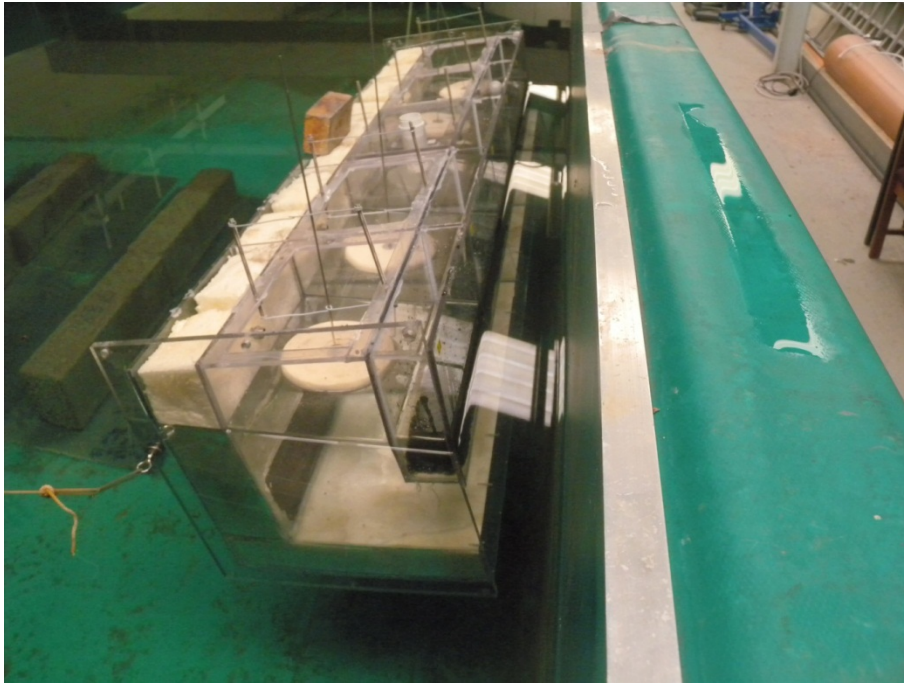


**Figure D.13: Hydrostatic stability of the Delta OWC Array chamber beam**

**Figure D.14: Chamber beam section during hydrostatic stability tests**

Figure D.14 illustrates the chamber beam section in the flume tank undergoing a test in roll backwards.

### D.4.2   Platform and Chamber Motion RAOs

The results presented here are for uni-directional waves with incident direction parallel to the symmetrical central axis of the platform. Figure D.15-D.16 are the translational and rotational RAO plots of the platform respectively. Figures D.17-D.21 are the chamber water surface elevation RAO plots.
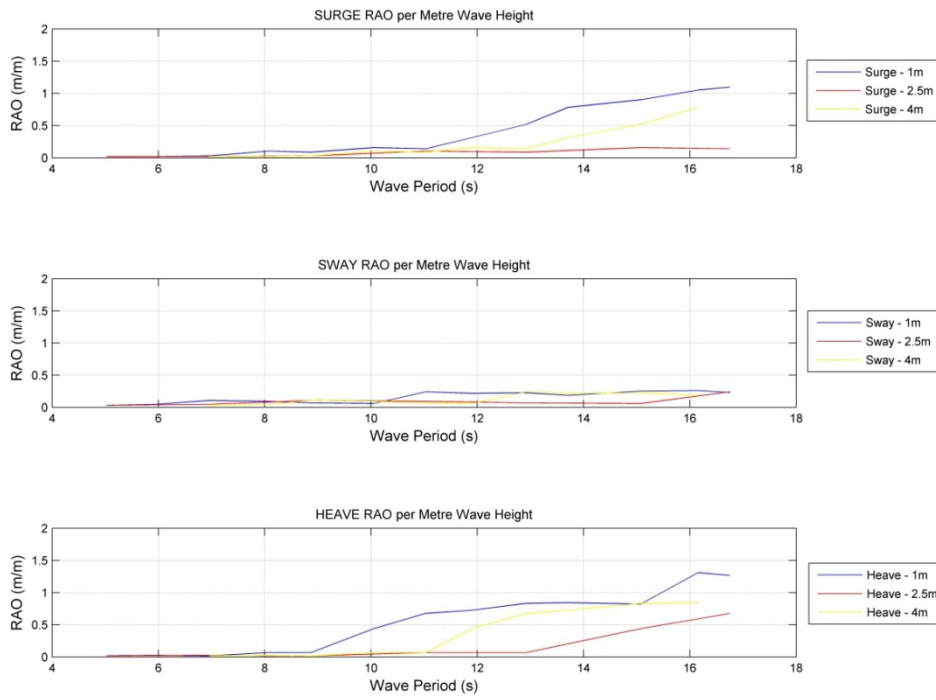
**Figure D.15: Surge, Sway and Heave Motion RAOs of the Delta OWC Array Platform for Varying Wave Heights**
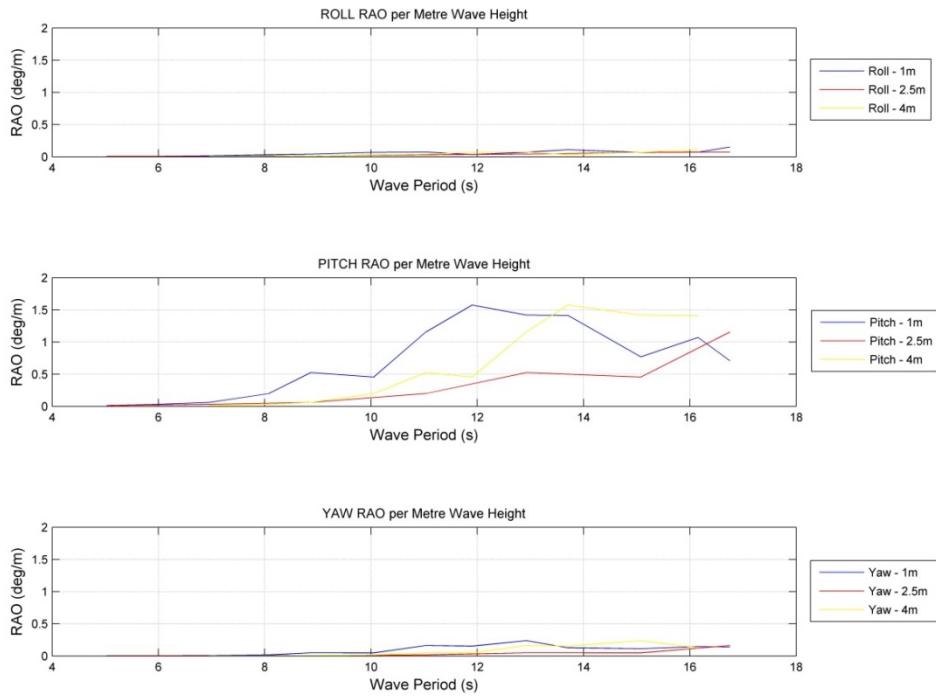


**Figure D.16: Roll, Pitch and Yaw Motion RAOs of the Delta OWC Array Platform for Varying Wave Heights**
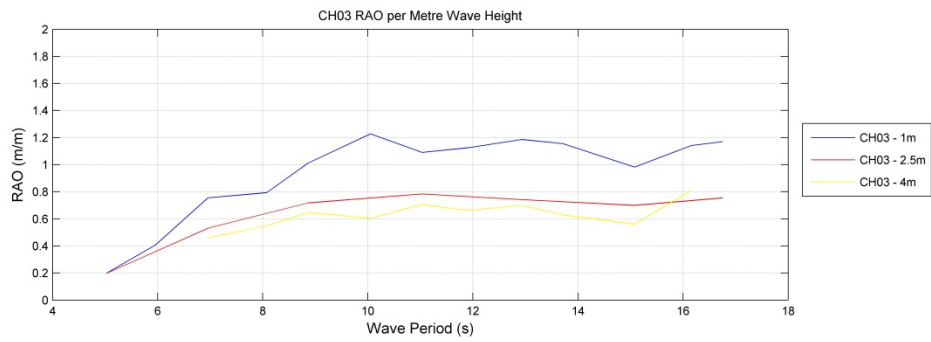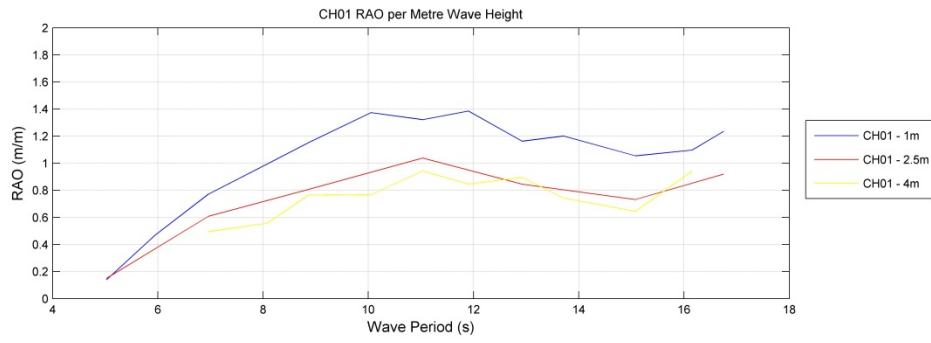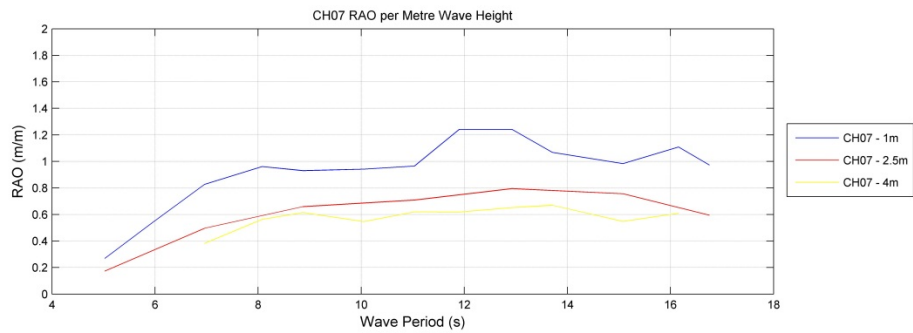
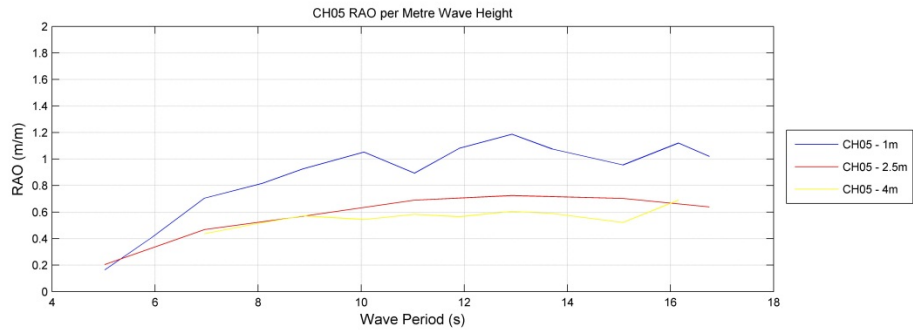**Figure D.17: Chamber 1&3 Water Surface Elevation RAOs**
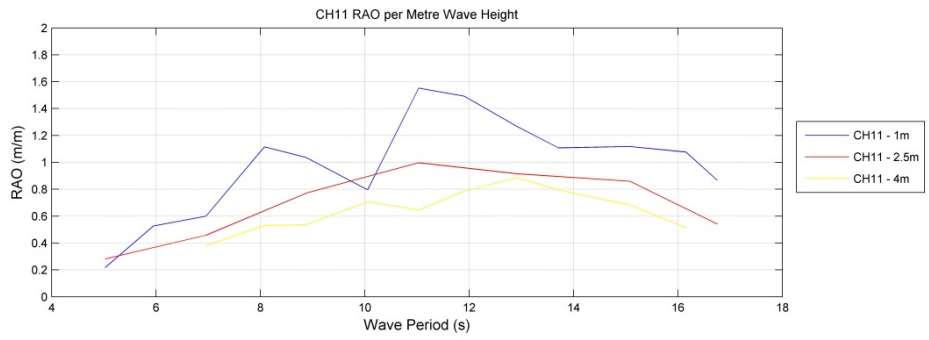


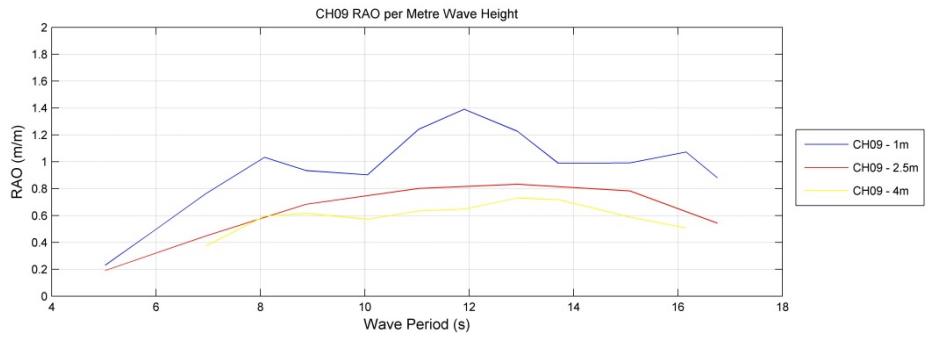**Figure D.18: Chamber 5&7 Water Surface Elevation RAOs**

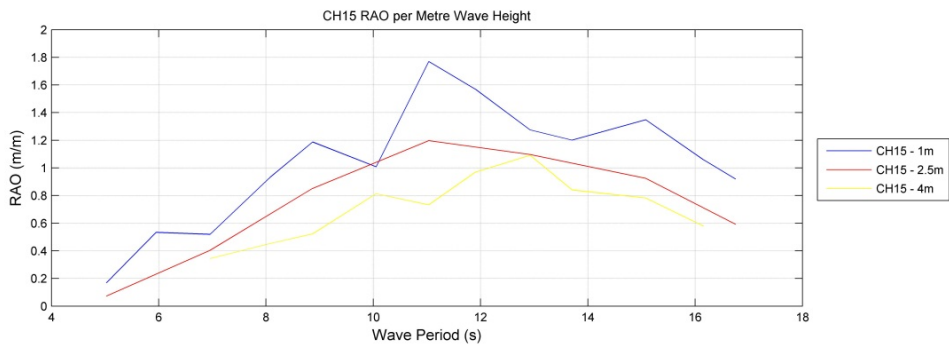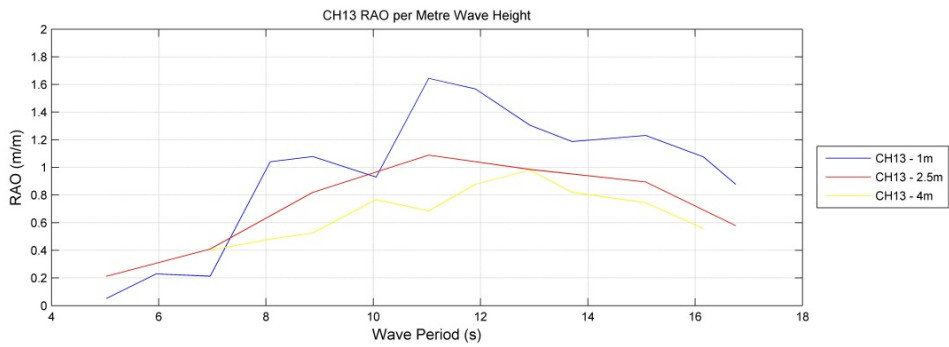**Figure D.19: Chamber 9&11 Water Surface Elevation RAOs**

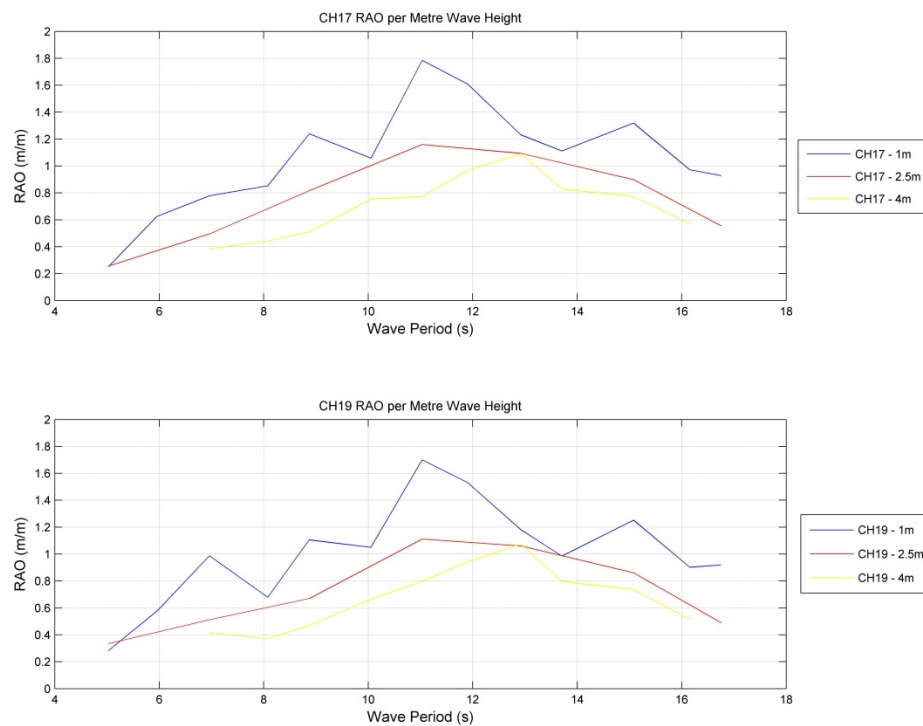**Figure D.20: Chamber 13&15 Water Surface Elevation RAOs**



**Figure D.21: Chamber 17&19 Water Surface Elevation RAOs**

The main observation from the plots above is that there is a clear dependency on wave period and wave height signalling there is a non-linear dependency between platform and water column response to incident wave conditions. Therefore the use of linear based numerical modelling tools to predict the performance of the system is perhaps not the best option. For a more accurate representation of the system, it would be recommended to use a second order frequency domain solver to model the system responses. In summary, it is critical to note that the pitch response and also the chamber water column RAO response reduces with increasing wave height for most of the wave periods tested.

### D.4.3    Chamber Pressure – Flow Relationship

The pressure-flow relationship, or the damping of the water column, is a critical aspect in the characterisation of an OWC. As discussed previously, the pressure and water level elevation of the water column chamber were measured by a pressure transducer and surface following float respectively. On plotting the instantaneous pressure and associated flow inferred from elevation measurements against one another, an unusual trend resulted as shown in blue in Figure D.22.
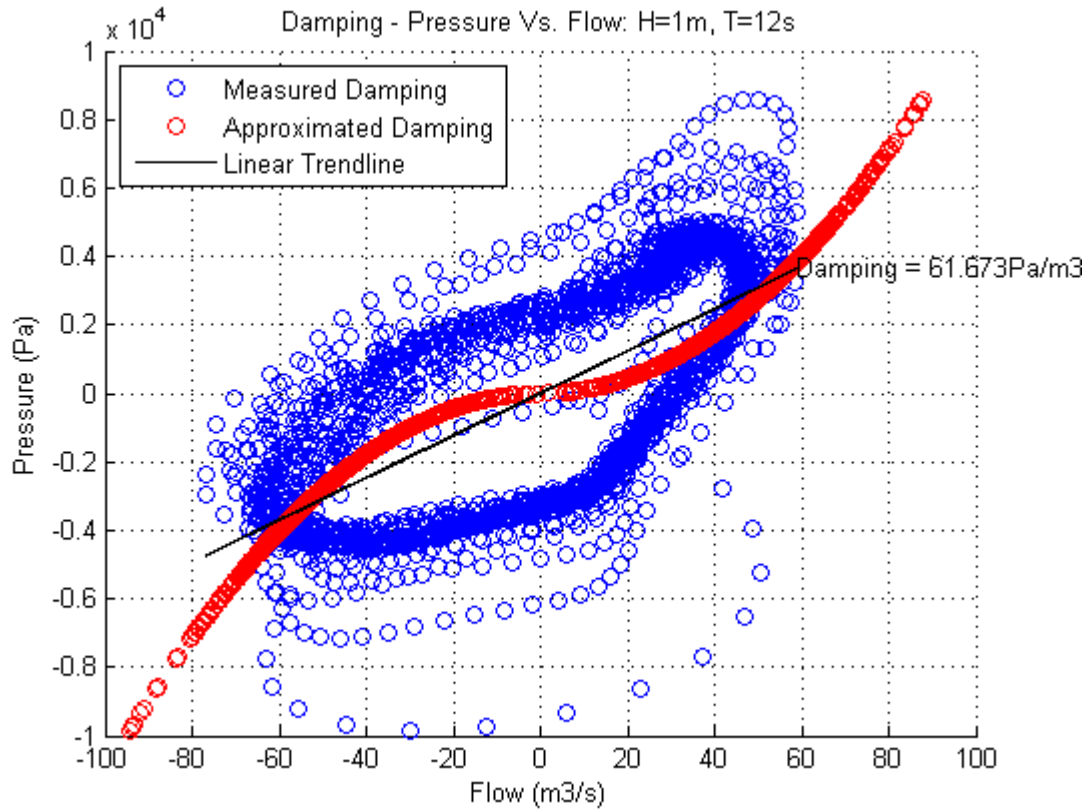
**Figure D.22: Damping Measures – Pressure Vs. Flow Diagram for one Chamber**

Also plotted in red is the pressure-flow relationship using Bernoulli's equation and the instantaneous chamber pressure. A linear trendline through the data is also plotted as an indication of the damping value. The origins of the scatter in the measured damping was puzzling as one would expect to see a trend matching the red line, with perhaps, depending on the pressures experienced, an element of hysteresis. To determine the source of this scatter, further detailed investigations were carried out on the time series data.
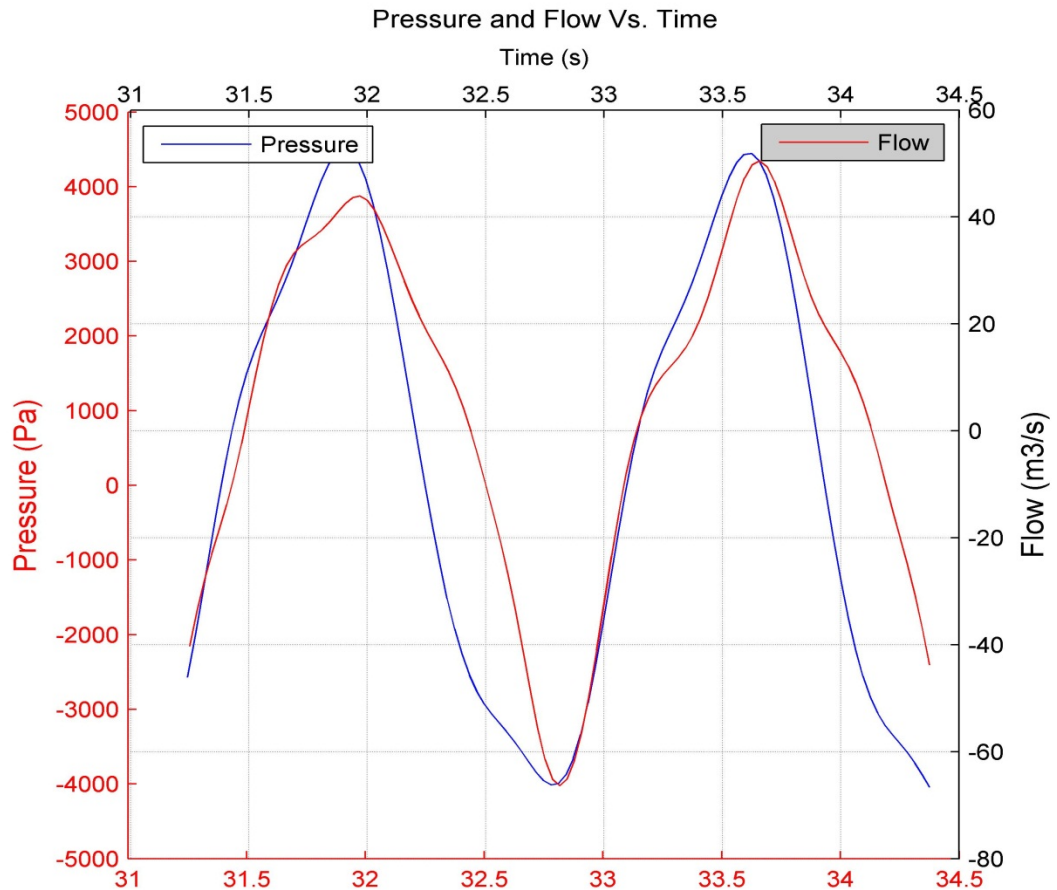
**Figure D.23: Pressure and Flow Time Series Superimposed**

Figure D.23 illustrates the instantaneous pressure-flow time series superimposed on the same time axis (with flow shifted back by ~3 timesteps due to a suspected phase lag in surface elevation by the float system). It may be seen that the peaks are broadly coincident. The axes make it difficult to determine the source of the scatter in the damping plot in Figure D.23. Therefore Figure D.24 was plotted. This is the instantaneous flow time series both inferred from the water column elevation measurements and inferred from pressure through Bernoulli's equation. This plot makes it more obvious what the source of the scatter in the measured damping may be. Similar to Figure D.23, the peaks of the signals are broadly coincident, however; the magnitude of the peaks on the 'up stoke' are considerably different and this difference is in general constant. In contrast the troughs of both signals are very close indeed. On the 'down stroke' it can be seen that the measured blue line is continually higher than the approximated flow. It is due to these variations in instantaneous flow that are the source of the scatter in the damping plot in Figure D.22. In terms of the reason for this discrepancy, it is reasonable to assume that it is as a result of the measurements from the float-guide system for measuring chamber water surface elevation. In order to confirm this, further tests are required on the float system used. Ideally this should be set up alongside a wave probe in a wave

tank and the instantaneous response from the float-guide-marker combination and the wave probe compared. In the event that a phase shift occurs between the signals due to the inertia of the float system, this should be quantified and can then be applied to the time series from the chamber water surface elevation. This should rectify the difference. For the purposes of quantifying power output, it was deemed more reasonable to use the flow time series inferred from pressure through Bernoulli's equation as this is consistent with measurements taken from the test rig used to characterise the orifice caps used in the original OWC Array tank testing described in APPENDIX A.
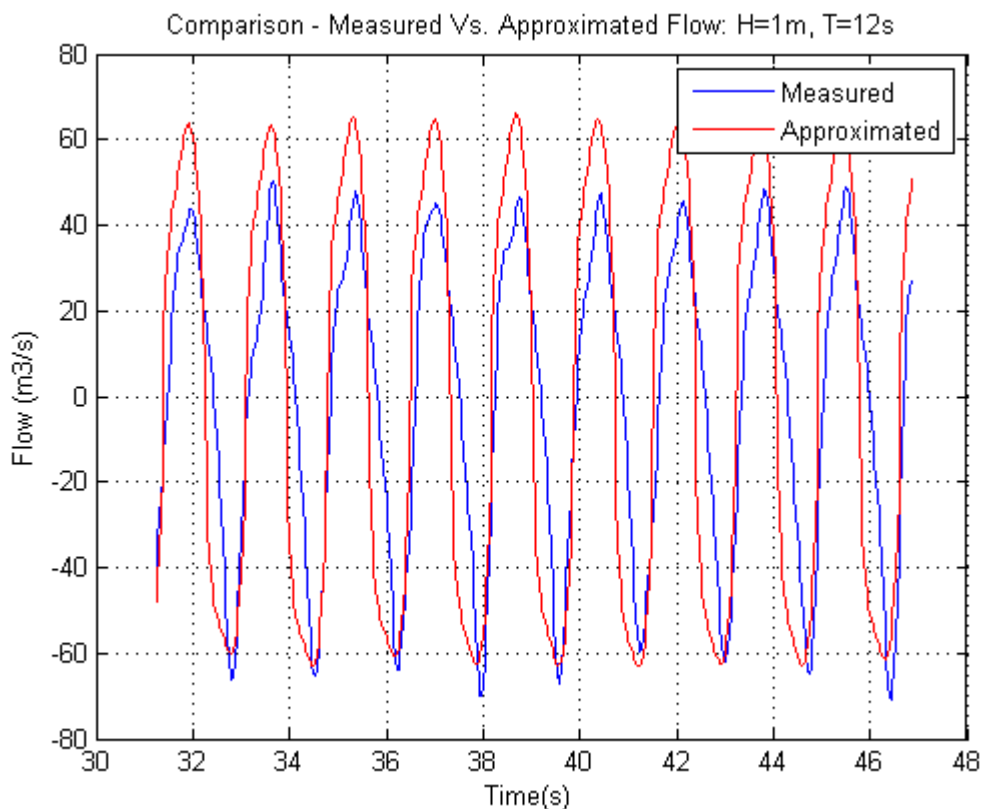


**Figure D.24: Comparison of Flow Time Series from Measurements from Surface Float and Inferred from Pressure Measurement**

### D.4.4    Power Performance Metrics

From the substantial bank of data from the tests, the power performance of the Delta OWC Array platform may be summarised in two main plots. Firstly, Figure D.25 illustrates the absorbed power RAO for monochromatic waves. Aside from the spurious result for 4m at 12s, the power performance is as expected. This plot illustrates the potential power output of the platform in idealised conditions and shows that the Delta OWC Array is a multi-MegaWatt output machine in most conditions.
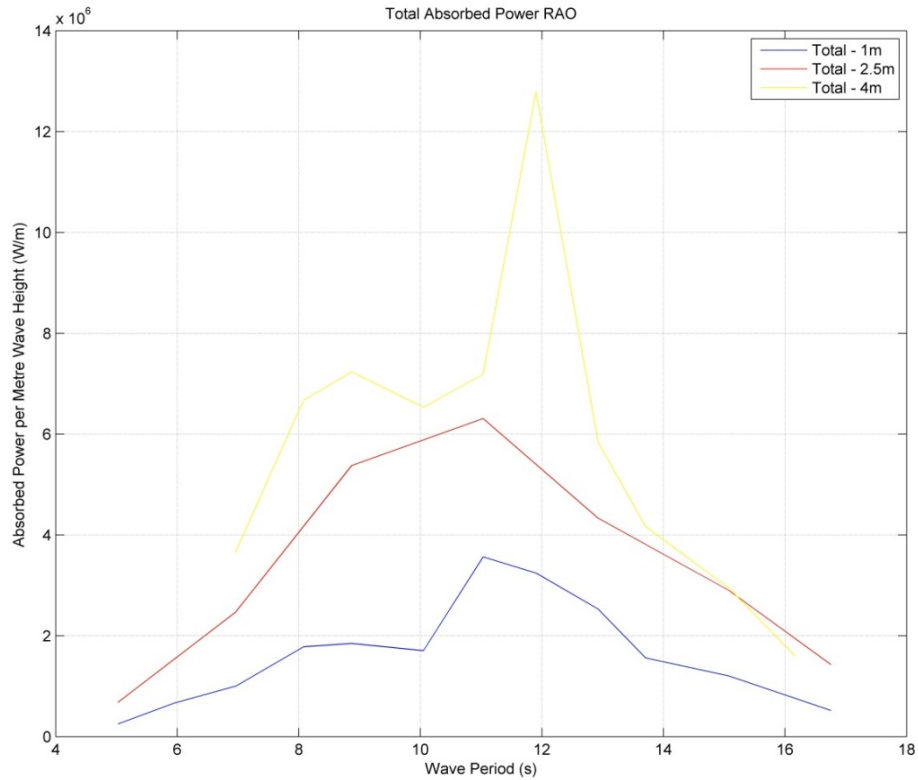
**Figure D.25: Power RAO for the Delta OWC Array in monochromatic wave conditions**

While Figure D.25 illustrated the idealised output of the machine, Figure D.26 illustrates the output in panchromatic waves. The results presented here are for uni-directional waves with incident directions of 0°, 22.5° and 45° to the symmetrical central axis of the platform.
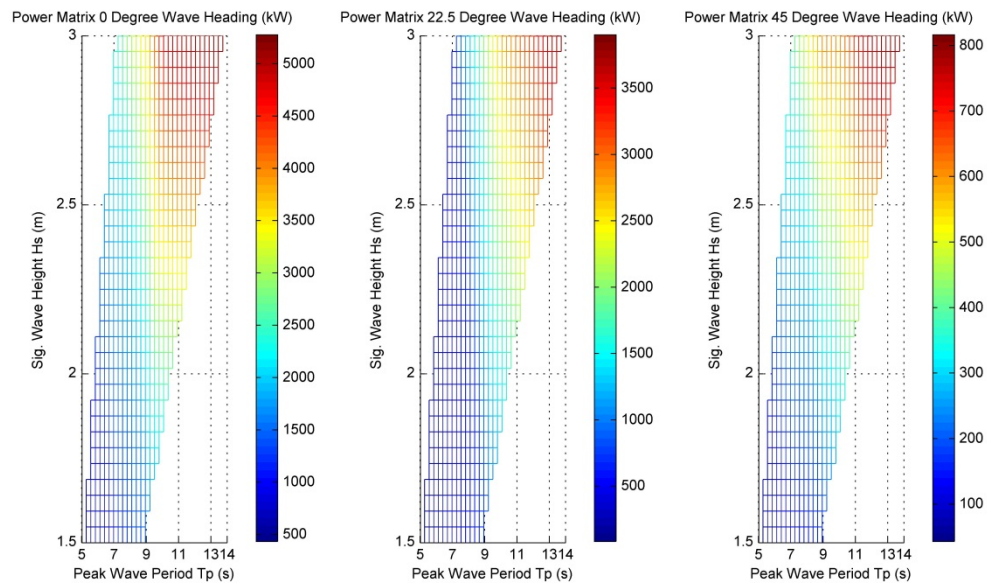


**Figure D.26: Prototype Absorbed Power Matrices for the Delta OWC Array Platform for Varying Incident Wave Direction in Panchromatic Waves**

325

It may be seen from Figure 5-44 that the Delta OWC Array platform is capable of absorbing 5MW of power in 3m $H_s$ sea states. This may be adjusted according to the approximate PTO efficiency of 54% to give 2700kW which is broadly in line with that suggested by the numerical simulations. However, with increasing wave directional angle relative to the central axis of the platform, the absorbed power drops considerably to a mere 800kW in 3m $H_s$ sea states for a wave directional angle of 45°. This is a substantial drop and clearly indicates the directional dependence of the platform. This suggests that a weather vaning mooring system is preferred for this platform but a full cost-benefit analysis is required based on the mooring system design.

## D.4    Challenges Faced During Tank Testing

### D.4.1    Water tightness of 60 buoyancy tanks

The construction of the model presented a number of issues, not just the size and mass of the model but also the water tightness criteria which had to be met for a total of 60 chambers. This proved impossible in the time allowed for construction using the low viscosity adhesive provided for the polycarbonate material. A decision was taken to pump each chamber with water resistant expandable foam in order to displace the required volume of water. This reduced the ability to shift mass blocks for fine tuning of tilt and draft, however due to the design of the chamber cross-section, only one configuration allowed correct stability and this was determined for one section prior to filling the chambers.

### D.4.2    Underestimated excitation of moonpool and associated structural failure of back beam

During the first Round of testing, an issue presented itself through the sloshing motion of the large moonpool and the lack of lateral stiffness of the back beam. As testing continued through increasing wave periods, the back beam began to warp and eventually cracked in one section. This section then filled with water until equilibrium was met again. The lateral stiffness of the back beam was clearly not sufficient, and additional steel bracing was fitted to the model to ensure sufficient stiffness during the remainder of the testing schedule. The addition of this bracing prevented the ability to change the internal angle of the structure to determine the effect on power absorption and motion characteristics.

### D.4.3    Failure of pressure sensors – corrosion and wetting of atmospheric opening from overtopping

Due to the angular excursions of the bow during testing at particular wave periods, the phenomenon of wave overtopping occurred to varying extents at higher wave heights. Particularly those at 6m prototype scale (120mm 1:50 scale). This caused significant wetting of the top sections of the model including some pressure sensors. These sensors operate by gauge pressure, or increase/decrease of pressure relative to atmospheric pressure. The port venting to atmosphere then became wet and

condensation resided in the port for a time. This, even minute amount of water, caused some sensors to fail and were beyond repair. For future survivability testing in ECN, a network of pneumatic tubing may be used to connect all atmospheric ports of the sensors with the ultimate atmospheric port being open well away from the model and/or water level.

## APPENDIX E Peer-Reviewed Papers Associated with this Thesis

Due to the broad nature of the topics considered throughout the development of this thesis, a significant number of peer-reviewed papers have either been written directly from the research carried out or the research carried out has contributed to papers by other lead authors. The following is a list of these papers and the conferences and/or journals they have been submitted to for publication in chronological order.

"Deterministic Economic Model for Wind-Wave Hybrid Energy Conversion Systems", 2012, K. O'Sullivan, J. Murphy, *Proceedings of the 2012 4th International Conference on Ocean Energy (ICOE2012)*, Dublin, Ireland

"Economic and Environmental Impact Appraisal of Commercial Scale Offshore Renewable Energy Installations on the west coast of Ireland", 2013, A.J. Posner, K. O'Sullivan, J. Murphy, *Proceedings of the 2013 International Coastal Symposium (ICS2013)* (Plymouth, UK), *Journal of Coastal Research*, Special Issue 65, pp.1639-1644, ISSN 0749-0208

"Power Output Performance and Smoothing Ability of an Oscillating Water Column Array Wave Energy Converter", 2013, K. O'Sullivan, J. Murphy, *Proceedings of the ASME 2013 32nd International Conference on Ocean, Offshore and Arctic Engineering (OMAE2013)*, June 9th-14th, Nantes, France

"Techno-Economic Optimisation of an Oscillating Water Column Array Wave Energy Converter", 2013, K. O'Sullivan, J. Murphy, *Proceedings of the 10th European Wave and Tidal Energy Conference (EWTEC2013)*, September 2nd-5th, Aalborg, Denmark

"Dynamic Responses of a Scaled Tension Leg Platform, Wind Turbine Support Structure in a Wave Tank", 2013, J. Murphy, R. O'Shea, K. O'Sullivan, V. Pakrashi, *Key Engineering Materials*, 569-570, 563-570

"Structural Design Implications when a Combined Wind and Wave Energy Platform is Applied in Different Site Scenarios", 2013, V. Pakrashi, J. Murphy, K. O'Sullivan, C. Long, P. O' Kelly-Lynch, *Proceedings of the Hydro 2013 International*, Chennai, India.

"Experimental Responses of a Monopile Foundation with a Wave Energy Converter Attached", 2013, V. Pakrashi, K. O'Sullivan, R. O'Shea, J. Murphy, *Proceedings of the Hydro 2013 International*, Chennai, India.

"Numerical Hydrodynamic and Structural Analysis of a Floating OWC at Three Irish Sites", 2014, K. O'Sullivan, J. Murphy, *Proceedings of the ASME 33rd International Conference on Ocean, Offshore and Arctic Engineering (OMAE2014)*, June 8th-13th, San Francisco, CA, USA

"Risk-Based Approach for the Development of Guidelines and Standards on Combined Marine Renewable Energy Platforms", 2014, L. Macadré, K. O'Sullivan,

A. Breuillard, S. le Diraison, *Proceedings of the ASME 33rd International Conference on Ocean, Offshore and Arctic Engineering (OMAE2014)*, June 8th-13th, San Francisco, CA, USA

"Structural Design Implications of Combining a Point Absorber with a Wind Turbine Monopile for East and West Coast of Ireland", 2014, V. Pakrashi, J. Murphy, K. O'Sullivan, C. Long, P. O' Kelly-Lynch, *Engineering Structures* – In Review

"The Hydrodynamics of the BBDB in the west of Ireland – Implications for Power Performance, Accessibility and Maintainability", K. O'Sullivan, J. Murphy

This paper is in preparation for submission to a leading offshore engineering journal in 2014 and is based on the work carried out in Chapter 3 of this thesis.

"Visualising the levelised cost of offshore energy around Europe", 2014, L. Cradden, K. O'Sullivan, D. Ingram

This paper is in preparation for the 5th International Conference on Ocean Energy (ICOE2014), Halifax, Canada in co-operation with the University of Edinburgh. A further journal publication is anticipated detailing the extension of the coupled LCOE model and GIS model to wave and tidal energy as well as offshore wind.

"Proposed Methodology for Assessing Cost Synergies Between Offshore Renewable Energy and Other Sea Uses", 2014, L. Margheritini, J.E. Hanssen, K. O'Sullivan, P. Mayorga

This paper is in preparation for the 2nd Asian Wave and Tidal Energy Conference (AWTEC2014), Tokyo, Japan in co-operation with 1-Tech, a MARINA Platform project consortium member.

"Hybrid offshore platforms for cost-efficient development of deepwater renewable energies", 2014, J.E. Hanssen, L. Margheritini, P. Mayorga, J. Hals, I. Martinez, A. Arrieta, R. Hezari, K. O'Sullivan, J. Steynor, D. Ingram

This paper is in preparation for the 5th International Conference on Ocean Energy (ICOE2014), Halifax, Canada in co-operation with a number of MARINA consortium members.